Current Oncological Abstract Service

COAS (Monthly)

May 2025, Volume 2 Issue 5

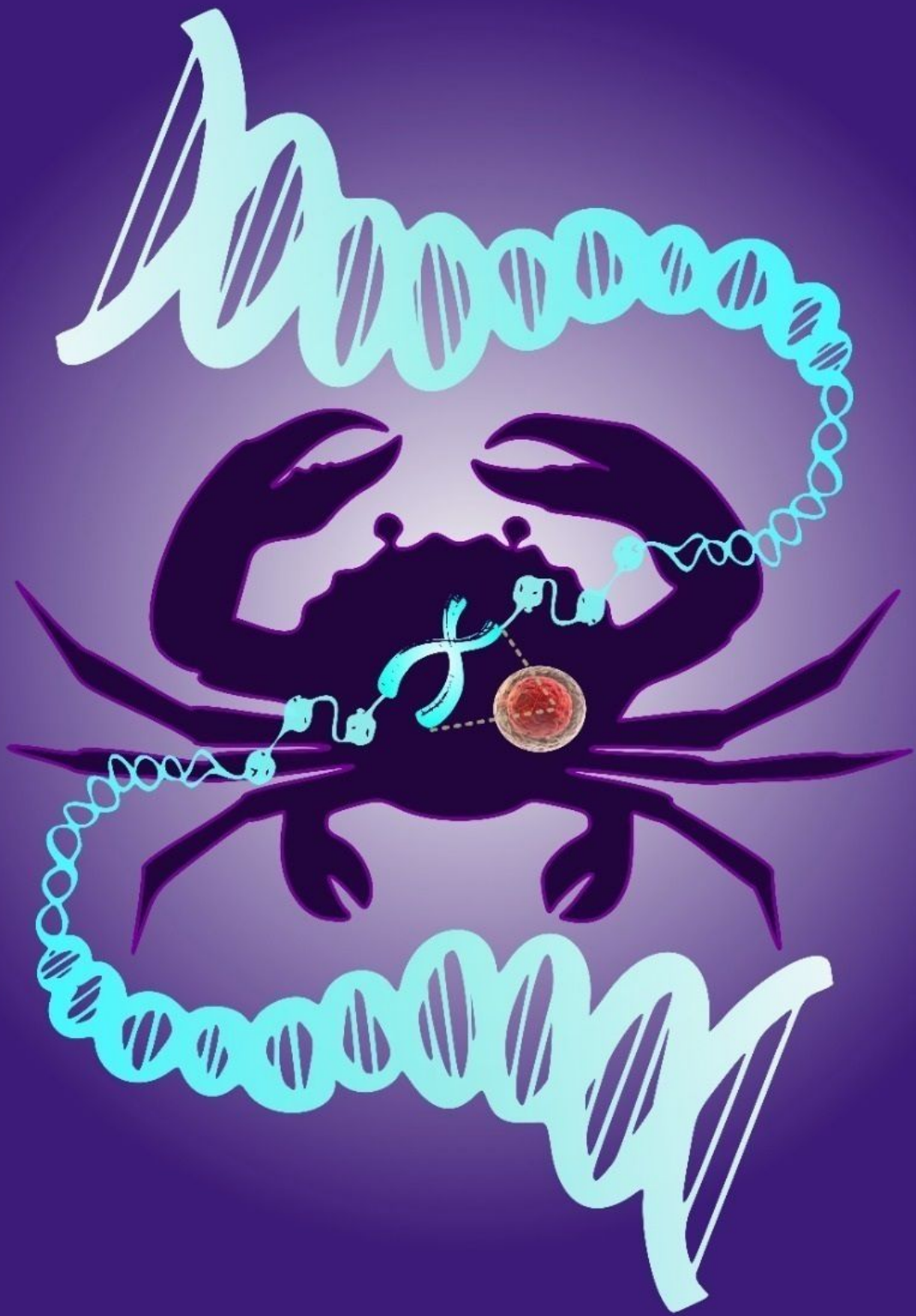

Compiled by:
Chittaranjan National Cancer Institute Library, Kolkata
(An Autonomous Body under Govt. of India, Ministry of Health & Family Welfare)

Current Oncological Abstract Service (COAS)

Monthly

Aims of the Abstracts

The Current Oncological Abstract Service (COAS) aims to provide timely, curated abstracts from a broad spectrum of oncological literature. The objectives of the service are:

1. To deliver concise, up-to-date abstracts of recently published oncological research, covering various subfields such as medical oncology, radiation oncology, anesthesiology, surgical oncology, and hematology.
2. To assist healthcare professionals, researchers, and students in staying informed about the latest advances and trends in oncology.
3. To support clinical and research-based decision-making by providing quick access to relevant, high-impact studies.
4. To foster knowledge exchange across disciplines, promoting a broader understanding of cancer-related topics.

Scope of the Abstracts

1. COAS includes abstracts from areas such as cancer biology, genetics, epidemiology, clinical trials, and treatment modalities (e.g., chemotherapy, immunotherapy, and targeted therapies), as well as patient care practices.
2. Abstracts are sourced from global research publications, offering a comprehensive view of international advancements in oncology.
3. Priority is given to high-impact studies, systematic reviews, meta-analyses, and research with significant implications for clinical practice.
4. In addition to core oncology, abstracts may cover related fields such as molecular biology, pharmacology, palliative care, and psychological support in oncology, reflecting the interdisciplinary nature of cancer care.

Layout

The "Current Oncological Abstract Service" is designed as a targeted information resource that provides clinicians, researchers, and students in oncology with the latest research abstracts and developments in cancer-related fields. It offers a regularly updated collection of abstracts from recently published articles, journals, and reports in oncology to keep users informed about current research trends, treatments, diagnostic methods, and advancements in oncology. The service is delivered monthly via email and as a downloadable PDF available on the CNCI website.

Content Sections - The COAS includes summaries of:

- The latest and most impactful research papers.
- Updates on new treatments, drugs, and clinical trials.
- Abstracts on new diagnostic tools, biomarkers, and techniques.
- Insights into cancer prevention research and epidemiological studies.
- Information on palliative care, patient management, and supportive therapies.

Abstract Formatting Each entry in the Current Oncological Abstract Service (COAS) includes:

- The title of the article or study.
- Authors and publication details.
- A summary focused on key findings and relevance.
- Keywords for easier navigation.
- A direct link to the original source (if online access is available).

User Navigation

- An index organized by cancer types, treatment methods, and research areas to facilitate easy navigation.
- A searchable database on the web platform, allowing users to quickly locate relevant abstracts.

User Engagement

- **Feedback Mechanism**: Users can provide feedback on abstracts and suggest improvements.
- **Personalization**: Users can subscribe to specific categories or topics of interest.

Bibliographical Citation:

Title-The title of the paper is invariably given in English and non-English titles are translated into English.

Author-A maximum of ten author's names are given. In case of more than ten authors, names of first ten authors are given followed by et al.

Details-The title of the paper is followed by volume number, issue number (in parenthesis), pagination and the of publication. Late publication or late receipt of the journals (if any), language(s) and number of references cited in the publication are given in parenthesis.

Abstract-Abstracts are informative and comprehensive. New data or findings are specifically indicated.

Current Oncological Abstract Service (COAS)

Editorial Board Members

Compiled by Central Library, Chittaranjan National Cancer Institute, Kolkata
Published by Chittaranjan National Cancer Institute Library, Kolkata

Current Oncological Abstract Service (COAS)

Monthly Abstracting Journal

VOLUME 2 ISSUE 5 MAY 2025

Compiler:

Dr. Sanmoy Chakraborty
Assistant Library & Information Officer

&

Ganesh Gorai
Assistant Library & Information Officer

Phone: 033 2475-9313, 033 3506-0600
Website: https://www.cnci.ac.in/
Email: cnci.library@gmail.com

DTP and Computer Processing:
CNCI Central Library

The purpose of the Current Oncological Abstract Service (COAS) is to provide users with valuable, curated oncology-related abstracts for research, educational, and informational purposes. Access to COAS materials is granted only to authorized users within CNCI, Kolkata. Use of COAS content is restricted to non-commercial, academic, and research-oriented purposes. Every effort is made to present the abstracts accurately but COAS assumes no liability for any errors and omissions.

Current Oncological Abstract Service (COAS)

Monthly Abstracting Journal

VOLUME 2 ISSUE 5 MAY 2025

Contents

Anesthesiology

25COASMA1

Title: Racial and ethnic differences in acute post-operative pain management: Systematic review and meta-analysis,

Anastasia Jones, Erik J. Feldtmann, Carlos Bellido, Emily C. Coughlin, Rahul S. Mhaskar, Cameron R. Smith, B. Lee Green, Linda T. Le-Wendling,

Journal of Clinical Anesthesia, Volume 104, 2025,111858,
https://doi.org/10.1016/j.jclinane.2025.111858.

Abstract: There are significant racial and ethnic differences in healthcare outcomes, including pain treatment. We conducted a systematic review and meta-analysis to investigate the racial and ethnic differences in acute pain treatment of surgical patients. We searched PubMed, Embase, and Scopus databases for any studies that reported racial and ethnic minority groups and treating acute postoperative pain. Random-effect meta-analysis was used to compare the odds ratio of receipt of regional anesthesia among racial and ethnic groups. Non-White patients were 18 % less likely to have regional anesthesia for postoperative pain [OR 0.82 (95 % CI; 0.76, 0.9]. Racial minority groups had lower rates of regional anesthesia—Black patients with OR of 0.93 (95 % CI; 0.91, 0.95); Asian patients with OR of 0.84 (95 % CI; 0.81, 0.87); race indicated as Other with OR of 0.78 (95 % CI; 0.71, 0.86). Only 3 studies reported Native Hawaiian and Alaska Native groups and found higher rates of regional anesthesia. Hispanic patients were 20 % less likely to receive regional anesthesia [OR of 0.8 (95 % CI; 0.72, 0.87)]. Three studies found some differences in opioid administration associated with race and ethnicity. A formal meta-analysis was not possible because of the heterogeneity of follow-up and timepoint comparison. There are racial and ethnic differences in the treatment of acute pain, especially in receipt of regional anesthesia. The most important step forward is the appropriate reporting of racial and ethnic demographic information. Further studies are warranted to understand the process by which differences arise in acute pain management.

Keywords: Regional anesthesia; Racial disparities; Racial differences; Ethnic disparities; Ethnic differences; Acute pain; Opioids

25COASMA2

Title: Intraoperative Factors Associated With Mechanical Ventilation Duration Following Aortic Surgery,

Nan Leng, Aaron M. Mittel, Dov Levine, Suzuka Nitta, Mitchell F. Berman, May Hua, Virendra I. Patel,

Journal of Cardiothoracic and Vascular Anesthesia, Volume 39, Issue 5,2025, Pages 1205-1213,
https://doi.org/10.1053/j.jvca.2025.02.021.

Abstract: Prolonged postoperative mechanical ventilation is a common complication after major aortic surgery. The relationship between prolonged ventilation and intraoperative variables influenced by anesthesiologists, such as ventilation practices, fluid administration, and blood pressure control during major aortic surgery is unknown. We sought to identify perioperative factors, including intraoperative physiologic and anesthesia-related variables,

which are associated with ventilation duration following aortic surgery. Single-center retrospective observational study. A tertiary, high-volume cardiac surgery referral center. Adult patients undergoing major aortic surgery requiring cardiopulmonary bypass (CPB). None (retrospective observational study). The primary outcome was the duration of postoperative ventilation (hours). Mixed-effects regression was performed to identify factors associated with the primary outcome. Among the 647 patients included in this study, the median of postoperative mechanical ventilation duration was 9.0 (IQR 6.0, 14.4) hours, with 73 (11.3%) of patients receiving mechanical ventilation for more than 24 hours. Variables significantly associated with the outcome were increases in pre- to post-CPB driving pressure (β = 4.23; 95% CI [0.08, 8.39]; p = 0.04), reduction in pre- to post-CPB end-tidal carbon dioxide partial pressure (β = –5.12; 95% CI [–8.85, –1.39]; p < 0.001), and normalized transfusion volumes (β = 11.14; 95% CI [4.36, 17.91]; p < 0.001). Mechanical power was not associated with postoperative ventilation duration (β = –2.29; 95% CI [–6.48, 1.90]; p = 0.52). Patients undergoing major aortic surgery are at risk for prolonged mechanical ventilation. Transfusion volume and pre- to post-CPB changes in driving pressures and end-tidal carbon dioxide are significantly associated with postoperative ventilation duration. Intraoperative mechanical ventilator power is not a significant predictor of mechanical ventilation duration after major aortic surgery. These variables are potentially modifiable by anesthesiologists and may be future therapeutic targets.

Keywords: postoperative pulmonary complication; prolonged ventilation; major aortic surgery; cardiac surgery; driving pressure; outcome analysis

25COASMA3

Title: Evaluation of Angiotensin II in Patients With Catecholamine-Resistant Vasodilatory Shock Requiring Continuous Renal Replacement Therapy (ANGEL CRRT),

Meaghan A. Rettele, Adham M. Mohamed, Timothy P. Berry, Sydney S. Wilson, Julie A. Welge,

Journal of Cardiothoracic and Vascular Anesthesia, Volume 39, Issue 5, 2025, Pages 1250-1256,
https://doi.org/10.1053/j.jvca.2025.01.042.

Abstract: To compare clinical outcomes of patients with catecholamine-resistant vasodilatory shock (CRVS) receiving continuous renal replacement therapy who receive adjunctive angiotensin II (ANGII) to those who do not.Retrospective cohort analysis. Multicenter, single health system consisting of one academic medical center and four community hospitals. Critically ill adult patients with CRVS (norepinephrine or equivalent dose ≥0.5 mcg/kg/min). Adjunctive ANGII versus standard-of-care (SOC) vasopressors alone (norepinephrine, epinephrine, vasopressin, phenylephrine, dopamine). The primary outcome was intensive care unit mortality. Secondary outcomes included 30-day mortality, Sequential Organ Failure Assessment (SOFA) score at 72 hours, time to shock resolution, and adverse effects. A multivariate logistic regression was used for the primary analysis. The study included 265 patients, of which 70 received ANGII and 195 received SOC. Intensive care unit and 30-day mortality were lower in patients that received ANGII (61.4% v 75.4%, adjusted odds ratio 0.438, 95% confidence interval: 0.239-0.805, p = 0.008; and 67.1% v

78.5%, adjusted odds ratio 0.479, 95% confidence interval: 0.256-0.898, p = 0.022). Differences in time to shock reversal and SOFA score at 72 hours were not statistically significant. The adverse effects evaluated were not statistically significant, apart from an increase in fungal infections in the ANGII group (17.1% v 7.2%, p = 0.016). ANGII was associated with lower mortality in patients who received renal replacement therapy compared to SOC. This evaluation reaffirms a subgroup of patients that may benefit from the addition of ANGII.

Keywords: angiotensin II; shock; renal replacement therapy; renin; vasopressors

25COASMA4

Title: Pancreatic Stone Protein as Sepsis Biomarker in Patients Requiring Mechanical Circulatory Support: A Pilot Observational Study,

Alessandro Belletti, Matteo A. Bonizzoni, Rosa Labanca, Paul Osenberg, Samuele Bugo, Domenico Pontillo,

Journal of Cardiothoracic and Vascular Anesthesia,Volume 39, Issue 5,2025,Pages 1229-1235,
https://doi.org/10.1053/j.jvca.2025.01.037.

Abstract: To demonstrate for the first time the performance of the novel biomarker pancreatic stone protein (PSP) in predicting the occurrence of sepsis in cardiogenic shock patients requiring mechanical circulatory support. Many patients with cardiogenic shock develop sepsis and the timely identification and treatment of sepsis remains a key factor to improve outcome and avoid unnecessary antibiotics treatment. Observational study recording PSP values for 5 days or until intensive care unit discharge (whichever came first) to analyze its kinetic and evaluate a potential correlation with sepsis development.Setting Cardiac intensive care unit.Participants 32 adult patients with cardiogenic shock requiring mechanical circulatory support, 28% women with a median age of 68 years (range, 60-72 years). Measurements and Main Results The main causes of cardiogenic shock were postcardiotomy (50%) and acute myocardial infarction (25%). Patients were supported with and intra-aortic balloon pump (62.5%), Impella (6.3%), or venoarterial extracorporeal membrane oxygenation (3.1%); 28% of patients had more than 1 support device. Forty percent of patients developed sepsis during their intensive care unit stay. The overall median peak PSP reached was 389.5 ng/mL (interquartile range, 222-601 ng/mL), with a peak on day 2. The peak was higher in patients who developed sepsis (601 ng/mL [interquartile range, 556-601 ng/mL] in patients with sepsis v 257 ng/mL [interquartile range, 207-576 ng/mL] in patients without). In these patients also daily PSP values from day 2 to 5 were higher. Conclusions Patients supported with mechanical circulatory support who develop sepsis present with significantly higher PSP values than those who do not develop sepsis. PSP values are generally high in this population, even in patients not developing sepsis.

Keywords: sepsis; cardiogenic shock; mechanical circulatory support; pancreatic stone protein; C-reactive protein; biomarker

25COASMA5

Title: Heparin Versus Bivalirudin in Pediatric Patients Assisted With Mechanical Circulatory Support: A Retrospective Before-and-after Study,

Chiara Giorni, Nicoletta Cantarutti, Alessandro Olimpieri, Simona Benegni, Alessandra Rizza, Isabella Favia,
Journal of Cardiothoracic and Vascular Anesthesia, Volume 39, Issue 5,2025,Pages 1242-1249,
https://doi.org/10.1053/j.jvca.2025.01.041.
Abstract: Children assisted with mechanical circulatory support experience bleeding and thrombotic complications that may depend upon anticoagulation strategies. The primary aim of this study was to compare the incidence of thrombotic events in pediatric heart failure patients assisted with mechanical circulatory support with the use of bivalirudin versus heparin anticoagulation. A secondary aim was to compare the percentage of out-of-range partial thromboplastin time values between these anticoagulants. Design Retrospective cohort study. Setting Tertiary pediatric cardiac intensive care unit. Participants Pediatric patients undergoing mechanical circulatory support for cardiac failure. Measurements and Main Results A total of 36 pediatric patients on mechanical support treated with either heparin (n.18) or bivalirudin (n.18) during the first 30 days of intensive care unit admission were compared. Bivalirudin group data were retrieved from February 2018 to August 2020 while data on the heparin group were extrapolated from 2015 to 2017. A comparison of anticoagulation was conducted specifically in EXCOR Berlin Heart and extracorporeal membrane oxygenation patients. Berlin Heart patients showed 1 (12.5%) versus 8 (80%) thrombotic episodes in the bivalirudin and heparin groups, respectively ($p = 0.005$), 0 and 3 (30%) cerebrovascular events, and 0 versus 3 (30%) death episodes, respectively ($p = 0.054$). In extracorporeal membrane oxygenation patients, the bivalirudin and heparin groups showed 0 versus 1 (8.3%) patient with a thrombosis episode ($p = 0.40$), 0 and 0 cerebrovascular events, and 5 (50%) versus 3 (25%) death episodes, respectively ($p = 0.169$). The number of out-of-range partial thromboplastin time values was higher in the heparin group both in Berlin Heart and extracorporeal membrane oxygenation patients ($p < 0.0001$). Conclusions In a cohort of children with heart failure, bivalirudin use was associated with a reduction in thrombotic events in Berlin Heart patients compared with heparin over a period of 30 days.
Keywords: anticoagulation; extracorporeal membrane oxygenation; pediatrics; ventricular assist device; bivalirudin; heparin

25COASMA6

Title: Oxygen Targets for Mechanically Ventilated Adults with Sepsis: Secondary Analysis of the PILOT Trial,

Jack C. Shapiro and Jonathan D. Casey and Edward T. Qian and Kevin P. Seitz and Li Wang and Bradley D. Lloyd
Journal of Intensive Care Medicine, Vol. 40, Number-5, pages 486–494,year 2025,
https://doi.org/https://doi.org/10.1177/08850666241299378,
Abstract: Patients with sepsis frequently require invasive mechanical ventilation. How oxygenation during mechanical ventilation affects clinical outcomes for patients with sepsis remains uncertain. To evaluate the effects of different oxygen saturation targets on clinical outcomes for patients with sepsis receiving mechanical ventilation. We performed a secondary analysis of the Pragmatic Investigation of optimaL Oxygen Targets (PILOT) trial dataset among patients who met criteria for sepsis by the Sepsis-3 definition at the time of

enrollment. We compared patients randomized to a lower oxygen saturation target (90%; range, 88–92%), an intermediate target (94%; range, 92–96%), and a higher target (98%; range, 96–100%) with regard to the outcomes of 28-day in-hospital mortality and ventilator-free days to study day 28.Of 2541 patients in the PILOT dataset, 805 patients with sepsis were included in the current analysis. In-hospital mortality by day 28 did not differ significantly between the lower target group (48%; 95% confidence interval [CI], 42% to 54%), the intermediate target group (50%; 95% CI, 43% to 56%), and the higher target group (51%; 95% CI, 45% to 56%) (P = 0.83). The number of ventilator-free days to day 28 did not significantly differ between the trial groups, with a mean of 9.9 (standard deviation [SD], 11.8) in the lower oxygen saturation target group, 9.5 (SD, 11.2) in the intermediate group, and 9.4 (SD, 11.4) in the higher group (P = 0.65). Among mechanically ventilated patients with sepsis in a large, randomized trial, the incidence of 28-day in-hospital mortality was not statistically significantly different between the use of a lower, intermediate, or higher oxygen target. However, the confidence intervals included treatment effects that would be clinically meaningfully and further randomized trials of oxygen targets in sepsis are required.

25COASMA7

Title: Comparative Analysis of Percutaneous Dilatational Tracheotomy and Surgical Tracheotomy in Critically Ill Patients: Outcomes and Complications,

Şahin Temel, Hatice Metin, Mehmet Gökhan Gök, Recep Civan Yüksel, Murat Sungur, Emrah Gülmez, Gönül Sungur, Kürşat Gündoğan,

Journal of Cardiothoracic and Vascular Anesthesia,Volume 39, Issue 5,2025,Pages 1214-1220,

https://doi.org/10.1053/j.jvca.2025.02.008.

Abstract: To evaluate the outcomes of percutaneous dilatational tracheostomy (PDT) versus surgical tracheostomy (ST) in critically ill patients, focusing on complications, duration of mechanical ventilation (MV), intensive care unit (ICU) length of stay, and mortality. Design Retrospective trial Setting Single tertiary center Participants A total of 119 patients receiving invasive MV in a medical ICU Interventions PDT (n = 55) or ST (n = 64) methods Measurements and Main Results The 2 groups showed comparable outcomes in terms of MV duration (36 days for PDT vs 35 days for ST; p = 0.72), ICU stay (43 days for PDT vs 37 days for ST; p = 0.17), and all-cause mortality (71% for PDT vs 64% for ST; p = 0.42). PDT was associated with significantly lower rates of subcutaneous emphysema (0% vs 16%; p = 0.01). Multivariate analysis showed no statistically significant association between tracheostomy technique and ICU mortality or overall complication rates after adjustment for confounders. Conclusion PDT and ST yield comparable outcomes in critically ill ICU patients, with no significant difference in overall complication rates or mortality. The fewer specific complications for PDT, such as subcutaneous emphysema, highlight its advantages in suitable cases. Individualized patient assessment remains crucial, and further studies are needed to refine tracheostomy practices.

Keywords: intensive care; tracheostomy; comparative study; critical care; tracheostomy techniques

25COASMA8

Title: Hemodynamic Improvement in Acute Respiratory Distress Syndrome Patients After Venovenous Extracorporeal Membrane Oxygenation Implantation,

Rosa Labanca, Marina Pieri, Giacomo Monti, Stefano Fresilli, Pasquale Nardelli, Luca Baldetti, Evgeny Fominskiy,

Journal of Cardiothoracic and Vascular Anesthesia, Volume 39, Issue 5,2025,Pages 1221-1228,

https://doi.org/10.1053/j.jvca.2025.01.011.

Abstract: Severe acute respiratory distress syndrome (ARDS) is often complicated by hemodynamic instability requiring pharmacological support. Venovenous extracorporeal membrane oxygenation (VV ECMO) is a well-established technique that contributes to improved outcomes in this population. However, the effects of VV ECMO on inotropic and vasoconstrictor requirements have never been addressed in a large case series. Design Observational study. Setting University hospital. Participants Consecutive adult ARDS patients treated with VV ECMO. Measurements and Main Results From June 2009 to October 2023, 118 ARDS patients received VV ECMO and had available baseline data. The median patient age was 57 years, 65% of patients were male, and 76% had ongoing inotropic and/or vasoconstrictor support. Two hours after ECMO implantation, 61% of patients showed hemodynamic improvement, as documented by the reduced need for catecholaminergic support or increased mean arterial pressure with identical inotropic and/or vasoconstrictor support. This percentage increased to 63% at 12 hours, 83% at 24 hours, and 85% at 48 hours.Conclusion In the first 2 hours after VV ECMO implantation, hemodynamic improvement was observed in the majority of ARDS patients. This positive effect might therefore be considered in the decision-making process for VV ECMO implantation.

Keywords: acute respiratory distress syndrome; extracorporeal membrane oxygenation; respiratory failure; hemodynamic; Vasoactive Inotropic Score; right ventricular failure; septic shock; intensive care

25COASMA9

Title: Postoperative Liver Dysfunction After Lung Transplantation With Extracorporeal Life Support and 1-Year Mortality—A Cohort Study,

Cecilia Veraar, Stefan Schwarz, Caroline Hillebrand, Johanna Schlein, Clarence J. Veraar, Edda Tschernko, Konrad Hoetzenecker, Martin Dworschak, Johannes Menger,

Journal of Cardiothoracic and Vascular Anesthesia,Volume 39, Issue 5,2025,Pages 1266-1274,

https://doi.org/10.1053/j.jvca.2025.02.012.

Abstract: Extracorporeal life support, including venovenous and venoarterial extracorporeal membrane oxygenation (ECMO) or cardiopulmonary bypass (CPB), triggers a pronounced inflammatory response and has been linked to postoperative liver dysfunction. Such dysfunction may negatively affect clinical outcomes after lung transplantation. Given that double-lung transplantation increasingly involves venoarterial ECMO, this work was designed to analyze the incidence of liver injury post-transplant and its impact on outcomes, specifically duration of intensive care unit (ICU) stay and 1-year mortality.Data from 1,350 consecutive patients who underwent lung transplantation between January 2009 and April

2023 were analyzed. Hepatic injury occurring within the first 12 postoperative days was classified as hypoxic liver dysfunction, drug-induced liver injury, or cholestasis. The corresponding incidences were 4%, 23%, and 52%, respectively. All were associated with an increased length of ICU stay. Owing to the multiple medications these patients receive post-transplantation, a clear distinction between drug-induced liver injury and a mild form of hypoxic liver dysfunction is difficult. However, only the latter was independently linked with increased 1-year mortality amounting to 35%. Patients who developed hypoxic liver dysfunction were more frequently operated on CPB or required prolonged ECMO support. Lung transplantation involving CPB or extended perioperative ECMO support significantly increases the risk of severe postoperative liver dysfunction associated with poorer outcomes. However, brief intraoperative ECMO deployment does not appear to carry this risk.

Keywords: lung transplantation; extracorporeal membrane oxygenation; postoperative liver dysfunction; hypoxic liver failure; drug-induced liver failure; cholestasis

25COASMA10

Title: Perioperative Management and Outcome of Catecholamine-Induced Takotsubo and Dilated Cardiomyopathy in Pheochromocytoma and Paraganglioma,

Manjiao Ma, Xiuhua Zhang, Xuerong Yu, Lulu Ma,

Journal of Cardiothoracic and Vascular Anesthesia, Volume 39, Issue 5,2025,Pages 1275-1281,
https://doi.org/10.1053/j.jvca.2025.02.004.

Abstract: To outline and compare the clinical features, preoperative preparation, perioperative management, and outcome of Takotsubo cardiomyopathy (TCM) and dilated cardiomyopathy (DCM) associated with pheochromocytomas and paragangliomas (PPGLs).

A retrospective cohort study. A single tertiary hospital. All patients scheduled for elective surgery of PPGL resection with TCM and DCM between March 2005 and June 2023 were enrolled. Measurements and Main Results This study enrolled 29 patients: 20 patients were in the TCM group and 9 patients were in the DCM group. The tumor size of the DCM group was bigger and the level of 24-hour urine norepinephrine was higher than those in the TCM group. After the preoperative medication preparation (111 median days) and anti–heart failure treatment (if necessary), the mean preoperative ejection fraction in the TCM group was significantly higher than that in the DCM group (66.8% ± 4.4% v 48.8% ± 7.8%, $p<0.001$), both elevated compared to ejection fraction at presentation ($p<0.001$). The intraoperative hemodynamic instability score was rather high in PPGL-TCM and PPGL-DCM patients (84.6 points), as well as in the hemodynamic variables section (13.7 points). Patients with DCM were more prone to present hemodynamic disturbances and to require a lower volume of fluids but a higher infusion of vasoactive agents than patients with TCM. The incidence of complications was 6.9% and there was no perioperative mortality. Following the preoperative medication preparation and anti–heart failure treatment, patients with TCM had better left ventricular recovery before surgery and fewer cardiovascular risks compared to patients with DCM. Optimal perioperative management and individualized anesthetic strategies are essential for this unique patient population.

Keywords: pheochromocytoma; paraganglioma; Takostubo cardiomyopathy; dilated cardiomyopathy; catecholamine-induced cardiomyopathy

25COASMA11

Title: Implementation of a Multidisciplinary Team for Initiation of Extracorporeal Cardiopulmonary Resuscitation in Patients Presenting After Out-of-hospital Cardiac Arrest,

Sean Hickey, Christopher Ortiz, Wei-Ting Chen, Phoebe Johnson Black, Tristan Grogan, Peyman Benharash, Vadim Gudzenko,

Journal of Cardiothoracic and Vascular Anesthesia, Volume 39, Issue 5,2025,Pages 1236-1241,
https://doi.org/10.1053/j.jvca.2025.02.018.

Abstract: Patents with out-of-hospital cardiac arrest (OHCA) are at high risk of death or poor neurologic recovery if spontaneous circulation is not rapidly restored. Emergent mechanical circulatory support with venoarterial extracorporeal membrane oxygenation (VA-ECMO) in the setting of extracorporeal cardiopulmonary resuscitation (ECPR) offers a bridge to diagnostic and therapeutic interventions but can be challenging to provide in a timely fashion. Coordination of multidisciplinary institutional resources into an ECMO Shock Team (ECMO-ST) may improve the survival of ECPR patients while concurrently increasing the number of OHCA patients placed on ECMO. Retrospective cohort study. Single-center urban university hospital in the United States with an active mechanical circulatory support and cardiac transplantation program. 55 OHCA patients who received ECPR after presenting to the emergency department from May 2013 to December 2022. Ad hoc emergent ECPR support versus activation of the ECMO-ST. The primary outcome was survival to hospital discharge. Secondary outcomes included time to ECMO cannulation, duration of ECMO support, renal failure requiring dialysis, diagnosis of hypoxic brain injury, intensive care unit length of stay, 6-month survival, and functional neurologic recovery quantified by cerebral performance category score at discharge and 6 months. Implementation of the ECMO-ST was associated with an increase in the rate of survival to hospital discharge from 22% (2/9 patients) to 52% (24/46 patients), although the result was not statistically significant due to the small sample size of the preintervention cohort. A total of 69% of those discharged from the hospital had favorable neurologic function as defined by cerebral performance category scores of 1-2. The organization and implementation of a multidisciplinary institutional ECPR response team trended toward an association with higher rates of survival to hospital discharge, with favorable neurologic function in patients presenting to the emergency department after OHCA.

Keywords: extracorporeal membrane oxygenation; ECMO; extracorporeal cardiopulmonary resuscitation; ECPR; cardiac arrest; emergency medicine; critical care; resuscitation; intensive care; shock

25COASMA12

Title: Early extubations in children intubated prior to arrival in Paediatric Burn ICU: A single center retrospective study over 1520 admissions,

Sébastien Lebrun, Nicolas Louvet, Nada Sabourdin, Isabelle Constant,

Anaesthesia Critical Care & Pain Medicine, Volume 44, Issue 3,2025,101500,
https://doi.org/10.1016/j.accpm.2025.101500.

Abstract: In adult burns intensive care units, more than 30% of patients arriving intubated, are extubated within 2 days (potentially unnecessary intubation, PUNI). Such data are lacking in paediatric populations. Exploring this paediatric PUNI rate was the primary aim of the study. Data from all the admissions to our paediatric burn intensive care unit were retrospectively analyzed over an 8-years period. Extubations within the first two days among patients arriving intubated were assessed as the primary outcome (PUNI rate). Using a univariate logistic regression and a multivariate model, we analyzed factors associated with intubation lasting more than 2 days (potentially necessary intubation, PNI). Finally, we developed a score to predict the probability of PNI. Among the 1520 admitted children (age: 0–17; Percentage of Total Body Surface Area (%TBSA): 1%–97%), 56 (4%) arrived intubated, 20 (36%) of whom were considered PUNI. These patients had smaller %TBSA burned compared to those having PNI (24% ± 17% vs. 48% ± 24%, p = 0.002). We developed a score based on factors independently associated with PNI: %TBSA burned (OR = 1.12 [1.09–1.15] for each additional per cent), flame burns (OR = 4.43 [1.64–11.6]) and facial burns (OR = 12.28 [3.41–67.4]). Seven children (<0.5%) were intubated after admission. Intubation before admission to a burn intensive care unit was less frequent in children. The paediatric rate of PUNI, however, was close to findings reported in adults: approximately one-third of intubated children were extubated within 2 days.
Keywords: Burns; Pediatric; Intubation; Intensive care

25COASMA13

Title: Association between low income and ICU delirium among critically ill older patients: A retrospective cohort study in Japan,

Toshinori Nishizawa, Nobutoshi Nawa, Atsushi Mizuno, Takahiro Suzuki, Hiroko Arioka, Takeo Fujiwara,

Anaesthesia Critical Care & Pain Medicine, Volume 44, Issue 3,2025,101523,
https://doi.org/10.1016/j.accpm.2025.101523.

Abstract: The social determinants of delirium have yet to be well-studied. We explored the association between low-income and intensive care unit (ICU) delirium among critically ill older patients in Japan, where universal healthcare coverage is provided. This was a retrospective cohort study. Study patients included 2705 adults aged 70 years or older who were admitted to the ICU of St. Luke's International Hospital in Tokyo for a mean duration of 4.3 (SD = 6.0) days between March 2014 and April 2022. Patients classified in the low-income categories of the public health insurance system or receiving public assistance were designated as the low-income group. ICU delirium was assessed using the Confusion Assessment Method-ICU. The Cox proportional hazards model was used to estimate the associations between low income and delirium. 508 patients (18.8%) were categorized as low-income. Delirium occurred in 1055 patients (39.0%) during ICU stay. After adjustment for age, sex, hearing or vision impairment, alcohol abuse, psychiatric disorders, cognitive impairment, cerebrovascular disease, and physical function, low-income showed a 1.20 times greater risk of ICU delirium (95%CI: 1.04−1.39, p = 0.014). After adjustment for potential mediators in addition to the confounding factors, low-income remained at 1.17 times greater risk of ICU delirium (95%CI: 1.01−1.36, p = 0.035). In a Japanese ICU, low income was found to be an independent risk factor for ICU delirium. Future studies are needed to

elucidate the mechanism of the association between low income and delirium in Japanese critically ill older patients.

Keywords: Income; Delirium; Social determinants of health; Intensive care units

25COASMA14

Title: Comparative analysis of patient and family satisfaction in Spanish Intensive Care Units: A cross-sectional study of the impact of diagnosis,

Eva de Miguel-Balsa, Esther Rios-Albert, Beatriz Quevedo-Sánchez, Angela Jorda-Miñana, Cristina Portillo-Requena,

Anaesthesia Critical Care & Pain Medicine, Volume 44, Issue 3,2025,101515,
https://doi.org/10.1016/j.accpm.2025.101515.

Abstract: Analysing relatives and patients experiences and satisfaction can highlight areas for improving Intensive Care Units (ICUs) care. Patients and families may differ about satisfaction and experience, depending on the diagnosis and procedures. We aimed to compare the experience and satisfaction of patients according to diagnosis, severity, and the procedures received, and also between relatives and patients. Prospective analysis of voluntary responses to the FS (Family Satisfaction)- ICU 24 R questionnaire from surviving ICU patients and their relatives (January-April 2023) in four Spanish hospitals, according to diagnostic groups. Responses were scored on a Likert scale (0: worst score; 100: best score), and means and standard deviations were compared. 185 responses were analysed, mostly acute cardiac pathology patients (91, 50.83%), followed by septic shock patients (22.9%). Patients rated the team performance higher than their relatives (98.79 ± 5.37 vs 89.68 ± 18.43; $p < 0.0001$), also symptom management such as pain (95.62 ± 9.52 vs 89.64 ± 17.24; $p = 0.0001$, and dyspnoea (94.23 ± 12.27 vs 88.09 ± 17.87; $p = <0.001$), the information process (91.50 ± 13.43 vs 83.17 ± 21.00; $p < 0.001$), and decision-making (80.38 ± 13.60 vs 65.84 ± 23.60; $p < 0.001$). Patients found visits to be scarce (43.75 ± 20.79), although their families were satisfied with their involvement in care (85.49 ± 19.64). Patients with sepsis and septic shock rated pain management the lowest compared to other diagnostic groups (sepsis/septic shock 89.58 ± 12.5 vs 98.61 ± 5.89; $p < 0.001$). Open visiting policies and enhancing the protocols for conscious sedation/analgesia in invasive procedures are opportunities to improve the satisfaction and experience of ICU patients and their families.

Keywords: Satisfaction; Intensive care; Quality of care; Humanization; Visiting policy

25COASMA15

Title: Norepinephrine infusion for preventing hypotension during hepatic exteriorization in Kasai portoenterostomy in infants with biliary atresia: A randomized controlled trial,

Khaled Sarhan, Nehal Ashraf, Ahmed Hasanin, Marwa Zayed, Reham Saleh, Manal Elgohary, Ramy Alkonaiesy, Kareem Nawwar,

Anaesthesia Critical Care & Pain Medicine, Volume 44, Issue 3,2025,101519,
https://doi.org/10.1016/j.accpm.2025.101519.

Abstract: Hepatic exteriorization during Kasai portoenterostomy is usually associated with profound hypotension. This study aimed to assess the role of prophylactic norepinephrine infusion in maintaining blood pressure in infants undergoing Kasai portoenterostomy

operation. Thirty-two infants scheduled for Kasai portoenterostomy operation were randomly assigned to one of two groups: Norepinephrine group: this group received prophylactic intraoperative norepinephrine infusion, Control group: this group received placebo saline infusion. The primary outcome was the incidence of hypotension during liver exteriorization, defined as a persistent reduction of the mean arterial pressure (MAP) ≥20% of the baseline reading requiring release of the liver. Other outcomes included: the frequency of stoppage of surgery and release of the liver, liver function variables, arterial blood gases parameters, total volume of intraoperative infused fluids, and incidence of bradycardia and hypertension. The incidence of persistent hypotension (defined as the need for liver release after administering IV fluid and vasopressor boluses) during liver exteriorization, was 12.5% (2 patients) in the norepinephrine group compared to 75% (12 patients) in the control group, relative risk (95% confidence interval [CI]): 0.17 (0.04−0.63), p = 0.001. Rescue norepinephrine boluses were used in 3 patients (18.8%) in the norepinephrine group compared to 13 patients (81.3%) in the control group, relative risk (95% CI): 0.23 (0.08−0.66), p = 0.001. Among infants with biliary atresia undergoing Kasai portoenterostomy operation, norepinephrine infusion significantly reduced the incidence of persistent severe hypotension during hepatic exteriorization requiring liver release.

Keywords: Kasai portoenterostomy; Norepinephrine; Kasai; Biliary; Atresia; Infant

25COASMA16

Title: Adjuvant nefopam versus standard of care in mechanically ventilated surgical critically ill patients: A randomized, double-blind controlled study,

Mohammed Gamal Abdelraouf, Samar Farghali Farid, Ahmed Mohammed Mukhtar, Nirmeen Ahmed Sabry,

Anaesthesia Critical Care & Pain Medicine, Volume 44, Issue 3,2025,101518,
https://doi.org/10.1016/j.accpm.2025.101518.

Abstract: Multimodal analgesia, through combining different classes of analgesia that target pain pathways with different mechanisms reduces opioid consumption. This study aimed to determine the impact of adjunct nefopam infusion on opiate consumption when added to standard-of-care analgesia and sedation in mechanically ventilated critically ill patients. This was a prospective, randomized, active control, double-blind study. Patients admitted to the ICU, being mechanically ventilated and candidates for analgesia and sedation protocols were randomized to the intervention group (n = 30) or to the control group (n = 30). The primary outcome was the cumulative dose of fentanyl in the first 24 h after inclusion. The secondary outcomes were the proportion of patients with positive pain scores, change in mean arterial pressure (MAP), heart rate (HR), ICU mortality, and others. A total of 60 patients were included in the final analysis; median (Q1, Q3) cumulative fentanyl consumption mcg/24 h was significantly (p = 0.001) lower in the intervention group compared to the control group 1300 (575, 2087.5) vs. 2400 (1612.5, 2665) mcg/24 h respectively. Pain and sedation scores were comparable between the two study groups. ICU mortality was 25 (83.3%) in the intervention group vs. 20 (66.7%) in the control group (P = 0.136). Nefopam was found to be an effective non-opioid option for analgesia in mechanically ventilated surgical and trauma critically ill patients, and more studies are needed to evaluate its safety.

Keywords: Analgesia; Critically ill; Fentanyl; Mechanical ventilation; Nefopam; Vasopressors

25COASMA17

Title: Optimal brain perfusion pressure derived from the continuous monitoring of cerebral autoregulation status during neonatal heart surgery under cardiopulmonary bypass in relation to brain injury: An observational study,

Pierre Bourgoin, Erta Beqiri, Peter Smielewski, Alexis Chenouard, Aurélie Gaultier, Flavie Sadones, Ugo Gouedard, Nicolas Joram, Pascal Amedro,

Anaesthesia Critical Care & Pain Medicine, Volume 44, Issue 3,2025,101509,
https://doi.org/10.1016/j.accpm.2025.101509.

Abstract: Understanding cerebral blood flow regulation and later optimizing brain perfusion is part of neuroprotection during cardiopulmonary bypass (CPB) in neonates. A total of 38 neonates undergoing CPB were monitored using near-infrared spectrometry and mean arterial pressure (MAP). Cerebral autoregulation (CAR) was assessed through the continuous measurement of the Cerebral Oxygenation Index (COx), and CAR-derived metrics were determined by plotting averaged COx values by MAP: Optimal MAP (MAPopt), lower limit of CAR (LLA), upper limit of CAR (ULA). Out of 38, 17 (45%) neonates exhibited moderate to severe brain lesions post-operatively. The onset of CPB was associated with CAR disruption (mean COx pre-CPB = 0.16 ± 0.11; during CPB: 0.39 ± 0.37, $p < 0.001$). A LLA was identified in 31 out of 38 (82%), 23 out of 38 (61%), and 14 out of 38 (37%) patients before, during, and after CPB, respectively. An ULA was identified in 29 out of 38 (76%), 22 out of 38 (58%), and 14 out of 38 (37%) patients in the same time frames. Patients with abnormal post-operative brain MRI spent more time below the LLA during CPB: 28.3% [17.1–32.9] versus 9.9% [6.9–18.5] in patients without detected brain injury, $p = 0.039$. No differences were observed regarding the time spent above the upper limit of autoregulation. The study provides valuable insights into the intricate relationship between intraoperative cerebral hemodynamics and post-operative brain injury. Further research is warranted to explore potential interventions based on CAR-derived metrics during CPB in neonates.

Keywords: Cerebral autoregulation; Neonatal heart surgery; Cardiopulmonary bypass; Cerebral oximetry; Mean arterial pressure; Brain injury; MRI severity scoring

25COASMA18

Title: Post-induction hypotension during rapid sequence intubation in the operating room: A post hoc analysis of the randomized controlled REMICRUSH trial,

Nicolas Grillot, Victoire Gonzalez, Romain Deransy, Armine Rouhani, Guillaume Cintrat, Paul Rooze,

Anaesthesia Critical Care & Pain Medicine, Volume 44, Issue 3,2025,101502,
https://doi.org/10.1016/j.accpm.2025.101502.

Abstract: We explored the risk factors of post-induction hypotension during rapid sequence intubation.We performed an ancillary analysis of a multicenter randomized clinical trial comparing remifentanil versus neuromuscular blockers associated with hypnotic in patients at risk for aspiration who underwent tracheal intubation in the operating room. The primary outcome was post-induction hypotension, defined as an episode of hypotension

(MBP ≤ 55 mmHg and/or SBP ≤ 80 mmHg) within 10 min after anesthetic induction. From 15 hospitals, 1137 adult patients were included, and 291 (26%) had post-induction hypotension. Propofol was used in 1117 (98%) patients and was associated with low doses of ketamine in 209 (18 %) patients. The independent risk factors associated with post-induction hypotension were age (OR 1.03, 95% CI [1.02; 1.04] p < 0.0001), baseline heart rate (p = 0.0068), bowel occlusion requiring nasogastric tube placement before intubation (OR 1.96, 95% CI [1.33; 2.87] p = 0.0006) and use of remifentanil (OR 3.54, 95%CI (2.61; 4.81) p < 0.0001). Use of low doses of ketamine (OR 0.61, 95% CI [0.41; 0.92] p = 0.0175) and basal SBP (OR 0.98, 95% CI [0.97; 0.99] p < 0.0001) were protective factors. The precision of the final model including the above-mentioned variables gave an AUC of 0.74 [95% CI 0.71; 0.77] for post-induction hypotension prediction. Post-induction hypotension was frequent during rapid sequence intubation. Sedation associating propofol with low doses of ketamine was associated with a low risk of post-induction hypotension. Further studies are required to demonstrate a causal effect.

Keywords: Post-induction hypotension; Rapid sequence intubation; General anesthesia; Risk factors; Propofol; Ketamine

25COASMA19

Title: Weaning from external ventricular drainage after non-traumatic subarachnoid hemorrhage: Rapid vs. gradual weaning and predicting closure trial failure. The SEVDVE retrospective multicenter cohort study,

Henri Lomo, Joseph Brasselet, Hélène Gohel, Simon Praud, Vincent Roux, Julie Faule, Tiphaine Bernard,

Anaesthesia Critical Care & Pain Medicine, Volume 44, Issue 3,2025,101508,
https://doi.org/10.1016/j.accpm.2025.101508.

Abstract: Weaning from external ventricular drainage (EVD) following subarachnoid hemorrhage (SAH) typically requires an EVD closure trial, performed either straightforwardly (rapid weaning) or after gradual elevation of EVD (gradual weaning). We wanted to compare these two methods and build a sore to predict closure trial failure. Among adult SAH patients, this multicenter (n = 5) retrospective study, compared rapid and gradual EVD weaning methods, and identified factors associated with EVD closure trial failure through logistic regressions. We developed a score to predict closure trial failure by splitting the dataset into training (2/3) and testing (1/3) sets. Among 1141 patients with an EVD between 01/01/2018 and 12/31/2022, 407 were hospitalized for SAH and had at least one EVD weaning attempt, 249 (61%) underwent gradual and 158 (39%) rapid weaning. Rapid weaning was associated with more failure (72 (46%) vs. 86 (35%), p = 0.044), but shorter length of stay (LOS) in both ICU and hospital. EVD closure trial failure was independently associated with prolonged EVD maintenance (p < 0.001), prolonged ICU (p = 0.001) and hospital LOS (p = 0.05). We developed a failure closure score using the difference in intracranial pressures (from H0 to H3 after closure), time since EVD insertion, and EVD level. The model's area under the receiver operating curve was 0.63 [0.53–0.74], indicating fair discrimination ability. EVD weaning strategies vary across centres. Rapid weaning was associated with a high risk of closure trial failure, but shorter LOS. EVD closure trial failure was associated with worse outcomes. A simple 3-criteria score could help.

Keywords: External ventricular drainage; Subarachnoid hemorrhage; Weaning; Intracranial pressures

25COASMA20

Title: A core outcome set of measurement instruments for assessing effectiveness and efficacy of perioperative pain management: results of the international IMI-PainCare PROMPT Delphi consensus process,

Esther M. Pogatzki-Zahn, Sarah De Lucia, Claudia Weinmann, Hauke Heitkamp, Lone Hummelshoj,

British Journal of Anaesthesia, Volume 134, Issue 5,2025,Pages 1460-1473,
https://doi.org/10.1016/j.bja.2025.01.029.

Abstract: Effective perioperative pain management is crucial to prevent patient suffering, delayed recovery, chronic postsurgical pain, and long-term opioid use. However, the heterogeneous use of outcomes in studies complicates evidence synthesis and might not accurately reflect the experiences of individual patients. We initiated a consensus process to establish a core outcome set (COS) of patient-reported outcome measures (PROMs) in postoperative pain, building upon the earlier consensus on a COS of domains. Potential PROMs were identified via systematic literature searches for the domains pain intensity (with subdomains at rest and during activity), physical function, self-efficacy, and adverse events, followed by appraisal of psychometric properties according to the COnsensus-based Standards for the selection of health Measurement INstruments methodology. Then, a consensus meeting was convened, followed by a Delphi process with an international, multiprofessional panel of stakeholders, including those with lived experience. A conclusive consensus meeting approved the final COS of PROMs. The final COS consists of one unidimensional numerical rating scale for assessing pain intensity on average, worst pain intensity, pain intensity at rest, and procedure-specific pain intensity during activity; one unidimensional scale for pain interfering with activities in bed; one procedure-specific scale for assessing physical function; the IMI-PainCare PROMPT adaptation of the Arthritis Self-Efficacy Scale for assessing self-efficacy; and the IMI-PainCare PROMPT adaptation of the Opioid-Related Symptom Distress Scale for assessing adverse events. Comprehensive use of a core outcome set will help harmonise outcome assessment, facilitate comparisons between studies, promote patient-centred research, and improve postoperative pain care.

Keywords: consensus process; core outcome set; Delphi approach; patient-reported outcome measure; postoperative pain; psychometric properties; questionnaire

25COASMA21

Title: Dexmedetomidine mitigation of renal ischaemia–reperfusion injury: comprehensive insights from cellular mechanisms to clinical application,

Kevin Chotinaruemol, Prangmalee Leurcharusmee, Siriporn C. Chattipakorn, Nipon Chattipakorn, Nattayaporn Apaijai,

British Journal of Anaesthesia, Volume 134, Issue 5,2025,Pages 1350-1372,
https://doi.org/10.1016/j.bja.2025.02.006.

Abstract: Renal ischaemia–reperfusion injury (IRI) is a critical cause of acute kidney injury (AKI) after major surgery, leading to elevated morbidity, mortality, and long-term renal

dysfunction. Despite advances in perioperative care, the occurrence of IRI remains high. The renoprotective properties of dexmedetomidine (DEX), a selective α2-adrenergic receptor agonist, have been demonstrated, reducing oxidative stress, inflammation, apoptosis, ferroptosis, cellular senescence, and renal fibrosis while enhancing mitochondrial function and autophagy. From cellular studies to clinical applications, DEX has been effective in mitigating renal IRI, enhancing postoperative renal outcomes, and lowering the incidence of AKI in various surgical settings. This review comprehensively discusses and summarises the renoprotective effects and the underlying mechanisms of DEX, with a focus on its application across various surgical and clinical scenarios. In conclusion, DEX effectively mitigates renal IRI, as evidenced by robust in vitro, in vivo, and clinical studies. It significantly reduces kidney damage and improves surgical outcomes. However, its efficacy is less pronounced in kidney transplantation, suggesting that its renoprotective effects vary depending on the clinical context.

Keywords: α2-adrenergic receptor agonist; acute kidney injury; dexmedetomidine; renal ischaemia–reperfusion injury; renoprotection

25COASMA22

Title: Balanced electrolyte solution with 1% glucose as intraoperative maintenance fluid in infants: a prospective study of glucose, electrolyte, and acid–base homeostasis,

Ulf Lindestam, Åke Norberg, Peter Frykholm, Olav Rooyackers, Andreas Andersson, Urban Fläring,

British Journal of Anaesthesia, Volume 134, Issue 5,2025,Pages 1432-1439,
https://doi.org/10.1016/j.bja.2024.08.041.

Abstract: Optimal composition and infusion rates of intravenous maintenance fluids for children undergoing surgery are not well defined. Avoidance of hypoglycaemia, ketosis, and hyponatraemia is important, and current guidelines recommend isotonic fluids containing 1.0–2.5% glucose. However, evidence for its safe use in infants is insufficient. The aim of this study was to investigate whether normoglycaemia is maintained in infants using a balanced electrolyte maintenance infusion with 1% glucose. Infants 1–12 months of age undergoing surgery were included in this prospective two-centre study. Intravenous maintenance fluid was given with infusion rates of 4–8 ml kg−1 h−1. Blood gas and ketone body analysis were performed at induction and at the end of anaesthesia. Plasma glucose concentration was monitored intraoperatively. For the 365 infants included in this study, the median infusion rate of maintenance fluid was 3.97 (interquartile range 3.21–5.35) ml kg−1 h−1. Mean plasma glucose concentration increased from 5.3 mM at induction to 6.1 mM at the end of anaesthesia (mean difference 0.8 mM; 95% confidence interval 0.6–0.9, P<0.001). No cases of hypoglycaemia (<3.0 mM) occurred. Mean sodium concentration remained stable during anaesthesia. Chloride and ketone body concentration increased and base excess decreased, but these were within the normal range. In infants undergoing surgery, maintenance infusion with a balanced electrolyte solution containing 1% glucose, at rates similar to those proposed by Holliday and Segar is a safe alternative with regards to homeostasis of glucose, electrolytes, and acid–base balance.

Keywords: acid–base physiology; glucose; infants; ketone bodies; perioperative fluid management; sodium

25COASMA23

Title: An updated systematic review and consensus definitions for standardised endpoints in perioperative medicine: patient comfort and pain relief,

Paul S. Myles, Sophie Wallace, Oliver Boney, Mari Botti, Frances Chung, Allan M. Cyna, Tong J. Gan,

British Journal of Anaesthesia, Volume 134, Issue 5,2025,Pages 1450-1459,
https://doi.org/10.1016/j.bja.2025.02.025.

Abstract: Improving comfort during and after surgery is a key concern for anaesthetists and other clinicians. With the inclusion of patient and public involvement, we undertook a Delphi consensus process to update previously recommended endpoints to be used in clinical trials evaluating treatments aiming to improve patient comfort after surgery. We undertook a systematic review to identify domains and outcome measures of patient comfort used in perioperative studies. Focus groups, workshops, and a multi-round Delphi consensus process that included clinician-researchers and a patient experience and consumer group updated a recommended list of standardised endpoints focused on patient comfort. Consensus was defined as a median item score of 7 or greater and at least 70% of responses achieving a score of 7 or greater on a 9-point Likert scale. Additional ratings were done to determine validity, reliability, feasibility, and patient-centredness. Qualitative analyses were undertaken to identify themes. Response rates for each of the Delphi rounds were 100%. A final list of eight defined endpoints was identified: supplementary analgesic use, subjective analgesic effectiveness, pain intensity (at rest, during movement, and at 12, 24, and 72 h), postoperative nausea and vomiting (PONV, at 0–6 h, at 6–24 h, and overall), postdischarge nausea and vomiting (PDNV), severe PONV, quality of recovery (QoR-15), and time to mobilisation. All endpoints were assessed as valid, reliable, and feasible measures of patient comfort and were considered patient-centred. Patient and public involvement highlighted the importance of clear communication and shared decision-making to enhance comfort through the surgical journey. We recommend that at least some of these standardised endpoints be included as outcome measures in clinical trials assessing patient comfort and pain after surgery.

Keywords: analgesia; clinical trials; Delphi; nausea; patient experience; patient-reported outcomes; postoperative pain; vomiting

25COASMA24

Title: Altered thrombin generation with prothrombin complex concentrate is not detected by viscoelastic testing: an in vitro study,

Nikolaus Hofmann, Herbert Schöchl, Johannes Zipperle, Johannes Gratz, Felix C.F. Schmitt, Daniel Oberladstätter,

British Journal of Anaesthesia, Volume 134, Issue 5,2025,Pages 1392-1401,
https://doi.org/10.1016/j.bja.2024.10.047.

Abstract: Bleeding guidelines currently recommend use of viscoelastic testing (VET) to direct haemostatic resuscitation in severe haemorrhage. However, VET-derived parameters of clot initiation, such as clotting time (CT) and activated clotting time (ACT), might not adequately reflect a clinically relevant interaction of procoagulant and anticoagulant activity, as revealed by thrombin generation assays. The aim of this study was to evaluate the ability of CT and ACT to indicate thrombin generation activity. Citrated whole blood obtained from

13 healthy volunteers underwent a 50% crystalloid dilution (DL-50%), followed by spiking with four-factor prothrombin complex concentrate (DL-50% + 4F-PCC). Changes in thrombin generation activity were compared with the VET parameters CT and ACT derived from four commercially available viscoelastic devices (ROTEM® Delta, ClotPro®, TEG®6s, and Quantra®) and standard coagulation tests. Dilution of whole blood resulted in a marked increase in velocity index, peak height, and endogenous thrombin potential (all $P<0.01$), with a further substantial increase after spiking with 4F-PCC (all $P<0.001$). In contrast, CT and ACT were significantly prolonged in response to DL-50% on all devices (all $P<0.05$). Subsequent spiking of diluted blood with 4F-PCC had no impact on CT and ACT derived from VET analysers, but it restored standard coagulation tests without reaching baseline values (all $P<0.01$). Upregulated thrombin generation parameters after PCC spiking were not displayed by CT, ACT, or standard tests. Our results do not support treatment algorithms using prolonged CT or ACT as a trigger for administration of PCC to augment thrombin generation.

Keywords: point-of-care coagulation testing; prothrombin complex concentrate; thrombin generation; trauma-induced coagulopathy; viscoelastic testing

25COASMA25

Title: Evaluation of AI-based nerve segmentation on ultrasound: relevance of standard metrics in the clinical setting,

Bernard V. Delvaux, Olivier Maupain, Thomas Giral, James S. Bowness, Luc Mercadal,
British Journal of Anaesthesia, Volume 134, Issue 5,2025, Pages 1497-1502,
https://doi.org/10.1016/j.bja.2024.12.040.

Abstract: In artificial intelligence for ultrasound-guided regional anaesthesia, accurate nerve identification is essential. The technology community typically favours objective metrics of pixel overlap on still-frame images, whereas clinical assessments often use subjective evaluation of cine loops by physician experts. No clinically acceptable threshold of pixel overlap has been defined for nerve segmentation. We investigated the relationship between these approaches and identify thresholds for objective pixel-based metrics when clinical evaluations identify high-quality nerve segmentation. cNerve™ is a deep learning segmentation tool on GE Healthcare's Venue™ ultrasound systems. It highlights nerves of the interscalene–supraclavicular-level brachial plexus, femoral, and popliteal-level sciatic block regions. Expert anaesthesiologists subjectively rated overall segmentation quality of cNerve™ on ultrasound cine loop sequences using a 1–5 Likert scale (1 = poor; 5 = excellent). Objective assessments of nerve segmentation, using the Intersection over Union and Dice similarity coefficient metrics, were applied to frames from sequences rated 5. A total of 173 still image frames were analysed. The median Intersection over Union for nerves was 0.49, and the median Dice similarity coefficient was 0.65, indicating variable performance based on objective metrics, despite subjective clinical evaluations rating the artificial intelligence-generated nerve segmentation as excellent. Variable objective segmentation metric scores correspond to excellent performance on clinically oriented assessment and lack the context provided by subjective expert evaluations. Further work is needed to establish standardised evaluation criteria that incorporate both objective pixel-

based and subjective clinical assessments. Collaboration between clinicians and technologists is needed to develop these evaluation methods for improved clinical applicability.

Keywords: artificial intelligence; machine learning; medical devices; translational AI; ultrasound-guided regional anaesthesia

25COASMA26

Title: Neurodevelopmental and behavioural disorders after perioperative invasive mechanical ventilation in paediatric surgical admissions,

Oliver G. Isik, Ling Guo, Ariel Ben-Ezra, Sandya Ganesh, May Hua, Caleb H. Miles, Mark Olfson, Andrew S. Geneslaw, Caleb Ing,

British Journal of Anaesthesia, Volume 134, Issue 5,2025,Pages 1440-1449,
https://doi.org/10.1016/j.bja.2024.12.042.

Abstract: Children with a respiratory disease requiring invasive mechanical ventilation (IMV) in the paediatric intensive care unit (PICU) have an elevated risk for subsequent neurodevelopmental and behavioural disorders (NDBD). This study evaluates NDBD in children receiving IMV during surgical admissions. Children enrolled in Texas Medicaid between 1999 and 2012 with a surgical admission were evaluated. Children in the PICU receiving IMV, in the PICU not receiving IMV, and in the intermediate medical care unit (IMCU) were identified and matched to children admitted to the general ward. The primary outcome was post-discharge NDBD. Secondary analyses evaluated NDBD risk by IMV duration and post-discharge psychotropic medication use. Of 35 161 children with surgical admissions meeting eligibility criteria, 993 were in the PICU with IMV, 7670 in the PICU without IMV, and 1027 in the IMCU. Increased rates of NDBD were observed in children receiving IMV (hazard ratio [HR] 1.91, 95% confidence interval [CI] 1.27–2.89, P=0.002), but not in those in the PICU without IMV (HR 1.12, 95% CI 0.98–1.29, P=0.10) or IMCU (HR 0.88, 95% CI 0.61–1.26, P=0.48). Elevated rates of NDBD were detected primarily in children receiving IMV for 96 h or more. Increased psychotropic medication use was observed only in the IMV group. Children receiving invasive mechanical ventilation during a surgical admission are at increased risk of neurodevelopmental and behavioural disorders after hospital discharge. Further research is needed to clarify the mechanisms behind this association and to identify potentially modifiable risk factors.

Keywords: behavioural disorders; child neurodevelopment; critical care medicine; mechanical ventilation; paediatric critical care; surgical critical care

25COASMA27

Title: Validation of Pediatric Sequential Organ Failure Assessment (pSOFA) Scores to Predict Critical Events in the Pediatric Intensive Care Unit,

Colleen M. Badke and Austin Wang and Latasha A. Daniels and L. Nelson Sanchez-Pinto,

Journal of Intensive Care Medicine,Vol. 40, Number-5, pages 565–570,year 2025,
https://doi.org/10.1177/08850666241307630

Abstract: To determine the prognostic value of the Pediatric Sequential Organ Failure Assessment (pSOFA) to discriminate critical events, including code events and intubations, in the pediatric intensive care unit (PICU). We performed an observational cohort study of all critical events in a quaternary care PICU between 5/2020 and 4/2023. Critical events were

extracted from our hospital communications platform and from the electronic health record (EHR). The pediatric sequential organ failure assessment (pSOFA) scores were prospectively calculated in real-time in our EHR every 15 min during the study period for data-driven situational awareness and were retrospectively analyzed for this study. Each encounter was divided into 6-h time blocks and we assessed the performance of the highest pSOFA score in each block at discriminating the occurrence of a critical event in the subsequent block. There were 5687 unique patient encounters included in the analysis. Critical events were identified in 578 out of 169 486 time blocks (prevalence 0.3%), which included 103 code events and 498 intubation events, in 392 unique PICU encounters. The total pSOFA score in a 6-h time block was significantly associated with a subsequent code event (odds ratio [OR] 1.19, 95% CI 1.13-1.24) or intubation (OR 1.13, 95% CI 1.10-1.15). Several organ-specific pSOFA subscores were also significantly associated with the outcomes. Area under the receiver operating characteristic curve (AUROC) for the total pSOFA score was 0.67 for a code event and 0.65 for intubation. Using a pSOFA score cutoff of ≥8, the positive predictive value was 0.8% and the negative predictive value was 99.7% for any critical event. The pSOFA score is significantly associated with critical events in the PICU, however, it does not have adequate performance to be used for situational awareness by itself.

25COASMA28

Title: Ig-M and Ig-A Enriched Ig-G Infusion as Adjuvant Therapy in the Critically ill Patients Experiencing SARS-CoV-2 Severe Infection,

Alberto Corona and Sara Simoncini and Giuseppe Richini and Ivan Gatti and Clemente Santorsola and Andrea Patroni and Giacomina Tomasini and Alice Capone and Elena Zendra and Myriam Shuman,

Journal of Intensive Care Medicine,Vol. 40, Number-5, pages 536–546,year 2024,
https://doi.org/10.1177/08850666241301689,

Abstract: SARS-CoV-2 in patients who need Intensive Care (ICU) is associated with a mortality rate ranging from 10 to 40%-45%, with an increase in morbidity and mortality in presence of sepsis. We assumed that immunoglobulin (Ig) M and IgA enriched IgG (IGAM) therapy may support SARS COV-2 sepsis-related phase improving patient outcome. We conducted a retrospective case-control study on all the patients admitted to our ICU during the three pandemic waves between February 2020 and April 2021. Upon ICU admission, patients received anticoagulants with the standard supportive treatment (ST) ± IGAM therapy. After matching for the baseline characteristics and treatments, the patients receiving IGAM therapy too (group A), were compared with those undergoing ST (group B) only. 85 patients were enrolled in group A, whereas 111 in group B. The mortality resulted lower in group A [37.6% versus 55.8%, OR: 0.7 (02-08), P = .01)]. A logistic regression analysis identified IGAM treatment as a survival predictor [OR: 0.35 (95%CI, 0.2-0.8)], whereas experiencing a super-infection [OR: 1.88 (95%CI, 1.5-4.9)] and a septic shock [OR: 1.92 (95%CI, 1.4-4.3)] as predictors of death. On day 7, the probability of dying was 3 times higher in patients treated with ST only. Variable life adjustment display (VLAD) was equal to 2.4 in group A, while – 2.2 group B (in terms of lives saved in relation with those expected, in according with Simplified Acute Physiology Score II (SAPS II) score. The treatment based on IGAM

infusion seems to give an advantage chance of survival in SARS-CoV-2 severe infection. Further prospective studies are warranted.

25COASMA29

Title: Exploring Rapid Response Team Activation Impact in Patients with Cirrhosis with Acute Decompensation,

Joelle N. Friesen and Mackenzie Maberry and Jody C. Olson and Alice Gallo de Moraes,

Journal of Intensive Care Medicine,Vol. 40, Number-5, pages 528–535,year 2024,
https://doi.org/https://doi.org/10.1177/08850666241302024,

Abstract: Cirrhosis is associated with significant healthcare utilization, yet data about in-hospital decompensations remain sparse. Additionally, the impact of liver transplant candidacy status on resuscitation and outcomes is largely unknown. We aimed to evaluate the characteristics of resuscitation events for patients with cirrhosis with acute decompensation, analyzing liver transplant candidacy and intensive care unit (ICU) transfer parameters. Retrospective single-center review of adult patients with liver cirrhosis who had a rapid response team (RRT) activation during hospitalization and no prior liver transplantation. Patients with cirrhosis who were liver transplant candidates were more likely to be younger ($p = .003$), have a higher serum total bilirubin ($p = .015$), higher INR ($p < .001$), and higher MELD 3.0 ($p = .006$). There was no significant difference in ICU transfer ($p = .170$) after RRT activation. Liver transplant candidates had a lower 30- and 60-day mortality ($p = .008$, $p = .014$) and were less likely to have a code status discussion after decompensation ($p = .001$). Lower serum albumin was associated with ICU transfer ($p = .001$). Patients who transferred to the ICU were more likely to have a code status discussion within 24 h after RRT ($p = .011$) without significant difference in 30- or 60-day mortality ($p = .059$, $p = .277$). Liver transplant candidacy in patients with cirrhosis with acute decompensation is not clearly correlated with ICU transfer. Liver transplant candidates are more likely to be younger, have higher MELD 3.0 scores, less likely to have code status discussed after RRT, and have lower 30- and 60-day mortality rates. Patients who transfer to the ICU are more likely to have a code status discussion without any significant difference in 30- or 60-day mortality.

25COASMA30

Title: Reducing Chest Compression Pauses During Pediatric ECPR,

Elena M. Insley and Andrew S. Geneslaw and Tarif A. Choudhury and Anita I. Sen,

Journal of Intensive Care Medicine, Vol. 40, Number-5, pages 495–502,year 2024,
https://doi.org/https://doi.org/10.1177/08850666241301023,

Abstract: To quantify chest compression (CC) pauses during pediatric ECPR (CPR incorporating ECMO) and implement sustainable quality improvement (QI) initiatives to reduce CC pauses during ECMO cannulation. Methods: We retrospectively identified baseline CC pause characteristics during pediatric ECPR events (pre-intervention), deployed QI interventions to reduce CC pause length, and then prospectively quantified CC pause metrics post-QI interventions (post-intervention). Data were gathered from a single center review of CC-pause characteristics in children less than 18 years old with a PICU ECPR arrest. QI Interventions included: (1) sharing baseline CC data with ECPR stakeholders, (2) establishing consensus among providers regarding areas for improvement, and (3) creating a

communication aid to encourage counting CC pauses out loud. Multidisciplinary ECPR simulations allowed for practice of these skills. Using telemetry data, CC pause metrics were analyzed in the medical (CPR before cannulation) and surgical (CPR during ECMO cannulation, demarcated by the sterile draping of the patient) phases of ECPR, pre- and post-intervention. Results: Pre-intervention, 11 ECPR events (5 central cannulation, 6 peripheral cannulation) met inclusion criteria compared with 14 ECPR events (2 central, 12 peripheral) post-intervention. Pre-intervention analysis identified longer CC pauses and lower chest compression fraction (CCF) during the surgical versus medical phase of ECPR. Compared to pre-intervention data, CCF during the surgical phase of ECPR improved from 66% to 81% (73-85%) post-intervention (P = .02). Median CC pause length was significantly reduced from 20 s pre-intervention to 10.5 (9-13) seconds post-intervention (P = .01). There was no change in the surgical phase of ECPR duration (44 min pre- vs 41 min post-intervention, P = .8) or survival to hospital discharge (45% vs 21%, P = .4). Conclusion: Simple and feasible communication interventions during ECPR can minimize CC pauses, increase CCF and improve CPR quality without prolonging the time needed for ECMO cannulation.

25COASMA31

Title: Examination of Risk Factors Affecting the Development of BSI and Mortality in Critically Ill COVID-19 Patients Hospitalized in Intensive Care Unit (ICU): A Single-Center Retrospective Study,

Çağla Keskin Sarıtaş and Halit Özsüt and Aysun Benli and Seniha Başaran,

Journal of Intensive Care Medicine,Vol. 40, Number-5, pages 547–555,year 2024, https://doi.org/https://doi.org/10.1177/08850666241305347,

Abstract: Various studies have shown that the incidence of BSI is greater in COVID-19 patients hospitalized in the intensive care unit (ICU). Our study aimed to determine the risk factors for BSI, mortality rates, and factors affecting mortality in adult COVID-19 patients hospitalized in the ICU. All COVID-19 patients who met the study criteria and stayed in intensive care for more than 2 days at a tertiary university hospital during the two-year pandemic period were included in the study. Logistic regression analysis was used to determine the risk factors for BSI and mortality. We found that respiratory rate (RR) ≥ 30 breaths per minute at the time of admission [OR: 2.342 (95% CI: 1.12-4.897)] and antibiotic use in the month before admission ICU [OR: 3.137 (95% CI: 1.321-7.451)] were independent risk factors for BSI in COVID-19 patients. Subanalysis was also performed according to the doses of immunomodulators such as anakinra, tocilizumab, and corticosteroids, and it was found that they had no effect on the BSI (P > .05). The predominant causative pathogens were K. pneumoniae, A. baumannii and enterococci. The multidrug resistant rate among bacteria was 78%. Although their comorbidities and disease severity at the time of ICU admission were similar, patients with BSIs had a higher mortality rate (58.1 to 81.9%, P = .000). The SAPS-2 score at ICU admission [OR: 3.095 (95% CI: 1.969-4.865)] and mechanical ventilation requirement throughout the ICU admission [OR: 9.314 (95% CI: 3.878-22.37)] were found to be independent risk factors for mortality by multivariate analysis. BSI was not found to be a risk factor for mortality (> .05). Antibiotic use in patients with severe COVID-19 significantly increases the risk of BSI; unnecessary antibiotic use should be avoided.

25COASMA32

Title: Pathogenic Burden, Antimicrobial Resistance Pattern and Clinical Outcome of Nosocomial Bloodstream Infections in Intensive Care Unit,

Deepak Kumar and Monika Chaudhary and Naresh Kumar Midha and Gopal Krishana Bohra

Journal of Intensive Care Medicine, Vol. 40, Number-5, pages 556–564,year 2024,
https://doi.org/https://doi.org/10.1177/08850666241305043,

Abstract: Purpose: Nosocomial bloodstream infections with multidrug-resistant microorganisms have become a common health threat in intensive care settings worldwide. Understanding antimicrobial resistance and the outcomes of these infections is crucial for addressing this issue. This study aimed to investigate the burden, antimicrobial resistance, and 28-day outcomes of nosocomial bloodstream infections in the intensive care unit. Materials and Methods: This retrospective study was conducted in a multispecialty intensive care unit at a tertiary care hospital in western India. Adult patients aged ≥18 years with bloodstream infections acquired after 48 h of admission were included in the analysis. Results: A total of 245 patients suspected of having nosocomial infections in the intensive care unit were evaluated, and 179 were included in the study. Gram-negative bacteremia was identified in the majority of cases, affecting 111 (62%) patients. Carbapenem-resistant Acinetobacter baumannii was the most prevalent pathogen, found in 21.2% (38/179) of patients. Candida species were detected in 37 (20.6%) cases, and gram-positive cocci were identified in 31 (17.3%) patients, with vancomycin-sensitive Enterococci being the most common gram-positive cocci isolated from blood. The central venous catheter was the most frequent source of bloodstream infection, identified in 66 (36.9%) patients. Among all patients, 28-day mortality was observed in 102 (57%) patients. Higher quick sepsis-related organ failure (qSOFA) scores at the onset of bloodstream infection, central venous catheters as a source of infection, inability to initiate early appropriate therapy and septic shock at the onset of bloodstream infection were identified as independent predictors of mortality in patients with nosocomial bloodstream infections. Conclusion: An increased burden of gram-negative bacilli and Candida was found to cause nosocomial bloodstream infections, with very high rates of antimicrobial resistance. Early appropriate diagnosis and treatment play a critical role in improving survival. Additionally, enhanced infection prevention and control practices are necessary to mitigate the heavy burden of infections caused by multidrug-resistant organisms in critical care settings.

25COASMA33

Title: Valproic Acid for Hyperactive Delirium and Agitation in Critically Ill Patients,

Olivia Nuti and Cristian Merchan and Tania Ahuja and Serena Arnouk and John Papadopoulos and Alyson Katz,

Journal of Intensive Care Medicine, Vol. 40, Number-5, pages 519–527,year 2024,
https://doi.org/https://doi.org/10.1177/08850666241302760,

Abstract: Delirium and agitation are common syndromes in critically ill patients. Valproic acid (VPA) has shown benefit in intensive care unit (ICU)-associated delirium and agitation, but further evaluation is needed. The purpose of this study was to evaluate the effectiveness and safety of VPA for hyperactive delirium and agitation in critically ill adult patients. A retrospective cohort study at NYU Langone Health was conducted in critically ill patients

treated with VPA for hyperactive delirium or agitation from October 1, 2017 to October 1, 2022. The primary outcome was effectiveness of VPA, defined as a reduction in the total number of any concomitant psychoactive medication by day 3 of VPA treatment. Secondary outcomes included the effect of VPA on the doses of concomitant medications and adverse events. A total of 87 patients were included in the final analysis. By day 3 of VPA treatment, a 33% reduction ($P < .001$) in the total number of concomitant psychoactive medications was observed. VPA decreased the need for sedatives, as assessed by midazolam equivalents, but no significant changes were seen with dexmedetomidine alone, opioids, or antipsychotics. A 10 mg/kg loading dose was utilized in 36% of the cohort and its use decreased the risk for initiating additional psychoactive medications by day 3 of therapy (OR 2.8, 95% CI 1.0-7.8, $P = .047$), with benefits noted as early as 48 h after initiation. Adverse events were low in the total cohort (10.3%). The addition of VPA to a complex pharmacologic regimen for hyperactive delirium and agitation is safe and can assist in the prevention of polypharmacy and overall workload in critically ill patients admitted primarily for cardiogenic shock and respiratory failure requiring mechanical ventilation.

25COASMA34

Title: Palliative Care Outcomes for Critically ill Children After Rapid Whole Genome Sequencing,

Katherine Perofsky and Ami Doshi and Zaineb Boulil and Julia Beauchamp Walters and Euyhyun Lee and David Dimmock and Stephen Kingsmore and Nicole G. Coufal,

Journal of Intensive Care Medicine, Vol. 40, Number-5, pages 509–518,year 2024,
https://doi.org/https://doi.org/10.1177/08850666241304320,

Abstract: Clinical utility of rapid whole genome sequencing (rWGS) has been reported in 30–70% of pediatric ICU patients who receive a molecular diagnosis. Rapid molecular diagnostic techniques have been increasingly integrated into critical care, yet the influence of genetic test results on palliative care related decision making is largely unknown. This study evaluates palliative care related outcomes after rWGS. Retrospective chart review Tertiary children's hospital Acutely ill children 18 years of age who received rWGS due to suspected genetic disease between July 2016 and November 2019 rWGS with associated precision medicine 536 patients underwent rWGS, of whom 152 (28.4%) received a molecular diagnosis. Diagnostic rWGS was associated with more code status modifications, an increase in palliative care inpatient consultations, and greater enrollment in home-based palliative services. A comparison of diagnostic and nondiagnostic rWGS groups where palliative decisions were made prior to reporting of genomic testing results did not identify differences between the groups. In the subset of patients who had palliative care interventions ($n = 57$, 53% with diagnostic rWGS), time to palliative care consultation and time to compassionate extubation were shorter for patients with rWGS-based diagnoses (Kaplan-Meier method, $P = .008$; $P = .015$). Significantly more patients in this subgroup with diagnostic rWGS received home-based palliative care (Chi-squared, $P = .025$, 95% CI [−0.47, −0.05]). Univariate Poisson regression indicated that diagnostic rWGS is associated with significantly fewer emergency visits, PICU admissions, and unplanned intubations. Diagnostic rWGS correlates with more rapid engagement of pediatric palliative care services, higher enrollment rates in home-based palliative care, and shorter time to compassionate extubation. Further

studies are needed with larger cohort sizes and validated pediatric palliative care outcome measurement tools to accurately determine if this change in care is driven by the underlying condition or knowledge of a molecular diagnosis.

Cancer Research

25COASMA1:

Title: Inhibition of Plasminogen Activator Inhibitor-1 (PAI-1) by Tiplaxtinin Reduces Aggressiveness of Cervical Carcinoma Cells

Sarah Wehbe, Julia Gallwas And Carsten Gründker

Anticancer Research May 2025, 45 (5) 1793-1805;
https://doi.org/10.21873/anticanres.17559

Abstract: Background/Aim: The effect of G-protein-coupled estrogen receptor 1 (GPER1) on tumors depends on tumor entity, with its expression level influencing signal transduction and function. Recent research suggests that GPER1 promotes tumor suppression in cervical carcinoma (CC). In contrast, silencing GPER1 increases expression of serpin family E member 1 (SERPINE1) and its protein, plasminogen activator inhibitor-1 (PAI-1), and promotes tumor progression, raising the question of whether PAI-1 might be a suitable target for the treatment of CC. To explore this, we examined the impact of PAI-1 inhibition using Tiplaxtinin (PAI-039, TPX).Materials and Methods: The effects of TPX treatment on viability, colony formation, migration, and invasion of SiHa cervical squamous cell carcinoma (CSCC) and HeLa cervical adenocarcinoma (CAC) cells were assessed using AlamarBlue, colony formation, gap closure, and Boyden chamber assays, respectively. Apoptosis was examined using the Annexin/PI assay, while the cell cycle was analyzed in more detail using the PI assay.Results: With increasing TPX concentration, viability and colony formation of SiHa and HeLa cells decreased significantly. Cell migration was strongly reduced under PAI-1 inhibitor treatment, while invasion showed a slight decline. Apoptosis and cell cycle were only minimally affected by TPX.Conclusion: PAI-1 inhibitor TPX showed a strong inhibitory effect on both SiHa CSCC and HeLa CAC cells, significantly reducing their viability, colony formation, and migratory capacity. The observed effects suggest that TPX could potentially be used to target and hinder the growth and spread of both CSCC and CAC cells.

Keywords: Cervical carcinoma (CC)G-protein-coupled estrogen receptor 1 (GPER1)serpin family E member 1 (SERPINE1)plasminogen activator inhibitor-1 (PAI-1)inhibitorTiplaxtinin

25COASMA2:

Title: Expression of YAP1 and TAZ in Melanoma-, Bronchial- and Breast Carcinoma Brain Metastasis: Primary vs. Relapsed Tumors

Jill Dicke, Laura Hero, Saskia Kuhl, Roland Goldbrunner And Marco Timmer

Anticancer Research May 2025, 45 (5) 1807-1812;
https://doi.org/10.21873/anticanres.17560

Abstract: Background/Aim: Brain metastases from the most common primary sites – lung carcinoma, breast carcinoma, and melanoma – are more frequent than primary brain tumors. YAP1/TAZ are regulators of tissue growth and epithelial-mesenchymal transition (EMT) within the hippo pathway. The aim of the study was the evaluation of the role of YAP1/TAZ in brain metastasis.Materials and Methods: Expression levels of YAP1 and TAZ were measured in samples of primary and relapsed brain metastases from patients with melanoma,

breast carcinoma, and bronchial carcinoma using qPCR and western blot.Results: Expression of YAP1 and TAZ was highest in melanoma followed by bronchial carcinoma and lowest in breast carcinoma. For YAP1, expression in primary metastasis was higher than in relapsed metastasis.Conclusion: Because of the important role of YAP1/TAZ in EMT, targeting these genes could be a promising approach to reduce the risk of metastasis.
Keywords: YAP1TAZmelanomabronchial carcinomabreast cancerbrain metastasis

25COASMA3:
Title: Advantages and Disadvantages of Drug Combination Treatment: Riluzole, Metformin and Dexamethasone Effect on Glioblastoma Cell
Jonathan Keul, Swetlana Sperling, Veit Rohde And Milena Ninkovic
Anticancer Research May 2025, 45 (5) 1813-1823;
https://doi.org/10.21873/anticanres.17561
Abstract: Background/Aim: In glioblastoma multiforme (GBM), a deadly brain tumor, glucose is one of the main fuels for accelerated growth. Patients with GBM are also exposed to excess glucose through hyperglycemia in diabetes mellitus. In addition, dexamethasone (Dex), a corticosteroid commonly administered for controlling cerebral oedema, causes additional excess glucose. Therefore, targeting glucose metabolism is an attractive therapeutic intervention for GBM treatment. We have recently shown that riluzole (Ril), a drug used to treat amyotrophic lateral sclerosis (ALS), has an effect on some detrimental Dex-induced metabolic changes in GBM. Therefore, we examined the effect of the combination of metformin (Met), widely used to treat type 2 diabetes, and Ril on GBM cells.Materials and Methods: The 3-(4, 5-dimethylthiazol)-2, 5-diphenyltetrazolium bromide(MTT) assay was used to determine cell viability of U87MG after treatment with Ril, Met, Ril plus Met (Ril+Met) and the addition of Dex to this co-treatment. Cell migration was assessed by the xCELLigence system, matrix metalloproteinase 2 (MMP2) activation by zymography assay and gene expression by real-time polymerase chain reaction (RT-PCR).Results: Co-treatment with Ril and Met was effective in killing GBM cells and reducing the expression of genes involved in glucose and stem cell metabolism. Furthermore, combination of Ril and Met reduced MMP2 activation. But co-administration increased the migration of U87MG cells. The addition of Dex to this combination reversed the unfavorable effects of Ril+Met on cell migration.Conclusion: Ril+Met co-treatment had a positive effect in terms of GBM cell death, decreased expression of genes involved in glucose metabolism and stemness, and reduced MMP2 activation. Disadvantage of Ril+Met treatment was increased cell migration. Taken together, these drug combinations may also allow the reduction of the concentration of Dex to minimize its side effects.
Keywords: Glioblastoma cellsriluzolemetformindexamethasoneinvasion

25COASMA4:
Title: Ubiquitin-proteasome Pathway-linked Gene Signatures as Prognostic Indicators in Prostate Cancer
Yasuo Takashima, Kengo Yoshii, Masami Tanaka And Kei Tashiro
Anticancer Research May 2025, 45 (5) 1825-1841;
https://doi.org/10.21873/anticanres.17562

Abstract: Background/Aim: Prostate cancer (PCa) is the most frequently diagnosed cancer in men and a leading cause of cancer-related death. While prostate-specific antigen is a widely used biomarker, its specificity is limited. This study investigated the prognostic significance of gene subsets associated with the ubiquitin-proteasome pathway in PCa.Materials and Methods: We analyzed transcriptomic and clinical data of 94 early-onset (age <55) patients with prostate cancer using public dataset. Differentially expressed genes linked to the ubiquitin-proteasome system were identified across cancer progression stages. Kaplan–Meier survival analysis, Cox regression, and least absolute shrinkage and selection operator (LASSO) modeling were applied to assess their prognostic potential.Results: Differential expression of IKBKB, UBQLN3, TMUB2, UBE2S, and BRCA1 was observed at relative-early stages of pT3a and Gleason 3+4. Similarly, HERPUD1, CDC20, UHRF1, PSMD7, PIAS3, MALT1, TNF, UBD, CD3E, CD247, SOCS1, UBE2C, CARD16, ZAP70, UBA7, and UBE3C expression levels also changed at pT3b and Gleason 4+3. At metastatic stages (pT4 and Gleason ≥8) OASL expression was up-regulated, whereas that of DDB1, RPN1, UBE3B, UBE2H, PPIL2, WWP2, and CDH1 was down-regulated. In addition, higher expression of PSMD2, CDC20, NFKB1, and STIP1 or lower expression of HERPUD2, NEDD4, ANAPC16, LNX1, and HERPUD1 was associated with poor prognoses according to the Kaplan–Meier or receiver operating characteristic analyses for biochemical recurrence-free survival. A LASSO-Cox model identified six gene candidates including LNX1, PSMD2, SUMO4, UBE2C, UBR5, and UHRF1.Conclusion: The identified gene subset provides novel prognostic insights into PCa progression and survival. These findings highlight potential biomarkers and therapeutic targets within the ubiquitin-proteasome pathway, offering new avenues for personalized treatment strategies.

Keywords: Prostate cancerubiquitin-proteasome systemtranscriptomeGleason scoredifferentially expressed genesLASSO-Cox model

25COASMA5:

Title: Potential Role of PTEN and AKT/PKB Proteins in the Pathogenesis of Ovarian Mature Teratomas

Jarosław Bal, Lukasz Fulawka, Marian Gabryś, Marek Murawski And Agnieszka Halon

Anticancer Research May 2025, 45 (5) 1843-1851;
https://doi.org/10.21873/anticanres.17563

Abstract: Background/Aim: Mature teratomas constitute over 95% of ovarian teratomas and account for more than 44% of all ovarian tumors and over 58% of benign ovarian lesions. The pathogenesis of these tumors is hypothesized to involve disruptions in primary germ cell development, with the PI3K/AKT signaling pathway potentially playing a crucial role. This study aimed to analyze the importance of the PTEN protein and its associated signalling pathway, particularly in relation to AKT kinase activation, in the pathogenesis of mature ovarian teratomas.Materials and Methods: Surgical specimens from 117 patients with mature ovarian teratomas and control tissues from contralateral ovaries were analyzed. Immunohistochemical analysis was conducted to evaluate the expression of PTEN and phosphorylated AKT (P-AKT/PKB), a key component of the PI3K/AKT pathway regulated by PTEN. Expression levels were assessed using the semi-quantitative Remmele Immunoreactive Score (IRS).Results: An inverse pattern was observed in PTEN expression,

with a higher overall IRS score in the study group despite a lower proportion of PTEN-positive cells. The expression of P-AKT protein was elevated in the studied group, both in terms of IRS score and the percentage of P-AKT reactive cells.Conclusion: The study supports a potential role of the PI3K/AKT pathway in the pathogenesis of mature ovarian teratomas, as evidenced by increased P-AKT expression. The role of PTEN, however, remains unclear due to contradictory findings. Further research with larger control groups is warranted to clarify these observations.

Keywords: Ovarian mature teratomaPTENAKT/PKBPI3K/AKT pathwayRemmele immunoreactive score

25COASMA6:

Title: Combination of Recombinant Methioninase With Rapamycin or Chloroquine Is Synergistic to Highly Inhibit Triple-negative Breast Cancer Cells In Vitro

Jinsoo Kim, Qinghong Han, Byung Mo Kang, Kohei Mizuta, Yohei Asano, Michael Bouvet And Robert M. Hoffman

Anticancer Research May 2025, 45 (5) 1853-1859;
https://doi.org/10.21873/anticanres.17564

Abstract: Background/Aim: Triple-negative breast cancer (TNBC) is a highly aggressive and heterogeneous subtype of breast cancer with a poor prognosis despite multimodal treatment. New therapeutic approaches for TNBC are necessary. We very recently showed that the triple combination of recombinant methioninase (rMETase), rapamycin (RAPA), and chloroquine (CQ) synergically eradicated osteosarcoma cells in vitro. The present study aimed to determine whether rMETase has synergistic efficacy with either RAPA or CQ on a TNBC cell line.Materials and Methods: The half-maximal inhibitory concentrations (IC50) of rMETase, RAPA, and CQ were determined on the human MDA-MB-231 TNBC cell line in vitro. The efficacy of rMETase, combined with RAPA or with CQ, at their respective IC50 values, on MDA-MB-231 cell viability was determined using the WST-8 assay.Results: The IC50 of rMETase was 0.56 U/ml, for RAPA the IC50 was 3.9 μM, and for CQ the IC50 was 5.0 μM. The viability of the MDA-MB-231 cells was significantly decreased after treatment with rMETase plus RAPA or rMETase plus CQ, compared to the control cells or cells treated with one drug only.Conclusion: rMETase, when combined with either RAPA or CQ, is synergistic on the MDA-MB-231 TNBC cell line. The present findings suggest the potential for future clinical applications of rMETase plus chemotherapy, such as RAPA or CQ, for recalcitrant TNBC.

Keywords: Methionine addiction, Hoffman effect, methioninase, rapamycin, chloroquine, combination, synergy, triple-negative breast cancerMDA-MB-231 cells

25COASMA7:

Title: Contribution of Methylenetetrahydrofolate Reductase Genotypes to Brain Tumor Risk Determination in Taiwan

Chao-Hsuan Chen, Chun-Chung Chen, Xian-Xiu Chen, Wen-Shin Chang, Chia-Wen Tsai, Mei-Chin Mong, Shih-Wei Hsu And Da-Tian Bau

Anticancer Research May 2025, 45 (5) 1861-1870;
https://doi.org/10.21873/anticanres.17565

Abstract: Background/Aim: Methylenetetrahydrofolate reductase (MTHFR) is an essential enzyme in folate metabolism, playing a critical role in DNA methylation and nucleotide synthesis. Variants of the MTHFR gene have been associated with varying susceptibility to brain tumors, particularly gliomas. This study aimed to investigate the role of MTHFR genotypes in determining brain tumor risk in Taiwan.Materials and Methods: In this hospital-based case-control study, we assessed the contribution of MTHFR C677T (rs1801133) and A1298C (rs1801131) genotypes to brain tumor risk. A total of 52 patients with brain tumor and 520 age- and sex-matched non-cancer healthy controls were included. Genotyping of MTHFR rs1801133 and rs1801131 was performed using polymerase chain reaction-restriction fragment length polymorphism (PCR-RFLP).Results: Our findings revealed a significant difference in the genotypic distribution of MTHFR rs1801131 between brain tumor cases and non-cancer controls (p for trend=0.0099). Specifically, individuals with the MTHFR rs1801131 homozygous CC genotype demonstrated a 3.69-fold increased risk of brain tumors [95% confidence interval (95%CI)=1.52-9.00, p=0.0062]. In contrast, the AC genotype did not show a statistically significantly increased risk [odds ratio (OR)=1.54, 95%CI=0.83-2.85, p=0.2278]. Allelic frequency analysis revealed that the C allele of MTHFR rs1801131 was associated with an elevated risk of brain tumors (OR=1.83, 95%CI=1.20-2.80, p=0.0071). No significant association was found for MTHFR rs1801133. Stratified analysis showed that the MTHFR rs1801131 CC genotype particularly increased the risk in individuals older than 60 years (OR=4.68, 95%CI=1.42-15.42, p=0.0202) and in females (OR=3.79, 95%CI=1.22-11.77, p=0.0410).Conclusion: The CC genotype of MTHFR rs1801131 may serve as a valuable marker for brain tumor susceptibility. Stratifying patients with brain tumors based on their MTHFR genotypes could help identify individuals at high risk, enabling more frequent monitoring and preventive measures to reduce the occurrence of brain tumors in Taiwan.

Key Words: Brain tumor, genotype, methylenetetra, hydrofolate reductase (MTHFR) polymorphismTaiwan

25COASMA8:

Title: Recombinant Methioninase and Cisplatinum Act Synergistically to Inhibit Lewis Lung Carcinoma Cells But Not Normal Fibroblasts

Yohei Asano, Qinghong Han, Kohei Mizuta et.al.

Anticancer Research May 2025, 45 (5) 1871-1876;
https://doi.org/10.21873/anticanres.17566

Abstract: Background/Aim: Cisplatinum (CDDP) is used as first-line therapy in lung cancer. To further improve the therapeutic efficacy of CDDP, we focused on methionine addiction of cancer, known as the Hoffman effect. The present study aimed to determine the synergistic efficacy of the combination of CDDP and recombinant methioninase (rMETase) to target methionine addiction of lung cancer.Materials and Methods: In the present in vitro study, we used the Lewis lung carcinoma (LLC) cell line and Hs27 normal human fibroblasts, as a control. Both cell lines were cultured in 96-well plates (1,000 cells/well) overnight at 37°C and treated with CDDP (from 1 μM to 40 μM) or rMETase (from 0.5 U/ml to 8 U/ml) for 72 h. Then, we measured the half-maximal inhibitory concentration (IC50) values of CDDP and rMETase for both cell lines using the WST-8 reagent to determine cell viability. We then

determined the synergistic efficacy of the combination of CDDP and rMETase at their respective IC50 concentrations on cell viability for both cell lines.Results: For LLC cells the IC50 of CDDP was 0.55 μM and the IC50 of rMETase was 0.45 U/ml. For Hs27 cells, the IC50 was 1.21 μM for CDDP and 0.69 U/ml for rMETase. The combination of rMETase and CDDP, at their respective IC50 concentrations, showed synergistic efficacy on LLC cells, but not on Hs27 cells.Conclusion: Combination therapy with rMETase and CDDP shows promise for treating lung cancer and may be readily translated to the clinic.
Keywords: Lewis lung carcinoma, skin fibroblasts, recombinant methioninase, cisplatinum, methionine addiction, Hoffman effect, synergy

25COASMA9:

Title: Development of Acquired Resistance in Alpelisib-treated Gastric Cancer Cells With PIK3CA Mutations and Overcoming Strategies

Minsu Kang, Kui-Jin Kim, Ji Hea Sung, et.al.

Anticancer Research May 2025, 45 (5) 1877-1896;
https://doi.org/10.21873/anticanres.17567

Abstract: Background/Aim: Alpelisib has shown promise in preclinical studies for treating PIK3CA-mutant gastric cancer (GC), and its combination with chemotherapy has progressed to clinical trials. However, acquired resistance to alpelisib remains a significant challenge. This study aimed to elucidate the mechanisms underlying acquired alpelisib resistance and propose potential therapeutic strategies to overcome it.Materials and Methods: Acquired alpelisib-resistant GC cell lines were developed by prolonged drug exposure. Mechanistic studies included whole-exome sequencing, western blotting, immunoprecipitation, Cdc42 and Rac1 activity assays, caspase-3/7 assays, colony formation assays, and sphere formation assays to investigate resistance pathways and therapeutic interventions.Results: Two GC cell lines with acquired resistance to alpelisib, SNU601-R and AGS-R, were successfully developed from SNU601 and AGS. Both acquired alpelisib-resistant cell lines exhibited PTEN functional loss, leading to activation of SRC, STAT1, AKT, and PRAS40 signaling pathways. Combination treatments with pan-PI3K inhibitors or AKT inhibitors successfully overcame resistance. Among these, the combination of capivasertib, an AKT inhibitor, with SN38 demonstrated superior cytotoxic effects. Furthermore, the combination of capivasertib and SN38 significantly reduced the colony forming ability and sphere formation compared to each treatment alone in SNU601-R and AGS-R cells.Conclusion: In alpelisib-treated GC cells with PIK3CA mutations, PTEN functional loss and changes in the associated signaling pathway were identified as important mechanisms of acquired alpelisib resistance. The combination of capivasertib and SN38 effectively overcomes acquired resistance to alpelisib in PIK3CA-mutant GC, providing a preclinical rationale for future clinical trials targeting acquired alpelisib-resistant GC with PIK3CA mutations.
Keywords: Gastric cancer, PIK3CAalpelisib resistance, AKT inhibitor, capivasertib, SN38

25COASMA10:

Title: Correlation Analysis Between IFIT2 and HLA Class II in Oral Cancer

Kuo-Chu Lai, Chi-Wei Chen, Peter Mu-Hsin Chang, et.al.

Anticancer Research May 2025, 45 (5) 1897-1914;

https://doi.org/10.21873/anticanres.17568

Abstract: Background/Aim: Interferon (IFN)-induced protein with tetratricopeptide repeats 2 (IFIT2) depletion is associated with tumor progression in oral cancer. The induction of human leukocyte antigen (HLA) class II molecules by IFN has also been reported in cancer cells. However, the correlation between IFIT2 and HLA class II in oral cancer remains unclear.Materials and Methods: Xenograft and experimental metastasis animal models and cDNA microarray analysis were used to evaluate in vivo oral cancer progression. Western blotting and immunohistochemical staining were used to examine human leukocyte antigen (HLA) class II and IFIT2 protein levels in oral cancer cells and oral cancer patients.Results: HLA class II genes exhibited increased expression in xenograft oral cancer sublines; however, no increases were detected in IFIT2-depleted xenograft and metastatic sublines, indicating that the loss of HLA class II expression may be related to IFIT2 depletion. In addition, IFIT2 may play a role in enhancing the responsiveness of oral cancer cells to IFN-γ-induced HLA class II expression. Clinically, IFIT2 protein expression is positively correlated with HLA class II protein expression in oral cancer. HLA class II expression was significantly negatively associated with lymph node metastasis compared with patients with negative HLA class II expression. Analysis of the TCGA database indicated that HLA class II expression, along with the enrichment of CD4+ T cells in the tumor microenvironment, may predict a better prognosis for patients with head and neck cancer, including oral cancer.Conclusion: HLA class II expression may be positively correlated with IFIT2 expression in oral cancer cells. Clinically, low expression of HLA II molecules may be related to lymph node metastasis in oral cancer patients.

Keywords: Oral cancer, interferon-induced proteins with tetratrico, peptide repeats 2human leukocyte antigen class IIlymph node metastasis

25COASMA11:

Title: Elevated PD-L1 Expression on Circulating Classical Monocytes Upon Checkpoint Inhibitor Therapy Is Associated With Increased Plasma Interleukin 5 in Patients With Lung Cancer

Eva Probst, Christian Idel, Jonas Fleckner, et.al.

Anticancer Research May 2025, 45 (5) 1915-1925;
https://doi.org/10.21873/anticanres.17569

Abstract: Background/Aim: Lung cancer remains one of the most prevalent cancers worldwide, with high morbidity and mortality rates. Besides established treatment options such as surgery and radio(chemo)therapy, advanced approaches such as anti-programmed death 1 (PD-1)/anti-programmed death ligand 1 (PD-L1) immune checkpoint inhibitors (ICIs) have been introduced as effective therapeutic options. In this context, PD-L1 expression on myeloid cells has been correlated with poor clinical outcomes in patients with cancer. This study aimed to investigate the influence of ICI treatment on the immunologic alterations of circulating monocyte subsets as potential bioliquid indicators for therapy response assessment in patients with lung cancer.Materials and Methods: Flow cytometry was employed to analyze the distribution of circulating CD14/CD16 monocyte subsets and the expression of adhesion molecules CD11a (integrin-α L; LFA-1), CD11b (integrin-α M; Mac-1), CD11c (integrin-α X), CX3CR1 (CX3CL1 receptor) and the checkpoint molecule PD-L1 in 22

patients with lung cancer. Furthermore, plasma concentrations of ICI-associated cytokine interleukin (IL-5) were quantified using ELISA the course of therapy.Results: The study revealed a significant increase in intermediate monocyte abundance, coupled with altered adhesion molecule expression and elevated PD-L1 levels in patients with lung cancer. Moreover, non-responders exhibited significantly increased plasma IL-5 levels after one month of ICI therapy. A significant positive correlation was also observed between plasma IL-5 concentrations and PD-L1 expression on peripheral blood classical monocytes.Conclusion: The identification of liquid biomarkers, such as peripheral blood monocyte subsets and plasma IL-5 levels, could serve as valuable indicators for ICI therapy decision-making and response prediction in lung cancer patients.

Keywords: Lung cancer, immune checkpoint inhibitor (ICI)monocyte subsets, PD1/PD-L1adhesion molecules, interleukin-5

25COASMA12:

Title: **Role of Platelet Interactions in Promoting Melanoma Malignancy With Insights into Proliferation, Cyclin D1 Expression, and Migration**

Noriko Yoshikawa, Chinami Ikushima, Nanako Tanaka, et.al.

Anticancer Research May 2025, 45 (5) 1927-1934;
https://doi.org/10.21873/anticanres.17570

Abstract: Background/Aim: Metastasis is a major obstacle in cancer treatment and hematogenous metastasis plays a critical role in tumor progression. Platelets have been implicated in facilitating this process by interacting with circulating tumor cells, promoting immune evasion, extravasation, and metastatic colonization.Materials and Methods: We explored the effects of platelet interactions on the malignancy of mouse melanoma cells, focusing on cell proliferation, cyclin D1 expression, and migration.Results: Co-culturing melanoma cells with platelets significantly increased their proliferative capacity, an effect that was also induced by the platelet culture supernatant alone. This suggests that soluble factors released from platelets, such as transforming growth factor-β (TGF-β) and platelet derived growth factor (PDGF), mediate this effect independently of direct cell-cell interactions. Furthermore, cyclin D1, a key regulator of the G1/S phase transition, is up-regulated in melanoma cells upon exposure to platelet-derived factors, indicating enhanced cell cycle progression. Migration assays revealed the role of platelets in melanoma cell motility, whereas pre-treatment with platelets significantly increased their migratory ability in a transwell assay. This suggests that platelets enhanced cell motility via phenotypic changes and epithelial-mesenchymal transition in mouse melanoma cells.Conclusion: Platelets promote melanoma metastasis by enhancing cell proliferation and migration through soluble factor-mediated mechanisms. Targeting platelet-tumor interactions may represent a potential therapeutic strategy for mitigating metastatic progression.

Keywords: Platelets, melanoma, cancer metastasis, cyclin D1migration

25COASMA13:

Title: Epigallocatechin Gallate Induces miR-192/215 Suppression of EGR1 in Gastric Cancer

Nan Zhou, Yuan Yuan, Huijuan Lin, Jian Wang, et. al.

Anticancer Research May 2025, 45 (5) 1935-1951;
https://doi.org/10.21873/anticanres.17571

Abstract: Background/Aim: Gastric cancer (GC) is a leading cause of cancer-related deaths worldwide. MicroRNAs (miRNAs) are key regulators of tumorigenesis. This study investigated the role of the miR-192/215–early growth response protein 1 (EGR1) axis in GC and explored its therapeutic implications.Materials and Methods: Combinatorial molecular approaches including dual-luciferase reporter assays and western blot analyses were employed to authenticate EGR1 as a direct target of miR-192/215. Multi-modal data analysis incorporating The Cancer Genome Atlas datasets and our institutional cohort (n=56) was conducted to delineate EGR1 expression profiles across clinicopathological GC stages. Pharmacological modulation studies were implemented to characterize the dose- and time-dependent effects of epigallocatechin-3-gallate (EGCG) on the miR-192/215–EGR1 axis.Results: EGR1 is a direct target of miR-192/215, with its expression negatively regulated by these miRNAs. Clinical analysis revealed significantly reduced EGR1 expression in tumors of early-stage GC (stage I) and cases with superficial invasion depth (T1) ($p<0.05$), suggesting a tumor-promoting role in the early stages of the disease. Higher EGR1 levels were associated with poorer overall survival, highlighting its potential as a prognostic biomarker ($p<0.05$). Furthermore, treatment of cells with EGCG transiently up-regulated miR-192/215 and down-regulated EGR1, highlighting its therapeutic potential.Conclusion: This study highlights the miR-192/215–EGR1 axis as a critical regulator of GC progression and a promising therapeutic target. EGCG may serve as an adjunct therapy for GC. Future studies should focus on the regulatory mechanisms of EGR1, its interaction with the tumor microenvironment, and clinical validation of EGCG and other agents targeting this axis.

Keywords: Gastric cancer, miR-192, miR-215EGR1, epigalloca, techin gallate.

25COASMA14:

Title: Light Bladder Net: Non-invasive Bladder Cancer Prediction by Weighted Deep Learning Approaches and Graphical Data Transformation

Chi-Hua Tung, Shih-Huan Lin, Kai-Po Chang, et.al.

Anticancer Research May 2025, 45 (5) 1953-1964;
https://doi.org/10.21873/anticanres.17572

Abstract: Background/Aim: Bladder cancer (BCa) is associated with high recurrence rates, emphasizing the importance of early and accurate detection. This study aimed to develop a lightweight and fast deep learning model, Light-Bladder-Net (LBN), for non-invasive BCa detection using conventional urine data.Materials and Methods: We improved LBN's generalization by applying data transformations, adding uniform noise, and employing feature selection methods (mRMR, PCA, SVD, t-SNE) to extract key vectors from its fully connected layer. These vectors were integrated into the original dataset, and multiple machine learning models were trained to enhance classification accuracy. Lastly, weighted voting was used to assign importance across these models.Results: Our approach achieved an accuracy of 0.83, a sensitivity of 0.85, a specificity of 0.80, and a precision of 0.81, indicating robust performance in detecting BCa from urine data.Conclusion: This non-invasive diagnostic method offers rapid, cost-effective predictions. A free online tool is available for clinicians and patients to conveniently detect BCa using standard urine samples at

http://merlin.nchu.edu.tw/LBN/

Keywords: Conventional urine examination, data image transformation, weighted voting, deep feature extraction, non-invasive bladder cancer prediction

25COASMA15:

Title: SH003 Inhibits Proliferation and Induces Apoptosis in Colon Cancer Through the RTK-STAT3 Pathway

Hyun-Ha Hwang, Ji-Sung Yoo, Jeong-Hui Je, et.al.

Anticancer Research May 2025, 45 (5) 1965-1980;
https://doi.org/10.21873/anticanres.17573

Abstract: Background/Aim: Colon cancer is the most prevalent type of gastrointestinal cancer, characterized by high incidence and mortality rates despite advancements in diagnosis and treatment. Although chemotherapy is the standard treatment for advanced cases, survival benefits are often limited, highlighting the need for innovative therapeutic strategies. SH003, an herbal mixture composed of Astragalus membranaceus, Angelica gigas, and Trichosanthes kirilowii Maximowicz, has demonstrated anticancer properties across various cancer types. This study aimed to explore the anticancer effects of SH003 on colon cancer through in vitro and in vivo experiments.Materials and Methods: In vitro studies were conducted using human colon cancer cell lines, including HCT116, HT29, SW480, SW620, LoVo, LS174T, H508, and LS1034. Cell viability assays were performed to determine IC50 values over time. Apoptosis induction was assessed through Western blot analysis. Cell cycle progression was analyzed by examining the expression of cell cycle-related proteins. The disruption of the RTK-STAT3 signaling pathway was evaluated by measuring the phosphorylation of ALK using RTK-array. In vivo experiments involved establishing an HCT116 xenograft mouse model to assess tumor growth inhibition and systemic toxicity following SH003 administration.Results: SH003 significantly reduced cell viability in all tested colon cancer cell lines, with IC50 values decreasing over time, indicating a time-dependent cytotoxic effect. Apoptosis induction was confirmed by increased levels of cleaved PARP, caspase-3, caspase-8, and caspase-9. SH003 also induced G1/S phase cell cycle arrest, as evidenced by decreased expression of p-Rb, CDK2, CDK4, and Cyclin D1. Furthermore, SH003 disrupted the RTK-STAT3 signaling pathway by reducing ALK phosphorylation and decreasing the levels of p-STAT3, c-Myc, and cyclin D1. In vivo, SH003 significantly suppressed tumor growth in the HCT116 xenograft mouse model, reducing tumor volumes without causing notable systemic toxicity.Conclusion: These findings suggest that SH003 possesses robust anticancer effects against colon cancer by inducing apoptosis, causing cell cycle arrest, and disrupting RTK-STAT3 signaling. The in vivo results further confirm SH003's efficacy and safety, supporting its potential as a promising therapeutic option for colon cancer treatment. Further studies are warranted to elucidate its mechanisms and clinical applicability.

Keywords: SH003, apoptosis, colon cancer, RTK/STAT3 signaling pathway

25COASMA16:

Title: SH003 Inhibits Proliferation and Induces Apoptosis in NSCLC Cell Lines by Inhibiting the Receptor Tyrosine Kinase-related Pathway

Hyun-Ha Hwang, Ji-Sung Yoo, Jeong-Hui Je et.al.

Anticancer Research May 2025, 45 (5) 1981-1995;
https://doi.org/10.21873/anticanres.17574

Abstract: Background/Aim: SH003, a novel herbal mixture consisting of Astragalus membranaceus, Angelica gigas, and Trichosanthes kirilowii Maximowicz, has shown promising anti-cancer effects in various cancers, including non-small cell lung cancer (NSCLC), which comprises approximately 85% of all lung cancer cases. Characterized by high mortality rates due to late-stage diagnosis and frequent development of resistance to traditional therapies, NSCLC is a significant clinical challenge. This study investigated the anti-cancer effects of SH003 on NSCLC cells, focusing on its role in modulating receptor tyrosine kinase (RTK) signaling pathways.Materials and Methods: NSCLC cell lines (A549, H460, HCC827) were treated with SH003 to evaluate cell viability (MTT assay), colony formation, apoptosis (Annexin V/7-AAD staining, western blot), and cell cycle distribution (PI staining). Phosphorylation of RTKs and related signaling molecules was analyzed using a phospho-RTK array and western blot. In vivo anti-tumor effects were assessed using an A549 xenograft mouse model treated orally with SH003.Results: NSCLC cell lines A549, H460, and HCC827 treated with SH003 showed significant, dose-dependent cell viability and colony formation reductions. SH003 induced apoptosis, evidenced by increased cleaved PARP and caspase-8 levels, and caused G1/S cell cycle arrest. Additionally, SH003 treatment decreased phosphorylation of multiple receptor tyrosine kinases (RTKs), including ErbB4, FGFR1, FGFR3, and PDGFRβ, as confirmed by an RTK array. In an A549 xenograft mouse model, SH003 inhibited tumor growth without affecting body weight, indicating low systemic toxicity.Conclusion: SH003 is a promising multi-target therapeutic agent for NSCLC, offering a novel strategy to improve patient outcomes.

Keywords: SH003, apoptosis, NSCLC, receptor tyrosine kinase

25COASMA17:

Title: High Expression of OR1F1 Protein as a Potential Prognostic Biomarker for Esophageal Squamous Cell Ca rcinoma

Shunsuke Yamagishi, Mitsuro Kanda, Takahiro Shinozuka, et. al.

Anticancer Research May 2025, 45 (5) 1997-2009;
https://doi.org/10.21873/anticanres.17575

Abstract: Background/Aim: In patients with esophageal squamous cell carcinoma (ESCC), the identification of biomarkers that enable precise stratification of postoperative prognostic risk is crucial for developing personalized treatment strategies. Biomarker reproducibility across multiple independent cohorts is a key consideration in biomarker discovery.Materials and Methods: Transcriptome analysis was performed on primary tumor tissues from patients with ESCC who experienced recurrence in distant organs, thus identifying olfactory receptor family 1 subfamily F member 1 (OR1F1) as a candidate biomarker. OR1F1 protein expression and prognostic value were analyzed in two independent cohorts of patients with ESCC who underwent curative esophagectomy using immunohistochemical staining.Results: In Cohort 1, high expression of OR1F1 protein in ESCC tissues was significantly correlated with reduced overall survival (OS) and disease-free survival (DFS). Multivariate analysis of OS after surgery identified high OR1F1 protein expression as an independent adverse prognostic factor. Likewise, high OR1F1 protein expression in tissues was strongly

associated with reduced OS and DFS in Cohort 2. In both cohorts, patient prognosis could be stratified into three distinct risk levels based on the expression level of OR1F1 protein.Conclusion: Tissue OR1F1 protein expression could serve as a valuable prognostic biomarker for patients with ESCC.

Keywords: Biomarkers, esophageal squamous cell carcinoma, OR1F1prognosis

25COASMA18:

Title: MAP17 as a Mediator of HGF-induced Proliferation and Invasion in Gastric Cancer

Byeong Il Jang, Ji Yoon Jung, Sung Ae Koh, et.al.

Anticancer Research May 2025, 45 (5) 2011-2024;
https://doi.org/10.21873/anticanres.17576

Abstract: Background/Aim: The 17 kDa membrane-associated protein (MAP17) is a non-glycosylated protein localized to the Golgi apparatus and plasma membrane. It is overexpressed in various cancer cells and has been implicated in promoting cancer progression. This study aimed to investigate the role of MAP17 in the proliferation and invasion of gastric cancer cells.Materials and Methods: To examine the role of MAP17 in carcinoma progression, we performed a series of in vitro and in vivo experiments. In vitro analyses included cell culture experiments, reverse transcription polymerase chain reaction (RT-PCR), complementary DNA (cDNA) microarray, western blot analysis, zymography, 3-(4,5-dimethylthiazol-2-yl)-2,5-diphenyltetrazolium bromide (MTT) assay, standard two-chamber invasion assay, and MAP17 knockdown using short hairpin RNA (shRNA). For in vivo analysis, MAP17 enzyme-linked immunosorbent assays (ELISA) were performed on thirty-five blood samples from patients who underwent surgical resection for gastric cancer.Results: MAP17 expression was up-regulated by HGF in human gastric cancer cells, leading to increased MMP9 expression. Treatment with the PI3K inhibitor LY294002 reduced MMP9 levels. MAP17 knockdown resulted in decreased MMP9 and increased Rac1 expression. Furthermore, MAP17 suppression reduced HGF-induced cell proliferation and invasion while promoting reactive oxygen species (ROS) accumulation. In vivo, a statistically significant decrease in serum MAP17 levels was observed after subtotal or total gastrectomy.Conclusion: MAP17 plays a crucial role in the proliferation and invasion of gastric cancer cells, suggesting its potential as a biomarker and therapeutic target for gastric cancer.

Keywords: Hepatocyte growth factor, MAP17reactive oxygen species, matrix metallo, proteinase gastric cancer

25COASMA19:

Title: Long-term Outcomes of Helical Tomotherapy in Lymph Node-positive Breast Cancer Following Breast-conserving Surgery

Felix Zwicker, Luis-Philipp Raether, Rudolf Klepper, et.al.

Anticancer Research May 2025, 45 (5) 2025-2040;
https://doi.org/10.21873/anticanres.17577

Abstract: Background/Aim: Adjuvant radiotherapy is an integral component of the interdisciplinary curative treatment of lymph node-positive breast cancer. We investigated

long-term clinical outcomes of helical tomotherapy following breast-conserving surgery.Patients and Methods: This single-center analysis included 80 female patients with breast cancer stages T1-T4 and lymph node metastasis (N1-N3) who underwent breast-conserving surgery, sentinel node biopsy, and/or axillary lymph node dissection. Patients received adjuvant fractionated radiation therapy to the whole breast and regional lymph node areas using helical tomotherapy. Boost irradiation was delivered sequentially or through the simultaneous integrated boost technique. Local control (LC), metastasis, survival, toxicity, and secondary malignancy rates were retrospectively analyzed.Results: The mean follow-up duration was 75 months. The 5- and 8-year overall survival rates were 89.4% and 87.0%, respectively. LC rates at 5- and 8-year were 98.7%, and metastasis-free survival rates were 91.2% and 85.2%, respectively. Acute erythema occurred in 70% (Grades 1-2) and 26% (Grade 3) of patients. Ipsilateral arm lymphedema of Grade 1 and Grade 2 developed in 10% and 1.3% of the treated patients, respectively. Acute or late toxicities exceeding Grade 3 were not observed.Conclusion: Helical tomotherapy showed excellent long-term results and low toxicity rates as adjuvant radiotherapy in patients with lymph node-positive breast cancer. The incidence of secondary malignancies was relatively low and corresponded to the preexisting records on radiation therapy. Broader clinical implementation of helical tomotherapy could benefit patients.

Keywords: Helical tomotherap, ylymph node-positive breast cancer, adjuvant radiotherapy

25COASMA20:

Title: Role of Stromal CD25+/CD8+ Lymphocyte Ratio in Patients With Grade 2-3 Cervical Intraepithelial Neoplasia (CIN 2-3): A Retrospective Single-center Study

Enrico Simonetti, Sabina Pistolesi, Amerigo Ferrari, et.al.

Anticancer Research May 2025, 45 (5) 2041-2050;
https://doi.org/10.21873/anticanres.17578

Abstract: Background/Aim: This study aimed to assess the role of the stromal CD25+/CD8+ (Cluster of Differentiation) lymphocyte ratio and other immunohistochemical markers in predicting the risk of recurrence and human papillomavirus (HPV) persistence after Loop Electrosurgical Excision Procedure (LEEP) conization in patients with grade 2-3 cervical intraepithelial neoplasia (CIN2-3).Patients and Methods: A retrospective analysis was conducted on 72 patients who underwent LEEP for CIN2-3 in our Department. Criteria for enrollment included HPV genotyping before and after surgery and a follow-up time ≥18 months. Immunohistochemical analysis assessed CD8+ cytotoxic T cells and CD25+ regulatory T cells in the cervical stroma, and the CD25+/CD8+ ratio was computed. Recurrence of CIN2-3 and HPV persistence after LEEP were the endpoints of the study.Results: CIN2-3 recurrence occurred in 13.9% of patients with smoking, HPV-16/18 infection, positive surgical margins, and CIN3 histology being significant risk factors. A CD25+/CD8+ ratio >1.25 was associated with a shorter disease-free survival (DFS) (p=0.033) and HPV persistence at 18 months (p=0.017) after LEEP at univariate analysis. Adjuvant HPV vaccination reduced the recurrence risk (p=0.004). A lympho-monocyte infiltrate consisting of at least 10% CD25+ T cells was significantly associated with HPV persistence at 18 months (p=0.0046).Conclusion: The CD25+/CD8+ ratio is a promising biomarker for identifying patients at higher risk of CIN2-3 recurrence and HPV persistence

post-LEEP. These findings highlight the role of immune profiling in the management of patients affected by CIN2-3 and support the integration of vaccination and personalized follow-up strategies.

Keywords: Cervical intraepithelial neoplasia (CIN2-3), CD25+/CD8+ lymphocyte ratiostromal lymphocyte infiltrate, HPV persistence, recurrence risk, loop electrosurgical excision procedure (LEEP), cytotoxic T cells (CD8+), regulatory T cells (CD25+), HPV genotyping

25COASMA21:

Title: Efficacy of Esophagectomy Following Neoadjuvant Chemotherapy for Esophageal Neuroendocrine Carcinoma

Takeshi Yamashita, Koichiro Fujimasa, Koji Otsuka, et.al.

Anticancer Research May 2025, 45 (5) 2051-2058;
https://doi.org/10.21873/anticanres.17579

Abstract: Background/Aim: Esophageal neuroendocrine carcinoma (E-NEC) is a rare malignancy. Although treatment for E-NEC involves a combination of surgery, chemotherapy, radiotherapy, and immunotherapy, E-NEC prognosis is poor and the treatment strategy remains unclear. Surgery after neoadjuvant chemotherapy is the standard treatment for advanced esophageal squamous cell carcinoma; however, limited reports exist on its application for E-NEC. This study aimed to examine the surgical outcomes of patients with E-NEC based on the pathological findings of endoscopic biopsies before surgery and surgical specimens.Patients and Methods: We examined patients who underwent thoracoscopic subtotal esophagectomy for esophageal or esophagogastric junction cancer and were diagnosed with E-NEC based on endoscopic biopsy or surgical pathology.Results: This study included 12 patients. Preoperative endoscopic biopsy confirmed a diagnosis of E-NEC in five patients. Six patients had a mixture of squamous cell carcinoma and NEC components (including suspected cases), and one patient had adenocarcinoma. Neoadjuvant chemotherapy was administered to 10 patients, including four who received 5-fluorouracil with cisplatin, three who received etoposide with cisplatin, two who received etoposide with carboplatin, and one who received S-1 with oxaliplatin. R0 resection was performed through thoracoscopic esophagectomy. Histopathological diagnosis after surgery identified NEC in eight patients, a mixed type in three patients, including MiNEN in two patients, and SCC in one patient. Recurrence occurred within one year in seven patients, and three of these patients died within one year due to hematogenous metastasis. The one-year overall survival rate was 67% (9/12 cases), and the median survival time was 41.7 months.Conclusion: Esophagectomy combined with preoperative chemotherapy for E-NEC may contribute to improved prognosis.

Keywords: Esophageal neuroendocrine carcinoma, neoadjuvant chemotherapy, esophagectomy

25COASMA22:

Title: Sex-related Survival Differences in Patients With Glioblastoma – Results From a Retrospective Analysis

Jan Leppert, Claudia Ditz, Jakob Matschke, et.al.

Anticancer Research May 2025, 45 (5) 2059-2069;
https://doi.org/10.21873/anticanres.17580

Abstract: Background/Aim: Glioblastoma is more common in men than in women. The aim of this analysis was to investigate sex-specific differences with a particular focus on their impact on survival including overall survival (OS) and progression-free survival (PFS).Patients and Methods: This retrospective study analyzed 209 GBM patients (91 females, 118 males) treated according to the Stupp regimen. Data on patient demographics, O6-methylguanine-DNA methyltransferase (MGMT) methylation status, treatment details [radiotherapy (RT) doses and temozolomide (TMZ) cycles], and survival endpoints were statistically analyzed using univariable Kaplan-Meier [and 95% confidence intervals (CI)] and multivariable Cox regression hazards models.Results: In the whole cohort, median follow-up was 14 (2-119) months. We observed a trend towards a higher prevalence of multifocal tumors in males (30.5% vs. 22%, p=0.092). In univariable analysis, MGMT-negative male patients who received >58 Gy RT had a significantly longer OS (14 vs. 5 months, log-rank p<0.001). In multivariable analysis, OS was not significantly influenced by patient age (p=0.579), total RT dose (Gy) (p=0.348), and MGMT status (p=0.262). Female patients (HR=3.252, p=0.028) and patients with higher tumor volume (HR=1.031, p=0.005) had a significantly higher mortality risk. Better Karnofsky-performance-status (HR=0.918, p=0.008), complete resection (HR=6.759, p=0.022), and higher numbers of adjuvant TMZ cycles (HR=0.739, p=0.003) led to prolonged OS.Conclusion: Sex seems to impact survival in patients suffering from glioblastoma, although underlying mechanisms are not yet completely understood. Treatment intensity (complete resection and the maximum possible number of TMZ cycles) had a significant effect on the patients' mortality risk.

Keywords: Sex-related differences, MGMT-methylation negative male patients, radiotherapy, dose intensity, temozolomide

25COASMA23:

Title: Efficacy and Prognostic Factors of Surgical Resection for Pulmonary Metastases From Ovarian Cancer

Yo Tsukamoto, Takashi Ohtsuka, Yoshikane Yamauchi, et.al.

Anticancer Research May 2025, 45 (5) 2071-2078;
https://doi.org/10.21873/anticanres.17581

Abstract: Background/Aim: Pulmonary metastases (PMs) from ovarian cancer are rare, and the efficacy of surgical intervention is unclear. This study aimed to validate the efficacy of surgical intervention for pulmonary metastases from ovarian cancer.Patients and Methods: Cases were taken from the database of the Metastatic Lung Tumor Study Group of Japan from 1996 to 2021, which prospectively registers surgical cases of pulmonary metastases at participating centers. Only patients who underwent radical surgery for pulmonary metastases from ovarian cancer were included. Factors associated with overall survival (OS) were analyzed.Results: The analysis included 48 patients with a mean age of 53.2 years old. The 5-year overall survival rate was 69.9% [95% confidence interval (CI)=51.9%-82.2%], with a median survival period of 121 months (95% CI=64-134 months). Predictors of poorer OS included preoperative extrapulmonary metastasis [hazard ratio (HR)=5.354, 95% CI=1.248-22.97; p=0.024], elevated preoperative tumor marker levels (HR=2.999, 95% CI=1.028-

8.705; p=0.044), and a disease-free interval of less than 24 months (HR=4.355, 95% CI=1.004-18.89; p=0.049). On multivariable analysis, preoperative extrapulmonary metastasis remained an independent prognostic factor (HR=6.229, 95% CI=1.216-31.92; p=0.028).Conclusion: This report includes the largest number of patients who underwent resection of PMs from OC. Preoperative extrapulmonary metastasis was identified as an adverse prognostic factor, emphasizing the need for careful consideration of surgical indications. Our results significantly contribute to understanding the prognosis and prognostic factors associated with surgical intervention for PMs from OC.

Keywords: Pulmonary metastasesmetastasectomy, ovarian cancer, prognostic factor

25COASMA24:

Title: HOX-PBX Up-regulation Predicts Favorable Prognosis in NPM1-mutated Normal Cytogenetic AML via WNT Signaling

Ghaleb Elyamany, Sultan Alotaibi, Bander Alharbi, et.al.

Anticancer Research May 2025, 45 (5) 2079-2089;
https://doi.org/10.21873/anticanres.17582

Abstract: Background/Aim: Acute myeloid leukemia (AML) is a genetically heterogeneous malignancy. HOX gene dysregulation, particularly within the HOXA cluster, plays a critical role in leukemogenesis. This study investigated the impact of HOX-PBX gene expression and its association with clinical outcomes in NPM1-mutated cytogenetically normal (CN)-AML.Materials and Methods: Gene expression analysis was performed on diagnostic bone marrow samples from 35 CN-AML patients using the NanoString nCounter platform. Differential expression of HOXA9, HOXA10, and PBX3 was assessed, along with correlations with NPM1 mutation status and WNT pathway activation. Kaplan–Meier survival analysis was conducted to evaluate prognostic significance.Results: HOXA9 and HOXA10 were significantly up-regulated in NPM1-mutated AML compared to NPM1-negative cases ($p<0.001$). PBX3 expression strongly correlated with HOXA10 ($r=0.86$, $p<0.001$), suggesting a cooperative role in leukemogenesis. Elevated HOXA9 (>589.7) was associated with improved survival (hazard ratio=0.3, p=0.021). Up-regulated WNT pathway targets (MYC, RUNX1) in NPM1-mutated cases indicate active WNT/β-catenin signaling, potentially promoting differentiation and favorable prognosis.Conclusion: HOX-PBX-WNT interactions contribute to the distinct biology of NPM1-mutated CN-AML. Targeting this axis may offer novel therapeutic strategies for AML, warranting further research into molecular-driven treatments for AML.

Keywords: Acute myeloid leukemi, acytogenetically normal AMLHOX genesPBX3 gene expression, WNT signaling

25COASMA25:

Title: Impact of Nivolumab Plus Chemotherapy on Conversion Therapy in Clinical Stage IVB HER2-negative Gastric Cancer

Yudai Hojo, Toshihiko Tomita, Masataka Igeta, et.al.

Anticancer Research May 2025, 45 (5) 2091-2102;
https://doi.org/10.21873/anticanres.17583

Abstract: Background/Aim: The approval of first-line nivolumab plus chemotherapy marks a

breakthrough in treating human epidermal growth factor receptor 2 (HER2)-negative unresectable advanced gastric and gastroesophageal junction (G/GEJ) cancer. This study aimed to evaluate the impact of nivolumab plus chemotherapy on conversion therapy in clinical stage (cStage) IVB HER2-negative G/GEJ adenocarcinoma.Patients and Methods: Patients with cStage IVB HER2-negative G/GEJ adenocarcinoma who underwent systemic chemotherapy at Hyogo Medical University Hospital from January 2017 to March 2023 were included. Nivolumab plus chemotherapy was initiated following its approval in Japan in November 2021. Conversion surgery (CS) was performed when distant metastases had disappeared, except for resectable liver metastases.Results: In total, 103 patients were eligible: 28 received nivolumab plus chemotherapy, and 75 received chemotherapy as first-line treatment. The conversion rate in the nivolumab plus chemotherapy group was significantly higher than that in the chemotherapy group (28.6% vs. 8.0%, p=0.011). Multivariate analysis revealed a significant association between first-line nivolumab plus chemotherapy and undergoing CS [odds ratio=3.540, 95% confidence interval (CI)=1.059-12.157]. R0 resection was achieved in all eight patients who underwent CS, and delayed immune-related adverse events did not occur perioperatively. In the nivolumab plus chemotherapy group, the median survival time in patients who underwent CS was significantly longer than that in patients treated with chemotherapy alone [not reached (95%CI=22.7-not reached) vs. 11.8 months (95%CI=5.1-33.3), p=0.035].Conclusion: First-line nivolumab plus chemotherapy increased the conversion rate compared with chemotherapy in patients with cStage IVB HER2-negative G/GEJ adenocarcinoma. CS following nivolumab plus chemotherapy was safe, and patients who underwent CS survived longer than those who received chemotherapy alone.

Keywords: Gastric cancer, nivolumab chemotherapy, conversion surgery, conversion therapy

25COASMA26:

Title: Palliative Radiotherapy for Large Osteolytic Metastatic Tumors Involving the Iliac Bone: A Report of 16 Cases

Federico Ampil, Russell Anderson, Troy Richards, et.al.

Anticancer Research May 2025, 45 (5) 2103-2108;
https://doi.org/10.21873/anticanres.17584

Abstract: Background/Aim: Among the bones that compose the pelvis, the ilium is the most commonly affected by metastatic tumors. The objective of our study was to describe the outcomes after palliative radiotherapy (PRT) of osteolytic metastatic tumors involving the iliac bone (OMTIB).Patients and Methods: Sixteen symptomatic patients with OMTIB were treated with PRT during a six-year period. The mean maximum diameter of the pelvic bone lesions was 9.3 cm (range=3.4-16 cm). OMTIB affected the iliac bone alone (six patients), the adjacent pelvic bones or muscles (seven patients), or both structures (three patients). The irradiation dose-fractionation scheme was ≥30 Gy given in 10 to 15 fractions.Results: Pain response rates were: good in 44% (7/16) of cases, fair in 25% (4/16), and poor in 31% (5/16). After treatment, mobility outcomes exhibited ambulation in 69% (9/13) and non-ambulation in 31% (4/13). During follow-up, the effects of PRT on OMTIB were reflected as stability in 28% (3/11), enlargement in 36% (4/11), and re-calcification in 36% (4/11). The overall

survival rates at one and two years were 44% (7/16) and 19% (3/16), respectively; median survival was two months. Conclusion: Although the prognosis of OMTIB is poor, PRT is an effective treatment for pain relief, improving mobility and promotion of bone repair.
Keywords: Metastatic tumor, palliative radiotherapy, chemotherapy, bone metastases, iliac bone

25COASMA27:

Title: Rare Upper Mediastinal Oligometastasis from Early Esophagogastric Adenocarcinoma: A Case Report

Larry Weng-Hong Lai, Takeshi Yamashita, Koji Otsuka, et.al.

Anticancer Research May 2025, 45 (5) 2109-2114;
https://doi.org/10.21873/anticanres.17585

Abstract: Background/Aim: Esophagogastric junction (EGJ) adenocarcinoma is an aggressive cancer with poor prognosis. Metastasis to the upper mediastinal lymph nodes is rare, with reported rates of 3.8% to 6.1%. This case report highlights the diagnostic and therapeutic challenges of oligometastatic recurrence in EGJ adenocarcinoma, emphasizing the role of surgery in selected cases.Case Report: A 63-year-old male underwent proximal gastrectomy for a Siewert type 2 poorly differentiated EGJ adenocarcinoma. Postoperative histopathology confirmed the diagnosis of stage 1 cancer. At 30 months, contrast-enhanced computed tomography (CT) scan detected a right paratracheal lymph node recurrence. Subsequent follow-up CT and positron emission tomography (PET) scan revealed progressive enlargement of the same lymph node with negative PET uptake. Owing to strong clinical and radiological suspicion of oligometastasis, thoracoscopic lymphadenectomy was performed with the patient in the left lateral decubitus position under one-lung ventilation. The postoperative histopathological examination confirmed metastatic adenocarcinoma. The patient was discharged uneventfully on postoperative day 5 and prescribed with adjuvant tegafur–gimeracil–oteracil (S-1). He remained asymptomatic during ongoing surveillance.Conclusion: This case highlights the challenges in diagnosing oligometastatic recurrence of EGJ adenocarcinoma, particularly when typical imaging signs are absent. It also demonstrates the importance of a multidisciplinary treatment approach, including careful surveillance and timely intervention. Surgery is one of the options for oligometastasis.
Keywords: Esophagogastric junction adenocarcin, omajunctional adenocarcinomao, ligometa, stasislymphatic invasion, salvage lymphadenectomy, surveillance

25COASMA28:

Title: Two Scoring Tools to Estimate the Risk of Taxane-induced Peripheral Sensory Neuropathy (PNP) in Patients Irradiated for Non-metastatic Breast Cancer

Dirk Rades, Tobias Bartscht, Achim Rody And Martin Ballegaard

Anticancer Research May 2025, 45 (5) 2115-2121;
https://doi.org/10.21873/anticanres.17586

Abstract: Background/Aim: Many patients with non-metastatic breast cancer assigned to radiotherapy already received taxane-based chemotherapy, often associated with peripheral neuropathy (PNP). Since treatment options are limited, identification of high-risk patients is important. Therefore, we developed two risk scores.Patients and Methods: Previously, we

identified risk factors for moderate to severe PNP. Now, risk scores were developed including four (Score A=performance score, cardiovascular disease, smoking history, beta blocker medication) or five (Score B=plus autoimmune disease) factors, respectively. For each existing factor, patients received 1 point; three risk groups were formed.Results: PNP rates using Score A were 11.1% (0 points), 37.5% (1-2 points), and 100% (3 points). Positive (PPV) and negative (NPV) predictive values were 100% and 88.9%. PNP rates using Score B were 7.4% (0 points), 33.8% (1-2 points), and 90.9% (3-4 points). PPV and NPV were 90.9% and 92.6%, respectively.Conclusion: Both risk scores provided high accuracy with respect to identification of patients with low or high risk of moderate to severe PNP.

Keywords: Non-metastatic breast cancer, adjuvant irradiation, paclitaxel, docetax, elperipheral sensory neuropathy, risk scores

25COASMA29:

Title: Chemotherapy-induced Moderate to Severe Peripheral Neuropathy in Patients Receiving Adjuvant Radiotherapy for Breast Cancer

Dirk Rades, Tobias Bartscht, Achim Rody, Nathan Y. Yu And Martin Ballegaard

Anticancer Research May 2025, 45 (5) 2123-2135;
https://doi.org/10.21873/anticanres.17587

Abstract: Background/Aim: A significant number of breast cancer patients assigned to adjuvant radiotherapy receive pre- or postoperative chemotherapy that can cause peripheral sensory and autonomic neuropathy (PNP). Identifying and grading PNP using a mobile application (app) may facilitate early detection and management. This study evaluated the prevalence of pre-radiotherapy PNP, providing essential baseline data for the prospective validation of such an app.Patients and Methods: Data of 133 breast cancer patients receiving chemotherapy prior to adjuvant radiotherapy were retrospectively analyzed regarding the incidence and risk factors of chemotherapy-induced moderate to severe PNP.Results: The incidence of moderate to severe PNP was 27.8%. On multivariate analysis, it was significantly associated with KPS ≤80 (p=0.030), history of significant cardiovascular disease (p=0.024), ≥10 pack years of smoking (p=0.023), and beta blocker medication (p=0.014). A trend was found for history of autoimmune disease (p=0.057).Conclusion: A considerable proportion of breast cancer patients assigned for adjuvant radiotherapy experienced moderate to severe PNP, which radiation oncologists should be aware of. The risk factors identified in this study likely contribute to earlier detection of PNP and inform the development of a prospective trial to validate a mobile-based PNP assessment tool.

Keywords: Breast cancer, adjuvant radiotherapy, chemotherapy, peripheral sensory neuropathy, incidence, risk factors

25COASMA30:

Title: Radiomics for Growth Prediction of Vestibular Schwannomas in Neurofibromatosis Type 2

Nina Boe, Victor F. Mautner, Reinhard E. Friedrich, et.al.

Anticancer Research May 2025, 45 (5) 2137-2146;
https://doi.org/10.21873/anticanres.17588

Abstract: Background/Aim: NF2-related schwannomatosis, formerly known as

Neurofibromatosis type 2 (NF2) is characterized by bilateral vestibular schwannomas (VS). Managing NF2 requires balancing watchful waiting with surgical intervention, each carrying inherent risks. While these risks are acknowledged, they have not yet been subjected to systematic investigation. Accurate prognosis of tumor growth is crucial for clinical decision-making. This study investigated radiomics features from longitudinal magnetic resonance imaging (MRI) data to predict VS growth.Patients and Methods: Radiomics features were extracted from cranial MRIs of 32 NF2 patients, each with at least two or more imaging time points. The association between these features and tumor growth was analyzed through correlation, visual inspection, and the Boruta algorithm.Results: Correlations between growth rates and radiomics features were weak ($\rho \leq 0.23$, $p < 0.016$). Three features exhibited a bimodal distribution, with cluster affiliation linked to tumor growth rate [cluster A: 7.9%/month, cluster B: 2.0%/month; Fisher exact odds ratio (OR)=2.55, p=0.010]. When considering only the first tumors in the MRI series, the Fisher exact OR was 2.29 (p=0.223). Boruta analysis identified wavelet.HLH_glcm_InverseVariance as a key feature, also relevant in the bimodal distribution. The Fisher exact OR of wavelet.HLH_glcm_InverseVariance for tumor growth was 2.64 (p=0.011) for all tumors and 2.21 (p=0.229) for initial tumors in the MRI series.Conclusion: Bimodally distributed radiomics features from initial MRIs did not reliably predict rapid tumor growth (error probability: 23%) but may aid in planning MRI follow-up intervals.

Keywords: NF2, radiomics, vestibular schwannomas, growth prediction, Boruta analysis

25COASMA31:

Title: Survival and Chemotherapy in the Last 30 Days as a Quality Indicator for Pancreatic Cancer

Mina M. Solheim, Carsten Nieder And Ellinor C. Haukland

Anticancer Research May 2025, 45 (5) 2147-2159;
https://doi.org/10.21873/anticanres.17589

Abstract: Background/Aim: This study aimed to investigate survival, treatment patterns, and the use of chemotherapy during the last 30 days of life in patients with pancreatic cancer, with the latter serving as a quality indicator.Patients and Methods: The data were collected through a retrospective review of electronic patient journals. The initial cohort consisted of 163 patients coded with ICD10-C25 pancreatic cancer at Nordland hospital trust from January 2021 till August 2023. A total of 113 patients were included, of whom 86 had histologically or cytologically confirmed pancreatic ductal adenocarcinoma, while 27 were diagnosed based on radiological findings.Results: The most common first-line chemotherapy regimen was nab-paclitaxel/gemcitabine, followed by FOLFIRINOX. The median survival was 4.0 months for all patients, 15.1 months for surgical patients, 7.0 months for patients treated with chemotherapy, and 1.5 months for patients who did not receive any treatment. Eight patients (18%) received chemotherapy during the last 30 days of life. All were treated with nab-paclitaxel/gemcitabine as first-line therapy, with an average of 0.75 treatment courses administered. Six of these patients were affiliated with small local hospitals without an oncologist present, and five were aged 75 years or older.Conclusion: Our findings largely align with the 2022 report from the Norwegian Quality Registry, though some deviations are observed due to better coverage and more detailed patient information in our study. The

slightly shorter survival rates may reflect the inclusion of radiologically diagnosed patients. To establish treatment in the last 30 days of life as a quality indicator and support longitudinal quality improvement, further in-depth analysis of at-risk patients is needed.
Keywords: Pancreatic cancer, palliative chemotherapy, treatment last 30 days, survival, quality indicator

25COASMA32:

Title: The Impact of State-trait Anxiety Inventory (STAI) Self-evaluation versus 25-year Outcome: A Prospective Follow-up Study in Patients With Breast Cancer Symptoms

Matti Eskelinen, Riika Koskela, Tuomas Selander et.al.
Anticancer Research May 2025, 45 (5) 2161-2169;
https://doi.org/10.21873/anticanres.17590
Abstract: Background/Aim: This study evaluated whether self-evaluation using the State-Trait Anxiety Inventory (STAI) questionnaire could predict long-term outcomes – specifically 25-year relapse-free survival (RFS) and overall survival (OS) – in patients presenting with breast cancer (BC) symptoms.Patients and Methods: A total of 115 patients with BC symptoms completed the STAI questionnaire pre-diagnosis. Associations between STAI scoring and long-term outcomes were analyzed using Kaplan–Meier and Cox proportional hazards models.Results: STAI scores correlated significantly with Beck Depression Inventory (BDI) ($r=0.634$, $p<0.001$) and Montgomery–Asberg Depression Rating Scale (MADRS) ($r=0.550$, $p<0.001$). A lower STAI score (<36) was associated with improved 25-year RFS (hazard ratio=2.753, $p=0.02$). The 25-year RFS rate was 80% for patients with low STAI scores versus 54% for those with higher scores. OS was also higher in the low-STAI group (80% vs. 65.9%), though the difference did not reach statistical significance ($p=0.100$).Conclusion: Although widely used to assess anxiety, STAI's long-term prognostic relevance in patients with BC symptoms has been largely overlooked. This 25-year prospective study is the first to demonstrate that lower STAI scores significantly predict better RFS. Given its correlation with established depression inventories, STAI could offer additional diagnostic and prognostic value. Integrating STAI assessments into the diagnostic workflow for patients with BC symptoms may improve long-term risk stratification and personalized care planning.
Keywords: Anxiety, inventory, breast disease, breast cancer, 25-year outcome

25COASMA33:

Title: Prediction of Severe Anemia and Neutropenia Induced by Abemaciclib in Patients With Breast Cancer

Shinya Takada, Kengo Umehara, Tahatsu Kanae, et.al.
Anticancer Research May 2025, 45 (5) 2171-2183;
https://doi.org/10.21873/anticanres.17591
Abstract: Background/Aim: Neutropenia and anemia are common and potentially serious adverse events associated with abemaciclib use in breast cancer, but their risk factors remain underexplored. This study aimed to identify the clinical predictors of severe neutropenia and anemia following the initiation of abemaciclib.Patients and Methods: The medical records of

252 patients with breast cancer who received abemaciclib therapy between August 2011 and November 2024 were retrospectively reviewed. The risk factors for severe neutropenia and anemia were identified based on clinical characteristics and laboratory values. Moreover, the timing of dose reduction after the initiation of abemaciclib treatment was compared with progression-free survival and overall survival using log-rank analysis.Results: Body mass index (BMI) <22.4 kg/m2 and pre-treatment neutrophil count <2,800×106 cells per liter were associated with an increased risk of grade ≥3 neutropenia [odds ratio (OR) (95% confidence interval, CI)=2.1 (1.1-4.0), p=0.03; OR (95%CI)=3.2 (1.5-6.7), p=0.003, respectively]. Also, BMI <22.4 kg/m2, hemoglobin level <8.9, and alanine aminotransferase (ALT) ≥60 U/l were significantly associated with an increased risk of grade ≥3 anemia [OR (95%CI)=5.0 (1.1-22.4), p=0.04; OR (95%CI)=1.6 (1.1-2.5), p=0.03; OR (95%CI)=9.6 (1.5-60.1), p=0.02, respectively].Conclusion: BMI and neutrophil count before treatment were significantly associated with an increased risk of abemaciclib-induced grade ≥3 neutropenia. Moreover, BMI, ALT, and hemoglobin were significantly associated with grade ≥3 anemia following abemaciclib initiation. These factors should be considered in determining individual risk of neutropenia and anemia and risk-benefit ratio of abemaciclib.
Keywords: Breast cancer, severe anemia, severe neutropenia, abemaciclib, predictor marker

25COASMA34:

Title: Treatment Outcomes After Progression With Enfortumab Vedotin in Patients With Advanced Urothelial Carcinoma

NOBUKI FURUBAYASHI, MANABU MOCHIDA, ATSUHIRO KIJIMA, et.al.

Anticancer Research May 2025, 45 (5) 2185-2193;
https://doi.org/10.21873/anticanres.17592

Abstract: Background/Aim: Enfortumab vedotin (EV) has been approved for the treatment of advanced urothelial carcinoma (UC) following platinum-based chemotherapy and immune checkpoint inhibitors (ICIs). However, there is no established treatment for patients whose disease progresses while on EV, and the clinical outcomes post-EV treatment are unclear.Patients and Methods: From December 2021 to January 2025, 33 patients with advanced UC received EV monotherapy. After excluding those who discontinued EV due to adverse events or continued treatment without progression, 18 patients were retrospectively analyzed.Results: The median follow-up was 4.1 months, and 16 patients (88.9%) died at the last follow-up. Ten patients received post-EV treatment (five received chemotherapy and five received ICIs), and eight opted for best supportive care (BSC). The overall survival (OS) was not significantly different between the post-EV and BSC groups (4.6 vs. 3.7 months, p=0.425). No significant differences in the progression-free survival (2.5 vs. 3.2 months, p=0.945) or OS (2.6 vs. 5.1 months, p=0.832) were observed between chemotherapy and ICI treatment in the post-EV treatment group. Patients with lymph node-only metastases had significantly longer OS than those with other metastases (13.5 vs. 3.3 months, p=0.039) in the post-EV treatment group.Conclusion: Post-EV treatment did not significantly improve the survival compared with BSC in patients with advanced UC. However, patients with lymph node-only metastases may show better outcomes than others. Further research is required to identify effective treatment strategies for this population.
Keywords: Urothelial carcinoma, enfortumab vedotin, chemotherapy

25COASMA35:

Title: Comparison of BRCA2 Single Nucleotide Variants Between Japanese Patients With Familial Prostate Cancer, Sporadic Prostate Cancer, and Benign Prostatic Hyperplasia

MASANORI AOKI, HIROSHI MATSUI, SOTA KURIHARA, et.al.

Anticancer Research May 2025, 45 (5) 2195-2204;
https://doi.org/10.21873/anticanres.17593

Abstract: Background/Aim: A family history of prostate cancer is an established risk factor for its development. The BRCA2 gene frequently harbors pathogenic mutations in patients with prostate cancer. This study compared single nucleotide variants (SNVs) in BRCA2 among patients with familial prostate cancer, primarily treated at our institution.Patients and Methods: SNVs in the BRCA2 gene were analyzed in 141 patients with benign prostatic hyperplasia (BPH), 202 patients with sporadic prostate cancer (SPC), and 151 patients with familial prostate cancer (FPC). We aimed to identify SNVs that were significantly more prevalent in FPC.Results: The analysis revealed that the G8187T variant was significantly more prevalent in the FPC group than in the BPH and SPC groups. Compared with the BPH group, the odds ratio was 4.93 (95% confidence interval=1.07-22.70, p=0.024). Among 75 cases with available prognostic information, the G8187T (+) variant was identified in six cases, whereas the G8187T (−) variant was found in 69 cases. Kaplan–Meier analysis showed no significant differences in overall (OS) or cancer-specific (CSS) survival between the two groups (OS, p=0.5734; CSS, p=0.2241).Conclusion: The G8187T variant in BRCA2 was significantly associated with familial prostate cancer in Japanese patients, suggesting that it constitutes a risk factor for disease development.

Keywords: Prostate cancer, familial prostate cancer, BRCA2SNV

25COASMA36:

Title: Appendectomy Mitigates Ulcerative Colitis Activity and Delays Colorectal Cancer Onset: A Retrospective Cohort Study

Yusuke Izutani, Takayuki Ogino, Makoto Fujii, et.al.

Anticancer Research May 2025, 45 (5) 2205-2214;
https://doi.org/10.21873/anticanres.17594

Abstract: Background/Aim: Ulcerative colitis (UC) is an idiopathic inflammatory disease with rising global incidence, influenced by genetic, environmental, and immunological factors whose interactions remain unclear. Although the appendix appears to influence UC onset and disease activity, few studies have investigated how the timing of appendectomy affects disease activity and colorectal cancer risk. This study aimed to clarify the impact of appendectomy on disease activity and colorectal cancer risk in patients with UC.Patients and Methods: We retrospectively analyzed 368 patients with UC treated at Osaka University Hospital and Kinshukai Infusion Clinic between April 2008 and December 2023. Participants were divided into two groups, namely the appendectomy (n=18) and non-appendectomy groups (n=350). We compared background characteristics, clinicopathological factors, and disease course, including Partial Mayo scores, relapse rates, proximal disease extension, medication use, and colorectal cancer development.Results: The appendectomy group showed significantly lower Partial Mayo scores at the most severe flare (4.5 vs. 8; p<0.001),

fewer relapses (p=0.016), lesser proximal disease extension (p=0.049), and lower use of steroids (p=0.032) and biologics or small molecules (p=0.006). Although colorectal cancer incidence was similar in the groups, the appendectomy group had a significantly longer duration from UC diagnosis to cancer diagnosis (29.3±16.0 vs. 16.0±9.9 years; p=0.033). Patients who underwent appendectomy after UC diagnosis exhibited milder disease activity, while those who underwent appendectomy before diagnosis were older at UC onset (p=0.004).Conclusion: Appendectomy is associated with milder UC activity and may delay disease onset. These findings offer insights into UC pathogenesis and suggest potential preventive approaches.

Keywords: Appendectomy, carcinogenesis, colorectal cancer, disease activity, ulcerative colitis

25COASMA37:

Title: Immune Checkpoint Inhibitor-induced Uveitis: Disproportionality and Timing Analyses of the Japanese Pharmacovigilance Database

Naohito Ide, Ken-Ichi Sako And Tomoji Maeda

Anticancer Research May 2025, 45 (5) 2215-2223;
https://doi.org/10.21873/anticanres.17595

Abstract: Background/Aim: Immune checkpoint inhibitors (ICIs) are widely used anticancer drugs, but they can trigger immune-related adverse events (irAEs), including rare but potentially blinding uveitis. In this study, the associations between ICIs and uveitis, and the time to uveitis onset, were evaluated using data from the Japanese Adverse Drug Event Report (JADER) database.Patients and Methods: We performed disproportionality analysis using data from the JADER database (April 2004–June 2024). Positive signals were identified using reporting odds ratios (RORs) with 95% confidence intervals (CIs). Time-to-onset analyses were performed with the Weibull distribution model, and sex-based differences were assessed with Kaplan–Meier curves and the log-rank test.Results: Among 914,713 cases in the JADER database, 346 were suspected ICI-induced uveitis. Positive signals were detected for nivolumab [ROR, 9.05 (95%CI=7.81-10.50)], ipilimumab [9.82 (8.20-11.76)], and pembrolizumab [4.94 (4.05-6.01)] but not for other ICIs. The median onset time was approximately 2 months (65 days for nivolumab, 61 days for ipilimumab, and 70 days for pembrolizumab). Pembrolizumab-induced uveitis occurred significantly earlier in female patients than in male patients (29.5 vs. 91 days, p=0.015). Onset patterns were classified as early failure for nivolumab and random failure for ipilimumab and pembrolizumab. The outcomes were mostly good, and severe cases of uveitis were rare.Conclusion: ICI-induced uveitis typically occurs within two months of treatment initiation, with pembrolizumab-induced uveitis occurring earlier in females than in males. Because causation cannot be established on the basis of this analysis, large-scale prospective clinical studies are needed.

Keywords: Adverse reactions, immune checkpoint inhibitors, Japanese Adverse Drug Event Report database, time-to-onset, uveitis

25COASMA38:

Title: The Long-term Outcomes of Borderline Resectable T3 in Locally Advanced

Esophageal Squamous Cell Carcinoma Treated With Neoadjuvant Triplet Chemotherapy

Junya Kitadani, Keiji Hayata, Taro Goda, et.al.

Anticancer Research May 2025, 45 (5) 2225-2235;
https://doi.org/10.21873/anticanres.17596

Abstract: Background/Aim: This study compared the clinical characteristics and outcomes between patients with resectable clinical T3 (cT3r) and borderline resectable clinical T3 (cT3br) esophageal squamous cell carcinoma (ESCC) who underwent neoadjuvant triplet chemotherapy.Patients and Methods: The study cohort comprised patients treated at our institution between January 2010 and November 2020 who underwent neoadjuvant chemotherapy using a triplet regimen – either DCF or DCS – followed by esophagectomy for cT3. Eligible patients were divided into cT3r and cT3br groups.Results: A total of 127 patients with cT3 ESCC were included, comprising 101 in the cT3r group and 26 in the cT3br group. The numbers of patients with complete response, partial response, stable disease, and progressive disease were significantly different between the cT3r and cT3br groups (4.9%, 52.5%, 8.9% and 3.0% vs. 3.9%, 42.3%, 19.2% and 23.1%, respectively; p=0.003). Anastomotic leakage (≥Clavien-Dindo grade III) occurred significantly more frequently in the cT3br group than in the cT3r group (38.5% vs. 9.9%, respectively; p=0.001). Surgical radicality of R0, R1, and R2 was significantly different between the cT3r and cT3br groups (93.0%, 4.0% and 3.0% vs. 57.6%, 7.7% and 34.7%, respectively; p<0.001). In survival analysis, the three-year recurrence-free and overall survival rates were significant different between the groups (53.1% vs. 24.9%; p<0.001, 59.8% vs. 32.6%, respectively; p<0.001). Multivariate analysis identified cT3br status (p=0.016) and poor histological response ≤1a (p<0.001) as independent prognostic factors for overall survival.Conclusion: cT3br and poorer histological response were identified as prognostic factors of overall survival in this retrospective cohort study. Neoadjuvant chemotherapy alone may be insufficient to achieve curative outcomes in cT3br cases. For patients who do not respond adequately to initial chemotherapy, the addition of preoperative chemoradiotherapy may be necessary to enhance local tumor control and improve long-term survival.

Keywords: Esophageal cancer, esophagectomy, T3brborderline resectable

25COASMA39:

Title: Gender-specific effects of prenatal polystyrene nanoparticle exposure on offspring lung development

Wenxia Bu, Mengjiao Yu, Xinyi Ma

Toxicology Letters, Volume 407, 1 May 2025, Pages 1-16
https://doi.org/10.1016/j.toxlet.2025.03.001

Abstract: Nanoplastics are widely present in the environment. Exposure to environmental pollutants during pregnancy can have adverse effects on fetal development and health. Establishing a link between nanoplastics and Bronchopulmonary Dysplasia (BPD) requires further investigation. In this study, we examined the impact of prenatal exposure to 80 nm polystyrene nanoparticles (PS-NPs) on offspring lung development, taking into account potential gender-specific effects. Pregnant female mice were exposed to PS-NPs through oropharyngeal aspiration, and critical data on lung development were collected at postnatal

days 1, 7, and 21. We found that exposure to PS-NPs reduced birth weight in female offspring and significantly increased lung weight in both male and female offspring by PND 21. Maternal exposure led to a reduction in alveolar numbers across offspring, with distinct underlying mechanisms observed between sexes. In female offspring, the reduction in alveolar numbers was linked to disrupted surfactant protein expression, significant inflammation, and increased apoptosis and fibrosis. In male offspring, impaired angiogenesis was the primary factor contributing to the increased risk of BPD. The impact on alveolar development was substantial in both genders. This study underscores the gender-specific impacts of prenatal nanoplastic exposure on lung development and offers new evidence and direction for future research on the cross-generational respiratory toxicity of PS-NPs.

25COASMA40:

Title: Analysis of structure phototoxicity relationship towards the de-risking of phototoxic liabilities in early drug discovery

Takafumi Takai

Toxicology Letters, Volume 407, 1 May 2025, Pages 17-23

https://doi.org/10.1016/j.toxlet.2025.03.002

Abstract: The in vitro phototoxicity assay using the 3T3 cell line is a widely used screening system to identify toxicity risk in humans after exposure to sunlight. The chemical structure of drugs itself is considered to be primarily involved in the process of eliciting phototoxicity. Therefore, various structure-based chemical descriptors have been utilized as a part of in silico prediction model for phototoxicity. Herein, we analyzed the relationship between chemical descriptors and phototoxicity using in-house diverse data sets (2201 compounds). HOMO-LUMO gaps worked best to discriminate phototoxic and non-phototoxic compounds among the descriptors we assessed. Furthermore, it was revealed that the prediction power was enriched, especially for a subset of compounds not having a fused ring.

25COASMA41:

Title: Protective role of hepatic non-parenchymal cells against drug-induced hepatocyte toxicity using perfluoropolyether-based microfluidic devices

Mengyang Wang, Qiyue Zhang,Kazuma Aoki et.al.

Toxicology Letters, Volume 407, 1 May 2025, Pages 24-31

https://doi.org/10.1016/j.toxlet.2025.03.004

Abstract: The role of hepatic non-parenchymal cells (NPCs) in drug-induced liver injury has been controversial. Utilizing our previously developed perfluoropolyether-based microfluidic devices—characterized by significantly reduced chemical absorption compared to conventional polydimethylsiloxane (PDMS)—we investigated the interactions between primary hepatocytes (PCs) and NPCs under physiologically relevant conditions. When exposed to coumarin or acetaminophen, PCs underwent severe cytotoxicity and showed glutathione (GSH) depletion. Notably, co-culture with NPCs restored drug-induced cytotoxicity and cellular GSH levels, accompanied by increased interleukin-6 (IL-6) secretion. Given previous reports linking IL-6 to cytochrome P450 expression modulation and glutathione synthesis, these findings suggest that IL-6 might be a critical mediator of protective effects exerted by NPCs. Using these microfluidic devices, we clearly

demonstrated the protective roles of NPCs without interference from innate immune systems, offering novel insights into hepatocellular protection mechanisms.

25COASMA42:

Title: Comparative effects of e-cigarette and conventional cigarette smoke on in vitro bronchial epithelial cell responses

K.L. Pleiss, D.D. Mosley, C.D. Bauer et.al.

Toxicology Letters, Volume 407, 1 May 2025, Pages 32-40
https://doi.org/10.1016/j.toxlet.2025.03.003

Abstract: Because of cigarette smoking, chronic lung diseases are the third leading cause of death in the United States. Electronic cigarettes (e-cig) were originally marketed as harm reduction devices for cigarette smokers due to low success rates with traditional smoking cessation methods. While several studies show that cigarette smoke causes damage to the lungs, comparative research assessing the injury profile of e-cig to traditional cigarettes is still limited. Comparative lung injury studies are crucial in determining the validity of e-cig as a harm reduction device for chronic smokers and can be used to assess the quality of alternate nicotine delivery options to reduce the morbidity and mortality caused by cigarettes. We hypothesize that exposure to JUUL to e-cig vapor produces decreased in vitro markers of lung injury in comparison to cigarette smoke extract at equivalent and higher nicotine concentrations to that from CSE. We compared the extent of injury to airway epithelial tissue from cigarettes and e-cig using various assays of cellular function, including ciliary beat frequency (CBF), wound closure, barrier function, cytokine release, and kinase activity. Cells were treated with various concentrations of Virginia Tobacco-flavored JUUL™ vapor extract (JVE) and cigarette smoke extract (CSE) either normalized for nicotine concentration or equivalent % dilutions from a 100 % stock extract. CSE stimulated cilia in the short term, but slowed cilia after several hours of exposure, whereas cells treated with JVE showed no significant changes in CBF. CSE slowed wound repair, but nicotine-equivalent doses of JVE did not significantly slow wound repair. CSE increased epithelial cell monolayer permeability and interleukin release in a concentration-dependent manner, but these were not observed with JVE treatment. Kinase activity assays revealed activation translocation of protein kinase C (PKC) activity in cells treated with CSE, but no such change in PKC activity was observed in JVE groups. The results of these in vitro assays suggest that at nicotine-equivalent doses, JVE from Virginia Tobacco-flavored JUUL does not impact the airway epithelium in the same manner as CSE. The lack of evidence for in vitro tissue injury in this study caused by JUUL™ vapor extract is not a justification for the harm posed by nicotine addiction, particularly at the high levels of nicotine contained in these products which are several times the legal limit of many countries.

25COASMA43:

Title: Cigarette smoking modulates m6A modification, affecting the induction of CYP1A1 mRNA by regulating human ARNT and AHRR in A549 cells

Takumi Nakano, Masataka Nakano, Tatsuki Fukami et.al.

Toxicology Letters, Volume 407, 1 May 2025, Pages 41-49
https://doi.org/10.1016/j.toxlet.2025.03.005

Abstract: N6-Methyladenosine (m6A) modification is a common epitranscriptomic mark of eukaryotic RNAs. This modification is installed by a methyltransferase like 3 (METTL3)-METTL14 complex and is eliminated by fat mass and obesity-associated protein (FTO) and AlkB homolog 5 (ALKBH5). Aberrant m6A modification is associated with the development and progression of cancer. Cigarette smoking is a major lifestyle habit and risk factor for lung cancer. This study aimed to clarify the effects of cigarette smoking on the expression of m6A modification-regulating enzymes and the significance of m6A modification in the biological responses to cigarette smoking. Treatment of cigarette smoke extract (CSE) significantly decreased METTL3 and METTL14 protein levels in human lung adenocarcinoma-derived A549 cells. The induction of CYP1A1 mRNA by 2,3,7,8-tetrachlorodibenzo-p-dioxin, a typical ligand of the aryl hydrocarbon receptor (AHR), was attenuated by the knockdown (KD) of METTL3 or ALKBH5, whereas it was enhanced by the KD of FTO. As the underlying mechanisms, significantly decreased expression of AHR nuclear translocator (ARNT) by the KD of METTL3 or ALKBH5, and significantly decreased expression of AHR repressor (AHRR) by the KD of FTO were demonstrated. Formaldehyde-assisted isolation of regulatory elements assay revealed that the KD of METTL3 or ALKBH5 resulted in the compaction of the chromatin structure of ARNT promoter, suggesting that METTL3 and ALKBH5 promote the transcription of ARNT through the rearrangement of chromatin structure. Collectively, we found that CSE treatment decreased METTL3 and METTL14 protein levels, and m6A modification have impact on the induction of CYP1A1 by modulating ARNT and AHRR expression.

25COASMA44:

Title: Extended sub-chronic exposure to heavy metal mixture induced multidrug resistance against chemotherapy agents in ovarian cancer cells

Gözde Sahin, Zeynep Banu Doğanlar et.al.

Toxicology Letters, Volume 407, 1 May 2025, Pages 50-62
https://doi.org/10.1016/j.toxlet.2025.03.006

Abstract: Recent scientific findings suggest that persistent, minimal quantity exposure to heavy metals combinations can instigate negative reactions across various cell types, tissues, and organs. However, the interplay between heavy metals present in blood and cancerous cells remains largely unclear. We aimed to examine the capability of a Pb, Cd, and Co at very low concentrations blend to trigger multidrug resistance against chemotherapeutic remedies such as cisplatin, 5-fluorouracil, and doxorubicin in the NIH-Ovcar3 human ovarian cancer cell line. Additionally, we sought to dissect the molecular mechanisms bolstering this resistance. Our results illustrate that consistent administration of the heavy metal mixture at extraordinarily low concentrations fosters pronounced chemotherapy resistance in Ovcar3 cells via cross resistance. This resistance endured and was propagated through ensuing cell generations. We observed that ATP-binding cassette (ABC) membrane transporters, specifically P-gp/ABCB1, BRCP/ABCG2, and ABCC1-type cellular detoxification functions, were markedly overexpressed, playing a crucial role in multidrug resistance. This finding supports the molecular evidence of the acquired multidrug resistance phenotype and provides preliminary insights into the potential resistance mechanism. We also found decreased mortality rates in the resistant ovarian cancer cells, with the mitochondrial apoptosis pathway

activating at a reduced rate post-chemotherapy relative to the non-resistant control cells. Furthermore, multidrug-resistant cells exhibited increased motility and enhanced wound-healing abilities, hinting at a higher metastatic potential. These findings suggest that analysing P-gp, BRCP, and ABCC1 multidrug resistance gene expression and/or protein levels within biopsy samples from ovarian cancer patients at risk of heavy metal exposure could prove advantageous in determining chemotherapy dosage and prolonging patient lifespan.

25COASMA45:

Title: Toxic effects of sterigmatocystin on porcine oocyte maturation and subsequent embryo development

Yumin Lee, Dabin Cha, Seunghyun Choi et.al.

Toxicology Letters, Volume 407, 1 May 2025, Pages 63-72

https://doi.org/10.1016/j.toxlet.2025.03.007

Abstract: Sterigmatocystin (STE), a precursor of aflatoxin B1, is one of the mycotoxins that easily contaminates feed. Although previous studies have suggested the toxic effects of aflatoxin B1 on oocyte maturation, little attention has been given to the effects of STE. Therefore, we investigated the effects of STE on porcine oocyte maturation. In this study, porcine oocytes were subjected to in vitro maturation supplemented with various concentrations of STE (0, 5, 10, and 25 μM). The results showed that the cumulus cell expansion indexes of all STE-treated groups were significantly decreased compared to the control group, with 10 μM significantly decreasing the transcript expression of cumulus expansion-related genes. Regarding nuclear maturation, metaphase II rates in all STE-treated groups were significantly lower than in the control group, with 10 μM significantly decreasing the transcript expression of oocyte competence-, mitogen-activated protein kinase-, and maturation-promoting factor-related genes. While cleavage rates showed no significant differences, the blastocyst formation rates significantly declined in groups treated with more than 10 μM of STE. Based on these findings, the 10 μM STE group was selected for subsequent experiments. STE supplementation significantly increased reactive oxygen species levels and decreased glutathione levels in oocytes compared to the control group. Furthermore, STE significantly decreased mitochondrial quantity and membrane potential, while increasing the percentage of γ-H2AX-positive oocytes. The number of LC3-positive dots and Annexin-V-positive oocytes was also significantly higher in the STE-treated group than in the control group. In conclusion, STE impairs porcine oocyte maturation and subsequent embryo development by inducing oxidative stress, mitochondrial dysfunction, DNA damage, excessive autophagy, and early apoptosis.

25COASMA46:

Title: Dose-dependent effects of chlorpyrifos on liver injury, intestinal dysbiosis, and metabolic perturbations in C57BL/6J mice

Shuilin Wei, Mengjing Wu, Quanzhi Qin et.al.

Toxicology Letters, Volume 407, 1 May 2025, Pages 73-82

https://doi.org/10.1016/j.toxlet.2025.03.011

Abstract: The organophosphorus pesticide chlorpyrifos (CPF) is widely utilized in

agriculture to protect crops from pests and diseases. Concerns regarding its extensive use have emerged due to the substance's persistence, bioaccumulation, endocrine disruption, and associated toxicity, which may lead to various adverse reactions. In this study, 32 male C57BL/6 J mice were orally administered varying doses of CPF over a period of two weeks. Metabolic perturbations resulting from subacute exposure to CPF were assessed using LC-MS/MS-based untargeted metabolomics, alongside biochemical analysis and histopathological techniques. The 16S rRNA gene sequencing method was employed to evaluate changes in the gut microbial community within the cecal contents of mice exposed to CPF. In vivo studies have shown that CPF exposure induced dose-dependent damage and dysregulation of the intestinal microbiota in mouse colonic tissues. This was characterized by significant alterations in the gut microbiota, increased intestinal permeability and elevated levels of lipopolysaccharides. These changes may have compromised intestinal barrier function and facilitated the transfer of intestinal microbial metabolites and endotoxins to the liver, subsequently leading to liver injury. Collectively, this study elucidates a potential mechanism by which CPF triggers liver injury through alterations in the intestinal microbial community and increased intestinal permeability. These findings not only enhance our understanding of the toxicological effects of CPF but also contribute to the assessment of health risks associated with CPF exposure.

25COASMA47:

Title: Environmental pesticide exposure and its association with hematological parameters and inflammation indices among school-aged children in Mexico

Miguel Alfonso Ruiz-Arias, Yael Yvette Bernal-Hernández, Irma Martha Medina-Díaz et.al.

Toxicology Letters, Volume 407, 1 May 2025, Pages 83-94
https://doi.org/10.1016/j.toxlet.2025.03.009

Abstract: Few studies have investigated the association between pesticide exposure and immune-inflammatory indices in children. We conducted a cross-sectional study of 369 school-aged children from three Mexican communities with varying levels of agricultural production. Blood samples were collected to calculate immune-inflammatory indices, and pooled hand-washing samples from 30 randomly selected children per community were analyzed for pesticide metabolites. Urinary dialkylphosphates (DAP) were determined in pooled samples per community. Multivariable logistic regression models assessed associations between pesticide exposure and immune-inflammatory indices (>median vs. <median). We detected ten classes of pesticides in hand-washing samples, including benzimidazoles, carbamates, neonicotinoids, organochlorines, organophosphates, and N-(phosphonomethyl)glycine. Total pesticide residue concentrations were 6.6 µg/L and 5.5 µg/L in the two highest production communities, compared to 0.3 µg/L in the reference community. Bifenthrin, chlorpyrifos, malathion, and carbendazim were present across all communities, with AMPA (a glyphosate metabolite) in the highest concentrations in agricultural areas. Urinary DAP were significantly higher in children from agricultural communities. Children in the largest agricultural community had lower hemoglobin and lymphocyte counts but higher neutrophil and eosinophil counts. Regression models showed increased odds of elevated systemic inflammation indices, particularly in children from the two highest production areas. Our adjusted models revealed significant associations between

pesticide exposure and platelet-to-lymphocyte ratio (PLR), neutrophil-to-lymphocyte ratio (NLR), and eosinophil-to-lymphocyte ratio (ELR), in community B compared to community C, emphasizing the need for targeted interventions in high-exposure communities.

25COASMA48:

Title: Measuring and manipulating mechanical forces during development

Clémentine Villeneuve, Kaitlin P. McCreery & Sara A. Wickström

Nature Cell Biology volume 27, pages575–590 (2025)
https://doi.org/10.1038/s41556-025-01632-x

Abstract: Tissue deformations are a central feature of development, from early embryogenesis, growth and building the body plan to the establishment of functional organs. These deformations often result from active contractile forces generated by cells and cell collectives, and are mediated by changes in their mechanical properties. Mechanical forces drive the formation of functional organ architectures, but they also coordinate cell behaviour and fate transitions, ensuring robustness of development. Advances in microscopy, genetics and chemistry have enabled increasingly powerful tools for measuring, generating and perturbing mechanical forces. Here we discuss approaches to measure and manipulate mechanical forces with a focus on developmental processes, ranging from quantification of molecular interactions to mapping the mechanical properties of tissues. We focus on contemporary methods, and discuss the biological discoveries that these approaches have enabled. We conclude with an outlook to methodologies at the interface of physics, chemistry and biology to build an integrated understanding of tissue morphodynamics.

Keyword: Biological techniques, Developmental biology

25COASMA49:

Title: Modulation of bone marrow haematopoietic stem cell activity as a therapeutic strategy after myocardial infarction: a preclinical study

Jasmin Rettkowski, Mari Carmen Romero-Mulero, Indranil Singh

Nature Cell Biology volume 27, pages591–604 (2025)
https://doi.org/10.1038/s41556-025-01639-4

Abstract: Myocardial infarction (MI) is a major global health concern. Although myeloid cells are crucial for tissue repair in emergency haematopoiesis after MI, excessive myelopoiesis can exacerbate scarring and impair cardiac function. Bone marrow (BM) haematopoietic stem cells (HSCs) have the unique capability to replenish the haematopoietic system, but their role in emergency haematopoiesis after MI has not yet been established. Here we collected human sternal BM samples from over 150 cardiac surgery patients, selecting 49 with preserved cardiac function. We show that MI causes detrimental transcriptional and functional changes in human BM HSCs. Lineage tracing experiments suggest that HSCs are contributors of pro-inflammatory myeloid cells infiltrating cardiac tissue after MI. Therapeutically, enforcing HSC quiescence with the vitamin A metabolite 4-oxo-retinoic acid dampens inflammatory myelopoiesis, thereby modulating tissue remodelling and preserving long-term cardiac function after MI.

Keyword: Acute inflammation, Haematopoietic stem cells

25COASMA50:

Title: Multipotent neural stem cells originating from neuroepithelium exist outside the mouse central nervous system

Dong Han, Wan Xu, Hyun-Woo Jeong et.al.

Nature Cell Biology volume 27, pages605–618 (2025)
https://doi.org/10.1038/s41556-025-01641-w

Abstract: Conventional understanding dictates that mammalian neural stem cells (NSCs) exist only in the central nervous system. Here, we report that peripheral NSCs (pNSCs) exist outside the central nervous system and can be isolated from mouse embryonic limb, postnatal lung, tail, dorsal root ganglia and adult lung tissues. Derived pNSCs are distinct from neural crest stem cells, express multiple NSC-specific markers and exhibit cell morphology, self-renewing and differentiation capacity, genome-wide transcriptional profile and epigenetic features similar to control brain NSCs. pNSCs are composed of Sox1+ cells originating from neuroepithelial cells. pNSCs in situ have similar molecular features to NSCs in the brain. Furthermore, many pNSCs that migrate out of the neural tube can differentiate into mature neurons and limited glial cells during embryonic and postnatal development. Our discovery of pNSCs provides previously unidentified insight into the mammalian nervous system development and presents an alternative potential strategy for neural regenerative therapy.

Keyword: Neural stem cells

25COASMA51:

Title: Proteostasis and lysosomal repair deficits in transdifferentiated neurons of Alzheimer's disease

Ching-Chieh Chou, Ryan Vest, Miguel A. Prado et.al.

Nature Cell Biology volume 27, pages619–632 (2025)
https://doi.org/10.1038/s41556-025-01623-y

Abstract: Ageing is the most prominent risk factor for Alzheimer's disease (AD). However, the cellular mechanisms linking neuronal proteostasis decline to the characteristic aberrant protein deposits in the brains of patients with AD remain elusive. Here we develop transdifferentiated neurons (tNeurons) from human dermal fibroblasts as a neuronal model that retains ageing hallmarks and exhibits AD-linked vulnerabilities. Remarkably, AD tNeurons accumulate proteotoxic deposits, including phospho-tau and amyloid β, resembling those in APP mouse brains and the brains of patients with AD. Quantitative tNeuron proteomics identify ageing- and AD-linked deficits in proteostasis and organelle homeostasis, most notably in endosome–lysosomal components. Lysosomal deficits in aged tNeurons, including constitutive lysosomal damage and ESCRT-mediated lysosomal repair defects, are exacerbated in AD tNeurons and linked to inflammatory cytokine secretion and cell death. Providing support for the centrality of lysosomal deficits in AD, compounds ameliorating lysosomal function reduce amyloid β deposits and cytokine secretion. Thus, the tNeuron model system reveals impaired lysosomal homeostasis as an early event of ageing and AD.

Keyword: Organelles, Protein folding

25COASMA52:

Title: In situ architecture of the human prohibitin complex

Felix Lange, Michael Ratz, Jan-Niklas Dohrke, et.al.

Nature Cell Biology volume 27, pages633–640 (2025)
https://doi.org/10.1038/s41556-025-01620-1

Abstract: Prohibitins are a highly conserved family of proteins that have been implicated in a variety of functions including mitochondrial stress signalling and housekeeping, cell cycle progression, apoptosis, lifespan regulation and many others. The human prohibitins prohibitin 1 and prohibitin 2 have been proposed to act as scaffolds within the mitochondrial inner membrane, but their molecular organization has remained elusive. Here we determined the molecular organization of the human prohibitin complex within the mitochondrial inner membrane using an integrative structural biology approach combining quantitative western blotting, cryo-electron tomography, subtomogram averaging and molecular modelling. The proposed bell-shaped structure consists of 11 alternating prohibitin 1 and prohibitin 2 molecules. This study reveals an average of about 43 prohibitin complexes per crista, covering 1–3% of the crista membrane area. These findings provide a structural basis for understanding the functional contributions of prohibitins to the integrity and spatial organization of the mitochondrial inner membrane.

Keyword: Cryoelectron tomography, Mitochondria.

25COASMA53:

Title: PRMT5-mediated arginine methylation stabilizes GPX4 to suppress ferroptosis in cancer

Yizeng Fan, Yuzhao Wang, Weichao Dan, et.al.

Nature Cell Biology volume 27, pages641–653 (2025)
https://doi.org/10.1038/s41556-025-01610-3

Abstract: The activation of ferroptosis has shown great potential for cancer therapy from an unconventional perspective, but revealing the mechanisms underlying the suppression of tumour-intrinsic ferroptosis to promote tumorigenesis remains a challenging task. Here we report that methionine is metabolized into S-adenosylmethionine, which functions as a methyl-group donor to trigger symmetric dimethylation of glutathione peroxidase 4 (GPX4) at the conserved arginine 152 (R152) residue, along with a prolonged GPX4 half-life. Inhibition of protein arginine methyltransferase 5 (PRMT5), which catalyses GPX4 methylation, decreases GPX4 protein levels by impeding GPX4 methylation and increasing ferroptosis inducer sensitivity in vitro and in vivo. This methylation prevents Cullin1-FBW7 E3 ligase binding to GPX4, thereby abrogating the ubiquitination-mediated GPX4 degradation. Notably, combining PRMT5 inhibitor treatment with ferroptotic therapies markedly suppresses tumour progression in mouse tumour models. In addition, the levels of GPX4 are negatively correlated with the levels of FBW7 and a poor prognosis in patients with human carcinoma. In summary, we found that PRMT5 functions as a target for improving cancer therapy efficacy, by acting to reduce the counteraction of ferroptosis by tumour cells by means of PRMT5-enhanced GPX4 stability.

Keyword: Cancer therapy, Cell death, Prostate cancer.

25COASMA54:

Title: Supra-second tracking and live-cell karyotyping reveal principles of mitotic chromosome dynamics

Rumen Stamatov, Sonya Uzunova, Yoana Kicheva et.al.

Nature Cell Biology volume 27, pages654–667 (2025)
https://doi.org/10.1038/s41556-025-01637-6

Abstract: Mitotic chromosome dynamics are essential for the three-dimensional organization of the genome during the cell cycle, but the spatiotemporal characteristics of this process remain unclear due to methodological challenges. While Hi-C methods capture interchromosomal contacts, they lack single-cell temporal dynamics, whereas microscopy struggles with bleaching and phototoxicity. Here, to overcome these limitations, we introduce Facilitated Segmentation and Tracking of Chromosomes in Mitosis Pipeline (FAST CHIMP), pairing time-lapse super-resolution microscopy with deep learning. FAST CHIMP tracked all human chromosomes with 8-s resolution from prophase to telophase, identified 15 out of 23 homologue pairs in single cells and compared chromosomal positioning between mother and daughter cells. It revealed a centrosome-motion-dependent flow that governs the mapping between chromosome locations at prophase and their metaphase plate position. In addition, FAST CHIMP measured supra-second dynamics of intra- and interchromosomal contacts. This tool adds a dynamic dimension to the study of chromatin behaviour in live cells, promising advances beyond the scope of existing methods.

Keyword: Bioinformatics, Chromosomes, Mitosis, Super-resolution microscopy, Time-lapse imaging

25COASMA55:

Title: ADSL-generated fumarate binds and inhibits STING to promote tumour immune evasion

Yuran Duan, Zhiqiang Hu, Peng Han, et.al.

Nature Cell Biology volume 27, pages668–682 (2025)
https://doi.org/10.1038/s41556-025-01627-8

Abstract: Highly aggressive tumours have evolved to restrain the cGAS–STING pathway for immune evasion, and the mechanisms underlying this hijacking remain unknown. Here we demonstrate that hypoxia induces robust STING activation in normal mammary epithelial cells but not in breast cancer cells. Mechanistically, adenylosuccinate lyase (ADSL), a key metabolic enzyme in de novo purine synthesis, is highly expressed in breast cancer tissues and is phosphorylated at T350 by hypoxia-activated IKKβ. Phosphorylated ADSL interacts with STING at the endoplasmic reticulum, where ADSL-produced fumarate binds to STING, leading to the inhibition of cGAMP binding to STING, STING activation and subsequent IRF3-dependent cytokine gene expression. Disrupting the ADSL–STING association promotes STING activation and blunts tumour growth. Notably, a combination treatment with ADSL endoplasmic reticulum translocation-blocking peptide and anti-PD-1 antibody induces an additive inhibitory effect on tumour growth accompanying a substantially increased immune response. Notably, ADSL T350 phosphorylation levels are inversely correlated with levels of STING activation and predicate poor prognosis in patients with breast cancer. These findings highlight a pivotal role of the metabolite fumarate in inhibiting

STING activation and uncover new strategies to improve immune-checkpoint therapy by targeting ADSL-moonlighting function-mediated STING inhibition.
Keyword: Breast cancer, Immune evasion, Innate immunity, Tumour immunology.

25COASMA56:
Title: Selective translational control by PABPC1 phase separation regulates blast crisis and therapy resistance in chronic myeloid leukaemia
Chenguang Sun, Xi Xu, Zhongyang Chen et.al.
Nature Cell Biology volume 27, pages683–695 (2025)
https://doi.org/10.1038/s41556-024-01607-4
Abstract: Tyrosine kinase inhibitors (TKIs) targeting the BCR-ABL1 fusion tyrosine kinase have revolutionized the treatment of chronic myeloid leukaemia (CML). However, the development of TKI resistance and the subsequent transition from the chronic phase (CP) to blast crisis (BC) threaten patients with CML. Accumulating evidence suggests that translational control is crucial for cancer progression. Our high-throughput CRISPR–Cas9 screening identified poly(A) binding protein cytoplasmic 1 (PABPC1) as a driver for CML progression in the BC stage. PABPC1 preferentially improved the translation efficiency of multiple leukaemogenic mRNAs with long and highly structured 5′ untranslated regions by forming biomolecular condensates. Inhibiting PABPC1 significantly suppressed CML cell proliferation and attenuated disease progression, with minimal effects on normal haematopoiesis. Moreover, we identified two PABPC1 inhibitors that inhibited BC progression and overcame TKI resistance in murine and human CML. Overall, our work identifies PABPC1 as a selective translation enhancing factor in CML-BC, with its genetic or pharmacological inhibition overcoming TKI resistance and suppressed BC progression.
Keyword: Cancer, Cancer therapeutic resistance, Translation.

25COASMA57:
Title: Emerging roles of prohibitins in cancer: an update
Yunliang Gao & Yuanyuan Tang et.al.
Cancer Gene Therapy volume 32, pages357–370 (2025)
https://doi.org/10.1038/s41417-025-00883-y
Abstract: The prohibitin (PHB) family, including PHB1 and its homolog PHB2, is ubiquitously located in different cellular compartments and plays roles in fundamental cellular processes such as proliferation, differentiation, and apoptosis. Accumulating evidence has indicated that this family contributes to the development of numerous diseases in particular cancers. Aberrant expressions of PHBs can been observed in diverse types of human cancer. Depending on their cell compartment-specific attributes and interacting proteins, PHBs are tightly linked to almost all aspects of cancer biology and have distinct bidirectional functions of tumor-suppression or tumor-promotion. However, the roles of PHBs in cancer have yet to be fully characterized and understood. This review provides an updated overview of the pleiotropic effects of PHBs and emphasizes their characteristic roles in each cancer respectively, with the great expectation to identify potential targets for therapeutic approaches and promising molecular biomarkers for cancer diagnosis and prognostic monitor.

Keywords: Cancer genetics, Drug development

25COASMA58:

Title: MDSC checkpoint blockade therapy: a new breakthrough point overcoming immunosuppression in cancer immunotherapy

Abdulrahman Ibrahim, Nada Mohamady Farouk Abdalsalam et.al.

Cancer Gene Therapy volume 32, pages371–392 (2025)
https://doi.org/10.1038/s41417-025-00886-9

Abstract: Despite the success of cancer immunotherapy in treating hematologic malignancies, their efficacy in solid tumors remains limited due to the immunosuppressive tumor microenvironment (TME), which is mainly formed by myeloid-derived suppressor cells (MDSCs). MDSCs not only exert potent immunosuppressive effects that hinder the success of immune checkpoint inhibitors (ICIs) and adaptive cellular therapies, but they also promote tumor advancement through non-immunological pathways, including promoting angiogenesis, driving epithelial-mesenchymal transition (EMT), and contributing to the establishment of pre-metastatic environments. While targeting MDSCs alone or in combination with conventional therapies has shown limited success, emerging evidence suggests that MDSC checkpoint blockade in combination with other immunotherapies holds great promise in overcoming both immunological and non-immunological barriers. In this review, we discussed the dual roles of MDSCs, with a particular emphasis on their underexplored checkpoints blockade strategies. We discussed the rationale behind combination strategies, their potential advantages in overcoming MDSC-mediated immunosuppression, and the challenges associated with their development. Additionally, we highlight future research directions aimed at optimizing combination immunotherapies to enhance cancer therapeutic effectiveness, particularly in solid tumor therapies where MDSCs are highly prevalent.

Keyword: Tumour immunology.

25COASMA59:

Title: Therapeutic targeting of the tryptophan-kynurenine-aryl hydrocarbon receptor pathway with apigenin in MED12-mutant leiomyoma cells

Takashi Iizuka, Azna Zuberi, Helen Wei, et.al.

Cancer Gene Therapy volume 32, pages393–402 (2025)
https://doi.org/10.1038/s41417-025-00881-0

Abstract: Approximately 77.4% of uterine leiomyomas carry MED12 gene mutations (mut-MED12), which are specifically associated with strikingly upregulated expression and activity of the tryptophan 2,3-dioxygenase (TDO2) enzyme, leading to increased conversion of tryptophan to kynureine. Kynurenine increases leiomyoma cell survival by activating the aryl hydrocarbon receptor (AHR). We used a leiomyoma-relevant model, in which a MED12 Gly44 mutation was knocked in by CRISPR in a human uterine myometrial smooth muscle (UtSM) cell line, in addition to primary leiomyoma cells from 26 patients to ascertain the mechanisms responsible for therapeutic effects of apigenin, a natural compound. Apigenin treatment significantly decreased cell viability, inhibited cell cycle progression, and induced apoptosis preferentially in mut-MED12 versus wild-type primary leiomyoma and UtSM cells.

Apigenin not only blocked AHR action but also decreased TDO2 expression and kynurenine production, preferentially in mut-MED12 cells. Apigenin did not alter TDO2 enzyme activity. TNF and IL-1β, cytokines upregulated in leiomyoma, strikingly induced TDO2 expression levels via activating the NF-κB and JNK pathways, which were abolished by apigenin. Apigenin or a TDO2 inhibitor decreased UtSM cell viability induced by TNF/IL-1β. We provide proof-of-principle evidence that apigenin is a potential therapeutic agent for mut-MED12 leiomyomas.

Keyword: Cell biology, Oncogenes.

25COASMA60:

Title: Ferroptosis enhances the therapeutic potential of oncolytic adenoviruses KD01 against cancer

Wenhuan Li, Teng Ji, Jiaqi Ye et.al.

Cancer Gene Therapy volume 32, pages403–417 (2025)
https://doi.org/10.1038/s41417-025-00882-z

Abstract: Oncolytic virotherapy has emerged as a promising strategy for cancer treatment by selectively targeting and lysing tumor cells. However, its efficacy is often limited in certain tumor types due to multiple factors. This study explores the combination of oncolytic adenoviruses with Erastin, a potent ferroptosis inducer, to enhance antitumor efficacy in oncolytic virus-insensitive cancer cell lines. In vitro experiments demonstrated that Erastin significantly increased the cytotoxicity of oncolytic virotherapy, leading to greater inhibition of cell proliferation and elevated rates of cell death compared to monotherapies. The combination treatment further promoted ferroptosis, as evidenced by increased reactive oxygen species (ROS) levels, enhanced lipid peroxidation, and disrupted redox homeostasis. RNA sequencing identified the downregulation of Dickkopf-1 (DKK1) as a key mediator of the enhanced ferroptotic effect. Restoring the expression of DKK1 partially mitigated the cytotoxic effects of the combination therapy, highlighting its crucial role in mediating the enhanced ferroptosis-induced oncolytic virotherapy efficacy. In vivo studies further validated these findings, demonstrating that the combined treatment significantly reduced tumor growth without inducing notable toxicity. This novel therapeutic approach has great potential to enhance the efficacy of oncolytic virotherapy in cancers resistant to oncolytic viruses by inducing ferroptosis. Further investigation in clinically relevant models is warranted to fully elucidate the underlying mechanisms and to optimize this combination strategy for potential clinical applications.

Keyword: Tumour immunology

25COASMA61:

Title: Chimeric Ad5/35 oncolytic adenovirus overcome preexisting neutralizing antibodies and enhance tumor targeting efficiency

Zhoutong Dai, Yao Si, Shengfeng Xiong et.al.

Cancer Gene Therapy volume 32, pages418–436 (2025)
https://doi.org/10.1038/s41417-025-00884-x

Abstract: KD01, a third-generation conditionally replicating adenovirus serotype 5 developed by our team, has approved by the China Center for Drug Evaluation (CDE) for

Phase I clinical trials (NCT06552598). However, 60% seroprevalence of anti-Ad5 neutralizing antibodies is a major hurdle for Ad5-based oncolytic viruses. To address this issue, we developed oAd5/35-HF, a fourth-generation oncolytic adenovirus vector designed to enhance infection efficiency and evade pre-existing neutralizing antibodies (NABs). To achieve this, we introduced targeted capsid modifications, replacing hexon hypervariable regions (HVRs) 1 and 5 with those from adenovirus serotype 35 (Ad35), along with alterations to the fiber region. These combined modifications significantly improved infection efficiency, maintained high viral titers, and enabled the virus to resist NABs. This is the first report of replacing both the Ad5 hexon HVRs and fiber regions with those from Ad35 in an oncolytic adenovirus, resulting in potent antitumor activity across multiple cancer types, even in the presence of high NAB levels. The oAd5/35-HF backbone provides a versatile platform for developing new chimera oncolytic adenovirus and adenovirus vector-based vaccine.
Keyword: Cancer, Tumour immunology

25COASMA62:

Title: Targeted inactivation of EWSR1 : : FLI1 gene in Ewing sarcoma via CRISPR/Cas9 driven by an Ewing-specific GGAA promoter

Saint T. Cervera, Selene Martínez, María Iranzo-Martínez et.al.

Cancer Gene Therapy volume 32, pages437–449 (2025)
https://doi.org/10.1038/s41417-025-00887-8

Abstract: We have recently demonstrated that genetic inactivation of EWSR1 : : FLI1 by CRISPR/Cas9, successfully blocks cell proliferation in a cell model of Ewing sarcoma. However, CRISPR/Cas9-mediated gene editing can exhibit off-target effects, and thus, precise regulation of Cas9 expression in target cells is essential to develop gene-editing strategies to inactivate EWSR1 : : FLI1 in Ewing sarcoma cells. In this study, we demonstrate that Cas9 can be specifically expressed in Ewing sarcoma cells when located downstream a promoter consisting of GGAA repeats and a consensus TATA box (GGAAprom). Under these conditions, Cas9 is selectively expressed in Ewing sarcoma cells that express EWSR1 : FLI1 oncoproteins, but not in cells expressing wild-type FLI1. Consequently, Ewing sarcoma cells infected with GGAAprom>Cas9 and a specific gRNA designed to inactivate EWSR1 : : FLI1, showed successful EWSR1 : : FLI1 inactivation and the subsequent blockade of cell proliferation. Notably, GGAAprom>Cas9 can be efficiently delivered to Ewing sarcoma cells via adenoviral vectors both in vitro and in vivo, highlighting the potential of this approach for Ewing sarcoma treatment. Our results demonstrate that the CRISPR/Cas9 machinery is safe and specific for Ewing sarcoma cells when driven under a GGAAprom, paving the way for the development of cancer gene therapies based on the selective expression of genes with therapeutic potential.
Keyword: Paediatric cancer, Sarcoma, Targeted therapies

25COASMA63:

Title: IER3: exploring its dual function as an oncogene and tumor suppressor

Meena Kanduri, Santhilal Subhash, Rossana Putino et.al.

Cancer Gene Therapy volume 32, pages450–463 (2025)
https://doi.org/10.1038/s41417-025-00891-y

Abstract: The IER3 gene has a complex role in cancer biology, acting either as a tumor suppressor or an oncogene, depending on the cancer type. This duality underscores the complexity and importance of molecular pathways in modulating cancer behavior. Despite its significance in cancer development, there is a dearth of studies elucidating the exact mechanisms underlying IER3's involvement in modulating cancer behavior. Here, utilizing cervical carcinoma and neuroblastoma (NB) cell lines as model systems we characterized the pathways that mediate the functional switch between the oncogenic and tumor suppressor roles of IER3. In HeLa cells, IER3 expression promotes an oncogenic program that includes immediate early response pathway genes such as EGR2, FOS, and JUN. However, in NB cells, IER3 suppresses the EGR2-dependent oncogenic program. This differential regulation of EGR2 by IER3 involves epigenetic modulation of the EGR2 promoter. IER3 dependent tumor suppressor pathway in NB cells relies on ADAM19 gene. Thus, our findings uncover the molecular pathways that dictate the context-dependent roles of IER3 in cancer, providing insights into its dual functionality in different cancer types.
Keyword: Cancer genetics, Oncogenes.

25COASMA64:

Title: BAIAP2L2 facilitates hepatocellular carcinoma progression and immune evasion of via targeting JAK1-mediated pathway and PD-L1 expression

Zhiyue Xie, Yanxia Wu, Nan Peng et.al.

Cancer Gene Therapy volume 32, pages464–474 (2025)
https://doi.org/10.1038/s41417-025-00890-z

Abstract: Hepatocellular carcinoma (HCC) poses a serious threat to human health due to its high mortality rate. Recently, breakthrough progress has been made in immunotherapy field. However, the mechanisms underlying HCC progression and immune escape are still unclear. This study aimed to investigate the impact of brain-specific angiogenesis inhibitor 1-associated protein 2-like 2 (BAIAP2L2) in HCC and elucidate its potential mechanisms in this context. Clinical data revealed that the overexpression of BAIAP2L2 correlated with tumor progression and poor prognosis in HCC patients. Functional assays demonstrated that BAIAP2L2 facilitates HCC proliferation, metastasis, invasion, and PD-L1-mediated immune evasion both in vitro and in vivo. Mechanistically, we observed co-localization and interaction between BAIAP2L2 and JAK1 within HCC cells, in turn enhancing the activation of the JAK1/STAT3 signaling pathway. Utilizing the JAK1 inhibitor Ruxolitinib effectively reversed BAIAP2L2-induced cellular processes such as proliferation, migration, invasion, and PD-L1 upregulation. Overall, our results emphasize that BAIAP2L2 plays a crucial role in driving tumor progression and immune evasion in HCC through the JAK1-mediated signaling pathway, thus proposing BAIAP2L2 as a promising therapeutic target for HCC treatment.
Keyword: Liver cancer, Targeted therapies

25COASMA65:

Title: Pbx3-mediated suppression of type I interferon response contributes to leukemia progression driven by MLL-AF9

Li Tang, Meng Lu, Yulong Du & Jianlong Sun et.al.

Cancer Gene Therapy volume 32, pages475–485 (2025)
https://doi.org/10.1038/s41417-025-00888-7

Abstract: Cell-intrinsic repression of inflammatory signaling supports the survival of acute myeloid leukemia blasts. However, how the cell-intrinsic inflammation status changes during AML progression remains elusive. Here, we used CRISPR-mediated genome editing to create a murine AML model driven by a chromosomal translocation between the mixed-lineage leukemia (Mll) gene and the Mllt3/Af9 gene. The resulting MLL-AF9 (MA9) fusion protein is sufficient to immortalize hematopoietic stem and progenitor cells (HSPCs) in vitro but insufficient to induce an overt leukemia phenotype in vivo rapidly. Leukemia progression in vivo is associated with a downregulation of type I interferon response genes, and this process depends on the upregulation of MA9 transcriptional target Pbx3 in the progenitor cell compartment. Accordingly, enhancing interferon response by interferon-α (IFNα) administration induces leukemic cell differentiation, and inhibiting MA9 transcriptional activity on top of the enhanced IFN signaling further delays leukemia progression. Our study underscores the importance of Pbx3-mediated suppression of interferon response genes in the progression of MA9-induced AML and highlights the potential application of type I interferon for its treatment.

Keyword: Leukaemia, Tumour immunology

25COASMA66:

Title: Therapeutic potential of synthetic microRNA mimics based on the miR-15/107 consensus sequence

Glen Reid, Marissa Williams, Yuen Yee Cheng, et.al.

Cancer Gene Therapy volume 32, pages486–496 (2025)
https://doi.org/10.1038/s41417-025-00885-w

Abstract: MicroRNA expression is frequently suppressed in cancer, and previously we demonstrated coordinate downregulation of multiple related microRNAs of the miR-15/107 group in malignant pleural mesothelioma (PM). From an alignment of the miR-15 family and the related miR-103/107, we derived a consensus sequence and used this to generate synthetic mimics. The synthetic mimics displayed tumour suppressor activity in PM cells in vitro, which was greater than that of a mimic based on the native miR-16 sequence. These mimics were also growth inhibitory in cells from non-small cell lung (NSCLC), prostate, breast and colorectal cancer, and sensitised all cell lines to the chemotherapeutic drug gemcitabine. The increased activity corresponded to enhanced inhibition of the expression of target genes and was associated with an increase in predicted binding to target sites, and proteomic analysis revealed a strong effect on proteins involved in RNA and DNA processes. Applying the novel consensus mimics to xenograft models of PM and NSCLC in vivo using EGFR-targeted nanocells loaded with mimic led to tumour growth inhibition. These results suggest that mimics based on the consensus sequence of the miR-15/107 group have therapeutic potential in a range of cancer types.

Keyword: Gene delivery, Mesothelioma, Non-small-cell lung cancer

25COASMA67:

Title: Natural trajectory subclasses of cognitive impairment in breast cancer patients

experiencing insomnia

Oxana Palesh PhD, MPH, Sarah E. Braun PhD, LCP, Tina Truong BS et.al.

Cancer, Volume131, Issue8, 15 April 2025,e35816
https://doi.org/10.1002/cncr.35816

Abstract: BackgroundCancer-related cognitive impairment (CRCI) has traditionally been assessed in a dichotomous manner. Identifying subclasses of CRCI and novel biomarkers can improve the accuracy of identifying patients most at risk for CRCI.MethodsA total of 139 breast cancer patients undergoing chemotherapy completed neurocognitive batteries over 12 months. Growth mixture modeling (GMM) was used to determine latent subgroups based on different trajectories of cognitive test performance across the four time points. Additionally, the authors collected peripheral blood to measure neuron-derived exosomes (NDE).ResultsMean cognitive performance improved significantly over time ($p < .001$). However, GMM identified three distinct latent subgroups: patients with stable, high performance (class 1, N = 45), patients with variable low performance (class 2, N = 15), and patients with average performance who improved over time (class 3, N = 79). Cognitive subclass 2 was characterized by significantly lower education levels than the other two classes ($p = .001$). Cognitive subclass 1 had fewer racial/ethnic minority patients than the other two classes ($p = .015$). Cognitive subclasses did not differ significantly in any other demographic or clinical characteristic. There were no significant differences observed by NDE.ConclusionsThere are multiple distinct longitudinal trajectories of CRCI and these may be influenced by social determinants of health such as education and race/ethnicity. Future research can focus on ways to administer interventions earlier to those at most risk for CRCI and continue to explore novel biomarkers of CRCI.

25COASMA68:

Title: Multilevel mortality risk factors among pediatric hematology-oncology patients with deterioration

Asya Agulnik MD, MPH, Maricela Robles-Murguia MS et.al.

Cancer, Volume131, Issue8, 15 April 2025, e35818
https://doi.org/10.1002/cncr.35818

Abstract: Background Hospitalized pediatric hematology-oncology patients have frequent clinical deterioration events (CDEs) requiring intensive care unit (ICU) interventions and resulting in high mortality, particularly in resource-limited settings. This study identifies independent risk factors for CDE mortality in hospitals providing childhood cancer care in Latin America and Spain.MethodsCenters implemented a prospective CDE registry, defined as unplanned transfer to a higher level of care, use of ICU-level interventions on the ward, or nonpalliative ward death. The authors analyzed registry data from April 2017 to December 2022. The primary outcome was CDEs mortality, defined as death occurring during ICU admission, <24 hours of ICU discharge, or end of ward-based ICU interventions. Multilevel modeling identified event-, patient-, and hospital-level independent risk factors for CDE mortality.ResultsAmong 69 participating hospitals in 18 countries, 4134 CDEs were reported in 3319 pediatric hematology-oncology patients with an event mortality of 26.8% (1108 events). Of all CDEs, 33.7% used ICU interventions on the ward and 87.5% were transferred to a higher level of care. In multilevel modeling, significant independent risk factors for event

mortality present at the start of deterioration included patient (disease relapse) and event (e.g., reason for hospital admission, use of ICU intervention on wards, abnormal lactate, platelets, or C-reactive protein, reason for deterioration, and number of organs with dysfunction); hospital factors were not significant predictors of mortality.Conclusions Hospitalized pediatric hematology-oncology patients with CDE have high mortality with significant variability across centers. Mortality, however, is largely driven by modifiable event-level factors, demonstrating the need for targeted interventions to improve survival.

25COASMA69:

Title: Olverembatinib in chronic myeloid leukemia—Review of historical development, current status, and future research

Hagop Kantarjian MD, Yifan Zhai MD, PhD, Vivian G. Oehler MD et.al.

Cancer, Volume131, Issue8, 15 April 2025, e35832
https://doi.org/10.1002/cncr.35832

Abstract: Once considered an incurable disease with a poor prognosis (median survival, 3–6 years), chronic myeloid leukemia (CML) is now managed with a diverse clinical armamentarium that includes BCR::ABL1 tyrosine kinase inhibitors (TKIs), which have largely normalized life expectancy in most patients in the chronic phase of the disease (CML-CP). Clinical challenges remain, including ABL1 mutation–driven treatment resistance (under the selection pressures exerted by TKIs), as well as treatment intolerance, which can involve potentially serious arterial occlusive events. Olverembatinib is a third-generation TKI approved in China for TKI-resistant CML-CP and accelerated-phase CML with the T135I mutation, as well as for CML-CP resistant to or intolerant of first- and/or second-generation TKIs. Olverembatinib exhibits a broad coverage of ABL1 mutants, including the gatekeeper T315I variant and compound mutations. In preclinical models, olverembatinib inhibited multiple downstream protein kinases, which has potentially opened avenues for future management of other malignancies, including acute myeloid and lymphoid leukemias, gastrointestinal tumors, and others. The pharmacokinetic profile of olverembatinib is compatible with alternate-day dosing. In clinical trials, olverembatinib exerted potent antileukemic effects in heavily pretreated patients with CML, including those with ponatinib or asciminib resistance or intolerance, and was well tolerated. Future studies include the phase 3 registrational POLARIS-1 (NCT06051409; in patients with newly diagnosed Philadelphia chromosome–positive acute lymphoblastic leukemia), POLARIS-2 (NCT06423911; in patients with CML with or without the T315I mutation), and POLARIS-3 (NCT06640361; in patients with succinate dehydrogenase–deficient gastrointestinal stromal tumors) clinical trials.

25COASMA70:

Title: Associations between experiences of discrimination and quality of life in Black breast cancer survivors

Nur Zeinomar PhD MPH, Marley Perlstein MS, Bo Qin PhD, et.al.

Cancer, Volume131, Issue8, 15 April 2025
https://doi.org/10.1002/cncr.35836

Abstract: BackgroundRacial discrimination has been associated with decreased health-

related quality of life (QOL) in the general population; however, its impact on QOL in cancer survivors is unclear. This study aims to examine how experiences of discrimination (EOD) impact QOL in breast cancer survivors and whether these associations vary by individual- and structural-level factors.MethodsThe association of EOD assessed at baseline (~12 months post-diagnosis) was assessed in the Women's Circle of Health Follow-up Study, a population-based longitudinal cohort study of Black breast cancer survivors in New Jersey. QOL was assessed at follow-up (~24 months postdiagnosis) using the Functional Assessment of Cancer Therapy – Breast (FACT-B). Multivariable linear regression models adjusted for confounders assessed the association of EOD (none, low, high) with QOL. We also examined statistical interaction by individual-level factors (coping and spirituality) and structural-level factors (neighborhood socioeconomic status and residential segregation).ResultsOf 216 study participants, 74% reported experiencing discrimination. In fully adjusted models, women with high EOD had lower overall QOL (no discrimination, mean FACT-B: 114.8; 95% CI, 107.9–121.7; high discrimination, mean FACT-B: 101.1; 95% CI, 94.2–108.0). Although no evidence was observed of statistically significant interaction, women with high spirituality had better overall QOL, regardless of EOD (high spirituality/low discrimination: 128.2; 95% CI, 121.9–134.5; high spirituality/high discrimination: 115.4; 95% CI, 108.5–122.3; low spirituality/no discrimination: 103.5; 95% CI, 93.8–113.2).Conclusions Among Black breast cancer survivors, discrimination was associated with poorer QOL. Spirituality may mitigate the harmful effects, as women with high spirituality, even in the context of high discrimination, reported higher QOL.

25COASMA71:

Title: Cladribine, idarubicin, and cytarabine (CLIA) for patients with relapsed and/or refractory acute myeloid leukemia: A single-center, single-arm, phase 2 trial

Hannah Goulart MD, Hagop Kantarjian MD, Gautam Borthakur MD et.al.

Cancer, Volume131, Issue8, 15 April 2025

https://doi.org/10.1002/cncr.35840

Abstract: The treatment of relapsed and/or refractory (R/R) acute myeloid leukemia (AML) remains challenging because of poor responses to chemotherapy. Efforts to improve outcomes have included the use of high-dose cytarabine in combination with nucleoside analogs, such as cladribine. The authors evaluated combined cladribine, idarubicin, and cytarabine (CLIA) in a phase 2 trial of 66 patients with R/R AML.Methods Patients received induction with cladribine 5 mg/m2 intravenously (days 1–5), cytarabine 1000 mg/m2 intravenously (days 1–5), and idarubicin 10 mg/m2 intravenously (days 1–3; CLIA). Sorafenib 400 mg twice daily (days 1–14) was added for FLT3-mutated AML.Results The composite response rate (complete remission [CR] plus complete remission with incomplete hematologic recovery [CRi]) was 33%; salvage 1 (S1) patients (n = 35) had a CR/CRi rate of 49%. After a 61-month median follow-up, the median overall survival (OS) was 7.9 months, with a median relapse-free survival (RFS) of 9.1 months for those in CR/CRi. The median OS for S1 patients was 12 months, with a median RFS of 10.3 months. For those who received CLIA with sorafenib (n = 22), the CR/CRi rate was 41%, median OS was 8.8 months, and median RFS was 3.8 months. Landmark analysis demonstrated superior OS for patients who proceeded to transplantation compared with patients who did not (median OS,

78 vs. 8.8 months, respectively; p < .001). The 4-week and 8-week mortality rates were 6% and 17%, respectively. Most grade >3 adverse events were related to infection and elevated liver function tests.Conclusions CLIA is effective for patients with R/R AML and offers a safety profile similar to that of other intensive regimens (ClinicalTrials.gov identifier NCT02115295).

25COASMA72:

Title: In vitro fertilization with cryopreserved oocytes or embryos after cancer: The role of gestational carriers

Taylor D. Ellington MPH, Alexis C. Wardell MS, Allison M. Deal MS et.al.

Cancer, Volume131, Issue8, 15 April 2025
https://doi.org/10.1002/cncr.35844

Abstract: Background: Fertility preservation counseling is recommended for reproductive-age cancer patients. Gestational carriers are individuals who carry a pregnancy for someone else. This service creates a path to biological children when cancer treatment necessitates the removal of the uterus. The authors examined the involvement of gestational carriers among women diagnosed with cancer.Methods Using data from eight statewide cancer registries linked with the Society for Assisted Reproductive Technology Clinic Outcomes Reporting System, the authors identified women with a cancer diagnosis who subsequently initiated in vitro fertilization (IVF) procedures during 2004 to 2018. Modified Poisson models were used to estimate prevalence ratios (PR) and 95% confidence intervals (CI). Discrete Cox regression models were used to calculate hazard ratios (HR) and CI. Multivariable models adjusted for age, state, and calendar year.Results Among 1095 women with cancer who used IVF with cryopreserved oocytes or embryos to attempt pregnancy, 19.1% worked with a gestational carrier. Involving gestational carriers was more common among those who initiated IVF for fertility preservation versus after cancer treatment (PR, 1.96; 95% CI, 1.54–2.50) and had chemotherapy versus no chemotherapy (PR, 1.92; 95% CI, 1.50–2.47). Using donor oocytes or embryos (vs. autologous) was more common among women who worked with a gestational carrier (PR, 1.62; 95% CI, 1.17–2.24). Working with a gestational carrier was not associated with conception (HR, 1.06; 95% CI, 0.82–1.37).Conclusions Approximately one in five women diagnosed with cancer who used IVF to attempt pregnancy worked with a gestational carrier. The results of this study emphasize the need for information on gestational carriers during fertility preservation counseling.

25COASMA73:

Title: Real-world treatment patterns and outcomes with oral azacitidine maintenance therapy in patients with acute myeloid leukemia

Brian Leber MD, Marcia T. Ruiz PhD, Hany Elgendy MD, et.al.

Cancer, Volume131, Issue8 , 15 April 2025
https://doi.org/10.1002/cncr.35845

Abstract: Introduction This study describes baseline and clinical characteristics, treatment patterns, survival, and safety outcomes of patients with acute myeloid leukemia (AML) who received oral azacitidine (oral-AZA) maintenance therapy in Canada following its approval in 2021.Methods A retrospective, observational medical record review was conducted of

patients with AML in remission after induction therapy and who initiated treatment with oral-AZA between March 2021 and July 2023 in Canada. Real-world relapse-free survival and overall survival outcomes were estimated using Kaplan–Meier methodology.Results Data from 119 patients were analyzed. The median age at oral-AZA initiation was 62.5 years. Most patients had favorable (39.5%) or intermediate (39.5%) genetic risk per the 2017/2022 European LeukemiaNet classification. Nearly all patients (99.2%) received cytarabine-based induction regimens. A total of 55.5% of patients received consolidation therapy, with a median of two cycles. After a median follow-up of 9.4 months, 68.1% of all patients were still receiving oral-AZA at last follow-up. After oral-AZA treatment, 21.0% of patients relapsed. Rates of real-world relapse-free survival and overall survival at 12 months from oral-AZA initiation were 66.9% and 74.5%, respectively. During oral-AZA treatment, 67.2% of patients experienced ≥1 adverse event. Concomitant antiemetic treatment was received by 78.2% of patients.Conclusion These findings provide real-world evidence further supporting the use of oral-AZA as a standard-of-care maintenance therapy in current routine clinical practice for patients with AML in remission who do not receive hematopoietic stem cell transplantation. These results may inform a broader clinical audience because of the inclusion of patients with diverse demographic and clinical characteristics.

25COASMA74:

Title: Characteristics and clinical outcomes of patients with myeloid malignancies and cohesin mutations

Maria R. Khouri MD, Bofei Wang PhD, Laurie K. Pearson MD et.al.

Cancer, Volume131, Issue8, 15 April 2025

Abstract: Background The prognostic impact of cohesin mutations in patients with acute myeloid leukemia (AML) and myelodysplastic syndromes (MDS) is controversial.Methods In patients with AML and MDS who underwent next-generation sequencing at the authors' center during 2017–2023, the authors assessed the landscape of cohesin mutations and the impact of co-occurring mutations on overall survival (OS) and compared outcomes between patients with cohesin mutations and those with wild-type (WT) cohesin genes.Results The study included 83 patients, 36 with cohesin mutations (STAG2, n = 28; SMC1A, n = 7; SMC3, n = 3; co-expression of cohesin mutations, n = 2) and 47 with WT cohesin genes. Of the 36 patients with cohesin mutations, 17 (47%) had AML (six de novo and 11 secondary), and 19 (53%) had MDS. Patients who had STAG2 mutations had better median OS than patients who had only SMC1A and SMC3 mutations (26 vs. 10 months; p = .043). SRSF2 mutation was the most frequent co-occurring mutation (n = 12; 33%) and was associated with worse median OS than WT SRSF2 (13 vs. 43 months; p = .016). Seven patients (19%) with cohesin mutations underwent hematopoietic transplantation; their median OS was 70 months. Compared with the WT cohesin group, patients who had cohesin mutations were more likely to have adverse-risk AML (82% vs. 53%). The median OS was similar among patients with adverse-risk AML in the cohesin-mutation and WT cohesin groups (10 vs. 14 months, respectively; p = .9).Conclusions The current study provides insight into the prognostic impact of cohesin mutations and co-occurring mutations in patients with myeloid malignancies.

25COASMA75:

Title: Contemporary neighborhood redlining and racial mortgage lending bias and disparities in prostate cancer survival

Wayne R. Lawrence DrPH, Neal D. Freedman PhD, Jennifer K. McGee-Avila et.al.

Cancer, Volume131, Issue8, 15 April 2025
https://doi.org/10.1002/cncr.35850

Abstract: Background Mortgage lending bias is a critical driver of residential segregation, and may contribute to disparities in cancer survival. This study investigated the association between contemporary redlining and racial lending bias and prostate cancer survival.Methods This cohort study used a Surveillance, Epidemiology, and End Results–Medicare database that included 34,163 Black and White men diagnosed with prostate cancer between 2010 and 2013. Home Mortgage Disclosure Act data were used to calculate the census-tract redlining index (the systematic denial of mortgages based on property location) and racial lending bias index (the systematic denial of a mortgage application for a Black applicant compared with a White applicant in the local area). Both indices were assessed continuously and categorically (low, moderate, or high). Multivariable-adjusted Cox models were used to estimate hazard ratios (HRs) for prostate cancer–specific and all-cause mortality.Results Overall, as the redlining index increased, men experienced poorer prostate cancer survival. Compared to men residing in low-redlined neighborhoods, those in high-redlined neighborhoods had an increased risk of prostate cancer–specific mortality (HR, 1.21; 95% confidence interval [CI], 1.03–1.42) and all-cause mortality (HR, 1.25; 95% CI, 1.17–1.34). Similar results were observed for redlining in a race-stratified analysis among Black and White men. Among White men, compared with those residing in low racial lending bias neighborhoods, those in high racial lending bias neighborhoods had an increased all-cause mortality risk (HR, 1.11; 95% CI, 1.03–1.21).Conclusions Contemporary redlining was associated with poorer prostate cancer survival in the overall population. However, an association between racial lending bias and elevated mortality was only observed among White men. Findings suggest that mortgage lending discrimination may contribute to disparities in prostate cancer survival.

25COASMA76:

Title: Evaluating the impact of hurricanes and the COVID-19 pandemic on colorectal cancer incidence in Puerto Rico: An interrupted time-series analysis

Tonatiuh Suárez-Ramos MS, Samantha Verganza MPH, Yisel Pagán-Santana DrPH, et.al.

Cancer, Volume131, Issue8, 15 April 2025
https://doi.org/10.1002/cncr.35793

Abstract: Background Major events, such as Hurricanes Irma and Maria and the coronavirus disease 2019 (COVID-19) pandemic disrupted Puerto Rico's health system. Lack of access to colorectal cancer (CRC) screening services may have impeded timely diagnosis. The authors examined the impact of these events on CRC incidence in Puerto Rico.Methods The Puerto Rico Central Cancer Registry database allowed the authors to obtain CRC cases from 2012 to 2021. An interrupted time-series analysis was performed to examine changes in CRC incidence immediately after and during the periods after the hurricanes and the pandemic. Analysis periods included: pre-hurricanes, post-hurricanes, and post-COVID-19 lockdown restrictions.Results We observed a level change of −8.3 CRC cases was observed in the

month the hurricanes struck Puerto Rico, corresponding to an immediate decrease of 17.5%. After a slight upward trend, a second decline of 39.4 CRC cases was estimated after the COVID-19 lockdown restrictions, representing an immediate change of −24.2%. By the end of the study, the estimated numbers of patients with early stage CRC patients and those aged 50–75 years did not reach the expected numbers. In addition, CRC cases in patients with late-stage disease and in those aged younger than 50 years and aged 76 years and older exceeded the expected numbers.Conclusions Hurricanes Irma and Maria and the COVID-19 pandemic caused a decrease in CRC incidence in Puerto Rico. This analysis suggests that limited access to CRC screening services during these events likely hindered CRC diagnoses. To fully understand the long-term effects, monitoring of CRC trends will be necessary in the coming years.

25COASMA77:

Title: Ovarian juvenile granulosa cell tumor: A report from the International Ovarian and Testicular Stromal Tumor and International Pleuropulmonary Blastoma/DICER1 Registries

Anne K. Harris MPH, Alexander T. Nelson MD, Dave Watson PhD et.al.

Cancer, Volume131, Issue9, 1 May 2025
https://doi.org/10.1002/cncr.35862

Abstract : Background Ovarian juvenile granulosa cell tumors (juvGCT) are rare sex cord-stromal tumors that occur primarily in children and adolescents. This study summarizes the clinical presentation and outcomes of patients with juvGCT. Methods Patients were enrolled in the International Ovarian and Testicular Stromal Tumor and/or International Pleuropulmonary Blastoma/DICER1 Registries. Available medical records were abstracted, and pathology was centrally reviewed. Surgical staging was classified using the 2014 International Federation of Gynecology and Obstetrics (FIGO) criteria. Results In total, 70 patients with juvGCT enrolled and were diagnosed between 2001 and 2024; most patients (81%, 57 of 70) presented with FIGO stage I disease. Adjuvant chemotherapy was given in 30% (21 of 70); all regimens were platinum-based. Three-year event-free survival among patients with stage IA tumors was 80.2% (95% confidence interval [CI], 62.4%–100.0%), IC1 was 87.4 (95% CI, 72.4%–100.0%), IC2-IC3 was 63.6% (95% CI, 40.7%–99.5%), and II-IV was 48% (95% CI, 24.6%–93.8%). Of the patients with recurrent juvGCT with known mitotic index (MI), all had MI greater than 19 mitoses per 10 high power fields (HPF) at diagnosis.Conclusion Outcomes were worse for patients with FIGO stage ≥IC2 disease and for tumors with >19 mitoses per 10 HPF. Given the prognostic significance of MI, the authors strongly recommend the assessment of MI for all juvGCTs. More information about tumor biology is critical to identify which patients may benefit from adjuvant chemotherapy and to facilitate the development of novel therapies.

25COASMA78:

Title: Recent advances in gynecologic radiation oncology

Christina C. Huang MD, MS, Diandra N. Ayala-Peacock MD, Sarah J. Stephens MD, Junzo P. Chino MD et.al.

Cancer, Volume131, Issue9 , 1 May 2025

https://doi.org/10.1002/cncr.35888

Abstract : Significant advances have been made in the treatment of patients with gynecologic malignancies in the past few years. Integration of molecular testing in endometrial cancer now allows for more accurate risk stratification and personalized treatment recommendations for patients, with PORTEC-4a investigating outcomes after treatment de-escalation based on molecular subgroup. In several clinical trials, mismatch repair-deficiency (MMR-d) status has been proven to be a strong predictor for response to immunotherapy in the advanced/metastatic setting, and the role of immunotherapy in early-stage endometrial cancer is now being investigated. For patients with locally advanced cervical cancer, results from INTERLACE demonstrate that induction chemotherapy is now a viable treatment option, and KEYNOTE A-18 shows promise for the addition of concurrent and maintenance pembrolizumab to chemoradiation. Meanwhile, EMBRACE 1 and 2 have demonstrated the benefits of high-quality image guided brachytherapy, providing patients with locally advanced cervical cancer excellent control with improved toxicity. For patients with vulvar cancer, GOG279 demonstrated that addition of multi-agent chemotherapy with intensity modulated radiation therapy resulted in high rates of complete pathologic response, and GROINS-V III is currently investigating the role of chemotherapy and nodal radiation for patients with macrometastases on sentinel lymph node biopsy. This work summarizes the findings of recent landmark trials in endometrial, cervical, and vulvar cancer and their implications for the radiation oncologist.

25COASMA79:

Title: Annual Report to the Nation on the Status of Cancer, featuring state-level statistics after the onset of the COVID-19 pandemic

Recinda L. Sherman MPH, PhD, ODS-C, Albert U. Firth BS, S. Jane Henley MSPH, Rebecca L. Siegel MPH, et.al.

Cancer, Volume131, Issue9, 1 May 2025
https://doi.org/10.1002/cncr.35833

ABSTRACT: Background This report represents a collaborative effort by the major cancer surveillance organizations to present the definitive US statistics for cancer incidence and mortality. Methods Cancer incidence data were obtained from population-based cancer registries funded by the Centers for Disease Control and Prevention and the National Cancer Institute and compiled by the North American Association of Central Cancer Registries. Cancer death data were obtained from the National Center for Health Statistics' National Vital Statistics System. Statistics are reported by cancer type, sex, race and ethnicity, and age. The potential impact of the coronavirus disease 2019 (COVID-19) pandemic on incidence was assessed by using state-level changes compared with previous years, the stringency of COVID-19 policy restrictions, the magnitude of COVID-19 death rates, and changes in the use of mammography. Results Overall cancer incidence rates per 100,000 were 500 among males and 437 among females. Excluding 2020, cancer incidence rates remained stable (2013–2021) among males and increased 0.3% per year on average (2003–2021) among females. The overall cancer death rate per 100,000 was 173 among males and 126 among females. Cancer death rates decreased by 1.5% per year (2018–2022), slowing from a previous 2.1% decline. Cancer incidence in 2020 declined from prepandemic levels for all

demographic groups examined. However, the magnitude of decline was not strongly associated with the study's proxies for health care capacity, health care access, or COVID-19 policies. Conclusions Overall cancer mortality declined over 20 years, even during the COVID-19 pandemic. Disruptions in health care use early in the pandemic resulted in incidence declines in 2020, but 2021 incidence returned to prepandemic levels.

25COASMA80:

Title: Gender equity gap persists, addressing the root cause through the lens of gynecologic oncology: An evidenced-based review

Jasmine Ebott MD, Kelsea R. Grant MD, John Farley MD et.al.

Cancer, Volume131, Issue9, 1 May 2025

https://doi.org/10.1002/cncr.35843

Abstract: Many studies have addressed the inequities of gender within medicine. And although more attention has been brought to this topic in the past couple of decades, studies demonstrate that there is an equity gap in the workplace, in the research sphere, and in pay compensation. Internet searches prove that leadership in academic spaces as well as private practice both remain predominantly male. As an example, the field of gynecologic oncology is a field that specifically addresses and serves the health needs of patients who identify as women. However, although the specialty should be at the forefront of the effort to address gender inequities, it still has considerable progress to make in this area. This article seeks to describe the literature regarding gender disparities in medicine, and what gender equity can look like while laying out strategies to address the inequities that persist – using gynecologic oncology as an example.

25COASMA81:

Title: Implementing artificial intelligence in breast cancer screening: Women's preferences

Alison Pearce BAppSci(OT), MPH, PhD, Stacy Carter BAppSci, MPH(Hons), PhD, Helen ML Frazer et.al.

Cancer, Volume131, Issue9, 1 May 2025

https://doi.org/10.1002/cncr.35859

Abstract: Background Artificial intelligence (AI) could improve accuracy and efficiency of breast cancer screening. However, many women distrust AI in health care, potentially jeopardizing breast cancer screening participation rates. The aim was to quantify community preferences for models of AI implementation within breast cancer screening. Methods An online discrete choice experiment survey of people eligible for breast cancer screening aged 40 to 74 years in Australia. Respondents answered 10 questions where they chose between two screening options created by an experimental design. Each screening option described the role of AI (supplementing current practice, replacing one radiologist, replacing both radiologists, or triaging), and the AI accuracy, ownership, representativeness, privacy, and waiting time. Analysis included conditional and latent class models, willingness-to-pay, and predicted screening uptake. Results The 802 participants preferred screening where AI was more accurate, Australian owned, more representative and had shorter waiting time for results (all $p < .001$). There were strong preferences ($p < .001$) against AI alone or as triage. Three

patterns of preferences emerged: positive about AI if accuracy improves (40% of sample), strongly against AI (42%), and concerned about AI (18%). Participants were willing to accept AI replacing one human reader if their results were available 10 days faster than current practice but would need results 21 days faster for AI as triage. Implementing AI inconsistent with community preferences could reduce participation by up to 22%.

25COASMA82:

Title: Testicular and ovarian Juvenile granulosa cell tumors in children and adolescents: Analysis of 113 patients registered to the German Registry for Rare Pediatric Tumors (STEP)

Dominik T. Schneider MD, PhD, Andrea Witowski MD, Michael Abele MD, Martin Benesch MD et.al.

Cancer, Volume131, Issue9, 1 May 2025
https://doi.org/10.1002/cncr.35861

Abstract: Background In juvenile granulosa cell tumors (juvGCTs), impaired survival was reported after preoperative tumor rupture, peritoneal metastases, or high mitotic rate (≥20 mitoses per 10 high-power fields). Therefore, a risk stratification was developed to select patients for chemotherapy. Methods Between 2001 and 2019, 89 female patients and 24 male patients were prospectively enrolled. Histopathologic classification was according to the World Health Organization classification, and staging was according to Children's Oncology Group and International Federation of Gynecology and Obstetrics classification.Results Testicular juvGCTs were detected as scrotal swelling during infancy. No recurrences were reported after orchiectomy. Patients with ovarian juvGCTs presented at a median age of 9.8 years with abdominal discomfort, isosexual precocity, or amenorrhea. After tumor resection, two of 52 patients with stage IA disease, one of 14 with stage IC1 disease (intraoperative rupture), 13 of 18 with stage IC2 or IC3 disease (preoperative rupture), and all five patients with stage II/III disease received chemotherapy. Four recurrences with two deaths were reported. Three recurrent tumors were initially stage IA with a high mitotic rate, and one was a stage II tumor. No recurrences were observed among patients who had stage IC2/IC3 disease, who had unfavorable prognoses in historical cohorts. The 5-year event-free survival was 0.95 ± 0.03 (85 of 89 patients), and overall survival was 0.97 ± 0.02 (87 of 89 patients).Conclusions Testicular and ovarian juvGCTs are clinically distinct entities. Although testicular juvGCTs exclusively present during infancy and have an excellent prognosis, ovarian juvGCTs may arise at any age and constitute potentially aggressive tumors. Centralized reference diagnostics and the establishment of counseling structures for the treatment of patients with ovarian juvGCTs improved prognosis compared with historical groups. The mitotic rate and incomplete surgery were identified as important risk factors in addition to tumor stage and should be considered in the risk-stratification of therapy.

25COASMA83:

Title: Impact of neighborhood archetypes on overall mortality among young patients with acute leukemia in California

Lena E. Winestone MD, MSHP, Juan Yang MS, Tanushree Banerjee PhD et.al.

Cancer, Volume131, Issue9, 1 May 2025

https://doi.org/10.1002/cncr.35863

Abstract: Introduction Residence in lower socioeconomic neighborhoods is associated with lower survival in children, adolescents, and young adults with leukemia. We sought to evaluate the impact of neighborhood archetypes on acute lymphoblastic leukemia (ALL) and acute myeloid leukemia (AML) survival.Methods Patients aged 0 to 39 years diagnosed with ALL or AML from 2006 through 2016 in the California Cancer Registry were included. Nine-class neighborhood archetypes, generated by latent class analysis of 39 social and built environment attributes at the census tract level, were the primary exposure of interest. Cox proportional hazards models were used for statistical analyses, stratified by age. Results Among 8776 patients, 72% had ALL and 28% had AML. For ALL, increased risk of mortality was observed in mixed socioeconomic status suburbs (adjusted hazard ratio, 1.39; 95% CI, 1.06–1.84) and Hispanic small towns (adjusted hazard ratio, 1.33; 95% CI, 1.03–1.84) relative to upper middle-class suburbs. For AML, neighborhood archetypes were not associated with mortality. When stratified by age, we observed associations between neighborhood archetypes (mixed socioeconomic status class suburb, inner city, Hispanic small towns) and mortality in pediatric but not young adult ALL patients. Conclusions Our findings demonstrate that neighborhood archetypes efficiently account for complex interactions across social and built environment attributes with leukemia survival. The greater effects of neighborhood archetype in pediatric ALL survival, as compared to AML, may be related to the prolonged, outpatient nature of ALL maintenance therapy and the challenges associated with treatment adherence among patients residing in disadvantaged neighborhoods.

25COASMA84:

Title: Impact of resistance training on inflammatory biomarkers and associations with treatment outcomes in colon cancer

Seohyuk Lee MD, Chao Ma MS, Bette J. Caan DrPH et.al.

Cancer, Volume131, Issue9, 1 May 2025
https://doi.org/10.1002/cncr.35865

Abstract: Introduction Among patients with colon cancer undergoing adjuvant chemotherapy, the impact of resistance training with supplemental dietary protein on inflammatory changes during treatment, whether baseline or changes in inflammatory markers are associated with relative dose intensity (RDI), and the associations of inflammation with body composition were investigated.Methods A multicenter randomized clinical trial of 174 patients with colon cancer undergoing adjuvant chemotherapy assigned to a home-based resistance training program or usual care was conducted. High-sensitivity C-reactive protein (hsCRP), interleukin-6, tumor necrosis factor-α receptor-II, and growth differentiation factor-15 levels were assessed preintervention and following chemotherapy completion. Baseline body composition was evaluated via dual-energy X-ray absorptiometry. Multivariate analyses were adjusted for sociodemographic and clinical factors.Results Patients randomized to resistance training versus usual care experienced similar changes in all inflammatory markers. Those in the highest versus lowest tertile of baseline hsCRP were more likely to have received RDI >70% (odds ratio, 4.11; 95% CI, 1.29–13.1); however, changes across any of the inflammatory markers were not associated with RDI. Patients in

the highest versus lowest tertiles of hsCRP, interleukin-6, and tumor necrosis factor-α receptor-II were more likely to have higher baseline body mass index, total lean mass, and total fat mass.Conclusion Inflammatory markers in patients with colon cancer undergoing adjuvant chemotherapy were not significantly impacted by randomization to a resistance training program but were associated with baseline body composition measures. Further investigations are needed to better elucidate the potential role of inflammatory markers and body composition in predicting important treatment outcomes.

25COASMA85:

Title: Impact of Medicaid expansion on racial disparities among patients with gastrointestinal cancer

Naveen Manisundaram MD, MPH, Rebecca A. Snyder MD, MPH, Chung-Yuan Hu PhD et.al.

Cancer, Volume131, Issue9, 1 May 2025

Abstract : Background Racial minority groups experience disparities in cancer treatment and mortality. This study aimed to investigate the effect of Medicaid expansion on the existing racial disparities in all-cause mortality among patients with gastrointestinal malignancies.Methods A cross-sectional cohort study of patients with pancreatic ductal adenocarcinoma (PDAC), colorectal cancer (CRC), and gastric adenocarcinoma (GC) of any stage was conducted using data from the National Cancer Database (2009–2019). Using difference-in-difference (DID) analysis, the authors compared adjusted 2-year mortality rates among Black and White patients residing in states with expanded Medicaid benefits (MES) and non-MES before (2009–2013) and after (2014–2019) Medicaid expansion.Results A total of 86,052 patients were included in this analysis, including 19,188 patients with PDAC, 60,404 with CRC, and 6460 with GC. Two-year mortality rates decreased among Black patients with PDAC residing in MES but not those residing in non-MES following Medicaid expansion (DID, –9.4%; 95% confidence interval [CI], –14.4% to –4.4%; $p < .001$). Mortality decreased more among Black and White patients with CRC in MES compared to those in non-MES following Medicaid expansion (DID, –2.9%; 95% CI, –5.7 to –0.04; $p = .047$ and DID, –4.2%; 95% CI, –5.8 to –2.5; $p < .001$, respectively). Black patients with GC in MES experienced a marked reduction in mortality compared to those in non-MES (DID, –7.7%, 95% CI, –16.1 to 0.56; $p = .07$).Conclusion Medicaid expansion was associated with a greater reduction in 2-year mortality rates among Black patients residing in MES compared to those residing in non-MES. Existing racial disparities in mortality remained the same or worsened in non-MES but were mitigated in MES following Medicaid expansion in almost all comparisons.

25COASMA86:

Title: Investigating structural inequities in area-level socioeconomic and health care access measures among people with HIV and cancer (2004–2020)

Jessica Y. Islam PhD, MPH, Gita Suneja MD, MS, Yu Chen Lin et.al.

Cancer, Volume131, Issue9, 1 May 2025

https://doi.org/10.1002/cncr.35881

Abstract: Background People with HIV (PWH) are less likely to receive cancer treatment

compared to those without HIV. The objective of this study was to evaluate the role of area-level social determinants of health (SDoH) in cancer treatment receipt among PWH and cancer in the United States. Methods The authors used the National Cancer Database (NCDB; 2004–2020) and included adult patients (18–89 years) with HIV, identified via International Classification of Diseases (ICD)-9 and ICD-10 codes. We focused on the 14 most common cancers common among PWH. The primary outcome was receipt of first-line curative cancer treatment as documented by NCDB. Key SDoH exposures were area-level educational attainment (percent of adults without a high school degree) and income (median income quartiles) by zip code. Hierarchical multivariable logistic regression models, clustered by cancer treatment facility, were used to estimate adjusted odds ratios (aORs) with 95% confidence intervals (CIs).Results The authors included 31,549 people with HIV and cancer, 16.5% of whom did not receive first-line curative cancer treatment. Overall, 43% were ≥60 years old, 38% were non-Hispanic Black, 68% were male, and 39% resided in the Southern United States. The most common cancers were lung (21%), diffuse large B-cell lymphoma or DLBCL (12%), colorectal (9%), and prostate (9%). PWH living in areas of lowest educational attainment (quartile [Q]4 vs. Q1: aOR, 0.73; 95% CI, 0.66–0.82) and lowest-income (Q4 vs. Q1: aOR, 0.73; 95% CI, 0.65–0.81) areas were less likely to receive cancer treatment, after adjusting for age, sex, stage, year, and cancer type. Conclusion Area-level SDoH are associated with cancer treatment receipt among PWH, suggesting structural factors may impact this long-standing observed inequity.

25COASMA87:

Title: Artificial intelligence–driven microsatellite instability profiling reveals distinctive genetic features in patients with lung cancer

Quentin Dominique Thomas MD, Julie Adèle Vendrell PhD, Lakhdar Khellaf MD et.al.

Cancer, Volume131, Issue9, 1 May 2025
https://doi.org/10.1002/cncr.35882

Abstract: Background Microsatellite instability (MSI) has emerged as a predictive biomarker for immunotherapy response in various cancers, but its role in non–small cell lung cancer (NSCLC) is not fully understood.Methods The authors used the bioinformatics tool MIAmS to assess microsatellite status from next-generation sequencing (NGS) data using a tailored microsatellite score. Immunohistochemistry (IHC) assays were also performed to evaluate the correspondence between MSI and deficient mismatch repair (dMMR) status. A retrospective analysis of 1547 lung cancer patients was conducted, focusing on those with an MSI phenotype. Clinical characteristics, co-occurring molecular alterations, tumor mutation burden (TMB), and homologous recombination deficiency (HRD) status were evaluated in this subset.Results Of the 1547 patients analyzed, eight (0.52%) were identified as having MSI through MIAmS, with six (0.39%) of these cases also being dMMR on IHC. All patients with dMMR had an MS score ≥2 and a history of smoking. Most patients showed loss of MLH1 and PMS2 staining on IHC. No correlation was found between MSI status and programmed death-ligand 1 expression, although all MSI patients exhibited high TMB, averaging 21.4 ± 5.6 mutations per megabase. Discussion MSI/dMMR in lung cancer is exceedingly rare, affecting less than 1% of cases. NGS-based analysis combined with bioinformatics tools provides a robust method to identify MSI/dMMR patients, potentially

guiding immunotherapy decisions. This comprehensive approach integrates molecular genotyping and MSI detection, offering personalized treatment options for lung cancer patients. NGS-based MSI testing is emerging as the preferred method for detecting microsatellite instability in various tumor types, including rare cancers.

25COASMA88:

Title: Feasibility and acceptability of the Comprehensive Oncology Rehabilitation and Exercise (CORE) clinical workflow algorithm in patients with newly diagnosed stage I–III breast cancer who undergo surgery as first-line treatment

Lea Haverbeck Simon PhD, MA, Carson Saviers-Steiger BS, Emily R. Dunston PhD et.al.

Cancer, Volume131, Issue9, 1 May 2025

https://doi.org/10.1002/cncr.35798

Abstract: Background This pilot, mixed-methods, randomized controlled trial determined the feasibility and acceptability of the Comprehensive Oncology Rehabilitation and Exercise (CORE) clinical workflow algorithm. CORE was designed to connect patients with newly diagnosed breast cancer to exercise and rehabilitation services from the time of diagnosis throughout cancer care. Methods In total, 72 patients with newly diagnosed, stage I–III breast cancer who required surgery as first-line treatment were randomized 2:1 to CORE or standard of care. CORE included a triaging tool of two questionnaires regarding self-reported exercise (the Godin Leisure Time physical activity questionnaire) and functional status (the Patient-Reported Outcomes Measurement Information System physical function questionnaire), which were administered at the check-in desk for routine breast surgical oncology clinic visits at the initial surgical consultation, postoperatively, and 24 weeks after surgery. Responses to questionnaires in the triaging tool triaged participants to one of three pathways within the algorithm: exercise service, rehabilitation service, or exercise self-management (not a service). Service pathways required referral by clinic staff. Feasibility was determined based on completing the triaging tool (≥66%) and referral completion (≥50%) at the initial surgical consultation visit. Acceptability was determined by four study participant focus groups and one clinic team focus group (≥50% positive response). Results Ninety-three percent of participants in CORE (n = 40) completed the triaging tool. Among those triaged to a service pathway (n = 29), 62% completed their referral. Focus group feedback was primarily positive. Conclusions The CORE clinical workflow algorithm is feasible and acceptable among women who have newly diagnosed stage I–III breast cancer with plans for surgery as first-line treatment. CORE was also acceptable among clinic staff.

25COASMA89:

Title: Triple-negative breast cancer molecular subtypes and potential detection targets for biological therapy indications

Yanchuan Zhang , Qinghua Li , Jie Lan et.al.

Carcinogenesis, Volume 46, Issue 2, February 2025, bgaf006, https://doi.org/10.1093/carcin/bgaf006

Abstract: Triple-negative breast cancer (TNBC) is a highly aggressive subtype of breast cancer associated with poor prognosis. While chemotherapy remains the conventional treatment approach, its efficacy is limited and often accompanied by significant toxicity.

Advances in precision-targeted therapies have expanded treatment options for TNBC, including immunotherapy, poly (ADP-ribose) polymerase inhibitors, androgen receptor inhibitors, cell cycle-dependent kinase inhibitors, and signaling pathway inhibitors. However, the heterogeneous nature of TNBC contributes to variations in treatment outcomes, underscoring the importance of identifying intrinsic molecular subtypes for personalized therapy. Additionally, due to patient-specific variability, the therapeutic response to targeted treatments is inconsistent. This highlights the need to strategize patients based on potential therapeutic targets for targeted drugs to optimize treatment strategies. This review summarizes the classification strategies and immunohistochemical (IHC) biomarkers for TNBC subtypes, along with potential targets for identifying indications for targeted drug therapy. These insights aim to support the development of personalized treatment approaches for TNBC patients.

Keyword: triple-negative breast cancer, biomarkers, molecular subtypes, targeted therapy

25COASMA90:

Title: Multifaceted role of transgelin isoforms in cancer hallmarks Get access Arrow

Ana Maria Jimenez Jimenez , Yazan Haddad , Vendula Jemelikova et.al.

Carcinogenesis, Volume 46, Issue 2, February 2025, bgaf014, https://doi.org/10.1093/carcin/bgaf014

Abstract: Transgelins (TAGLNs) are actin-binding proteins within the calponin family, playing a crucial role in modulating actin-myosin interactions and maintaining actin filament stability. These proteins are expressed in both smooth and non-smooth muscle cells, contributing to the regulation of muscle contractility and cell migration. TAGLNs family has three isoforms that differ in their isoelectric point, namely: TAGLN1, TAGLN2, and TAGLN3. TAGLNs regulation is involved in the development of many diseases, such as pulmonary arterial hypertension, asthma, atherosclerosis, obstructive nephropathy, diabetes, and cancer. Recent research indicates TAGLNs involvement in carcinogenesis and chemoresistance. This review investigates TAGLNs as potential cancer biomarkers, exploring their versatile tissue-specific impact on patient outcomes. We also highlight their roles as, tumor suppressor agents and tumor progression oncogenes depending on the tumor type, tumor genetic variations, and TAGLNs expression profiles. Furthermore, emerging evidence suggests that the interplay between TAGLN2 and chemoresistance to anticancer drugs is mediated by its interaction with the chemoresistance double agent MT-2, with possible bidirectional implications. TAGLNs present a promising avenue for novel therapeutic strategies against cancer, owing to their tissue-specific duality in promoting/suppressing tumor growth and cell migration in cancer cells. Thus, they can serve as a potential prognostic/diagnostic biomarker. The focus should be on leveraging, in future therapeutics, the interplay between TAGLNs and MTs to reverse tumor progression and chemoresistance, transforming them into tumor suppression.

Keyword: transgelins, cancer, chemoresistance, metallothionein.

25COASMA91:

Title: Olfactomedin 4 promotes gastric cancer cell G2/M progression and serves as a therapeutic target in gastric adenocarcinoma

Wenli Liu , Hongzhen Li , Istvan Botos et.al.
Carcinogenesis, Volume 46, Issue 2, February 2025, bgaf010, https://doi.org/10.1093/carcin/bgaf010

Abstract: Olfactomedin 4 (OLFM4) is a member of the olfactomedin domain-containing olfactomedin glycoprotein family and plays important roles in innate immunity, inflammation, and cancer. It exhibits increased expression in gastric cancer patient tissues and has been shown to regulate proliferation and apoptosis in gastric cancer cells. However, the molecular mechanism(s) underlying OLFM4's role in gastric cancer remain unknown. In this study, we found that OLFM4 knockdown significantly inhibited YCC3 gastric cancer cell proliferation and induced G2/M cell cycle arrest. Yeast two-hybridization screening revealed that OLFM4 directly interacts with cyclin B1 interacting protein 1 (CCNB1IP1), an E3 ubiquitin protein ligase. In YCC3 cells, OLFM4 co-immunoprecipitated and colocalized with CCNB1IP1 and underwent cell cycle phase-specific nucleo-cytoplasmic shuttling. OLFM4 knockdown decreased both cyclin B1 protein levels and CDK1 activity in YCC3 cells. Screening of a cohort of OLFM4-targeted microRNAs (miRNAs) for their impact on cell proliferation identified several that significantly downregulated OLFM4 protein levels and inhibited YCC3 cell proliferation in vitro. Rescue experiments demonstrated that these miRNAs' inhibitory effect on cell proliferation was partially related to their downregulation of OLFM4. When three of these miRNAs were individually administered intratumorally to nude mice bearing YCC3 cell xenografts, tumor growth was significantly inhibited when compared with tumors treated with a negative control miRNA. These results suggest that OLFM4 promotes cell cycle progression and cell proliferation in gastric cancer cells and may have utility as a therapeutic target in gastric adenocarcinoma.

25COASMA92:

Title: Dysregulation of G6PD by HPV E6 exacerbates cervical cancer by activating the STAT3/PLOD2 pathway

Jie Zhang , Wei Dong , Qin Yang et.al.
Carcinogenesis, Volume 46, Issue 2, February 2025, bgaf005, https://doi.org/10.1093/carcin/bgaf005

Abstract: High-risk human papillomavirus (HPV) infection is strongly linked to the initiation and progression of cervical cancer (CC), yet the precise molecular mechanisms involved remain partially understood. This investigation examined differential protein expression profiles in various cohorts, including healthy controls and HPV-positive CC patients with different expression levels of glucose-6-phosphate dehydrogenase (G6PD), shedding light on the dysregulation of oncogenic proteins by HPV. Proteomic analysis of cervical tissues revealed specific protein signatures, indicating significant upregulation of HPV E6, G6PD, STAT3, phosphorylated STAT3, and procollagen-lysine 2-oxoglutarate 5-dioxygenase 2 (PLOD2) in HPV-infected CC tissues and cell lines. Functional experiments, involving the manipulation of G6PD and STAT3 activities in CC cells with HPV E6 modulation, demonstrated that dysregulated G6PD enhanced cell proliferation, migration, and invasion while suppressing apoptosis, primarily through the STAT3/PLOD2 pathway. Integrating these findings with the existing literature underscores the role of G6PD as an oncogene, potentially under STAT3 regulation, and highlights the role of PLOD2 as a pivotal

factor in CC progression. This study also proposed a mechanism in which HPV E6-induced dysregulation of G6PD activates the STAT3-PLOD2 axis to promote CC progression. Understanding the intricate interplay between HPV E6, G6PD, STAT3, and PLOD2 offers valuable insights into the molecular landscape of CC. These findings may pave the way for targeted therapeutic approaches aimed at disrupting this axis to mitigate the progression of CC.

Keyword: high-risk human papillomavirus 16, glucose-6-phosphate dehydrogenase, signal transducer and activator of transcription 3, procollagen-lysine 2-oxoglutarate 5-dioxygenase 2, cervical cancer

25COASMA93:

Title: Smoking behavior-related genetic variants and lung cancer risk in Japanese: an assessment by mediation analysis

Sayaka Yamamoto, Yuriko N Koyanagi , Yuji Iwashita et.al.

Carcinogenesis, Volume 46, Issue 2, February 2025, bgaf011, https://doi.org/10.1093/carcin/bgaf011

Abstract: Cigarette smoking is one of the most important risk factors for lung cancer. Genetic studies have shown that smoking behavior-related genetic variants are directly associated with lung cancer, independent of smoking behavior, mainly in European populations. A recent genome-wide association study in Japan identified five loci associated with the number of cigarettes smoked per day. This study aimed to evaluate whether these loci are associated with lung cancer risk directly or indirectly through changing smoking behavior. Here, we conducted a case-control study (1427 cases and 5595 controls) and a prospective cohort study (128 incident cases in 10 520 subjects). Using mediation analysis, we decomposed the total effect of the lead single nucleotide polymorphism (SNP) at each locus on lung cancer risk into direct and indirect effects. The results of the two studies were pooled using a random-effects model to estimate summary relative risks (RRs) and their 95% confidence intervals (CIs). Two studies showed that: (i) rs78277894 (EPHX2-CLU, G > A) had a protective direct effect (RR: 0.84; 95% CI: 0.77–0.93) on lung cancer risk; and (ii) rs56129017 (CYP2A6, C > T) had carcinogenic direct and indirect effects on lung cancer risk (RR: 1.26; 95% CI: 1.15–1.39 and RR: 1.01; 95% CI: 1.00–1.01, respectively). This mediation analysis revealed that two smoking behavior-related SNPs, EPHX2-CLU rs78277894 and CYP2A6 rs56129017, were associated with lung cancer risk through pathways independent of changing smoking behavior. Our findings may contribute to our understanding of lung carcinogenesis pathways that cannot be addressed by changes in smoking behavior.

Keyword: smoking behavior-related SNP, lung cancer risk, mediation analysis, case-control study, prospective cohort study

25COASMA94:

Title: Reactions of [13C]-labelled tobacco smoke with DNA to generate selected adducts formed without metabolic activation

Mei-Kuen Tang , Trevor Ostlund , Nour F Dameh et.al.

Carcinogenesis, Volume 46, Issue 2, February 2025, bgaf008,

https://doi.org/10.1093/carcin/bgaf008

Abstract: DNA adducts are central in the carcinogenic process because they can cause miscoding leading to permanent mutations in important genes involved in carcinogenesis. While it is known that tobacco smoking leads to increased levels of multiple DNA adducts, most DNA adducts detected to date in humans cannot be explicitly attributed to smoking but instead have various possible exogenous and endogenous sources. We plan to probe the tobacco source of DNA adducts by providing carbon-13 labelled ([13C]-labelled) cigarettes to smokers and analyzing [13C]-labelled DNA adducts in their oral cells to determine which adducts arise from smoking. Prior to conducting studies in humans, we first report here proof-of-principle machine smoking experiments to evaluate carbon isotopologues of (a) selected carbonyls and (b) DNA adducts resulting from direct exposure of cigarette smoke vapour-phase to calf-thymus DNA. The smoke of the study cigarettes, made from a 50:50 mixture of [13C]-labelled tobacco and a popular commercial tobacco, yielded similar concentrations of carbonyl compounds and their respective DNA adducts compared with the smoke of 1R6F reference cigarettes and the popular brand of cigarettes. We detected [13C]-isotopologues of DNA adducts such as 1,N6-etheno-dA, (8R/S)-3-(2'-deoxyribos-1-yl)-5,6,7,8-tetrahydro-8-hydroxypyrimido[1,2-a]purine-10(3H)-one (γ-OH-Acr-dG), and (6S,8S and 6R,8R)-3-(2'-deoxyribos-1-yl)-5,6,7,8-tetrahydro-8-hydroxy-6-methylpyrimido[1,2-a]purine-10(3H)-one [(6S,8S)-γ-OH-Cro-dG and (6R,8R)-γ-OH-Cro-dG], proving that they have a direct source from tobacco smoke and providing important new insights regarding their mechanisms of formation. These unique results form the basis for further studies in cell culture and in cigarette smokers to establish how carcinogens in tobacco smoke cause DNA adduct formation.

Keyword: DNA adducts, [13C]-labelled cigarettes, 13-carbon, LC–NSI–HRMS/MS, machine smoking

25COASMA95:

Title: Establishing a new-onset diabetes-related metabolism signature for predicting the prognosis and immune landscape in pancreatic cancer

Yilei Yang , Luyao Liu , Haochen Cui et.al.

Carcinogenesis, Volume 46, Issue 2, February 2025,
https://doi.org/10.1093/carcin/bgae072

Abstract: New-onset diabetes (NOD) is a common condition among patients with pancreatic adenocarcinoma (PAAD) and is related to poor clinical outcomes. The potential impact of NOD on PAAD progression and the tumor microenvironment remains unclear. Here, we revealed that NOD in PAAD was associated with metabolic disorders. Utilizing three machine-learning algorithms, an NOD-related metabolism signature (NRMS) was established. Validated in three independent cohorts, patients with a high NRMS score exhibited a worse prognosis. Moreover, an elevated NRMS score was associated with an immunosuppressive microenvironment and diminished response to immunotherapy. Further experiments demonstrated that ALDH3A1, a key feature in NRMS, was significantly upregulated in tissues from PAAD patients with NOD and played a crucial role in tumor progression and immune suppression. Our findings highlight the potential of NRMS as a prognostic biomarker and an indicator of immunotherapy response for patients with PAAD.

Keyword: pancreatic adenocarcinoma, new-onset diabetes, metabolism, tumor microenvironment

25COASMA96:

Title: Role of the nucleotide excision repair function of CETN2 in the inhibition of the sensitivity of hepatocellular carcinoma cells to oxaliplatin

Hengcheng Tang , Huaduan Zi , Donghu Zhou et.al.

Carcinogenesis, Volume 46, Issue 2, February 2025, bgaf003,
https://doi.org/10.1093/carcin/bgaf003

Abstract: Resistance to platinum-based chemotherapy agents like oxaliplatin (OXA) poses significant challenges in the treatment of cancers such as hepatocellular carcinoma (HCC). Centrin 2 (CETN2), which functions in nucleotide excision repair (NER) of DNA damage, is overexpressed in HCC. We investigated the potential role of CETN2 in modulating the sensitivity of HCC cells to OXA. CETN2 expression correlated with decreased OXA sensitivity in Huh7 and Hep3B HCC cell lines. CETN2 forms a complex with XPC, which is crucial for the initial DNA damage recognition in NER, thereby enhancing NER and reducing the efficacy of OXA. siRNA-mediated knockdown of CETN2 increased OXA-induced cytotoxicity and apoptosis, confirming its role in chemoresistance. Moreover, overexpression of CETN2 inhibited OXA-induced DNA damage, an effect partially reversed by XPC knockdown. Our findings highlight CETN2 as a potential biomarker and therapeutic target in overcoming OXA resistance in HCC and suggest the possibility for CETN2 inhibitors in enhancing chemotherapeutic efficacy in the treatment of HCC.

Keyword: Centrin 2, oxaliplatin, hepatocellular carcinoma, nucleotide excision repair, intrinsic apoptosis.

25COASMA97:

Title: Nature of the Reactive Biferric Peroxy Intermediate P′ in the Arylamine Oxygenases and Related Binuclear Fe Enzymes

Lars H. Böttger, Dory E. De Weese, Shyam R. Iyer et.al.

J. Am. Chem. Soc. 2025, 147, 14, 11707–11725
https://doi.org/10.1021/jacs.4c11712

Abstract: Binuclear nonheme iron enzymes activate O2 to perform a wide range of chemical transformations. The process of O2 activation typically involves a biferric peroxy-level intermediate P. It has been previously found that this intermediate undergoes further activation, either protonation or rearrangement to form P′ or further oxidation to form high-valent intermediates Q or X. This study defines the structure of the P′ intermediate in the N-oxygenases CmlI (and AurF based on previous data) using nuclear resonance vibrational spectroscopy (NRVS) in conjugation with density functional theory (DFT) calculations. These results, combined with variable temperature variable field (VTVH) magnetic circular dichroism (MCD) spectroscopy on the 1-electron cryoreduced P′, define the structure of the P′ intermediate as a μ-1,2-hydroxoperoxo biferric site with a second hydroxide bridge. Reaction coordinate calculations demonstrate that single electron transfer (SET) is facilitated by protonation of the peroxo, activating its reductive cleavage, and that the additional hydroxide bridge does not impact this reaction. VTVH MCD studies further reveal that the

hydroxide bridge is absent in the biferrous site, suggesting that during the O2 reaction with the biferrous site, a water molecule forms the hydroxide bridge in providing the proton that activates the peroxide in P′ for reactivity.

25COASMA98:

Title: Encoded Display of Chemical Libraries on Nanoparticles as a Versatile Selection Tool To Discover Protein Ligands

Kang Ju Lee, Hee Myeong Wang, Minkyung Kim et.al.

J. Am. Chem. Soc. 2025, 147, 14, 11726–11740
https://doi.org/10.1021/jacs.4c13487

Abstract: DNA-encoded library (DEL) technology is a powerful tool for discovering potent ligands for biological targets but constrained by limitations, including the insolubility of DNA in organic solvents and its instability under various reaction conditions, which restrict the reactivity scope and structural diversity achievable in library synthesis. Here, we present a new strategy called nanoDEL, where library molecules and DNA tags are displayed on the surface of nanoparticles. Since nanoparticles disperse well in both organic solvents and aqueous solutions, DEL synthesis can be accomplished using well-established organic solvent-based conditions, eliminating the need for aqueous conditions. Moreover, nanoDEL enables air-sensitive reactions that are inaccessible with conventional DEL methods relying on aqueous conditions. Notably, in nanoDEL, multiple copies of a DNA tag are attached to an individual nanoparticle to encode a single compound, significantly enhancing tolerance to DNA-damaging conditions. Even when most DNA tags are damaged, sequence analysis remains feasible via amplification of intact tags. Consequently, nanoDEL facilitates the convenient use of existing organic reactions without the necessity to develop DNA-compatible reactions. The potential of nanoDEL was validated by affinity selection against streptavidin as a model system and successfully applied to the discovery of potent small-molecule inhibitors for a kinase and stapled peptide inhibitors targeting a protein–protein interaction, exhibiting dissociation constants in the nanomolar range. Furthermore, we demonstrated that a large combinatorial library can be efficiently synthesized on nanoparticles using a synthetic scheme including moisture-sensitive reaction steps, which are not feasible with conventional DELs.

25COASMA99:

Title: Rational Design Principles for De Novo α-Helical Peptide Barrels with Dynamic Conductive Channels

Ai Niitsu, Andrew R. Thomson, Alistair J. Scott et.al.

J. Am. Chem. Soc. 2025, 147, 14, 11741–11753
https://doi.org/10.1021/jacs.4c13933

Abstract: Despite advances in peptide and protein design, the rational design of membrane-spanning peptides that form conducting channels remains challenging due to our imperfect understanding of the sequence-to-structure relationships that drive membrane insertion, assembly, and conductance. Here, we describe the design and computational and experimental characterization of a series of coiled coil-based peptides that form transmembrane α-helical barrels with conductive channels. Through a combination of rational

and computational design, we obtain barrels with 5 to 7 helices, as characterized in detergent micelles. In lipid bilayers, these peptide assemblies exhibit two conductance states with relative populations dependent on the applied potential: (i) low-conductance states that correlate with variations in the designed amino-acid sequences and modeled coiled-coil barrel geometries, indicating stable transmembrane α-helical barrels; and (ii) high-conductance states in which single channels change size in discrete steps. Notably, the high-conductance states are similar for all peptides in contrast to the low-conductance states. This indicates the formation of large, dynamic channels, as observed in natural barrel-stave peptide channels. These findings establish rational routes to design and tune functional membrane-spanning peptide channels with specific conductance and geometry.

25COASMA100:

Title: Plasmonic Charge Localization and C–H Activation at Single-Atom Sites in Dilute Copper Platinum Alloys

Emma-Rose Newmeyer, Yicheng Wang, Zachary Alexander Long et.al.

J. Am. Chem. Soc. 2025, 147, 14, 11789–11799

https://doi.org/10.1021/jacs.4c14842

Abstract: The role of energy transfer in plasmonic alloys is critical for advancing photocatalysis to industrially and societally relevant chemical processes. In this study, we synthesized and characterized CuPt dilute alloy catalysts to explore the impact of dopant concentration on energy transfer in plasmon-assisted nonoxidative propane dehydrogenation. By leveraging the localized surface plasmon resonance (LSPR) in copper nanoparticles, we examined how single-atom and ensemble Pt sites influence (photo)catalytic performance. In situ diffuse reflectance infrared Fourier transform spectroscopy, along with kinetic analysis of photocatalytic experiments, provided evidence that Pt single-atom sites enhance nonthermal charge carrier generation and energy transfer processes, accelerating C–H scission, resulting in a significant increase in light-driven reaction rates compared to CuPt alloys with ensemble Pt sites. The photochemical enhancement enabled by dilute plasmonic alloys is proposed to result from transient oxidative potentials (i.e., hot holes) localized on isolated dopant sites. These findings demonstrate the potential of engineering active sites in dilute plasmonic alloys for tailored electronic properties, paving the way for broader applications in plasmonic photocatalysis.

25COASMA101:

Title: Structural Context Modulates the Conformational Ensemble of the Intrinsically Disordered Amino Terminus of α-Synuclein

Rania Dumarieh, Dominique Lagasca, Sakshi Krishna et.al.

J. Am. Chem. Soc. 2025, 147, 14, 11800–11810

https://doi.org/10.1021/jacs.4c15653

Abstract: Regions of intrinsic disorder play crucial roles in biological systems, yet they often elude characterization by conventional biophysical techniques. To capture conformational distributions across different time scales, we employed a freezing approach coupled with solid-state NMR analysis. Using segmentally isotopically labeled α-synuclein (α-syn), we investigated the conformational ensembles of the six alanines, three glycines, and a single site

(L8) in the disordered amino terminus under three distinct conditions: in 8 M urea, as a frozen monomer in buffer, and within the disordered regions flanking the amyloid core. The experimental spectra varied significantly among these conditions and deviated from those of a statistical coil. In 8 M urea, monomeric α-syn exhibited the most restricted conformational sampling, rarely accessing chemical shifts characteristic of α-helices or β-strands. In buffer, monomeric α-syn showed a broader conformational sampling, favoring α-helical conformations and, to a lesser extent, random coil states. Notably, amino acids in the disordered regions flanking the amyloid core demonstrated the most extensive conformational sampling, with broad peaks encompassing the entire range of possible chemical shifts and a marked increase in highly extended β-strand conformations. Collectively, this work demonstrates that intrinsically disordered regions exhibit distinct conformational ensembles, which are influenced not only by the chemical environment but also by the conformations of adjacent protein sequences. The differences in the conformational ensembles of the disordered amino terminus may explain why the monomer and the amyloid form of α-syn interact with different biomolecules inside cells.

25COASMA102:

Title: Interface Preconstruction Enables Robust Passivation of the Ah-Level Aqueous Li-ion Batteries

Anxing Zhou, Jinkai Zhang, Ming Chen et.al.

J. Am. Chem. Soc. 2025, 147, 14, 11811–11820

https://doi.org/10.1021/jacs.4c15852

Abstract: The solid electrolyte interphase (SEI) offers effective passivation on the anode for aqueous lithium-ion batteries (ALIBs). Conventional passivation in ALIBs mainly relies on the LiF-contained SEI originating from anion reduction in the electrolyte. However, such SEI formation is a competitive reaction negatively impacted by the parasitic hydrogen evolution reaction (HER), resulting in high Li+ irreversible consumption and imperfect bare flaws. To address this issue, we propose preconstructing an artificial interphase by introducing a multifunctional interface additive CsF to build superior passivation on the anode in ALIBs. CsF first undergoes a displacement reaction with LiTFSI from the fresh electrolyte to form the LiF in situ on the interface of the anode before the cycles, avoiding the extra Li+ irreversible consumption. Meanwhile, we uncover that the dissolving Cs+ in the electrolyte can destroy the hydrogen bond network of the water to lower water activity on the anode interface and strongly interact with TFSI– to form the cation–anion complex, facilitating the anion proximity to the anode interface. The anion reduction based on the artificial interphase can finally help achieve the robust SEI in ALIBs. Such passivation stabilizes the aqueous electrolyte, significantly suppressing the side reaction of the HER that allows ALIBs to obtain a superior long life above 2000 cycles. The ampere-hour-level (Ah-level) pouch cell achieves an energy density of 57 Wh/kg and 176 Wh/L with high energy efficiency (~94%).

25COASMA103:

Title: 3D Imaging Reveals Widespread Stacking Disorder in Single Crystal 2D Covalent Organic Frameworks

Priti Kharel, Patrick T. Carmichael, Anusree Natraj et.al.

J. Am. Chem. Soc. 2025, 147, 14, 11821–11828
https://doi.org/10.1021/jacs.4c16207
Abstract: Although tailored porosity is a defining feature of layered, two-dimensional (2D) polymers known as 2D covalent organic frameworks (COFs), understanding the interplanar stacking of 2D COFs and their resulting three-dimensional (3D) pore structure remains challenging. Here, we use scanning transmission electron microscopy and ptychography, an emerging 3D angstrom-scale imaging method, to study single-crystalline particles of the imine-linked 2D COF TAPB-DMPDA. Previously assumed to adopt an average-eclipsed structure with only angstrom-level stacking disorder, we find the crystals contain widespread stacking disorder of larger magnitudes, including interplanar shifts up to a half unit cell and nanoscale inhomogeneities in stacking and tilt. 3D visualizations show pore channels are distorted by this stacking disorder. The extensive stacking disorder found in even high-quality 2D COFs has profound implications for envisioned applications and should motivate the development of design strategies to control their 3D structures.

25COASMA104:

Title: An Atomically Dispersed Mn Photocatalyst for Vicinal Dichlorination of Nonactivated Alkenes

Prakash Kumar Sahoo, Rakesh Maiti, Peng Ren et.al.
J. Am. Chem. Soc. 2025, 147, 14, 11829–11840
https://doi.org/10.1021/jacs.4c16413
Abstract: A novel Mn-based single-atom photocatalyst is disclosed in this study, designed for the dichlorination of alkenes to achieve vicinal dichlorinated products using N-chlorosuccinimide as a mild chlorinating agent, which have widespread applications as pest controlling agents, polymers, flame retardants, and pharmaceuticals. In developing this innovative catalyst, we achieved the atomic dispersion of Mn on aryl-amino-substituted graphitic carbon nitride (f-C3N4). This marks the first instance of a heterogeneous version, offering an operationally simple, sustainable, and efficient pathway for dichlorination of alkenes, including drugs, bioactive compounds, and natural products. This material was extensively characterized by using techniques such as UV–vis spectroscopy, X-ray absorption near-edge structure (XANES), extended X-ray absorption fine structure (EXAFS), high-resolution transmission electron microscopy (HR-TEM), X-ray photoelectron spectroscopy (XPS), magic-angle spinning (MAS), and solid-state nuclear magnetic resonance (ssNMR) spectroscopy to understand it at the atomic level. Furthermore, mechanistic studies based on multiscale molecular modeling, combining classical reactive molecular dynamics (RMD) simulations and quantum chemistry (QC) calculations, illustrated that the controlled formation of Cl radicals from the in situ formed Mn–Cl bond is responsible for the dichlorination reaction of alkenes. In addition, gram-scale and reusability tests were also performed to demonstrate the applicability of this approach on an industrial scale.

25COASMA105:

Title: Solvent Medium-Induced Changes to Internal Pressure in the Layered Host VOPO4·2H2O and the Influence on Intercalation Reactions

Jiahui Liu, Yuan Liu, Timothy Yoo et.al.
J. Am. Chem. Soc. 2025, 147, 14, 11841–11850
https://doi.org/10.1021/jacs.4c16643
Abstract: Layered vanadium phosphate dihydrate, VOPO4·2H2O, has been chosen as a host for ferrocene intercalation to explore the influence of solvent-guest and solvent-host interactions on rates and product selection. After eliminating solvents that react directly with the VOPO4·2H2O host, ferrocene intercalation was evaluated in a series of seven solvents that do not themselves intercalate or otherwise alter the host structure. The intercalation kinetics are analyzed in acetone, butanone, pentanone, acetonitrile, propionitrile, butyronitrile, and DMF. No intercalation is observed in DMF, but all other solvents yield a mixture of stage 1 and stage 2 ferrocenium intercalation products with reaction rates and product ratios varying across the series of solvents. Using ex situ as well as in situ PXRD methods, faster reactions yield more stage 1 product, while a higher degree of stage 2 product is seen for slower kinetics. The results are interpreted in the context of competition between intercalation rates and the buildup of elastic strain between intercalated domains and unintercalated host. To understand solvent effects, both solvent-guest and solvent-host effects are considered. None of the typically considered solvent-guest effects, such as guest desolvation energy, dielectric constant, and guest oxidation potential, correlate with the observed reaction kinetics. On the other hand, different solvent environments are shown to change the internal pressure, Peff, within the layered hosts, a consequence of changing surface energy and surface tension (stress) in particles with nanometer scale dimensions. The VOPO4·2H2O interlayer spacing decreases when particles are suspended in DMF and organonitrile solvents, while the layers separate slightly in acetone, butanone, and pentanone. Using calculated elastic constants, the structural changes correspond to changes in Peff in the range 0.22 GPa > ΔPeff > −0.11 GPa across the series of solvents. A density functional theory analysis of the influence of pressure on ferrocene diffusion adds support for the idea that intercalation kinetics are altered by changing internal pressure. The results show solvent environments can be responsible for altering the effective pressure within intercalation hosts, influencing intercalation rates and product selection, even if the solvents do not react directly with the host solids.

25COASMA106:
Title: Synthesis and Superconductivity of Ternary A15-(Lu, Y)4H23 at High Pressures
Kexin Zhang, Jingkun Yu, Yuchen Zhang et.al.
J. Am. Chem. Soc. 2025, 147, 14, 11879–11885
https://doi.org/10.1021/jacs.4c16805
Abstract: Ternary hydrides, formed by introducing new elements into binary hydrides, are a crucial pathway for enhancing superconducting transition temperatures (Tc) or reducing the stable pressures. In this work, we have acquired the ternary hydride formed by Lu and Y atoms, inspired by the low stabilization pressure of the Lu–H system with its fully filled 4f electrons, as well as the higher Tc of the Y–H system. By effectively controlling the high-pressure and high-temperature conditions, we have successfully synthesized Pm-3n (Lu, Y)4H23 (A15-type). The synthesized Pm-3n (Lu, Y)4H23 reveals the highest Tc of 112 K at 215 GPa, which is the record Tc among A15-type superconductors. Compared to the binary

Pm-3n Lu4H23, the Pm-3n (Lu, Y)4H23 exhibits a 60% increase in Tc and a 61% enhancement in the upper critical field μ0Hc2(0). Interestingly, Pm-3n (Lu, Y)4H23 displays minimal volume expansion and a slight increase in the H–H bond distance relative to Pm-3n Lu4H23 due to the introduction of Y atoms. Combined theoretical and experimental analyses indicate that the substitution of Lu atoms with Y atoms enhances electron–phonon coupling (EPC) through modified electronic bands and phonon softening caused by the expansion of H–H bonds, collectively driving the significant enhancement of Tc in Pm-3n (Lu, Y)4H23. Our work demonstrates a crucial strategy for adjusting and enhancing the superconducting performance of hydrides and offers valuable practical experience for developing ternary hydrides.

25COASMA107:

Title: Low-Temperature Direct Arylation Polymerization for the Sustainable Synthesis of a Library of Low-Defect Donor–Acceptor Conjugated Polymers via Pd/Ag Dual-Catalysis

Hwangseok Kim, Hyeonjin Yoo, Hongsik Kim et.al.

J. Am. Chem. Soc. 2025, 147, 14, 11886–11895

https://doi.org/10.1021/jacs.4c16831

Abstract: Donor–acceptor alternating conjugated polymers (D–A CPs) are one of the best materials for high-performance organic electronic devices, owing to their low bandgap and high charge carrier mobility. However, most of the D–A CPs are synthesized by less sustainable polymerization methods. To address this issue, direct arylation polymerization (DArP), eliminating the need for transmetalating agents, was developed over the past two decades. Nevertheless, C–H activation during DArP still requires significantly harsh reaction conditions, limiting the precision and applicability of CPs. In this report, we demonstrate a versatile and sustainable Pd/Ag dual-catalytic DArP conducted at low or even room temperatures, thereby yielding low-defect D–A CPs. Initially, electron-deficient acceptor substrates with various electronic properties and pKa underwent successful concerted-metalation-deprotonation (CMD) via Ag catalysis with mild conditions and highly chemoselective Pd-catalyzed C–C coupling. This synergistic dual-catalysis allowed for the library synthesis of D–A and A–A CPs from acceptor C–H monomers and aryl halide monomers at low temperatures (25–70 °C) in sustainable solvents such as p-cymene. Interestingly, the D–A CPs obtained via Pd/Ag DArP displayed higher structural regularity and crystallinity, eventually outperforming those prepared by conventional synthetic methods in device performances of ambipolar organic field-effect transistors (μe up to 0.80 cm2 V–1 s–1) and complementary metal-oxide semiconductor inverters (gain up to 102).

25COASMA108:

Title: Mechanistic Characterization of Diterpene Synthase Pairs for Tricyclic Diterpenes from Cyanobacteria

Jiayi Yu, Taro Shiraishi, Kizerbo A. Taizoumbe et.al.

J. Am. Chem. Soc. 2025, 147, 14, 11896–11905

https://doi.org/10.1021/jacs.4c16710

Abstract: In recent years, genome mining in cyanobacteria has revealed abundant gene

clusters related to natural product biosynthesis. However, only a few terpene synthases (TSs) have been identified from this bacterial phylum. Pfam profiles, such as PF03936 and PF19086, which are frequently used for TS retrieval, are built from plant, bacterial, and fungal TSs. Herein, we constructed a new hidden Markov model (HMM) specific to bacterial TSs on the basis of 110 bacterial TSs experimentally validated in recent years. Using this model, we identified a pair of diterpene synthases, Cpt11 (class II TS) and Cts11 (class I TS), in the cyanobacterium Scytonema tolypothrichoides. In vitro experiments demonstrated that Cpt11 catalyzes the formation of syn-copalyl diphosphate from geranylgeranyl diphosphate and that Cts11 subsequently converts syn-copalyl diphosphate into a rare 6,6,7-tricyclic diterpene alcohol. Its biosynthesis was established through isotope labeling experiments, which revealed a unique sequence of a 1,6-proton shift and ring expansion to a seven-membered ring. We solved the crystal structure of Cts11 at a resolution of 1.76 Å. Additionally, via site-directed mutagenesis experiments, we identified two amino acid residues whose exchanges affected the formation of the original diterpene alcohol, leading to the formation of two new compounds: a 6,6,7-tricyclic diterpene hydrocarbon and another 6,6,6-tricyclic diterpene alcohol. A BLAST search revealed several sequences that shared over 70% identity with Cts11 from cyanobacteria that could produce diverse diterpenes. This study demonstrates the potential for cyanobacteria to produce unprecedented terpenoids and lays the foundation for studying the physiological activities of terpenoids in cyanobacteria.

25COASMA109:

Title: Ligand-Controlled Regioselective Dearomative Vicinal and Conjugate Hydroboration of Quinolines

Chao Hu, Chen-Yan Cai, Elizabeth S. Barta et.al.

J. Am. Chem. Soc. 2025, 147, 14, 11906–11914

https://doi.org/10.1021/jacs.4c17247

Abstract: A dearomative strategy to regioselectively modify arenes using a “diene” synthon within aromatic rings provides access to highly functionalized heterocycles from abundant aromatic feedstocks and represents an alternative synthetic approach besides traditional cross-coupling and C–H functionalization methodologies. In this study, we present an efficient method for selectively introducing boron onto quinolines through dearomative hydroboration using easily accessible and stable phosphine-ligated borane complexes. The vicinal 5,6- and conjugate 5,8-hydroborated products could be obtained regioselectively by modifying the phosphine ligand. Drawing inspiration from diverse organoboron transformations, these borane building blocks were diversified by a range of downstream functionalizations, providing modular pathways for the skeletal modifications of quinolines to access a variety of challenging functionalized heterocycles.

25COASMA110:

Title: Precision Self-assembly of 3D DNA Crystals Using Microfluidics

Xugen Chen, Pan Fu, Karol Woloszyn et.al.

J. Am. Chem. Soc. 2025, 147, 14, 11915–11924

https://doi.org/10.1021/jacs.4c17455

Abstract: Controlling the uniformity in size and quantity of macroscopic three-dimensional

(3D) DNA crystals is essential for their integration into complex systems and broader applications. However, achieving such control remains a major challenge in DNA nanotechnology. Here, we present a novel strategy for synthesizing monodisperse 3D DNA single crystals using microfluidic double-emulsion droplets as nanoliter-scale microreactors. These uniformly sized droplets can shrink and swell without leaking their inner contents, allowing the concentration of the DNA solution inside to be adjusted. The confined volume ensures that, once a crystal seed forms, it rapidly consumes the available DNA material, preventing the formation of additional crystals within the same droplet. This approach enables precise control over crystal growth, resulting in a yield of one DNA single crystal per droplet, with a success rate of up to 98.6% ± 0.9%. The resulting DNA crystals exhibit controlled sizes, ranging from 19.3 ± 0.9 μm to 56.8 ± 2.6 μm. Moreover, this method can be applied to the controlled growth of various types of DNA crystals. Our study provides a new pathway for DNA crystal self-assembly and microengineering.

25COASMA111:

Title: Bilayer Kagome Ferrimagnet Exhibiting Exceptional Spontaneous Exchange Bias in TbMn6(Ge,Ga)6

Hankun Xu, Wenjie Li, Junjie Chen et.al.

J. Am. Chem. Soc. 2025, 147, 14, 11941–11948

https://doi.org/10.1021/jacs.4c17505

Abstract: Manipulating interlayer interactions in two-dimensional (2D) materials has led to intriguing behaviors. Borrowing these 2D signatures to bulk materials is likely to unlock exceptional properties. Here, we report an emergent 2D-like bilayer Kagome ferrimagnet through reducing the interbilayer magnetic interaction to nearly zero. This concept is realized within bulk TbMn6(Ge,Ga)6 compounds, characterized by an isolated and pure Mn Kagome lattice, simply by the chemical substitution of Ge with Ga. Specifically, the targeted compound TbMn6Ge5Ga1 exhibits a giant spontaneous exchange bias (SEB) of approximately 1.6 T, which is more than twice that observed in known materials. Field-dependent neutron diffraction reveals the robust nature of the compensated ferrimagnetic (FiM), characterized by almost two-thirds of the moments being pinned and irreversible under fields up to 9 T. Through magnetic and structural analysis, alongside theoretical calculations, we demonstrate that the substantial SEB is related to the intense competition between local robust and weak FiM states within the bilayer Kagome configuration, which are stabilized by an incommensurate spin arrangement. The concept of a bilayer Kagome magnet offers new opportunities for discovering attractive properties in 2D-like materials.

25COASMA112:

Title: O-Cyanobenzaldehydes Irreversibly Modify Both Buried and Exposed Lysine Residues in Live Cells

Huan Ling, Lin Li, Liping Duan et.al.

J. Am. Chem. Soc. 2025, 147, 14, 11955–11963

https://doi.org/10.1021/jacs.4c18006

Abstract: Lysine residue represents an attractive site for covalent drug development due to its high abundance (5.6%) and critical functions. However, very few lysines have been

characterized to be accessible to covalent ligands and perturb the protein functions, owing to their protonation state and adjacent steric hindrance. Herein, we report a new lysine bioconjugation chemistry, O-cyanobenzaldehyde (CNBA), that enables selective modification of the lysine ε-amine to form iso-indolinones under physiological conditions. Activity-based proteome profiling enabled the mapping of 3451 lysine residues and 85 endogenous kinases in live cells, highlighting its potential for modifying hyper-reactive lysines within the proteome or buried catalytic lysines within the kinome. Further protein crystallography and mass spectrometry confirmed that K271_ABL1 and K162_AURKA are covalently targetable sites in kinases. Leveraging a structure-based drug design, we incorporated CNBA into the core structure of Nutlin-3 to irreversibly inhibit the MDM2-p53 interaction by targeting an exposed lysine K94 on the surface of murine double minute 2. Importantly, we have demonstrated the potential application of CNBA as a lysine-recognized bioconjugation agent for developing new antibody-drug conjugates. The results collectively validate CNBA as a new selective and efficient modifying agent with broad applications for both buried and exposed lysine residues in live cells.

25COASMA113:

Title: A Lanthanide Nanoparticle–Aggregation-Induced Emission Photosensitizer Complex System Drives Coupled Triplet Energy Transfer for Enhanced Radio-Photodynamic Therapy

Yibo An, Dazhuang Xu, Pan He et.al.

J. Am. Chem. Soc. 2025, 147, 14, 11964–11974

https://doi.org/10.1021/jacs.4c18033

Abstract: Cerenkov light (CL), utilized as an internal excitation source for photodynamic therapy (PDT), addresses the limitations of laser penetration and has substantial potential for seamlessly integrating clinical radiotheranostics with phototheranostics. Nevertheless, the effectiveness of CL-mediated PDT is significantly hindered by challenges, such as the low intensity of CL and inadequate energy transfer between the CL donor and photosensitizers (PSs). In this study, a novel approach is introduced for enhanced radionuclide-activated radio-photodynamic therapy utilizing a hybrid nanoparticle system composed of lanthanide nanoparticles and an aggregation-induced emission photosensitizer (AIE PS), designated LnNP–TQ NPs. This system enables lanthanide nanoparticles to optimize the decay energy of radionuclides, effectively sensitizing the AIE PS through triplet energy transfer (TET)-mediated processes with an efficiency approaching 100%. When activated by the clinical radionuclide 18F for positron emission tomography imaging, the LnNP–TQ NPs substantially inhibited tumor growth via effective singlet oxygen (1O2) generation. This strategy, which optimally harnesses radionuclide energy and achieves efficient energy transfer, offers a promising pathway for enhancing radiotherapy–phototherapy efficacy in tumor treatment.

25COASMA114:

Title: Chemoselective Hydrogenation of Halonitrobenzenes by Platinum Nanoparticles with Auxiliary Co–N4 Single Sites in Sandwiched Catalysts

Tian Lin, Zhouwen Cao, Junqi Pei et.al.

J. Am. Chem. Soc. 2025, 147, 14, 11975–11987

https://doi.org/10.1021/jacs.4c18288

Abstract: The chemoselective hydrogenation of halonitrobenzenes to haloanilines is of great importance but remains challenging to simultaneously achieve high catalytic activity, excellent selectivity, and good reusability, especially for ortho-substituted substrates. This is due to the occurrence of hydrogenolysis of halogen groups, as well as the easy migration and aggregation of active species on the catalyst surface during the hydrogenation of nitro groups. In this study, we integrate Pt nanoparticles (NPs) with auxiliary Co–N4 single sites from a porphyrinic metal–organic framework [known as PCN-221(Co)] in a sandwiched nanostructure as a catalyst for the chemoselective hydrogenation of ortho-halonitrobenzenes at 80 °C and 1 MPa H2 in a 50 mL batch microreactor. This sandwiched catalyst achieves 97.3% selectivity for ortho-chloroaniline at nearly complete conversion of ortho-chloronitrobenzene, with an exceptionally high turnover frequency (TOF) of 11,625 h–1 and good reusability over ten cycles, outperforming state-of-the-art heterogeneous supported metal catalysts. Theoretical and experimental investigations reveal that the nitro group in ortho-chloronitrobenzene is preferentially hydrogenated by Pt NPs, while the ortho-chloro group is selectively adsorbed by Co–N4 single sites in PCN-221(Co), preventing its hydrogenolysis and enhancing selectivity for ortho-chloroaniline. Furthermore, the PCN-221(Co) shell in the sandwiched catalyst plays a key role in enriching ortho-chloronitrobenzene and stabilizing the supported Pt NPs, thus leading to high catalytic activity and good reusability. Additionally, at nearly complete conversion of ortho-fluoronitrobenzene and ortho-bromonitrobenzene, this sandwiched Pt catalyst displays 100% selectivity for ortho-fluoroaniline with a TOF of 8680 h–1 and 99.2% selectivity for ortho-bromoaniline with a TOF of 5859 h–1, respectively. When meta- and para-halonitrobenzenes are used as substrates, high activity and excellent selectivity for the corresponding haloanilines are also achieved by the sandwiched Pt catalysts.

25COASMA115:

Title: How Temperature Change Affects the Lattice Parameters, Molecular Conformation, and Reaction Cavity in Enantiomeric and Racemic Crystals of Thalidomide

Ayaka Matsumoto, Kenta Nakagawa, Takuya Nakanishi et.al.

J. Am. Chem. Soc. 2025, 147, 14, 11988–11997
https://doi.org/10.1021/jacs.4c18394

Abstract: For the single crystals of thalidomide (C13H10N2O4, TD) grown by the solvent evaporation method, the temperature dependences of the crystal structures have been investigated over a wide temperature range between 100 and 423.15 K. Comparing the α-form of a racemic TD crystal, which consists of symmetric heterochiral dimers and belongs to P21/n space group, with the enantiomeric TD crystal, which belongs to P21 and consists of asymmetric (pseudosymmetric) homochiral dimers, there have been clear differences in the temperature-dependent changes of the lattice parameters, the isobaric linear thermal expansion coefficients (along the crystallographic and the principal Cartesian axes), the volumetric expansion coefficients of the unit cell, and the structures of hydrogen-bonded dimer in the crystal such as intra- and intermolecular dihedral angles, cavities (reaction cavities), and the hydrogen-bond length. In the asymmetric homochiral dimers, one monomer

with a larger reaction cavity changes its intramolecular dihedral angle with temperature, while the other monomer with a smaller cavity does not. In contrast, in the symmetric heterochiral dimers, two monomers with the same cavity volume similarly change their intramolecular dihedral angles with the temperature. Such differences in the temperature-dependent conformational changes between asymmetric and symmetric dimers cause differences between enantiomeric and racemic crystals.

25COASMA116:

Title: Bacillus subtilis Utilizes Decarboxylated S-Adenosylmethionine for the Biosynthesis of Tandem Aminopropylated Microcin C, a Potent Inhibitor of Bacterial Aspartyl-tRNA Synthetase

Alexey Kulikovsky, Eldar Yagmurov, Anastasiia Grigoreva et.al.

J. Am. Chem. Soc. 2025, 147, 14, 11998–12011

https://doi.org/10.1021/jacs.4c18468

Abstract: The biosynthetic pathways of natural products involve unusual biochemical reactions catalyzed by unique enzymes. Aminopropylation, although apparently simple, is an extremely rare modification outside polyamine biosynthesis. The canonical pathway used in the biosynthesis of peptide-adenylate antibiotic microcin C of E. coli (Eco-McC) entails alkylation by the S-adenosyl-methionine-derived 3-amino-3-carboxypropyl group of the adenylate moiety and subsequent decarboxylation to yield the bioactive aminopropylated compound. Here, we report the structure and biosynthesis of a new member of the microcin C family of antibiotics, Bsu-McC, produced by Bacillus subtilis MG27, which employs an alternative aminopropylation pathway. Like Eco-McC, Bsu-McC consists of a peptide moiety that facilitates prodrug import into susceptible bacteria and a warhead, a nonhydrolyzable modified isoasparaginyl-adenylate, which, when released into the cytoplasm, binds aspartyl-tRNA synthetase (AspRS) inhibiting translation. In contrast to the Eco-McC, whose warhead carries a single aminopropyl group attached to the phosphate moiety of isoasparaginyl-adenylate, the warhead of Bsu-McC is decorated with a tandem of two aminopropyl groups. Our in silico docking of the Bsu-McC warhead to the AspRS-tRNA complex suggests that two aminopropyl groups form extended interactions with the enzyme and tRNA, stabilizing the enzyme–inhibitor complex. We show that tandem aminopropylation results in a 32-fold increase in the biological activity of peptidyl-adenylate. We also show that B. subtilis adopted an alternative pathway for aminopropylation in which two homologous 3-aminopropyltransferases utilize decarboxylated S-adenosylmethionine as a substrate. Additionally, Bsu-McC biosynthesis alters the social behavior of the B. subtilis producer strain, resulting in a sharp decrease in their ability to form biofilms.

25COASMA117:

Title: Polarization Rearrangement Induced High-Efficiency Piezocatalytic Overall Pure Water Splitting in Ultrathin (001)-Confined PbTiO3

Peixi Zhang, Qiang Li, Ran Su et.al.

J. Am. Chem. Soc. 2025, 147, 14, 12012–12023

https://doi.org/10.1021/jacs.4c18542

Abstract: Facing the emergencies of global warming and energy shortages, nano

ferroelectrics, which exhibit superior charge separation capabilities and polarization tunability, are extensively utilized in piezocatalytic H2 production. However, acquiring polarized structures that behave with robust ferroelectricity and strong piezoelectricity in ultralow dimension nanomaterials for efficient piezocatalysis remains a huge challenge. This research achieved exceptional piezocatalytic overall pure water splitting performance in 3.5 nm-thick (001)-confined PbTiO3 nanosheets, reaching a H2 evolution rate of 1068 μmol g–1 h–1, exceeding those of similar ferroelectric oxides. The highly confined crystallographic polarization orientation in nanosheets induced polarization rearrangement from the c-axis to other nonpolarized crystallographic orientations, as evidenced by piezoelectric force microscopy and phase field simulations, which improve piezoelectricity and boost piezocatalytic behavior significantly. Local structure investigations jointly by neutron pair distribution function, X-ray absorption spectrum, and atomic-scale scanning transmission electron microscopy methods show that the rearranged structure arises from the lattice inhomogeneous tensile strain. TiO6 octahedrons were distorted, with the Ti atom moving diagonally toward the symmetry center. Such ferroelectric reconstruction of a practical nanopolarized structure with remarkable performance in this work will promote the development of high-performance nano ferroelectrics.

25COASMA118:

Title: Inner–Outer Sheath Synergistic Shielding of Polysulfides in Asymmetric Solvent-Based Electrolytes for Stable Sodium–Sulfur Batteries

Weiqi Yao, Min-Hao Pai, Arumugam Manthiram et.al.

J. Am. Chem. Soc. 2025, 147, 14, 12061–12074
https://doi.org/10.1021/jacs.4c18374

Abstract: Room-temperature sodium–sulfur (RT Na–S) batteries are garnering interest owing to their high theoretical energy density and low cost. However, the notorious shuttle behavior of sodium polysulfides (NaPS) and uncontrollable dendrite growth lead to the poor cycle stability of RT Na–S cells. In this work, we report the use of 1,2-dimethoxypropane (DMP) and 1,1,2,2-tetrafluoroethyl-2,2,2-trifluoroethyl ether (TFTFE) as inner solvent and outer diluent, respectively, in a localized high-concentration electrolyte system. Impressively, the asymmetric DMP as the inner solvent, introduced to replace the conventional solvent 1,2-dimethoxyethane (DME), shields NaPS effectively from incorporation into the inner solvation structure due to the extra methyl groups in the molecular structure. Furthermore, the TFTFE diluent, which contains electron-withdrawing perfluoro segments (−CF3– and −CF2−), exhibits significantly low solvation power. Consequently, the outer sheath TFTFE diluent further minimizes NaPS dissolution, thereby enhancing the cycle stability. This inner–outer sheath synergistic effect leads to the formation of highly effective cathode-electrolyte interphase (CEI) and solid-electrolyte interphase (SEI) layers simultaneously, significantly alleviating the shuttle effect and reducing the side reactions between NaPS and sodium metal. Remarkably, the Na–S cells with the designed electrolyte present long-cycling reversibility with 530 mAh g–1 over 600 cycles at a C/2 rate and a low capacity decay rate of 0.077% per cycle. This study provides a profound understanding of the electrolyte structure involving NaPS and offers a firm basis for the rational design of electrolytes for rechargeable metal–sulfur battery systems.

25COASMA119:

Title: Exquisite Complex Reaction Cascade in the Natural 1,2,4-Triazine Assembly

Yiyuan Cheng, Haoran Pang, Wenjun Zhang et.al.

J. Am. Chem. Soc. 2025, 147, 14, 12075–12081
https://doi.org/10.1021/jacs.4c18761

Abstract: 1,2,4-Triazine ring is a scaffold widely found in biologically active compounds, but how nature makes it remains enigmatic. In this study, we unveil the complex enzymatic and nonenzymatic cascade reactions that assemble the 1,2,4-triazine moiety found in the structures of the natural products pseudoiodinine and toxoflavin. Through biochemical studies, isotope labeling, and the application of substrate analogues, we propose a plausible pathway for the 1,2,4-triazine assembly from a common precursor in riboflavin biosynthesis. This process involves four two-electron oxidation steps, C–N bond formation, decarboxylation, and the N–N bond forming step catalyzed by a metal-dependent WD40-repeat (WDR) protein. This study thus not only provides the first biocatalytic route for the 1,2,4-triazine assembly but also identifies a previously unrecognized catalytic role of a large WDR protein family.

25COASMA120:

Title: Single-Crystal X-ray Structures of Homochiral Brønsted Acidic Covalent Organic Frameworks

Bang Hou, Xing Han, Haomiao Xie et.al.

J. Am. Chem. Soc. 2025, 147, 14, 12127–12137
https://doi.org/10.1021/jacs.5c00458

Abstract: Determining the crystal structures of covalent organic frameworks (COFs) with atomic precision is pivotal for uncovering their properties and optimizing functionalities. However, the synthesis of high-quality single crystals of COFs suitable for X-ray diffraction analysis, especially chiral COFs (CCOFs), remains a formidable challenge. In this work, we report two three-dimensional (3D) CCOFs synthesized via imine condensation of tetrahedral tetraamine and tetraaldehydes derived from optically active 1,1′-biphenol phosphoryl chloride or thiophosphoryl chloride. Single crystals of varying sizes are obtained through either a low-temperature modulation strategy, yielding large crystals up to 100 μm, or a solvothermal method. The large single crystals are structurally characterized by single-crystal X-ray diffraction, achieving a resolution of 0.90 Å. These two CCOFs are isostructural and each features a 4-fold interpenetrated diamondoid open framework with all phosphoric acid groups periodically aligned within tubular helical channels, displaying enhanced Brønsted acidity compared to non-immobilized acids. The frameworks exhibit permanent porosity, chemical resistance in boiling water, 14 M NaOH, and 0.1 M HCl, and thermal stability up to 400 °C. Notably, these CCOFs serve as efficient and recyclable heterogeneous Brønsted acid catalysts in the asymmetric addition to aromatic aldehydes, enantioselective transfer hydrogenation of ketimines, and three-component direct asymmetric Mannich reactions involving aldimines and cyclic ketones, achieving good to high enantioselectivities (up to 99.5% ee) that surpass those obtained in analogous systems with homogeneous catalysts. This work represents the first successful demonstration of single-crystal structures of homochiral COFs, paving the way for in-depth investigations into structure–property relationships in enantioselective

processes and facilitating the design of novel functional chiral organic materials.

25COASMA121:

Title: Catalytic Aldehyde Decarbonylase Activity by a Thiolate-Bound Iron Porphyrin: Observation of a Peroxyhemiacetal Intermediate during Catalysis

Soumya Samanta, Srijan Sengupta, Triparna Roy, Apurba Pal, Abhishek Dey

J. Am. Chem. Soc. 2025, 147, 14, 12285–12297

https://doi.org/10.1021/jacs.5c01859

Abstract: Aldehyde decarbonylation is a key chemical step in nature that is involved in the biosynthesis of hormones and long-chain hydrocarbons where O2 is the oxidant. A cytochrome P450 enzyme, aromatase, catalyzes this reaction, where a thiolate-bound ferric peroxide is proposed to be the oxidant. Despite several attempts, only substoichiometric yields have been reported by synthetic iron porphyrins in organic solvents using peroxide. Several synthetic nonheme complexes have been reported to catalyze decarbonylation in stoichiometric yields using peroxides as oxidants. Catalytic decarbonylation with molecular O2 using either heme or nonheme complexes remains elusive. Iron picket-fence porphyrin is attached to thiol-terminated self-assembled monolayers. In situ resonance Raman spectroscopy reveals the accumulation of an Fe(III)-OOH intermediate with Fe–O and O–O vibrations at 579 cm–1 and 798 cm–1, respectively, during heterogeneous electrocatalytic O2 reduction in a pH 7 buffer solution. In the presence of different aldehydes in solution, catalytic aldehyde decarbonylase reactivity is observed with TON and TOF of ∼ 83000 and 277 s–1, respectively, for 2-methyl-2-phenylpropionaldehyde and ∼ 13000 and 45 s–1, respectively, for undecanal using molecular O2 in a pH 7 buffer solution. In situ SERRS-RDE in the presence of 2-phenylpropionaldehyde indicates the formation of a peroxyhemiacetal species with Fe–O, O–O, and C–O vibrations at 520 cm–1, 833 cm–1, and 1185 cm–1, respectively, as an intermediate in catalytic aldehyde decarbonylase activity.

25COASMA122:

Title: Subnanometric Nickel Phosphide Heteroclusters with Highly Active Niδ+–Pδ− Pairs for Nitrate Reduction toward Ammonia

Qi Hu, Chunyan Shang, Xinbao Chen et.al.

J. Am. Chem. Soc. 2025, 147, 14, 12228–12238

https://doi.org/10.1021/jacs.5c01455

Abstract: The development of efficient electrocatalysts for the neutral nitrate reduction reaction (NO3–RR) toward ammonia (NH3) is essential to address the environmental issues caused by NO3– but remains considerably challenging owing to the sluggish reaction kinetics of NO3–RR in neutral media. Herein, we report subnanometric heteroclusters with strongly coupled nickel–phosphorus (Ni–P) dual-active sites as electrocatalysts to boost the neutral NO3–RR. Experimental and theoretical results reveal that the subnanometric feature of Ni–P heteroclusters promotes the electron transfer from Ni to P, generating Niδ+–Pδ− active pairs, in which Niδ+ species are highly active for the NO3–RR and Pδ− tunes the interfacial water hydrogen bonding network to promote the water dissociation step and accelerate proton transfer during the NO3–RR. Consequently, in the neutral NO3–RR, Ni–P heteroclusters exhibit a large NH3 yield rate of 0.61 mmol h–1 cm–2 at −0.8 V versus reversible hydrogen

electrode, which is 2.8- and 3.3-fold larger than those on Ni–P nanoparticles and Ni clusters, respectively, and the generated NH3 exists as NH4+ in electrolytes. This study offers an efficient approach to boosting electrocatalytic reactions with multiple intermediates by designing subnanometric heteroclusters with strongly coupled active sites.

25COASMA123:

Title: Catalytic Enantioselective Smiles Rearrangement Enabled by the Directed Evolution of P450 Radical Aryl Migratases

Wenzhen Fu, Katherina Murcek, Jasper Chen et.al.

J. Am. Chem. Soc. 2025, 147, 14, 12197–12205

https://doi.org/10.1021/jacs.5c01179

Abstract: Despite its synthetic potential, catalytic enantioselective Smiles rearrangement has remained elusive. Through the directed evolution of P450 radical aryl migratases (P450Smiles's), we describe the first example of catalytic enantioselective Smiles rearrangement. A range of racemic N-arylsulfonyl-α-chloroamides could be transformed by P450Smiles in an enantioconvergent manner, affording acyclic amide products possessing an all-carbon quaternary stereocenter with excellent chemo- and enantioselectivity. Both electron-rich and electron-deficient substituents were compatible with the migrating aryl group, demonstrating this P450-catalyzed Smiles rearrangement is insensitive to the electronic properties of the migrating group. Importantly, our evolved P450 variants were capable of overriding the innate cyclization activity of the N-alkyl amidyl radical intermediate, allowing the chemoselective reductive formation of acyclic products. Classical molecular dynamics (MD) simulations revealed this unusual enzyme-controlled chemoselectivity stems from the restricted conformation of the amidyl radical within the enzyme active site, disfavoring the cyclization pathway. This new-to-nature biocatalytic asymmetric Smiles rearrangement showcases the synthetic potential of enzymatic chemo- and enantioselectivity control over highly reactive radical intermediates eluding small-molecule catalysts.

25COASMA124:

Title: Chiral Lewis Acid-Catalyzed Intramolecular [2 + 2] Photocycloaddition: Enantioselective Synthesis of Azaarene-Functionalized Azabicyclo[2.1.1]hexanes and Bicyclo[1.1.1]pentanes

Dong Tian, Yixing Pan, Xiaowei Zhao et.al.

J. Am. Chem. Soc. 2025, 147, 15, 12410–12417

https://doi.org/10.1021/jacs.5c03542

Abstract: We present an asymmetric intramolecular [2+2] photocycloaddition reaction enabled by a dual catalyst system involving DPZ as a photosensitizer and chiral Sc(III) complex, leading to azaarene-functionalized 2-azabicyclo[2.2.1]hexanes (aza-BCHs). The approach efficiently preventing racemization during subsequent nitrogen-deletion skeletal editing of aza-BCHs to yield 2-substituted bicyclo[1.1.1]pentanes (BCPs). The method achieves high ee and broad substrate scope, including the successful formation of all-carbon quaternary stereocenters. Furthermore, the successful activation of simple azaarene substrates by chiral Lewis acids in asymmetric photocatalysis highlights a notable contribution to this

field.

25COASMA125:

Title: Empowering Diastereoselective Cyclopropanation of Unactivated Alkenes with Sulfur Ylides through Nucleopalladation

Nityananda Ballav, Chandan Kumar Giri, Shib Nath Saha

J. Am. Chem. Soc. 2025, 147, 15, 13017–13026
https://doi.org/10.1021/jacs.5c03146

Abstract: Regio- and stereoselective cyclopropanation of unactivated alkenes under mild conditions remains a challenging yet fundamental transformation. We present a versatile palladium(II)-catalyzed method for the diastereoselective cyclopropanation of alkenyl amines and alkenyl acids, which leverages the nucleopalladation mechanism and the unique ambiphilic reactivity of sulfur ylides. This Pd(II)/Pd(IV) catalytic protocol selectively delivers anti-cyclopropanes for allylamines with a removable isoquinoline-1-carboxamide auxiliary, while enabling excellent syn-selectivity for alkenyl acid derivatives containing a 2-(aminomethyl)pyridine derivative as a directing group. The protocol is operationally simple and scalable, features a wide substrate generality, and also remains effective in the presence of various medicinally relevant scaffolds. The cyclopropane products were further transformed into 1,2,3-trifunctionalized cyclopropanes and engaged in an aza-Piancatelli reaction, introducing additional molecular complexity. DFT studies were performed to shed light on the reaction mechanism and the origins of the observed stereoselectivity.

25COASMA126:

Title: Palladium-Catalyzed Transfer Iodination from Aryl Iodides to Nonactivated C(sp3)–H Bonds

Emilien Le Saux, Bill Morand

J. Am. Chem. Soc. 2025, 147, 15, 12956–12961
https://doi.org/10.1021/jacs.5c02553

Abstract: We report a new strategy for the catalytic iodination of nonactivated C(sp3)–H bonds. The method merges the concepts of shuttle and light-enabled palladium catalysis to employ aryl iodides as both hydrogen atom transfer reagents and iodine donors. A noncanonical Pd0/PdI catalytic cycle is harnessed to transfer iodine from a C(sp2) to a C(sp3)–H bond under mild conditions, which tolerate sensitive functional groups. This mechanism is also applied to implement a C(sp3)–H thiolation that exploits reversible steps of the system.

25COASMA127:

Title: Spontaneous Exciton Dissociation in Sc-Doped Rutile TiO2 for Photocatalytic Overall Water Splitting with an Apparent Quantum Yield of 30%

Fei Qin, Yuyang Kang, Xingyuan San et.al.

J. Am. Chem. Soc. 2025, 147, 15, 12897–12907
https://doi.org/10.1021/jacs.5c01936

Abstract: Achieving high-efficiency photocatalytic overall water splitting with earth-abundant materials like TiO2 under ambient conditions is a compelling renewable energy

solution. However, this remains challenging due to both the presence of rich deep-level defects and lack of strong driving force in particulate photocatalysts, limiting the separation of photogenerated charges. Here, we developed a scandium (Sc)-doped rutile TiO2 with fully passivated detrimental Ti3+ defects and very strong built-in electric field arising from engineered (101)/(110) facet junctions. The Sc3+ doping enables a much lower exciton binding energy of 8.2 meV (28.6 meV for undoping) than room-temperature thermal fluctuation energy, indicating spontaneous exciton dissociation. These features enable the photogenerated electrons and holes to selectively transfer to the (110) and (101) facets, respectively. The resulting Sc-doped TiO2 with cocatalyst delivers photocatalytic overall water splitting with an apparent quantum yield of 30.3% at 360 nm and a solar-to-hydrogen conversion efficiency of 0.34%, representing the highest values reported for TiO2-based photocatalysts under ambient conditions.

25COASMA128:

Title: Investigating Reactivity and Selectivity in a Palladium-Catalyzed Heteroleptic Ligand System for Electrophilic Arene Fluorination

Shubham Deolka, Mohammad H. Samha, Aleria Garcia Roca et.al.

J. Am. Chem. Soc. 2025, 147, 15, 12878–12889

https://doi.org/10.1021/jacs.5c01738

Abstract: Methods to access fluorinated molecules are of significant interest to the medicinal and agrochemical industries. We report a series of high-valent PdIV complexes stabilized by two distinct ligand cores, which mediate electrophilic fluorination reactions with excellent yields and good regioselectivity. Using high-throughput experimentation and kinetic analysis, the distinct roles of each ligand were uncovered. Synthetic modulation of the catalyst alongside density functional theory transition state modeling provided evidence into the turnover-limiting step while revealing key insights into the origin of regioselectivity. This workflow presents a general strategy for exploring heteroleptic systems as well as synthetic enhancements to electrophilic fluorination reactions relevant to both industrial and academic settings.

25COASMA129:

Title: Enantioselective Desymmetrization of Biaryls via Cooperative Photoredox/Brønsted Acid Catalysis and Its Application to the Total Synthesis of Ancistrobrevolines

Junsoo Moon, Eunjoo Shin, Yongseok Kwon et.al.

J. Am. Chem. Soc. 2025, 147, 15, 12800–12810

https://doi.org/10.1021/jacs.5c01480

Abstract: Photoredox catalysis has emerged as a powerful tool for forming and breaking chemical bonds, further taking hold with its integration with asymmetric catalysis. While the dual-catalytic approach has led to successful examples of the control of stereogenic centers, the control of stereogenic axes has remained underexplored. In this study, an acylimine intermediate was generated through photoredox catalysis, and a symmetric substrate, 2-arylresorcinol, was desymmetrized with the aid of chiral phosphoric acid catalysis. Using this approach, a stereogenic center and stereogenic axis were successfully controlled to provide a

natural-product-driven compound. The origins of enantioselectivity and diastereoselectivity were investigated through a density functional theory study of four possible enantiodetermining transition states. Consequently, the first total syntheses of the ring-contracted naphthylisoquinoline alkaloid ancistrobrevolines A and B were accomplished concisely. This approach provides not only a novel methodology and strategy to synthesize naphthylisoquinoline alkaloids but also a direction to advance catalytic research and total synthesis studies.

25COASMA130:

Title: Cooperative Heterobimetallic CO2 Activation Involving a Mononuclear Aluminum(II) Intermediate

Roushan Prakash Singh, Kevin P. Quirion, Joshua Telser et.al.

J. Am. Chem. Soc. 2025, 147, 15, 12715–12721

https://doi.org/10.1021/jacs.5c00944

Abstract: Molecular chemistry of aluminum most commonly involves AlIII ions due to their noble gas electronic configurations. In contrast, the chemistry of AlII ions is underexplored and may contain undiscovered reaction manifolds. Here, we report the CO2 activation chemistry of a transient AlII intermediate supported by a chelating, dianionic ligand and investigate the electronic structure details and reaction mechanisms required to access this reactivity. We found that a heterobinuclear complex, (NON)Al–FeCp(CO)2 (1), undergoes Al–Fe bond homolysis at ambient conditions to reveal the [(NON)Al]•/[CpFe(CO)2]• radical pair in situ. The presence of predominantly Al-centered spin density (i.e., an AlII ion) within this radical pair was established by quantum-chemical calculations and with experiments in which radical scavengers (TEMPO, benzophenone) induce Al–Fe bond homolysis. Exposure of 1 to CO2 atmosphere resulted in insertion of CO2 into the Al–Fe bond. This net 2-electron CO2 reduction process was computationally modeled using density functional theory and direct dynamics simulations, revealing that reduction involves two 1-electron steps and, thus, depends on stabilization of high-energy [CO2]•– by coordination to aluminum. This mechanism for CO2 activation is unexpected given the canonical predisposition of CO2 for multielectron reduction processes and demonstrates the possibility of discovering new reaction profiles using earth-abundant elements in unusual oxidation states.

25COASMA131:

Title: Donor–Acceptor-π-Acceptor–Donor-Type Photosensitive Covalent Organic Framework for Effective Photocatalytic Aerobic Oxidation

Tian-Xiang Luan, Ling-Bao Xing, Ning Lu et.al.

J. Am. Chem. Soc. 2025, 147, 15, 12704–12714

https://doi.org/10.1021/jacs.5c00750

Abstract: Developing effective photocatalysts for the oxidation reaction is of great significance in chemical synthesis but is still challenging. Herein, linking photochromic triphenylamine with pyrene units by the in situ formed robust imidazole moieties, a covalent organic framework (COF), PyNTB-COF, containing a rare donor–acceptor-π-acceptor–donor (D-A-π-A-D) fragment, was successfully synthesized for photocatalytic aerobic oxidation. Structure characterizations confirm its crystalline framework, high porosity, and good

stability. Property studies reveal its photoelectric semiconductor feature with high photoresponsive charge separation and migration activity derived from the D-A-π-A-D fragments, proven by the experimental results and theoretical calculations. Photocatalytic experiments not only display its highly effective photoresponsive activity in triggering the generation of ·O2– under visible light irradiation but also exhibit its high photocatalytic efficiency in the aerobic oxidations of toluene and the amidation of aldehydes. This work demonstrates that the integration of photochromic units into framework materials to construct π-conjugated D–A moieties could enhance photocatalytic charge separation and migration efficiency, achieving promising photocatalysts for photocatalytic aerobic oxidation.

25COASMA132:

Title: Molecular Anodes for Electrocatalytic Water Oxidation Based on Self-Assembled Bilayers Driven by Electron Transfer Mediators

Paula Tris-Marzo, Daniele Veclani, Alessandro Venturini et.al.

J. Am. Chem. Soc. 2025, 147, 15, 12686–12695

https://doi.org/10.1021/jacs.5c00489

Abstract: The generation of solar fuels via water splitting with sunlight requires, among others, robust and efficient electrodes for the water oxidation reaction. For this purpose, the combination of powerful molecular catalysts and graphitic materials has been shown to work outstandingly well. However, in oxide-based materials, that are of enormous importance as conductive or semiconductive materials, the molecular catalysts either do not work or are transformed into the corresponding oxides. Here, we use a supramolecular strategy based on self-assembled bilayers where a silanolate with long alkyl chains is bonded to the electrode surface and acts as a platform to supramolecularly interact with multiple long alkyl chains attached to the water oxidation catalyst. In this manner, the catalyst and the electrolyte assembly are isolated from the oxide surface, conferring great stability, but at the same time, they are sufficiently close so that efficient electron transfer can take place from the catalyst to the electrode. Our best hybrid molecular anode works efficiently as a water oxidation catalyst at pH 7 without practically any activity losses, at current densities of 0.40 mA/cm2 for 15 h, giving more than 33,800 TONs and with a Faradaic efficiency of over 92% while maintaining intact its molecular nature. This work provides a successful proof of concept of the benefit of properly combining molecular catalysts with oxide-based materials to obtain the best of both worlds.

25COASMA133:

Title: Bioinspired Chloride-Assisted Protein Channels: Enhancing Proton Transport for Sustainable Energy Harvesting from Acidic Wastewater

Wenxiu Jiang, Xuan Ding, Zihao Huang et.al.

J. Am. Chem. Soc. 2025, 147, 15, 12604–12613

https://doi.org/10.1021/jacs.4c18730

Abstract: Highly efficient proton transfer in biological processes has driven the pursuit of synthetic analogs; however, replicating high proton permeance in natural systems remains a significant challenge. Herein, inspired by the function of the ClC-ec1 protein, we report the design of Cl–-assisted proton transport channels within a hybrid membrane composed of

covalent organic frameworks (COFs) integrated with aramid nanofibers (ANFs). By leveraging buffer layer-mediated interfacial polymerization and the flocculation behavior of ANF in aqueous environments, we establish robust hydrogen-bonding interactions between COFs and ANFs. The hydride material enables Cl– binding, significantly accelerating proton transport in a manner similar to that of the ClC-ec1 protein channel. In the presence of a small concentration of Cl– ions (0.1% of the proton concentration), the proton permeation rate is enhanced approximately by 3 times, reaching 9.8 mol m–2 h–2. Notably, the membrane facilitates sustainable osmotic power generation from acidic wastewater, delivering an output power density of 434.8 W m–2. Theoretical calculations revealed that ANF preferentially binds Cl–, promoting proton hopping and lowering the energy barrier for proton transport. This study establishes a new paradigm for bioinspired ion-assisted proton transport, presenting an approach for sustainable energy harvesting from acidic wastewater.

25COASMA134:

Title: s-Block Metal-Lanthanide Bonding: Direct Comparison of Mg–Yb and Mg–Ca Complexes

Sandeep Kumar Thakur, Nil Roig, Johannes Maurer et.al.

J. Am. Chem. Soc. 2025, 147, 15, 12555–12561
https://doi.org/10.1021/jacs.4c17853

Abstract: Despite considerable progress in understanding the fundamental aspects of metal–metal bonding, lanthanide-metal bonding is limited to interactions between lanthanide (Ln) metals and electron-rich p- or d-block metals. Exemplified by a Mg–Yb complex, we present synthesis and extensive computational analyses of the first s-block metal-Ln bond. Key to its formation is the unique Mg0 complex [(BDI*)MgNa]2 (1) which can be viewed as a dimer consisting of two magnesyl anions, (BDI*)Mg–, bridged by two Na+ cations (BDI* = HC[C(tBu)N-DIPeP]2, DIPeP = 2,6-CHEt2-phenyl). Reaction of dimeric 1 with (YbN’’2)2 (N’’ = N(SiMe3)2) quantitatively gave the mixed complex [(BDI*)MgNa/YbN’’2] (2-Yb) in which (BDI*)Mg– anions bridge between Yb2+ and Na+ cations (Mg–Yb: 3.466(1), Mg–Na: 3.415(1) Å). Atoms-In-Molecules shows Mg–Yb and Mg–Na bond paths corresponding to weak electrostatic interactions. Complex 2-Yb is isostructural to previously reported [(BDI*)MgNa/CaN’’2] (2-Ca). Weak Mg0-M2+ (M = Ca, Yb) bonding is supported by facile exchange reactions with (SrN’’2)2 leading to formation of [(BDI*)MgNa/SrN’’2] (2-Sr). Energy decomposition analysis (EDA-NOCV) confirmed major electrostatic Mg0-M2+ bonding (63–66%), while orbital interactions are less significant (19–20%). Both, 2-Ca and 2-Yb show considerable Mg0 → M2+ electron transfer leading to oxidation-state ambiguities (Mg0-M+II ↔ Mg+I-M+I). Effective-Oxidation-State calculations assign the following metal oxidation states, Na+I-Mg0-M+II, with a reliability index of 69–72%. Despite structural and electronic similarities, there are differences in reactivities. Complex 2-Ca reacts only as a 2-electron reducing agent whereas 2-Yb can deliver up to three electrons. This study includes reactions with N2O, TEMPO, and Me3PX (X = O, S, Se). While only 2-Ca could be converted in a complex with incorporated O2–, complexes with S2– or Se2– have been isolated for both.

25COASMA135:

Title: Selective Electrochemical Capture of Monovalent Cations Using Crown Ether-Functionalized COFs

Dong Jiang, Jonathan P. Hill, Joel Henzie et.al.

J. Am. Chem. Soc. 2025, 147, 15, 12460–12468
https://doi.org/10.1021/jacs.4c16346

Abstract: Electrochemical adsorption offers a promising approach for the separation of monovalent cations, which is an important but challenging subject in separation science. However, progress in this area has been hampered by the lack of suitable materials with effective ion selectivity. In this work, we present the synthesis of covalent organic frameworks (COFs) functionalized with a series of crown ethers (NCx-TAB-COFs, x donate 12, 15, 18, indicating the size of crown ether) for the efficient and highly selective electrochemical capture of monovalent cations. In our design, crown ether moieties act as confinement sites, imparting high selectivity for different monovalent cations depending on the cavity dimensions of the crown ether present. COFs electrodes prepared using the novel crown-COFs exhibit superior performance for the selective sequestration of monovalent (alkali metal) cations. Notably, 18-crown-6 ether-substituted COF (NC18-TAB-COF) shows a remarkable selectivity (14.26) for K+ over Na+ and a substantial Rb+/Na+ selectivity of 22.4. Furthermore, NCx-TAB-COFs maintain their remarkable selectivity and capacity under mixed-cation conditions. Density functional theory calculations and molecular dynamics simulations suggest that the unexpectedly high selectivity for larger cations is likely due to diverse binding modes in conjunction with the porous structure of the COFs. Given their lower dehydration-free energies and smaller hydrodynamic radii, K+, Rb+, and Cs+ more readily permeate the confined channels of COFs. In contrast, Na+ and Li+, with higher dehydration-free energies and hydrodynamic radii, diffuse into the NCx-TAB-COFs structure at a much slower rate and are bound predominantly to the surfaces of the COFs.

25COASMA136:

Title: Oxide Support Inert in Its Interaction with Metal but Active in Its Interaction with Oxide and Vice Versa

Cui Dong, Rongtan Li, Zhenping Qu et.al.

J. Am. Chem. Soc. 2025, 147, 16, 13210–13219
https://doi.org/10.1021/jacs.4c17075

Abstract: Supported metal or oxide nanostructures catalyze many industrial reactions, where the interaction of metal or oxide overlayer with its support can have a substantial influence on catalytic performance. In this work, we show that small Pt species can be well stabilized on CeO2 under both H2-containing and O2-containing atmospheres but sintering happens on SiO2, indicating that CeO2 is active whereas SiO2 is inert in Pt–support interaction. On the other hand, Co oxide (CoOx) supported on SiO2 can maintain a low-valence Co2+ state both in air and during CO2 hydrogenation to CO, indicating a strong interaction of CoOx with SiO2. However, the CoOx overlayer has a weak interaction with CeO2 and is easily reduced to metallic Co during the CO2 hydrogenation reaction producing CH4. Thus, SiO2 is active, but CeO2 is inert for CoOx–support interaction, which is counter to the common sense from the Pt/oxide systems. Systematic studies in stability behaviors of Pt and CoOx nanocatalysts

supported on various oxides show that the reducibility of the oxide supports can be used to describe the catalyst–support interaction. Oxide supports with high reducibility or low metal–oxygen bond strength interact strongly with Pt and other metals, showing high metalphilicity. Conversely, oxide supports with low reducibility or high metal–oxygen bond strength have strong interaction with CoOx and other oxides, having high oxidephilicity.

25COASMA137:

Title: Cyclometallated Co(III) Complexes with Lowest-Energy Charge Transfer Excited States Accessible with Visible Light

Spencer T. Burton, Gyunhee Lee, Curtis E. Moore et.al.

J. Am. Chem. Soc. 2025, 147, 16, 13315–13327

https://doi.org/10.1021/jacs.4c18299

Abstract: The Co(III) complexes, cis-[Co(ppy)2(L)]PF6, where ppy = 2-phenylpyridine and L = bpy (2,2′-bipyridine; 1), phen (1,10-phenanthroline; 2), and DAP (1,12-diazaperylene; 3), are reported and their photophysical properties were investigated to evaluate their potential as sensitizers for applications that include solar energy conversion schemes and photoredox catalysis. Calculations show that cyclometallation in the cis-[Co(ppy)2(L)]PF6 series affords strong Co(dπ)/ppy(π) orbital interactions that result in a Co/ppy(π*) highest occupied molecular orbital (HOMO) and a lowest unoccupied molecular orbital (LUMO) localized on the diimine ligand, L(π*). Complexes 1–3 exhibit relatively invariant oxidation potentials, whereas the reduction event is dependent on the identity of the diimine ligand, L, consistent with the theoretical predictions. For 3 a broad Co/ppy(π*) → L(π*) metal/ligand-to-ligand charge transfer (ML-LCT) absorption band is observed in CH3CN with a maxima at 507 nm, extending beyond 600 nm. Upon excitation of the 1ML-LCT transition, transient absorption features consistent with the population of a 3ML-LCT excited state with lifetimes, τ, of 3.0 ps, 4.6 and 42 ps for 1, 2 and 3 in CH3CN respectively are observed. Upon irradiation with 505 nm, 3 is able to reduce methyl viologen (MV2+), an electron acceptor commonly in photocatalytic schemes. To our knowledge, 3 represents the first heteroleptic molecular Co(III) complex that combines cyclometallation with a diimine ligand with lowest-lying metal-to-ligand charge transfer excited states able to undergo photoinduced charge transfer with low-energy green light. As such, the structural design of 3 represents an important step toward d6 photosensitizers based on earth abundant metals.

25COASMA138:

Title: Versatile Solid-State Medical Superglue Precursors of α-Lipoic Acid

Subhajit Pal, Erika E. Salzman, Dominic Ramirez et.al.

J. Am. Chem. Soc. 2025, 147, 16, 13377–13384

https://doi.org/10.1021/jacs.4c18448

Abstract: α-Lipoic acid (αLA) is an attractive building block for medical adhesives. However, due to poor water solubility of αLA and high hydrophobicity of poly(αLA), elevated temperatures, organic solvents, or complex preparations are typically required to obtain and deliver αLA-based adhesives to biological tissue. Here, we report αLA-based powder and low-viscosity liquid superglues that polymerize and bond rapidly upon contact with wet tissue. A monomeric mixture of αLA, sodium lipoate, and an activated ester of

lipoic acid was used to formulate the versatile adhesives. Stress–strain measurements of the wet adhesives confirmed the high flexibility of the adhesive. Moreover, a small molecule regenerative drug was successfully incorporated into and released from the adhesive without altering the physical and adhesive properties. In vitro and in vivo studies of the developed adhesives confirmed their cell and tissue compatibility, biodegradability, and potential for sustained drug delivery. Moreover, due to the inherent ionic nature of the adhesives, they demonstrated high electric conductivity and sensitivity to deformation, allowing for the development of a tissue-adherent strain sensor.

25COASMA139:

Title: Electrochemical Benzylic C–H Carboxylation

Weimei Zeng, Chengyi Peng, Youai Qiu et.al.

J. Am. Chem. Soc. 2025, 147, 16, 13461–13470

https://doi.org/10.1021/jacs.5c00259

Abstract: Direct benzylic C–H carboxylation stands as a high atom economy, efficient, and convenient route for the synthesis of valuable benzylic carboxylic acids, which are of great significance in many pharmaceuticals and bioactive molecules. However, the inherent inertness of both benzylic C–H bonds and carbon dioxide presents a great challenge for further transformations. Herein, we report our efforts to overcome this obstacle via halide-promoted linear paired electrolysis to generate various benzylic carboxylic acids. Remarkably, this process is transition-metal- and base-free, making it environmentally benign and cost-effective. Besides, it is suitable for constructing a wide range of primary, secondary, and tertiary benzylic carboxylic acids under mild reaction conditions, demonstrating broad substrate scopes and good functional group tolerance. Furthermore, our protocol enables the direct synthesis of some drug molecules, including Flurbiprofen, Ibuprofen, and Naproxen, and facilitates the late-stage modification of complex compounds, showcasing the practical application in synthetic chemistry and underscores its potential to advance the synthesis of benzylic carboxylic acids and related compounds.

25COASMA140:

Title: Rapid Fluorochromic Sensing of Tertiary Amines and Opioids via Dual-Emissive Ground and Excited Charge-Transfer States

Aoyuan Cheng, Xuewen Gu, Chengze Yang et.al.

J. Am. Chem. Soc. 2025, 147, 16, 13512–13521

https://doi.org/10.1021/jacs.5c00425

Abstract: The recognition and differentiation of organic amines are crucial for applications in drug analysis, food spoilage, biomedical assays, and clinical diagnostics. Existing luminescence-based recognition methods for amines predominantly rely on fluorescence quenching, limiting the scope of sensitive and selective detection. Here, we present a fluorochromic approach for rapidly distinguishing different organic amines based on their unique excited-state and ground-state interactions with a naphthalimide derivative under ultraviolet light. Our findings reveal that the photoluminescence quantum yield and emission color are significantly influenced by the substituent group and the molecular flexibility of the amine. Specifically, primary amines, together with other common lone-pair donors, such as

alcohol, ether, thiol, thioether, and phosphine, did not exhibit photoluminescence changes, while secondary amines exhibited only weak emission. For tertiary amines, however, bright green photoluminescence activation was rapidly produced for molecules containing at least one methyl group; red-shifted yellow emission was observed for ones with bulkier side groups other than methyl; and for conformationally locked bicycloamines, no emission was observed. In addition, this fluorochromic process of the naphthalimide derivative not only depends on tertiary amine substituent groups but also shows distinctly different ground- and excited-state photoluminescence dynamics in time-resolved spectroscopy. Based on these differences, a qualitative method is developed for visual recognition of natural and synthetic opioids, including heroin, fentanyl, and metonitazene, which is more facile and rapid compared to current methods such as the Marquis reagent kit, and could facilitate onsite testing, real-time monitoring, and streamlined workflows in both laboratory and field settings.

25COASMA141:

Title: Harnessing Mechanochemistry for Direct Synthesis of Imine-Based Metal–Organic Frameworks

Zhuorigebatu Tegudeer, Luke C. Davenport, Martin E. Kordesch et.al.

J. Am. Chem. Soc. 2025, 147, 16, 13522–13530

https://doi.org/10.1021/jacs.5c00460

Abstract: The growth of metal–organic frameworks (MOFs) is most frequently accessed by the direct assembly of metal cations and multitopic ready-to-connect ligands under solvothermal conditions. However, such nonambient conditions are expected to impose a synthetic challenge to incorporate degradable ligands into MOFs. This explains why imine-based MOFs are scarce as the imine motif is usually prone to decompose through hydrolysis. This work not only showcases mechanochemistry as an ambient, sustainable, and high-yield strategy for synthesizing a variety of imine-based MOFs but also achieves the integration of ligand synthesis and MOF growth into a single tandem step. Thus, this work provides straightforward access to imine-based MOFs, a subfamily of historically challenging MOF materials.

25COASMA142:

Title: Hydrodealkenylative C(sp3)–C(sp2) Bond Fragmentation Using Isayama–Mukaiyama Peroxidation

Jeremy H. Dworkin, Zhuoxi M. Chen, Kathleen C. Cheasty et.al.

J. Am. Chem. Soc. 2025, 147, 16, 13531–13544

https://doi.org/10.1021/jacs.5c00540

Abstract: Advancements in radical capture strategies have expanded the range of products accessible from alkenes through dealkenylative synthesis. These methods, however, are still limited, as they rely on ozonolysis to generate the key peroxide intermediates from alkenes. Ozonolysis has several limitations. It is not compatible with alkenes containing electron-rich aromatics. It is also inapplicable to certain alkene substitution patterns in the context of dealkenylative synthesis. Additionally, it struggles with sterically hindered alkenes, internal nucleophiles and electrophiles, and allylic alcohols. In this paper, using Isayama–Mukaiyama peroxidation (IMP), we address the limitations of ozonolysis to rescue previously

inaccessible alkene substrates and broaden the applicability of dealkenylative functionalization. In particular, we apply IMP in hydrodealkenylation and describe a novel radical hydrogenation condition─employing catalytic [FeIII], catalytic benzenethiol, and γ-terpinene in refluxing methanol─to resolve β-scission issues associated with IMP-generated alkyl silylperoxides.

25COASMA143:

Title: Single-Atom Saturation: A Fundamental Principle for Single-Atom-Site Catalyst Design

Chunjin Ren, Yu Cui, Qiang Li et.al.

J. Am. Chem. Soc. 2025, 147, 16, 13610–13617

https://doi.org/10.1021/jacs.5c00643

Abstract: Single-atom alloys (SAAs), with twin advantages of alloys and single-atom catalysts, have emerged as an innovative class of electrocatalysts. This uniqueness is expected to achieve unattainable catalytic performance but simultaneously gives rise to the absence of guidelines for designing desired SAAs. Herein, we proposed a fundamental principle, single-atom saturation (SSA), to quantify the binding strength of different intermediates on SAAs, enabling the rapid and qualitative evaluation of the catalytic activity across various reactions. SSA is rationalized by combining the variation of electronic structure (d electron occupancy saturation) and geometrical structure (coordination saturation) of the single guest atom as well as the effect of the host atom type and the intermediate adsorption configuration. Based on the insights given by SSA, Pd1Cu(111), Ru1Cu(111), Ir1Ag(111), Pt1Ag(111), and Pt1Cu(111) are predicted to possess excellent activity for CO2 reduction, N2 reduction, O2 evolution, O2 reduction, and H2 evolution reactions, respectively, most of which are supported by reported experiments. Moreover, SSA is also applicable to nitrogen-doped graphene-supported single-atom catalysts (SACs) with ultrahigh accuracy. In general, single-atom saturation is a concise, interpretable, and universal descriptor that deciphers the structure–activity relation of SAAs across various reactions, where the insights revealed also offer a simple and fundamental principle for the design of excellent single-atom-site catalysts.

25COASMA144:

Title: Aqueous-Phase Synthesis of Cyclic Trinuclear Cluster-Based Metal–Organic Frameworks

Kun Wu, Wei Zhao, Ling Huang et.al.

J. Am. Chem. Soc. 2025, 147, 16, 13711–13720

https://doi.org/10.1021/jacs.5c01434

Abstract: The synthesis of metal–organic frameworks (MOFs) often involves high-boiling-point organic solvents, which can have extensive environmental impact and limit their large-scale applications. Here, we present a one-pot aqueous-phase approach for the rapid preparation of 33 trinuclear-copper-cluster-based MOFs (1 to 33) with different pyrazoles under ultrasonic irradiation. To address the water-solubility challenge of organic linkers, we employ aromatic amines/aldehydes and pyrazole aldehydes/amines to in situ generate imine-based pyrazoles. This linker dismantling strategy enables the formation of low-concentration

pyrazoles, which are essential for the assembly of trinuclear-copper-cluster-based MOFs in the aqueous phase. The use of preassembled trinuclear gold complexes instead of aromatic amines affords an Au–Cu-based MOF (34) of alternating gold and copper clusters, a rare example of MOFs with mixed yet precise arrangement of metal compositions. Additionally, the direct addition of pyruvic acid to the reaction mixture results in the facile synthesis of a carboxylic-acid-functionalized MOF (35), eliminating the need for preinstallation or postmodification steps in traditional MOF synthesis. Furthermore, we demonstrate 11-AA as an efficient photocatalyst for cross-dehydrogenative coupling (CDC) reactions, exploiting the synergetic effect of substrate activation on the copper sites and subsequent coupling initiated by the photosensitive organic linkers. This work offers a simple solution for making MOFs with minimal environmental impact; it also opens up possibilities for developing multifunctional MOFs for diverse applications.

25COASMA145:

Title: Minimally Protected and Stereoselective O-Glycosylation of Carboxylic Acid Allows Rapid Access to α-1-O- and 2-O-Acyl Glycosides

Bangxing Hao, Rongxia Li, Panpan Wang et.al.

J. Am. Chem. Soc. 2025, 147, 16, 13744–13753

https://doi.org/10.1021/jacs.5c01845

Abstract: We herein reported a catalytic, minimally protected, and highly α-stereoselective glycosylation protocol using carboxylic acid as an acceptor and glycosyl 8-alkynyl-1-naphthoate as a donor, enabling efficient access to unprotected α-1-O- and 2-O-acyl glycosides. This method demonstrates excellent functional compatibility and scope generality, allowing for the glycosylation of a wide range of complex carboxylic acids. Notably, we successfully synthesized two natural products, α-penta-O-galloyl-d-glucopyranose and nyctanthesin A, using this protocol. Mechanistic studies highlighted the crucial role of the 1-O ester functionality in ensuring chemoselectivity and the important contribution of the 2-O functionality in facilitating the reaction.

25COASMA146:

Title: Unraveling the Unique Behavior of Atomically Dispersed Pt on Zeolite Fe-DeAlBEA for Catalyzing Propane Dehydrogenation with Cofed Hydrogen

Afnan Alghannam, Alexander J. Pattison, Sonali Das et.al.

J. Am. Chem. Soc. 2025, 147, 16, 13784–13798

https://doi.org/10.1021/jacs.5c01730

Abstract: Propene, used on a large scale to manufacture polypropylene and several commodity chemicals, is increasingly produced by catalytic propane dehydrogenation (PDH). Atomically dispersed Pt has emerged as a promising candidate catalyst for PDH; however, stabilizing atomically dispersed Pt at high temperatures is challenging. Here, we demonstrate the use of dealuminated zeolite beta with a high Fe content as a host for stabilizing isolated Pt, which is anchored strongly to the zeolite support by Pt–Fe bonds. The isolated Pt–Fe sites exhibit promising PDH performance, including a high apparent forward rate coefficient for propene formation (404.8–26.4 mol propene/mol Pt·bar·s) and a high selectivity (≥96%) at 823 K in the presence of H2. Kinetics data characterizing the rate of PDH with a range of Pt

loadings show that atomically dispersed Pt catalyzes propene formation at rates independent of H2 partial pressure, whereas metallic Pt clusters, formed at high Pt loadings, catalyze the reaction with a slightly negative dependence on H2 partial pressure. The shift in Pt speciation with Pt loading, confirmed by infrared spectroscopy of adsorbed CO, X-ray absorption spectroscopy, and high-angle angular dark field scanning transmission electron microscopy, suggests that the observed change in kinetics with Pt dispersion is a consequence of a change in the reaction mechanism.

25COASMA147:

Title: Total Synthesis of (+)-Hazuntiphylline, (−)-Anhydrohazuntiphyllidine, and (−)-Hazuntiphyllidine

Robert-Cristian Raclea, Marius Mewald, Kolby L. White et.al.

J. Am. Chem. Soc. 2025,

https://doi.org/10.1021/jacs.5c01932

Abstract: The first total synthesis of the bisindole alkaloids (+)-hazuntiphylline, (−)-anhydrohazuntiphyllidine, and (−)-hazuntiphyllidine is described. We envisioned an efficient synthetic strategy based on a plausible biosynthetic hypothesis for the rapid assembly of these complex alkaloids via successive methylenation of an oxidized variant of the natural product (−)-mehranine. Our concise synthesis of these alkaloids required the development of completely stereoselective double alkylation sequences of transiently formed C3-enamines and precise timing for hydration of intricate intermediates. Whereas homodimerization of a C3-methylene mehranine-derivative exclusively gave (−)-3-epi-anhydrohazuntiphyllidine, an alternative alkylation cascade was developed to afford the natural products (−)-anhydrohazuntiphyllidine and (+)-hazuntiphylline. Insights gained in these studies concerning the intermediacy of hydrated intermediates enabled a completely stereoselective synthesis of (−)-hazuntiphyllidine, the most complex member of the Hazunta alkaloids. We discuss our hypothesis for the rapid assembly of these intriguing alkaloids, including our completely controlled access to both the natural and epimeric C3-quaternary stereochemistry of anhydrohazuntiphyllidine, and analysis of plausible biosynthetic intermediates including a sensitive methylenebisdesmethylmehranine-derivative, highlighting divergent pathways to each natural alkaloid based on the order of C–C and C–N bond formation and the hydration of putative intermediates.

25COASMA148:

Title: Sulfenylcarbene-Mediated Carbon Atom Insertion for the Late-Stage Functionalization of N-Heterocycles

Prakash Kafle, Deacon Herndon, Indrajeet Sharma et.al.

J. Am. Chem. Soc. 2025, 147, 16, 13824–13832

https://doi.org/10.1021/jacs.5c02012

Abstract: Late-stage functionalization (LSF) is a crucial strategy in drug discovery, allowing the modification of complex molecules, including pharmaceuticals, to enhance chemical diversity in drug libraries. We harness the chemoselectivity of sulfenylcarbenes, which selectively react with alkenes even in the presence of more reactive functional groups such as alcohols, carboxylic acids, and amines. This reactivity allows sulfenylcarbenes to insert a

single carbon atom bearing diverse functional groups, transforming pyrroles, indoles, and imidazoles into synthetically challenging pyridines, quinolines, and pyrimidines, respectively. Sulfenylcarbene precursors are easily synthesized in two steps from commercially available reagents. Our metal-free LSF approach employs benchtop-stable sulfenylcarbene precursors and enables late-stage modification of natural products, amino acids, pharmaceuticals, and C-glycosides. Mechanistic studies and density functional theory (DFT) calculations were conducted to investigate the regio- and chemoselectivity outcomes.

25COASMA149:

Title: Ultrasound-Energized OX40L-Expressing Biohybrid for Multidimensional Mobilization of Sustained T Cell-Mediated Antitumor Immunity and Potent Sono-Immunotherapy

Mengyun Liang, Xiaoying Kang, Hanwen Liu et.al.

J. Am. Chem. Soc. 2025, 147, 16, 13833–13850

https://doi.org/10.1021/jacs.5c02025

Abstract: Harnessing immunostimulation to reinvigorate antitumor effector immune cells represents a promising strategy for tumor eradication. However, achieving durable clinical outcomes necessitates multidimensional activation to sustain robust immune responses. Here, we present an ultrasound-empowered living biohybrid that strategically mobilizes T-cell-mediated immunity for potent tumor sono-immunotherapy. Through synthetic biology, we engineer bacteria to express a fusion protein encoding the costimulatory OX40 ligand (OX40L), and further functionalize them with a high-performance polymer sonosensitizer tethered via a reactive oxygen species-cleavable linker. Upon ultrasound irradiation, the sono-activated nanocargoes detach from the bacterial surface, facilitating cellular entry and exposing immune-stimulating OX40L. The potent sonodynamic effects, coupled with the native immunogenicity of bacteria, promotes tumor-associated antigen release, fosters a proinflammatory microenvironment, and drives dendritic cell maturation, thereby priming cytotoxic T-cell activation. The OX40L expressed by the engineered bacteria amplifies and sustains T-cell activity, orchestrating a robust and durable antitumor response. This cascade-amplified immune activation effectively suppresses tumor growth, induces long-lasting immune memory, and provides protection against tumor metastasis and recurrence, significantly enhancing survival outcomes. By integrating ultrasound-energized nanoadjuvants with costimulatory immune boosters, this hybrid living biotherapeutic platform offers a versatile and powerful strategy for multidimensional immune activation, advancing the frontier of cancer sono-immunotherapy.

25COASMA150:

Title: Involving Carbene or Not? Mechanism of Corey–Winter Reaction

Pan Zhang, Zhi-Xiang Yu et.al.

J. Am. Chem. Soc. 2025, 147, 16, 13915–13927

https://doi.org/10.1021/jacs.5c02629

Abstract: The mechanism of the Corey–Winter reaction is unclear, even though this reaction, discovered more than 60 years ago, has evolved as an indispensable method of synthesizing olefins from diols. We report a computational study of the mechanism of the Corey–Winter

reaction, ruling out three well-known pathways of this reaction and proposing a new pathway consistent with the experimental observations. This new pathway starts from nucleophilic addition of phosphite to the carbon (not the sulfur) atom of the cyclic thionocarbonates. This step is followed by the intramolecular addition of S to P, generating thiaphosphirane intermediates. Elimination of phosphorothioates then takes place, giving oxygen-heterocyclic carbenes (OHCs). Finally, the cycloreversion of the OHCs gives carbon dioxide and the target olefin products. Calculations support that the OHC intermediates are involved in the Corey–Winter reaction. In addition, the Woodward–Hoffmann orbital correlation and electron flow pattern for the cycloreversion process of the OHCs to olefins and carbon dioxide have been revised. Moreover, why diazaphospholidine can accelerate the Corey–Winter reaction has been rationalized in this study by multivariable linear regression analysis.

25COASMA151:

Title: A Bimolecular Diels–Alder Reaction Mediated by Inclusion in a Polar Bis-calix[4]pyrrole Octa-Imine Cage

Jiaming Huang, Pablo Ballester et.al.

J. Am. Chem. Soc. 2025, 147, 16, 13962–13972

https://doi.org/10.1021/jacs.5c03361

Abstract: We describe using a dynamically self-assembled octa-imine cage as a molecular flask to accelerate a bimolecular Diels–Alder reaction. We investigate the cage's binding properties using 1H NMR spectroscopic titrations, ITC experiments, and X-ray crystallography. We detect and characterize the formation of the ternary complex (Michaelis) in solution. A detailed kinetic analysis of the reaction data supports that the cage's acceleration is provided by including the two reactants, resulting in an effective molarity (EM) of ∼40 M. Exo-selectivity and shift of the reaction's chemical equilibrium are also encountered in the cage's confined space. Our results mimic enzymes' ability to bind two substrates in a polar cavity, using directional interactions, and accelerate their stereoselective reaction, with the potential for cavity engineering to enable other reactions.

25COASMA152:

Title: After 75 Years, an Alternative to Edman Degradation: A Mechanistic and Efficiency Study of a Base-Induced Method for N-Terminal Peptide Sequencing

Harnimarta Deol, Ava Raeisbahrami, Phuoc H.T. Ngo et.al.

J. Am. Chem. Soc. 2025, 147, 16, 13973–13982

https://doi.org/10.1021/jacs.5c03385

Abstract: The sequencing of peptides via N-terminal amino acid removal is a classic reaction termed Edman degradation. This method involves repeated treatment of the N-terminal amino group of a peptide with phenyl isothiocyanate (PITC), followed by treatment with trifluoroacetic acid. Spurred by the need for an alternative non-acid-based chemistry for next-generation protein sequencing technologies, we developed a base-induced N-terminal degradation method. Several N-terminal derivatization reagents carrying supernucleophiles were tested. After rounds of iterative designs, compound DR3, with a N-hydroxysuccinimide as a leaving group and hydrazinecarboxamide as the supernucleophile, demonstrated the highest yield for the peptide derivatization step and the most efficient elimination of the N-

terminal amino acid in just 1% of a hydroxide salt. The method successfully removed all 20 amino acids at the N-terminus in high yield. The technique demonstrates compatibility with oligonucleic acids, which differs from Edman degradation due to their inherent sensitivity to acidic environments. To demonstrate the practical application of our approach, we sequenced amino acids sequentially from a peptide, effectively determining the sequence of an unknown peptide. Notably, our methodology was successfully applied to mixtures of peptides derived from protein samples, where a significant fraction of the peptides derivatized with DR3 underwent elimination of their N-terminal amino acid upon addition of base. Overall, although our method does not outperform Edman degradation in efficiency, it serves as a valuable alternative in cases where base-induced cleavage is advantageous, particularly for preserving acid-sensitive functionalities.

25COASMA153:

Title: Regiodivergent Hydroamidation of Alkenes via Cobalt-Hydride Catalysis

Bingxue Liu, Qianqian Lu, Xiao Hu et.al.

J. Am. Chem. Soc. 2025, 147, 16, 13983–13992

https://doi.org/10.1021/jacs.5c03484

Abstract: Regiodivergent hydroamin(d)ation of alkenes presents a valuable strategy for the synthesis of diverse amines or amides from a common set of starting materials, yet achieving controlled regioselectivity remains a significant challenge. In this work, we present a cobalt-catalyzed regiodivergent hydroamidation of alkenes, enabling enantioselective ipso- and migratory hydroamidation of heterocyclic alkenes. The ability to finely tune various reaction parameters allows for a seamless switch in regioselectivity. Notably, ipso- and migratory selectivity are governed by the choice of cobalt catalyst anions. Mechanistic studies reveal a neutral Co–H species mediating ipso-hydroamidation and a cationic Co–H intermediate promoting migratory hydroamidation. This protocol exhibits a broad substrate scope, high functional group tolerance, and provides an efficient pathway for synthetizing structurally diverse amides.

25COASMA154:

Title: Electrocatalytic Ethylene Glycol to Long-Chain C3+ α-Hydroxycarboxylic Acids via Cross-Coupling with Primary Alcohols

Qiujin Shi, Yu-Quan Zhu, Xiang Liu et.al.

J. Am. Chem. Soc. 2025, 147, 16, 14004–14014

https://doi.org/10.1021/jacs.5c04034

Abstract: Electrocatalytic conversion of ethylene glycol (EG) into α-hydroxycarboxylic acids (α-HCAs) holds great importance for advancing sustainable chemical development since EG is widely accessible in polyethylene terephthalate (PET) plastic and biomass. Herein, we report the direct electrocatalytic cross-coupling of EG and primary C1–C4 alcohol, producing carbon-chain-propagated C3–C6 α-HCAs over a gold (Au) catalyst. Taking EG and methanol (MeOH) cross-coupling to lactic acid (LA) as an example, experimental evidence shows that stabilization of the aldehyde intermediates (glycolaldehyde and formaldehyde from EG and MeOH, respectively) without overoxidation is important for the following cross-coupling via aldol condensation and thus LA formation. Based on this

understanding, we systematically modulate the catalyst and reaction conditions, achieving a high LA productivity of 268.1 μmol cm–2 h–1 with a Faradaic efficiency of 28.7% at a constant current of 100 mA cm–2. The carbon-chain propagation strategy shows generality for EG cross-coupling with C1–C4 primary alcohols, successfully producing C3–C6 α-HCAs. As a proof of concept, a postconsumer PET bottle is converted to LA with a good productivity of 224.5 μmol cm–2 in a 2 h electrolysis. This work demonstrates the possibility of the electrocatalytic strategy to convert EG into long-chain compounds via C–C bond cross-coupling, representing a crucial step toward building a sustainable society.

25COASMA155:

Title: Electric-Double-Layer Mechanism of Surface Oxophilicity in Regulating the Alkaline Hydrogen Electrocatalytic Kinetics

Yaling Jiang, Peimeng Qiu, Qinghua Liu et.al.

J. Am. Chem. Soc. 2025, 147, 17, 14122–14130

https://doi.org/10.1021/jacs.4c14511

Abstract: Regulating the surface oxophilicity of the electrocatalyst is known as an efficient strategy to mitigate the order-of-magnitude kinetic slowdown of hydrogen electrocatalysis in a base, which is of great scientific and technological significance. So far, its mechanistic origin remains mainly ascribed to the bifunctional or electronic effects that revolve around the catalyst–intermediate interactions and is under extensive debate. In addition, the understanding from the perspective of interfacial electric-double-layer (EDL) structures, which should also strongly depend on the electrode property, is still lacking. Here, by decorating a Pt electrode with Mo, Ru, Rh, and Au metal atoms to tune surface oxophilicity and systematically combining electrochemical activity tests, in situ surface-enhanced infrared absorption spectroscopy, density functional theory calculation, and ab initio molecular dynamics simulation, we found that there exist consistent volcano-type relationships between *OH adsorption strength and alkaline hydrogen evolution activity, the stretching/bending vibration information on interfacial water, and the potential of zero charge (PZC) of the electrode. This demonstrates that the origin of surface oxophilicity in impacting the alkaline hydrogen electrocatalytic activity lies in its modification toward the electrode PZC, which thereby dictates the electric field strength, rigidity, and hydrogen bonding network structure in EDL and ultimately governs the interfacial proton transfer kinetics. These findings emphasize the importance of focusing on electrocatalytic interface structures to understand electrode property-dependent reaction kinetics.

25COASMA156:

Title: Photo-Switchable Supramolecular Interactions Regulate K+ Transmembrane Transport and Cancer Cell Apoptosis

Cong Li, Yaqi Wu, Sheng Bao et.al.

J. Am. Chem. Soc. 2025, 147, 17, 14139–14153

https://doi.org/10.1021/jacs.4c14583

Abstract: Natural channel proteins (NCPs) have numerous ion transport modes, but it remains a big challenge to replicate this trait by artificial ion transport systems. Herein, we present an azobenzene-incorporated single-chain random heteropolymers (RHPs)-derived

biomimetic K+ channel P3, which can switch between three ion transport states ("ON," "Partially OFF," and "Totally OFF") in both liposomes and cancer cells. The conformational adjustments of P3 activated by light-modulating two groups of supramolecular interactions ((1) hydrogen bonding and π–π interactions; (2) host–guest interactions) realize these switches, resembling the protein mechanisms that govern activity. Underlying molecular mechanisms are the photoisomerization of azobenzene moieties in P3 and their complexation with β-cyclodextrin (β-CD), enabling the exploit of a "one stone (azobenzene moiety), two birds (supramolecular interactions)" strategy. Mechanistic investigations demonstrate that P3-induced substantial K+ efflux (a 50% drop within just 4 min) causes endoplasmic reticulum (ER) stress, intriguing Ca2+ sparks, enhanced reactive oxygen species (ROS), and finally severe mitochondria-dependent apoptosis. This NCP-like channel (P3) is expected to provide new opportunities for a deeper understanding of the internal mechanisms of NCPs, as well as for treating cancer and other diseases.

25COASMA157:

Title: Terminal Vanadium Hydride through Oxidative C–H Cleavage and Its Application in Reduction of O2

Lei Zheng, Yun-Shu Cui, Dong-Ping Chen et.al.

J. Am. Chem. Soc. 2025, 147, 17, 14154–14162

https://doi.org/10.1021/jacs.4c14758

Abstract: We reported the synthesis and characterization of a novel vanadium hydride complex {[DippN2NCH2C6H4]VH}2{K}2 (2) obtained through intramolecular Caryl-H oxidative addition with an in situ-generated low-valent vanadium intermediate. This vanadium hydride exhibits strong reducing properties and is capable of activating O2 through a 4-electron reduction process. Simultaneously, it forms dioxovanadate complex 5 with a regenerated Csp2-H bond and oxovanadium complex 6. Feasible mechanisms for the formation of 5 and 6 were proposed based on the deuterium-labeled experiments and DFT calculations.

25COASMA158:

Title: The Role of Boron Reagents in Determining the Site-Selectivity of Pyridine(dicarbene) Cobalt-Catalyzed C–H Borylation of Fluorinated Arenes

Haozheng Li, Hanna H. Cramer, Jose B. Roque et.al.

J. Am. Chem. Soc. 2025, 147, 17, 14163–14173

https://doi.org/10.1021/jacs.4c15596

Abstract: The origin of the meta- and ortho-to-fluorine site-selectivity in the C(sp2)–H borylation of fluorinated arenes with B2Pin2 and HBPin promoted by pyridine(dicarbene)cobalt catalysts has been investigated. In situ generation of the cobalt(I)-boryl complex and treatment with three representative fluoroarenes established meta-selective C(sp2)–H oxidative addition to form predominantly the meta isomers of the corresponding cobalt(I)-aryl complexes. Attempts to observe or isolate the four-coordinate cobalt(I)-boryl complex yielded the cobalt-hydride dimer, [(iPrACNC)CoH]2, borohydride (iPrACNC)CoH2BPin, or diboryl hydride, (iPrACNC)CoH(BPin)2 depending on the amounts of B2Pin2 and HBPin present. The phosphite derivatives (iPrACNC)CoH(P(OiPr)3)

and (iPrACNC)CoBPin(P(OiPr)3) were prepared and crystallographically characterized. In the catalytic borylation of 1,3-difluorobenzene, ortho-to-fluorine cobalt(I)-aryl and borohydride complexes were identified as resting states despite meta-to-fluorine borylation being the major product of catalysis. Deuterium kinetic isotope effects support irreversible but not turnover-limiting C(sp2)–H oxidative addition. Stoichiometric borylation of isolated cobalt(I)-aryl intermediates with B2Pin2 established that the meta-cobalt(I)-aryl was more reactive than the ortho-isomer and accounts for the observed cobalt(I)-aryl resting states. All cobalt(I)-aryl compounds reacted more quickly with HBPin. While ortho-cobalt(I)-aryl compounds yielded arylboronate products with high site-selectivity, meta-cobalt-aryl counterparts yielded a mixture of arylboronate isomers and free arene. Deuterium labeling experiments with DBPin confirmed that HBPin mediates reversible C(sp2)–H oxidative addition. Thus, the overall site-selectivity arises from two reinforcing effects: (i) kinetically meta-selective oxidative addition and (ii) faster reaction of the meta-cobalt-aryl isomer with B2Pin2. As B2Pin2 is converted to HBPin, C(sp2)–H reductive elimination competes against borylation of the meta-cobalt-aryl isomer, resulting in increased ortho-selective borylation.

25COASMA159:

Title: Multiplicity of Regulatory Subunit Conformations Defines Structural Ensemble of Reset Protein Kinase A Holoenzyme

Varun Venkatakrishnan, Tatiana N. Laremore, Theresa S.C. Buckley

J. Am. Chem. Soc. 2025, 147, 17, 14174–14190

https://doi.org/10.1021/jacs.4c16269

Abstract: How protein kinase A (PKA) is reset to a basal state following 3′5′-cyclic adenosine monophosphate (cAMP)-mediated activation is unknown. Here we describe the mechanism of cAMP-PKA type I signal termination leading to a reset of PKA by holoenzyme formation through the obligatory action of phosphodiesterases (PDEs). We report a catalytic subunit (Cα)-assisted mechanism for the reset of type I PKA and describe for the first time multiple structures of the reset PKA holoenzyme (RIα2:Cα2) that capture an ensemble of multiple conformational end-states through integrative electron microscopy and structural mass spectrometry approaches. Together these complementary methods highlight the large conformational dynamics of the regulatory subunit (RIα) within the tetrameric reset PKA holoenzyme. The cAMP-free reset PKA holoenzyme adopts multiple distinct conformations of RIα with contributions from the N-terminal linker and CNB-B dynamics. Our findings highlight the interplay between RIα, Cα, and PDEs (PDE8) in cAMP-PKA signalosomes to offer a new paradigm for PDE-mediated regulation of cAMP-PKA signaling.

25COASMA160:

Title: Pd-Catalyzed Counter-Steric Site- and Chemoselective Glycosylation: Total Synthesis of Fridamycin A and Himalomycin B

Jihun Kang, Seungsoo Moon, Young Ho Rhee et.al.

J. Am. Chem. Soc. 2025, 147, 17, 14432–14441

https://doi.org/10.1021/jacs.5c00855

Abstract: Here, we report a de novo synthetic strategy toward fridamycin-type glycoside natural products. A salient feature of the method is highlighted by the Pd-catalyzed

asymmetric hydroalkoxylation of fridamycin A methyl ester with alkoxyallene, which enables site- and chemoselective introduction of 2,3,6-trideoxyglycosysides to various hydroxyl positions in a highly controlled manner. A unique advantage of this method is demonstrated by the total synthesis of himalomycin B and a C4′-epi derivative of the proposed structure of amicenomycin B.

25COASMA161:

Title: Short-Range Magnetic Correlations and Thermally Assisted Spin Tunnelling in Distorted Diamond Lattices RTaO4 (R = Tb and Dy)

Jogendra Kumar, K. Mukherjee

J. Am. Chem. Soc. 2025, 147, 17, 14442–14454

https://doi.org/10.1021/jacs.5c00872

Abstract: Rare earth-based frustrated systems provide an excellent platform to study novel magnetic phenomena owing to their localized moment and unquenched orbital momentum. Here, we present a comprehensive investigation of crystallographic and thermodynamic properties of TbTaO4 and DyTaO4, wherein the magnetic ions form a distorted diamond structure. The former exhibits a crossover from short-ranged magnetic correlations to long-ranged antiferromagnetic ordering at ∼2.2 K, while the latter manifests only short-ranged magnetic correlations down to 1.8 K. Interestingly, a field-induced frequency dependence is observed in AC susceptibility in both cases, similar to that observed in spin ice systems. Analysis using the Casimir–duPre plot and Arrhenius law confirms that the origin behind this spin relaxation is thermal in nature, with activation energy close to the first excited crystal electric field gap. Our studies suggest that the observed frequency-dependent behavior is not only limited to spin ice materials, but it is a generic phenomenon in a broader class of rare earth-based frustrated magnetic systems.

25COASMA162:

Title: Harnessing the Deubiquitinase USP1 for Targeted Protein Stabilization

Chao Qian, Zhen Wang, Yan Xiong et.al.

J. Am. Chem. Soc. 2025, 147, 17, 14564–14573

https://doi.org/10.1021/jacs.5c01662

Abstract: Deubiquitinase-targeting chimera (DUBTAC) has emerged as a promising technology for targeted protein stabilization (TPS) by harnessing deubiquitinases (DUBs) to remove polyubiquitin chains from target proteins. Despite the presence of over 100 human DUBs, only OTUB1 and USP7 have been utilized in the development of DUBTAC. Hence, there is an urgent need to harness additional DUBs to expand the DUBTAC arsenal. In this work, we demonstrate for the first time that the USP1 deubiquitinase, which is overexpressed in several human cancers, can be leveraged for TPS. We report the development of novel USP1-recruiting DUBTACs by utilizing a noncovalent small-molecule inhibitor of USP1. First, we generated a USP1-based CFTR DUBTAC, MS5310, which effectively stabilized CFTR and is more potent than previously reported CFTR DUBTACs. Next, we developed first-in-class USP1-recruiting UTX DUBTACs, including MS7131, from a small-molecule inhibitor of UTX and JMJD3. Notably, MS7131 effectively stabilized the tumor suppressor UTX in a concentration- and time-dependent manner, while sparing the oncoprotein JMJD3,

despite it retaining potent inhibition of JMJD3. Furthermore, UTX stabilization induced by MS7131 was dependent on the engagement of both USP1 and UTX. Consequently, MS7131, but not the parent USP1 inhibitor or UTX inhibitor, effectively reduced histone H3 lysine 27 trimethylation and significantly suppressed the proliferation and clonogenicity of cancer cells. Overall, this study highlights that USP1 can be harnessed for DUBTAC development. Moreover, we developed a valuable chemical tool, MS7131, for the investigation of UTX's distinct functions. This advancement paves the way for leveraging DUBTACs in the treatment of related diseases.

25COASMA163:

Title: Access to Enantiopure Spiropyridines Enabled by Enantio-Relay Double [2 + 2 + 2] Cycloaddition and Kinetic Resolution [2 + 2 + 2] Cycloaddition of Alkynes and Nitriles

Li-Gang Bai, Yu-Qing Zheng, Han-Nan Chen et.al.

J. Am. Chem. Soc. 2025, 147, 17, 14574–14584

https://doi.org/10.1021/jacs.5c01653

Abstract: The synthesis of enantiopure and structurally unique spiro-type molecules is of utmost significance in catalysis, synthetic chemistry, and related fields. We present here a general solution, a nickel-catalyzed [2 + 2 + 2] cycloaddition, for accessing enantioenriched spiropyridines from readily available nitriles and alkynes in a single synthetic step, including (1) enantio-relay double [2 + 2 + 2] cycloaddition of malononitriles with alkynes and (2) kinetic resolution [2 + 2 + 2] cycloaddition of racemic pyridine-containing nitriles with alkynes. Both strategies feature a broad substrate scope and exclusive regioselectivities, and are scalable to multigram. Remarkably, the double [2 + 2 + 2] cycloaddition integrates enantio-induction by desymmetrizing dinitriles during the initial catalytic cycle with additional enantio-enhancement during the second cycloaddition (enantio-relay), yielding excellent enantioselectivities (>99% ee for all examined examples). Furthermore, the highly efficient kinetic resolution strategy enables the achievement of exceptionally high enantioselectivities without compromising yields (s > 200 for most examples), overcoming the general challenges of kinetic resolution toward yield and enantioselectivity. The ability to construct previously inaccessible spiro structures lays the groundwork for advancing spiropyridine derivatives, especially the multinitrogen-containing compounds as potential ligands. Due to the perpendicular molecular orientation and inherent rigidity of the architectures obtained, we anticipate significant promise of the presented synthetic approaches for enhancing efforts in synthesis and catalysis.

25COASMA164:

Title: Photocatalytic Synthesis of Substituted 2-Aryl Morpholines via Diastereoselective Annulation

Tiffany A. Brisco, Simon De Kreijger, Vaishnavi N. Nair et.al.

J. Am. Chem. Soc. 2025, 147, 17, 14605–14613

https://doi.org/10.1021/jacs.5c01832

Abstract: Morpholines are prevalent in medicinal chemistry due to their favorable pharmacokinetic properties and widespread presence in FDA-approved drugs. Existing

methods for morpholine synthesis often require prefunctionalized or protected reagents, limiting their versatility and efficiency. Here, we present a photocatalytic, diastereoselective annulation strategy for the synthesis of morpholines directly from readily available starting materials. This method employs a visible-light-activated photocatalyst, Lewis acid, and Brønsted acid to achieve high yields and stereoselectivity. It also provides access to diverse substitution patterns, including challenging tri- and tetra-substituted morpholines. Mechanistic studies reveal that the reaction proceeds through the formation of a radical cation intermediate, with triflic acid playing critical roles in protonating the substrate, preserving the photocatalyst, and preventing product oxidation. Beyond morpholines, this strategy is extended to piperidines, pyrrolidines, and other privileged nitrogen heterocycles. Our findings provide a modular approach for constructing complex, medicinally valuable scaffolds, advancing both synthetic and medicinal chemistry.

25COASMA165:

Title: Decoding the Competing Effects of Dynamic Solvation Structures on Nuclear Magnetic Resonance Chemical Shifts of Battery Electrolytes via Machine Learning

Qi You, Yan Sun, Feng Wang et.al.

J. Am. Chem. Soc. 2025, 147, 17, 14667–14676

https://doi.org/10.1021/jacs.5c02710

Abstract: Understanding the solvation structure of electrolytes is critical for optimizing the electrochemical performance of rechargeable batteries as it directly influences properties such as ionic conductivity, viscosity, and electrochemical stability. The highly complex structures and strong interactions in high-concentration electrolytes make accurate modeling and interpretation of their “structure–property” relationships even more challenging with spectroscopic methods. In this study, we present a machine learning-based approach to predict dynamic 7Li NMR chemical shifts in LiFSI/DME electrolyte solutions. Additionally, we provide a comprehensive structural analysis to interpret the observed chemical shift behavior in experiments, particularly the abrupt changes in 7Li chemical shifts at high concentrations. Using advanced modeling techniques, we quantitatively establish the relationship between the molecular structure and NMR spectrum, offering critical insights into solvation structure assignments. Our findings reveal the coexistence of two competing local solvation structures that shift in dominance as electrolyte concentration approaches the concentrated limit, leading to an anomalous reversal of 7Li NMR chemical shift in the experiment. This work provides a detailed molecular-level understanding of the intricate solvation structures probed by NMR spectroscopy, leading the way for an enhanced electrolyte design.

25COASMA166:

Title: Unsupervised Machine Learning Prediction of a Novel 1:3 Intermetallic Phase with the Synthesis of TbIr3 (PuNi3-type) as Experimental Validation

Siddha Sankalpa Sethi, Arnab Dutta, Emil I. Jaffal et.al.

J. Am. Chem. Soc. 2025, 147, 17, 14739–14755

https://doi.org/10.1021/jacs.5c03510

Abstract: Crystal structure classification of binary intermetallic structures with 1:3

stoichiometry was done with machine learning algorithms. The data set included 97 features and a total of 2366 reported compounds adopting six different structure types. An unsupervised learning method based on principal component analysis (PCA) followed by clustering using the K-means method was applied to cluster compounds belonging to different structure types. With the recommendation engine, we predicted the expansion of the clusters and then identified the cluster/structure-type overlap. The PuNi3-type was among the clearly segregated structure types according to the unsupervised model, and a novel representative, TbIr3, was selected for experimental validation, adopting this structure. The final supervised machine learning predictions were done with partial least squares discriminant analysis (PLS-DA), support vector machine (SVM), and XGBoost, confidently predicting that the novel TbIr3 belongs to the PuNi3-type with accuracies of 96.6, 99.8, and 99.9% respectively. Successful crystal structure segregation was attributed to a novel set of descriptors comprising both compositional and structural features. Given that the predicted PuNi3-type of the TbIr3 phase could be controversial due to the extensive study of the Tb–Ir phase diagram and the reports of the TbIr3 in two different structure types, we conducted two independent experimental structural validations to confirm the existence of TbIr3 in the PuNi3-type structure. Subsequent theoretical validation explained that Ir–Ir contacts are the primary stability factor of TbIr3 in the PuNi3-type structure compared to other structure types.

25COASMA167:

Title: Mechanistic Insights into Copper-Catalyzed Asymmetric Cyanation of Allylic C–H Bonds

Jiayuan Li, Tilong Yang, Pinhong Chen et.al.

J. Am. Chem. Soc. 2025, 147, 17, 14756–14768
https://doi.org/10.1021/jacs.5c03680

Abstract: Direct C–H bond functionalization has emerged as one of the most powerful and practical strategies for the modification of drug molecules. We have recently disclosed a Cu/NFAS (NFAS = N-fluoroalkyl sufonamide) catalytic system that exhibits high site-, regio-, and enantioselectivity for the direct cyanation of allylic C–H bonds. Here, we present a mechanistic investigation of this catalyst system, including the elucidation of side reactions involved in the transformation. This work focuses on an in-depth analysis of the catalytic cycle based on kinetic studies by NMR spectroscopy and characterization of the catalyst speciation by EPR and UV–vis spectroscopy. These studies indicate that a fraction of NFAS is sacrificed to the side reactions of the Cu(II)-bounded N-centered radical (Cu(II)–NCR) species for the generation of silylated sulfonamides and (CN)2. The data also show a great dependence of the reaction yield and selectivity (hydrogen atom abstraction or HAA over side reactions) on the structure of the Cu(II)–NCR species. Kinetic studies and DFT calculations further reveal that oxidation of the CuCN species by NFAS, HAA process, and cyanation of Cu(II)–NCRs with TMSCN have comparable energy barriers, which collectively determine the rate of the overall C–H cyanation reaction.

25COASMA168:

Title: Synergistic LMCT and Ni Catalysis for Methylative Cross-Coupling Using tert-Butanol: Modulating Radical Pathways via Selective Bond Homolysis

Lingfei Duan, Yunzhi Lin, Qing An et.al.

J. Am. Chem. Soc. 2025, 147, 17, 14785–14796
https://doi.org/10.1021/jacs.5c03711

Abstract: Ligand-to-metal charge transfer (LMCT) excitation has emerged as a potent strategy for the selective generation of heteroatom-centered radicals, yet its full potential in modulating open-shell radical pathways remains underexplored. Here, we present a photocatalytic methylative cross-coupling reaction that capitalizes on the synergistic interplay between LMCT and Ni catalysis, enabling the use of tert-butanol as an efficient and benign methylating reagent. The electron-deficient ligand 2,6-ditrifluoromethyl benzoate facilitates Ce(IV)-mediated bond scission of tert-butanol, generating a methyl radical that is subsequently captured by the Ni catalytic cycle to form C–CH3 bonds. Under mild reaction conditions, this strategy affords efficient methylation of sp3 carbons adjacent to carbonyls and sp2 centers, demonstrating broad functional group tolerance and applicability in late-stage functionalization of bioactive molecules. Additionally, trideuteromethylative coupling can be facilely achieved using commercial tert-butanol-d10. This approach circumvents the need for traditional tert-butoxy radical precursors, such as peroxides, while strategically modulating the radical pathway to favor β-scission and suppress unwanted tert-butoxy radical formation in solution. Mechanistic studies reveal that the benzoate ligand plays a crucial role in enabling LMCT excitation and facilitating methyl radical generation, supporting a concerted Ce–OR and β-C–C bond homolysis mechanism, further evidenced by the modulation of regioselectivity in alkoxy radical-mediated β-scission.

Diagnostic Services
(Pathology**, C**ancer Screening **& R**adio-diagnosis**)**

25COASMA1:
Title: SALL4 as a Useful Marker for the Distinction of Various Gestational Trophoblastic Disease Subtypes
Choriocarcinoma From Other Trophoblastic Lesions and Early Complete Hydatidiform Mole From Partial Mole and NonMolar Villi
Trecourt, Alexis MD; Donzel, Marie MD; Gaillot-Durand, Lucie MD et.al
The American Journal of Surgical Pathology 49(5):p 417-428, May 2025.
https://doi.org/10.1097/PAS.0000000000002358
Abstract: The distinction between choriocarcinoma and residual trophoblastic cell proliferation from a complete hydatidiform mole/invasive mole (CHM/IM) without villi is challenging on curettage materials. We investigated whether SALL4 immunostaining could help differentiate various gestational trophoblastic diseases. Placental site nodules (PSN; n=10), atypical PSN (APSN; n=8), placental site trophoblastic tumors (PSTT; n=9), epithelioid trophoblastic tumors (ETT; n=5), gestational choriocarcinomas (n=31), partial hydatidiform moles (PHM; n=13), CHM/IM (n=47), and nonmolar products of conception (POC) (n=26) were included. SALL4 immunostaining was quantified (0 [1% to 10%], [11% to 100%]) and characterized (scattered single-cell or clustered nuclear positivity) in 2 locations: cytotrophoblast/intermediate trophoblast and villous stromal fibroblasts. A diffuse (11% to 100%) and clustered pattern of SALL4 immunostaining in cytotrophoblast/intermediate trophoblast was statistically associated with choriocarcinomas (74.2%, 23/31) as compared with PSN (0/10; P<0.0001), APSN (0/8; P=0.0002), PSTT (0/9; P<0.0001), ETT (0/5; P=0.0034), PHM (0/13; P<0.0001), CHM/IM (0/47; P<0.0001), and nonmolar POC (0/26; P<0.0001). Most nonchoriocarcinoma samples showed no SALL4 expression; when present, it was of low level (1% to 10%) and with a scattered single-cell staining in 3/9 PSTT (33%), 1/13 PHM (7.7%), 19/47 CHM/IM (40%), and 1/26 nonmolar POC (1.7%). These results were confirmed using a validation cohort. In addition, 66% (31/47) of CHM/IM villous stromal fibroblasts showed SALL4 expression (11% to 100%) (all before 14 gestational weeks), whereas this level of expression was never observed in PHM (0/13), nor in nonmolar POC (0/26; P<0.0001). Finally, a clustered and >10% SALL4 immunostaining in cytotrophoblast/intermediate trophoblast favors choriocarcinoma diagnosis. SALL4 expression in >10% villous stromal fibroblasts before 14 gestational weeks favors CHM/IM rather than PHM and nonmolar POC.
Keywords: gestational trophoblastic disease; gestational trophoblastic neoplasia; SALL4; immunohistochemistry

25COASMA2:
Title: BRAF Gene Fusions in Melanoma: First Kinase Domain Duplication, New Fusion Partners, and Clinical Outcomes
Odintsov, Igor; Davis, Dale; Pissaloux, Daniel; More
The American Journal of Surgical Pathology. 49(5):429-438, May 2025.
https://doi.org/10.1097/PAS.0000000000002370

Abstract: BRAF gene fusions have been well-described in Spitzoid melanocytic lesions but can also occur uncommonly in conventional melanomas. Here we report a series of 17 melanomas harboring BRAF gene fusions as their putative primary genetic driver. All but one of these tumors occurred in adults (age range 13 to 96) with a relatively even sex distribution (41% female) and a broad distribution of anatomic sites. None of the tumors showed typical Spitzoid histomorphologic features. Molecular analysis identified the first example of BRAF kinase domain duplication in melanoma, which raises interesting questions regarding the mechanism of fusion-induced BRAF activation. Although we did not identify histomorphologic features that could distinguish BRAF-fused melanomas from more conventional melanomas, we did observe a generally low tumor mutational burden and a lower rate of UV-associated mutational signatures (3/17; 18%), suggesting that BRAF-fused melanomas are molecularly and mechanistically distinct from conventional cutaneous melanomas. We report detailed treatment information and clinical outcomes for this series, with most patients having shown disease progression on systemic immunotherapy (8/12; 67%). Our results highlight the need for continued molecular subclassification to yield a comprehensive understanding of melanoma pathogenesis and have potential implications for therapeutic selection in BRAF-fused and perhaps other unconventional forms of melanoma.

25COASMA3:

Title: Insights into the Clinical Prognosis of High-grade Appendiceal Mucinous Neoplasms

Dartigues, Peggy MD; Kepenekian, Vahan MD; Illac-Vauquelin, Claire MD

The American Journal of Surgical Pathology 49(5):p 499-507, May 2025.
https://doi.org/10.1097/PAS.0000000000002373

Abstract: High-grade appendiceal mucinous neoplasm (HAMN) is used to describe a rare epithelial neoplasm of the appendix characterized by pushing-type invasion and high-grade cytologic atypia. Its implications regarding lymph node spread and the necessity of right colectomy are currently debate. The objective of the present study was to assess the clinicopathologic characteristics, the risk of lymph node and peritoneal metastasis, and long-term outcomes of patients diagnosed as HAMN in comparison to low-grade appendiceal mucinous neoplasm (LAMN) and appendiceal adenocarcinoma, treated by right hemicolectomy. A total of 443 patients diagnosed with LAMN (n=246), HAMN (n=34), or appendiceal adenocarcinoma (n=163) and who underwent right colectomy with lymph node dissection in all cases within 32 institutions of the French Network for Rare Peritoneal Malignancies (RENAPE) were included. The median age was 56.5 years (range: 21 to 91), and the majority were female (n=250, 56.4%) without difference between groups (P=0.604). Lymph node metastases were identified in 17.8% of appendiceal adenocarcinoma cases (29/163); none were found among LAMN or HAMN cases. A higher number of lymph nodes were analyzed in those treated for appendiceal adenocarcinoma than LAMN (P<0.001) and HAMN (P=0.035). Regarding peritoneal metastasis, a higher proportion of cases were classified as high-grade with/without signet cells in patients treated for HAMN (P<0.001) and appendiceal adenocarcinoma (P<0.001) than those treated for LAMN. Among patients with perforation of the appendix, those treated for LAMN had longer overall survival (OS; P<0.001) and progression-free survival (PFS; P<0.0001) than those treated for

appendiceal adenocarcinoma or those treated for HAMN; among patients without perforation, those treated for LAMN and HAMN had longer OS (P=0.042) and PFS (P=0.012) than those treated for appendiceal adenocarcinoma. No lymph node metastases were observed in patients treated for HAMN, and those without appendix perforation had a similar prognosis to LAMN. This study supports staging HAMN using the same system as LAMN and treating it with appendectomy alone in the absence of appendix perforation.

Keywords: high-grade appendiceal mucinous neoplasms; pseudomyxoma; lymph nodes; metastasis

25COASMA4:

Title: European Myeloma Network Group review and consensus statement on primary plasma cell leukemia

P. Musto · M. Engelhardt[3] · N.W.C.J. van de Donk

Annals of Oncology, Volume 36, Issue 4P361-374
https://doi.org/10.1016/j.annonc.2025.01.022

Abstract: Background-Primary plasma cell leukemia (PPCL) is the most aggressive disorder among plasma cell malignancies, with new diagnostic criteria recently established by the International Myeloma Working Group. Studies have shown that PPCL patients receiving a combination of novel agents, but not eligible for transplantation, may have a median survival up to 2 years, extended to 3 years or more in those undergoing transplant procedures. These findings remain unsatisfactory, particularly if compared with progresses obtained in multiple myeloma. Design-A European Myeloma Network (EMN) expert panel reviewed the most recent literature and selected the areas of major concern in the management of PPCL by generating and rank ordering key questions using the criterion of clinical relevance. Multistep procedures were utilized to achieve a consensus on recommendations. The Delphi questionnaire method was used and a consensus of at least 80% was reached for all final statements. Results-An extended overview of current biological, clinical, prognostic, and therapeutic aspects of PPCL, including ongoing and close to start clinical trials, is presented. Furthermore, updated guidelines for the management of PPCL and practical recommendations are provided, in the context of current knowledge about this disease, also looking at possible future perspectives to ameliorate the outcome of these patients. Conclusions-PPCL still remains an unmet clinical need. Notwithstanding, some not negligible progresses have been recently achieved. The European Myeloma Network panel strongly support ongoing and planned clinical trials, as well as biological studies based on novel technologies, strategies, and treatment options that could represent breakthroughs we have been waiting for too long.

Keywords: primary plasma cell leukemia**,** high-risk multiple myeloma**,** practical recommendations**,** guidelines**,** Delphi consensus

25COASMA5:

Title: Biomarker analyses from the phase III randomized CLEAR trial: lenvatinib plus pembrolizumab versus sunitinib in advanced renal cell carcinoma

R.J. Motzer ,C. Porta[2] · M. Eto

Annals of Oncology, Volume 36, Issue 4, P375-386

https://doi.org/10.1016/j.annonc.2024.12.003 External Link

Abstract: Background-In CLEAR, lenvatinib + pembrolizumab (L + P) significantly improved efficacy versus sunitinib in first-line treatment of patients with advanced renal cell carcinoma (aRCC). We report results from CLEAR biomarker analyses.

Patients and methods- Programmed death-ligand 1 (PD-L1) immunohistochemistry (IHC) and next-generation sequencing assays (whole exome sequencing/RNA sequencing) were carried out on archival tumor specimens. For IHC-derived/RNA sequencing analyses, a continuous analysis was carried out adjusting by Karnofsky performance status (KPS) score for: PD-L1 combined positive score (CPS) versus best overall response (BOR)/progression-free survival (PFS); and each gene signature score [T-cell inflamed gene expression profile ($Tcell_{inf}$GEP)/non-$Tcell_{inf}$GEP signatures including proliferation and angiogenesis] versus BOR/PFS. Association between mutation status of RCC driver genes and PFS were analyzed for genes for which ≥20 patients per arm had oncogenic alterations. Association of molecular subtypes with outcome was evaluated with baseline KPS adjustments. The set of biomarkers evaluated and statistical significance criteria for PD-L1 CPS, gene signature scores, and molecular subtypes were prespecified. Results- Within-arm analyses using continuous values showed no association between PD-L1 levels and BOR/PFS for either treatment. PFS hazard ratios between arms were similar regardless of the mutant or wild-type subgroups of RCC driver genes (VHL, PBRM1, SETD2, BAP1, KDM5C). No associations between PFS and gene signature scores were observed for L + P. With sunitinib, high proliferation and MYC signature scores showed shorter PFS; high angiogenesis and microvessel density signature scores showed longer PFS. Six new molecular subtypes were defined. Tumors of patients with favorable/intermediate risk were enriched in angiogenesis and angiogenesis/stromal clusters; those with poor risk were enriched in proliferative and unclassified (low-$Tcell_{inf}$GEP/low-angiogenesis/low-proliferation) clusters. No association between molecular subtypes and PFS for L + P/sunitinib was observed (after adjustment for KPS and gene signatures that were individually associated with PFS). Conclusions- Improvements in objective response rate and PFS for L + P versus sunitinib in aRCC were observed consistently across a range of biomarker subgroups defined using RCC driver mutations, PD-L1, gene expression signatures, and molecular subtypes.

Keywords: Urogenital tumors, biomarkers, lenvatinib, pembrolizumab

25COASMA6:

Title: Avelumab + axitinib versus sunitinib as first-line treatment for patients with advanced renal cell carcinoma: final analysis of the phase III JAVELIN Renal 101 trial

T.K. Choueiri[1] K. Penkov[2] · H. Uemura

Annals of Oncology, Volume 36, Issue 4, P387-392
https://doi.org/10.1016/j.annonc.2024.12.008

Abstract: Background-In the phase III JAVELIN Renal 101 trial (NCT02684006), first-line treatment with avelumab + axitinib resulted in significantly longer progression-free survival (PFS) and a higher objective response rate (ORR) versus sunitinib in patients with advanced renal cell carcinoma (aRCC). We report the final analysis, including the primary analysis of overall survival (OS). Patients and methods-Patients with untreated aRCC (any prognostic risk score) were enrolled. The primary endpoints were OS and PFS in the programmed death-

ligand 1-positive (PD-L1+) population. ORR, duration of response, safety, and patient-reported outcomes (PROs) were also assessed. Results- The minimum follow-up was 68 months in all patients. The median OS with avelumab + axitinib versus sunitinib, respectively, was 43.2 months [95% confidence interval (CI) 36.5-51.7 months] versus 36.2 months (95% CI 29.8-44.2 months) in the PD-L1+ population [hazard ratio (HR) 0.86 (95% CI 0.701-1.057); P = 0.0755] and 44.8 months (95% CI 39.7-51.1 months) versus 38.9 months (95% CI 31.4-45.2 months) in the overall population [HR 0.88 (95% CI 0.749-1.039); P = 0.0669]. Investigator-assessed PFS remained prolonged with avelumab + axitinib versus sunitinib [5-year event-free rate in the overall population, 12.0% (95% CI 8.9% to 15.6%) versus 4.4% (95% CI 2.5% to 7.3%)]. ORR in the overall population was 59.7% (95% CI 55.0% to 64.3%) with avelumab + axitinib versus 32.0% (95% CI 27.7% to 36.5%) with sunitinib; duration of response was ≥5 years in 16.4% (95% CI 12.0% to 21.4%) versus 9.2% (95% CI 4.6% to 15.7%), respectively. Rates of grade ≥3 treatment-related adverse events were 66.8% versus 61.5%, respectively. PROs were similar between arms. Conclusions-JAVELIN Renal 101 provides the longest follow-up to date for immune checkpoint inhibitor + tyrosine kinase inhibitor combination treatment from a phase III trial in aRCC. OS analyses favored avelumab + axitinib versus sunitinib but did not reach statistical significance; subsequent treatment may have impacted results. Avelumab + axitinib provided long-term efficacy benefits versus sunitinib, including prolonged PFS, a nearly doubled ORR, and more durable responses, with a manageable long-term safety profile.

Keywords: Urogenital tumors, avelumab, axitinib, sunitinib, phase III, advanced renal cell carcinoma

25COASMA7:

Title: Correlation between progression-free and overall survival in patients with Hodgkin lymphoma: a comprehensive analysis of individual patient data from randomized German Hodgkin Study Group (GHSG) trials

P.J. Bröckelmann[1] · H. Müller[1] · M. Fuchs

Annals of Oncology, Volume 36, Issue 4
https://doi.org/10.1016/j.annonc.2024.12.009

Abstract: Background-This study aimed to evaluate the correlation between progression-free (PFS) and overall survival (OS) after first-line treatment of classical Hodgkin lymphoma (HL) and to assess the potential of PFS as a surrogate parameter for OS. Patients and methods- We analyzed individual patient data collected during and after treatment with polychemotherapy in nine randomized phase III trials [German Hodgkin Study Group (GHSG) HD7-HD15] between January 1993 and August 2018. The effects of 16 experimental treatments on PFS and OS at the trial level were evaluated using Cox proportional hazards (PH) regression and linear weighted least squares regression. At the patient level, marginal Cox PH models for multiple endpoints were applied using the Wei–Lin–Weissfeld method. Results- At least one PFS and OS event was recorded in 1682 and 1064 of 10 605 patients, respectively. At the trial level, there was a strong correlation between treatment effects on PFS and OS (weighted Pearson r = 0.72, R^2 = 0.54, P < 0.001). At the patient level, a moderate to strong correlation between treatment effects on PFS and OS was observed, with Pearson r values ranging between 0.61 and 0.85 (each P < 0.001) and

an overall r = 0.74. A regression model that accounted for different types of experimental treatments and historical progress across trial generations achieved a very strong correlation (R^2 = 0.93). When applied to data from the contemporary first-line ECHELON-1 trial, this model successfully predicted OS from PFS {prognosticated ln[HR(OS)] = −0.68 as compared with observed ln[HR(0.59)] = −0.53}. Conclusion-In first-line trials of HL, PFS and OS, as well as treatment effects and prognostic effects on these endpoints, are strongly correlated. PFS serves as a strong predictor of treatment effects on OS, providing valuable insights many years before OS can be reliably assessed.

Keywords: Leukemias, myeloma and hematological malignancies, Hodgkin lymphoma, progression-free survival, overall survival, correlation

25COASMA8:

Title: Prognostic value of residual disease (RD) biology and gene expression changes during the neoadjuvant treatment in patients with HER2-positive early breast cancer (EBC)☆

A. Fernandez-Martinez[1,2] · M. Tanioka[3] · S.G. Ahn

Annals of Oncology, Volume 36, Issue 4, P403-413
https://doi.org/10.1016/j.annonc.2024.12.010

Abstract: Background-In human epidermal growth factor receptor 2 (HER2)-positive early breast cancer (EBC), we investigated tumor and immune changes during neoadjuvant treatment and their impact on residual disease (RD) biology and prognostic implications across four neoadjuvant studies of trastuzumab with or without lapatinib, and with or without chemotherapy: CALGB 40601, PAMELA, NeoALTTO, and NSABP B-41. Patients and methods- We compared tumor and immune gene expression changes during neoadjuvant treatment and their association with event-free survival (EFS) by uni- and multivariable Cox regression models in different cohorts and timepoints: 452 RD samples at baseline including 169 with a paired RD, and biomarker changes during neoadjuvant therapy, evaluating model performance via the c-index. Results-Analysis of 169 paired tumor samples revealed a shift in intrinsic subtype proportions from HER2-enriched at baseline (50.3%) to normal-like (49.1%) followed by luminal A (18.9%) in RD. This luminal phenotypic change was supported by decreased correlation to the HER2-enriched centroid, ERBB2, and HER2 amplicon genes and increased correlation to the luminal A centroid (Wilcoxon test P < 0.001). Additionally, RD showed relative immune activation marked by significant increases in B-cell, CD8 T-cell, and natural killer cell signatures (Wilcoxon test P < 0.05). In multivariable Cox models, intrinsic subtypes at baseline provided more prognostic information, while immune gene expression signatures provided more prognostic information in RD. Notably, the best multivariable EFS model (c-index = 0.77) integrated the immunoglobulin G signature from RD samples (adjusted hazard ratio 0.45, 95% confidence interval 0.30-0.67, adjusted P = 0.002). Conclusions-In patients with HER2-positive EBC and RD, tumor biomarkers provide more prognostic information at baseline. In contrast, immune biomarkers perform better for EFS prognosis in RD.

Keywords: HER2-positive early breast cancer**,** residual disease**,** genomic biomarkers gene expression, prognostic, post-treatment

25COASMA9:

Title: Genomic correlates of response and resistance to the irreversible FGFR1-4 inhibitor futibatinib based on biopsy and circulating tumor DNA profiling

L. Goyal,, D. DiToro,, A. Hollebecque,

Annals of Oncology, Volume 36, Issue 4P414-425
https://doi.org/10.1016/j.annonc.2024.11.017

Abstract: Background-Futibatinib is the only covalent inhibitor of FGFR1-4 to gain regulatory approval in oncology. In this article, we present genomic analyses of tissue biopsies and circulating tumor DNA (ctDNA) from patients with 1 of nearly 20 tumor types treated with futibatinib in the phase I/II FOENIX study. Patients and methods-Eligible patients included those with ctDNA samples collected per protocol at baseline and/or progression on futibatinib in the phase Ib portion of the study for FGF/FGFR-altered advanced solid tumors or the phase II portion of the study for FGFR2 fusion/rearrangement-positive cholangiocarcinoma. Assessments included analytical concordance between tumor and ctDNA analyses for detection of FGFR alterations, association of ctDNA-detected co-occurring genomic alterations with response to futibatinib, and determination of patterns of acquired resistance following progression on futibatinib. Results- Among 300 patients treated with futibatinib, 226 were eligible for this analysis, including 139 (62%) with cholangiocarcinoma. FGFR1 fusions, FGFR3 fusions, or FGFR2 amplifications per tissue analysis, detection rates in ctDNA for these aberrations were 84%, 0%, 11%, and 59%, respectively. Objective response rates on futibatinib were not significantly different between patients with TP53-altered versus -unaltered solid tumors; progression-free survival was reduced in patients with CDKN2B-altered versus -unaltered cholangiocarcinoma (median 4.8 versus 11.0 months; P = 0.03). Acquired resistance to futibatinib was frequently polyclonal and driven by an array of mutations within the relevant FGFR kinase domain, predominantly V565L, V565F, and N550K variants. Conclusions-In this largest and most systematic analysis of acquired resistance to an FGFR inhibitor from prospective clinical trials, emergence of secondary FGFR2 kinase domain mutations was observed in most patients receiving clinical benefit to futibatinib. ctDNA analysis shows clinically relevant potential as a noninvasive method for assessing genomic profiles, identifying patients who may benefit from FGFR inhibitor treatment, and exploring acquired resistance mechanisms.

Keywords: fibroblast growth factor receptor**,** cholangiocarcinoma**,** futibatinib**,** circulating tumor DNA

25COASMA10:

Title: A model for decoding resistance in precision oncology: acquired resistance to FGFR inhibitors in cholangiocarcinoma

L. Goyal, D. DiToro, F. Facchinetti

Annals of Oncology, Volume 36, Issue 4P426-443
https://doi.org/10.1016/j.annonc.2024.12.011

Abstract: Background-Fibroblast growth factor receptor (FGFR) inhibitors have significantly improved outcomes for patients with FGFR-altered cholangiocarcinoma, leading to their regulatory approval in multiple countries. As with many targeted therapies, however, acquired resistance limits their efficacy. A comprehensive, multimodal approach is crucial to

characterizing resistance patterns to FGFR inhibitors. Patients and methods -This study integrated data from six investigative strategies: cell-free DNA, tissue biopsy, rapid autopsy, statistical genomics, in vitro and in vivo studies, and pharmacology. We characterized the diversity, clonality, frequency, and mechanisms of acquired resistance to FGFR inhibitors in patients with FGFR-altered cholangiocarcinoma. Clinical samples were analyzed longitudinally as part of routine care across 10 institutions. Results-Among 138 patients evaluated, 77 met eligibility, yielding a total of 486 clinical samples. Patients with clinical benefit exhibited a significantly higher rate of FGFR2 kinase domain mutations compared with those without clinical benefit (65% versus 10%, $P < 0.0001$). We identified 26 distinct FGFR2 kinase domain mutations, with 63% of patients harboring multiple. While IC50 assessments indicated strong potency of pan-FGFR inhibitors against common resistance mutations, pharmacokinetic studies revealed that low clinically achievable drug concentrations may underly polyclonal resistance. Molecular brake and gatekeeper mutations predominated, with 94% of patients with FGFR2 mutations exhibiting one or both, whereas mutations at the cysteine residue targeted by covalent inhibitors were rare. Statistical genomics and functional studies demonstrated that mutation frequencies were driven by their combined effects on drug binding and kinase activity rather than intrinsic mutational processes. Conclusion-Our multimodal analysis led to a model characterizing the biology of acquired resistance, informing the rational design of next-generation FGFR inhibitors. FGFR inhibitors should be small, high-affinity, and selective for specific FGFR family members. Tinengotinib, a novel small molecule inhibitor with these characteristics, exhibited preclinical and clinical activity against key resistance mutations. This integrated approach offers a blueprint for advancing drug resistance research across cancer types.

Keywords: acquired resistance, targeted therapy, FGFR, cholangiocarcinoma, cell-free DNA

25COASMA11:

Title: European cancer mortality predictions for the year 2025 with focus on breast cancer

C. Santucci[1] · S. Mignozzi[1] · F. Levi

Annals of Oncology, Volume 36, Issue 4P460-468
https://doi.org/10.1016/j.annonc.2025.01.014

Abstract: Background-We predicted the number of cancer deaths and rates for 2025 in the European Union (EU), its five most populous countries, and the UK, focusing on breast cancer. Materials and methods-We derived population data and death certificates for all cancers and major sites for the EU, France, Germany, Italy, Poland, Spain, and the UK since 1970, from the World Health Organization and United Nations databases. Estimates for 2025 were computed by linear regression on recent trends identified through Poisson joinpoint regression, considering the slope of the most recent trend segment. Deaths averted from 1989 to 2025 were calculated by applying the 1988 peak rate to subsequent population data.

Results-We estimated 1 280 000 cancer deaths in the EU in 2025, corresponding to age-standardised rates (ASRs) of 120.9/100 000 males (−3.5% versus 2020) and 79.1/100 000 females (−1.2%). In the UK, we predicted 173 000 cancer deaths and ASRs of 101.2/100 000 males (−10.1%) and 82.1/100 000 females (−6.3%). In the EU, favourable trends are

predicted for major neoplasms, except pancreatic cancer, in males (+2.0%) and females (+3.0%), and lung (+3.8%) and bladder (+1.9%) cancers among females. Breast cancer mortality showed favourable trends in all countries. Substantial decreases were predicted for EU females aged 50-69 years (−9.8%) and 70-79 years (−12.4%). Between 1989 and 2025, we estimated about 6.8 million averted cancer deaths in the EU, including over 373 000 breast cancer deaths. Corresponding numbers for the UK were 1 500 000 and 197 000. Conclusion-EU breast cancer rates have fallen by 30% since 1990, due to advances in prevention, treatment, and early detection. Contrasting trends in lung cancer among males and females reflect differing tobacco smoking patterns. Female lung cancer mortality is still increasing in the EU, though less than in the previous decade. Persistent unfavourable pancreatic cancer trends can be related to the increasing prevalence of obesity and limited therapeutic advances, requiring continued attention.

Keywords: Epidemiology, cancer mortality, predictions, breast cancer, European Union UK

25COASMA12:

Title: Airway associated inflammation in post- transplant cystic fibrosis patients as a predictor of chronic lung allograft dysfunction (CLAD)

Journal of Clinicl Pathology,Volume 78, Issue 4
https://doi.org/10.1136/jcp-2024-209899

Abstract: Aims In cystic fibrosis lung transplant recipients (LTRs), graft dysfunction due to acute infections, rejection or chronic lung allograft dysfunction (CLAD) is difficult to distinguish. Characterisation of the airway inflammatory milieu could help detect and prevent graft dysfunction. We speculated that an eosinophil or neutrophil- rich milieu is associated with higher risk of CLAD. Methods A retrospective, single- centre observational study of cystic fibrosis LTRs between 2002 and 2021 was performed. Data from biopsy slides, pulmonary function testing and bronchoalveolar lavage fluid microbiology tests were collected. The primary outcome was bronchiolitis obliterans syndrome (BOS) or death after transplant, with an 8- year follow- up period. Results 40 patients were identified with an average age of 35.3 at first transplantation, including 5 redo lung transplants. Fungal infections were associated with significantly worsened outcomes ($p \leq 0.001$). Eosinophils in large airways was associated with worse BOS-free survival ($p=0.03$). **Conclusions-** Subcategorisation of the inflammatory milieu (particularly noting eosinophils) in surveillance biopsies may help detect CLAD earlier and improve long-term outcomes in cystic fibrosis LTRs.

25COASMA13:

Title: Prevalence and clinical outcomes of germline variants among patients with myeloid neoplasms

Sunisa Kongkiatkamon, Pimjai Niparuck
Journal of clinical Pathology, Volume 78, Issue 4
https://doi.org/10.1136/jcp-2023-209264

Abstract: Aims- Myeloid neoplasms (MNs) with germline predisposition have been recognised as a distinct entity. Emerging evidence suggests that sporadic myelodysplastic

syndromes may also harbour undetected germline predispositions. We investigated germline alterations in a cohort of 122 adult Thai MNs. **Methods-** MN patients were recruited and tested for germline variants using deep targeted next-generation sequencing. The germline variant was filtered using American College of Medical Genetics classifications and then evaluated for the association with clinical characteristics and outcomes. **Results-** Our findings revealed pathogenic/likely pathogenic germline alterations in 12 (10%) of the patients. These germline lesions were commonly found in the DNA damage response pathway (n=6, 50%). We also identified novel deleterious FANCA ^{A1219GfsTer59} variants in two patients diagnosed with secondary acute myeloid leukaemia (sAML) from aplastic anaemia and AML with myelodysplasia related. Among sAML, individuals with germline mutations had inferior overall survival compared with those with wild-type alleles (2 months vs 12 months) with HR 4.7 (95% CI 1.0 to 20), p=0.037. Therefore, the presence of pathogenic or likely pathogenic mutations may be linked to inferior survival outcomes. **Conclusions**- Our study highlighted that the prevalence of germline predisposition in Southeast Asian populations is comparable to that in Caucasians. This underscores the importance of germline genetic testing within the Asian population.

25COASMA14:

Title: Attitudes of UK pathologists and judicial officers towards medicolegal view and grant examinations: a cross-sectional mixed-methods study

Jacob Foster, David Sadler, Sam Taylor

Journal of clinical Pathology, Volume 78, Issue 4
https://doi.org/10.1136/jcp-2024-209413

Abstract: Aims- Despite the 1988 'Dundee Initiative', which maximised the use of view and grant examinations to reduce the invasive forensic autopsy rate in Tayside, the view and grant itself remains controversial. This is the first study to measure attitudes towards view and grants, applying the Theory of Planned Behaviour to investigate what attitudes are held, the reasons behind them and their association with deciding the scope of postmortem examinations**. Methods-** A mixed-methods cross-sectional study examined 62 UK pathologists, coroners and procurators fiscal using an online questionnaire. Participants were asked their demographics and attitudes towards view and grants before allocating five fictitious reportable deaths to either view and grant or invasive forensic autopsy (both in ideal and real world conditions), explaining their decisions using free-text. **Results** Participants held both positive and negative attitudes towards view and grants, and most were relatively strong and ambivalent. Attitudes predicted respondents' decisions- to favour view and grant or invasive forensic autopsy in all ideal world scenarios, but no real world scenarios. There were significant differences in attitudes and decisions when comparing pathologists and judicial officers, and respondents working in Coroner and Fiscal systems. Thematic analysis was conducted on free-text responses. **Conclusions-** Discrepancies between attitudes, and ideal and real world choices suggest that what respondents wanted to do did not necessarily translate to what they would actually do in the scenarios tested. Applying concepts of attitudes, norms and perceived control can help to understand decision-making by death investigators, and why some jurisdictions favour more invasive procedures.

25COASMA15:

Title: Prognostic implications, genomic and immune characteristics of lung adenocarcinoma with lepidic growth pattern

Yue Li1, Yi Xu1, Qifeng Ding

Journal of clinical Pathology, Volume 78, Issue 4
https://doi.org/10.1136/jcp-2024-209603

Abstract: **Aims** Conflicting data were provided regarding the prognostic impact and genomic features of lung adenocarcinoma (LUAD) with lepidic growth pattern (LP+A). Delineation of the genomic and immune characteristics of LP+A could provide deeper insights into its prognostic implications and treatment determination. **Methods**- We conducted a search of articles in PubMed, EMBASE and the Cochrane Library from inception to January 2024. A domestic cohort consisting of 52 LUAD samples was subjected to whole-exome sequencing as internal validation. Data from The Cancer Genomic Atlas and the Gene Expression Omnibus datasets were obtained to characterise the genomic and immune profiles of LP+A. Pooled HRs and rates were calculated. **Results** The pooled results indicated that lepidic growth pattern was either predominant (0.35, 95% CI 0.22 to 0.56, p<0.01) or minor (HR 0.50, 95% CI 0.36 to 0.70, p<0.01) histological subtype was associated with favourable disease-free survival. Pooled gene mutation rates suggested higher EGFR mutation (0.55, 95% CI 0.46 to 0.64, p<0.01) and lower KRAS mutation (0.14, 95% CI 0.02 to 0.25, p=0.02) in lepidic-predominant LUAD. Lepidic-predominant LUAD had lower tumour mutation burden and pooled positive rate of PD-L1 expression compared with other subtypes. LP+A was characterised by abundance in resting CD4+memory T cells, monocytes and γδ T cells, as well as scarcity of cancer-associated fibroblasts. **Conclusions**-LP+A was a unique histological subtype with a higher EGFR mutation rate, lower tumour mutation burden and immune checkpoint expression levels. Our findings suggested potential benefits from targeted therapy over immunotherapy in LP+A.

25COASMA16:

Title: Cytopathology of follicular and oncocytic follicular thyroid neoplasms: A Bethesda System perspective

André Lametti MD, Fadi Brimo MD, Yonca Kanber MD, Derin Caglar MD, Manon Auger MD

Cancer Cytopathology, Volume133, Issue5
https://doi.org/10.1002/cncy.70016

Abstract: The third edition of The Bethesda System for Reporting Thyroid Cytopathology includes category IV, follicular neoplasm (FN), which is used to classify fine-needle aspirates of thyroid nodules that may correspond to invasive follicular-derived neoplasia other than papillary thyroid carcinoma. This diagnosis is infrequently rendered, and may represent a challenge for pathologists. This review presents a practical approach to FN and its subtype oncocytic follicular neoplasm (OFN). First, minimal criteria for the diagnosis must be achieved, namely sufficient cellularity, architectural features consistent with neoplasia, and follicular cell or oncocytic cytomorphology. Second, select diagnoses that are common or important differential diagnoses for FN or OFN must be ruled out, via a combination of morphological findings and limited ancillary tests, when available. These include follicular

nodular disease, parathyroid sampling, metastatic carcinoma, noninvasive follicular thyroid neoplasm with papillary-like nuclear features, medullary thyroid carcinoma, certain subtypes of papillary thyroid carcinoma, and lymphocytic thyroiditis. This approach should allow for a careful selection of cases where diagnostic thyroid lobectomy is an appropriate therapeutic modality.

25COASMA17:

Title: Clinicopathological and molecular characterization of non–small cell lung cancer with pericardial effusions

Weijie Ma MD, Nathalie J. Rodrigues Simoes MD, Peter P. Seery, Tianhong Li MD

Cancer Cytopathology, Volume133, Issue5
https://doi.org/10.1002/cncy.70015

Abstract: Background- Cytological evaluation is essential for assessing pericardial effusions (PEs) in non–small cell lung cancer (NSCLC). This study retrospectively examined the clinicopathological, molecular, and prognostic characteristics of patients with NSCLC with PE. Methods- Clinical data from 80 patients with NSCLC with PE treated at an academic center over the course of 15 years were reviewed. PE specimens were categorized according to the International System for Reporting Serous Fluid Cytopathology (ISRSFC). The analysis included patient demographics, molecular alterations, cytopathology, histology, and survival outcomes. Results- Of the 80 patients, 36 (45%) were female and 90% had stage IV disease. A smoking history was noted in 58 patients (72.5%), and 22 patients (27.5%) presented with tamponade. Lung adenocarcinoma predominated (87.5%). The ISRSFC categorized 25% of the specimens as negative for malignancy (NFM), 7.5% as atypia of undetermined significance (AUS), 3.75% as suspicious for malignancy (SFM), and 63.75% as malignant (MAL). Immunohistochemistry in 57 specimens identified thyroid transcription factor 1 (65%) as the most frequently positive marker. Molecular analysis revealed p53 mutations (59.1%) as the most prevalent, followed by KRAS (34.1%) and EGFR (15.9%). Kaplan–Meier analysis showed significantly better survival for NFM patients than non-NFM patients (MAL, SFM, and AUS; $p = .0036$). Bloody PEs and tamponade were associated with worse outcomes. The immunotherapy group achieved the most prolonged survival among stage IV patients (9.07 months; $p = .017$). Cox regression confirmed cytology-negative status as an independent prognostic factor. Conclusions- Cytological evaluation and ISRSFC classification are crucial for NSCLC-associated PEs. A multidisciplinary approach integrating cytology, immunohistochemistry, and molecular profiling is essential for optimal management and prognosis.

25COASMA18:

Title: Selection of neuroendocrine markers in diagnostic workup of neuroendocrine neoplasms: The real-world data and machine learning model algorithms

Haiming Tang MD, PhD, Haoran Xia PhDet.al.

Cancer Cytopathology, Volume133, Issue5
https://doi.org/10.1002/cncy.70018

Abstract: Background- Accurate diagnosis of neuroendocrine neoplasms (NENs) is challenging, especially in poorly differentiated neuroendocrine carcinomas (NECs). This

study was aimed to search the best or best combination of neuroendocrine markers in the diagnostic workup of NENs via analysis of the real-world data and machine learning algorithms. Methods- Cytology cases with a workup of four neuroendocrine markers (chromogranin, synaptophysin, CD56, and INSM1) were retrieved. Sensitivity, specificity, and area under the curve of receiver operating characteristic curve (AUC-ROC) were calculated for each marker alone or in combination. Two machine learning algorithms, neural network and random forests, were also tested. Results- The study cohort included 106 NENs (64 NECs and 42 well-differentiated neuroendocrine tumors [NETs]) and 36 non-NEN cases. The combination of synaptophysin and INSM1 had sensitivity of 0.95, specificity of 0.92, and AUC-ROC of 0.93. Addition of CD56 to the combination further increased the sensitivity and AUC-ROC to 1 and 0.96, respectively, in all NENs as well as NEC cases. In addition, the combination of chromogranin, synaptophysin and INSM1 had sensitivity of 1, specificity of 0.92, and AUC-ROC of 0.96 in NETs. Machine learning models, specifically random forests and neural network, confirmed the efficacy of combining synaptophysin, INSM1, and CD56. Conclusions- The combination of synaptophysin, INSM1, and CD56 has the best performance in diagnostic workup of all NENs, although chromogranin may be selected for NETS. The random forests and neural network models support the common practice rule of requiring at least two out of three markers to be positive for optimal marker utilization.

25COASMA19:

Title: Comparison of conventional and novel rotational FNA needles using conventional microscopy and image analysis to quantitatively assess yield

Mohammed Amer Swid MD, Alivia E. Shen, Amanda J. Young MS, Tariq Rahman MD, Sara E. Monaco MD

Cancer Cytopathology, Volume133, Issue5
https://doi.org/10.1002/cncy.70014

Abstract: Background-There is increasing interest in designing new fine-needle aspiration (FNA) needles to maximize tissue acquisition. This study compares cytological preparations from a new rotating FNA needle (CytoCore) with conventional FNA (ConvFNA) using semiquantitative evaluation and quantitative image analysis (IA). Methods- FNA were performed on ex vivo tissue in quadruplicate for each needle type (ConvFNA and CytoCore), including different sizes (22 G and 25 G) and variable procedure time (5 and 20 s). The Nikon Elements (v5.41.02) was used to quantify the cellularity and size of the largest tissue fragment on cell blocks. Results- A total of 96 cytology specimens were evaluated were evaluated from benign and malignant specimens. For both ConvFNA and CytoCore, a longer procedure time (20 s) tended to produce greater cellularity and larger tissue fragments in the cell block specimens for both needles when analyzed with image analysis and was statistically significant for the CytoCore needle ($p < .01$). The ConvFNA tended to perform better with short procedure time. There was no statistically significant difference using different needle gauges. Conclusion- This study shows that IA can help to quantitatively evaluate sample cellularity in the cell blocks from specimens acquired with different needles. A longer procedure time tended to produce more cellular samples and larger tissue fragments in the cell block for both ConvFNA and CytoCore needles and was statistically significant for

CytoCore. Additional larger studies, including those with true clinical cases, should be considered to evaluate the different needle types further.

25COASMA20:

Title: Performance Characteristics of Incisional and Core Needle Biopsies for Diagnosis in Parotid Gland: Single-Institutional Experience and Assessment of the Value of a Milan System for Reporting Salivary Gland Cytopathology–Like Risk Stratification Model

Rayan Rammal, MD; Qian Wang, MD et.al.

Arch Pathol Lab Med (2025) 149 (4): 328–339.
https://doi.org/10.5858/arpa.2024-0051-OA

Abstract: Context-Unlike parotid fine-needle aspiration biopsy, standardized reporting for core needle biopsy (CNB) and incisional biopsy (IB) is not established. Objective-To examine the value of risk stratification by a Milan System for Reporting Salivary Gland Cytopathology (MSRSGC)–like classifier for parotid CNB/IB. Design -Five hundred ninety-two parotid biopsy records (CNB = 356, IB = 236) were retrieved (1994–2022) along with clinicopathologic data. Diagnoses were transformed to an MSRSGC-like classifier and compared with end points including risk of malignancy. Results -Over time, CNB was progressively more used compared with IB. Overall malignancy call rate was 223 of 592 (37.7%). Common specific diagnoses included Warthin tumor, lymphoma subtypes, and metastatic squamous cell carcinoma for CNB and IB, in addition to pleomorphic adenoma for CNB. Descriptive diagnoses were still frequent. Nondiagnostic rates were higher in CNB (26 of 356; 7.30%) than IB (5 of 236; 2.12%; $P < .001$). Tissue volumes significantly influenced CNB adequacy, with minimum and optimal volumes of 4.76 mm^3 (J index, receiver operating characteristic curve) and 12.92 mm^3 (95th percentile of distribution), respectively. One hundred forty-four patients (112 CNBs) had follow-up resections; diagnoses were concordant for 66 of 73 adequate CNBs (90.41%). Our restructured risk grouping of MSRSGC categories performed robustly in terms of risk of malignancy (sensitivity = 85.5%, specificity = 100%, accuracy = 92.3%, area under the curve = 0.9677). Conclusions-Although CNB and IB are amenable to a risk stratification system, there are some differences as compared with fine-needle aspiration biopsy, particularly given the high baseline prevalence of malignancy. Specific diagnoses are often feasible and concordant with resection. CNB tissue volume can inform optimal and minimal sampling recommendations for adequacy.

25COASMA21:

Title: Assessment of Breast Pathology Reporting Needs and Development of Tumor Synoptic Templates in Sub-Saharan Africa

Gilbert Z. Nkya, MD, MMed; Oluwatosin Zainab Omoyiola, MBChB;et.al.

Arch Pathol Lab Med (2025) 149 (4): 340–346.
https://doi.org/10.5858/arpa.2024-0101-OA

Abstract: Context-Breast pathology reports include many important details to guide clinical management. Reports with missing critical data elements are commonly seen in non-subspecialized pathology practices. The use of synoptic templates has been shown to improve pathology reports. Although synoptic templates are readily available from professional

societies, many are not tailored to low-resource settings. Objective- To perform an assessment of current breast pathology reporting at 3 referral hospitals in sub-Saharan Africa and design a locally adapted breast cancer synoptic template. Design-We conducted semi-structured interviews with key stakeholders involved in breast cancer care, including pathologists, radiologists, oncologists, and surgeons, from Nigeria, Tanzania, and Mozambique. Moreover, each stakeholder reviewed a preliminary synoptic template that was compiled by using templates from the College of American Pathologists, Royal College of Pathologists, and International Collaboration on Cancer Reporting and was asked to score each data element as essential, optional, or exclude. A locally adapted synoptic template was then designed from the needs assessment. Using the adapted templates, a retrospective review of breast cancer pathology reports from 2020 to 2022 was conducted to determine the completeness of reports at the 3 institutions. Results-A total of 17 physicians were interviewed. Review of pathology reports revealed that none of the reports across all 3 sites contained all data elements considered essential by local physicians. Conclusions-There is an urgent need to improve breast pathology reporting in sub-Saharan Africa. Development and implementation of synoptic templates in collaboration with key stakeholders has the potential to improve pathology reporting practices in low-resource settings.

25COASMA22:

Title: Adverse Prognostic Impact of Transitional and Pleomorphic Patterns in Pleural Nonepithelioid Mesothelioma: Insights From Comprehensive Analysis and Reticulin Stain

Francesco Fortarezza, MD; Federica Pezzuto, MD, PhD et.al.

Arch Pathol Lab Med (2025) 149 (4): 347–353.
https://doi.org/10.5858/arpa.2023-0523-OA

Abstract: Context- Mesothelioma subtyping into epithelioid and nonepithelioid categories plays a crucial role in prognosis and treatment selection, with emerging recognition of the impact of various histologic patterns. Objective-To investigate the prognostic implications of transitional and pleomorphic patterns in sarcomatoid mesothelioma. Design-A total of 132 mesothelioma cases (87 biphasic, 45 sarcomatoid) were analyzed. Histologic slides were assessed, treatment data collected, and cases categorized into predominant epithelioid or sarcomatoid patterns. The sarcomatoid mesotheliomas were classified into usual, pleomorphic, and transitional patterns, with reticulin staining for the latter. Statistical analysis included Cox regression and Kaplan-Meier methods. Results-Younger age ($P = .02$) and receiving therapy ($P < .001$) correlated with improved survival for both histotypes. Advanced stage was associated with shorter survival in sarcomatoid cases ($P = .02$). Predominant epithelioid pattern in biphasic cases led to longer survival ($P < .001$). Transitional and pleomorphic patterns were indicative of worse prognosis, with significantly lower survival in cases with both patterns than in cases with the usual sarcomatoid pattern ($P = .046$). Multivariate analysis identified independent survival factors, including predominant epithelioid component in biphasic mesothelioma ($P = .001$) and chemotherapy ($P < .001$).
Conclusions-Histologic subtyping in mesothelioma plays a pivotal role in prognosis. Transitional and pleomorphic patterns, even in low percentages, indicate poorer outcomes. This study highlights the need for standardized diagnostic support and suggests the potential

utility of histochemical staining in identifying more aggressive morphologic aspects. Recognizing the significance of these patterns can guide treatment decisions and patient care strategies.

25COASMA23:

Title: Neoadjuvant Chemotherapy Response in Triple-Negative Apocrine Carcinoma: Comparing Apocrine Morphology, Androgen Receptor, and Immune Phenotypes

Inwoo Hwang, MD; Yoojoo Lim, MD et.al…

Arch Pathol Lab Med (2025) 149 (4): 354–362.

https://doi.org/10.5858/arpa.2023-0561-OA

Abstract: Context-Apocrine differentiation and androgen receptor (AR) positivity represent a specific subset of triple-negative breast cancer (TNBC) and are often considered potential prognostic or predictive factors. Objective-To evaluate the response of TNBC to neoadjuvant chemotherapy (NAC) and to assess the impact of apocrine morphology, AR status, Ki-67 labeling index (Ki-67LI), and tumor-infiltrating lymphocytes (TILs). Design-A total of 232 TNBC patients who underwent NAC followed by surgical resection in a single institute were analyzed. The study evaluated apocrine morphology and AR and Ki-67LI expression via immunohistochemistry from pre-NAC biopsy samples. Additionally, pre-NAC intratumoral TILs and stromal TILs (sTILs) were quantified from biopsies using a deep learning model. The response to NAC after surgery was assessed based on residual cancer burden. Results-Both apocrine morphology and high AR expression correlated with lower Ki-67LI ($P < .001$ for both). Apocrine morphology was associated with lower postoperative pathologic complete response (pCR) rates after NAC ($P = .02$), but the difference in TILs between TNBC cases with and without apocrine morphology was not statistically significant ($P = .09$ for sTILs). In contrast, AR expression did not significantly affect pCR ($P = .13$). Pre-NAC TILs strongly correlated with postoperative pCR in TNBCs without apocrine morphology ($P < .001$ for sTILs), whereas TNBC with apocrine morphology demonstrated an indeterminate trend ($P = .82$ for sTILs). Conclusions-Although TIL counts did not vary significantly based on apocrine morphology, apocrine morphology itself was a more reliable predictor of NAC response than AR expression. Consequently, although apocrine morphology is a rare subtype of TNBC, its identification is clinically important.

25COASMA24:

Title: Navigating the 2022 International Consensus and World Health Organization Classifications of Hematopathology: A Call for Unified Diagnostic Language

Hadil Zureigat, MD; Bridget Adcock, MD et.al.

Arch Pathol Lab Med (2025) 149 (4): 363–367.

https://doi.org/10.5858/arpa.2024-0031-OA

Abstract: Context-In 2022, 2 distinct guidelines for the diagnosis of myeloid neoplasms became available: the 5th edition of the World Health Organization guideline (WHO2022) solely and the International Consensus Classification (ICC). Despite major overlap, there are important differences that can have important implications.Objective-To explore the current opinions and diagnostic practices of hemato-oncologists and hematopathologists across the United States. Design-An online anonymous survey was created using REDCap, and a secure

link was shared via email to fellowship program leadership and via posts on social media. Results-A total of 310 responses were obtained. Only 33 of 309 respondents (10.7%) reported using solely the 2016 World Health Organization guideline to make diagnoses, whereas 167 of 309 (54%) supplemented it with other guidelines. The rest were either not sure (17; 5.5%), used WHO2022 solely (46; 14.9%), or used ICC solely (6; 1.9%). The choice of guideline was not related to region (P = .15), practice setting (P = .86), or hospital size (P = .22). More than 90% reported having 2 distinct guidelines is a source of confusion in clinical diagnosis, management, trial design, and other areas. Conclusions-Overall, our study found that having 2 distinct guidelines could be a source of confusion for physicians and it highlights the need for a unified diagnostic language.

25COASMA25:

Title: Effects of the Paris System on the Unsatisfactory Category in a Cytohistologic Correlation Study of Patients With Urothelial Carcinoma

Karina Munhoz de Paula Alves Coelho, MD, PhD, MSc; Hercilio Fronza, Jr, MD; Paula de Carvalho, MD; Giordano Barzotto Tagliari, MD;

Arch Pathol Lab Med (2025) 149 (4): 368–371.

https://doi.org/10.5858/arpa.2023-0506-OA

Abstract: Context-The main objectives of the Paris System are to detect high-grade urothelial carcinoma, to standardize morphologic criteria and the cytopathologic report, to reduce the prevalence of the atypia category, and to improve the malignancy risk stratification. Objective-To compare the results and sensitivity of cytologic classification before and after reclassification by the Paris System.Design-Urinary cytology samples from patients with a histologic diagnosis of urothelial carcinoma were reclassified on the basis of the Paris System categories. The diagnoses before reclassification were divided into 5 categories (A, B, C, D, E) and compared with the Paris System (I, II, III, IV, V). Sensitivity was calculated considering cytohistologic agreement in relation to high-grade urothelial carcinoma. Results-A total of 111 urinary cytology samples from patients were analyzed, corresponding to 40 histologic samples; of these, 12 (30%) were high grade and the remaining were low grade. Comparison of the correlated categories showed an increase from 3 (3 of 111; 2.7%) (A) to 31 (31 of 111; 27.9%) (I) in unsatisfactory cases and a decrease from 67 (67 of 111; 60.0%) to 30 (30 of 111; 27.0%) in negative cases, while the atypia category remained unchanged (15 cases [15 of 111; 13.5%]) (C and III). Suspicious cases increased from 5 (5 of 111; 4.5%) (D) to 14 (14 of 111; 12.6%) (IV) and cases of urothelial carcinoma were unchanged (21 cases [21 of 111; 18.9%]) (E and V). Sensitivity was 69% for the previous classification and 90% for the Paris System. Conclusions-The Paris System improved the sensitivity of urinary cytology and the standardization of the unsatisfactory criteria, with an increase of cases in this category and a decrease of cases previously classified as negative among patients with a subsequent histologic diagnosis of urothelial carcinoma.

25COASMA26:

Title: Advances in Human Leukocyte Antigen Testing Technologies and Management Strategies for Platelet Transfusion Refractoriness

H. Cliff Sullivan, MD; P. Dayand Borge, Jr, MD, PhD; Richard R. Gammon, MD; Manish Gandhi, MD; Mary C. Philogene, PhD; YanYun Wu, MD, PhD; Patricia M. Kopko, MD
Arch Pathol Lab Med (2025) 149 (4): 372–380.
https://doi.org/10.5858/arpa.2023-0484-RA
Abstract: Context-The blood bank is often consulted for transfusion support of patients with suspected platelet transfusion refractoriness (PTR). The workup is complex because testing includes specialized assays that are uncommonly ordered with limited availability. Add to this the variety of possible products—crossmatched platelets, human leukocyte antigen (HLA)–matched platelets, HLA antigen–negative platelets—and the approach to PTR can be overwhelming. Moreover, most literature on the subject is published in transfusion medicine journals aimed at transfusion medicine physicians and blood bank specialists in academic settings. Resources tailored to community hospital blood banks are lacking. Objective-
To provide pathologists who may not have subspecialized training in transfusion medicine and who direct blood bank algorithmic workflows based on clinical scenario and test availability to provide appropriate transfusion support for patients with PTR. Data Sources-
This review is a comprehensive overview of terminology, HLA testing procedures, interpretations, and practical recommendations for managing PTR in various scenarios based on expert opinion as well as relevant medical literature published from 2007 to 2022. Conclusions-Consultation on PTR is complicated and encompasses many clinical and laboratory aspects. The lack of guidelines derived from high-quality prospective studies poses challenges in the workup and management of PTR. Hindering the process further are limited test availability, unfamiliarity with the technical assays, and the various specialized platelet products. The clinical evaluation algorithm presented herein along with the workflow pathways offer pathologists user-friendly and best-practice guidelines with different options based on the clinical scenario and the tests available.

25COASMA27:

Title: The Diagnostic Accuracy of Claudin-4 Immunochemistry in Differentiating Metastatic Carcinomas From Mesothelial Processes in Serous Effusion Cytology: A Systematic Review and Meta-analysis

Maria Kleinaki, MD; Johannes A. Vey, MSc; Sinclair Awounvo, MSc; Angela Ishak, MD; Maria Arnaouti, MD; Han Suk Ryu, MD, PhD; Ilias P. Nikas, MD
Arch Pathol Lab Med (2025) 149 (4): 381–388.
https://doi.org/10.5858/arpa.2023-0560-RA
Abstract: Context-Distinguishing metastatic carcinomas from mesotheliomas or reactive mesothelial cells in pleural, peritoneal, and pericardial effusions is a common diagnostic problem cytopathologists encounter. Objective-To perform the first meta-analysis on the pooled diagnostic accuracy of claudin-4 immunochemistry in serous effusion cytopathology.
Design-This report followed the PRISMA (Preferred Reporting Items for Systematic Reviews and Meta-Analyses) guidelines for diagnostic test accuracy studies. Three databases (PubMed, Scopus, and the Cochrane Library) were searched until October 9, 2023, followed by study selection using specific inclusion and exclusion criteria and data extraction. The study quality assessment was performed by using the Quality Assessment of Diagnostic Accuracy Studies 2 (QUADAS-2) tool. Statistical analysis was performed by using R to

calculate the pooled sensitivity and specificity of claudin-4 immunochemistry. In addition, the diagnostic odds ratio was measured, representing the odds ratio of a positive result indicating a carcinoma rather than a mesothelial process in serous effusion cytology.
Results-Fourteen observational studies, published between 2011 and 2023, fulfilled the selection criteria and were included. All 14 studies used the 3E2C1 clone. Claudin-4 immunochemistry showed a high diagnostic accuracy in serous effusion cytology. The pooled sensitivity and specificity were 98.02% (95% CI, 93.96%–99.37%) and 99.72% (95% CI, 97.36%–99.97%), respectively. Lastly, the pooled diagnostic odds ratio was 1660.5 (95% CI, 760.0–3627.8), and no evidence of statistical heterogeneity between the included studies was found ($I^2 = 0\%$, $\tau^2 = 0$). Conclusions-Claudin-4 may be used as a single pan-carcinoma immunochemical biomarker in the differential diagnosis between metastatic carcinomas and mesotheliomas or reactive mesothelial cells in serous effusion cytology.

25COASMA28:

Title: Neoadjuvant Therapy and Lung Cancer: Role of Pathologists

Sanja Dacic, MD, PhD

Arch Pathol Lab Med (2025) 149 (4): e78–e81.
https://doi.org/10.5858/arpa.2024-0203-RA

Abstract: Context-Recent neoadjuvant clinical trials in lung cancer have demonstrated the survival benefits in carefully selected patients. Standardization of the assessment of pathologic response to neoadjuvant therapy in surgically resected specimens is required.
Objective-To review the current pathology practices in the gross processing and microscopic assessment of surgically resected non–small cell lung carcinoma specimens after neoadjuvant therapy. Data Sources-PubMed publications and experience of the author. Conclusions-Gross processing of the surgically resected lung carcinoma after neoadjuvant therapy needs further refinement and standardization in clinical trials and in a real-world clinical practice. Microscopic assessment of the response includes quantification of viable tumor, necrosis, and stroma. The best approach would be to use a single standardized and most reproducible scoring system. Published studies on gross processing of lung carcinoma specimens in the neoadjuvant setting and microscopic assessment of pathologic response provide a good foundation for the future standardization of pathology practice.

25COASMA29:

Title: Pulmonary Adenocarcinoma Updates: Histology, Cytology, and Grading

Jake Sharma, DO; Fang Zhou, MD; Andre L. Moreira, MD, PhD

Arch Pathol Lab Med (2025) 149 (4): e82–e86.
https://doi.org/10.5858/arpa.2023-0540-RA

Abstract: Context-Adenocarcinomas are the most common histologic subtype of lung cancer, and exist within a widely divergent clinical, radiologic, molecular, and histologic spectrum. There is a strong association between histologic patterns and prognosis that served as the basis for a recently described grading system. As the study of molecular pathology rapidly evolves, all targetable mutations so far have been found in adenocarcinomas, thus requiring accurate diagnosis and classification for the triage of molecular alterations and adequate therapy. Objective-To discuss the rationale for adenocarcinoma classifications

within the 2021 5th edition of the World Health Organization Classification, with a focus on nonmucinous tumors, including tumor grading and biopsy/cytology diagnosis.
Data Sources-PubMed search. Conclusions-A grading system for adenocarcinoma has improved prognostic impact of the classification of pulmonary adenocarcinoma. An accurate diagnosis of adenocarcinoma in small biopsy material is important for tissue triage for molecular studies and ultimately for patient management and treatment.

25COASMA30:

Title: Uncommon Tumors of the Lung: Recently Described and Rediscovered Tumors

Cesar A. Moran, MD

Arch Pathol Lab Med (2025) 149 (4): e87–e92.

https://doi.org/10.5858/arpa.2023-0414-RA

Abstract: Context- The great majority of primary pulmonary neoplasms are represented by non–small cell carcinomas—adenocarcinoma and squamous cell carcinoma. In addition, there is another group of neoplasms such as those of neuroendocrine origin that also represent a meaningful subset of primary lung neoplasms. Basically, any other tumor that is not in these groups of tumors may represent an unusual lung neoplasm. Objective- To highlight more recently described unusual tumoral entities that may represent a challenge in diagnosis and that require awareness of their existence. Data Sources- This is a review of 3 different entities: bronchiolar adenoma, adenofibroma, and hemangioblastoma-like clear cell stromal tumor. These tumoral conditions are rare, and a review of the literature is presented. The most relevant morphologic, immunohistochemical, and molecular aspects of bronchiolar adenoma, adenofibroma, and hemangioblastoma-like clear cell stromal tumor are presented. The difficulty of arriving at an unequivocal diagnosis in small biopsies is highlighted. Conclusions- The 3 entities represent uncommon tumors occurring primarily in the lung and a diagnostic challenge not only in biopsy specimens but also often in surgically resected specimens. The use of immunohistochemical stains and in some cases of molecular diagnostics is of aid in arriving at final interpretation.

25COASMA31:

Title: Thoracic Frozen Section Pitfalls: Lung Adenocarcinoma Versus Selected Mimics

Sanjay Mukhopadhyay, MD

Arch Pathol Lab Med (2025) 149 (4): e93–e99.

https://doi.org/10.5858/arpa.2024-0023-RA

Abstract: Context- Intraoperative (frozen section) analysis of lung lesions (nodules, masses, ground-glass opacities) can occasionally be diagnostically challenging. Objective- To describe selected pitfalls in thoracic frozen sections with a focus on the differential diagnosis between adenocarcinoma and its mimics, and to provide tips to prevent misinterpretation.
Data Sources- Peer-reviewed literature and the author's experience. Conclusions- A common challenge in thoracic frozen sections is the differential diagnosis between lung adenocarcinoma and its mimics. Diagnostic difficulties arise because mimics of adenocarcinoma often entrap reactive lung epithelium that can appear atypical on frozen section slides. Entities that can be misinterpreted as adenocarcinoma include ciliated muconodular papillary tumor/bronchiolar adenoma, hamartoma, inflammatory

myofibroblastic tumor, and pulmonary Langerhans cell histiocytosis. Knowledge of the key clinical, radiologic, and histologic features of these entities can help prevent overdiagnosis of adenocarcinoma. Pathologic findings that facilitate the distinction between adenocarcinoma and its mimics at frozen section include the appearance and contour of the lesion at low magnification, growth patterns, cilia, stromal features, shape of the epithelial cells (cuboidal versus columnar), nuclear features of malignancy (crowding, hyperchromasia, irregular contours), and abruptness of the junction between the lesion and adjacent uninvolved lung. Knowledge of the clinical context, imaging findings, and the surgical consequence of the intraoperative diagnosis can also prevent diagnostic errors. Finally, since adenocarcinomas of the lung are often relatively bland and lack the stromal desmoplasia seen in adenocarcinomas of other organs, familiarity with the morphologic spectrum of lung adenocarcinomas at frozen section analysis is important.

25COASMA32:

Title: Progressive Pulmonary Fibrosis and Interstitial Lung Abnormalities: AJR Expert Panel Narrative Review

Jeffrey P. Kanne, MD , Christopher M. Walker, MD, Anupama G. Brixey, MD, Kevin K. Brown, MD, Lydia Chelala, MD, Ella A. Kazerooni, MD, MS, Simon L. F. Walsh, MD, PhD

American Journal of Roentgenology, Volume 224, Issue 3

https://doi.org/10.2214/AJR.24.31125

Abstract: Progressive pulmonary fibrosis (PPF) and interstitial lung abnormalities (ILA) are relatively new concepts in interstitial lung disease (ILD) imaging and clinical management. Recognition of signs of PPF and identification and classification of ILA are important tasks during chest high-resolution CT interpretation to optimize management of patients with ILD and those at risk of developing ILD. However, in professional society guidance, the role of imaging surveillance remains unclear for stable patients with ILD, asymptomatic patients with ILA who are at risk of progression, and asymptomatic patients at risk of developing ILD without imaging abnormalities. In this AJR Expert Panel Narrative Review, we summarize the current knowledge regarding PPF and ILA and describe the range of clinical practice with respect to imaging patients with ILD, those with ILA, and those at risk of developing ILD. In addition, we offer suggestions to help guide surveillance imaging in areas with an absence of published guidelines, where such decisions are currently driven primarily by local pulmonologists' preference.

25COASMA33:

Title: Training and Verification Requirements for Interpretation of Cardiac CT and MRI: AJR Expert Panel Narrative Review

Prabhakar Shantha Rajiah, MBBS, MD Matthew Budoff, MD, Brian Ghoshhajra, MD,

American Journal of Roentgenology, Volume 224, Issue 3

https://doi.org/10.2214/AJR.24.31524

Abstract: The use of cardiac CT and MRI is rapidly expanding based on strong evidence from large international trials. The number of physicians competent to interpret cardiac CT and MRI may be unable to keep pace with the increasing demand. Societies and

organizations have prescribed training requirements for interpreting cardiac CT and MRI, with recent updates focusing on the increased breadth of competency that is now required due to ongoing imaging advances. In this AJR Expert Panel Narrative Review, we discuss several aspects of cardiac CT and MRI training, focusing on topics that are uncertain or not addressed in existing society statements and guidelines, including determination of competency in different practice types in real-world settings and the impact of artificial intelligence on training and education. The article is intended to guide updates in professional society training requirements and also inform institutional verification processes.

25COASMA34:

Title: Breast Cryoablation, From the AJR "How We Do It" Special Series

Jothika V. Challapalli, MD , Jessica H. Yoon, MD,

American Journal of Roentgenology, Volume 224, Issue 3
https://doi.org/10.2214/AJR.24.31025

Abstract: Breast cryoablation is a minimally invasive image-guided percutaneous procedure for the treatment of fibroadenomas and early-stage breast cancer that uses liquid nitrogen or argon gas to create extremely cold temperatures that devitalize targeted tissue. Although more long-term data are needed, this outpatient procedure is well-tolerated and carries minimal risks, including nontarget thermal injury that can be mitigated by careful planning and proper technique. Building a sustainable breast cryoablation service in a radiology practice poses several practical considerations, such as training proceduralists, purchasing equipment, recruiting patients, and understanding the revenue cycle. This Special Series Review describes aspects of the radiologist's role in this procedure, including implementation of a breast ablation program, patient selection, technical details related to intervention, and expected postprocedural outcomes.

25COASMA35:

Title: Bosniak Classification of Cystic Renal Masses Version 2019: Proportion of Malignancy by Class and Subclass—Systematic Review and Meta-Analysis

Trevor A. McGrath, MD, PhD, Matthew S. Davenport, MD, Stuart G. Silverman, MD, Christopher S. Lim, MD, Yassir E. Almalki, MD, Yuki Arita, MD, PhD, Xu Bai, MD

American Journal of Roentgenology, Volume 224, Issue 3
https://doi.org/10.2214/AJR.24.32342

Abstract: BACKGROUND. Bosniak classification version 2019 (v2019) was a major revision to version 2005 (v2005) that defined cystic renal mass subclasses on the basis of wall or septa features. OBJECTIVE. The purpose of the study was to determine the proportion of malignancy within cystic renal masses stratified by Bosniak classification v2019 class and feature-based subclass. EVIDENCE ACQUISITION. MEDLINE and Embase databases were searched on July 24, 2023, for studies published in 2019 or later that reported cystic renal masses that underwent renal-mass CT or MRI, were assessed using Bosniak classification v2019, and had a reference standard (histopathology indicating benignancy or malignancy or ≥ 5 years of imaging follow-up indicating benignancy). Study authors were contacted to provide subclass-stratified data. Pooled proportions of malignancy

stratified by v2019 class and subclass were determined using meta-analysis. EVIDENCE SYNTHESIS. The analysis included 12 studies reporting 966 patients with 975 cystic masses. No class I mass was malignant. Pooled proportions of malignancy by class were as follows: II, 9% (95% CI: 5–17%); IIF, 26% (95% CI: 13–46%); III, 80% (95% CI: 71–87%); and IV, 88% (95% CI: 83–91%). Pooled proportions of malignancy by subclass were as follows: IIF with many smooth, thin septa, 10% (95% CI: 2–33%); IIF with minimal wall or septal thickening, 47% (95% CI: 18–77%); IIF with heterogeneous T1 hyperintensity, 26% (95% CI: 8–57%); III with a thick, smooth wall or septa, 78% (95% CI: 60–90%); III with obtuse protrusion(s) 3 mm or less, 84% (95% CI: 77–90%); IV with acute protrusion(s) of any size, 88% (95% CI: 80–93%); and IV with obtuse protrusion(s) 4 mm or greater, 86% (95% CI: 77–91%). The proportion of malignancy was 41% for IIF masses with histopathology reference versus 2% for IIF masses with imaging follow-up reference. In four studies performing intraindividual comparisons of v2005 versus v2019, the proportions of malignancy were as follows: class IIF, 24% versus 42% (p = .13); III, 74% versus 77% (p = .72); and IV, 79% versus 84% (p = .22). CONCLUSION. Bosniak IIF masses had higher malignancy rates when histopathology rather than imaging follow-up was the reference standard, indicating verification bias. All Bosniak III and IV subclasses had high malignancy rates.

25COASMA36:

Title: Digital Mammography, Tomosynthesis, and Contrast-Enhanced Mammography: Intraindividual Comparison of Mean Glandular Dose for Screening Examinations

JeremiahW. Sanders, PhD William Pavlicek, PhD, Wolfgang Stefan, PhD, James Hanson, ME, Richard E. Sharpe, Jr., MD, MBA,

American Journal of Roentgenology, Volume 224, Issue 3
https://doi.org/10.2214/AJR.24.32150

Abstract: BACKGROUND. Contrast-enhanced mammography (CEM) is growing in clinical use due to its increased sensitivity and specificity compared with full-field digital mammography (FFDM) and/or digital breast tomosynthesis (DBT), particularly in patients with dense breasts. OBJECTIVE. The purpose of this study was to perform an intraindividual comparison of mean glandular dose (MGD) with FFDM, DBT, a combination protocol using both FFDM and DBT (hereafter, combined FFDM-DBT), and CEM in patients undergoing breast cancer screening. METHODS. This retrospective study included 389 women (median age, 57.4 years) with an elevated risk of breast cancer who, as part of participation in an earlier prospective clinical trial, underwent breast cancer screening with combined FFDM-DBT and CEM between February 2019 and April 2021. A total of 764 breasts (383 left, 381 right) were evaluated. One craniocaudal (CC) view and one mediolateral oblique (MLO) view were evaluated per breast for each of FFDM, DBT, and CEM. MGD values were extracted from DICOM metadata. BI-RADS breast density categories were extracted from clinical radiology reports. Data were summarized descriptively, including determination of corresponding effective doses. RESULTS. The breast density category was A in zero patients, B in 44 patients (88 breasts), C in 306 patients (599 breasts), and D in 39 patients (77 breasts). The median MGD per breast (CC and MLO views combined) was 4.07 mGy for FFDM alone, 4.97 mGy for DBT alone, 9.38 mGy for combined FFDM-DBT, 3.96 mGy for

low-energy CEM, 1.90 mGy for high-energy CEM, and 5.87 for CEM overall. Corresponding effective dose values were 0.49, 0.60, 1.13, 0.48, 0.23, and 0.70 mSv, respectively. The median MGD for density categories B, C, and D, respectively, was 4.01, 4.22, and 2.70 mGy for FFDM; 5.93, 4.93, and 3.17 mGy for DBT; and 5.90, 6.02, and 4.52 mGy for CEM. CONCLUSION. In this intraindividual comparative study of screening examinations, the MGD per breast was higher for CEM than for FFDM or DBT alone. However, these differences were small, and MGD was lower for CEM than for combined FFDM-DBT.

25COASMA37:

Title: Role of MRI in Assessing the Feasibility of Fertility-Sparing Treatments for Early-Stage Endometrial and Cervical Cancers

Mihan Lee, MD, PhD, Pamela I. Causa Andrieu, MD, Stephanie Nougaret, MD, PhD, Luca Russo, MD, Sara Moufarrij, MD, Jennifer J. Mueller, MD, Nadeem R. Abu-Rustum, MD, Christine O. Menias, MD, and Yulia Lakhman, MD

American Journal of Roentgenology, , Volume 224, Issue 3

https://doi.org/10.2214/AJR.24.32157

Abstract: Fertility-sparing treatment (FST) has become a key aspect of managing gynecologic cancers in reproductive-age patients who wish to preserve fertility. Several leading clinical societies, including the European Society of Gynecological Oncology, the European Society for Radiotherapy and Oncology, the European Society of Pathology, and the European Society of Human Reproduction and Embryology, have published evidence-based guidelines on fertility-sparing strategies and post-treatment surveillance of patients with early-stage gynecologic cancers, in particular endometrial and cervical cancers. These guidelines highlight MRI as essential to initial patient selection and follow-up. Properly tailored pelvic MRI protocols and clear MRI reports are key to performing accurate staging, assessing eligibility, and confirming the initial and ongoing feasibility of FST. Accordingly, radiologists, particularly those specializing in gynecologic imaging, play a critical role in the multidisciplinary approach to FST. They should be well-versed in FST eligibility criteria and key MRI findings before and after FST, ensuring these details are comprehensively communicated in structured MRI reports.

25COASMA38:

Title: Machine Learning to Detect Cervical Spine Fractures Missed by Radiologists on CT: Analysis Using Seven Award-Winning Models From the 2022 RSNA Cervical Spine Fracture AI Challenge

Yingming Amy Chen, MD , Zixuan Hu, MSc, Kevin D. Shek, MD, Jefferson Wilson, MD, Fahad Saud S. Alotaibi, MD, Christopher D. Witiw, MD, Hui Ming Lin, HBSc, MRT,

American Journal of Roentgenology, Volume 224, Issue 3

https://doi.org/10.2214/AJR.24.32076

Abstract: BACKGROUND. Available data on radiologists' missed cervical spine fractures are based primarily on studies using human reviewers to identify errors on reevaluation; such studies do not capture the full extent of missed fractures. OBJECTIVE. The purpose of this study was to use machine learning (ML) models to identify cervical spine fractures on CT

missed by interpreting radiologists, characterize the nature of these fractures, and assess their clinical significance. METHODS. This retrospective study included all cervical spine CT examinations performed in adult patients in the emergency department between January 1, 2018, and December 31, 2022. Examinations reported as negative for cervical spine fracture were processed by seven award-winning ML models from the 2022 Radiological Society of North America Cervical Spine Fracture AI Challenge; examinations classified as positive by at least four of the seven models were considered to have ML-detected fractures. Two neuroradiologists independently reviewed examinations with ML-detected fractures using ML-derived heat maps to identify those representing true missed fractures. The neuroradiologists further assessed the fractures' extent. Two spine surgeons independently assessed whether missed fractures were clinically significant (i.e., warranting at least one of surgical consultation, MRI, CTA, or collar immobilization). RESULTS. The study included 6671 patients (2414 women, 4257 men; mean age, 54.6 ± 22.1 [SD] years) who underwent a total of 6979 cervical spine CT examinations. Interpreting radiologists reported 6378 examinations as negative for fracture. Of these, 356 had ML-detected fractures (i.e., positive by at least four of seven models). The neuroradiologists classified 40 of these examinations, in 39 unique patients, as having true fractures. ML-detected missed true fractures involved 51 unique sites, most commonly the C7 transverse process (n = 12), C5 spinous process (n = 12), and C6 spinous process (n = 8). The surgeons considered missed fractures clinically significant in 15 of 40 examinations (MRI and collar immobilization [n = 7], MRI and surgical evaluation [n = 1], CTA [n = 9]). Interobserver agreement, expressed as kappa, was 0.88 between neuroradiologists for true fracture classification and 0.94 between surgeons for clinical significance classification. CONCLUSION. ML models identified cervical spine fractures missed by radiologists. These fractures were further characterized to systematically highlight radiologists' common misses.

25COASMA39:

Title: CT-Based Body Composition Measures and Systemic Disease: A Population-Level Analysis Using Artificial Intelligence Tools in Over 100,000 Patients

B. Dustin Pooler, MD, John W. Garrett, PhD, Matthew H. Lee, MD, Benjamin E. Rush, PhD, MPH, Adam J. Kuchnia, PhD, Ronald M. Summers, MD, PhD

American Journal of Roentgenology, Volume 224, Issue 3
https://doi.org/10.2214/AJR.24.32216

Abstract: BACKGROUND. CT-based abdominal body composition measures have shown associations with important health outcomes. Advances in artificial intelligence (AI) now allow deployment of tools that measure body composition in large patient populations. OBJECTIVE. The purpose of this study was to assess associations of age, sex, and common systemic diseases with CT-based body composition measurements derived using a panel of fully automated AI tools in a population-level adult patient sample. METHODS. This retrospective study included 140,606 adult patients (67,613 men and 72,993 women; mean age, 53.1 ± 17.6 [SD] years) who underwent abdominal CT at a single academic institution between January 1, 2000, and February 28, 2021. CT examinations were not restricted on the basis of patient setting, clinical indication, or IV contrast media use. Thirteen fully automated AI body composition tools quantifying liver, spleen, and kidney volume and attenuation;

vertebral trabecular attenuation; skeletal muscle area and attenuation; and abdominal fat area and attenuation were applied to each patient's first available abdominal CT examination. EHR review was performed to identify common systemic diseases, including cancer,cardiovascular disease (CVD), diabetes mellitus (DM), and cirrhosis, on the basis of relevant ICD-10 codes; 64,789 patients (46.1%) had at least one systemic disease diagnosed. Multiple linear regression models were performed for the 118,141 patients (84.0%) with no systemic disease or a single systemic disease, to assess age, sex, and the presence of systemic disease as predictors of body composition measures; effect sizes were characterized using the unstandardized regression coefficient B. RESULTS. Multiple linear regression models using age, sex, and systemic disease as predictors were overall significant for all 13 body composition measures (all $p < .001$) with variable goodness of fit ($R^2 = 0.03–0.43$ across models). In the models, age was predictive of all 13 body composition measures; sex, 12 measures; cancer, nine measures; CVD, 11 measures; DM, 13 measures; and cirrhosis, 12 measures (all $p < .05$). CONCLUSION. Age, sex, and the presence of common systemic diseases were predictors of AI-derived CT-based body composition measures.

25COASMA40:

Title: BRAF Gene Fusions in Melanoma : First Kinase Domain Duplication, New Fusion Partners, and Clinical Outcomes

Odintsov, Igor MDDavis, Dale MDPissaloux, Daniel PhDTirode, Franck PhDde la Fouchardiere, Arnaud MD, PhDHanna, John MD, PhD

The American Journal of Surgical Pathology, 49 (5), 429-438.

https://doi.org/10.1097/PAS.0000000000002370

Abstract: BRAF gene fusions have been well-described in Spitzoid melanocytic lesions but can also occur uncommonly in conventional melanomas. Here we report a series of 17 melanomas harboring **BRAF** gene fusions as their putative primary genetic driver. All but one of these tumors occurred in adults (age range 13 to 96) with a relatively even sex distribution (41% female) and a broad distribution of anatomic sites. None of the tumors showed typical Spitzoid histomorphologic features. Molecular analysis identified the first example of **BRAF** kinase domain duplication in melanoma, which raises interesting questions regarding the mechanism of fusion-induced BRAF activation. Although we did not identify histomorphologic features that could distinguish **BRAF** -fused melanomas from more conventional melanomas, we did observe a generally low tumor mutational burden and a lower rate of UV-associated mutational signatures (3/17; 18%), suggesting that **BRAF** -fused melanomas are molecularly and mechanistically distinct from conventional cutaneous melanomas. We report detailed treatment information and clinical outcomes for this series, with most patients having shown disease progression on systemic immunotherapy (8/12; 67%). Our results highlight the need for continued molecular subclassification to yield a comprehensive understanding of melanoma pathogenesis and have potential implications for therapeutic selection in **BRAF** -fused and perhaps other unconventional forms of melanoma.

.

25COASMA41:

Title: Clinicopathologic and Molecular Characterization of Gynecologic Carcinosarcomas With a Mesonephric-Like Carcinomatous Component

Mendoza, Rachelle P. MDTjota, Melisa Y. MD, PhDChoi, Donghyuk N. BSChapel, David B. MD[§]Kolin, David L. MD, PhD[‖]Euscher, Elizabeth D. MD
The American Journal of Surgical Pathology, 49 (5), 439-447.
https://doi.org/10.1097/PAS.0000000000002368.
Abstract: Carcinosarcoma with a mesonephric-like carcinomatous component (MLCS) is a rare subtype of gynecologic malignancy recently described in the literature. This study aims to expand the genomic characterization of MLCS by performing independent molecular analysis of the carcinomatous and sarcomatous components in a series of MLCS. Eight cases of gynecologic MLCS (endometrial, lower uterine segment, and ovarian) were identified and underwent clinicopathologic evaluation. Genomic DNA extraction and next-generation sequencing (NGS) were performed separately from the carcinomatous and sarcomatous components of 4 tumors, while 2 tumors underwent NGS of combined carcinomatous and sarcomatous components. The average age at diagnosis was 65.6 years (range 50 to 83 years). MLCS patients were diagnosed at FIGO stage I (n=3), stage II (n=2), stage III (n=2), and stage IV (n=1). The carcinomatous and sarcomatous components were observed to harbor the same single nucleotide variations. All cases had less than 10 mutations/Mb and were microsatellites stable. All cases (6/6, 100%) harbored **KRAS** point mutations in codon 12, including the following variants: p.G12D (n=2), p.G12A (n=2), and p.G12V (n=2). Five cases showed additional alterations in **ARID1A** (case 1), **PTEN** (case 2), **PIK3CA** (case 4), **SPOP** (case 6), **TET1** (case 6), **BUB1** (case 7), **LYN** (case 7) and **PTPRD** (case 7). The presence of both **KRAS** and **PTEN** / **PIK3CA** alterations suggests a combined endometrioid and mesonephric differentiation in MLCS.

25COASMA42:

Title: Breast Carcinomas Resembling Acinic Cell Carcinoma : Comprehensive Analysis of 14 Cases and Review of the Literature

Qin, Fengxia MD, PhDLi, Jiazhen MMedZheng, Yi MD, PhDJiang, Chengying MD, PhD
The American Journal of Surgical Pathology, 49 (5), 448-457.
https://doi.org/10.1097/PAS.0000000000002363.
Abstract: Acinic cell carcinoma (AciCC) of the breast is an exceptionally rare subtype of invasive breast carcinoma, often exhibiting a triple-negative phenotype and relatively indolent behavior. Since the first case reported by Roncaroli and colleagues in 1996, no more than 60 additional cases have been described in English medical journals, usually as case reports or small case series. In this study, we presented an in-depth analysis of 14 cases of AciCC of the breast, including 4 pure AciCCs and 10 AciCCs mixed with other histologic types. We reported the clinicopathologic characteristics, histologic components, treatment modalities including response to neoadjuvant treatment in 3 patients, and outcomes. In addition, we assessed the expression of nuclear transcription factor nuclear receptor subfamily 4 group A member 3 by immunohistochemistry and gene rearrangements by fluorescence in situ hybridization, which has been implicated in AciCC of the salivary gland. All 14 cases were negative for nuclear receptor subfamily 4 group A member 3 expression, and no gene rearrangements were detected. We also conducted a thorough review of the literature to highlight advancements in understanding this rare breast cancer subtype. This study aims to enhance clinical knowledge of AciCC of the breast and contributed to growing

evidence that AciCC of the breast and AciCC of the salivary glands appear to be unrelated entities, despite sharing a similar histologic appearance.

25COASMA43:

Title: Clinicopathologic Features and Viral Status of Low-risk HPV6 and HPV11-Associated Squamous Cell Carcinoma of the Uterine Cervix and Vulva

Williams, Guy A. II MDWu, Annie A. MD, PhDEugene, Henrietta C. MS

The American Journal of Surgical Pathology, 49 (5), 458-470.
https://doi.org/10.1097/PAS.0000000000002367.

Abstract: Despite being designated as “noncarcinogenic” human papillomavirus (HPV) types, mono-infection with HPV6 or HPV11 has been found in squamous cell carcinomas (SCCs) at specific sites, including the larynx, penis, anus, and rarely, the lower female genital tract. The association between clinicopathologic features, viral status, and the carcinogenic mechanisms related to these low-risk HPVs remains unclear. The current study characterizes a series of low-risk HPV6 and HPV11-associated SCCs of the uterine cervix (6 cases) and vulva (2 cases). The diagnosis of SCC was made through the identification of stromal invasion in 6 cases. In case 2, the diagnosis of cancer was made after metastases to the sigmoid colon and liver. The patient in case 6 was diagnosed with intramucosal papillary SCC given multiple recurrences. While all tumors displayed a similar verruco-papillary architecture, the cytologic features, and immunostaining patterns suggest 2 groups of lesions: one with high-grade cytology and a high Ki-67 proliferation index (>60% of lesional cells), and the other with low-grade cytology and a low Ki-67 (20% to 30% of lesional cells). The detection of HPV6 in 7 of 8 cases underscores its critical role in carcinogenesis at these anatomic sites. Case 8 represented the only patient who was infected with HPV11 and who had a well-controlled human immunodeficiency virus infection. Correlating with viral status, all cases, except case 7, demonstrated a negative or focal p16 staining pattern. In case 7, despite a block pattern of p16 staining often seen in predicting high-risk HPV, we employed several methods to confirm HPV6 as the sole HPV infection. Although this descriptive study does not establish an etiological mechanism for how HPV6/11 leads to malignant transformation, our results exclude the possibility of viral integration through a quantitative polymerase chain reaction-based analysis of the E2/E6 ratio. Our study highlights and expands upon the clinicopathologic features of a distinct group of low-risk HPV6/11-associated SCCs in the cervix and vulva. Although rare, recognizing this group of lesions is important for pathologists and oncologists, as it provides a basis for guiding appropriate prevention strategies and treatment modalities based on the viral type.

25COASMA44:

Title: Extensive Pathologic Invasion and Prognostic Implication of Gastric-Type Cervical Adenocarcinoma : A Comparative Analysis With Human Papillomavirus-Associated Adenocarcinoma

Kamijo, Kyosuke MDMiyamoto, Tsutomu MD, PhDet.al.

The American Journal of Surgical Pathology, 49 (5), 471-480.
https://doi.org/10.1097/PAS.0000000000002369.

Abstract: Gastric-type adenocarcinoma (GAS) is the most common subtype of human

papillomavirus (HPV)-independent cervical adenocarcinomas and is associated with a poor prognosis. We used a gross morphologic classification system and imaging analysis to compare the clinicopathological features of GAS and HPV-associated adenocarcinoma (HPVA) and identify factors contributing to the poor prognosis of GAS. This retrospective 2-center study analyzed 33 patients with GAS and 70 with HPVA (stages IB-IVB) who underwent surgery between 1997 and 2023. GAS had a higher rate of positive surgical margins (21.2% vs. 0%, respectively, **P** <0.001) and unclear tumor boundaries on gross morphologic findings (47.8% vs. 8.8%, respectively, **P** <0.001). Discrepancies between clinical and pathologic T classifications were more common in GAS, leading to frequent upstaging (51.5% vs. 28.6%, respectively, **P** =0.029). Imaging analysis revealed that GAS was associated with a smaller median tumor cell area (19.8% vs. 55.7%, respectively, **P** <0.001), which was significantly correlated with unclear tumor boundaries. Perineural invasion (PNI) was significantly more frequent in GAS (69.7% vs. 10.0%, respectively, **P** <0.001). A Kaplan-Meier analysis showed that patients with PNI had significantly poorer overall survival (**P** <0.001). A Cox multivariate analysis identified an advanced pathologic stage, positive peritoneal cytology, and positive surgical margins as independent risk factors. The present results indicate that GAS has a unique "stealth" invasion pattern, possibly caused by low tumor density, leading to undetectable tumor boundaries and positive surgical margins. This suggests a greater risk of incomplete resection than HPVA, leading to a poorer prognosis.

25COASMA45:

Title: High-Grade Papillary Thyroid Carcinoma, Diffuse Sclerosing Subtype : A Series of 18 Cases Detailing the Pathologic Features, Potential for Misdiagnosis, and Aggressive Clinical Behavior

Ghossein, Ronald A. MDScholfield, Daniel W. MDQin, HowardShaha, Ashok R. MD

American Journal of Surgical Pathology, 49 (5), 481-489.
https://doi.org/10.1097/PAS.0000000000002371.

Abstract: High-grade differentiated thyroid carcinoma is a novel classification defined by elevated mitotic count (MC) of ≥5/2 mm^2 and/or tumor necrosis. It may assume a phenotype of papillary thyroid carcinoma, diffuse sclerosing subtype (PTC-DS), and can be termed HGPTC-DS. A detailed clinicopathologic review was conducted on a large series of 18 cases of HGPTC-DS. A control group of 41 PTC-DSs with genomic data was also included. Histologically, HGPTC-DS showed typical features of PTC-DS and HG areas, often exhibiting solid architecture of uniform squamoid cells admixed with tumor necrosis, frequently the comedo type. All HGDTC-DSs had tumor necrosis. The MC was often low (median 1/2 mm^2). PTC nuclear features were retained and no nuclear pleomorphism was seen. HGPTC-DS was often subjected to misdiagnosis. Among the 7 external cases, the initial diagnosis was anaplastic carcinoma in 1 and PTC in 5. Compared with PTC-DS, HGPTC-DS was associated with positive resection margin, AJCC eighth edition pT3b and pT4a/4b disease, gross extrathyroidal extension (ETE), a higher number of regional lymph nodes metastasis, a larger size of nodal metastasis, decreased recurrence-free survival (RFS) and regional recurrence-free survival (**P** <0.05). Among the 9 HGPTC-DSs sequenced, 5 harbored **RET** fusions, 2 had **STRN::ALK** fusion, and 1 had **BRAF** p.V600E mutation. In

conclusion, HGPTC-DS is a rare high-grade carcinoma characterized by uniform squamoid area with comedo-type tumor necrosis, high pT stage, gross ETE, large volume nodal metastasis, poor RFS, and RRFS. Given its rarity, it may be subjected to misdiagnosis as PTC and anaplastic carcinoma.

25COASMA46:

Title: High-accuracy Detection of PD-L1 3'-UTR Disruption by Immunohistochemistry and Fluorescence in Situ Hybridization on Formalin-fixed Paraffin-embedded Sections

Fujimoto, Ayumi MDSakata, Seiji MD, PhDKataoka, Keisuke MD, PhDǁKogure, Yasunori MD

The American Journal of Surgical Pathology, 49 (5), 490-498.

https://doi.org/10.1097/PAS.0000000000002372.

Abstract: Programmed death-ligand 1 (PD-L1/CD274) structural variation (SV) disrupting the 3′-untranslated region has been highlighted as being associated with PD-L1 overexpression. In the present study, we evaluated lymphoma tissue samples to investigate the applicability of immunohistochemistry (IHC) and fluorescence in situ hybridization (FISH) for detecting the PD-L1 SV involving the 3′-untranslated region. In total, 1052 lymphoma samples were screened using IHC, and 99 IHC screening-positive samples were evaluated with FISH (non-Hodgkin lymphoma [NHL, n=58] and Hodgkin lymphoma [HL, n=41]). Of these, 92 samples showed strong PD-L1 expression with 2 PD-L1 antibodies (E1J2J and SP142) (concordant PD-L1 IHC), whereas 7 samples showed strong PD-L1 expression only with E1J2J (discordant PD-L1 IHC). Abnormal FISH findings for PD-L1 were detected in all evaluated samples (51 NHLs and 41 HLs). A structural abnormality pattern was observed in 17 of the 51 evaluated NHL samples (33%). In contrast, all 41 HL samples showed a copy number abnormality pattern, with 1 exhibiting a structural abnormality pattern. Target-capture sequencing of the PD-L1 gene was performed on 73 of the 99 IHC screening-positive samples, comprising 41 NHLs and 32 HLs. PD-L1 SVs were detected in 16 (39%) of the 41 NHL samples and in only one of the 32 HL samples (3%). Samples exhibiting discordant PD-L1 IHC and/or FISH structural abnormality patterns were shown to harbor PD-L1 SV by target-capture sequencing, with positive and negative predictive values of 94% and 96%, respectively. Our approach is an alternative to target-capture sequencing for evaluating PD-L1 gene abnormalities.

25COASMA47:

Title: Insights into the Clinical Prognosis of High-grade Appendiceal Mucinous Neoplasms

Dartigues, Peggy MDKepenekian, Vahan MDIllac-Vauquelin, Claire MD

The American Journal of Surgical Pathology, 49 (5), 499-507.

https://doi.org/10.1097/PAS.0000000000002373.

Abstract: High-grade appendiceal mucinous neoplasm (HAMN) is used to describe a rare epithelial neoplasm of the appendix characterized by pushing-type invasion and high-grade cytologic atypia. Its implications regarding lymph node spread and the necessity of right colectomy are currently debate. The objective of the present study was to assess the clinicopathologic characteristics, the risk of lymph node and peritoneal metastasis, and long-

term outcomes of patients diagnosed as HAMN in comparison to low-grade appendiceal mucinous neoplasm (LAMN) and appendiceal adenocarcinoma, treated by right hemicolectomy. A total of 443 patients diagnosed with LAMN (n=246), HAMN (n=34), or appendiceal adenocarcinoma (n=163) and who underwent right colectomy with lymph node dissection in all cases within 32 institutions of the French Network for Rare Peritoneal Malignancies (RENAPE) were included. The median age was 56.5 years (range: 21 to 91), and the majority were female (n=250, 56.4%) without difference between groups (**P** =0.604). Lymph node metastases were identified in 17.8% of appendiceal adenocarcinoma cases (29/163); none were found among LAMN or HAMN cases. A higher number of lymph nodes were analyzed in those treated for appendiceal adenocarcinoma than LAMN (**P** <0.001) and HAMN (**P** =0.035). Regarding peritoneal metastasis, a higher proportion of cases were classified as high-grade with/without signet cells in patients treated for HAMN (**P** <0.001) and appendiceal adenocarcinoma (**P** <0.001) than those treated for LAMN. Among patients with perforation of the appendix, those treated for LAMN had longer overall survival (OS; **P** <0.001) and progression-free survival (PFS; **P** <0.0001) than those treated for appendiceal adenocarcinoma or those treated for HAMN; among patients without perforation, those treated for LAMN and HAMN had longer OS (**P** =0.042) and PFS (**P** =0.012) than those treated for appendiceal adenocarcinoma. No lymph node metastases were observed in patients treated for HAMN, and those without appendix perforation had a similar prognosis to LAMN. This study supports staging HAMN using the same system as LAMN and treating it with appendectomy alone in the absence of appendix perforation.

25COASMA48:

Title: Novel Histologic Features in Ameloblastoma With RAS Q61R Mutation

Stojanov, Ivan J. DMDTrzcinska, Anna M. DMDQaisi, Mohammed DMD, MD‖Kmeid, Michel MDAzzato, Elizabeth M. MDShah, Akeesha A. MD

The American Journal of Surgical Pathology, 49 (5), 508-514.
https://doi.org/10.1097/PAS.0000000000002375.

Abstract: Ameloblastoma is characterized histologically by evidence of ameloblastic differentiation and molecularly by MAPK pathway alterations, most frequently **BRAF** $^{\mathbf{V600E}}$ mutation and **RAS** mutations, as well as by **SMO** mutations. This mutational profile is present across all histologic variants, including those occasionally lacking overt histologic evidence of ameloblastic differentiation, such as desmoplastic ameloblastoma and granular cell ameloblastoma. Recently, we have come across 4 cases of maxillary ameloblastoma demonstrating peculiar histologic features not accounted for by recognized histologic variants. Three intraosseous tumors were remarkably similar in histologic appearance and demonstrated a proliferation of spindled to basaloid cells in solid/sheet-like, cystic, and ribbon-like growth patterns within dense fibrous connective tissue. One case had numerous squamous morules and only 1 case, focally, demonstrated ameloblastic differentiation, yet all 3 cases harbored **NRAS** $^{\mathbf{Q61R}}$ mutation. A fourth case harbored **HRAS** $^{\mathbf{Q61R}}$ mutation and arose peripherally, in palatal (maxillary) gingiva, as a follicular-patterned neoplasm with bland squamoid morphology and scattered foci of ameloblastic differentiation. RAS Q61R immunohistochemistry was positive in both the tumor and overlying surface epithelium, in support of surface derivation. These 4 cases

demonstrate that ameloblastoma may occasionally present with non-traditional histologic features, lacking categorization into known histologic variants and sometimes lacking any evidence of ameloblastic differentiation. In this setting, the differential diagnosis may be broad and include more indolent odontogenic neoplasms such as adenomatoid odontogenic tumor or squamous odontogenic tumor, odontogenic carcinomas, and non-odontogenic neoplasms. A high index of suspicion, followed by confirmatory molecular testing or mutation-specific immunohistochemistry, is necessary for accurate diagnosis.

25COASMA49:

Title: Atypical Intraductal Proliferation in Prostate Needle Core Biopsy : Validation as a Marker of Unsampled Adverse Pathology in a Clinicopathologic Series of 142 New Patients

Bhattarai, Roshan MD, McKenney, Jesse K. MD Alaghehbandan, Reza MDLiu, Xuefeng PhDCox, Roni M. MD§Myles, Jonathan L. MDPrzybycin, Christopher G. MD

American Journal of Surgical Pathology, 49 (5), 515-522.
https://doi.org/10.1097/PAS.0000000000002376.

Abstract: Atypical intraductal proliferation (AIP) of the prostate is characterized by morphologic features exceeding that of high-grade prostatic intraepithelial neoplasia but not meeting strict diagnostic criteria for intraductal carcinoma. We examined the clinical significance of AIP in biopsy specimens. Patients with AIP diagnosed on biopsy were identified from surgical pathology archives. Initial biopsies, any repeat biopsies, and any radical prostatectomy (RP) slides were rereviewed. We also identified a control group of 50 consecutive patients with available prostate biopsies showing invasive prostatic adenocarcinoma but no AIP and having paired RP for comparison. Medical records were searched for nonsurgical treatment and clinical outcome status. Patients with initial biopsies showing invasive adenocarcinoma with either grade group (GG) ≥3 and/or unfavorable histology (as recently defined) were excluded from both the study and control groups. Correlation with subsequent adverse pathology at rebiopsy or RP, as defined by separate criteria: unfavorable histology, large cribriform/intraductal carcinoma, GG ≥3, pN1, and/or pM1, was assessed for both groups. Phosphate and tensin (PTEN) homolog and ETS-related gene (ERG) immunohistochemistry were performed on biopsies with available paired RP, using standard protocols. One hundred forty-two patients with AIP met inclusion criteria. At initial biopsy, 16 patients (11.3%) had AIP without concomitant invasive carcinoma, whereas 126 (88.7%) also had invasive adenocarcinoma. Of the 126 invasive tumors with AIP meeting study criteria, 19 (15.1%) were GG 1 and 107 (84.9%) GG 2. One hundred thirty-nine of 142 patients with AIP (97.9%) had available clinical follow-up (mean: 36.9 mo). Fifty-two (36.3%) patients with AIP underwent RP, 36 (25.4%) had brachytherapy, 28 (19.7%) had radiotherapy, 17 (12%) remained on active surveillance, 2 (1.4%) had cryoablation, 2 (1.4%) received androgen deprivation therapy, and 1 (0.7%) had high-intensity focused ultrasound. Forty-seven of 52 patients undergoing prostatectomy (90.3%) had glass slides available for review: 30 (63.8%) were GG2, 13 (27.7%) GG3, 1 (2.1%) GG4, and 3 (6.4%) GG5. Seventeen (36.2%) patients were staged as pT2, 25 (53.2%) pT3a, and 5 (10.6%) pT3b. Forty-two of 47 (89.4%) patients had associated unfavorable histology on prostatectomy, including 41 (87.2%) with large cribriform/intraductal carcinoma, 17 (36.2%)

GG≥3, and 5 (10.6%) with metastatic disease. In the 36 AIP lesions examined for PTEN and ERG immunoreactivity, 14 (38.9%) had concomitant PTEN loss and ERG over-expression, 6 (16.7%) showed PTEN loss only, and 6 (16.7%) had ERG overexpression only. AIP morphology was more predictive of risk for unfavorable histology at RP than PTEN/ERG immunophenotype. Seventeen patients not undergoing RP had rebiopsy, of which 5 (29.4%) had at least one adverse feature identified on repeat biopsy. Nineteen of 50 patients (38%) in the non-AIP control group had adverse pathology at RP (by any definition), compared with 89.4% in the AIP study group (**P** < 0.0001). In conclusion, AIP in prostate needle core biopsy is strongly associated with unsampled adverse pathology, defined by unfavorable histology and other traditional definitions of aggressive disease. For optimal patient risk stratification and active surveillance management, AIP should gain better recognition as a standard reporting element given its association with an increased likelihood of unsampled high-risk disease.

Medical Oncology
(Chemotherapy**, H**ematology **& R**adiotherapy**)**

25COASMA1:
Title: Nodal Burden and Oncologic Outcomes in Patients With Residual Isolated Tumor Cells After Neoadjuvant Chemotherapy (ypN0i+): The OPBC-05/ICARO Study
Giacomo Montagna, MD, MPH , Alison Laws, MD,MPH ht6705, Massimo Ferrucci, MD, PhD
Journal of Clinical Oncology, Volume 43, Number 7
https://doi.org/10.1200/JCO.24.01052
Abstract: Purpose-The nodal burden of patients with residual isolated tumor cells (ITCs) in the sentinel lymph nodes (SLNs) after neoadjuvant chemotherapy (NAC) (ypN0i+) is unknown, and axillary management is not standardized. We investigated rates of additional positive lymph nodes (LNs) at axillary lymph node dissection (ALND) and oncologic outcomes in patients with ypN0i+ treated with and without ALND. Methods- The Oncoplastic Breast Consortium-05/ICARO cohort study retrospectively analyzed data from patients with stage I to III breast cancer with ITCs in SLNs after NAC from 62 centers in 18 countries. The primary end point was the 3-year rate of any axillary recurrence. The rate of any invasive recurrence was the secondary end point. Results-In total, 583 patients were included, of whom 182 (31%) had completion ALND and 401 (69%) did not. The median age was 48 years. Most patients (74%) were clinically node-positive at diagnosis and 41% had hormone receptor–positive/human epidermal growth factor receptor 2–negative tumors. The mean number of SLNs with ITCs was 1.2. Patients treated with ALND were more likely to present with cN2/3 disease (17% v 7%, P < .001), have ITCs detected on frozen section (62% v 8%, P < .001), have lymphovascular invasion (38% v 24%, P < .001), and receive adjuvant chest wall (89% v 78%, P = .024) and nodal radiation (82% v 75%, P = .038). Additional positive nodes were found at ALND in 30% of patients, but only 5% had macrometastases. The 3-year rates of any axillary and any invasive recurrence were 2% (95% CI, 0.95 to 3.6) and 11% (95% CI, 8 to 14), respectively, with no statistical difference by type of axillary surgery. Conclusion-The nodal burden in patients with ypN0(i+) was low, and axillary recurrence after ALND omission was rare in patients selected for this approach. These results do not support routine ALND in all patients with ypN0(i+).

25COASMA2:
Title: Axillary Surgery for Patients With Residual Isolated Tumor Cells (ypN0i+) After Neoadjuvant Systemic Therapy for Early Breast Cancer
Elisa Agostinetto, MD, Carmela Caballero, MD ,Michail Ignatiadis, MD, PhD
Journal of Clinical Oncology, Volume 43, Number 7
https://doi.org/10.1200/JCO-24-01711
Abstract: The Oncology Grand Rounds series is designed to place original reports published in the Journal into clinical context. A case presentation is followed by a description of diagnostic and management challenges, a review of the relevant literature, and a summary of the authors' suggested management approaches. The goal of this series is to help readers

better understand how to apply the results of key studies, including those published in Journal of Clinical Oncology, to patients seen in their own clinical practice.

25COASMA3:

Title: Zanubrutinib Versus Bendamustine and Rituximab in Patients With Treatment-Naïve Chronic Lymphocytic Leukemia/Small Lymphocytic Lymphoma: Median 5-Year Follow-Up of SEQUOIA

Mazyar Shadman, MD,MPH Talha Munir, PhD,MBBS,MRCP,FRCPath, Tadeusz Robak, M D, PhD

Journal of Clinical Oncology, Volume 43, Number 7

https://doi.org/10.1200/JCO-24-02265

Abstract: Clinical trials frequently include multiple end points that mature at different times. The initial report, typically based on the primary end point, may be published when key planned co-primary or secondary analyses are not yet available. Clinical Trial Updates provide an opportunity to disseminate additional results from studies, published in JCO or elsewhere, for which the primary end point has already been reported. SEQUOIA (ClinicalTrials.gov identifier: NCT03336333) is a phase III, randomized, open-label trial that compared the oral Bruton tyrosine kinase inhibitor zanubrutinib to bendamustine plus rituximab (BR) in treatment-naïve patients with chronic lymphocytic leukemia/small lymphocytic lymphoma (CLL/SLL). The initial prespecified analysis (median follow-up, 26.2 months) and subsequent analysis (43.7 months) found superior progression-free survival (PFS; the primary end point) in patients who received zanubrutinib compared with BR. At a median follow-up of 61.2 months, median PFS was not reached in zanubrutinib-treated patients; median PFS was 44.1 months in BR-treated patients (hazard ratio [HR], 0.29; one-sided P = .0001). Prolonged PFS was seen with zanubrutinib versus BR in patients with mutated immunoglobulin heavy-chain variable region (IGHV) genes (HR, 0.40; one-sided P = .0003) and unmutated IGHV genes (HR, 0.21 [95% CI, 0.14 to 0.33]; one-sided P < .0001). Median overall survival (OS) was not reached in either treatment arm; estimated 60-month OS rates were 85.8% and 85.0% in zanubrutinib- and BR-treated patients, respectively. No new safety signals were detected. Adverse events were as expected with zanubrutinib; rate of atrial fibrillation was 7.1%. At a median follow-up of 61.2 months, the results supported the initial SEQUOIA findings and suggested that zanubrutinib was a favorable treatment option for untreated patients with CLL/SLL.

25COASMA4:

Title: Phase II Study of Acalabrutinib, Venetoclax, and Obinutuzumab in a Treatment-Naïve Chronic Lymphocytic Leukemia Population Enriched for High-Risk Disease

Matthew S. Davids, MD, MMSc , Christine E. Ryan, MD

Journal of Clinical Oncology, Volume 43, Number 7

https://doi.org/10.1200/JCO-24-02503

Abstract: Purpos-The AMPLIFY trial recently established fixed-duration acalabrutinib, venetoclax, and obinutuzumab (AVO) as a new standard-of-care option for patients with

previously untreated chronic lymphocytic leukemia (CLL) with wild-type TP53; however, due to the chemoimmunotherapy control arm, AMPLIFY excluded patients with high-risk TP53 aberration, for whom current standards of care are continuous Bruton tyrosine kinase inhibitor therapy or alternatively fixed-duration venetoclax-based doublets. AVO has not previously been evaluated in patients with CLL with TP53 aberration. Methods-This investigator-sponsored, multicenter, phase II study enrolled patients with treatment-naïve CLL enriched for high-risk CLL, defined by TP53 aberration (ClinicalTrials.gov identifier: NCT03580928). Patients received acalabrutinib, obinutuzumab, and then venetoclax, with each treatment introduced sequentially and in combination, with the duration guided by measurable residual disease (MRD). Patients who achieved undetectable MRD (uMRD) after either 15 or 24 cycles could discontinue treatment. The primary end point was complete remission (CR) with bone marrow uMRD (BM-uMRD) at the start of cycle 16. Results-Seventy-two patients were accrued, including 45 patients with TP53 aberration. The CR with BM-uMRD rates at the start of cycle 16 were 42% in patients with TP53 aberration and 42% in all-comers, and the BM-uMRD rates were 71% and 78%, respectively. Hematologic toxicities were mainly low grade, and cardiovascular toxicities and bleeding complications were infrequent. After a median follow-up of 55.2 months, 10 patients had progressed, including four with transformation, and three patients died. Four-year progression-free survival and overall survival for patients with or without TP53 aberration were 70%/96% and 88%/100%, respectively. Conclusion-AVO was highly active and well tolerated in patients with previously untreated high-risk CLL, supporting its use as a new standard-of-care treatment option.

25COASMA5:

Title: High Omega-3, Low Omega-6 Diet With Fish Oil for Men With Prostate Cancer on Active Surveillance: The CAPFISH-3 Randomized Clinical Trial

WilliamJ. Aronson, MD , Tristan Grogan, MS

Journal of Clinical Oncology, Volume 43, Number 7
https://doi.org/10.1200/JCO.24.00608

Abstract: Purpose-Men on active surveillance (AS) for prostate cancer are extremely interested in dietary changes or supplements to prevent progression of their disease. We sought to determine whether a high omega-3, low omega-6 fatty acid diet with fish oil capsules (D + FO) decreases proliferation (Ki-67) in prostate biopsies in men with prostate cancer on AS over a 1-year time period. Methods-In this phase II, prospective randomized trial, men (N = 100) with grade group 1 or 2 prostate cancer who elected AS were randomly assigned to the D + FO or a control group. Same-site prostate biopsies were obtained at baseline and 1 year. The primary end point was the change in Ki-67 index from baseline to 1 year from same-site biopsies compared between the groups. Results-The Ki-67 index decreased in the D + FO group by approximately 15% from baseline to 1 year (1.34% at baseline, 1.14% at 1 year) and increased in the control group by approximately 24% from baseline to 1 year (1.23% at baseline, 1.52% at 1 year), resulting in a statistically significant difference in the change of Ki-67 index between the groups (95% CI, 2% to 52%, P = .043). There was no significant difference in the secondary outcomes grade group, tumor length, Decipher genomic score, or prostate-specific antigen between the two groups. Four patients

in the D + FO group were withdrawn from the trial because of adverse events related to the FO. Conclusion-A high omega-3, low omega-6 diet with FO for 1 year resulted in a significant reduction in Ki-67 index, a biomarker for prostate cancer progression, metastasis, and death. These findings support future phase III trials incorporating this intervention in men on AS.

25COASMA6:

Title: Longitudinal Results From the Nationwide Just ASK Initiative to Promote Routine Smoking Assessment in American College of Surgeons–Accredited Cancer Programs

Jessica L. Burris, PhD Jamie S. Ostroff, PhD

Journal of Clinical Oncology, Volume 43, Number 7
https://doi.org/10.1200/JCO.24.00304

Abstract: Purpose-Persistent smoking after cancer diagnosis causes adverse outcomes while smoking cessation can improve survival. Thus, integration of smoking assessment and cessation assistance into routine cancer care is critical. Aiming for incremental practice change that could be sustained and built upon through future quality improvement (QI) projects, the American College of Surgeons initiated Just ASK in 2022 to increase implementation of smoking assessment among its accredited Cancer Programs. This manuscript describes outcomes from Just ASK. Methods-Seven hundred sixty-two programs enrolled in this cohort study, followed Plan Do Study Act methodology, and used local QI teams to facilitate practice change. The primary outcome was the ask rate (ie, patients asked/patients seen). Programs completed three surveys across the 1-year study (89.8% retention), answering questions about their program plus organizational readiness, implementation barriers, implementation strategies, and clinical practices related to assessing smoking among patients newly diagnosed with cancer. Data analysis involved descriptive statistics and analysis of change over time (eg, McNemar chi-squares). Results- Programs (53.1% community-based) tended to report moderate organizational readiness, multiple implementation barriers, and adoption of 4.63 ± 1.49 of eight possible implementation strategies (eg, training staff/providers). Programs reported frequency of assessing smoking status, documenting it in the electronic health record, advising patients who smoke to quit, and documenting advice and treatment increased over time (all $P < .001$). The ask rate increased from baseline to mid to final survey ($P < .01$; 87.79% v 88.65% v 91.92%, respectively). Conclusion-Just ASK is the latest, and by far the largest, endeavor to improve assessment of cancer patients' smoking status. Participants reported significant advances within a short time span and study results underscore the potential for national accreditation organizations to transform oncology practice.

25COASMA7:

Title: Intermittent or Continuous Panitumumab Plus Fluorouracil, Leucovorin, and Irinotecan for First-Line Treatment of RAS and BRAF Wild-Type Metastatic Colorectal Cancer: The IMPROVE Trial

Antonio Avallone, MD Francesco Giuliani, MD, Alfonso De Stefano, MD, PhD

Journal of Clinical Oncology, Volume 43, Number 7

https://doi.org/10.1200/JCO.24.00979

Abstract: Purpose-To investigate whether intermittent treatment after an induction phase of first-line schedule of fluorouracil, leucovorin, and irinotecan (FOLFIRI) plus panitumumab (PAN) prevents or delays the onset of resistance and improves safety and compliance with treatment in patients with unresectable RAS/BRAF wild-type (wt) metastatic colorectal cancer (mCRC). Patients and Methods-IMPROVE (ClinicalTrials.gov identifier: NCT04425239) was an open-label, multicenter, randomized phase II noncomparative trial. Patients with unresectable RAS/BRAF wt mCRC were randomly assigned (1:1) to receive FOLFIRI plus PAN continuously until progression (arm A) or intermittently, with treatment-free intervals (arm B) until progression on treatment, toxicity, or death. The primary end point was progression-free survival on treatment (PFSot) at 12 months. Assuming a null hypothesis of median PFSot time ≤7 months and target PFSot ≥10 months, 65 patients per arm were needed to achieve 80% power and 10% type I error, according to the binomial test. Results-Between May 2018 and June 2021, 69 patients were randomly assigned to arm A and 68 to arm B. The median number of treatment cycles was 13 in arm A and 16 in arm B. At a median follow-up of 43.2 months (IQR, 35.0-50.5), median PFSot was 11.2 and 17.5 months with 12-month PFSot rates of 45.7% and 58.5%, for arms A and B, respectively. The overall response rates were 68.1% and 61.2%, and median overall survival rates were 36.3 and 35.1 months in arms A and B, respectively. The overall rate of grade >2 skin PAN-related adverse events was 30.3% in arm A and 17.9% in arm B. Conclusion- Intermittent FOLFIRI plus PAN after the induction phase was feasible, and the primary end point was met with reduced toxicity while allowing patients more time off treatment.

25COASMA8:

Title: Onvansertib in Combination With Chemotherapy and Bevacizumab in Second-Line Treatment of KRAS-Mutant Metastatic Colorectal Cancer: A Single-Arm, Phase II Trial

Daniel H. Ahn, DO Maya Ridinger, PhD

Journal of Clinical Oncology, Volume 43, Number 7
https://doi.org/10.1200/JCO-24-01266

Abstract: Purpose-This phase II study evaluated the efficacy and tolerability of onvansertib, a polo-like kinase 1 (PLK1) inhibitor, in combination with fluorouracil, leucovorin, and irinotecan (FOLFIRI) + bevacizumab for the second-line treatment of KRAS-mutant metastatic colorectal cancer (mCRC). Patients and Methods- This multicenter, open-label, single-arm study enrolled patients with KRAS-mutated mCRC previously treated with oxaliplatin and fluorouracil with or without bevacizumab. Patients received onvansertib (15 mg/m^2 once daily on days 1-5 and 15-19 of a 28-day cycle) and FOLFIRI + bevacizumab (days 1 and 15). The primary end point was the objective response rate (ORR), and secondary endpoints included progression-free survival (PFS), duration of response (DOR), and tolerability. Translational and preclinical studies were conducted in KRAS-mutant CRC. Results-Among the 53 patients treated, the confirmed ORR was 26.4% (95% CI, 15.3 to 40.3). The median DOR was 11.7 months (95% CI, 9.4 to not reached). Grade 3/4 adverse events were reported in 62% of patients. A post hoc analysis revealed that patients with no

prior bevacizumab treatment had a significantly higher ORR and longer PFS compared with patients with prior bevacizumab treatment: ORR of 76.9% versus 10.0% (odds ratio of 30.0, P < .001) and median PFS of 14.9 months versus 6.6 months (hazard ratio of 0.16, P < .001). Our translational findings support that prior bevacizumab exposure contributes to onvansertib resistance. Preclinically, we showed that onvansertib inhibited the hypoxia pathway and exhibited robust antitumor activity in combination with bevacizumab through the inhibition of angiogenesis. Conclusion- Onvansertib in combination with FOLFIRI + bevacizumab showed significant activity in the second-line treatment of patients with KRAS-mutant mCRC, particularly in patients with no prior bevacizumab treatment. These findings led to the evaluation of the combination in the first-line setting (ClinicalTrails.gov identifier: NCT06106308).

25COASMA9:

Title: Hyperthermic Intraperitoneal Chemotherapy in Platinum-Sensitive Recurrent Ovarian Cancer: A Randomized Trial on Survival Evaluation (HORSE; MITO-18)

Anna Fagotti, MD, PhD Barbara Costantini, MD

Journal of Clinical Oncology, Volume 43, Number 7
https://doi.org/10.1200/JCO.24.00686

Abstract: Purpose-To investigate whether the addition of hyperthermic intraperitoneal chemotherapy (HIPEC) to secondary cytoreductive surgery (SCS) without neoadjuvant chemotherapy has a benefit on progression-free survival (PFS), as opposed to SCS alone in patients with platinum-sensitive recurrent epithelial ovarian cancer (platinum-free interval, >6 months). Methods-This was a multicenter randomized phase III study. Random assignment was performed at the time of surgery in cases with residual tumor ≤0.25 cm. HIPEC with cisplatin (CDDP) 75 mg/m^2 for 60 minutes at 41.5°C was administered at the end of surgery in the experimental arm. Both groups received postoperative platinum-based chemotherapy. The primary end point was PFS. The safety profile and postrecurrence survival (PRS) were the secondary end points. Results- A total of 167 patients underwent random assignment, 82 patients to SCS plus HIPEC (experimental arm) and 85 to SCS alone (control arm). The median follow-up was 83 months (IQR, 64-102). The median PFS was 23 months (95% CI, 17 to 29) in the group that underwent surgery alone and 25 months (95% CI, 18 to 32) in the group that underwent cytoreductive surgery with HIPEC. The probability of PRS at 5 years was 61.6% (95% CI, 50.8 to 72.4) in the SCS group and 75.9% (95% CI, 66.5 to 85.3) in the SCS plus HIPEC group. The incidence of postoperative adverse events of any grade was similar between the two groups. Conclusion-The addition of HIPEC to complete or nearly complete primary SCS did not confer a benefit in terms of PFS in patients with platinum-sensitive peritoneal recurrence.

25COASMA10:

Title: Clonal Hematopoiesis in Women With Breast Cancer

Christina Mayerhofer, MD , Rachel A. Freedman, MD, MPH

Journal of Clinical Oncology, Volume 43, Number 7
https://doi.org/10.1200/JCO-24-01848

Abstract: Purpose- Clonal hematopoiesis (CH) has been associated with a variety of adverse outcomes, most notably hematologic malignancy and ischemic cardiovascular disease. A series of recent studies also suggest that CH may play a role in the outcomes of patients with solid tumors, including breast cancer. Here, we review the clinical and biological data that underlie potential connections between CH, inflammation, and breast cancer, with a focus on the prevalence and impact of clonal hematopoiesis of indeterminate potential in patients with breast cancer. Methods- We summarize data from multiple studies, including a series of cohorts of patients with breast cancer, to assess the prevalence of CH, the relationship between CH and exposure to cytotoxic therapy, and the correlation between CH and breast cancer–specific outcomes. Results-Our findings indicate that CH is prevalent among patients with breast cancer, particularly those treated with cytotoxic therapies. However, there are no definitive data to support an association between the presence of CH and breast cancer–specific outcomes. Conclusion-Current data do not support routine CH testing in patients with breast cancer, nor should the presence of CH influence decisions regarding breast cancer therapy in most patients. However, larger, long-term studies are necessary to further define the implications of CH in patients with breast cancer and guide clinical decision making.

25COASMA11:

Title: Fulvestrant Versus Anastrozole in Endocrine Therapy–Naïve Women With Hormone Receptor–Positive Advanced Breast Cancer: Final Overall Survival in the Phase III FALCON Trial

JohnF.R. Robertson, MD ,Zhimin Shao, MD, Shinzaburo Noguchi, PhD, Igor Bondarenko, P hD

Journal of Clinical Oncology, Volume 43, Number 13
https://doi.org/10.1200/JCO.24.00994

Abstract: The randomized phase III FALCON trial demonstrated significant improvement in progression-free survival (PFS) with fulvestrant versus anastrozole in postmenopausal women with endocrine therapy–naïve, hormone receptor–positive/human epidermal growth factor receptor 2–negative advanced breast cancer. Herein, the prespecified final overall survival (OS) analysis is reported. After the primary PFS analysis, data were collected on survival, serious adverse events, and health-related quality of life. The final OS analysis was triggered at ≥65% maturity and ≥8 years since the last patient was enrolled. Analyses were descriptive with nominal P values (one-sided α threshold .01845). At the data cutoff (July 11, 2022), 314 (68.0%) of 462 patients had died (fulvestrant, 157/230 [68.3%], anastrozole, 157/232 [67.7%]). The final OS analysis of FALCON demonstrated no significant difference between fulvestrant and anastrozole (medians, 44.8 and 42.7 months, respectively; hazard ratio [HR], 0.97 [95% CI, 0.77 to 1.21]; P = .7579). Among patients with nonvisceral disease (n = 208), a trend showed a 15% reduction in the relative risk of death with fulvestrant versus anastrozole (median OS, 65.2 v 47.8 months; HR, 0.85 [95% CI, 0.60 to 1.20]). Data from FALCON are consistent with published evidence of long-term clinical benefit with fulvestrant and other endocrine therapies in the subset of patients with nonvisceral disease.

25COASMA12:

Title: Improved Patient-Reported Outcomes With Post-Transplant Cyclophosphamide: A Quality-of-Life Evaluation and 2-Year Outcomes of BMT CTN 1703

ShernanG. Holtan, MD , Javier Bolaños-Meade, MD, Monzr M. Al Malki, MD

Journal of Clinical Oncology, Volume 43, Number 8
https://doi.org/10.1200/JCO.24.00921

Abstract: The BMT CTN 1703 phase III trial confirmed that graft-versus-host disease (GVHD) prophylaxis with post-transplantation cyclophosphamide (PTCy), tacrolimus (Tac), and mycophenolate mofetil (MMF) results in superior GVHD-free, relapse-free survival (GRFS) compared with Tac/methotrexate (MTX) prophylaxis. This companion study assesses the effect of these regimens on patient-reported outcomes (PROs). Using the Lee Chronic GVHD Symptom Score and PROMIS subscales (physical function, GI symptoms, social role satisfaction) as primary end points and hemorrhagic cystitis symptoms and Lee subscales as secondary end points, responses from English and Spanish speakers were analyzed at baseline and days 100, 180, and 365 after transplant. PRO scores were compared between the arms using inverse probability weighted-independent estimating equation models. The PTCy arm had significantly lower scores on the Lee Chronic GVHD Symptom Scale (P = .01), indicating lower GVHD symptom burden. Lee Scale nutrition and mouth subscores were also better in the PTCy arm compared with the Tac/MTX arm (P < .01 for both). Older participants (age >65 years) reported better Lee Scale psychological subscores than younger participants (P = .003). No significant differences were identified in hemorrhagic cystitis or in the PROMIS subscales between treatment arms. The updated clinical end points at 2 years for the parent trial confirmed that PTCy/Tac/MMF maintained a significant advantage over Tac/MTX in GRFS (42.4% v 28.8%, P = .001). In addition to improved GRFS, patients randomly assigned to the PTCy arm reported lower symptom burden during the first year after transplant.

25COASMA13:

Title: Development and Validation of the RSClinN+ Tool to Predict Prognosis and Chemotherapy Benefit for Hormone Receptor–Positive, Node-Positive Breast Cancer

Lajos Pusztai, MD,DPhil , Kathy S. Albain, MD

Journal of Clinical Oncology, Volume 43, Number 8
https://doi.org/10.1200/JCO-24-01507

Abstract: Purpose-Clinicopathological factors and the 21-gene Oncotype DX Breast Recurrence Score (RS) test both influence prognosis. Our goal was to develop a new tool, RSClinN+, to individualize recurrence risk and chemotherapy benefit predictions by menopausal status for patients with HR+/human epidermal growth factor receptor 2–negative, lymph node–positive breast cancer by integrating the RS result with clinicopathological factors (grade, tumor size, age). Methods-We used patient-level data from 5,283 patients treated with chemoendocrine therapy (CET) versus endocrine therapy alone (ET) in the S1007 (N = 4,916) and S8814 (N = 367) trials to develop the tool. Cox

proportional hazards regression models stratified by trial were used to estimate 5-year invasive disease-free survival for pre- and postmenopausal woman, respectively. The integrated RSClinN+ model was compared with RS alone and clinicopathological models using likelihood ratio tests. Absolute CET benefit was estimated as the difference between ET and CET risk estimates. Validation of RSClinN+ was performed in 592 patients with node-positive disease in the Clalit Health Services registry. Results-RSClinN+ provides better prognostic information than RS model alone (premenopausal P = .034; postmenopausal P < .001) or clinicopathological model alone (premenopausal P = .002; postmenopausal, P < .001). In postmenopausal women, RS showed interaction with CET benefit (P = .016), with RSClinN+ absolute CET benefit ranging from <0.1% to 21.5% over RS ranges 0-50. In premenopausal patients with RS ≤25, there was no significant interaction between RS and CET benefit. In external validation, RSClinN+ risk estimates were prognostic (hazard ratio, 1.75 [95% CI, 1.38 to 2.20]) and concordant with observed risk (Lin's concordance, 0.92). Conclusion- RSClinN+ provides improved estimates of prognosis and absolute CET benefit for individual patients compared with RS or with clinical data alone and could be used in patient counseling.

25COASMA14:

Title: Estimating Long-Term Survivorship Rates Among Patients With Resected Stage III/IV Melanoma: Analyses From CheckMate 238 and European Organization for Research and Treatment of Cancer 18071 Trials

JeffreyS. Weber, MD,PhD , Mark R. Middleton, PhD, FRCP

Journal of Clinical Oncology, Volume 43, Number 8
https://doi.org/10.1200/JCO.24.00237

Abstract: Purpose-Standard-of-care treatments for patients with resected stage III/IV melanoma include the immuno-oncology (IO) agents nivolumab (NIVO) and ipilimumab (IPI). This study used mixture cure models (MCMs) to estimate cure rates among patients treated with NIVO or IPI in the phase III CheckMate 238 (ClinicalTrials.gov identifier: NCT02388906) and European Organization for Research and Treatment of Cancer (EORTC) 18071 (ClinicalTrials.gov identifier: NCT00636168) trials, and to assess the impact of use of adjuvant immunotherapy on cure rates versus watchful waiting. Methods-MCMs were applied to patient-level recurrence-free survival data from CheckMate 238 and EORTC 18071. Cured patients were assumed to experience no disease recurrence and mortality risks similar to the general population. Uncured patients were at risk of disease recurrence and all-cause death. The survival trend of the cured patients was estimated using life expectancy data for a general population with the same baseline demographic characteristics. A regression model assessed the odds ratios (ORs) of cure across key subgroups on the basis of baseline characteristics of the study populations. Results
In CheckMate 238, estimated cure rates were 48.3% (95% CI, 41.8 to 54.9) with NIVO and 38.2% (95% CI, 32.7 to 44.1) with IPI. In EORTC 18071, estimated cure rates were 38.0% (95% CI, 32.1 to 44.2) with IPI and 29.2% (95% CI, 24.4 to 34.6) with placebo. In the indirect comparison of the two trials, the odds of cure were significantly higher with NIVO than with placebo (OR, 2.33 [95% CI, 1.49 to 3.65]). Conclusion-Analyses involving two large phase III trials investigating adjuvant IO treatment for resected melanoma demonstrate

higher cure rates for both NIVO and IPI than placebo, with NIVO providing the highest cure rate. Similar cure rates were estimated for patients treated with IPI in both trials, despite staging and dosing differences.

25COASMA15:

Title: Pooled Long-Term Outcomes With Nivolumab Plus Ipilimumab or Nivolumab Alone in Patients With Advanced Melanoma

Georgina V. Long, PhD, MBBS, FRACP , James Larkin, MD, PhD, FRCP

Journal of Clinical Oncology, Volume 43, Number 8
https://doi.org/10.1200/JCO.24.00400

Abstract: Purpose-Nivolumab (NIVO) + ipilimumab (IPI) combination and NIVO monotherapy have demonstrated durable clinical benefit in patients with unresectable/metastatic melanoma. This analysis describes long-term overall survival (OS) with the combination or monotherapy pooled across all major company-sponsored trials, as well as clinical factors associated with survival, in patients with immune checkpoint inhibitor (ICI) treatment–naïve unresectable/metastatic melanoma. Methods-Data were pooled from six CheckMate studies in ICI treatment–naïve patients receiving NIVO + IPI (NIVO 1 mg/kg + IPI 3 mg/kg or NIVO 3 mg/kg + IPI 1 mg/kg) or NIVO monotherapy (3 mg/kg). OS was assessed for each treatment, as well as in select subgroups. Cox proportional multivariate analysis (MVA) and classification and regression tree (CART) analyses were performed within treatment arms. Results-Median follow-up for OS was 45.0 months for patients treated with NIVO + IPI (n = 839) and 35.8 months for patients treated with NIVO (n = 536). OS was longer with NIVO + IPI versus NIVO monotherapy (hazard ratio, 0.78 [95% CI, 0.67 to 0.91]), with 6-year OS rates of 52% versus 41%, respectively. Consistent benefit was observed in BRAF-mutant and BRAF-wild-type patients and those with normal and elevated lactate dehydrogenase (LDH). Numerical difference in OS was also observed across PD-L1 expression levels, although more pronounced with no/low PD-L1 expression. Clinical factors associated with decreased survival in both the MVA and CART analyses were LDH > upper limit of normal with either treatment, age ≥65 years with NIVO + IPI, and the presence of liver metastases with NIVO monotherapy. Conclusion-In this large, pooled nonrandomized retrospective analysis, we observed that NIVO + IPI provides longer OS than NIVO in patients with ICI treatment–naïve advanced melanoma and identifies clinical factors that appear to be associated with survival for each treatment, which may assist with treatment decision making.

25COASMA16:

Title:Randomized Controlled Trial of a Virtually Delivered Exercise and Stress Management Program to Improve Physical Performance of Hematopoietic Cell Transplant Survivors

DavidD. Ma, MBBS,DM, Zhixin Liu, PhD, Kimberley Au, BSc

Journal of Clinical Oncology, Volume 43, Number 8
https://doi.org/10.1200/JCO.24.00333

Abstract: Purpose Because of advances in hematopoietic cell transplant (HCT), meeting the long-term health needs of increasing numbers of HCT survivors remains challenging. This

multicenter trial aimed to assess the short- and long-term effects of an exercise and mindfulness intervention delivered by telehealth. Methods-One hundred thirty-nine participants >6 months post-HCT were randomly assigned 1:1 to a 6-week personalized exercise and mindfulness training with three motivation sessions at 3-6 months via an online meeting platform or usual care. Physical and quality-of-life (QOL) assessments were conducted online for 12 months. The primary end point was the 6-minute walk test (6-MWT) at 3 months. Results-The median time post-HCT was 21 months (range, 7-67 months). Improvement in mean difference of 6-MWT was found in the intervention group compared with control (intention-to-treat) at 3 months (51.4 m [95% CI, 27.3 to 75.5]; P < .001; effect size [ES], 0.52) and was maintained at 12 months (59.3 m, P = .003; ES, 0.60). Sustained improvements in mean difference for sit-to-stand (STS) at 3 and 12 months were seen. There were no significant changes in hand grip strength or QOL outcomes between groups. A significant difference in serum soluble intercellular adhesion molecule-1 (sICAM-1) concentration was observed between the intervention and control groups in the exploratory study. No intervention adverse events were found. Conclusion-The supervised multimodal telehealth intervention provided clinically meaningful and durable improvement of physical capacity in HCT survivors. This home-based program has the potential to provide an unmet need for HCT survivors. Similar programs may benefit survivors of other cancers, organ transplants, and chronic disorders.

25COASMA17:

Title: Oxaliplatin-Based Versus Alkylating Agent in Neuroendocrine Tumors According to the O^6-Methylguanine-DNA Methyltransferase Status: A Randomized Phase II Study (MGMT-NET)

Thomas Walter, MD,PhD , Thierry Lecomte, MD, PhD

Journal of Clinical Oncology, Volume 43, Number 8

https://doi.org/10.1200/JCO.23.02724

Abstract: Purpose Alkylating agents (ALKY) are the main chemotherapies used for advanced neuroendocrine tumors (NETs). O^6-Methylguanine-DNA methyltransferase (MGMT) status, as proficient (p) or deficient (d), may predict the response to ALKY. Patients and Methods-MGMT-NET (ClinicalTrials.gov identifier: NCT03217097) was a phase II trial randomly assigning 1:1 for pMGMT or 2:1 for dMGMT-NETs to either ALKY or oxaliplatin (Ox). Inclusion criteria were a confirmed advanced pancreatic, thoracic, or unknown primary NETs with an indication for chemotherapy and tissue available. The primary aim was to detect a difference of 35% between the 3-month objective response rate (ORR) in pMGMT-NETs versus in dMGMT-NETs when treated with ALKY. A biomarker-stratified design was performed to compare ALKY and Ox in the dMGMT and pMGMT strata for the secondary end points. dMGMT was defined using pyrosequencing (PSQ; methylated MGMT ≥9%) and using immunochemistry (H-score of MGMT <50) when PSQ was not interpretable. Results-From October 2018 to October 2021, 105 patients (55 pancreas, 38 thorax, 12 unknown) started either ALKY (n = 62) or Ox (n = 43). The median age was 63 years (range, 30-84), and 59% were males. NETs were G1 (19%), G2 (69%), or G3 (10%). Among patients with interpretable MGMT status, 56.9% (58 of 102) had a dMGMT-NET. The primary end point was not reached; the 3-month ORR was 10 (29.4%)

versus 2 (8%), and the odds ratio was 3.5 (0.58-21.16), P = .172. However, best ORR (18 [52.9%] v 3 [11.5%]) and median progression-free survival (14.6 [95% CI, 7.2 to 22.1] v 11.3 [9.4 to 13.2] months) were higher for dMGMT-NETs versus pMGMT-NETs. MGMT status does not seem to affect the Ox efficacy. Conclusion- Despite the fact that the primary end point was not reached, ALKY has clinical activity in patients with dMGMT-NETs.

25COASMA18:

Title: Influence of Nucleophosmin (NPM1) Genotypes on Outcome of Patients With AML: An AIEOP-BFM and COG-SWOG Intergroup Collaboration

Claudia Tregnago, PhD , Maddalena Benetton, PhD

Journal of Clinical Oncology, Volume 43, Number 8
https://doi.org/10.1200/JCO-24-01715

Abstract: Purpose-Several genomic subsets of NPM1 mutations with varying sequences (type A, B, D, etc) have been identified. Despite molecular heterogeneity, NPM1 mutations cumulatively portend a more favorable outcome, but biology and prognostic implications of different genomic subsets have not been extensively studied. In this multicentric study, we investigated the impact of NPM1 genotypes on patient's outcomes and interrogated the underlying biology of the different subtypes. Materials and Methods-Of more than 4,000 patients enrolled in multiple pediatric cooperative (AIEOP, BFM, ELAM02, NOPHO, DCOG, and COG trials), or adult (SWOG) trials, 348 pediatric and 75 adult AML patients with known NPM1 genotype and available outcome were selected for this study. Diverse NPM1 variants were correlated with the probabilities of overall survival (OS) and event-free survival. Nuclear localization and translational efficiency of the NPM1 variants was studied. Results-Evaluation of clinical outcome on the basis of NPM1 genotypes showed that patients with type A, B, and other rare variants had similarly favorable outcomes, whereas those with type D had a significantly worse outcome (OS of 63% for type D v 86% for type non-D, P = .005). Multivariate analysis confirmed type D as an independent prognostic factor associated with inferior OS (hazard ratio, 3; P = .005). In vitro, we demonstrated that in type D versus type A synonymous variants, codon optimality plays major roles in determining gene expression levels, and translation efficiency, which resulted in a more expressed NPM1-D mRNA and protein, mediating peculiar mitochondrial gene expression. Conclusion- The evaluation of specific NPM1 genotypes identified AML patients with type D mutations being significantly associated with inferior outcomes, suggesting a reclassification of D cases to higher-risk groups.

25COASMA19:

Title: Phase II Trial of Nivolumab Plus Doxorubicin, Vinblastine, Dacarbazine as Frontline Therapy in Older Adults With Hodgkin Lymphoma

Pallawi Torka, MD , Tatyana Feldman, MD, Kerry J. Savage, MD

Journal of Clinical Oncology, Volume 43, Number 8
https://doi.org/10.1200/JCO-24-01278

Abstract: Purpose-We conducted a phase I/II study evaluating nivolumab plus doxorubicin, vinblastine, dacarbazine (N-AVD) as frontline therapy for treatment-naïve older adults (OA) with classical Hodgkin lymphoma (cHL; ClinicalTrials.gov identifier: NCT03033914).

Methods- Patients age ≥60 years with newly diagnosed, any stage, cHL were treated with six cycles of AVD at standard doses plus nivolumab 240 mg intravenously once every 2 weeks (on days 1 and 15) of each cycle. A geriatric assessment was performed before therapy initiation. The primary end point was progression-free survival (PFS). Results-Patient characteristics (N = 40) included median age of 66 years (range, 60-78 years) with 38% ≥70 years, 78% with stage III/IV disease, 68% with International Prognostic Score of ≥3, 82% dependent in ≥1 activities of daily living, 23% dependent in ≥1 instrumental activities of daily living, 50% with impaired timed up and go test, and 40% with polypharmacy. Among 37 response-evaluable patients, the median follow-up was 49 months and 3-year PFS and overall survival (OS) were 79% and 97%, respectively. Overall, 50% patients experienced grade 3/4 treatment-related adverse events (TRAEs), including febrile neutropenia in 8%. Four (10%) patients stopped therapy due to TRAEs. There was no correlation between baseline geriatric impairments and survival outcomes or toxicities. Positron emission tomography-2 was not predictive of PFS or OS. Conclusion-N-AVD is a highly effective and well-tolerated frontline regimen in OA with cHL across a wide range of geriatric impairments.

25COASMA20:

Title: Chimeric Antigen Receptor-T Cells in Colorectal Cancer: Pioneering New Avenues in Solid Tumor Immunotherapy

Shaida Ouladan, MD, PhD, MSc, Elias Orouji, MD, PhD

Journal of Clinical Oncology, Volume 43, Number 8

https://doi.org/10.1200/JCO-24-02081

Abstract: Colorectal cancer (CRC) remains a major global health burden, being one of the most prevalent cancers with high mortality rates. Despite advances in conventional treatment modalities, patients with metastatic CRC often face limited options and poor outcomes. Chimeric antigen receptor-T (CAR-T) cell therapy, initially successful in hematologic malignancies, presents a promising avenue for treating solid tumors, including CRC. This review explores the potential of CAR-T cell therapy in CRC by analyzing clinical trials and highlighting prominent CRC-specific targets. We discuss the challenges such as immunosuppressive microenvironment, tumor heterogeneity, and physical barriers that limit CAR-T efficacy. Emerging strategies, such as logic-gated and dual-targeting CAR-T cells, offer practical solutions to overcome these hurdles. Furthermore, we explore the combination of CAR-T cell therapy with immune checkpoint inhibitors to enhance T-cell persistence and tumor infiltration. As the field continues to evolve, CAR-T cell therapies hold significant potential for revolutionizing the treatment landscape of CRC.

25COASMA21:

Title: Treatment of Pleural Mesothelioma: ASCO Guideline Update

Hedy L. Kindler, MD , Nofisat Ismaila, MD

Journal of Clinical Oncology, Volume 43, Number 8

https://doi.org/10.1200/JCO-24-02425

Abstract: Purpose-To provide evidence-based recommendations to practicing physicians and others on the management of pleural mesothelioma (PM). Methods- ASCO convened an Expert Panel of medical oncology, thoracic surgery, radiation oncology, pathology, cancer genetics, and advocacy experts to conduct an updated literature search, which included systematic reviews, meta-analyses, randomized controlled trials, and prospective and retrospective comparative observational studies published from 2016 through 2024. Outcomes of interest included survival, disease-free or recurrence-free survival, and quality of life. Expert Panel members used available evidence and informal consensus to develop evidence-based guideline recommendations. Results- The literature search identified 110 additional relevant studies to inform the evidence base for this guideline.

25COASMA22:

Title: The prevalence of post-therapy epilepsy in patients treated for high-grade glial tumors: a systematic review and meta-analysis.

Ferreira, M.P., Carvalho, R.L., Borges, D.F. et al.

Med Oncol 42, 128 (2025).

https://doi.org/10.1007/s12032-025-02677-6

Abstract: Gliomas are the most prevalent type of primary brain tumor of the adult central nervous system. High-grade gliomas (HGG) are the most common type of glioma. Epilepsy is often the first clinical manifestation of HGG. Since epilepsy leads to increased morbidity and mortality rates, seizure control is one of the main therapeutic goals for patients with glioma-related epilepsy. Post-therapy epilepsy is observed in a significant percentage of patients, hence, this work aimed to quantify the prevalence of post-therapy epilepsy after HGG treatment. Our search was conducted across PubMed®, EMBASE®, Web of Science™, Cochrane Library, Sicelo and Scopus, adhering to the Preferred Reporting Items for Systematic Reviews and Meta-Analyses guidelines. This review included articles published in Portuguese or English that evaluate adult patients with newly diagnosed HGG, who were treated with at least surgery or radiation. Thirty-six studies reporting on 4036 HGG patients were included in our meta-analysis. The mean age ranged from 44 to 73 years. Glioblastoma was the most commonly observed HGG, representing 77,8% of all glioma patients. The pre-treatment seizure frequency was observed in 21,2%. All patients underwent surgery as the main therapy, and 1842 patients received standard adjuvant therapy. We also observed a pooled prevalence of post-therapy seizures of 25.5% (95% confidence interval of [19.9%; 31.1%]). Substantial heterogeneity in all assessed variables was observed. Conducting larger prospective studies with suitable epilepsy diagnostic methods would help provide a more precise estimate of the number of HGG patients who develop post-therapy epilepsy.

Keywords: High-grade glioma, Post-therapy epilepsy, Glioblastoma, Astrocytoma, Oligodendroglioma, Systematic review

25COASMA23:

Title: Efficacy and safety of KRAS -G12C inhibitors in colorectal cancer: a systematic review of clinical trials.

Sayed, M.S., Alami Idrissi, Y., Ahmed, O. et al.

Med Oncol 42, 127 (2025).
https://doi.org/10.1007/s12032-025-02684-7

Abstract: Patients with colorectal cancer (CRC) who have KRAS mutations often see poor results with standard treatments, leaving them with fewer viable options. Over the past few years, new KRAS G12C inhibitors have emerged as a targeted approach for a specific subset of these mutations, though their effectiveness and safety in advanced CRC remain areas of ongoing research. In this systematic review, we identified nine clinical trials including a total of 668 patients, by searching PubMed, Web of Science, CENTRAL, and Embase through October 2024. When sotorasib was used alone, the objective response rate (ORR) ranged from 7.1 to 9.7%, with disease control (DC) rates of 73.8 to 82.3% and a median progression-free survival (PFS) spanning 4–5.6 months. Combining sotorasib with panitumumab, especially at higher doses, raised its ORR to 26.4%. Meanwhile, pairing adagrasib with cetuximab led to a 42% ORR and a median PFS of 6.9 months, surpassing the 19% ORR observed with adagrasib alone. Divarasib monotherapy produced a 36% ORR and an 85.5% DC rate, with a PFS of 5.6 months; in tandem with cetuximab, those numbers climbed to a 62.5% ORR and a PFS of 8.1 months. Common side effects across these trials included diarrhea, nausea, fatigue, and various skin reactions. Overall, KRAS G12C inhibitors appear to offer meaningful benefits for CRC patients, particularly when used alongside EGFR inhibitors like cetuximab or panitumumab. However, further large-scale, randomized trials are needed to refine dosing strategies and gain a clearer picture of both efficacy and potential risks.

25COASMA24:

Title: An investigative study on the impact of DLK1 and NCoR1 knockdown by siRNA transfection on endometrial cancer proliferation: unveiling notch interactions.

Chandran Manimegalai, S., Krishnamoorthy, S.P., Kalimuthu, V. et al.

Med Oncol **42**, 124 (2025).
https://doi.org/10.1007/s12032-025-02676-7

Abstract: Endometrial cancer is the most common gynecological malignancy. Despite advances in treatment, many patients experience disease recurrence or metastasis. This study investigates the impact of siRNA-mediated gene knockdown of NCoR1 and DLK1 genes in the proliferation of endometrial cancer cell lines Ishikawa and AN3CA and normal HEK 293 cells. Cellular growth and survival before and after the treatment of predesigned siRNAs in the endometrial cancer cell lines were evidenced using fluorescent stains. The mRNA expression of BID, BAX, BCL2, Caspases 3, 8, and 9 GPR78, EGFR, VEGF, NCoR1, DLK1 and ARID1A was analyzed in the untreated HEK 293, Ishikawa, and AN3CA cell lines to substantiate the oncogenic property of Ishikawa and AN3CA cell lines. Then, to evidence the successful transfection of NCoR1 and DLK1 gene in endometrial cancer cells, the mRNA and protein expression of targeted genes before and after being transfected were also validated. As a result, the mRNA expression significantly increased in BID, BAX, BCL2, GPR78, EGFR and VEGF. On the other hand, Caspases 3, 8, and 9 were down-regulated in Ishikawa and AN3CA compared to the control cell line (HEK 293). The mRNA and protein expression of NCoR1 and DLK1 in siRNA-mediated transfection supported the reduced proliferation in endometrial cancer cells by interfering with certain pathways like Notch,

MAPK, SWI/SNF, and NF-κB, which have crucial roles in the grade of receptor to the histone remodeling. With these findings, the study recommends exploring the possible role and interactions of NCoR1 and DLK1, signaling pathways that favor the progression of endometrial cancer.

25COASMA25:

Title: Integrative analysis of ubiquitination-related genes identifies HSPA1A as a critical regulator in colorectal cancer progression.

Gao, X., Yan, T., Yu, X. et al. Med Oncol **42**, 123 (2025).
https://doi.org/10.1007/s12032-025-02662-z

Abstract: Colorectal cancer (CRC) is a prevalent and lethal malignancy, with ubiquitination significantly influencing cellular processes involved in cancer progression. However, the contributions of ubiquitination-related genes in CRC remain unclear. This study conducted a detailed analysis of gene expression profiles associated with ubiquitination in CRC, evaluating 1006 genes across 46 pathways. By comparing CRC tissues to adjacent normal tissues, we identified differentially expressed genes and developed a ubiquitination-related pathway gene signature (URPGS) using LASSO regression analysis on genes with prognostic significance. The prognostic capability of the URPGS was validated in independent cohorts, and its associations with clinical characteristics, including post-chemotherapy survival outcomes, were examined. Machine learning techniques identified HSPA1A as a key gene relevant to CRC both in vitro and in vivo. Our analysis revealed 307 differentially expressed ubiquitination-related genes, with 24 significantly associated with patient prognosis. The developed 14-gene URPGS exhibited strong prognostic value, effectively stratifying patients into high-risk and low-risk groups for overall survival. The URPGS correlated with advanced clinical stages, lymph node metastasis, and recurrence, with higher scores linked to poorer post-chemotherapy survival outcomes. Knockdown of HSPA1A significantly inhibited CRC cell proliferation, migration, and invasion in vitro, as well as tumor growth and metastasis in vivo. This research establishes a novel URPGS that effectively predicts prognosis and chemotherapy outcomes in CRC, enhancing our understanding of ubiquitination's role and suggesting personalized treatment strategies.

25COASMA26:

Title: ADAM9 mediates Cisplatin resistance in gastric cancer cells through DNA damage response pathway.

Zhang, Xy., Zhao, Cy., Dong, Jm. et al
Med Oncol **42**, 122 (2025).
https://doi.org/10.1007/s12032-025-02645-0

Abstract: Gastric cancer is one of the most common malignant tumors in the world. The occurrence of chemotherapy resistance seriously affects the survival and prognosis of middle and advanced patients. Enhancing DNA repair ability is one of the important mechanisms of chemotherapy resistance. ADAM9, a member of the disintegrin and metalloproteinase family, is involved in many biological processes, such as tumor cells proliferation, apoptosis, invasion and migration, vascular invasion, and drug resistance. In this study, we found that the high expression of ADAM9 in gastric cancer tissues was associated with a variety of

clinicopathological factors and poor prognosis in patients. Gastric cancer cells with high ADAM9 expression reduced sensitivity to Cisplatin, decreased DNA damage, increased expression of ATM and CHK2, the key proteins in DNA damage repair pathway, and improved cancer cells survival rate. Further studies showed that the expression of ADAM9 was selectively interfered with gastric cancer cells, the expression levels of ATM and CHK2 were decreased, while the expression of damage protein γ-H2AX was significantly increased, the degree of DNA damage was increased, and the sensitivity of gastric cancer cells to Cisplatin was significantly enhanced. It is suggested that ADAM9 is involved in Cisplatin resistance in gastric cancer cells, and its mechanism is related to the activation of ATM-CHK2 pathway in DNA damage repair. These data demonstrate that ADAM9 plays a pro-cancer role and mediates Cisplatin resistance in gastric cancer, which may be a new target to overcome chemotherapy resistance.

25COASMA27:

Title: Addition of thalidomide for prevention of chemotherapy-induced nausea and vomiting in the second cycle after the failure of four-drug regimen in the first cycle.

Gowda, N., Ravichandran, M., Indrajithu, J. et al

Med Oncol **42**, 121 (2025).

https://doi.org/10.1007/s12032-025-02655-y

Abstract: Four-drug antiemetic prophylaxis achieves emesis control in 70–90% of patients receiving highly emetogenic chemotherapy (HEC). However, less than half achieve control of nausea. We added thalidomide to OAOD (ondansetron, aprepitant, dexamethasone, and olanzapine) to try and improve nausea control. Adults (> 18 years) who had failed ("any nausea" in 0–120 h after HEC) OAOD prophylaxis in cycle 1, were randomly assigned to thalidomide (T = 50 mg OD for 5 days) + OAOD or placebo (P) + OAOD in cycle 2. The primary endpoint was the proportion of patients achieving "no nausea" in 0–120 h from chemotherapy in the second cycle. A sample size of 50 (including dropouts) would be able to detect 30% "no nausea" in the T arm ($\beta = 80\%$, $\alpha = 0.05$). We enrolled 105 patients in cycle 1 and randomized 49 patients (25 thalidomide/ 24 placebo; median age 45(30–60) years; all anthracycline/ cyclophosphamide for breast cancer). The addition of thalidomide did not improve the proportion with "no nausea" in the overall (0-120 h) [T (16%) vs. P (21%); $p = 0.72$)], acute (0-24 h) (32% vs. 25%, $p = 0.58$), and delayed (24-72 h) (32% vs. 25%, $p = 0.46$) periods. Severe nausea (VAS ≥ 7) in the delayed period was reduced (T = 4% vs. P = 30%, $p = 0.02$). Sedation and dizziness were not increased, but mild constipation was higher with thalidomide [T (84%) vs. P (58%), $p = 0.047$)]. The addition of thalidomide to standard 4-drug CINV prophylaxis in cycle 2 did not improve nausea control among patients who "failed" the 4-drug regimen in cycle 1.

25COASMA28:

Title: NEK2 promotes the progression of osteosarcoma through the AKT/p-AKT pathway and interacts with FoxM1.

Tan, X., Liang, X., Feng, Y. et al.

Med Oncol **42**, 120 (2025).

https://doi.org/10.1007/s12032-025-02657-w

Abstract: Osteosarcoma is a highly invasive and metastatic primary malignant bone tumor, and resistance to chemotherapy remains a major therapeutic challenge. Our previous studies showed that increased Forkhead box protein M1 (FoxM1) expression promotes osteosarcoma progression. While NIMA-related kinase 2 (NEK2) has emerged as a potential oncogenic factor, its functional role and molecular mechanisms in osteosarcoma remain poorly understood. Pearson's correlation analysis was performed to assess the relationship between FoxM1 and NEK2 expression using the GSE33382 dataset from GEO. Coimmunoprecipitation (Co-IP) was employed to investigate FoxM1–NEK2 interactions. NEK2 expression was modulated in the HOS and U2OS osteosarcoma cell lines through pharmacological inhibition (MBM-55), siRNA-mediated knockdown, and plasmid-mediated overexpression. Cellular proliferation was evaluated via CCK-8 and colony formation assays. Transwell migration/invasion assays and flow cytometry were performed to assess the metastatic potential and apoptosis, respectively. The protein levels of FoxM1, NEK2, and AKT/p-AKT were analyzed by Western blotting. Western blot analyses of FoxM1-overexpressing cell lines and RCM-1-treated cells revealed a positive correlation between NEK2 and FoxM1 levels. Co-IP confirmed their interaction. NEK2 knockdown significantly suppressed proliferation, migration, and invasion; enhanced cisplatin sensitivity (reduced the IC_{50}); and promoted apoptosis. Conversely, NEK2 overexpression exacerbated malignant phenotypes and decreased chemosensitivity. Mechanistically, NEK2 activation was shown to drive osteosarcoma progression via AKT/p-AKT pathway activation. This study revealed that NEK2 promotes osteosarcoma proliferation, invasion, migration, and chemoresistance while inhibiting apoptosis, likely through AKT/p-AKT signaling. These effects may be regulated by FoxM1.

25COASMA29:

Title: Pan-cancer analysis unveils the role and mechanisms of neddylation modifications in tumorigenesis.

Hu, Q., Li, X., Wang, P. et al.
Med Oncol 42, 119 (2025).
https://doi.org/10.1007/s12032-025-02658-9

Abstract: This study explores the roles of ubiquitin-like modification genes in pan-cancer, focusing on their regulatory mechanisms, prognostic implications, and drug sensitivity. Data on five key neddylation pathway genes (RBX1, NEDD8, NAE1, UBA3, UBE2M) were collected from TCGA and GTEx databases, covering mRNA expression, DNA methylation, SNVs, and CNVs. Gene expression differences between normal and cancer tissues, along with associations with genetic alterations, methylation, and cancer-related pathways, were analyzed. Drug sensitivity correlations were assessed using GDSC and CTRP databases. Neddylation pathway genes exhibit hypomethylation and overexpression across various cancers, correlating with poor prognosis. SNVs are predominantly missense mutations, while CNVs are mostly heterozygous deletions and amplifications. These genes regulate several key cancer-related pathways, such as DNA damage repair, cell cycle modulation, and inhibition of RTK/RAS/MAPK pathways. Ubiquitin-like modification genes are associated with poor prognosis due to their low methylation and high expression in cancers. Their

genetic alterations impact cancer pathways, underscoring their potential as therapeutic targets and prognostic biomarkers.

Keywords: Neddylation modification, Pan-cancer analysis, DNA methylation, Genetic alterations, Tumorigenesis, Drug sensitivity

25COASMA30:

Title: Isoliquiritigenin attenuates tumor progression and PD-L1 expression by inhibiting the phosphorylation of STAT3 in melanoma.

Zeng, H., Guo, A., Liu, Z. et al.
Med Oncol **42**, 118 (2025).
https://doi.org/10.1007/s12032-025-02666-9

Abstract: Isoliquiritigenin (ISL) has been reported with antitumor activities. While, the underlying molecular mechanisms remain largely unknown. The transcription factor of programmed cell death ligand 1 (PD-L1), STAT3, plays an important role in tumor metastasis. In this study, we first verified that ISL suppressed the growth and metastasis ability of melanoma cells both in vitro and in vivo. Then, we found that ISL could repress the expression of PD-L1 and STAT3 phosphorylation. TIMER algorithm analysis showed that the levels of immune infiltration were positively correlated with the expression of STAT3. Furthermore, the STAT3 phosphorylation inhibitor Stattic could enhance the effect of ISL in suppressing cell proliferation, promoting apoptosis, and restraining the ability of migration and invasion of melanoma cells. This study revealed that ISL inhibited melanoma metastasis and repressed PD-L1 expression by repressing the phosphorylation of STAT3, which help us to understand the mechanism of ISL in melanoma therapy.

25COASMA31:

Title: Tumor microenvironment: recent advances in understanding and its role in modulating cancer therapies.

Shah, D.D., Chorawala, M.R., Raghani, N.R. et al.
Med Oncol **42**, 117 (2025).
https://doi.org/10.1007/s12032-025-02641-4

Abstract: Tumor microenvironment (TME) denotes the non-cancerous cells and components presented in the tumor, including molecules produced and released by them. Interactions between cancer cells, immune cells, stromal cells, and the extracellular matrix within the TME create a dynamic ecosystem that can either promote or hinder tumor growth and spread. The TME plays a pivotal role in either promoting or inhibiting tumor growth and dissemination, making it a critical factor to consider in the development of effective cancer therapies. Understanding the intricate interplay within the TME is crucial for devising effective cancer therapies. Combination therapies involving inhibitors of immune checkpoint blockade (ICB), and/or chemotherapy now offer new approaches for cancer therapy. However, it remains uncertain how to best utilize these strategies in the context of the complex tumor microenvironment. Oncogene-driven changes in tumor cell metabolism can impact the TME to limit immune responses and present barriers to cancer therapy. Cellular and acellular components in tumor microenvironment can reprogram tumor initiation, growth, invasion, metastasis, and response to therapies. Components in the TME can

reprogram tumor behavior and influence responses to treatments, facilitating immune evasion, nutrient deprivation, and therapeutic resistance. Moreover, the TME can influence angiogenesis, promoting the formation of blood vessels that sustain tumor growth. Notably, the TME facilitates immune evasion, establishes a nutrient-deprived milieu, and induces therapeutic resistance, hindering treatment efficacy. A paradigm shift from a cancer-centric model to a TME-centric one has revolutionized cancer research and treatment. However, effectively targeting specific cells or pathways within the TME remains a challenge, as the complexity of the TME poses hurdles in designing precise and effective therapies. This review highlights challenges in targeting the tumor microenvironment to achieve therapeutic efficacy; explore new approaches and technologies to better decipher the tumor microenvironment; and discuss strategies to intervene in the tumor microenvironment and maximize therapeutic benefits.

25COASMA32:

Title: Nanotechnology in Imatinib delivery: advancing cancer treatment through innovative nanoparticles.

Ghadami, A., Fathi-karkan, S., Siddiqui, B. et al.

Med Oncol **42**, 116 (2025).

https://doi.org/10.1007/s12032-025-02660-1

Abstract: Nanotechnology-based drug delivery systems have improved target medicines' therapeutic efficacy and specificity in cancer therapy. Imatinib, one of the tyrosine kinase inhibitors widely used for treating chronic myeloid leukemia and gastrointestinal stromal tumors (GIST), faces many drawbacks, such as poor solubility, reduced bioavailability, and the development of resistance. The paper critically reviews advances in nanotechnology-based approaches toward the delivery of Imatinib, relating to polymeric, lipid-based, carbon-based, and stimuli-responsive nanoparticles. These methods enhance solubility, stability, and targeted distribution and are often used to facilitate the co-delivery of other anticancer drugs with considerable problems in cancer treatment. Although much potential for these technologies exists, scalability, safety, and regulatory approval, among other features, need resolution before real cost can meet clinical efficacy. Further directions would go toward bio-inspired system development, enhancing regulatory frameworks, and cost-effective manufacturing processes that bring nanotechnology into the realm of standard treatment for cancer.

25COASMA33:

Title: EM-12, a natural sesquiterpene lactone extracted from Elephantopus mollis, promotes cancer cell apoptosis by activating ER stress.

Huang, X., Zhou, J., Li, Z. et al.

Med Oncol **42**, 115 (2025).

https://doi.org/10.1007/s12032-025-02654-z

Abstract: The Elephantopus mollis H.B.K. contains various sesquiterpene lactones that have shown anti-proliferative and proapoptotic effects in various cancers, although the underlying mechanisms are partially understood. Inducing of excessive ER stress is a potential cancer therapeutic strategy. However, ER stress activator remain limited in current clinical

applications. In this study, we identified that EM-12, an uncovered sesquiterpene lactone isolated from Elephantopus mollis H.B.K., as a BiP ATPase activity inhibitor through BiP ATPase activity assay in vitro. This molecule also exhibits significantly greater cytotoxicity in numerous ovarian cancer cell lines, including paclitaxel-resistance ovarian cancer cell line, compared to transformed ovarian epithelial cell lines. In addition, EM-12 exerts broad-spectrum cytotoxicity against various human cancer cell lines, including liver, nasopharyngeal, and breast cancer cell lines. Mechanically, EM-12 promotes ER stress and ER-stress-related apoptosis to against cancer cells through inhibiting BiP ATPase activity.

25COASMA34:

Title: Exosomes derived from natural killer cells: transforming immunotherapy for aggressive breast cancer.

Alfawaz Altamimi, A.S., Arockia Babu, M., Afzal, M. et al.

Med Oncol **42**, 114 (2025).

https://doi.org/10.1007/s12032-025-02647-y

Abstract: Natural killer cell-derived exosomes (NK-Exos) hold great promise as immune modulators and immunotherapeutics against cancer due to their intrinsically latent anti-tumor effects. They use these nanosized vesicles to deliver cytotoxic molecules, such as perforin, granzymes, and miRNAs, directly to cancer cells to kill them, avoiding immune suppression. NK-Exos has particular efficacy for treating aggressive breast cancer by modulating the TME to activate the immune response and suppress immunosuppressive factors. Bioengineering advances have extended the therapeutic potential of NK-Exos, which permits precise tumor cell targeting and efficient delivery of therapeutic payloads, including small RNAs and chemotherapeutic agents. In engineered NK-Exos, sensitization of cancer cells to apoptosis, reduction of tumor growth, and resistance to drugs have been demonstrated to be highly effective. When combined, NK-Exos synergizes with radiotherapy, chemotherapy, or checkpoint inhibitors, enhancing therapeutic efficacy, and minimizing systemic toxicity. This review emphasizes the critical role of NK-Exos in breast cancer treatment, their integration into combination therapies, and the need for further research to overcome existing limitations and fully realize their clinical potential.

25COASMA35:

Tritle: Nanomedicine innovations in colon and rectal cancer: advances in targeted drug and gene delivery systems.

Razzaq, S., Fatima, I., Moafian, Z. et al.

Med Oncol **42**, 113 (2025).

https://doi.org/10.1007/s12032-025-02670-z

Abstract: Nanotechnology has revolutionized cancer diagnostics and therapy, offering unprecedented possibilities to overcome the constraints of conventional treatments. This study provides a detailed overview of the current progress and difficulties in the creation of nanostructured materials, with a specific emphasis on their use in drug and gene delivery systems. The study examines tactics that attempt to improve the effectiveness and safety of chemotherapeutic drugs such as doxorubicin (Dox) by focusing on the potential of antibody–drug conjugates and functionalized nanoparticles. Moreover, it clarifies the challenges

encountered in administering nanoparticles orally for gastrointestinal treatments, emphasizing the crucial physicochemical properties that affect their behavior in the gastrointestinal system. This study highlights the transformational potential of nanostructured materials in precision oncology by examining advanced breakthroughs such cell membrane-camouflaged nanoparticles and inorganic nanoparticles designed for gastrointestinal disorders. The text investigates the processes involved in the absorption of nanoparticles and their destruction in lysosomes, revealing the many methods in which enterocytes take up these particles. This study strongly supports the use of advanced nanoparticle-based methods to reduce the harmful effects on the whole body and improve the effectiveness of therapy, based on a thorough examination of current experiments on animals and humans. The main objective of this paper is to provide a fundamental comprehension that will stimulate more investigation and practical use in the field of cancer nanomedicine, advancing its boundaries.

25COASMA36:

Title: Cost-effective isolation of Viburnum opulus-derived nanovesicles and evaluation of their cytotoxic, anticancer, and antioxidant properties on human glioblastoma cell line U87MG.

Giritlioglu, N.I., Poyraz, F.S., Mansuroglu, B. et al.

Med Oncol **42**, 112 (2025).
https://doi.org/10.1007/s12032-025-02669-6

Abstract: Glioblastoma is the most common and highly invasive glial tumor, significantly reducing patient survival. Current therapeutic approaches have limited success rates. Plant-derived nanovesicles are a rapidly developing area, recognized for their exceptional biofunctional properties, and are emerging as a promising approach in cancer treatment. The present study focuses on the isolation of nanovesicles from Viburnum opulus fruits using a cost-effective method that includes a polymer-based exosome precipitation buffer and size exclusion chromatography, followed by their characterization. Morphological analysis via Field Emission Scanning Electron Microscopy and Transmission Electron Microscopy revealed nanovesicles ranging from oval to elliptical shapes, with average diameters of 54.23 nm and 41.21 nm, respectively. Dynamic light scattering analysis determined the average size of 45.36 nm indicating the presence of nanovesicles, and the zeta potential was − 2.87 mV. Biochemical characterization showed total protein and phenolic concentrations of 1534 ± 97.78 µg/ml and 4.270 ± 0.66 mg gallic acid equivalents/L, respectively, with total antioxidant status values of 3.83 ± 0.37 mmol Trolox equivalents/L. Based on IC50 values, these nanovesicles were 7.5 times more toxic to U87MG human glioblastoma cells compared to healthy human dermal fibroblasts. Analyses including clonogenic cell survival, wound healing, apoptosis, total antioxidant status, and total oxidant status were continued on only U87MG cells, as human dermal fibroblasts showed a low response to nanovesicle treatment. Qualitative and quantitative assessments demonstrated that Viburnum opulus-derived nanovesicles effectively inhibited cancer cell proliferation and migration. Due to their non-toxic, anticancer, and antioxidant properties, these nanovesicles hold significant potential in glioblastoma management.

25COASMA37:

Title:Role of hepatotropic viruses in promoting hepatocellular carcinoma—current knowledge and recent advances.

Starnawski, P., Nowak, K., Augustyn, Z. et al

Med Oncol **42**, 111 (2025).
https://doi.org/10.1007/s12032-025-02674-9

Abstract: Hepatocellular carcinoma (HCC) is a leading cause of cancer-related mortality worldwide, with chronic infections by hepatotropic viruses such as hepatitis B virus (HBV), and hepatitis C virus (HCV), being major risk factors. Chronic infections with these viruses are the leading cause of HCC worldwide, with HBV alone responsible for over 50% of cases. Despite advances in direct-acting antivirals (DAAs) for HCV and nucleos(t)ide analogues (NAs) for HBV, challenges remain in HCC prevention, early detection, and treatment. Recent research highlights the role of viral-induced metabolic alterations, such as the Warburg effect, mitochondrial dysfunction, and lipid dysregulation, in promoting HCC. Moreover, immune checkpoint inhibitors have emerged as effective treatments for advanced HCC, though responses vary between HBV- and HCV-related cancers. Additionally, novel therapeutic approaches and metabolic-targeted therapies offer promising avenues for virus-associated HCC treatment. Advancements in liquid biopsy biomarkers and artificial intelligence-driven diagnostics are improving HCC surveillance and risk stratification, potentially enabling earlier interventions. While HBV vaccination has significantly reduced HCC incidence, disparities in global vaccination coverage persist. Furthermore, antiviral therapies combined with structured surveillance programs have proven effective in reducing HCC incidence and mortality. This review highlights the complex connection between viral, genetic, and environmental factors in HCC development and underscores the importance of integrated prevention strategies to reduce its burden globally.

25COASMA38:

Title: Diagnosis and treatment of cardiac tumors.

Imai, T., Shimoi, T., Kawai, A. et al.

Med Oncol **42**, 110 (2025).
https://doi.org/10.1007/s12032-025-02661-0

Abstract: Cardiac tumors, though rare, present significant diagnostic and therapeutic challenges due to their diverse nature and potential severity. These tumors, which can be primary or metastatic, are often detected incidentally through imaging modalities such as echocardiography or CT scans. Differentiating between benign and malignant forms is crucial for guiding appropriate management strategies. This review synthesizes current diagnostic approaches and treatment modalities for cardiac tumors, with a focus on the role of imaging techniques like UCG, CT, MRI, and PET in tumor characterization. Multidisciplinary treatment plans are necessary, including surgical resection for benign tumors, chemotherapy, and radiotherapy for malignant tumors, and novel targeted therapies such as MDM2 inhibitors for selected cases. While primary malignant tumors like sarcomas and mesotheliomas exhibit rapid progression and poor prognosis, recent advances in multimodal therapy offer potential improvements in survival. The incidence of primary cardiac tumors is low, with an autopsy-reported occurrence rate of 0.02%. Benign cardiac tumors, such as

myxomas and fibromas, generally have favorable outcomes with surgical resection. In contrast, primary malignant tumors like sarcomas and mesotheliomas exhibit rapid progression and poor prognosis, necessitating aggressive treatment including surgery, chemotherapy, and radiotherapy. Metastatic cardiac tumors occur in approximately 10% of cancer patients at autopsy and are managed according to the treatment plan for the primary malignancy. The management of cardiac tumors requires a multidisciplinary approach tailored to tumor type, location, and systemic effects. While benign tumors often respond well to surgical management, malignant and metastatic tumors demand more complex strategies to optimize patient outcomes.

25COASMA39:

Title: LncRNA CCAT1 decreases the sensitivity to doxorubicin in lung cancer cells by regulating miR-181a/CPEB2 axis.

Muge, Q., Qing, Y., Bao, W. et al

Med Oncol **42**, 109 (2025).

https://doi.org/10.1007/s12032-025-02668-7

Abstract: Recently, long non-coding RNAs have gained an increasing amount of attention in treating lung cancer. However, a full understanding of how CCAT1 lncRNA works against proliferation is not yet available. Therefore, we assess the impact of CCAT1 on the lung cancer cell proliferation, apoptosis, and doxorubicin (DOX) sensitivity, and the involvement of miR-181a/CPEB2 pathway. For this purpose, lung cancer A549 cells were exposed to siRNA against CCAT1 and DOX and cell viability were measured by MTT assay. ELISA was used to evaluate cell apoptosis. The protein and mRNA expression levels of apoptotic markers, miR-181a and CPEB2 were measured by western blot and qRT-PCR. Knock-downing CCAT1 inhibited the cell viability of A549 cells. In addition, si-CCAT1 treatment increased apoptosis in both cell lines via modulating the anti- and pro-apoptotic markers. Si-CCAT1 increased the levels miR-181a and decreased CPEB2 in A549 cells. In conclusion, our study has provided strong evidence that lncRNA CCAT1 decreased the sensitivity to doxorubicin in lung cancer cells by regulating the miR-181a/CPEB2 axis.

25COASMA40:

Title: Evaluation of the antiangiogenic effect of AMG232 in multiple myeloma coculture systems.

Pooraskari, Z., Barri Ghazani, H., Piri, R. et al.

Med Oncol **42**, 107 (2025).

https://doi.org/10.1007/s12032-025-02659-8

Abstract: This study explored the efficacy of AMG232, a potent and selective MDM2 inhibitor, as an antiangiogenic agent in a multiple myeloma (MM) cell line (AMO-1) cocultured with endothelial cells (HUVECs) in vitro. HUVECs and AMO-1 cells were cocultured in transwell systems. Cell viability was assessed through an MTT assay after exposure to various concentrations of AMG232. Following treatment, gene expression changes were analyzed via quantitative real-time PCR. Wound healing and tube formation assays were also conducted to quantify the effects on cell migration and angiogenesis. AMG232 showed dose-dependent cytotoxicity in AMO-1 cells (IC_{50} = 386.1 nM), whereas

HUVECs were moderately sensitive (IC_{50}= 942.1 nM). In coculture, both cell types displayed increased resistance to AMG232, indicating a protective cell–cell interaction. Treatment with 250-nM AMG232 significantly downregulated the mRNA expression of angiogenic factors—including VEGF-A, VEGFR-2, MMP-2, IL-6, and HIF-1α—in both AMO-1 cells and HUVECs ($P < 0.05$). Wound healing assays revealed that AMG232 markedly inhibited HUVEC migration, with significantly reduced wound closure rates at 24 and 48 h compared with the controls ($P < 0.01$). Tube formation assays further revealed that AMG232 substantially decreased angiogenesis in HUVECs, as evidenced by reductions in junction number, mesh number, and total tube length ($P < 0.01$). Our research revealed that AMG232 effectively inhibited angiogenesis and exhibited cytotoxic effects on MM cells by downregulating key angiogenic factors and impairing endothelial cell functions. These results suggest that AMG232 has significant potential as a therapeutic agent for targeting angiogenesis in MM treatment.

25COASMA41:

Title: Dual targeting of CXC chemokine receptor 4 and multidrug resistance protein 1 by ZIN056 effectively combat daunorubicin resistance in acute myeloid leukemia cells.

Abohassan, M., Al Shahrani, M.M., AlOuda, S.K. et al.

Med Oncol **42**, 106 (2025).

https://doi.org/10.1007/s12032-025-02656-x

Abstract: Drug resistance, associated with the overexpression of CXC chemokine receptor CXCR4 and multidrug resistance protein 1 (MDR1) remains a significant barrier to effective therapy in Acute Myeloid Leukemia (AML). Targeting both CXCR4 and MDR1 could potentially enhance treatment efficacy in resistance. In silico computational screening of the Zinc natural product library using Discovery Studio Visualizer, Protein–Ligand Interaction Profiler, GROMACS, and GMX_MMPBSA techniques were used. THP-1, and SKM-1 cells were used for in vitro analysis. Flow cytometry was employed for target analysis and apoptosis enumerations. The virtual screening identified ZIN056 with favorable binding affinities of − 10.6 kcal/mol and − 9.1 kcal/mol for CXCR4 and MDR1, respectively. MD simulations demonstrated stable binding interactions, with Root Mean Square Deviation values around 0.2 nm for both proteins. The ΔG binding calculations further confirmed values of − 30.09 kcal/mol for CXCR4 and − 34.47 kcal/mol for MDR1, indicating energetically favorable binding. The compound inhibited the THP-1 and SKM-1 cell proliferation with GI_{50} values of 250.6 nM, and 346.7 nM, respectively. ZIN056 decreased CXCR-4 expression and MDR1-induced positive population ($MDR1^{+}$) in THP-1 and SKM-1 cells. ZIN056 inhibited the proliferation of the regular and $MDR1^{+}$ AML cells, while Daunorubicin exhibited a tenfold resistance in controlling $MDR1^{+}$ AML cell proliferation. ZIN056-induced apoptosis in MDR1 + AML cells, whereas Daunorubicin failed to promote apoptosis in these cells. The findings suggest that dual targeting of CXCR4 and MDR1 using ZIN056 may offer a promising strategy to overcome drug resistance in AML and provide a foundation for further development of dual inhibitors for AML patients.

25COASMA42:

Title: αKG-induced oxidative stress and mTOR inhibition as a therapeutic strategy for liver cancer.

Choi, S.K., Kim, M.J. & You, J.S.

Med Oncol **42**, 105 (2025).
https://doi.org/10.1007/s12032-025-02653-0

Abstract: Despite the availability of targeted therapies, liver cancer remains a severe health burden. The need for adjuvant therapy to improve treatment efficacy and prevent recurrence is emerging. Alpha-ketoglutarate (αKG) is an intermediate in the tricarboxylic acid cycle and a cofactor for various oxygenases. A critical role of this multifunctional metabolite has started to be revealed in physiological and pathological conditions. We found that αKG exerts various anti-tumor effects in liver cancer cells. Our kinetic transcriptome study suggested that increasing reactive oxygen species and inhibiting mTORC1 signaling underlies. Indeed, αKG treatment elevated oxidative stress and induced DNA damage, presumably caused by early downregulation of the antioxidant gene SLC7A11. Further, we validated impaired mTOR signaling and decreased cellular energy production. This unique mechanism underscores αKG's potential as a liver cancer therapy by harnessing oxidative stress and disrupting metabolic signaling. These findings could provide valuable insights into further exploration of αKG as a promising therapeutic agent in liver cancer.

25COASMA43:

Title: Fisetin as a chemoprotective and chemotherapeutic agent: mechanistic insights and future directions in cancer therapy.

Fatima, R., Soni, P., Sharma, M. et al.

Med Oncol **42**, 104 (2025).
https://doi.org/10.1007/s12032-025-02664-x

Abstract: Cancer remains a leading cause of mortality globally, characterized by the uncontrolled proliferation of abnormal cells, invasion of healthy tissues, and potential metastasis. Natural compounds have become a focus in cancer research due to their potential therapeutic roles. Among these, fisetin, a dietary flavonoid, demonstrates notable anti-cancer properties through various molecular mechanisms. This review evaluates the chemoprotective and chemotherapeutic potential of fisetin, focusing on its mechanisms of action against cancer and its capacity to enhance cancer treatment. A systematic literature search was conducted across PubMed, Web of Science, and Scopus databases using keywords related to fisetin and cancer. The review synthesizes findings from in vitro and in vivo studies examining fisetin's effects on signaling pathways, apoptosis induction, oxidative stress modulation, and synergistic potential with chemotherapeutic agents. Fisetin has shown the ability to suppress tumor growth and metastasis by modulating critical signaling pathways, including PI3K/Akt/mTOR, NF-κB, and MAPK. It induces apoptosis in cancer cells through mitochondrial and endoplasmic reticulum stress responses and demonstrates antioxidative properties by reducing reactive oxygen species. Additionally, fisetin enhances the efficacy of conventional chemotherapies, indicating its role as a potential adjuvant in cancer treatment. Fisetin presents a promising natural compound with diverse anti-cancer effects, impacting cell cycle arrest, apoptosis, and oxidative stress pathways. Further clinical studies are

warranted to fully elucidate its therapeutic potential and to optimize its delivery for improved bioavailability in cancer patients.

25COASMA44:

Title: Exosomal RNAs and EZH2: unraveling the molecular dialogue driving tumor progression.

Zwamel, A.H., Ahmad, A.T., Altalbawy, F. et al.

Med Oncol **42**, 103 (2025).

https://doi.org/10.1007/s12032-025-02648-x

Abstract: The EZH2 gene encodes an enzyme that is part of the epigenetic factor Polycomb Repressive Complex 2 (PRC2). In order to control gene expression, PRC2 mainly modifies chromatin structure. In this complex process, EZH2 methylates histone proteins, which in turn suppresses further RNA transcriptions. As a result, EZH2 dysregulations can occasionally induce abnormal gene expression patterns, which can aid in the development and progression of cancer. Non-coding RNAs significantly impact the expression of EZH2 through epigenetic mechanisms. Meanwhile, normal and cancerous cells frequently release vesicles into the extracellular matrix, also known as exosomes, that occasionally carry RNA molecules from their origin cells, including messenger RNAs, microRNAs, and other non-coding RNAs. Thus exosomes are granted the ability to regulate numerous physiological functions and act as crucial messengers between cells by influencing gene expression in the recipient cell. We conducted this review to focus on EZH2's substantial biological role and the mechanisms that regulate it, driven by the desire to understand the possible impact of exosomal RNAs on EZH2 expression.

25COASMA45:

Title: PKM2 knockout facilitates the activation of the AMPK/KLF4/ACADVL pathway, leading to increased oxidative degradation of fatty acids in TNBC.

Zhang, L., Cheng, L., Ma, Y. et al.

Med Oncol **42**, 102 (2025).

https://doi.org/10.1007/s12032-025-02671-y

Abstract: This study unveils PKM2 as a master metabolic coordinator in triple-negative breast cancer (TNBC), governing the glycolysis-lipolysis balance through the AMPK/KLF4/ACADVL axis. We demonstrate stage-specific PKM2 upregulation in TNBC, with CRISPR/Cas9 knockout inducing dual metabolic reprogramming—suppressed glycolysis and activated lipid catabolism. Mechanistically, PKM2 ablation triggers AMPK-dependent nuclear translocation of KLF4, which directly activates ACADVL (mitochondrial β-oxidation rate-limiting enzyme), explaining lipid droplet depletion. Therapeutically, synergistic lethality emerges from combining PKM2 knockout with ACADVL inhibition, suggesting metabolic redundancy disruption strategies. Unlike PKM2-SCAP-mediated lipogenesis reported elsewhere, our work establishes a KLF4-driven lipid catabolic pathway specific to TNBC. Crucially, this AMPK/KLF4/ACADVL network operates independently of BRCA status, proposing targeted therapy for chemoresistant non-BRCA mutant TNBC. Our findings redefine TNBC metabolic plasticity through

transcriptional-metabolic crosstalk, offering combinatorial therapeutic paradigms against metabolic adaptation.

25COASMA46:

Title: Recent advancements in genistein nanocarrier systems for effective cancer management.

Arora, D., Vanshita, Bhati, H. et al.

Med Oncol **42**, 101 (2025).

https://doi.org/10.1007/s12032-025-02649-w

Abstract: Cancer continues to be a significant global health concern, consistently ranking as one of the leading causes of mortality across diverse populations and socio-economic contexts. Genistein, a soy-derived isoflavonoid, has gained significant attention for its diverse health benefits, particularly its potent anticancer activity. Emerging pre-clinical and clinical evidences highlights its ability to modulate key cellular processes, including apoptosis, autophagy, angiogenesis, metastasis, immune responses and cell cycle regulation. Despite its therapeutic potential, the clinical translation of genistein is limited by its poor pharmacokinetics, low aqueous solubility, and rapid metabolic degradation, resulting in suboptimal bioavailability. To address these limitations, various nanotechnology-based formulations have been developed, significantly improving the bioavailability, stability, and therapeutic efficacy of genistein. Functionalized nanocarriers further enhance its effectiveness by enabling targeted drug delivery, reducing off-target toxicities, and achieving sustained release at the tumor site. This review provides a comprehensive overview of advanced nanoformulations for genistein delivery emphasizing their efficacy against prevalent cancers such as breast, lung, and colon cancer. By exploring the interplay between genistein's therapeutic potential and innovative drug delivery systems, this review underscores the transformative impact of nanotechnology in overcoming the limitations of conventional cancer therapies and improving patience compliance.

25COASMA47:

Title: Integrative approach to decipher pharmacological mechanism of Cinnamomum zeylanicum essential oil in prostate cancer.

Mohanty, D., Padhee, S., Priyadarshini, A. et al.

Med Oncol **42**, 100 (2025).

https://doi.org/10.1007/s12032-025-02665-w

Abstract: Prostate cancer has garnered much importance in recent years due to its rising incidence and mortality among men worldwide. The ineffectiveness of existing therapies and adverse events associated with conventional treatment have led patients to turn towards traditional medicine for the management of prostate cancer. Cinnamomum zeylanicum bark essential oil (CZEO) possesses promising anticancer properties, yet the exact mechanism of action of CZEO for the management of prostate cancer remains unclear. Therefore, the current study tried to elucidate the bioactive components and key potential targets through which CZEO may exert its anticancer effect for treating prostate cancer. Fifty-nine constituents were identified by GC–MS, of which 52 were drug-like constituents. A total of 2847 targets related to CZEO and 2283 targets related to prostate cancer were obtained from

public databases and the GEO dataset. Twenty-three overlapping targets exist between CZEO and disease targets. Compound-disease-target network analysis revealed camphor, eugenol, methyl eugenol, trans farnesyl acetate and nerol as the core bioactive ingredients of CZEO. The topological screening of the PPI network revealed BCL2, TNF, NFKBIA, CREBBP and IL7R as potential hub targets. These hub targets were validated based on mRNA expression level, pathological stages, overall survival, immune infiltrate and genetic alteration analysis in prostate adenocarcinoma and normal patients. KEGG enrichment analysis proposed that CZEO exhibits its anticancer effect mainly by modulating the PI3-AKT and MAPK signalling pathway. Moreover, molecular docking and dynamics simulation studies revealed a good binding affinity of these core compounds with TNF, NFKBIA and BCL2. CZEO exhibited a remarkable anti-proliferative effect against PC-3 cells with an IC_{50} value of 13.56 µg/mL. CZEO promoted apoptosis and cell cycle arrest in the G2/M phase in PC-3 cells. CZEO-induced apoptosis was due to loss of mitochondrial membrane potential, increase in reactive oxygen species levels and activation of caspases (caspase 3, caspase 8 and caspase 9). RT-qPCR analysis revealed that CZEO modulated the mRNA expression level of hub genes (BCL2, TNF, NFKBIA, CREBBP, and IL7R, caspase 3, caspase 8 and caspase 9). The present study provides a mechanistic approach of Cinnamomum zeylanicum essential oil against prostate cancer.

25COASMA48:

Title: Combination therapy using parthenolide and doxorubicin induces apoptosis in Raji cells: insights into miR-27b and signaling pathway alterations.

Zare-Badie, Z., Zare, F., Rastegari, B. et al.

Med Oncol **42**, 99 (2025).

https://doi.org/10.1007/s12032-025-02673-w

Abstract: Burkitt lymphoma, a highly aggressive form of non-Hodgkin lymphoma, have significant treatment challenges, such as chemotherapy-related toxicity and the risk of relapse, especially in older adults. Treatment of Raji cells, a Burkitt lymphoma cell line, with parthenolide in combination to doxorubicin may enhance therapeutic efficacy. This study aimed to evaluate cell viability and apoptosis following treatment with these agents, and to investigate the underlying molecular mechanisms involving miR-27b and the MET/PI3K/AKT signaling pathway. Raji cells were treated with varying concentrations of parthenolide and doxorubicin for 48 and 72 h, cell viability was assessed using the MTT assay, and apoptosis was quantified using flow cytometry. Subsequently, we performed quantitative RT-PCR to evaluate the expression levels of miR-27b, MET, PI3K, and AKT. The half-maximum inhibitory concentration (IC_{50}) values of 976.1 nM for doxorubicin and 4.39 µM for parthenolide were determined at 48 h. The apoptosis rate increased from 7.6% in the untreated control to 44.5% and 49.2% for doxorubicin and parthenolide, respectively, reached to 81.2% at higher doses of parthenolide in combination ($p < 0.001$). miR-27b expression was significantly upregulated, particularly in the combination group ($p < 0.001$). MET and PI3K expression was significantly downregulated by the combination treatments ($p < 0.05$). In conclusion, combination of parthenolide and doxorubicin exert enhanced cytotoxic effects via increased apoptosis and modulation of miR-27b and the MET signaling pathway in Raji cells, regulatory relationship between miR-27b and the MET

signaling pathway may contribute to the observed therapeutic benefits. Further research is required to clarify the molecular mechanisms and therapeutic applications of this combination strategy.

25COASMA49:

Title: FBXO32 ubiquitination of SUFU promotes progression and lenvatinib resistance in hepatocellular carcinoma via hedgehog signaling.

Wang, S., Peng, R., Chen, C. et al.

Med Oncol **42**, 98 (2025).

https://doi.org/10.1007/s12032-025-02644-1

Abstract: Lenvatinib is a prevalent treatment for hepatocellular carcinoma (HCC), yet resistance to the drug significantly limits its effectiveness. This study investigates the role of FBXO32 (F-Box Protein 32) in HCC progression and lenvatinib resistance. Methods: We utilized the GSE211850 and GSE46408 datasets to identify an E3 ubiquitin ligase that is highly expressed in both lenvatinib-resistant HCC cells and HCC tissues. The expression and clinical relevance of this E3 ubiquitin ligase were further validated using lenvatinib-resistant HCC cells, online databases, and HCC clinical tissue samples. The phenotype was verified by cell and animal experiments. Techniques such as RNA sequencing, western blotting, immunofluorescence, Co-immunoprecipitation (Co-IP), Ubiquitination, and cycloheximide (CHX) chase assay reveal the mechanism. FBXO32 is highly expressed in both lenvatinib-resistant HCC cells and HCC tissues. High FBXO32 expression correlated with increased ALT, AFP levels, larger tumors, and advanced TNM stages, serving as an independent risk factor for overall survival (OS) and recurrence-free survival (RFS). Functional assays demonstrated that FBXO32 overexpression enhanced cell proliferation, stemness, apoptosis resistance, and lenvatinib resistance, while knockdown had opposing effects. KEGG enrichment analysis indicated a link between FBXO32 and the Hedgehog signaling pathway. FBXO32-mediated degradation of SUFU, a Hedgehog pathway inhibitor, activated this pathway. Inhibiting Hedgehog signaling counteracted FBXO32's impact on HCC growth and resistance. Conclusion: FBXO32 is a critical marker for lenvatinib efficacy and HCC prognosis, suggesting that targeting FBXO32 or the Hedgehog pathway could provide innovative strategies for overcoming lenvatinib resistance in HCC.

25COASMA50:

Title: Targeting EGFR and PI3K/mTOR pathways in glioblastoma: innovative therapeutic approaches.

Singh, G., Rohit, Kumar, P. et al.

Med Oncol **42**, 97 (2025).

https://doi.org/10.1007/s12032-025-02652-1

Abstract: Glioblastoma (GBM) stands as the most aggressive form of primary brain cancer in adults, characterized by its rapid growth, invasive nature, and a robust propensity to induce angiogenesis, forming new blood vessels to sustain its expansion. GBM arises from astrocytes, star-shaped glial cells, and despite significant progress in understanding its molecular mechanisms, its prognosis remains grim. It is frequently associated with mutations or overexpression of the epidermal growth factor receptor (EGFR), which initiates several

downstream signaling pathways. Dysregulation of key signaling pathways, such as EGFR/PTEN/AKT/mTOR, drives tumorigenesis, promotes metastasis and leads to treatment resistance. The modest survival benefits of the conventional treatment of surgical resection followed by radiation and chemotherapy underscore the pressing need for innovative therapeutic approaches. In most the tumor, overexpression of EGFR is found associated with GBM and mutations in its several variants are important for promoting ongoing mitogenic signaling and tumor growth. This receptor inhibits apoptosis and promotes cell survival and proliferation by activating downstream PI3K/AKT/mTOR pathways. This route is typically blocked by PTEN, a crucial tumor suppressor, however, GBM frequently results in abnormalities in this protein. The aim of this review is to explore the molecular foundations of GBM, with a focus on the EGFR and PI3K/mTOR pathways and their impact on tumor behavior. Additionally, this review highlights EGFR and PI3K/AKT/mTOR inhibitors currently in clinical and preclinical trials, addressing treatment resistance, challenges, and future directions.

25COASMA51:

Title: Exosomal miR-92a-3p modulates M2 macrophage polarization in colorectal cancer: implications for tumor migration and angiogenesis.

Zhao, W., Wu, Y., Wang, Y. et al

Med Oncol **42**, 96 (2025).
https://doi.org/10.1007/s12032-025-02635-2

Abstract: Colorectal cancer (CRC) is one of the most prevalent malignant neoplasms globally. Its development and metastasis are closely associated with the polarization of macrophages within the tumor microenvironment (TME). In particular, the polarization of M2-type macrophages has been demonstrated to be related to the promotion of tumor growth, migration, and angiogenesis. This study aims to investigate the role of miR-92a-3p in colon cancer-derived exosomes in regulating M2-type macrophage polarization by targeting EID2B and to elucidate the impact of this process on tumor migration and angiogenesis. MicroRNAs that were differentially expressed in plasma exosomes from CRC patients were initially identified through a search of the GEO database. The results were then verified by RT-qPCR using miR-92a-3p. The uptake of exosomes was observed via laser confocal microscopy, and the impact of miR-92a-3p on the polarization of exosomes and macrophages was examined through the use of RT-qPCR and WB. A bioinformatics analysis and a dual-luciferase reporter assay were employed to identify the downstream target of miR-92a-3p and to investigate its effect on the MAPK/ERK pathway. miR-92a-3p was upregulated in plasma exosomes of colon cancer patients and exhibited a positive correlation with lymph node metastasis. The results demonstrated that miR-92a-3p was capable of promoting M0 macrophage polarization toward the M2 phenotype, and of enhancing the migratory and invasive capacities of CRC cells, as well as their angiogenic potential in vitro. Bioinformatic analysis and experimental validation demonstrated that miR-92a-3p targeted EID2B and that this target gene was negatively correlated with M2-type macrophage polarization. The results demonstrated that miR-92a-3p promotes macrophage M2 polarization by activating the MAPK/ERK pathway. miR-92a-3p activates the MAPK/ERK pathway and induces macrophage M2 polarization by targeting EID2B, thereby promoting migration and

angiogenesis in CRC. These findings offer new potential targets for the treatment of colon cancer.

25COASMA52:

Title: Young-onset metastatic colorectal cancer: an opportunity and a vision for progress in cancer.

Cooray, P.D., Cooper, N.J.

Med Oncol **42**, 95 (2025).
https://doi.org/10.1007/s12032-025-02640-5

Abstract: Metastatic young-onset colorectal cancer (yo-CRC) is a distinct and aggressive disease subtype that is becoming increasingly prevalent worldwide with Australia leading the world in this trend. This article provides an evidence-based perspective, through the prism of authors' personal experience, to craft an effective pathway not only to deliver improved outcomes for the patients but also to reduce disparities and foster collaboration amongst the cancer-treating community and indeed patients. It highlights an opportunity to re-define, re-design, and create a model that is rewarding to patients and cancer-treating community. Although our focus is on the high unmet needs group of yo-CRC, this model has the potential to expand to other cancer types and care models. We analyse the unique epidemiological trends, challenges, and burdens, emphasising the need for tailored treatment approaches for younger patients with colorectal cancer especially in the metastatic setting. We identify current gaps in clinical practice and research. To improve real-world outcomes, we propose a conceptual framework to enhance clinician–patient communication and treatment planning. Central to our approach is the integration of a Registry of Incidence, Intervention, and Outcomes (RIIO), which enables real-time data collection and analysis, improving treatment personalisation and efficacy. This registry could revolutionise patient care and drive research innovation through enhanced data sharing and collaboration. We advocate for a patient-centric integrated care model that utilises all available therapies to maximise survival and quality of life. Our perspective underscores the urgent need for a paradigm shift in how yo-CRC is viewed, researched and managed, proposing a pathway to significantly enhanced outcomes. Whilst it is feasible to expand the concepts discussed here for all colorectal cancer and indeed all cancer types, we believe this approach is most relevant and acutely needed in yo-CRC setting for reasons detailed in the manuscript.

25COASMA53:

Title: Selinexor in the treatment of liposarcoma: from preclinical evidence to clinical practice.

Remiszewski, P., Gaik, W., Skora, A. et al.

Med Oncol **42**, 94 (2025).
https://doi.org/10.1007/s12032-025-02651-2

Abstract: Selinexor is a new compound studied for the treatment of liposarcoma, particularly dedifferentiated liposarcoma (DDLPS), where treatment options remain limited. As a first-in-class oral exportin-1 (XPO1) inhibitor, selinexor has shown anti-tumour activity in preclinical models, particularly in MDM2- and CDK4-amplified DDLPS, where it induces apoptosis, inhibits tumour growth and promotes nuclear retention of p53. Preclinical studies have also

suggested potential synergy with doxorubicin and eribulin, although these findings have yet to be validated in randomised clinical trials. The phase II/III SEAL trial (NCT02606461) evaluated selinexor versus placebo in patients with advanced, previously treated DDLPS. While the study demonstrated a statistically significant, albeit modest, improvement in median progression-free survival (PFS) from 2.1 to 2.8 months, no overall survival benefit was observed. In addition, selinexor was associated with significant toxicity, including fatigue, nausea and weight loss. Similarly, a phase Ib/II study (NCT03042819) evaluating selinexor in combination with doxorubicin reported a 21% response rate and a median PFS of 5.5 months, although this regimen was also associated with high rates of neutropenia and fatigue. Despite these results, selinexor is not currently approved for the treatment of liposarcoma and its clinical utility remains under investigation. Ongoing studies, such as the SeliSarc trial (NCT04595994) evaluating selinexor in combination with gemcitabine and the NRSTS2021 trial (NCT06239272) evaluating selinexor in paediatric soft tissue sarcoma, aim to further define its role. The results of these studies will be critical in determining whether selinexor can be incorporated into standard sarcoma treatment.

25COASMA54:

Title: Nanomaterials in gastric cancer: pioneering precision medicine for diagnosis, therapy, and prevention.

Liu, T., Gu, Y., Zhao, Y. et al.

Med Oncol **42**, 93 (2025).

https://doi.org/10.1007/s12032-025-02650-3

Abstract: Gastric cancer (GC) continues to be a major health issue globally due to its high rates of both occurrence and mortality. Despite advancements in treatment, the outlook for those affected remains poor, highlighting the critical need for new diagnostic and treatment methods. Nanotechnology, especially nanoparticles, is emerging as a crucial innovation in cancer care by improving imaging, targeting drug delivery, and enhancing early detection. These nanoparticles are also enhancing the effectiveness of treatments like phototherapy, chemotherapy, and immunotherapy. Notably, they show potential in addressing infections like Helicobacter pylori (H. pylori), which is known to increase the risk of developing GC. This review underscores the pivotal role of nanotechnology in enhancing the integrated management of GC, offering a basis for future advancements in the field.

25COASMA55:

Title: Prodelphinidin from purple sweet potato induces apoptosis in human triple-negative breast cancer cells via ROS-mediated ER stress activation.

Zhang, J., Chen, Z., Wang, S. et al.

Med Oncol **42**, 92 (2025).

https://doi.org/10.1007/s12032-025-02642-3

Abstract: Triple negative breast cancer (TNBC), a highly aggressive and heterogeneous subtype of breast cancer, lacks an effective targeted therapy. Conventional medication has limited efficacy in treating TNBC, which highlights the potential of developing therapeutic agents from natural bioactive compounds. This study aimed to investigate the cytotoxicity of prodelphinidin (PD), an anthocyanin found in purple sweet potato, in human MDA-MB-231

and MDA-MB-436 cells. The results showed that PD selectively inhibited human breast cancer, particularly TNBC. Furthermore, PD demonstrated significant dose- and time-dependent inhibition of MDA-MB-231 and MDA-MB-436 cell activity. Flow cytometry and western blot analysis revealed that PD induced cell apoptosis by down-regulating Bcl-2, activating caspase-3/9, and cleaving PARP. Additionally, PD treatment upregulated the expression of p-elF2α, GRP78, and CHOP, indicating the involvement of endoplasmic reticulum stress (ERS). PD treatment also increased the production of reactive oxygen species (ROS) and decreased superoxide dismutase (SOD) activity in TNBC cells. The cytotoxicity of PD reduced significantly by pre-treatment with caspase inhibitors (Ac-DEVD-CHO and Z-LEHD-FMK). In conclusion, PD effectively inhibited the proliferation and induced apoptosis in TNBC cells through the activation of ROS and endoplasmic reticulum stress.

25COASMA56:

Title: Macrophage-derived lncRNAs in cancer: regulators of tumor progression and therapeutic targets.

Suliman, M., Saleh, R.O., Chandra, M. et al

Med Oncol **42**, 91 (2025).

https://doi.org/10.1007/s12032-025-02643-2

Abstract: Macrophages are key tumor microenvironment (TME) regulators, exhibiting remarkable plasticity that enables them to either suppress or promote cancer progression. Emerging evidence highlights the critical role of macrophage-derived long non-coding RNAs (lncRNAs) in shaping tumor immunity, influencing macrophage polarization, immune evasion, angiogenesis, metastasis, and therapy resistance. This review comprehensively elucidates the functional roles of M1- and M2-associated lncRNAs, detailing their molecular mechanisms and impact on cancer pathogenesis. In summary, elucidating the roles of lncRNAs derived from macrophages in cancer progression offers new avenues for therapeutic strategies, significantly improving patient outcomes in the fight against the disease. Further research into the functional significance of these lncRNAs and the development of targeted therapies is essential to harness their potential fully in clinical applications. We further explore their potential as biomarkers for cancer prognosis and therapeutic targets for modulating macrophage activity to enhance anti-cancer immunity. Targeting macrophage-derived lncRNAs represents a promising avenue for precision oncology, offering novel strategies to reshape the TME and improve cancer treatment outcomes.

25COASMA57:

Title: Bone marrow mesenchymal stem cells enrich breast cancer stem cell population via targeting metabolic pathways.

Movahed, Z.G., Mansouri, K., Mohsen, A.H. et al.

Med Oncol **42**, 90 (2025).

https://doi.org/10.1007/s12032-025-02632-5

Abstract: The role of cancer cell metabolic reprogramming in the formation and maintenance of cancer stem cells (CSCs) has been well established. This reprogramming involves alterations in the metabolic pathways of cancer cells, leading to the acquisition of

stem cell-like properties such as self-renewal and differentiation. This study aimed to investigate the potential effects of bone marrow mesenchymal stem cells (BM-MSCs) on the enrichment of breast CSCs. Exosomes (Exo) and conditioned media (CM) were isolated from BM-MSCs for use in this experimental study. The impact of BM-MSCs-Exo and BM-MSCs-CM on the expression of stemness genes NANOG and OCT-4, as well as CD24 and CD44 markers, was assessed in MCF-7 and MDA-MB-231 cell cultures to identify CSCs. Furthermore, the effects of BM-MSCs-Exo and BM-MSCs-CM on cancer cell metabolism were evaluated by examining changes in glycolysis, the pentose phosphate pathway (PPP), and amino acid profiles. Additionally, the influence of BM-MSCs-Exo and BM-MSCs-CM on tumor growth in vivo was also investigated. The analysis of stemness marker expression in cells treated with BM-MSCs-Exo and BM-MSCs-CM revealed an increase in stemness characteristics compared to the control group. Furthermore, the examination of changes in cell metabolism following these treatments showed alterations in glycolysis, PPP, and amino acid metabolism pathways. Additionally, it was demonstrated that BM-MSCs-Exo and BM-MSCs-CM can promote tumor growth in mice following transplantation of 4T1 cells. These findings suggest that BM-MSCs-Exo and BM-MSCs-CM can enrich the population of CSCs in MCF-7 and MDA-MB-231 cells by targeting metabolic pathways, however, further studies are required to elicit the exact mechanisms of these phenomena.

25COASMA58:

Title: Effects of royal jelly on ovary cancer cells proliferation and apoptosis.

Asmaz, E.D., Güler, S. & Zık, B.

Med Oncol **42**, 89 (2025).

https://doi.org/10.1007/s12032-025-02638-z

Abstract: The aim of the present study is to investigate the proliferative or apoptotic effects of different doses and durations of Royal jelly (RJ) on serous type epithelial ovarian cancer, which is the most common epithelial ovarian cancer. For this purpose, cells of the Skov-3 human ovarian adenocarcinoma cell line were grown in McCoy medium and seeded in 6-well plates. RJ was prepared as a stock solution (1000 mg RJ/10 ml dH_2O) and 1, 5, 10, 20, and 50 mg/ml RJ doses from the prepared stock solution were added to the medium for 24, 48, and 72 h incubated. After the treatment of RJ, the cell viability test (Tripan Blue), Ki-67 to determine the proliferative effect, cleaved-Caspase-3 and cleaved PARP expressions to determine its apoptotic effect were examined by immunocytochemical and immunofluorescence methods. In addition, findings were supported by the TUNEL method. As a result of the experiments, it was determined that 1 mg/ml and 24 h treatment of RJ did not affect cell proliferation and apoptosis, but generally, 50 mg/ml of RJ for 72 h inhibited proliferation in cancer cells and induced apoptosis. The use of royal jelly both monotherapeutically and in combination as an alternative treatment for ovarian cancer may provide the basis for new experimental protocols.

25COASMA59:

Title: Deciphering FOXM1 regulation: implications for stemness and metabolic adaptations in glioblastoma.

Swati, K., Arfin, S., Agrawal, K. et al.

Med Oncol **42**, 88 (2025).
https://doi.org/10.1007/s12032-025-02639-y

Abstract: The Forkhead box M1 (FOXM1) gene-mediated Wnt signaling pathway plays a significant role in the development and growth of glioblastoma multiforme (GBM), an exceptionally aggressive form of brain cancer. Our research explores the crucial involvement of the FOXM1 gene, a key transcription factor within the Wnt signaling pathway using bioinformatics techniques in both GBM and glioma stem cells (GSCs). Elevated FOXM1 gene expression is strongly associated with poor patient survival in GBM. Furthermore, FOXM1 gene expression is correlated with stemness-related factors, such as SOX2 and SOX9, which act as key drivers in the progression of cancer stem cells. Moreover, we specifically look into the direct associations of the FOXM1 gene with angiogenetic-related factors, metabolic genes, metastatic genes, pluripotency-related factors, immune cell infiltration, transcriptional networks, and functional category enrichment analysis, shedding light on the intricate molecular mechanisms involved in GBM initiation and progression. Additionally, our research identifies FOXM1-targeting miRNAs, revealing their potential as therapeutic candidates with implications for patient survival rates and DNA methylation patterns of the FOXM1 gene, uncovering insights into its epigenetic regulation. This knowledge contributes to a comprehensive understanding of the molecular landscape and potential avenues for developing more effective therapeutic approaches against GBM and GSCs.

25COASMA60:

Title: Botanical sources, biopharmaceutical profile, anticancer effects with mechanistic insight, toxicological and clinical evidence of prunetin: a literature review.

Bithi, S.A., Al Hasan, M., Bhuia, M.S. et al
Med Oncol **42**, 87 (2025).
https://doi.org/10.1007/s12032-025-02646-z

Abstract: Prunetin (PRU), a naturally occurring flavonoid, has gained recognition for its wide-ranging therapeutic benefits, though its anticancer properties have yet to be extensively reviewed. This study explores the potential of PRU in targeting critical molecular pathways involved in tumor progression, including oxidative stress, apoptosis, cell cycle regulation, and metastasis. Data were compiled from reputable sources, including PubMed, Springer Link, Scopus, Wiley Online, Web of Science, ScienceDirect, and Google Scholar. The findings emphasize PRU's ability to mitigate oxidative stress, promote apoptosis, and regulate the cell cycle in cancer cells. Its anti-inflammatory and anti-angiogenic properties further enhance its effectiveness against cancer. Mechanistic studies reveal that PRU suppresses oncogenic pathways such as PI3K/Akt/mTOR (Phosphoinositide 3-kinase/Protein kinase B/Mammalian target of rapamycin) while activating tumor-suppressor mechanisms. Experimental models show that PRU effectively inhibits cancer cell proliferation and metastasis. Additionally, PRU exhibits favorable pharmacokinetics, demonstrating high intestinal absorption (95.5%), good Caco-2 permeability, and metabolism via CYP1A2, CYP2C19, CYP2C9, and CYP3A4, though it has poor blood–brain barrier (BBB) permeability and limited aqueous solubility, posing challenges for systemic bioavailability. Beyond its anticancer properties, PRU displays broad pharmacological relevance, including

anti-inflammatory, cardioprotective, neuroprotective, anti-obesity, and osteoprotective effects, mediated through pathways, such as NF-κB, MAPK, and AMPK. Toxicological studies indicate a favorable safety profile, with low cytotoxicity in normal cells and no significant toxicity at high doses in preclinical models. While clinical evidence on PRU remains limited, studies on structurally related isoflavones suggest promising therapeutic potential, necessitating further clinical trials to establish its efficacy and safety in humans.

25COASMA61:

Title: The reciprocal effects of autophagy and the Warburg effect in pancreatic ductal adenocarcinoma: an in vitro study.

Azizzadeh, B., Majidinia, M. & Gheysarzadeh, A.

Med Oncol **42**, 86 (2025).

https://doi.org/10.1007/s12032-025-02631-6

Abstract: Autophagy and the Warburg effect are two common pathways in pancreatic ductal adenocarcinoma (PDAC). To date, the reciprocal effects of these pathways have not yet been elucidated. Therefore, this study was designed to investigate the relationship between these factors in vitro and may provide therapeutic targets in the future. The Mia-Paca-2 and AsPc-1 cell lines were cultured under normal conditions. To achieve autophagy, starvation was induced by Hank's balanced salt solution (HBSS), whereas autophagy was inhibited by 3-methyladenine (3-MA). The Warburg effect is mimicked by lactic acid, and the Warburg effect is inhibited by oxamate, the main inhibitor of lactate dehydrogenase. Cell viability was checked through the MTT assay method. Autophagy was checked via evaluation of Beclin-1 via western blotting. The amount of lactic acid was also measured with a lactate dehydrogenase (LDH) assay kit. The cells were incubated with different concentrations of 3-MA, lactic acid and oxamate. The viability of AsPc-1 cells decreased, and the IC_{50} values were 1195 µM, 23.06 mM and 8.617 mM for 3-MA, lactic acid and oxamate, respectively. Similarly, the IC_{50} values of Mia-Paca-2 were 873.9 µM, 35.9 mM and 26.74 mM for 3-MA, lactic acid and oxamate, respectively. Our data revealed that starvation increased the expression of the autophagy-related protein Beclin-1 (P value < 0.05); however, 3-MA significantly reduced its expression (P value < 0.05). In addition, lactic acid alone did not affect the expression level of Beclin-1 (P value > 0.05), but oxamate treatment increased its expression (P value < 0.05). We also showed that starvation reduced lactic acid levels, but an autophagy inhibitor, 3MA, significantly increased lactic acid production (P value < 0.05). Our findings showed that lactic acid alone has no significant effect on autophagy and that oxamate induces autophagy, possibly because of caloric restriction. On the other hand, autophagy inhibits lactic acid production, whereas the inhibition of autophagy leads to increased lactic acid production.

25COASMA62:

Title: Targeting the TGF-β-p21 axis: a critical regulator of bleomycin–induced cell cycle arrest and apoptosis in vitro-implication for progressive cervical cancer therapy.

Shrivastava, S., Ratnacaram, C.K.

Med Oncol **42**, 85 (2025).

https://doi.org/10.1007/s12032-025-02624-5

Abstract: Cervical cancer signifies a global health concern and is a major cause of cancer mortality in women worldwide. Dysregulation of apoptotic pathway and cell cycle play a role in cancer development. Aberrant signalling pathways leads to complex mechanisms leading to the severity. Bleomycin is an anti-tumor glycopeptide molecule which exhibits impressive cytotoxicity in cancer cells. However, its modulating significance on TGF-β induced cell cycle arrest and apoptosis in cervical cancer remains elusive. We confirmed the cytotoxicity, anti proliferative effect of bleomycin in HeLa cells. Meanwhile, bleomycin also led to the suppression of cell migration, invasion. Relative gene expression quantification for cell cycle regulatory, apoptotic, and TGF-β member's genes was done by qRT-PCR. Bleomycin markedly downregulated the expression of cyclin A2, cyclin B1 and cell cycle arrest at G_2/M phase in vitro. Dual AO/EB and Propidium iodide staining was done to evaluate early and late apoptosis in cervical cancer cells. Bleomycin prompts early and late apoptosis in cervical cancer cells by chromatin condensation and blebbing. Mechanistically, bleomycin activates TGF-β induced p21 cascade by upregulation of GADD45A and GDF11, stabilizing p53, to induce cell cycle arrest and apoptosis. Bleomycin induces DNA damage triggering TGF-β pathway. This study can broaden our understanding of the signalling mechanisms that could develop effective strategies for cancer therapy. Elucidation of these pathways in cervical cancer may ultimately lead to novel and more effective treatments. Here, we highlight apoptosis-inducing drug as a therapeutic strategy to regulate the process of carcinogenesis, and regulating apoptosis could benefit cancer treatment and prevention.

25COASMA63:

Title: Characterization of lncRNAs contributing to drug resistance in epithelial ovarian cancer.

Siahestalkhi, E.K., Demiray, A., Yaren, A. et al.
Med Oncol **42**, 84 (2025).
https://doi.org/10.1007/s12032-025-02628-1

Abstract: Epithelial ovarian cancer (EOC) is the second leading cause of death among women with gynecological cancers, particularly in high-income countries. Despite significant advancements in molecular oncology and an initially positive response to primary chemotherapy, the development of drug resistance remains a major challenge in the effective management of EOC. Consequently, there is an urgent need for innovative biological markers that can enable early diagnosis and provide more accurate predictions of recurrence risk in ovarian cancer patients. This study investigated the expression profiles of seven specific long noncoding RNAs (lncRNAs)—SNHG7, TUG1, XIST1, PRLB, TLR8-AS1, ZFAS1, and PVT1—associated with epithelial ovarian cancer and their relationship with drug resistance. To achieve this, drug-resistant subtypes of aggressive EOC cell lines, including carboplatin/paclitaxel-resistant OVCAR3 and SKOV3 lines, were developed. The expression profiles of the selected lncRNAs were quantitatively analyzed using RT-qPCR across various ovarian cancer cell lines and in serum samples from 25 patients before chemotherapy, six months after treatment, and 23 healthy controls. The findings revealed that the target lncRNAs were significantly upregulated under drug-resistant conditions and in post-chemotherapy serum samples, suggesting their involvement in a complex regulatory network. These results highlight the critical roles of lncRNAs in the progression and treatment

response of EOC, positioning them as potential therapeutic targets and biomarkers for early diagnosis and treatment stratification. Identifying reliable lncRNA biomarkers could enable the early detection of patients at risk for developing drug resistance, thereby facilitating personalized treatment strategies to improve patient outcomes and survival rates.

25COASMA64:

Title: Metal nanoparticles as a promising therapeutic approach for prostate cancer diagnosis and therapy: a comprehensive review.

Saadh, M.J., Khidr, W.A., Alfarttoosi, K.H. et al.

Med Oncol **42**, 83 (2025).
https://doi.org/10.1007/s12032-025-02633-4

Abstract: Prostate cancer is a leading cause of mortality among men worldwide, particularly in the USA and European nations, with an estimated 1.9 million new cases and over 580,000 deaths annually, according to recent global statistics. The treatment of prostate tumors presents significant clinical challenges, due to the disease's high metastatic potential, specifically to vital organs, such as the liver, lungs, bones, and brain. The intrinsic heterogeneity of prostate cancer cells, characterized by diverse genetic, molecular, and phenotypic profiles, complicates conventional therapeutic strategies, highlighting the need for advanced diagnostic and treatment modalities. Nanoparticles play a critical role in oncology field due to their unique physicochemical properties, including high surface area-to-volume ratio and the ability to be functionalized with targeting ligands. Metallic-based nanoparticles exhibits significant potential for applications in field of nanomedicine, drug delivery systems, gene silencing methods, radiotherapy enhancement, cancer diagnostics, and targeted therapeutic interventions. Metal nanoparticles have substantially improved the sensitivity and specificity of major imaging modalities and have demonstrated remarkable efficacy as biosensors for the detection of prostate cancer-specific biomarkers. This review article provides an in-depth analysis of the utilization of metal nanomaterials in prostate cancer, focusing on their roles in enhancing therapeutic efficacy, advancing diagnostic precision, and supporting the development of novel treatment strategies.

25COASMA65:

Title: Twice-Yearly Lenacapavir for HIV Prevention in Men and Gender-Diverse Persons

Colleen F. Kelley, M.D., M.P.H, Maribel Acevedo-Quiñones, M.D.,

N Engl J Med 2025; 392:1261-1276
https://doi.org/10.1056/NEJMoa2411858

Abstract: Twice-yearly subcutaneous lenacapavir has been shown to be efficacious for prevention of human immunodeficiency virus (HIV) infection in cisgender women. The efficacy of lenacapavir for preexposure prophylaxis (PrEP) in cisgender men, transgender women, transgender men, and gender-nonbinary persons is unclear. In this phase 3, double-blind, randomized, active-controlled trial, we randomly assigned participants in a 2:1 ratio to receive subcutaneous lenacapavir every 26 weeks or daily oral emtricitabine–tenofovir disoproxil fumarate (F/TDF). The primary efficacy analysis compared the incidence of HIV infection in the lenacapavir group with the background HIV incidence in the screened

population. The secondary efficacy analysis compared the incidence of HIV infection in the lenacapavir group with that in the F/TDF group. Among 3265 participants who were included in the modified intention-to-treat analysis, HIV infections occurred in 2 participants in the lenacapavir group (0.10 per 100 person-years; 95% confidence interval [CI], 0.01 to 0.37) and in 9 participants in the F/TDF group (0.93 per 100 person-years; 95% CI, 0.43 to 1.77). The background HIV incidence in the screened population (4634 participants) was 2.37 per 100 person-years (95% CI, 1.65 to 3.42). The incidence of HIV infection in the lenacapavir group was significantly lower than both the background incidence (incidence rate ratio, 0.04; 95% CI, 0.01 to 0.18; P<0.001) and the incidence in the F/TDF group (incidence rate ratio, 0.11; 95% CI, 0.02 to 0.51; P=0.002). No safety concerns were identified. A total of 26 of 2183 participants (1.2%) in the lenacapavir group and 3 of 1088 (0.3%) in the F/TDF group discontinued the trial regimen because of injection-site reactions. The HIV incidence with twice-yearly lenacapavir was significantly lower than the background incidence and the incidence with F/TDF.

25COASMA66:

Title: Left Atrial Appendage Closure after Ablation for Atrial Fibrillation

Oussama M. Wazni, M.D., Walid I. Saliba

N Engl J Med 2025; 392:1277-1287

https://doi.org/10.1056/NEJMoa2408308

Abstract: Oral anticoagulation is recommended after ablation for atrial fibrillation among patients at high risk for stroke. Left atrial appendage closure is a mechanical alternative to anticoagulation, but data regarding its use after atrial fibrillation ablation are lacking. We conducted an international randomized trial involving 1600 patients with atrial fibrillation who had an elevated score (≥2 in men and ≥3 in women) on the CHA_2DS_2-VASc scale (range, 0 to 9, with higher scores indicating a greater risk of stroke) and who underwent catheter ablation. Patients were randomly assigned in a 1:1 ratio to undergo left atrial appendage closure or receive oral anticoagulation. The primary safety end point, tested for superiority, was non–procedure-related major bleeding or clinically relevant nonmajor bleeding. The primary efficacy end point, tested for noninferiority, was a composite of death from any cause, stroke, or systemic embolism at 36 months. The secondary end point, tested for noninferiority, was major bleeding, including procedure-related bleeding, through 36 months.A total of 803 patients were assigned to undergo left atrial appendage closure, and 797 to receive anticoagulant therapy. The mean (±SD) age of the patients was 69.6±7.7 years, 34.1% of the patients were women, and the mean CHA_2DS_2-VASc score was 3.5±1.3. At 36 months, a primary safety end-point event had occurred in 65 patients (8.5%) in the left atrial appendage closure group (device group) and in 137 patients (18.1%) in the anticoagulation group (P<0.001 for superiority); a primary efficacy end-point event had occurred in 41 patients (5.3%) and 44 patients (5.8%), respectively (P<0.001 for noninferiority); and a secondary end-point event had occurred in 3.9% and 5.0% (P<0.001 for noninferiority). Complications related to the appendage closure device or procedure occurred in 23 patients.Among patients who underwent catheter-based atrial fibrillation ablation, left atrial appendage closure was associated with a lower risk of non–procedure-related major or clinically relevant nonmajor bleeding than oral anticoagulation and was noninferior to oral

anticoagulation with respect to a composite of death from any cause, stroke, or systemic embolism at 36 months.

25COASMA67:

Title: Alteplase for Posterior Circulation Ischemic Stroke at 4.5 to 24 Hours

Shenqiang Yan, M.D. Ying Zhou, Ph.D., Maarten G. Lansberg, M.D., Ph.D., David S. Liebeskind, M.D.,

N Engl J Med 2025; 392:1288-1296, VOL. 392 NO. 13
https://doi.org/10.1056/NEJMoa2413344

Abstract: The effects and risks of the use of intravenous thrombolysis between 4.5 and 24 hours after the onset of a posterior circulation ischemic stroke are not well studied. METHODS-In a trial conducted in China, we randomly assigned patients with posterior circulation stroke, without extensive early hypodensity on computed tomography and with no planned thrombectomy, to receive alteplase (0.9 mg per kilogram of body weight; maximum dose, 90 mg) or standard medical treatment 4.5 to 24 hours after the onset of symptoms. The primary outcome was functional independence (defined as a score of 0 to 2 on the modified Rankin scale; scores range from 0 to 6, with higher scores indicating greater disability) at 90 days. The key safety outcomes were symptomatic intracranial hemorrhage and death. RESULTS-A total of 234 patients were enrolled; 117 were assigned to the alteplase group and 117 to the standard treatment group. The median score on the National Institutes of Health Stroke Scale was 3 (interquartile range, 2 to 6) (scores range from 0 to 42, with higher scores indicating greater neurologic deficit). A higher percentage of patients in the alteplase group than in the standard treatment group had functional independence at 90 days (89.6% vs. 72.6%; adjusted risk ratio, 1.16; 95% confidence interval [CI], 1.03 to 1.30; P=0.01). The incidence of symptomatic intracranial hemorrhage within 36 hours was 1.7% in the alteplase group and 0.9% in the standard treatment group. At 90 days, 5.2% of the patients in the alteplase group and 8.5% of those in the standard treatment group had died.
CONCLUSIONS-Among Chinese patients with mainly mild posterior circulation stroke who did not receive thrombectomy, alteplase administered 4.5 to 24 hours after stroke onset resulted in a higher frequency of functional independence at 90 days than standard medical care.

25COASMA68:

Title: The Genetic Architecture of Congenital Diarrhea and Enteropathy

Zeenat Gaibee, M.D., Neil Warner, Ph.D., Katlynn Bugda Gwilt, Ph.D.,

N Engl J Med 2025;392:1297-1309, VOL. 392 NO. 13
https://doi.org/10.1056/NEJMoa2405333

Abstract: Next-generation sequencing has enabled precision therapeutic approaches that have improved the lives of children with rare diseases. Congenital diarrhea and enteropathies (CODEs) are associated with high morbidity and mortality. Although treatment of these disorders is largely supportive, emerging targeted therapies based on genetic diagnoses include specific diets, pharmacologic treatments, and surgical interventions. METHODS-We analyzed the exomes or genomes of infants with suspected monogenic congenital diarrheal disorders. Using cell and zebrafish models, we tested the effects of variants in newly

implicated genes. RESULTS-In our case series of 129 infant probands with suspected monogenic congenital diarrheal disorders, we identified causal variants, including a new founder NEUROG3 variant, in 62 infants (48%). Using cell and zebrafish models, we also uncovered and functionally characterized three novel genes associated with CODEs: GRWD1, MYO1A, and MON1A.CONCLUSIONS-We have characterized the broad genetic architecture of CODE disorders in a large case series of patients and identified three novel genes associated with CODEs.

25COASMA69:

Title: Association between Wealth and Mortality in the United States and Europe

Sara Machado, Ph.D. Ilias Kyriopoulos, Ph.D., E.John Orav, Ph.D.,and Irene Papanicolas, Ph.D.

N Engl J Med 2025;392:1310-1319, VOL. 392 NO. 13
https://doi.org/10.1056/NEJMsa2408259

Abstract: Amid growing wealth disparity, we have little information on how health among older Americans compares with that among older Europeans across the distribution of wealth. METHODS-We performed a longitudinal, retrospective cohort study involving adults 50 to 85 years of age who were included in the Health and Retirement Study and the Survey of Health, Ageing, and Retirement in Europe between 2010 and 2022. Wealth quartiles were defined according to age group and country, with quartile 1 comprising the poorest participants and quartile 4 the wealthiest. Mortality and Kaplan–Meier curves were estimated for each wealth quartile across the United States and 16 countries in northern and western, southern, and eastern Europe. We used Cox proportional-hazards models that included adjustment for baseline covariates (age group, sex, marital status [ever or never married], educational level [any or no college education], residence [rural or nonrural], current smoking status [smoking or nonsmoking], and absence or presence of a previously diagnosed long-term condition) to quantify the association between wealth quartile and all-cause mortality from 2010 through 2022 (the primary outcome). RESULTS-Among 73,838 adults (mean [±SD] age, 65±9.8 years), a total of 13,802 (18.7%) died during a median follow-up of 10 years. Across all participants, greater wealth was associated with lower mortality, with adjusted hazard ratios for death (quartile 2, 3, or 4 vs. quartile 1) of 0.80 (95% confidence interval [CI], 0.76 to 0.83), 0.68 (95% CI, 0.65 to 0.71), and 0.60 (95% CI, 0.57 to 0.63), respectively. The gap in survival between the top and bottom wealth quartiles was wider in the United States than in Europe. Survival among the participants in the top wealth quartiles in northern and western Europe and southern Europe appeared to be higher than that among the wealthiest Americans. Survival in the wealthiest U.S. quartile appeared to be similar to that in the poorest quartile in northern and western Europe. CONCLUSIONS-In cohort studies conducted in the United States and Europe, greater wealth was associated with lower mortality, and the association between wealth and mortality appeared to be more pronounced in the United States than in Europe.

25COASMA70:

Title: Extended Reduced-Dose Apixaban for Cancer-Associated Venous Thromboembolism

Isabelle Mahé, M.D., Ph.D. Marc Carrier, M.D
N Engl J Med 2025;392:1363-1373, VOL. 392 NO. 14
https://doi.org/0.1056/NEJMoa2416112
Abstract: In patients with active cancer and venous thromboembolism, whether extended treatment with a reduced dose of an oral anticoagulant is effective in preventing recurrent thromboembolic events and decreasing bleeding is unclear. METHODS-We conducted a randomized, double-blind, noninferiority trial with blinded central outcome adjudication. Consecutive patients with active cancer and proximal deep-vein thrombosis or pulmonary embolism who had completed at least 6 months of anticoagulant therapy were randomly assigned in a 1:1 ratio to receive oral apixaban at a reduced (2.5 mg) or full (5.0 mg) dose twice daily for 12 months. The primary outcome was centrally adjudicated fatal or nonfatal recurrent venous thromboembolism, assessed in a noninferiority analysis (margin of 2.00 for the upper boundary of the 95% confidence interval of the subhazard ratio). The key secondary outcome was clinically relevant bleeding, assessed in a superiority analysis. RESULTS-A total of 1766 patients underwent randomization at a median time since the index event of 8.0 months (interquartile range, 6.5 to 12.6); 866 patients were assigned to the reduced-dose group, and 900 to the full-dose group. The median treatment duration was 11.8 months (interquartile range, 8.3 to 12.1). Recurrent venous thromboembolism occurred in 18 patients (cumulative incidence, 2.1%) in the reduced-dose group and in 24 (cumulative incidence, 2.8%) in the full-dose group (adjusted subhazard ratio, 0.76; 95% confidence interval [CI], 0.41 to 1.41; P=0.001 for noninferiority). Clinically relevant bleeding occurred in 102 patients (cumulative incidence, 12.1%) in the reduced-dose group and in 136 (cumulative incidence, 15.6%) in the full-dose group (adjusted subhazard ratio, 0.75; 95% CI, 0.58 to 0.97; P=0.03). Mortality was 17.7% in the reduced-dose group and 19.6% in the full-dose group (adjusted hazard ratio, 0.96; 95% CI, 0.86 to 1.06). CONCLUSIONS-Extended anticoagulation with reduced-dose apixaban was noninferior to full-dose apixaban for the prevention of recurrent venous thromboembolism in patients with active cancer. The reduced dose led to a lower incidence of clinically relevant bleeding complications than the full dose.

25COASMA71:

Title: Endovascular Treatment for Stroke Due to Occlusion of Medium or Distal Vessels

Marios Psychogios, M.D. Alex Brehm, Ph.D., Marc Ribo, M.D.
N Engl J Med 2025;392:1374-1384
https://doi.org/10.1056/NEJMoa2408954
Abstract: Endovascular treatment (EVT) of stroke with large-vessel occlusion is known to be safe and effective. The effect of EVT for occlusion of medium or distal vessels is unclear. METHODS-We randomly assigned participants with an isolated occlusion of medium or distal vessels (occlusion of the nondominant or codominant M2 segment of the middle cerebral artery [MCA]; the M3 or M4 segment of the MCA; the A1, A2, or A3 segment of the anterior cerebral artery; or the P1, P2, or P3 segment of the posterior cerebral artery) to receive EVT plus best medical treatment or best medical treatment alone within 24 hours after the participant was last seen to be well. The primary outcome was the level of disability at 90 days, as assessed with the modified Rankin scale score. RESULTS-A total of 543

participants (women, 44%; median age, 77 years) were included in the analysis: 271 were assigned to receive EVT plus best medical treatment and 272 to receive best medical treatment alone. The median score on the National Institutes of Health Stroke Scale (range, 0 to 42, with higher scores indicating more severe symptoms) at admission was 6 (interquartile range, 5 to 9). Intravenous thrombolysis was given to 65.4% of the participants. The predominant occlusion locations were the M2 segment (in 44.0% of the participants), M3 segment (in 26.9%), P2 segment (in 13.4%), and P1 segment (in 5.5%). In the comparison between EVT plus best medical treatment and best medical treatment alone, no significant difference in the distribution of modified Rankin scale scores was observed at 90 days (common odds ratio for improvement in the score, 0.90; 95% confidence interval, 0.67 to 1.22; P=0.50). All-cause mortality was similar in the two groups (15.5% with EVT plus best medical treatment and 14.0% with best medical treatment alone), as was the incidence of symptomatic intracranial hemorrhage (5.9% and 2.6%, respectively). CONCLUSIONS-In persons with stroke with occlusion of medium or distal vessels, EVT did not result in a lower level of disability or a lower incidence of death than best medical treatment alone.

25COASMA72:

Title: Endovascular Treatment of Stroke Due to Medium-Vessel Occlusion

Mayank Goyal, M.D., Ph.D., Johanna M. Ospel, Ph.D., Aravind Ganesh, D.Phil.

N Engl J Med 2025;392:1385-1395
https://doi.org/10.1056/NEJMoa2411668

Abstract: Whether the large effect size of endovascular thrombectomy (EVT) for stroke due to large-vessel occlusion applies to stroke due to medium-vessel occlusion is unclear. METHODS- In a multicenter, prospective, randomized, open-label trial with blinded outcome evaluation, we assigned patients with acute ischemic stroke due to medium-vessel occlusion who presented within 12 hours from the time that they were last known to be well and who had favorable baseline noninvasive brain imaging to receive EVT plus usual care or usual care alone. The primary outcome was the modified Rankin scale score (range, 0 [no symptoms] to 6 [death]) at 90 days, reported as the percentage of patients with a score of 0 or 1. RESULTS-A total of 530 patients from five countries were enrolled between April 2022 and June 2024, with 255 patients assigned to the EVT group and 275 to the usual-care group. Most patients (84.7%) had primary occlusions in a middle-cerebral-artery branch. A modified Rankin scale score of 0 or 1 at 90 days occurred in 106 of 255 patients (41.6%) in the EVT group and in 118 of 274 (43.1%) in the usual-care group (adjusted rate ratio, 0.95; 95% confidence interval [CI], 0.79 to 1.15; P=0.61). Mortality at 90 days was 13.3% in the EVT group and 8.4% in the usual-care group (adjusted hazard ratio, 1.82; 95% CI, 1.06 to 3.12). Symptomatic intracranial hemorrhage occurred in 14 of 257 patients (5.4%) in the EVT group and in 6 of 272 (2.2%) in the usual-care group. CONCLUSIONS-Endovascular treatment for acute ischemic stroke due to medium-vessel occlusion within 12 hours did not lead to better outcomes at 90 days than usual care.

25COASMA73:

Title: Assessment of a Polygenic Risk Score in Screening for Prostate Cancer

Jana K. McHugh, F.F.R.C.S.I., Elizabeth K. Bancroft, Ph.D., Edward Saunders

N Engl J Med 2025;392:1406-1417, VOL. 392 NO. 14
https://doi.org/10.1056/NEJMoa2407934

Abstract: The incidence of prostate cancer is increasing. Screening with an assay of prostate-specific antigen (PSA) has a high rate for false positive results. Genomewide association studies have identified common germline variants in persons with prostate cancer, which can be used to calculate a polygenic risk score associated with risk of prostate cancer. METHODS- We recruited persons 55 to 69 years of age from primary care centers in the United Kingdom. Using germline DNA extracted from saliva, we derived polygenic risk scores from 130 variants known to be associated with an increased risk of prostate cancer. Participants with a polygenic risk score in the 90th percentile or higher were invited to undergo prostate cancer screening with multiparametric magnetic resonance imaging (MRI) and transperineal biopsy, irrespective of PSA level. RESULTS- Among 40,292 persons invited to participate, 8953 (22.2%) expressed interest in participating and 6393 had their polygenic risk score calculated; 745 (11.7%) had a polygenic risk score in the 90th percentile or higher and were invited to undergo screening. Of these 745 participants, 468 (62.8%) underwent MRI and prostate biopsy; prostate cancer was detected in 187 participants (40.0%). The median age at diagnosis was 64 years (range, 57 to 73). Of the 187 participants with cancer, 103 (55.1%) had prostate cancer classified as intermediate or higher risk according to the 2024 National Comprehensive Cancer Network (NCCN) criteria, so treatment was indicated; cancer would not have been detected in 74 (71.8%) of these participants according to the prostate cancer diagnostic pathway currently used in the United Kingdom (high PSA level and positive MRI results). In addition, 40 of the participants with cancer (21.4%) had disease classified as unfavorable intermediate risk or as high or very high risk according to NCCN criteria. CONCLUSIONS- In a prostate cancer screening program involving participants in the top decile of risk as determined by a polygenic risk score, the percentage found to have clinically significant disease was higher than the percentage that would have been identified with the use of PSA or MRI.

25COASMA74:

Title: Efficacy and Safety of Obinutuzumab in Active Lupus Nephritis

Richard A. Furie, M.D., Brad H. Rovin, M.D., Jay P. Garg, M.D

N Engl J Med 2025;392:1471-1483, VOL. 392 NO. 15
https://doi.org/10.1056/NEJMoa2410965

Abstract: Obinutuzumab, a humanized type II anti-CD20 monoclonal antibody, provided significantly better renal responses than placebo in a phase 2 trial involving patients with lupus nephritis receiving standard therapy. METHODS-In a phase 3, randomized, controlled trial, we assigned adults with biopsy-proven active lupus nephritis in a 1:1 ratio to receive obinutuzumab in one of two dose schedules (1000 mg on day 1 and at weeks 2, 24, 26, and 52, with or without a dose at week 50) or placebo. All patients received standard therapy with mycophenolate mofetil, along with oral prednisone at a target dose of 7.5 mg per day by week 12 and 5 mg per day by week 24. The primary end point was a complete renal response at week 76, defined by a urinary protein-to-creatinine ratio of less than 0.5 (with protein and creatinine both measured in milligrams), an estimated glomerular filtration rate of at least 85% of the baseline value, and no intercurrent event (i.e., rescue therapy, treatment failure,

death, or early trial withdrawal). Key secondary end points at week 76 included a complete renal response with a prednisone dose of 7.5 mg per day or lower between weeks 64 and 76 and a urinary protein-to-creatinine ratio lower than 0.8 without an intercurrent event. RESULTS- A total of 271 patients underwent randomization; 135 were assigned to the obinutuzumab group (combined dose schedules) and 136 to the placebo group. A complete renal response at week 76 was observed in 46.4% of the patients in the obinutuzumab group and 33.1% of those in the placebo group (adjusted difference, 13.4 percentage points; 95% confidence interval [CI], 2.0 to 24.8; P=0.02). A complete renal response at week 76 with a prednisone dose of 7.5 mg per day or lower between weeks 64 and 76 was observed in more patients in the obinutuzumab group than in the placebo group (42.7% vs. 30.9%; adjusted difference, 11.9 percentage points; 95% CI, 0.6 to 23.2; P=0.04), and a urinary protein-to-creatinine ratio lower than 0.8 without an intercurrent event was more common with obinutuzumab than with placebo (55.5% vs. 41.9%; adjusted difference, 13.7 percentage points; 95% CI, 2.0 to 25.4; P=0.02). No unexpected safety signals were identified. More serious adverse events, mainly infections and events related to coronavirus disease 2019, occurred with obinutuzumab than with placebo. CONCLUSIONS- Among adults with active lupus nephritis, obinutuzumab plus standard therapy was more efficacious than standard therapy alone in providing a complete renal response.

25COASMA75:

Title: Tecovirimat for Clade I MPXV Infection in the Democratic Republic of Congo

The PALM007 Writing Group

N Engl J Med 2025;392:1484-1496, VOL. 392 NO. 15
https://doi.org/10.1056/NEJMoa2412439

Abstract: Tecovirimat is available for the treatment of mpox (formerly known as monkeypox) in Europe and the United States, on the basis of findings from efficacy studies in animals and safety evaluations in healthy humans. Evidence from randomized, controlled trials of safety and efficacy in patients with mpox is lacking. METHODS- We conducted a double-blind, randomized, placebo-controlled trial of tecovirimat in patients with mpox in the Democratic Republic of Congo (DRC). Patients with at least one mpox skin lesion and positive polymerase-chain-reaction results for clade I MPXV were assigned in a 1:1 ratio to receive tecovirimat or placebo. All patients received supportive care. The primary end point was resolution of mpox lesions, measured in number of days after randomization. Safety was also assessed. RESULTS- From October 7, 2022, through July 9, 2024, a total of 597 patients underwent randomization — 295 to receive tecovirimat and 302 to receive placebo. The median time from randomization to lesion resolution was 7 days with tecovirimat and 8 days with placebo; the competing-risks hazard ratio for lesion resolution was 1.13 (95% confidence interval [CI], 0.97 to 1.31; P=0.14). Results were similar whether patients began the trial regimen within 7 days after the reported onset of symptoms (competing-risks hazard ratio, 1.16; 95% CI, 0.98 to 1.37) or more than 7 days after onset (competing-risks hazard ratio, 1.00; 95% CI, 0.71 to 1.40). Overall mortality was 1.7%, which was lower than the case fatality rate of 4.6% reported in the DRC in 2023. At 14 days, the percentages of patients who had blood, lesion, and oropharyngeal samples negative for MPXV by PCR were similar in the

two groups. Adverse events occurred in 72.9% of the patients in the tecovirimat group and 70.5% of those in the placebo group, and serious adverse events were reported in 5.1% and 5.0%, respectively. CONCLUSIONS -Tecovirimat did not reduce the number of days to lesion resolution in patients with mpox caused by clade I MPXV. No safety concerns were identified.

25COASMA76:

Title: Pulsed Field or Cryoballoon Ablation for Paroxysmal Atrial Fibrillation

Tobias Reichlin, M.D., Thomas Kueffer, Ph.D.

N Engl J Med 2025;392:1497-1507, VOL. 392 NO. 15

https://doi.org/10.1056/NEJMoa2502280

Abstract: Pulmonary-vein isolation is an effective treatment for paroxysmal atrial fibrillation. Pulsed field ablation (PFA) is a nonthermal ablation method with few adverse effects beyond the myocardium. Data are lacking on outcomes after PFA as compared with cryoballoon ablation as assessed with continuous rhythm monitoring. METHODS- In this randomized noninferiority trial in Switzerland, we randomly assigned patients with symptomatic paroxysmal atrial fibrillation in a 1:1 ratio to undergo PFA or cryoablation. All the patients received an implantable cardiac monitor to detect atrial tachyarrhythmias. The primary end point was the first recurrence of an atrial tachyarrhythmia between day 91 and day 365 after ablation. We assessed noninferiority using a margin of 20 percentage points for the difference in the cumulative incidence of recurrence. The safety end point was a composite of procedure-related complications. RESULTS- A total of 105 patients were assigned to undergo PFA, and 105 were assigned to undergo cryoablation. A recurrence of atrial tachyarrhythmia was observed between day 91 and day 365 in 39 patients in the PFA group and in 53 patients in the cryoablation group (Kaplan–Meier cumulative incidence, 37.1% and 50.7%, respectively; between-group difference, −13.6 percentage points; 95% confidence interval, −26.9 to −0.3; P<0.001 for noninferiority, P=0.046 for superiority). The safety end point occurred in 1 patient (1.0%) with PFA and in 2 patients (1.9%) with cryoablation. CONCLUSIONS- Among patients with symptomatic paroxysmal atrial fibrillation, PFA was noninferior to cryoballoon ablation with respect to the incidence of a first recurrence of atrial tachyarrhythmia, as assessed by continuous rhythm monitoring.

25COASMA77:

Titler: Fidanacogene Elaparvovec for Hemophilia B — A Multiyear Follow-up Study

John E.J. Rasko, M.B., B.S., Ph.D. , Benjamin J. Samelson-Jones, M.D., Ph.D., Lindsey A.

N Engl J Med 2025;392:1508-1517, VOL. 392 NO. 15

https://doi.org/10.1056/NEJMoa2307159

Abstract: Treatment with fidanacogene elaparvovec, a recombinant adeno-associated virus (AAV) vector developed for the treatment of hemophilia B, led to sustained expression of the high-activity factor IX variant (FIX-R338L, or FIX-Padua) in a phase 1–2a study. The long-term safety and efficacy of this treatment are not known. METHODS-In a 12-month study, 15 participants with severe or moderately severe hemophilia B (factor IX coagulant activity, ≤2% of the normal value) received fidanacogene elaparvovec at a dose of 5×10^{11} vector

genomes (vg) per kilogram of body weight; thereafter, participants could enroll in a 5-year follow-up study. Safety end points included adverse events and changes in laboratory measures. Efficacy end points included the annualized rate of treated bleeding events (annualized bleeding rate) and factor IX activity. RESULTS- A total of 14 participants provided consent and completed at least 3 years of follow-up (median, 5.5; range 3 to 6); participation was ongoing among 8 at the data cutoff. None of the participants reported treatment-related adverse events after year 1. Throughout follow-up, nine serious adverse events were noted in 4 participants; none were thrombotic or treatment-related. No factor IX inhibitors were detected. Throughout follow-up, mean factor IX activity was in the mild hemophilia range; the mean annualized bleeding rate was less than 1, and 10 participants had no treated bleeding episodes. Surveillance liver ultrasounds obtained from year 1 onward showed no evidence of cancer but showed steatosis in 4 participants who had weight gain and elevated aminotransferase levels (maximum alanine aminotransferase level, 77 U per liter). One participant with a history of hepatitis C, hepatitis B, human immunodeficiency virus infection, and an elevated body-mass index had progression of underlying advanced liver fibrosis. A total of 13 surgical procedures were performed in 8 participants; exogenous factor IX was administered for 10 procedures, and no associated unexpected bleeding complications occurred. CONCLUSIONS- Fidanacogene elaparvovec was associated with no or only low-grade adverse effects over a period of 3 to 6 years. Efficacy was maintained in the long term at 5×10^{11} vg per kilogram, one of the lowest intravenous doses of AAV used for any indication.

25COASMA78:

Title: Dapagliflozin in Patients Undergoing Transcatheter Aortic-Valve Implantation

Sergio Raposeiras-Roubin, M.D.,Ph.D., IgnacioJ. Amat-Santos, M.D.,Ph.D.,

N Engl J Med 2025;392:1396-1405, VOL. 392 NO. 14
https://doi.org/10.1056/NEJMoa2500366

Abstract: Sodium–glucose cotransporter 2 (SGLT2) inhibitors reduce the risk of heart-failure admission among high-risk patients. However, most patients with valvular heart disease, including those undergoing transcatheter aortic-valve implantation (TAVI), have been excluded from randomized trials. METHODS- We conducted this randomized, controlled trial in Spain to evaluate the efficacy of dapagliflozin (at a dose of 10 mg once daily) as compared with standard care alone in patients with aortic stenosis who were undergoing TAVI. All the patients had a history of heart failure plus at least one of the following: renal insufficiency, diabetes, or left ventricular systolic dysfunction. The primary outcome was a composite of death from any cause or worsening of heart failure, defined as hospitalization or an urgent visit, at 1 year of follow-up. RESULTS- A total of 620 patients were randomly assigned to receive dapagliflozin and 637 to receive standard care alone after TAVI; after exclusions, a total of 1222 patients were included in the primary analysis. A primary-outcome event occurred in 91 patients (15.0%) in the dapagliflozin group and in 124 patients (20.1%) in the standard-care group (hazard ratio, 0.72; 95% confidence interval [CI], 0.55 to 0.95; P=0.02). Death from any cause occurred in 47 patients (7.8%) in the dapagliflozin group and in 55 (8.9%) in the standard-care group (hazard ratio, 0.87; 95% CI,

0.59 to 1.28). Worsening of heart failure occurred in 9.4% and 14.4% of the patients, respectively (subhazard ratio, 0.63; 95% CI, 0.45 to 0.88). Genital infection and hypotension were significantly more common in the dapagliflozin group. CONCLUSIONS- Among older adults with aortic stenosis undergoing TAVI who were at high risk for heart-failure events, dapagliflozin resulted in a significantly lower incidence of death from any cause or worsening of heart failure than standard care alone.

25COASMA79:

Title: Pridopidine in Amyotrophic Lateral SclerosisThe HEALEY ALS Platform Trial

Writing Committee for the HEALEY ALS Platform Trial; for the HEALEY ALS Platform Trial Study Group

JAMA. 2025;333(13):1128-1137.
https://doi.org/10.1001/jama.2024.26429

Abstract: Importance Amyotrophic lateral sclerosis (ALS) is a fatal disease. The sigma-1 (σ1) receptor emerged as a target for intervention. Objective To determine the effects of pridopidine, a σ1-receptor agonist, in ALS. Design, Settings, and Participants Pridopidine was tested as a regimen of the HEALEY ALS Platform Trial, a phase 2/3, multicenter, randomized, double-blind, platform trial. The study was conducted at 54 sites in the US from January 2021 to July 2022 (final follow-up, July 14, 2022). A total of 163 participants with ALS were randomized to receive pridopidine or placebo. An additional 122 concurrently randomized participants were assigned to receive placebo in other regimens and included in the analyses. Interventions Eligible participants were randomized 3:1 to receive oral pridopidine 45 mg twice daily (n = 121) or matching oral placebo (n = 42) for a planned duration of 24 weeks. Main Outcomes and Measures The primary efficacy outcome was change from baseline through week 24 in ALS disease severity, analyzed using a bayesian shared parameter model, which has components for function (Revised Amyotrophic Lateral Sclerosis Functional Rating Scale [ALSFRS-R]) and survival that were linked through an integrated estimate of treatment-dependent disease slowing across these 2 components. This was denoted as the disease rate ratio (DRR), with DRR less than 1 indicating a slowing in disease progression on pridopidine relative to placebo. There were 5 key secondary end points: time to 2-point or greater reduction in ALSFRS-R total score among participants with bulbar dysfunction at baseline, rate of decline in slow vital capacity among participants with bulbar dysfunction at baseline, percentage of participants with no worsening in the ALSFRS-R bulbar domain score, time to 1-point or greater change in the ALSFRS-R bulbar domain score, and time to death or permanent assisted ventilation. Results Among 162 patients (mean age, 57.5 years; 35% female) who were randomized to receive the pridopidine regimen and included in the primary efficacy analysis, 136 (84%) completed the trial. In the primary analysis comparing pridopidine vs the combined placebo groups, there was no significant difference between pridopidine and placebo in the primary end point (DRR, 0.99 [95% credible interval, 0.80-1.21]; probability of DRR <1, 0.55) and no differences were seen in the components of ALSFRS-R or survival. There was no benefit of pridopidine on the secondary end points. In the safety dataset (pridopidine, n = 121; placebo, n = 163), the most common adverse events were falls (28.1% vs 29.3%, respectively) and muscular weakness (24.0% vs 31.7%, respectively).

Conclusions and Relevance In this 24-week study, pridopidine did not impact the progression of ALS.

25COASMA80:

Title:CNM-Au8 in Amyotrophic Lateral SclerosisThe HEALEY ALS Platform Trial

Writing Committee for the HEALEY ALS Platform Trial; for the HEALEY ALS Platform Trial Study Group

JAMA. 2025;333(13):1138-1149.
https://doi.org/10.1001/jama.2024.27643

Abstract: Importance Bioenergetic failure has been proposed as a driver of amyotrophic lateral sclerosis (ALS). CNM-Au8 is a suspension of gold nanocrystals that catalyzes the conversion of nicotinamide adenine dinucleotide hydride into NAD^+, resulting in an increase of cellular adenosine triphosphate production. Objective To determine the effects of CNM-Au8 on ALS disease progression. Design, Setting, and Participants CNM-Au8 was tested as a regimen of the HEALEY ALS Platform Trial, a phase 2/3, multicenter, randomized, double-blind platform trial. The study was conducted at 54 sites in the US from July 2020 to March 2022 (final follow-up, March 17, 2022). A total of 161 participants with ALS were randomized to receive CNM-Au8 (n = 120) or regimen-specific placebo (n = 41). Data from 123 concurrently randomized placebo participants in other regimens were combined for analyses. Interventions Eligible participants were randomized in a 3:3:2 ratio to receive CNM-Au8 60 mg daily (n = 61), CNM-Au8 30 mg daily (n = 59), or matching placebo (n = 41) for 24 weeks. Main Outcomes and Measures The primary efficacy outcome was change from baseline through week 24 in ALS disease severity measured by a bayesian shared parameter model of function (based on the Revised Amyotrophic Lateral Sclerosis Functional Rating Scale) and survival, which provided an estimate of the rate of disease progression measured by the disease rate ratio (DRR), with a DRR of less than 1 indicating treatment benefit. Secondary end points included a Combined Assessment of Function and Survival using a joint-rank test, rate of decline in slow vital capacity (percent predicted), and survival free of permanent assisted ventilation. Results Among 161 participants who were randomized within the CNM-Au8 regimen (mean age, 58.4 years; 61 [37.9%] female), 145 (90%) completed the trial. In the primary analysis comparing the combined CNM-Au8 dosage groups vs the combined placebo groups, the primary end point (DRR, 0.97 [95% credible interval, 0.783-1.175]; posterior probability of DRR <1, 0.65) and the 3 secondary end points suggested no benefit or harm of CNM-Au8. In the active (n = 120) vs placebo (n = 163) groups, the most common adverse events were diarrhea (23 [19%] vs 12 [7%]), nausea (17 [14.2%] vs 14 [8.6%]), fatigue (12 [10.8%] vs 30 [18.4%]), and muscular weakness (24 [20%] vs 45 [27.6%]). Conclusions and Relevance No benefit of CNM-Au8 on ALS disease progression was observed at 24 weeks.

25COASMA81:

Title: Adjuvant Atezolizumab for Early Triple-Negative Breast CancerThe ALEXANDRA/IMpassion030 Randomized Clinical Trial

Michail Ignatiadis, MD[1]; Andrew Bailey, MSc[2]; Heather McArthur, MD

JAMA. 2025;333(13):1150-1160.

https://doi.org/10.1001/jama.2024.26886

Abstract: Importance Triple-negative breast cancer is an aggressive subtype with a high incidence in young patients, a high incidence in non-Hispanic Black women, and a high risk of progression to metastatic cancer, a devastating sequela with a 12- to 18-month life expectancy. Until recently, one strategy for treating early-stage triple-negative breast cancer was chemotherapy after surgery. However, it was not known whether the addition of immune therapy to postsurgery chemotherapy would be beneficial. Objective To evaluate the addition of immune therapy in the form of atezolizumab to postoperative chemotherapy in patients with the high-risk triple-negative breast cancer subtype. Design, Setting, and Participants In this open-label international randomized phase 3 trial conducted in more than 330 centers in 31 countries, patients undergoing surgery as initial treatment for stage II or III triple-negative breast cancer were enrolled between August 2, 2018, and November 11, 2022. The last patient follow-up was on August 18, 2023. Interventions Patients were randomized (1:1) to receive standard chemotherapy for 20 weeks with (n = 1101) or without (n = 1098) the immune therapy drug atezolizumab for up to 1 year. Main Outcomes and Measures The primary end point was invasive disease-free survival (time between randomization and invasive breast cancer in the same or opposite breast, recurrence elsewhere in the body, or death from any cause). Results The median age of enrolled patients was 53 years and most self-reported as being of Asian or White race and neither Latino nor Hispanic ethnicity. The study independent data monitoring committee halted enrollment at 2199 of 2300 planned patients. All patients stopped atezolizumab following a planned early interim and futility analysis. The trial continued to a premature final analysis. With invasive disease-free survival events in 141 patients (12.8%) treated with atezolizumab-chemotherapy and 125 (11.4%) with chemotherapy alone (median follow-up, 32 months), the final stratified invasive disease-free survival hazard ratio was 1.11 (95% CI, 0.87-1.42; P = .38). Compared with chemotherapy alone, the regimen of atezolizumab plus chemotherapy was associated with more treatment-related grade 3 or 4 adverse events (54% vs 44%) but similar incidences of fatal adverse events (0.8% vs 0.6%) and adverse events leading to chemotherapy discontinuation. Chemotherapy exposure was similar in the 2 treatment groups. Conclusions and Relevance The addition of the immune therapy drug atezolizumab to chemotherapy after surgery did not provide benefit among patients with triple-negative breast cancer who are at high risk of recurrent disease.

25COASMA82:

Title: Evaluation of a Clinical Decision Support System for Imaging RequestsA Cluster Randomized Clinical Trial

Stijntje W. Dijk, MD, MSc[1,2,3,4]; Claudia Wollny, DrRerNat[5]; Joerg Barkhausen, MD[6]

JAMA. 2025;333(14):1212-1221.
https://doi.org/10.1001/jama.2024.27853

Abstract: Importance Given the widespread use of medical imaging, evaluating the effectiveness of interventions to improve appropriateness is crucial for optimizing health care resources and patient outcomes. Objective To assess the effects of implementing a clinical decision support system (CDSS), the European Society of Radiology iGuide, on the appropriateness of the medical imaging ordering behavior of physicians. Design and

Setting A cluster randomized clinical trial with 26 departments at 3 German university hospitals acting as clusters, incorporating a before and after discontinued design. All imaging requests originating from physicians in the participating departments over a 2.5-year period were included (between December 2021 and June 2024). Interventions All departments started without a CDSS and required structured clinical indication data entry and tracking of requested imaging. After randomization, 13 clusters (departments at hospitals) received the CDSS intervention (intervention clusters) and 13 clusters did not (control clusters). The CDSS intervention provided ordering physicians with information as to whether their imaging requests were appropriate, appropriate under certain conditions, or inappropriate; in addition, alternative diagnostic tests, including the corresponding appropriateness score, were suggested by the CDSS, after which physicians could choose to modify their imaging requests. Main Outcomes and Measures The primary outcome measure was the proportion of inappropriate imaging requests made per department. A difference-in-differences analysis was used to investigate changes in the proportion of inappropriate imaging requests between departments with vs those without the CDSS. Results A total of 65 764 imaging requests were scored using the CDSS; 50.1% of imaging requests were for female patients and the mean patient age was 64 years (SD, 17.1 years). Prior to implementation of the CDSS, there were 21 625 imaging requests from the control clusters, 1367 (6.3%) of which were categorized as inappropriate; and there were 13 338 imaging requests from the intervention clusters, 1007 (7.6%) of which were categorized as inappropriate. After implementation of the CDSS, there were 10 055 imaging requests from the control clusters, 518 (5.2%) of which were categorized as inappropriate; and there were 7206 imaging requests from the intervention clusters, 461 (6.4%) of which were categorized as inappropriate. The intervention clusters showed a similar reduction (mean difference, −0.5% [99% CI, −2.4% to 0.4%]) in inappropriate imaging requests compared with the control clusters (mean difference, −1.8% [99% CI, −4.3% to −0.4%]) and there was a difference-in-differences value of 1.3 percentage points (99% CI, −2.0 to 1.8 percentage points; P = .69), which was not statistically significant. Conclusions and Relevance The CDSS did not reduce the number of inappropriate imaging requests ordered by physicians in academic hospital settings.

25COASMA83:

Title: Illicit Substance Use and Treatment Access Among Adults Experiencing Homelessness

Ryan D. Assaf, PhD, MPH[1,2]; Meghan D. Morris, PhD, MPH[1,3]; Elana R. Straus, BA[4];

JAMA. 2025;333(14):1222-1231.
https://doi.org/10.1001/jama.2024.27922

Abstract: Importance The lack of representative research on homelessness risks mischaracterizing and misrepresenting the prevalence of illicit substance use.

Objective To estimate the population prevalence and patterns of illicit substance use, treatment, nonfatal overdose, and naloxone possession among people experiencing homelessness in 1 US state. Design, Setting, and Participants This representative survey study of adults experiencing homelessness from October 2021 to November 2022 in 8 California counties used multistaged probability-based sampling and respondent-driven

sampling. Eligible individuals were 18 years or older and met the federal definition of homelessness. Main Outcomes and Measures The primary outcome measures included lifetime and past–6-month illicit substance use and substance type (methamphetamine, nonprescription opioids, or cocaine). Lifetime and current substance use treatment, unmet treatment need, types of treatments received, nonfatal overdose (lifetime and current episode of homelessness), and current possession of naloxone were measured. Population prevalence estimates with 95% Wald CIs were calculated using survey replicate weights. Results Of 3865 individuals approached, 3042 (79%) participated and an additional 158 participants were recruited through respondent-driven sampling. Among 3200 participants, the mean age was 46.1 (95% CI, 45.3-46.9) years, 67.3% (95% CI, 65.2%-69.3%) were cisgender male, and there were similar proportions of Black and African American, Hispanic and Latine, and White participants. Overall, an estimated 65.3% (95% CI, 62.2%-68.4%) of participants used illicit drugs regularly (≥3 times per week) in their lifetime; 41.6% (95% CI, 39.4%-43.8%) began using regularly before their first episode of homelessness and 23.2% (95% CI, 20.5%-25.9%) began using regularly after. In the past 6 months, an estimated 37.1% (95% CI, 32.9%-41.3%) of participants reported regular use of any drug; 33.1% (95% CI, 29.4%-36.7%) reported use of methamphetamines, 10.4% (95% CI, 7.9%-12.9%) reported use of opioids, and 3.2% (95% CI, 1.8%-4.6%) reported use of cocaine. In their lifetime, an estimated 25.6% (95% CI, 22.8%-28.3%) injected drugs and 11.8% (95% CI, 9.8%-13.8%) injected drugs in the past 6 months. Among those with any regular lifetime use, an estimated 6.7% (95% CI, 3.8%-9.5%) of participants were currently receiving treatment. Of those with any regular use in the last 6 months, an estimated 21.2% (95% CI, 17.9%-24.5%) reported currently wanting but not receiving treatment. An estimated 19.6% (95% CI, 17.4%-21.8%) of participants had a nonfatal overdose in their lifetime and 24.9% (95% CI, 21.3%-28.5%) currently possessed naloxone. Conclusion and Relevance In a representative study of adults experiencing homelessness in California, there was a high proportion of current drug use, history of overdose, and unmet need for treatment. Improving access to treatment tailored to the needs of people experiencing homelessness could improve outcomes

25COASMA84:

Title: Emergency Clinician Buprenorphine Initiation, Subsequent Prescriptions, and Continuous Prescriptions

Annette M. Dekker, MD, MS[1]; David L. Schriger, MD, MPH[1,2]; Andrew A. Herring, MD

JAMA. 2025;333(14):1232-1241.
https://doi.org/10.1001/jama.2024.27976

Abstract: Importance Rates of opioid use disorder (OUD) and associated mortality in the US remain high. Treatment of OUD with buprenorphine reduces morbidity and mortality. There have been national efforts to expand buprenorphine initiation to the emergency department (ED), where many patients with low treatment access seek medical care. Adoption and trends of emergency clinician buprenorphine prescribing are unknown.

Objective To describe emergency clinician buprenorphine initiation for OUD, subsequent prescriptions, and changes over time in California. Design, Setting, and Participants Observational retrospective study of buprenorphine prescriptions in the California Controlled Substance Utilization Review and Evaluation System (CURES)

database from January 1, 2017, to December 31, 2022. Any patient aged 18 to 79 years with a California zip code who filled a buprenorphine prescription in CURES and their California prescribers were eligible for inclusion. Exposure Buprenorphine prescription by an emergency clinician. Main Outcomes and Measures Outcomes included (1) the number of patients prescribed buprenorphine; (2) the number of clinicians prescribing buprenorphine; (3) the number and characteristics of buprenorphine prescriptions; (4) the percentage of emergency clinician buprenorphine initiation prescriptions with subsequent linkage to a second prescription and continuous prescriptions, also reported as a continuation ratio; and (5) days and number of initiation prescriptions prior to continuous prescriptions. Results In this retrospective observational study, 345 024 patients received 3.8 million buprenorphine prescriptions from 21 099 clinicians in California from 2017 to 2022. The mean age of patients at the time of first buprenorphine prescription was 37 years; 8187 (67%) were male. Emergency clinicians increased from 2% (n = 78) to 16% (n = 1789) of buprenorphine prescribers in 2017 and 2022, respectively (P < .001). Buprenorphine initiation prescriptions by emergency clinicians increased from 0.1% (n = 53) to 5% (n = 4493) of all initiation prescriptions in 2017 and 2022, respectively (P = .001). The continuation ratio for patients to receive a second prescription within 40 days of an ED initiation was 2.8 (10 823/3916). The continuation ratio for patients to start 180 days or more of continuous prescriptions within 40 days of ED buprenorphine initiation was 18.3 (10 823/593) and 9.1 within 1 year (5989/655 [2017-2021 data]). Conclusions and Relevance These findings suggest increasing prescription of buprenorphine for OUD by California emergency clinicians from 2017 to 2022, with approximately 1 in 9 patients going on to receive continuous buprenorphine prescriptions within 1 year.

25COASMA85:

Title: Total testosterone, sex hormone-binding globulin, and free testosterone concentrations and risk of primary liver cancer: A prospective analysis of 200,000 men and 180,000 postmenopausal women

Cody Z. Watling, Rebecca K. Kelly, Eleanor L. Watts, Barry I

International Journal of Cancer, Volume156, Issue8

https://doi.org/10.1002/ijc.35244

Abstract: In most countries, males have ~2–3 times higher incidence of primary liver cancer than females. Sex hormones have been hypothesized to contribute to these differences, but the evidence remains unclear. Using data from the UK Biobank, which included ~200,000 males and ~180,000 postmenopausal females who provided blood samples at recruitment, we estimated hazard ratios (HR_2) and 95% confidence intervals (CI) for a doubling in hormone concentration from multivariable adjusted Cox regression for circulating total testosterone, sex-hormone binding globulin (SHBG), and free testosterone concentrations and risk of primary liver cancer. After a median of 11.8 years of follow-up, 531 cases of primary liver cancer were observed, of which 366 occurred in males and 165 occurred in females. Total testosterone and SHBG were shown to be positively associated with liver cancer risk in both males and females (Total testosterone HR_2: 3.42, 95% CI:2.42–4.84 and 1.29, 0.97–1.72, respectively; SHBG HR_2: 5.44, 4.42–6.68 and 1.52, 1.09–2.12, respectively). However, free testosterone was inversely associated with primary liver cancer in males (HR_2: 0.42, 0.32–

0.55) and no association was observed in females. When analyses compared two main liver cancer subtypes, hepatocellular carcinoma (HCC) and intrahepatic cholangiocarcinoma (ICC), there was evidence of heterogeneity; associations for total testosterone and SHBG concentrations were only positively associated with HCC in both males (HR_2: 3.56, 2.65–4.79 and 7.72, 6.12–9.73, respectively) and females (HR_2: 1.65, 1.20–2.27 and 6.74, 3.93–11.5, respectively) but not with ICC. Further research understanding the mechanisms of how sex-steroids may influence liver cancer risk is needed.

25COASMA86:

Title: Smoking behavior and the risks of tumor recurrence and progression in patients with non-muscle-invasive bladder cancer

Joann Kiebach, Ivy Beeren, Katja K. H. Aben, J. Alfred Witjes

International Journal of Cancer, Volume156, Issue8

https://doi.org/10.1002/ijc.35250

Abstract: Studies on the relationship of cigarette smoking with the risks of recurrence and progression of non-muscle-invasive bladder cancer (NMIBC) are inconsistent and prospective data are scarce. Therefore, we aimed to assess the association of smoking behavior with risks of NMIBC recurrence and progression. We used data of the prospective multi-center cohort study UroLife, including 1495 patients with NMIBC who reported information on smoking at 6 weeks post-diagnosis (baseline; reflecting present and pre-diagnosis). This included smoking status (also based on reporting 3 months post-diagnosis), intensity, duration, pack years, and time since smoking cessation, if applicable. Hazard ratios and 95% confidence intervals (CIs) for risks of first recurrence, multiple recurrences, and progression were computed using multivariable proportional hazards regression models. During a total median follow-up period of 4.6 years, 517 patients developed ≥1 recurrence and 163 had progression. Higher versus lowest categories of smoking intensities and pack years up to baseline were significantly associated with a higher risk of first recurrence. No significant linear associations were found, except for smoking intensity among BCG-treated patients (per 10 cigarettes/day increase: HR 1.23, 95%CI 1.02, 1.48). No associations for smoking status, duration, and time since cessation were observed. Analyses of multiple recurrence risk showed comparable results. Regarding progression risk, no consistent associations were found. In conclusion, heavier smoking was associated with higher recurrence risk, particularly among BCG-treated patients. This may be attributable to persistent damage through its carcinogenic compounds. Given the mixed results across different exposures, the effect of smoking behavior on NMIBC prognosis remains unclear.

25COASMA87:

Title: Fertility treatment and risk of ovarian cancer in a large nationwide cohort of infertile Danish women

Allan Jensen, Sonia Guleria, Vanna Albieri, Bugge Nøhr,

International Journal of Cancer, Volume156, Issue8

https://doi.org/10.1002/ijc.35251

Abstract: Whether fertility treatment increases the risk of ovarian cancer has been a concern for many decades, but previous research has yielded conflicting findings. We therefore

investigated this association within a large population-based cohort study of infertile women aged 20–45 years and living in Denmark between 1995 and 2017, as identified in the Danish Infertility Cohort (n = 146,110). The study cohort was linked to nationwide registers to obtain information on fertility drug use, cancer diagnoses, covariates, emigration, and vital status was. Hazard ratios (HR) and 95% confidence intervals (CI) with adjustment for potential confounders for ovarian cancer overall and for serous ovarian cancer were estimated using Cox proportional hazard models. During a median 10.3 years of follow-up, 114 women were diagnosed with ovarian cancer of which 65 had serous ovarian cancer. Our results showed that the rate of serous ovarian cancer (HR 1.92; 95% CI 1.16–3.17) was increased after every use of progesterone but the association was not affected by increased follow-up time since first use or with increased cumulative dose. We performed a secondary analysis adding less extensive data from 1971 through 1994 from the Danish Infertility Cohort. In this study cohort, 332 women developed ovarian cancer of which 192 had serous ovarian cancer. The overall results were similar, including the association between every use of progesterone and serous ovarian cancer (HR 2.05: 95% CI: 1.31–3.21). In conclusion, the novel finding that use of progesterone is associated with an increased rate of serous ovarian cancer warrants further investigation.

25COASMA88:

Title: Environmental tobacco smoking (ETS) and esophageal cancer: A population-based case-control study in Jiangsu Province, China

Zi-Yi Jin, Kuangyu Liu, Gina Wallar, Jin-Yi Zhou, Li-Na Mu, Xing Liu, Li-Ming Li, Na

International Journal of Cancer, Volume156, Issue8

https://doi.org/10.1002/ijc.35254

Abstract: Esophageal cancer continues to pose a significant public health issue in areas with increased incidence rates such as China. Although involuntary smoking was defined as a group 1 carcinogen for lung cancer, few studies have explored the impact of environmental tobacco smoking (ETS) on esophageal cancer. In this paper, we examined the association between ETS and esophageal cancer in high-risk groups in Jiangsu Province, China. Epidemiologic data were collected for 2969 newly diagnosed cases and 8019 population controls including exposure to active/passive smoking and risk factors. The unconditional logistic regression model and the semi-Bayes (SB) method were applied to assess adjusted odds ratios (ORs) and confidence intervals (CIs). ETS exposure (ever vs. never) was positively associated with esophageal cancer with an SB-adjusted OR (95% CI) of 1.44 (1.31–1.58) among overall population, and 1.56 (1.35–1.82) among non-smokers (i.e., non-active smokers), with corresponding population attributable fractions of 15.0% (95% CI: 10.3%–18.9%) and 12.1% (95% CI: 8.8%–19.8%), respectively. The association was more prominent in men at work and in women at home, with SB-adjusted OR (95% CI) of 1.36 (1.17–1.58) and 1.61 (1.35–1.58), respectively. A dose–response relationship between ETS exposure and the disease was detected across the entire population as well as in non-smokers. This is the largest population-based case–control study of ETS and esophageal cancer and the first study to evaluate such association among non-smokers in a Chinese population. We recommend strengthening the ongoing anti-tobacco public health initiatives in China with a particular emphasis on creating a tobacco-free work/home environment.

25COASMA89:

Title: Disparities in childhood leukemia survival for Asian, Native Hawaiian, and Pacific Islanders in the United States

Mia Hashibe, Kimberly A. Herget, Joshua D. Schiffman, Vivian Y. Chang

International Journal of Cancer, Volume156, Issue8

https://doi.org/10.1002/ijc.35259

Abstract: While some previous studies disaggregated the Asian, Native Hawaiian, and Pacific Islander (ANHPI) population to investigate survival for childhood leukemia, further studies are needed to understand the differences between subpopulations. The aim of our study was to estimate 5-year relative survival for patients with childhood leukemia and to investigate disparities in prognostic factors with disaggregation of the ANHPI population. We used the Surveillance, Epidemiology, and End Results Program 17 database and included 1881 ANHPI patients with childhood leukemia and 8772 non-Hispanic White (NHW) patients with childhood leukemia. The Cox proportional hazards model was used to estimate hazard ratios for the risk of death. We observed lower 5-year relative survival rates for Southeast Asian and East Asian compared to NHW patients with childhood leukemia for acute lymphoid leukemia (ALL). The survival rates were higher for patients diagnosed at 1–9 years of age, more recent years of diagnosis, and patients residing in urban areas. The risk of death was 42% higher for East Asian patients and 50% higher for Southeast Asian patients compared to NHW patients for childhood ALL. For prognostic factors among East Asian patients with childhood leukemia, higher risks of death were observed for patients diagnosed at <12 months old and for acute myeloid leukemia compared to ALL. Further studies are needed to elucidate the reasons behind the disparities in survival rates for Southeast Asian and East Asian patients with childhood leukemia, including socioeconomic and genetic contributions to leukemia risk and clinical responses to different therapeutic modalities.

25COASMA90:

Title: Comprehensive characterization of MCL-1 in patients with colorectal cancer: Expression, molecular profiles, and outcomes

Pooja Mittal, Francesca Battaglin, Yasmine Baca,

International Journal of Cancer, Volume156, Issue8

https://doi.org/10.1002/ijc.35304

Abstract: Myeloid cell leukemia 1 (MCL-1) is a member of the B-cell lymphoma 2 protein family and has anti-apoptotic functions. Deregulation of MCL-1 has been reported in several cancers, including lung and breast cancer. In the present study, the association of MCL-1 expression with molecular features in colorectal cancer (CRC) has been highlighted. CRC samples from Caris Life Sciences (Phoenix, AZ) were analyzed using NextGen DNA sequencing, whole transcriptome sequencing, whole exome sequencing, and immunohistochemistry (IHC); and stratified based on MCL-1 expression as top quartile MCL-1^{high} (Q4) and bottom quartile MCL-1^{low} (Q1). Immune cell infiltration (CI) in the tumor microenvironment (TME) was measured using RNA deconvolution analysis (QuanTIseq). MCL-1^{high} tumors were associated with an increased rate of programmed death ligand 1 IHC, higher T cell-inflamed signature, interferon score, microsatellite instability-high and tumor mutational burden-high status. MCL-1^{high} was associated with higher

mutation rates of BCOR, TP53, KMT2D, ASXL1, KDM6A, ATM, MSH6, SPEN, KRAS, STK11, GNAS, RNF43, and lower mutation rates of CDKN1B, NRAS, and APC, and copy number amplifications in several genes. MCL-1^{high} TME had higher CI of M1 and M2 macrophages, B cells, natural killer cells, neutrophils, and T-regulatory cells infiltration, and lower CI of myeloid dendritic cells. Higher MCL-1 expression is significantly associated with favorable clinical outcomes in CRC cohorts. Our data showed a strong correlation between MCL-1 and distinct immune biomarkers and TME CI in CRC. Our findings suggest MCL-1 is a potential modulator of antitumor immunity, TME, and biomarker in CRC.

25COASMA91:

Title: Participation and relative cost of attendance by direct-mail compared to opt-in invitation strategy for HPV self-sampling targeting cervical screening non-attenders: A large-scale, randomized, pragmatic study

Birgitte Tønnes Pedersen, Si Brask Sonne,

International Journal of Cancer, Volume156, Issue8

https://doi.org/10.1002/ijc.35263

Abstract: Broad accessibility to cervical cancer screening and high participation rate is essential to reduce cervical cancer incidence. HPV self-sampling is an alternative to clinician collected cervical samples to increase accessibility and screening coverage. To inform on deployment strategies of HPV self-sampling, this large-scale, randomized, pragmatic study compared two invitation modalities; direct-mail and opt-in. The study included screening non-attenders from the Capital Region of Denmark randomly allocated (1:4) to a direct-mail or opt-in invitation for cervical screening by HPV self-sampling. Primary endpoint was screening participation; secondary endpoints were HPV prevalence and histology outcome. Adherence to follow-up and cost were also evaluated. After exclusion of hysterectomized/non-accessible women, 49,393 women were invited: 9639 by direct-mail, and 39,754 by the opt-in offer. A direct-mail invitation for HPV self-sampling yielded a significant higher participation than an opt-in invitation. HPV self-sample participation for direct-mail was 25.2% (n = 2426), opt-in participation was 20.2% (n = 8047), adjusted OR = 1.27, 95% CI 1.20–1.34. Participation increased with age ($p < .0001$) for both strategies and decreased with screening history of non-attendance ($p < .0001$). Interaction between invitation strategy and age/screening history was found; more women below 50 years of age participated by direct-mail compared to opt-in ($p < .0001$) and higher participation by direct-mail group was found in women with a short history of non-attendance ($p < .0001$). Participation of long-term unscreened women was similar between arms. The relative cost was ≈14 HPV self-sample kits distributed per additional participant by direct-mail over opt-in. HPV prevalence, adherence to follow-up, and detection of high-grade cervical intraepithelial neoplasia was similar between invitation strategies.

25COASMA92:

Title: Prognostic and predictive implications of sterile alpha motif and HD domain-containing protein 1 (SAMHD1) expression in breast cancer

Maria Kouvaraki, Ioannis Zerdes, Emmanouil G. Sifakis, Michail Sarafidis,

International Journal of Cancer, Volume156, Issue8

https://doi.org/10.1002/ijc.35319

Abstract: Sterile alpha motif and HD domain-containing protein 1 (SAMHD1) is a dNTP hydrolase important for intracellular dNTP homeostasis and serves as tumor suppressor and modulator of antimetabolite efficacy in cancer, though largely unexplored in breast cancer (BC). A cohort of patients with early BC (n = 564) with available gene expression data (GEP) was used. SAMHD1 protein expression was assessed by immunohistochemistry performed on tissue microarrays. A large pooled transcriptomic dataset was used for validation (n = 2402). GEP data from the metastatic TEX randomized phase III trial (NCT01433614) were used for SAMHD1 predictive evaluation in response to capecitabine. SAMHD1 protein and mRNA levels were higher in HER2-enriched/HER2+ and basal-like (BL)/ER-/HER2- BC. Both SAMHD1 gene and protein expression were independently associated with favorable outcomes in BL tumors. In the pooled dataset, SAMHD1 gene expression was independently associated with favorable disease-free survival in the entire population and within the BL and HER2-enriched molecular subtypes. In metastatic BC, SAMHD1 mRNA levels were higher in responders receiving capecitabine. In conclusion SAMHD1 gene and protein expression represent promising prognostic biomarkers in BL early BC.

25COASMA93:

Title: Tissue-matched analysis of MRI evaluating the tumor infiltrating lymphocytes in hepatocellular carcinoma

Mengqi Huang, Chenyu Song, Xiaoqi Zhou,

International Journal of Cancer, Volume156, Issue8

https://doi.org/10.1002/ijc.35281

Abstract: Tumor-infiltrating lymphocytes (TILs) play critical roles in the tumor microenvironment and immunotherapy response. This study aims to explore the feasibility of multi-parametric magnetic resonance imaging (MRI) in evaluating TILs and to develop an evaluation model that considers spatial heterogeneity. Multi-parametric MRI was performed on hepatocellular carcinoma (HCC) mice (N = 28). Three-dimensional (3D) printing was employed for tissue sampling, to match the multi-parametric MRI data with tumor tissues, followed by flow cytometry analysis and next-generation RNA-sequencing. Pearson's correlation, multivariate logistic regression, and receiver operating characteristic (ROC) curve analyses were utilized to model TIL-related MRI parameters. MRI quantitative parameters, including T1 relaxation times and perfusion, were correlated with the infiltration of leukocytes, T-cells, CD4+ T-cells, CD8+ T-cells, PD1 + CD8+ T-cells, B-cells, macrophages, and regulatory T-cells (correlation coefficients ranged from −0.656 to 0.482, $p < .05$) in tumor tissues. TILs were clustered into inflamed and non-inflamed subclasses, with the proportion of T-cells, CD8+ T-cells, and PD1 + CD8+ T-cells significantly higher in the inflamed group compared to the non-inflamed group (43.37% vs. 25.45%, 50.83% vs. 34.90%, 40.45% vs. 29.47%, respectively; $p < .001$). The TIL evaluation model, based on the Z-score combining Kep and T1post, was able to distinguish between these subgroups, yielding an area under the curve of 0.816 (95% confidence interval 0.721–0.910) and a cut-off value of −0.03 (sensitivity 68.4%, specificity 91.3%). Additionally, the Z-score was related to the gene expression of T-cell activation, chemokine production, and

cell adhesion. The tissue-matched analysis of multi-parametric MRI offers a feasible method of regional evaluation and can distinguish between TIL subclasses.

25COASMA94:

Title: NMR-based metabolomics combined with metabolic pathway analysis reveals metabolic heterogeneity of colorectal cancer tissue at different anatomical locations and stages

Rongzhi Cai, LiXin Ke, Yan Zhao, Jiayun Zhao,

International Journal of Cancer, Volume156, Issue8

https://doi.org/10.1002/ijc.35273

Abstract: Colorectal cancer (CRC) still remains the leading cause of cancer death worldwide. This study aimed to profile the metabolic differences of colorectal cancer tissues (CCT) at different stages and sites, as compared with their distant noncancerous tissues (DNT), to investigate the temporal and spatial heterogeneities of metabolic characterization. Our NMR-based metabolomics fingerprinting revealed that many of the metabolite levels were significantly altered in CCT compared to DNT and esophageal cancer tissues, indicating deregulations of glucose metabolism, one-carbon metabolism, glutamine metabolism, amino acid metabolism, fatty acid metabolism, TCA cycle, choline metabolism, and so forth. A total of five biomarker metabolites, including glucose, glutamate, alanine, valine and histidine, were identified to distinguish between early and advanced stages of CCT. Metabolites that distinguish the different anatomical sites of CCT include glucose, glycerol, glutamine, inositol, succinate, and citrate. Those significant metabolic differences in CRC tissues at different pathological stages and sites suggested temporal and spatial heterogeneities of metabolic characterization in CCT, providing a metabolic foundation for further study on biofluid metabolism in CRC early detection.

25COASMA95:

Title: Impact of circulating tumor human papillomavirus DNA kinetics on disease outcomes in HPV-associated oropharyngeal cancer

Sachin R. Jhawar, Catherine Haring,

International Journal of Cancer,Volume156, Issue8

https://doi.org/10.1002/ijc.35291

Abstract: Circulating tumor tissue modified (TTMV)-HPV DNA has emerged as a promising biomarker in human papillomavirus associated oropharyngeal squamous cell carcinoma (HPV-OPSCC). The objective of this study was to assess ctHPVDNA TTMV clearance kinetics during RT and its relationship with progression in HPV-OPSCC. We identified 80 non-metastatic HPV-OPSCC patients with 366 TTMV samples who underwent prospective plasma TTMV testing before, during and after curative intent RT or CRT between June 2021 and February 2023. Patients with rapid favorable clearance (>95% decline from pre-treatment value) of TTMV were compared to those with suboptimal clearance (<95%). The primary objective was to evaluate the relationship between TTMV clearance during CRT and its impact on progression free survival (PFS). The median follow-up was 14.7 months. Clinical nodal stage was associated with higher TTMV-HPV DNA scores at baseline, with a median score of 128, 778, and 1219 for N0/N1, N2a/b, and N2c/3

patients, respectively. Patients who had persistent TTMV at the end of RT had an inferior PFS compared to those who cleared their TTMV at 2 years (91.7% vs. 71.7%) (log rank, p = .042). Among patients who had complete clearance of their TTMV at 3 months, those who had a negative, equivocal, and incomplete PET response had a 2-year PFS of 94.3%, 77.8%, and 59.3%, respectively (log-rank, p = .029). Our study indicates that persistent TTMV-HPV DNA is associated with worse PFS and may portend unfavorable outcomes. Thus, monitoring TTMV clearance kinetics could be a valuable biomarker for guiding treatment decisions in patients with HPV-OPSCC.

25COASMA96:

Title: Determining risk-adapted starting age and interval for breast cancer screening based on reproductive and hormonal factors

Tung Hoang, Jeonghee Lee, So-Youn Jung,

International Journal of Cancer, Volume156, Issue 9

https://doi.org/10.1002/ijc.35265

Abstract: This study aimed to elucidate the risk of developing breast cancer (BC) by reproductive and hormonal profiles to suggest risk-adapted starting screening ages and to investigate risks after negative mammography results to inform screening intervals in the Korean setting. Participants who performed health examinations between 2002 and 2023 at the National Cancer Center were analyzed. Risk-adapted starting age of screening was defined as the age at which women with various reproductive and hormonal profiles obtained a 10-year cumulative risk level similar to women aged 40 years in the general population. The Cox progression model was used to assess BC risk according to the reproductive and hormonal score and time since the last negative mammography. Of the 24,597 women enrolled in this study, 606 had BC (median follow-up 13.2 years, IQR = 9.5–16.5 years). The 10-year cumulative risk of BC at age 40 years in general women was estimated at 2.35%. Women with different reproductive and hormonal profiles reached this risk level 8.55 years earlier to 4.61 years later. We found that women with various reproductive and hormonal profiles had similar incident cases in both low- and high-score groups beyond 5 years after a negative finding from mammography (p > .05), compared to those screened within 0 to <2 years after negative screening results. This study identifies possible risk-based starting ages for BC screening based on reproductive and hormonal factors. Our findings suggest that extending the current biennial screening interval beyond 5 years may still detect a comparable number of cases.

25COASMA97:

Title: Prior antibiotics exposure is associated with an elevated risk of surgical site infections, including anastomotic leakage, after colon cancer but not rectal cancer surgery: A register-based study of 38,839 patients

Sai San Moon Lu, Martin Rutegård, Christel Häggström, Åsa Gylfe, Sophia Harlid, Bethany Van Guelpen

International Journal of Cancer, Volume156, Issue 9

https://doi.org/10.1002/ijc.35269

Abstract: Gut microbiota composition has been implicated in surgical site complications after colorectal cancer surgery. Antibiotics affect gut microbiota, but evidence for a role in surgical site complications is inconclusive. We aimed to investigate use of prescription antibiotics during the years before surgery in relation to the risk of surgical site infections, including anastomotic leakage, within 30 days after surgery. Cardiovascular/neurological complications and the urinary antiseptic methenamine hippurate, for which there is no clear link with the microbiota, were used as negative controls. We conducted a patient cohort study using complete population data from Swedish national registers between 2005 and 2020. The final study population comprised 26,527 colon cancer and 12,312 rectal cancer cases with a 4.5 year exposure window. In colon cancer patients, antibiotics use was associated with a higher risk of surgical site infections (adjusted odds ratio (aOR) for any versus no use = 1.20, 95% confidence interval (CI) 1.10–1.33) and anastomotic leakage in particular (aOR =1.19, 95% CI 1.03–1.36), both with dose–response relationships for increasing cumulative antibiotics use (P_{trend} = <0.001 and P_{trend} = 0.047, respectively). Conversely, associations in rectal cancer patients, as well as for the negative controls cardiovascular/neurological complications and methenamine hippurate, were null. In conclusion, prescription antibiotics use up to 4.5 years before colorectal cancer surgery is associated with a higher risk of surgical site infections, including anastomotic leakage, after colon cancer but not rectal cancer surgery. These findings support a role for antibiotics-induced intestinal dysbiosis in surgical site infections.

25COASMA98:

Title: Survival scenarios of patients with localized and metastatic pancreatic adenocarcinoma: A population-based study

Steven C. Kuijper, Anne M. Gehrels, Lydia G. van der Geest,

International Journal of Cancer, Volume156, Issue 9

https://doi.org/10.1002/ijc.35267

Abstract: Pancreatic adenocarcinoma (PAC) is notorious for its poor survival. The provision of survival scenarios—that is, best-case, typical and worst-case scenarios—could prove valuable to patients and clinicians. This study investigated survival scenarios and how these have changed over a period of 16 years for patients with PAC. Data from the Netherlands Cancer Registry were used to identify patients with localized and metastatic PAC (2005–2021). Survival scenarios, including best-case, upper-typical, typical (median), lower-typical, and worst-case, were estimated based on survival curve percentiles (p10, p25, p50, p75, and p90). Annual differences were assessed for significance using weighted linear regression analyses. Factors associated with these scenarios were identified through univariable tests. Overall, 14,622 patients with localized and 20,199 with metastatic PAC were included. For patients with localized PAC, the best, upper-typical and typical survival scenarios improved statistically significant with average annual improvement of 1.54 (95%CI: 1.2–1.88), 0.67 (0.56–0.78), and 0.24 (0.19–0.29) months, respectively. For patients with metastatic PAC the best and upper-typical survival scenarios increased statically significantly with annual improvement of 0.28 (0.21–0.34) and 0.06 (0.02–0.09) months, respectively. The best-case and upper-typical scenarios were associated with younger patients, more aggressive disease-focused treatments, fewer comorbidities, and better overall performance status. Over the past

16 years, survival improvements in patients with PAC have been most notable in these scenarios. Although the absolute gains were modest, these results offer encouraging potential for advancements in life-prolonging care for this type of cancer.

25COASMA99:

Title: Type II diabetes and metformin use does not affect colorectal cancer prognosis

Mehrnoosh Shahrivar, Caroline E. Dietrich, Bengt Glimelius, Deborah Saraste, Anna Martling, Christian Buchli, Caroline Nordenvall

International Journal of Cancer, Volume156, Issue 9

https://doi.org/10.1002/ijc.35266

Abstract: Previous studies on the impact of metformin and colorectal cancer (CRC) outcomes have been limited by small size and confounding by indication, yielding inconsistent results. The aim of this study was to assess whether diabetes and pre-diagnostic metformin use influence CRC prognosis. The study was performed using the Colorectal Cancer Data Base Sweden, a register-linkage originating from the Swedish Colorectal Cancer Register with linkage to national health care registers and demographic registers. All adult patients diagnosed with primary non-metastatic CRC between 2007 and 2016, treated with curative surgery, were identified and followed up from 90 days post-surgery until December 31, 2022. Antidiabetic medication use was defined as dispensed prescription ≥6 months of use within 1 year of surgery. Type II diabetes mellitus (T2DM) patients were divided into three treatment groups (i) diet only, (ii) metformin user, and (iii) non-metformin user. Cox regression models estimated hazard ratios (HRs) with 95% confidence intervals (CIs) for time to recurrence, CRC-specific, and all-cause mortality, adjusted for relevant covariates. Of 33,028 non-metastatic CRC patients, 4539 (13.7%) had T2DM, with 1745 using metformin. A T2DM diagnosis was not associated with increased recurrence rate or CRC-specific mortality; HR_{adj} 0.97 (95% CI 0.89–1.06) and HR_{adj} 0.95 (95% CI 0.87–1.05), respectively, compared with non-diabetic patients. Furthermore, no association between T2DM, metformin use, and recurrence or CRC-specific mortality was seen, HR_{adj} 0.98 (95% CI 0.86–1.12) and HR_{adj} 0.98 (95% CI 0.85–1.13), respectively. T2DM is not associated with an elevated recurrence or CRC-specific mortality. Additionally, metformin use does not impact CRC prognosis.

25COASMA100:

Title: Synchronous bilateral Wilms tumors are prone to develop independently and respond differently to preoperative chemotherapy

Ting Tao, Shuangai Liu, Min He, Manli Zhao, Chen Chen,

International Journal of Cancer, Volume156, Issue 9

https://doi.org/10.1002/ijc.35297

Abstract: Wilms tumor (WT) is the most common kidney cancer in infants and young children. The determination of the clonality of bilateral WTs is critical to the treatment, because lineage-independent and metastatic tumors may require different treatment strategies. Here we found synchronous bilateral WT (n = 24 tumors from 12 patients) responded differently to preoperative chemotherapy. Transcriptome, whole-exome and whole-genome analysis (n = 12 tumors from 6 patients) demonstrated that each side of bilateral WT was

clonally independent in terms of somatic driver mutations, copy number variations and transcriptomic profile. Molecular timing analysis revealed distinct timing and patterns of chromosomal evolution and mutational processes between the two sides of WT. Mutations in WT1, CTNNB1 and copy-neutral loss of heterozygosity of 11p15.5 provide possible genetic predisposition for the early initiation of bilateral WT. Our results provide comprehensive evidence and new insights regarding the separate initiation and early embryonic development of bilateral WT, which may benefit clinical practices in treating metastatic or refractory bilateral WT.

25COASMA101:

Title: Preclinical studies on the antitumor and non-toxic effect of combining pirfenidone with vinorelbine and carboplatin in non-small cell lung cancer

Helena Branco, Catarina A. Rodrigues, Júlio Oliveira, Nuno Mendes,

International Journal of Cancer, Volume156, Issue 9

https://doi.org/10.1002/ijc.35276

Abstract: Non-small cell lung cancer (NSCLC) shows limited therapeutic response to vinorelbine and carboplatin. Combining these drugs with an antifibrotic drug may enhance their antitumor effect. Pirfenidone is an antifibrotic drug whose antitumor activity has been described in different types of cancer. This work aimed to perform preclinical studies on the combination of pirfenidone with vinorelbine, or with vinorelbine plus carboplatin, in NSCLC. Our data revealed that pirfenidone sensitized three NSCLC cell lines to vinorelbine by reducing cell growth, viability and proliferation, inducing alterations in the cell cycle profile, and increasing cell death (%). Importantly, pirfenidone increased the sensitivity of the three NSCLC cell lines to the combined treatment of vinorelbine plus carboplatin. This combined drug treatment (triplet) did not induce cytotoxicity against non-tumorigenic cells. Notably, the triplet drug combination significantly reduced the growth and proliferation of A-549 xenografts in nude mice, as also reduced vimentin and collagen expression. Most interestingly, the triplet treatment exhibited a safer toxicological profile than the doublet (vinorelbine plus carboplatin) currently applied in the clinical practice. Altogether, these preclinical data support the possibility of repurposing pirfenidone in combination with vinorelbine or with vinorelbine plus carboplatin for NSCLC perioperative treatment, improving therapeutic efficacy while reducing toxicity.

25COASMA102:

Title: Head-to-head comparison of palbociclib and ribociclib in first-line treatment of HR-positive/HER2-negative metastatic breast cancer with real-world data from the OPAL registry

Marc Thill, Mark-Oliver Zahn, Anja Welt, Arnd Nusch

International Journal of Cancer, Volume156, Issue 9

https://doi.org/10.1002/ijc.35296

Abstract: Cyclin-dependent kinase 4/6 inhibitors (CDKIs) in combination with endocrine therapy (ET) are the standard-of-care in the first-line treatment of HR-positive, HER2-negative metastatic breast cancer. In the absence of direct head-to-head trials comparing the efficacy and safety of the different CDKIs, the individual choice of treatment in everyday

practice is complex. Inverse probability of treatment weighting was used to emulate a head-to-head comparison of palbociclib +ET (PALBO) and ribociclib +ET (RIBO) in patients recruited into the prospective, observational, multicenter registry platform OPAL (NCT03417115). Progression-free survival (PFS), overall survival (OS) and quality of life surveys were analyzed, also for subgroups stratified by treatment-free interval (TFI). A total of 623 patients with HR-positive, HER2-negative metastatic breast cancer received PALBO (n = 388) or RIBO (n = 235) in their first line of treatment. No difference between PALBO and RIBO was found for PFS (median 26.7 months [23.6, 30.7] vs. 27.0 months [21.1, 30.4], HR 1.01 [0.80, 1.27]) and OS (median 42.4 months [38.8, 50.3] vs. 49.3 months [36.9, NA], HR 0.96 [0.71, 1.28]). There was a trend for longer PFS and OS in patients with TFI <12 months receiving RIBO. Patients reported comparable side effects for both CDKIs. This head-to-head comparison revealed no difference in PFS and OS between PALBO and RIBO, however, a trend to longer PFS and OS with RIBO was observed in the subgroup of patients with TFI <12 months. Side effects experienced with PALBO and RIBO highlight the important toxicities to be addressed during treatment decision.

25COASMA103:

Title: Interval cancer risk after the upper age limit of screening has been reached: Informing risk stratification in FIT-based colorectal cancer screening

Brenda J. van Stigt, Iris Lansdorp-Vogelaar, Manon C. W. Spaander

International Journal of Cancer, Volume156, Issue 9

https://doi.org/10.1002/ijc.35294

Abstract: Upper age limits are currently fixed for all fecal immunochemical test (FIT)-based colorectal cancer (CRC) screening programs. A risk-stratified upper age limit may be beneficial. Therefore, we assessed differences in interval CRC risk among individuals who had reached the upper age limit of screening (75 years). Individuals with a negative FIT (<47 μg Hb/g feces) in the final round of the Dutch CRC screening program were selected from the national screening database and linked to the national cancer registry to identify CRCs diagnosed within 24 months (interval CRCs). Survival analyses assessed whether sex and last fecal hemoglobin (f-Hb) concentration were associated with interval CRC risk. A multivariable logistic regression assessed whether sex, last f-Hb concentration and screening round were associated with stage distribution (early vs. late). Last f-Hb concentrations were considered detectable when they were >0 μg Hb/g feces. Among 305,761 individuals with a complete follow-up (24 months), 661 were diagnosed with interval CRC (21.6 per 10,000 negative FITs). Individuals with detectable f-Hb (15%) were 5 times more likely to be diagnosed with interval CRC than those without (HR 4.87, 95%CI: 4.19–5.65). Moreover, their cancers were more often detected at a late stage compared to individuals without detectable f-Hb (OR 1.45, 95%CI: 1.06–2.01). Our results show that interval CRC risk among individuals aged ≥75 differs substantially by last f-Hb concentration, indicating a uniform age to stop screening is suboptimal. Future research, taking into account multiple screening rounds and FIT results, should determine the optimal risk-stratified screening strategy.

25COASMA104:

Title: Acceptability and somatic mutations in cervicovaginal self-sampling for earendometrial cancer detection in women with Lynch syndrome

Paula Peremiquel-Trillas, José Manuel Martínez, Sònia Paytubi, Jon Frias-Gomez,

International Journal of Cancer, Volume156, Issue 9

https://doi.org/10.1002/ijc.35368

Abstract: New molecular approaches are being developed to detect endometrial cancer using minimally invasive sampling methods. This study aims to evaluate the acceptability of self-collected cervicovaginal samples among women with Lynch syndrome, a group at high risk for developing endometrial cancer. Participants collected cervicovaginal self-samples and answered an at-home acceptability questionnaire in a cross-sectional study. Self-samples from a subset of these women were analyzed for somatic mutations using next-generation sequencing (NGS), targeting a panel of 47 genes. A total of 61 (88.4%) out of 69 eligible women participated in the study. The overall self-sampling experience was rated good or very good (N = 55, 90.2%). Most of the women were confident about correctly sampling (N = 58, 95.1%), and most reported no or mild pain (N = 56, 91.8%). During self-sample collection, most women reported feeling calm and comfortable and experiencing safety, privacy, and normality. In a pilot study using a subset of 15 samples, five somatic variants were identified in four self-samples (4/15, 26.7%) in ACVR2A, ARID1A, APC, and KMT2D. During follow-up, three out of four women with variants detected in the self-sample underwent prophylactic hysterectomy at a median of 9.1 months, while one out of four developed endometrial cancer after 3.9 years since the collection of the sample. Self-sampling is well-accepted and well-tolerated in women with Lynch syndrome and could potentially reduce some barriers associated with gynaecological surveillance. Further research is needed to evaluate the feasibility of implementing cervicovaginal self-collection and the accuracy of molecular testing for gynaecological surveillance in women with Lynch syndrome.

25COASMA105:

Title: "Cell dedifferentiation" versus "evolutionary reversal" theories of cancer: The direct contest of transcriptomic features

Alexander E. Vinogradov, Olga V. Anatskaya et.al.

International Journal of Cancer, Volume156, Issue 9

https://doi.org/10.1002/ijc.35352

Abstract: Cell dedifferentiation is considered an important hallmark of cancer. The atavistic reversal to a unicellular-like (UC) state is a less widely accepted concept, so far not included in the conventional hallmarks. The activated expression of ontogenetically earlier and evolutionary earlier genes in cancers supports both theories because ontogenesis partially recapitulates phylogenesis during cell differentiation (the cellular biogenetic law). We directly contested both types of gene signatures in stem vs. differentiated and cancer vs. normal cells, using meta-analysis of human single-cell transcriptomes (totally, 38 pairwise comparisons involving over 18,600 cells). Because compared cells can differ in proliferation rate, the correction for cell cycle activity was applied. Taken together as multiple variables in stem vs. differentiated cells analyses, the ontogenetic signature excluded the UC signature from predictive variables, usually even forcing it to change the sign of prediction (from plus

to minus). In contrast, in cancer vs. normal cells, the UC signature excluded the ontogenetic signature. Thus, the direct contest decided in favor of the atavistic theory and placed a UC-like state as a central hallmark of cancer, which has a plausible evolutionarily formed mechanism (UC attractor) and can generate other hallmarks. These data suggest a paradigm shift in the understanding of oncogenesis and propose an integrative framework for cancer research. In a practical sense, the upregulation of UC signature over ontogenetic signature indicates potential tumorigenicity, which can be used in early diagnostics and regenerative medicine. For therapy, these results suggest the UC center of cellular networks as a universal target.

25COASMA106:

Title: Hypoxia-inducible factor-targeting therapy augmented the sensitivity to programmed death ligand-1 blockade by enhancing interferon-γ-induced chemokines in tumor cells

Yohei Yabuki, Atsushi Mitsuhashi et.al.

International Journal of Cancer, Volume156, Issue 9

https://doi.org/10.1002/ijc.35301

Abstract: Immune checkpoint inhibitors (ICIs) targeting programmed death ligand-1 (PD-L1) provide clinical benefits for various advanced malignancies. However, the predictive factors that determine sensitivity to ICIs have not been fully elucidated. We focused on tumor-derived CXCL10/11 as a pivotal factor that determines the response to PD-L1 blockade by regulating T cell accumulation and tumor angiogenesis. We previously reported that CXCL10/11 was upregulated by interferon (IFN)-γ in ICI-sensitive tumor cells but not in ICI-resistant cells, including mouse Lewis lung carcinoma (LLC). In the present study, gene silencing of tumor-derived CXCL10/11 induced resistance to PD-L1 blockade in AB1-HA mesothelioma cell-bearing mice. To identify the mechanisms underlying ICI resistance, we performed a microarray analysis to compare the IFN-γ-inducible genes between ICI-sensitive AB1-HA and ICI-resistant LLC in vitro. A pathway analysis based on microarray data indicated that hypoxia-inducible factor (HIF) 1A is the key signal that inhibits CXCL10/11 expression. We revealed that the HIF1A inhibitors echinomycin (EC) and YC-1 upregulated CXCL10/11 genes induced by IFN-γ in tumor cells in vitro. In addition, combination therapy with PD-L1 blockade and EC demonstrated synergistic antitumor effects in LLC-bearing mice. Combination therapy enhanced tumor infiltration of CD8 T cells and suppressed tumor angiogenesis. The present study suggests that HIF1A signaling in tumor cells dominates ICI resistance via the downregulation of tumor-derived CXCL10/11.

25COASMA107:

Title: Aggressive characteristics of tumor deposits in colorectal cancer highlight the need for staging refinement in patients with 0–3 metastatic lymph nodes

Xi'e Hu, Shuang Xie, Zhenyu Yang, Xin Zhao, Li Gong, Ping Yang

International Journal of Cancer, Volume156, Issue 9

https://doi.org/10.1002/ijc.35306

Abstract: Accurate staging is essential for the optimal management of patients with colorectal cancer (CRC). The role of tumor deposits (TDs) in CRC staging has been

contentious due to a lack of comprehensive understanding of their clinical and biological traits. In this retrospective study, we analyzed large data from 5718 CRC patients diagnosed between 2011 and 2022, ensuring rigorous data collection and long-term follow-up. Patients with positive TDs displayed aggressive clinical features. The risk factors for TDs varied among patients with different backgrounds of lymph node (LN) involvement, and the numbers of TDs and metastatic LNs showed a significantly positive correlation. TDs significantly impacted CRC prognosis, resulting in unfavorable outcomes irrespective of LN status. To delve into the biological characteristics of TDs, we performed transcriptome sequencing, immunohistochemistry, and Kaplan–Meier analyses on tissue samples from the additional CRC cohort and The Cancer Genome Atlas datasets. TDs exhibited aggressive biological phenotypes that were distinct from primary tumors and metastatic LNs, characterized by elevated signatures of epithelial-mesenchymal transition, angiogenesis, and immune suppression. Cox proportional hazards analysis was then applied to reassess the appropriate role of TDs within the TNM staging system, revealing that the prognostic weightiness of TDs in CRC corresponded to N2a rather than N1 in patients with 0–3 LN metastases. Overall, our comprehensive analysis showed that TDs, with their aggressive clinical and biological characteristics, could optimize the staging of CRC, highlighting the need to refine their role within the TNM staging system.

25COASMA108:

Title: Long-term efficacy and safety of danicopan as add-on therapy to ravulizumab or eculizumab in PNH with significant EVH

Austin Kulasekararaj, Morag Griffin et.al.

Blood (2025) 145 (8): 811–822.
https://doi.org/10.1182/blood.2024026299

Abstract: Complement C5 inhibitor treatment with ravulizumab or eculizumab for paroxysmal nocturnal hemoglobinuria (PNH) improves outcomes and survival. Some patients remain anemic due to clinically significant extravascular hemolysis (cs-EVH; hemoglobin [Hb] ≤9.5 g/dL and absolute reticulocyte count [ARC] ≥120 × 10^9/L). In the phase 3 ALPHA trial, participants received oral factor D inhibitor danicopan (150 mg 3 times daily) or placebo plus ravulizumab or eculizumab during the 12-week, double-blind treatment period 1 (TP1); those receiving placebo switched to danicopan during the subsequent 12-week, open-label TP2 and continued during the 2-year long-term extension (LTE). There were 86 participants randomized in the study, of whom 82 entered TP2, and 80 entered LTE. The primary end point was met, with Hb improvements from baseline at week 12 (least squares mean change, 2.8 g/dL) with danicopan. For participants switching from placebo to danicopan at week 12, improvements in mean Hb were observed at week 24. Similar trends were observed for the proportion of participants with ≥2 g/dL Hb increase, ARC, proportion of participants achieving transfusion avoidance, and Functional Assessment of Chronic Illness Therapy–Fatigue scale scores. Improvements were maintained up to week 72. No new safety signals were observed. The breakthrough hemolysis rate was 6 events per 100 patient-years. These long-term data demonstrate sustained efficacy and safety of danicopan plus ravulizumab/eculizumab for continued control of terminal complement activity, intravascular hemolysis, and cs-EVH in PNH.

25COASMA109:

Title: Antibiotic-induced loss of gut microbiome metabolic output correlates with clinical responses to CAR T-cell therapy

Rishika Prasad, Abdur Rehman, et.al.

Blood (2025) 145 (8): 823–839.
https://doi.org/10.1182/blood.2024025366

Abstract: Antibiotic (ABX)–induced microbiome dysbiosis is widespread in oncology, adversely affecting outcomes and side effects of various cancer treatments, including immune checkpoint inhibitors and chimeric antigen receptor T-cell (CAR-T) therapies. In this study, we observed that prior exposure to broad-spectrum ABXs with extended anaerobic coverage such as piperacillin-tazobactam and meropenem was associated with worse anti-CD19 CAR-T therapy survival outcomes in patients with large B-cell lymphoma (N = 422) than other ABX classes. In a discovery subset of these patients (n = 67), we found that the use of these ABXs was in turn associated with substantial dysbiosis of gut microbiome function, resulting in significant alterations of the gut and blood metabolome, including microbial effectors such as short-chain fatty acids (SCFAs) and other anionic metabolites, findings that were largely reproduced in an external validation cohort (n = 58). Broader evaluation of circulating microbial metabolites revealed reductions in indole and cresol derivatives, as well as trimethylamine N-oxide, in patients who received ABX treatment (discovery, n = 40; validation, n = 28). These findings were recapitulated in an immune-competent CAR-T mouse model, in which meropenem-induced dysbiosis led to a systemic dysmetabolome and decreased murine anti-CD19 CAR-T efficacy. Furthermore, we demonstrate that SCFAs can enhance the metabolic fitness of CAR-Ts, leading to improved tumor killing capacity. Together, these results suggest that broad-spectrum ABX deplete metabolically active commensals whose metabolites are essential for enhancing CAR-T efficacy, shedding light on the intricate relationship between ABX exposure, microbiome function and their impact on CAR-T efficacy. This highlights the potential for modulating the microbiome to augment CAR-T immunotherapy.

25COASMA110:

Title: Serum free light chains in a racially diverse population including African Americans and populations from South Africa

Luca Bertamini, Jean-Baptiste Alberge et.al.

Blood (2025) 145 (8): 840–849.
https://doi.org/10.1182/blood.2024026078

Abstract: Detection of light chain (LC) monoclonal gammopathies (MGs) traditionally relies on serum free LC (FLC) κ, λ, and their ratio (κ/λ) reference ranges based on a mostly White population. We investigated FLC values in a racially diverse population by screening 10 035 individuals for heavy chain MG, identifying 9028 negative cases whose FLC were measured. Participants included 4149 from the PROMISE study (United States, n = 2383; South Africa, n = 1766) and 4879 from the Mass General Brigham Biobank, with 44% self-identifying as Black. Using standard FLC reference ranges, 1074 of 10 035 individuals (10.7%) were diagnosed with LC monoclonal gammopathy of undetermined significance (MGUS), with 99% being κ-restricted. In the United States, 14.8% of Black and 4% of White individuals

were diagnosed (P < .01). Among US participants of African (AFR) and European (EUR) genetic ancestry, 14.4% AFR and 2.9% EUR were diagnosed (P < .01). Among South Africans (100% Black), 27.8% were diagnosed using standard ranges. To avoid overdiagnosis, we propose a new κ/λ ratio reference range (0.686 to 2.10) for populations of AFR descent with normal renal function, with standard values for κ and λ being 7.97 to 77.50 mg/L and 6.20 to 49.20 mg/L, respectively. This reduces LC-MGUS overdiagnosis by 91% (10.7% vs 0.97%). Using the new reference, LC-MGUS accounts for 8.8% of MGUS cases, with 74% being κ-restricted, consistent with LC myeloma rates. These findings highlight the importance of basing disease definitions, such as MGUS, on diverse populations. Adopting our proposed FLC reference values would reduce MGUS overdiagnosis among Black individuals, avoiding unnecessary financial, psychological, and medical consequences. This study includes data from NCT03689595.

25COASMA111:

Title: Dexamethasone dose intensity does not impact outcomes in newly diagnosed multiple myeloma: a secondary SWOG analysis

Rahul Banerjee, Rachael Sexton, Andrew J. Cowan,et.al.

Blood (2025) 145 (1): 75–84.

https://doi.org/10.1182/blood.2024025939

Abstract: Dexamethasone is a key component of induction for newly diagnosed multiple myeloma (NDMM), despite common toxicities, including hyperglycemia and insomnia. In the randomized ECOG E4A03 trial, dexamethasone 40 mg once weekly was associated with lower mortality than higher doses. However, the performance of dexamethasone dose reductions below this threshold with regard to progression-free survival (PFS) and overall survival (OS) in NDMM has not been fully characterized. We conducted a secondary pooled analysis of the SWOG 0777 and SWOG 1211 studies of NDMM, which used lenalidomide and dexamethasone (Rd) alone, with or without bortezomib, and with or without elotuzumab. The planned dexamethasone intensity was 40 to 60 mg weekly in all arms. Patients were categorized into FD-DEX (full-dose dexamethasone maintained throughout induction) or LD-DEX (lowered-dose dexamethasone or discontinuation; only permitted for grade 3+ toxicities per both study protocols). Of the 541 evaluated patients, the LD-DEX group comprised 373 patients (69%). There were no differences in PFS or OS between the FD-DEX and LD-DEX groups, which were balanced in terms of age, stage, and performance status. Predictors of PFS and OS in the multivariate models were treatment arm, age ≥70 years, and thrombocytopenia. FD-DEX did not significantly improve either outcome. Our study suggests that dexamethasone dose reductions are common in multiple myeloma, even within clinical trials. Given the many toxicities and unclear benefits of dexamethasone in the era of modern treatment regimens, dexamethasone dose reduction during NDMM induction warrants further prospective studies

25COASMA112:

Title: Safety and efficacy of standard-of-care ciltacabtagene autoleucel for relapsed/refractory multiple myeloma

Surbhi Sidana,Krina K. Patel et.al.,

Blood (2025) 145 (1): 85–97.
https://doi.org/10.1182/blood.2024025945

Abstract: Ciltacabtagene autoleucel (cilta-cel) was approved in 2022 for patients with relapsed/refractory multiple myeloma (RRMM). We report outcomes with cilta-cel in the standard-of-care setting. Patients with RRMM who underwent leukapheresis for cilta-cel manufacturing between 1 March 2022 and 31 December 2022 at 16 US academic medical centers were included. Overall, 255 patients underwent leukapheresis and 236 (92.5%) received cilta-cel, of which 54% would not have met CARTITUDE-1 eligibility criteria. In treated patients (N = 236), cytokine release syndrome was seen in 75% (grade ≥3, 5%), immune effector cell–associated neurotoxicity syndrome in 14% (grade ≥3, 4%), and delayed neurotoxicity in 10%. Overall and complete response rates were as follows: all patients who received cilta-cel (N = 236), 89% and 70%; patients receiving conforming cilta-cel (n = 191), 94% and 74%; and conforming cilta-cel with fludarabine/cyclophosphamide lymphodepletion (n = 152), 95% and 76%, respectively. Nonrelapse mortality was 10%, most commonly from infection. After a median follow-up of 13 months from cilta-cel, the median progression-free survival (PFS) was not reached, with 12-month estimate being 68% (95% confidence interval, 62-74). High ferritin levels, high-risk cytogenetics, and extramedullary disease were independently associated with inferior PFS, with a signal for prior B-cell maturation antigen–targeted therapy (P = .08). Second primary malignancies excluding nonmelanoma skin cancers were seen in 5.5% and myeloid malignancies/acute leukemia in 1.7%. We observed a favorable efficacy profile of standard-of-care cilta-cel in RRMM, despite more than half the patients not meeting the CARTITUDE-1 eligibility criteria.

25COASMA113:

Title: Nanobody-based naturally selected CD7-targeted CAR-T therapy for acute myeloid leukemia

Peihua Lu, Xian Zhang,et.al.

Blood (2025) 145 (10): 1022–1033.
https://doi.org/10.1182/blood.2024024861

Abstract: Approximately 30% of patients with acute myeloid leukemia (AML) express CD7 on their myeloblasts. We have previously demonstrated that single-chain variable fragment (scFv)–based "naturally selected" CD7 chimeric antigen receptor T-cell (NS7CAR-T) therapy shows significant efficacy, with a favorable safety profile in T-cell lymphoid malignancies. Here, we derived dual variable heavy-chain domain of a heavy-chain antibody (dVHH) NS7CAR-Ts that have superior CD7 binding specificity, affinity to their scFv-based counterparts, and improved proliferative capability. In this phase 1 clinical trial, we evaluated the efficacy and safety of nanobody-based dVHH NS7CAR-Ts for patients with $CD7^+$ refractory/relapsed AML. A cohort of 10 patients received dVHH NS7CAR-Ts across 2 dosage levels of 5×10^5/kg and 1×10^6/kg. Before enrollment, patients had undergone a median of 8 (range, 3-17) prior lines of therapy. Seven patients had prior transplants. After NS7CAR-T infusion, 7 of 10 (70%) patients achieved complete remission (CR). The median observation time was 178 days (range, 28-776). Among 7 patients who achieved CR, 3 who relapsed from prior transplants underwent a second allogeneic hematopoietic stem cell transplant (allo-HSCT). One patient remained leukemia free on day 401, and the other 2 died

on day 241 and day 776, respectively, from nonrelapse-related causes. Three CR patients without consolidative (allo-HSCT) relapsed within 90 days. All the nonresponders and relapsed patients had CD7 loss. The treatment was well tolerated, with 80% experiencing mild cytokine release syndrome and none had neurotoxicity. This trial underscores the potential promising treatment of dVHH NS7CAR-Ts in providing clinical benefits with a manageable safety profile to patients with $CD7^+$ AML, warranting further investigation.

25COASMA114:

Title: Cullin-5 controls the number of megakaryocyte-committed stem cells to prevent thrombocytosis in mice

Maria Kauppi, Craig D. Hyland et.al.

Blood (2025) 145 (10): 1034–1046.

https://doi.org/10.1182/blood.2024025406

Abstract: Cullin-5 (Cul5) coordinates the assembly of cullin-RING-E3 ubiquitin ligase complexes that include the suppressors of cytokine signaling (SOCS)-box–containing proteins. The SOCS-box proteins function to recruit specific substrates to the complex for ubiquitination and degradation. In hematopoiesis, SOCS-box proteins are best known for regulating the actions of cytokines that utilize the JAK-STAT signaling pathway. However, the roles of most SOCS-box proteins have not been studied in physiological contexts and any actions for Cul5/SOCS complexes in signaling by several hematopoietic cytokines, including thrombopoietin (TPO) and interleukin-3 (IL-3), remain unknown. To define additional potential roles for Cul5/SOCS complexes, we generated mice lacking Cul5 in hematopoiesis; the absence of Cul5 is predicted to impair the SOCS-box–dependent actions of all proteins that contain this motif. Here, we show that Cul5-deficient mice develop excess megakaryopoiesis and thrombocytosis revealing a novel mechanism of negative regulation of megakaryocyte-committed stem cells, a distinct population within the hematopoietic stem cell pool that have been shown to rapidly, perhaps directly, generate megakaryocytes, and which are produced in excess in the absence of Cul5. Cul5-deficient megakaryopoiesis is distinctive in being largely independent of TPO/myeloproliferative leukemia protein and involves signaling via the β-common and/or β-IL-3 receptors, with evidence of deregulated responses to IL-3. This process is independent of the interferon-α/β receptor, previously implicated in inflammation-induced activation of stem-like megakaryocyte progenitor cells.

25COASMA115:

Title: Lasalocid A selectively induces the degradation of MYD88 in lymphomas harboring the MYD88 L265P mutation

Wei Li, Ruirui Wang, Junhao Wang et.al.

Blood (2025) 145 (10): 1047–1060.

https://doi.org/10.1182/blood.2024026781

Abstract: Myeloid differentiation primary response protein 88 (MYD88) is a key adaptor molecule in the signaling pathways of toll-like receptor and interleukin-1 receptor. A somatic mutation resulting in a leucine-to-proline change at position 265 of the MYD88 protein (MYD88 L265P) is one of the most prevalent oncogenic mutations found in patients with hematological malignancies. In this study, we used high-throughput screening to identify

lasalocid A as a potent small molecule that selectively inhibited the viability of lymphoma cells expressing MYD88 L265P and the associated activation of NF-κB. Further investigations using CRISPR-CRISPR–associated protein 9 genetic screening, proteomics, and biochemical assays revealed that lasalocid A directly binds to the MYD88 L265P protein, enhancing its interaction with the ubiquitin ligase RNF5. This interaction promotes MYD88 degradation through the ubiquitin-dependent proteasomal pathway, specifically in lymphomas with the MYD88 L265P mutation. Lasalocid A exhibited strong antitumor efficacy in xenograft mouse models, induced disease remission in ibrutinib-resistant lymphomas, and showed synergistic activity with the B-cell lymphoma 2 inhibitor venetoclax. This study highlights the potential of inducing MYD88 L265P degradation using small molecules, offering promising strategies for treating lymphomas that harbor the MYD88 L265P mutation.

Surgical Oncology

25COASMA1

Title: Combined preoperative and post-adjuvant-chemotherapy carcinoembryonic antigen levels are prognostic for early recurrence and survival in stage III colon cancer,

Erman Akkus, Beliz Bahar Karaoğlan, Barış Akçadağ, Barış Bahçekapılı, Cihangir Akyol, Güngör Utkan,

The American Journal of Surgery, Volume 243,2025,116256,
https://doi.org/10.1016/j.amjsurg.2025.116256.

Abstract: The definitive treatment of stage-III colon cancer is surgery and adjuvant chemotherapy. A combined assessment of pre-operative and post-adjuvant chemotherapy carcinoembryonic antigen (CEA) levels may better prognosticate early recurrence and survival. A cohort of patients who underwent surgery and adjuvant chemotherapy was assessed. The CEA-Square (CEA2) score was defined as the multiplication of preoperative and post-adjuvant chemotherapy CEA levels and was grouped as "≤25(ng/mL)2" and ">25(ng/mL)2. Among the 432 patients,137 were eligible. CEA2 score (>25 vs ≤ 25 (ng/mL)2) was significantly prognostic for early recurrence (34.5 % vs. 14.3 %, log-rank, $p < 0.001$). In the multivariable analysis, only the CEA2 score remained associated with early recurrence [HR:3.375, (95 % CI:1.488–7.655), $p = 0.004$]. In a median follow-up of 37.5 months (2.5–101.0), a high CEA2 score [>25 (ng/mL)2] was significantly associated with a worse OS (log-rank, $p < 0.001$). CEA2 is a simple, practical score combining prognostic values of preoperative and post-adjuvant chemotherapy CEA levels.

Keywords: Colon cancer; Stage III; Carcinoembryonic antigen; CEA; Preoperative; Adjuvant chemotherapy

25COASMA2

Title: Colorectal cancer care equity in underserved communities: Innovative solutions for screening, outreach & capacity in rural Washington,

Lauren Duffy, Marley Anderson, Evelyn Rowe, Michelle Yan, Aliya Abdelhak, Juliana Garcia, Clemma Muller, Anjali Kumar,

The American Journal of Surgery, Volume 243,2025,116246,
https://doi.org/10.1016/j.amjsurg.2025.116246.

Abstract: Colorectal cancer (CRC) mortality hotspots in rural Washington, notably Yakima and Richland, identified an 8-year earlier median age of death in non-white patients. Post-pandemic data from WA State Department of Health and MultiCare's electronic health records revealed a 40 % decrease in CRC screenings. During a 2023 CRC prevention summit, barriers and solutions were discussed focusing on rural Hispanic laborers as this population is often seen at partner locations, Yakima Valley Farm Workers Clinic (YVFWC). Community outreach—Our team established a presence at Yakima's largest health fair, Fiesta de Salud. We also provided screening resources at Richland's farmers' markets. Planned events -- We will network with local community leaders and health providers to actualize screening (stool-based testing, hands-on endoscopy training). Persistent CRC mortality disparities in Washington State underscores the need for targeted interventions. Partnering with

organizations and engaging in community outreach aims to increase screening rates and enhance education.

25COASMA3

Title: Association of immediate symmetrizing oncoplastic surgery with patient-reported outcomes in patients with breast cancer – A retrospective cohort study,

Martin Heidinger, Gilles Bilfeld, Nico Föge, Julie M. Loesch, Nadia Maggi, Rama Kiblawi, Ruth S. Eller,

The American Journal of Surgery, Volume 243,2025,116286,
https://doi.org/10.1016/j.amjsurg.2025.116286.

Abstract: Oncoplastic breast surgery (OPS) with immediate symmetrization is commonly performed. However, its impact on patient-reported outcomes (PROs) remains uncertain. Patients with stage 0-III breast cancer who underwent OPS (including oncoplastic breast conserving surgery, or nipple- or skin-sparing mastectomy) at a Swiss university hospital between 01/2013-12/2023 who completed a postoperative BREAST-Q questionnaire were identified from a prospectively maintained database. A generalized linear model was used to detect differences in PROs between those who underwent unilateral versus immediate symmetrizing surgery. Of 441 eligible patients, 333 (75.5 %) underwent unilateral OPS, while 108 (24.5 %) underwent bilateral OPS. Median time to PRO assessment was 35.1 months (Q1-Q3 13.4–49.5). No differences in PROs were identified between patients who underwent unilateral versus bilateral OPS. Short-term surgical morbidity was more common in patients who underwent symmetrizing surgery, which negatively impacted PROs. The present study did not demonstrate any impact of immediate symmetrization on PROs.

Keywords: Breast cancer; Oncoplastic surgery; Patient-reported outcomes; Quality of life

25COASMA4

Title: A modified Z-shaped incision combined with platysma and sternocleidomastoid muscle flaps to improve maxillofacial aesthetics of patients with total parotidectomy,

Xiao Luo, Shan Gao, Ming-Liang Dou, Yan-Li Lan, Xiao-Jiao Lan, Jia-Li Liao, Yi-Wen Wei,

Asian Journal of Surgery, Volume 48, Issue 5,2025,Pages 2891-2896,
https://doi.org/10.1016/j.asjsur.2024.12.126.

Abstract: To explore the safety and cosmetic effect of a modified z-shaped incision combined with platysma muscle flap and sternocleidomastoid muscle flap in improving maxillofacial aesthetics for patients with total parotidectomy. 44 patients with total parotidectomy were randomly divided into experimental group(n = 22) and control group(n = 22). The experimental group used a modified z-shaped incision combined with platysma muscle flap and sternocleidomastoid muscle flap to improve maxillofacial aesthetics of patients. The control group received traditional surgery. The differences of surgical duration, hospitalization days, surgical complications and maxillofacial aesthetics between the two groups were compared. The differences between the experimental group and the control group in terms of maxillofacial aesthetics and surgical duration were statistically significant($P < 0.05$),while there were no statistically significant differences in terms of hospitalization days and surgical complications ($P > 0.05$). The modified z-shaped incision

combined with platysma muscle flap and sternocleidomastoid muscle flap can significantly improve maxillofacial aesthetics of patients with total parotidectomy, and compared with traditional surgery,the safety is consistent,so it is worthy of clinical promotion and application.

Keywords: Cosmetic incision; Platysma; Sternocleidomastoid; Parotidectomy; Maxillofacial aesthetics; Maxillofacial depression

25COASMA5

Title: Long-term survival outcome of patients with femoral neck and trochanteric fractures: A nationwide population-based observational study,

Kun-Han Lee, Kao-Shang Shih, Sheng-Mou Hou, Chun-Chiao Chen, Ting-Yang Peng, Yu-Chun Liu, Mu-Chieh Chi, Mao-Yi Yang, Li-Wei Hung,

Asian Journal of Surgery, Volume 48, Issue 5,2025,Pages 2897-2901,
https://doi.org/10.1016/j.asjsur.2025.01.059.

Abstract: Hip fractures in the geriatric population are the significant medical and public health concern due to their adverse outcomes and high mortality. The purposes of the study were to compare the survival between trochanteric and femoral neck hip fracture on older patients and further compare the difference and prognosis in this population. Data were extracted from the Taiwanese National Health Insurance Research Database. A retrospective cohort study was conducted to analyze regarding patients ≥65 years who sustained a fragile hip fracture. Risk factors that had the potential to confound the correlation between hip fracture and mortality were recorded. Univariate analysis using the Cox proportional hazards model was performed to compute the unadjusted hazard ratios of each covariate for excess mortality. Subsequently, covariates that were significant in the univariate analysis were included in a multivariate model. A total of 61,346 patients were included nationwide. The femoral neck fracture population were significantly younger, have lower Charlson comorbidity index score, with less proportion to have comorbidities. The mortality rate was lower for femoral neck fracture patients compared to trochanteric fracture patients. Hazard ratios for trochanteric patients were 1.32, 0.96, 1.02 and 1.09 for 0–3 months, 3 months-1 year, 1–5 years and 5–10 years. The trochanteric fracture group showed a noticeably higher rate of mortality compared to the femoral neck fracture group in the first 3 months after injury. This suggests the need for extra careful postoperative care for individuals in the trochanteric fracture group.

Keywords: Hip fracture; Trochanteric fracture; Femoral neck fracture; Mortality; Risk factors

25COASMA6

Title: Comparative efficacy of indocyanine green and Tc-99m for sentinel lymph node biopsy in breast cancer: Upfront surgery and post-neoadjuvant chemotherapy,

Tanakorn Tarapongpun, Hung-Wen Lai, Chiung-Ying Liao, Shih-Lung Lin, Hsin-I Huang, Shou-Tung Chen, Dar-Ren Chen,

Asian Journal of Surgery,Volume 48, Issue 5,2025,Pages 2866-2873,
https://doi.org/10.1016/j.asjsur.2025.01.045.

Abstract: This retrospective study aimed to compare the sensitivity of sentinel lymph node (SLN) detection using indocyanine green (ICG), Technetium-99 (Tc-99m), and combined technique (ICG + Tc-99m) in clinical node-negative early-stage breast cancer patients, both in upfront surgery and post-neoadjuvant chemotherapy (NAC) settings. Breast cancer patients who underwent breast surgery with SLN biopsy from December 2021 to May 2024 were enrolled. Both ICG and Tc-99m were used in combination during the SLN biopsy. The primary outcome was the SLN detection rate (per case) and nodal detection rate (per node) compared between ICG, Tc-99m, and combined technique. 176 patients (128 upfront surgery, 48 post-NAC) were analyzed and a total of 326 SLNs were identified. The SLN detection rate was not different between ICG and Tc-99m in upfront surgery (96.1 % vs. 95.3 %, P = 0.65) and post-NAC (89.6 % vs. 85.4 %, P = 0.41). The mean number of identified SLNs was higher with ICG compared to Tc-99m (1.6 ± 1.0 vs. 1.4 ± 0.9, P < 0.001). ICG exhibited a higher overall nodal detection rate than Tc-99m (86.2 % vs. 74.2 %, P < 0.001). Using the combined technique significantly increased the SLN detection rate particularly in post-NAC compared to Tc-99m alone (93.8 % vs 85.4 %, P < 0.05) with a false negative rate of 2.1 %. ICG demonstrated high sensitivity for SLN detection, comparable to Tc-99m in both upfront surgery and NAC settings. Using dual tracers also significantly improved the SLN detection rate in post-NAC setting, suggesting that ICG may serve as an effective alternative tracer for SLN mapping, regardless of NAC.

Keywords: Indocyanine green (ICG); Radioisotope (RI); Technetium 99 (Tc-99m); Sentinel lymph node (SLN); Breast cancer; Neoadjuvant chemotherapy

25COASMA7

Title: Comparative efficacy of venous thromboembolism prophylaxis in patients with blunt trauma: Direct thrombin inhibitors vs low-molecular-weight heparin,

Jen-Fu Huang, Chih-Po Hsu, Sheng-Yu Chan, Ya-Chiao Lin, Chi-Tung Cheng, Po-Cheng Lo, Meng-Hsuan Lee,

Asian Journal of Surgery, Volume 48, Issue 5,2025,Pages 2874-2881,
https://doi.org/10.1016/j.asjsur.2025.03.123.

Abstract: Venous thromboembolism (VTE) includes deep vein thrombosis (DVT) and pulmonary embolism (PE) and poses a risk to patients with trauma. This study compared the efficacy of direct thrombin inhibitors (DTIs) and low-molecular-weight heparin (LMWH) for the prophylaxis of VTE in patients with blunt injuries. This study analyzed data from the American College of Surgeons Trauma Quality Improvement Program, focusing on patients with an injury severity score (ISS) of ≥10 who received VTE prophylaxis. It identified covariates associated with VTE and adverse events. Among 194,154 patients, those on DTIs (n = 205) were older and had higher ISS than those on LMWH (n = 193,949). The DTI group had higher rates of DVT (4.9 % vs 1.3 %), PE (3.4 % vs 0.7 %), unplanned visiting to the operating room (OR) (5.4 % vs 1.5 %), and mortality (8.8 % vs 2.5 %). After propensity score matching, DTIs were associated with increased incidences of DVT (4.9 % vs 1.8 %), PE (3.4 % vs 0.8 %), and unplanned visiting to the OR (5.4 % vs 1.5 %). Multivariate analysis indicated that DTIs significantly increased the odds of DVT (odds ratio, 2.945), PE (odds ratio, 4.250), and unplanned visiting to the OR (odds ratio, 4.175). DTIs are linked to more DVT and PE than LMWH in VTE prevention. LMWH is more effective than the other

options and causes fewer adverse events. LMWH is preferred for patients with blunt injuries and an ISS of ≥10.

Keywords: Direct thrombin inhibitors; Low-molecular-weight heparin; Venous thromboembolism

25COASMA8

Title: Mammographic microcalcifications as a predictor of neoadjuvant efficacy across different breast cancer molecular subtypes,

Zixuan Luo, Jiawei Hu, Deguang Kong, Junlong Song, Zhiyu Li, Chuang Chen,

Asian Journal of Surgery, Volume 48, Issue 5,2025,Pages 2902-2910,
https://doi.org/10.1016/j.asjsur.2024.12.023.

Abstract: Microcalcifications are significant indicators of breast cancer, particularly for distinguishing the different molecular subtypes. This study aimed to investigate the relationship between microcalcifications detected before treatment and various clinical indicators across different molecular types in breast cancer patients undergoing neoadjuvant chemotherapy (NAC). In this retrospective study, clinical data from 178 breast cancer patients who underwent NAC, and 369 cases total, were analyzed. The patients were categorized into microcalcification and non-microcalcification groups according to mammography results. Statistical methods, including chi-square tests, t-tests, and nonparametric tests, were used to compare clinical variables across different molecular subtypes in the presence and absence of microcalcifications. Additionally, multivariate analyses and regression equations were used to determine the ability of microcalcifications to predict HER2-positive breast cancer. Significant differences were identified between breast cancer subtypes ($X2 = 14.129$, $p < 0.001$) and type of breast surgery ($X2 = 5.073$, $p = 0.024$). Patients with breast microcalcifications demonstrated a higher likelihood of achieving pathologic complete response (pCR) than those without microcalcifications ($p = 0.041$), particularly with the HER2-positive subtype, $p = 0.004$, odd ratio (OR) = 0.115, 95.0 % confidence interval (CI): 0.026–0.498). Conversely, patients with the basal-like subtype exhibited the opposite trend ($p = 0.002$, OR = 15.000, 95.0 % CI: 2.782–80.867). The results obtained from residual cancer burden (RCB) analysis were consistent with the pCR findings. Patients with the HER2-positive subtype exhibited the highest likelihood of developing breast microcalcifications ($X2 = 14.129$, $p < 0.001$). We employed a logistic regression equation to predict the probability of achieving pCR in HER2-positive breast cancer and achieved an overall prediction accuracy of 82.72 %. Breast microcalcifications are valuable predictors of NAC effectiveness, particularly with respect to molecular subtypes. Microcalcifications are associated with higher pCR rates and a lower RCB in HER2-positive breast cancer, but may reduce NAC efficacy in basal-like breast cancer. The predictive value of breast microcalcifications for NAC efficacy has crucial clinical implications for the treatment of HER2-positive breast cancer.

Keywords: Breast cancer; Mammography; Microcalcifications; Neoadjuvant therapy; Pathologic complete response; HER2-Positive; Basal-like

25COASMA9

Title: The recurrence outcome with respect to treatment choices in idiopathic granulomatous mastitis: A retrospective cohort study with 10-year single-center experience,

Ercument Gurluler, Kazim Senol,

Asian Journal of Surgery,Volume 48, Issue 5,2025,Pages 2927-2932,
https://doi.org/10.1016/j.asjsur.2025.01.062.

Abstract: This study aimed to investigate the recurrence outcome with respect to treatment choices in patients with idiopathic granulomatous mastitis (IGM). A total of 175 female patients (mean ± SD age: 36.3 ± 8.9 years) with histopathologically confirmed IGM were included in this retrospective cohort study. Data on patient age, presenting symptoms, treatment protocols (medical and/or surgery), the recurrence rate, recurrence-free survival (RFS) and progression-free survival (PFS) were recorded. RFS time (month) and PFS and time (month) were compared across medical treatment subgroups (antibiotic, steroid, steroid-sparing immunosuppressant). The treatment protocols involved surgery plus medical treatment in 82(46.9 %) patients, medical treatment alone in 82(46.9) and surgery alone in 11(6.2 %) patients. The medical treatment included the immunosuppressive therapy (42.1 %), antibiotic therapy (29.3 %) and steroid therapy (28.7 %). Within a median 36 months of follow-up, recurrence was noted in 64(39.5 %) patients and was significantly more common in the surgery plus medical treatment group than in the medical treatment alone group (53.7 % vs. 25.0 %, $p < 0.001$). Overall, median (95 % CI) RFS time and PFS time were 29(21.9–36.1) months and 12(5.8–18.2) months, respectively. No significant difference was noted between medical treatment subgroups in terms of RFS time (log-rank p value: 0.176) and PFS time (log-rank p value: 0.421). Nonetheless, immunosuppressive therapy showed a non-significant tendency for longer RFS (vs. steroid therapy) and longer PFS (vs. both antibiotic and steroid therapy). In conclusion, this retrospective cohort study in patients with IGM revealed the association of systemic therapy, particularly the steroid-sparing immunosuppressive treatment, with favorable long-term RFS and PFS outcome.

Keywords: Idiopathic granulomatous mastitis; Antibiotic; Steroid; Immunosuppressive; Recurrence-free survival; Progression-free survival

25COASMA10

Title: Pulmonary entrapping predicts occult diaphragmatic injury in blunt thoracic trauma with rib fractures,

Po-Chih Chang, Chao-Wen Chen, Yu-Wei Liu, Shah-Hwa Chou, Ting-Wei Chang, Hsien-Pin Li, Hung-Hsing Chiang,

Asian Journal of Surgery,Volume 48, Issue 5,2025,Pages 2859-2865,
https://doi.org/10.1016/j.asjsur.2025.01.093.

Abstract: Blunt thoracic trauma (BTT) often leads to rib fractures (RFs), with an increasing trend in surgical stabilization of rib fractures (SSRF) combined with thoracoscopic exploration, revealing previously underestimated occult diaphragmatic injuries (ODIs) that can result in hernias if not promptly addressed. We present our experience managing ODIs following BTT with complex RFs in a tertiary hospital in Southern Taiwan. We conducted a retrospective study including patients undergoing SSRF for BTT with complex RFs from

January 2018 to March 2024. We analyzed demographic data, trauma details, clinical presentations, intraoperative findings, radiological features, and attempted to identify predictive factors for ODIs using logistic regression analysis. We also reviewed previous case series on ODIs. We identified 11 ODIs, primarily detected during thoracoscopic exploration performed concurrently with SSRF (n = 8) or excessive bloody pleural effusion (n = 3). One hundred and twenty-two patients underwent SSRFs for their complex RFs simultaneously. All these patients with incidental ODI findings during SSRF for complex RFs underwent successful diaphragm repair via thoracoscopy. Multivariate logistic regression analysis revealed a significant association between trapped lung and ODI occurrence in patients undergoing SSRF after BTT (odds ratio: 24.423; 95 % confidence interval: 2.77–215.369; p = 0.004). Our findings emphasize the importance of considering pulmonary entrapment as a significant predictive factor for ODI after BTT with complex RFs. Routine thoracoscopy during SSRF is crucial for early detection and management of this rare condition.

Keywords: Blunt injury; Diaphragm; Fracture fixation; Rib fractures; Pulmonary entrapping; Thoracoscopy

25COASMA11

Title: White matter lesions in brain MRI and cardiovascular risk factors in sudden sensorineural hearing loss patients: A comparative study,

Shadman Nemati, Negar Hosseinpoor, Mehrgan Khanhakimi, Sima Fallah Arzpeyma, Mohammad Ebrahim Ghaffari, Seyed Hassan Mostafavi, Pejman Kiani, Alia Saberi,

American Journal of Otolaryngology, Volume 46, Issue 3,2025,104607,
https://doi.org/10.1016/j.amjoto.2025.104607.

Abstract: Sudden Sensorineural Hearing Loss (SSNHL) is an otologic emergency characterized by a rapid decrease in hearing threshold. The etiology of SSNHL is often unclear, with potential links to vascular pathologies. This study investigates the association between white matter lesions (WMLs) observed in brain MRI and cardiovascular risk factors in SSNHL patients. This case-control study involved 34 SSNHL patients and 34 matched controls, none of them had migraine. Both groups underwent pure tone audiometry and brain MRI. WMLs were assessed using the Fazekas scale. Cardiovascular risk factors, including hypertension, diabetes, dyslipidemia, BMI, and smoking, were documented. While none of the cardiovascular risk factors showed a significant difference between the two groups, the presence of WMLs was significantly higher in the SSNHL group compared to controls (79.4 % vs. 32.4 %; p < 0.001). More specifically, 24 patients (70.6 %) and 10 controls (29.4 %) had periventricular white matter (PVWM) lesions, while 20 patients (58.8 %) and 8 controls (23.5 %) had deep white matter (DWM) lesions. Logistic regression analysis revealed that increased grades of PVWM lesions were associated with a 5.7-fold higher likelihood of moderate or greater hearing loss (p = 0.033). The degree of DWM lesions, according to the Fazekas scale, demonstrated a significant correlation with hearing recovery rate.White matter lesions (WMLs) are significantly associated with sudden sensorineural hearing loss (SSNHL), with higher grades of PVWM lesions increasing the likelihood of severe hearing loss and DWM lesions correlating with hearing recovery. These associations seem to be independent of cardiovascular risk factors.

Keywords: Sudden sensorineural hearing loss; SSNHL; White matter lesions; WMLs; Fazekas scale; Cardiovascular risk factor

25COASMA12

Title: Endonasal dome bind with incorporation of a columellar strut reduces Infratip fullness: a quantitative photographic analysis,

Jeewanjot S. Grewal, Michael Diffley, Yitzchok Greenberg, Suma Alzouhayli, Kylie Springer, Richard Westreich, Robert H. Deeb,

American Journal of Otolaryngology, Volume 46, Issue 3,2025,104619,
https://doi.org/10.1016/j.amjoto.2025.104619.

Abstract: To demonstrate the effectiveness of the dome bind suture technique with incorporation of a columellar strut in reducing infratip lobule fullness in closed rhinoplasty by use of quantitative photographic analysis. A retrospective review of patients who underwent rhinoplasty by two senior authors was carried out. All surgical maneuvers were documented. Photographic analysis was performed quantitatively using Rhinobase software. Results were recorded as ratio of change relative to a stable anatomic reference. This was chosen as the intercanthal distance on frontal view and lateral canthus to lateral commissure distance on lateral view. Sixty-three patients were included who underwent the dome bind suture technique. On frontal view, the ratio of the infratip lobule on post-surgical images versus preintervention was 0.88, which represents a reduction of 12 % ($P < 0.01$). This was not apparent on lateral view, with a postoperative/preoperative ratio of 1.02 ($P = 0.53$). We have demonstrated that the endonasal dome bind technique with incorporation of a columellar strut is useful at reducing infratip lobule fullness on frontal view and is a valuable tool in the armamentarium of the rhinoplasty surgeon.

Keywords: Endonasal rhinoplasty; Closed rhinoplasty; Dome bind suture; Infratip fullness; Infratip lobule

25COASMA13

Title: Synchronous versus asynchronous delivery of concurrent chemotherapy and radiation for head and neck cancer: Does timing matter?,

Allen M. Chen, Meng Gan, Tjoson Tjoa, Yarah Haidar, William B. Armstrong,

American Journal of Otolaryngology, Volume 46, Issue 3,2025,104612,
https://doi.org/10.1016/j.amjoto.2025.104612.

Abstract: To evaluate the impact of variations in the timing of chemotherapy and radiation on clinical outcome for patients treated with concurrent chemoradiation for head and neck cancer. The medical records of 264 consecutive adult patients treated with concurrent cisplatin-based chemoradiation for squamous cell carcinoma of the head and neck were reviewed. Among these 187 patients (71 %) had chemotherapy and radiation commencing on the same day (“synchronous delivery”) and 87 patients had chemotherapy and radiation commencing on different days (“asynchronous delivery”). The 3-year actuarial estimates of overall survival (74 % vs. 76 %), progression-free survival (75 % vs. 75 %), and local-regional control (71 % vs. 73 %) were not significantly different between concurrent chemoradiation patients treated by synchronous and asynchronous delivery methods, respectively ($p > 0.05$, for all). Exploratory subset analysis using the 1, 3, 7, 10, and 14 day

cutoffs as thresholds for starting chemotherapy and radiation together demonstrated that patients who had greater than a 7 day gap between chemotherapy and radiation had significantly worse 3-year overall survival (63 % vs. 78 %, p = 0.01), progression-free survival (59 % vs. 77 %, p = 0.01), and local-regional control (65 % vs. 74 %, p = 0.02) compared to those whose treatment commencement occurred within 7 days, respectively. While the clinical repercussions of not starting concurrent chemotherapy and radiation on the same day are likely of minimal consequence for patients with head and neck cancer, efforts to start treatments within 7 days of one another are recommended.

Keywords: Chemoradiation; Head and neck; Cancer; Multidisciplinary; Coordination

25COASMA14

Title: Comparison of cartilage myringoplasty for repairing non-cholesteatomatous chronic perforation with mastoid cavity pneumatization and opacification,

Qinghua Wang, Ningyu Feng, Zhengcai Lou,

American Journal of Otolaryngology, Volume 46, Issue 3,2025,104621,
https://doi.org/10.1016/j.amjoto.2025.104621.

Abstract: The objective of this study was to compare the graft outcomes of cartilage myringoplasty for the repair of chronic otitis media (COM) with a complete ossicular chain between mastoid cavity pneumatization and opacification. Chronic perforations with non-cholesteatomatous COM were allocated to either mastoid cavity pneumatization (MCP) group and opacification (MCO) group. All patients underwent endoscopic cartilage underlay myringoplasty alone. The graft success rate, audiometric outcomes, soft tissue opacification change, and complications were evaluated at 12 months after surgery. The postoperative infection was 2.7 % patients in the MCP group and 8.1 % patients in the MCO group (P = 0.607). Overall graft success rates were 91.9 % in the MCP group and 89.2 % in the MCO group (P = 0.691). MCO group exhibited more deterioration in preoperative air conduction (AC) PTAs (P = 0.047) or pre-operative ABG (P = 0.039) compared with MCP group, while there were no significant differences between the groups in postoperative AC PTAs, BC PTAs, or ABGs. Nevertheless, MCO group exhibited better ABG gain compared with MCP group (21.2 ± 6.9 vs 13.8 ± 2.6 dB; P = 0.024). Temporal bone CT at postoperative 12 months revealed no change in opacification in 56.8 % patients and reduced opacification or complete pneumatization in 43.2 % patients in the CMO group. Also, none of the patients developed worsening sensorineural hearing loss or postoperative tinnitus. Myringoplasty alone did not affect the graft success rate in the patients with mastoid cavity pneumatization or opacification, however, in comparison, the patients with mastoid cavity opacification had a worse preoperative hearing but better postoperative hearing recovery. In addition, myringoplasty alone could improve the mastoid cavity opacification.

Keywords: Chronic otitis media; Mastoid cavity; Pneumatization; Opacification; Myringoplasty; Hearing gain

25COASMA15

Title: Investigation of vascularization patterns in juvenile Angiofibroma and the impact of preoperative embolization on surgical excision,

Hon Minh Hao Nguyen, Minh Tran Quang Le, Hai Thanh Nguyen, Hong Viet Tran, Luan Viet Tran,
American Journal of Otolaryngology, Volume 46, Issue 3,2025,104632,
https://doi.org/10.1016/j.amjoto.2025.104632.

Abstract: Juvenile nasopharyngeal angiofibroma (JNA) is a rare, highly vascular tumor posing a significant challenge for endoscopic excision due to excessive intraoperative bleeding. Exploring feeding vessels and preoperative embolization could reduce intraoperative blood loss and improve surgical outcomes for JNA. This study investigates the vascularization patterns of JNA and the impact of preoperative embolization on surgical excision. This was a descriptive cross-sectional study of 30 histopathologically confirmed JNA patients who underwent preoperative embolization followed by endoscopic surgical excision from January 2019 to May 2023 at Ear Nose Throat Hospital of Ho Chi Minh City. The distribution of vascular supply of tumors, as well as the role of preoperative embolization, were analyzed. Most tumors received exclusive blood supply from the internal maxillary artery (IMA) accounting for 50%, with 20% of cases being supplied by bilateral IMAs. A combined supply pattern involving the IMA and other external carotid artery branches was observed in 26.6%. Three complex cases (10%) received blood from the internal carotid artery (ICA). Embolization was performed at branches originating from the external carotid artery (ECA) but not from the ICA to avoid complications. All patients achieved complete endoscopic JNA excision. The average intraoperative blood loss was 608 mL (range: 100 mL - 3000 mL), and the average Boezaart score was 2.63. No major surgical complications occurred in the perioperative period. Significant differences in blood loss were observed among different UPMC tumor stages ($p < 0.001$) and tumor sizes ($p = 0.008$). Advanced-stage tumors were more likely to have an ICA blood supply ($p = 0.038$). Understanding the vascularization patterns of juvenile angiofibroma and the role of preoperative embolization can facilitate endoscopic excision of these tumors.

Keywords: Juvenile nasopharyngeal angiofibroma; Preoperative embolization; Transarterial embolization; UPMC tumor stages; Internal maxillary artery (IMA); External carotid artery (ECA); Internal carotid artery (ICA)

25COASMA16

Title: Expansion sphincter pharyngoplasty with cartilage implant in uvulopalatal flap for treatment of obstructive sleep apnea,

Fereshte Shenavayi, Shayan Dasdar, Hamed Amirifard, Reza Erfanian, Arezu Najafi, Nika Kianfar, Amin Amali, Shohre Ghasemi, Reihaneh Heidari,
American Journal of Otolaryngology, Volume 46, Issue 3,2025,104608,
https://doi.org/10.1016/j.amjoto.2025.104608.

Abstract: Uvulopalatopharyngoplasty and its modifications, including expansion sphincter pharyngoplasty, are the most common surgical interventions for obstructive sleep apnea. To introduce a novel surgery technique in which expansion sphincter pharyngoplasty was performed accompanied by inserting a cartilage implant into the palate. Adult patients required septoplasty and pharyngoplasty were selected. In intervention group, expansion sphincter pharyngoplasty was performed with the insertion of a cartilage implant, obtained from their septum into the uvulopalatal flap site. In control group, similar procedures were

performed except for cartilage insertion. Surgery outcome was assessed at the 3rd and 6th month post-operation by STOP-Bang Questionnaire (SBQ), Epworth Sleepiness Scale (ESS), and snoring level. Thirty-one individuals with a mean age of 36.9 ± 9.0 years, consisting of 27 (87.1 %) men, were recruited. At follow-ups sessions of intervention group (n = 16), the SBQ decreased from 3.94 ± 1.39 to 2.33 ± 1.11 and 1.80 ± 1.21 ($p < 0.001$), ESS decreased from 10.31 ± 5.52 to 5.20 ± 2.83 and 3.33 ± 1.76 ($p < 0.001$), and snoring level decreased from 2 to 1 and 1 ($p < 0.001$). In control group (n = 15), the SBQ decreased from 4.23 ± 0.60 to 2.38 ± 0.96 and 2.08 ± 1.11 ($p < 0.001$), ESS decreased from 13.08 ± 5.88 to 7.69 ± 4.27 and 5.69 ± 4.05 ($p < 0.001$), and snoring level decreased from 3 to 2 and 1 ($p < 0.001$). Between group comparison indicated that ESS was marginal at the second follow-up ($p = 0.051$), and the snoring level was significantly different at first ($p = 0.019$) and second ($p = 0.031$) follow-ups. Performing expansion sphincter pharyngoplasty with a cartilage implant in selected individuals improved surgery outcome.

Keywords: Obstructive sleep apnea; Snoring; Palatopharyngoplasty; Palatal implant; Cartilage; Septoplasty

25COASMA17

Title: A geographical comparison between head & neck cancer incidence and distribution of otolaryngologists,

Henry C. Ideker, Ahmad Odeh, Angela Mazul, Sean T. Massa,
American Journal of Otolaryngology, Volume 46, Issue 3,2025,104625,
https://doi.org/10.1016/j.amjoto.2025.104625.

Abstract: The incidence of head and neck cancer (HNC) is increasing, and research is needed to identify and treat populations at higher risk. The Surveillance, Epidemiology, and End Result (SEER), Area Health Resource File (AHRF), and American Community Survey (ACS) databases were queried for incidence of HNC, provider demographics, and county demographics, respectively. The primary outcome was county-level incidence rate. Multivariate analysis of county variables identified risk factors associated with higher incidence. The geographic incidence of HNC is unequally distributed with higher incidence in counties with older age (3.68 % increase, CI: 3.46–3.89 %), white (1.71 %, CI: 1.08–2.35 %) and black (1.20 %, CI: 0.40–2.00 %) race, and higher percentage of smokers (1.36 %, CI: 1.17–1.55 %). The otolaryngology workforce was inversely related to the county-level incidence. Compared to counties with no Otolaryngologist, those with 11+ had 41.5 % (39.7–43.4 %) lower incidence. The otolaryngology workforce is not optimally distributed to address geospatial variation in HNC incidence.

Keywords: Head and neck cancer; ENT cancer; ENT as post graduate career; Population demographic studies; Disparities

25COASMA18

Title: Systematic review and meta-analysis of the correlation between tinnitus and mental health,

Yuyang Jiang, Qiang Liu, Yi Ding, Yongdong Sun,
American Journal of Otolaryngology, Volume 46, Issue 3,2025,104611,
https://doi.org/10.1016/j.amjoto.2025.104611.

Abstract: This paper assesses the correlation between tinnitus and mental health, including depression, anxiety, stress, insomnia, and suicide through meta-analysis. Web of Science, Embase, PubMed, and Cochrane databases were searched until January 2024. After article screening, data extraction, and quality evaluation, meta-analysis was performed using Stata 15.1. 22 papers were enrolled, including 5 case-control studies, 8 cohort studies, and 9 cross-sectional studies. Meta-analysis uncovered that tinnitus was associated with depression (OR = 1.92, 95 % CI: 1.56, 2.36), anxiety (OR = 1.63, 95 % CI: 1.34, 1.98), stress (OR = 1.17, 95 % CI: 1.01, 1.36), insomnia (OR = 3.07, 95 % CI: 2.36, 3.98), and suicide (OR = 5.31, 95 % CI: 4.34, 6.51). A correlation is indicated between tinnitus and mental health. Therefore, it is critical to incorporate psychological interventions in tinnitus treatment and to implement a comprehensive treatment program.
Keywords: Tinnitus; Mental health; Depression; Anxiety; Stress; Insomnia; Suicide; Meta-analysis

25COASMA19

Title: Effect of palatoplasty technique on otologic outcomes in children with cleft palate,

Shaina W. Gong, Paul Hung, Chioma G. Obinero, Jose Barrera, Zi Yang Jiang, Matthew R. Greives, Zhen Huang,

American Journal of Otolaryngology, Volume 46, Issue 3,2025,104610,
https://doi.org/10.1016/j.amjoto.2025.104610.

Abstract: In patients with cleft palate (CP), the impact of primary palatoplasty technique on otologic outcomes remains a major point of contention. While some studies report improved outcomes after certain techniques of palatal repair, there is a lack of consensus on the most effective procedure. We sought to characterize the effects of primary palatoplasty technique on otologic outcomes in children with CP. A single institution retrospective review of patients with CP who underwent primary palatoplasty (straight-line repair or Furlow Z-plasty) was performed. Primary outcomes of interest included time to placement of T-tubes, number of tympanostomy tube placements, tympanic membrane (TM) perforation, and 3-year and 6-year postoperative hearing thresholds. A total of 140 patients were included in this study. The mean number of tympanostomy tube placements in the straight-line repair group (1.93 ± 1.28) was significantly higher than in the Furlow Z-plasty group (1.42 ± 1.03, $p = 0.03$). Median time from primary palate repair to T-tube placement was 38.93 (IQR 33.03) months. Higher birth weight ($p < 0.01$) and multiple tympanostomy tube placements ($p < 0.05$) were associated with longer time to T-tube placement. T-tube replacement was associated with a 16.9 times higher likelihood of TM perforation ($p < 0.05$). The median PTA significantly improved from 16.25 (IQR 7) dB at 3 years to 11.00 (IQR 5.25) dB at 6 years ($p < 0.01$). Furlow palatoplasty technique was associated with fewer number of tympanostomy tube placements; however, palatoplasty technique did not significantly impact time to T-tube placement, TM perforation, or hearing outcomes. There were no significant differences in long-term hearing outcomes between patients who underwent Furlow Z-plasty and those who had straight-line repair. Most patients achieved normal hearing thresholds by 6 years after primary palatoplasty and tympanostomy tube placement. These are important considerations to discuss when counseling patients' families on surgical management of CP and otologic outcomes.

Keywords: Cleft palate; Otologic outcome; Palatoplasty technique; Hearing outcome

25COASMA20

Title: Impact of ipsilateral false vocal fold resection on swallowing following transoral laser cordectomies — A fibreoptic endoscopic evaluation of swallowing study,

A. Burián, K. Smatanová, T. Bocskai, János Girán, I. Szanyi,

American Journal of Otolaryngology, Volume 46, Issue 3, 2025, 104622,
https://doi.org/10.1016/j.amjoto.2025.104622.

Abstract: To investigate early and late impact of false vocal fold removal (vestibulectomy) on swallowing using FEES following type III, IV and V transoral laser cordectomies (TLC). Fifteen transorally resectable glottic cancers (10 T1a, 2 T1b, 2 T2, 1 selected T3) necessitating TLC with vestibulectomy were included. All participants underwent TLC in the investigation period. FEES was performed preoperatively and in the early and late postoperative period establishing modified penetration-aspiration scale (mPAS) and pharyngeal residue severity scale (PRSS) to statistically assess possible differences among the investigated timepoints. Laryngeal preservation and local recurrence were also noted. 2 type III, 9 type IV, 2 type Va and 2 type Vd cordectomies were performed. Early postoperative mPASs changed significantly compared to preoperative status ($p = 0.046$). Difference between early and late postoperative mPASs was also significant ($p = 0.046$). There was no difference between preoperative and late postoperative mPASs ($p = 1.0$). Regarding pharyngeal residue, significant changes were noted in the early postoperative period compared to preoperative values ($p = 0.002$). Regarding late postoperative PRSSs, statistically significant decline was found compared to early postoperative scores ($p = 0.004$). No remarkable difference was found between preoperative and late postoperative PRSSs ($p = 0.317$). Laryngeal preservation failed in only one case due to recurrence. In our serie, ipsilateral vestibulectomy during TLC did not deteriorate swallowing in the long term neither by increased pharyngeal residue nor by increased aspiration risk. Investigation of cases without co-morbidities may further confirm our observations. Nevertheless, TLC provided excellent laryngeal preservation.

Keywords: Aspiration; Cordectomy; False vocal fold; FEES; Vestibulectomy

25COASMA21

Title: Minimally invasive surgery for hyperacusis-enhanced round and oval window reinforcement procedure,

Herbert Silverstein, Neil Nayak, Sean Holmes, Allen Young, Kadie Nausha,

American Journal of Otolaryngology, Volume 46, Issue 3,2025,104615,
https://doi.org/10.1016/j.amjoto.2025.104615.

Abstract: Hyperacusis is an audiological disorder in which patients become persistently sensitive and intolerant to everyday environmental sounds. Patients suffering from hyperacusis not only experience pain and discomfort, but also undergo impairments in social, occupational, recreational, and day-to-day activities, resulting in poor quality of life. Previously, a senior author (HS) reported a minimally invasive surgical technique to help hyperacusis patients via reinforcement of the oval and round windows with temporalis fascia (Silverstein, 2015). In a recent publication (Young, 2024), patients with (Loudness

Discomfort Level) LDLs above 70 dB had an 80.1 % satisfaction with the round and oval window reinforcement and would recommend the surgery. However, in the group of patients whose LDLs were below 70 dB indicating extreme hyperacusis only 49 % were satisfied and would recommend the surgery. To improve the results, a modification of the original technique was used by enhancing the reinforcement in patients with severe hyperacusis. Enhanced reinforcement of the oval and round windows and tympanic membrane resulted in a superior reduction in hyperacusis symptoms.

Keywords: Hyperacusis; Enhanced oval and round window reinforcement; Decreased noise intolerance

25COASMA22

Title: Elastic scattering spectroscopy for intraoperative oral cancer mucosal margin guidance: Initial results from a 104 patient cohort,

G.P. Krisciunas, E. Rodriguez-Diaz, L. Berry, G. Spokas, O.M. A'Amar, M. Couey, H. Edwards,

American Journal of Otolaryngology, Volume 46, Issue 3,2025,104605,
https://doi.org/10.1016/j.amjoto.2025.104605.

Abstract: To assess Elastic Scattering Spectroscopy (ESS) classification accuracy of benign vs malignant tissue obtained during intra-operative oral cancer resection. The study comprised 104 patients with a biopsy positive for oral cancer (N = 85) or dysplasia (N = 19) who were scheduled to undergo surgical excision. ESS measurements were obtained intraoperatively on and immediately adjacent to the lesion within the planned resection margin prior to excision, and on contralateral normal-site control tissue. Two-millimeter biopsies were obtained from tumor and margin tissue. All measurements were evaluated using Leave One Person Out (LOPO) AI-assisted statistical algorithms. Three analyses evaluated ESS diagnostic accuracy: one at the sample level, one at the pooled sample patient level, and one using only diagnostically variable biopsy co-registered margin samples. Statistical analyses included sensitivity, specificity, negative predictive value (NPV), positive predictive value (PPV), and Area Under the Receiver Operating Characteristic Curve (AUC-ROC). Diagnostic accuracy at the sample level yielded sensitivity = 82 %, specificity = 84 %, and AUC = 0.91. Pooling samples within each patient yielded sensitivity = 94 %, specificity = 87 %, and AUC = 0.95. Sample level diagnostic accuracy at the margin yielded sensitivity = 76 %, specificity = 50 %, and AUC = 0.70, but prioritizing sensitivity, yielded a sensitivity = 90 %, specificity = 30 %, with AUC = 0.70. The ESS device demonstrated high sensitivity and appropriate specificity when differentiating benign from malignant tissue. Discriminant ability increased when samples were pooled within patients, informing future protocols for evaluating intraoperative ESS measures. These data are very promising and support the contention that ESS could be a valuable adjunct tool that facilitates comprehensive and efficient assessment of surgical margins.

Keywords: Elastic scattering spectroscopy; Machine learning; Non-invasive diagnostics; Oral cancer; Margin guidance

25COASMA23

Title: Association of nasal surgery with olfactory function among older adults,

Khamis T. Suleiman, Richard G. Chiu, Sharmilee M. Nyenhuis, Kamal Eldeirawi, Victoria S. Lee,
American Journal of Otolaryngology, Volume 46, Issue 3,2025, 104638,
https://doi.org/10.1016/j.amjoto.2025.104638.
Abstract: Olfactory Dysfunction (OD) is a prevalent condition that commonly presents in the older adult population. Various factors have been shown to contribute to OD, such as neurodegenerative disease, older age, and smoking status; however, the influence of nasal surgery on olfactory function is not well delineated. This study seeks to explore the potential effect of nose surgery on olfactory function. This cross-sectional study was conducted on data for 2285 adults from Round 1 of the National Social Life, Health, and Aging Project (NSHAP), a nationally representative sample of US older adults. The 5-item Sniffin' Sticks test was used to define olfactory function: correctly identifying ≥4 odors indicated normal olfactory function, while correctly identifying 0–3 odors was considered OD Associations between prior nasal surgery and OD were assessed using multivariable logistic regression, and adjusted odds ratios (OR) were calculated. Analyses were weighted using NSHAP-provided person-level weights to account for sampling design. OD was present in 18.4 % of adults. The weighted average age was 67.1 ± 7.2 years among those with normal olfaction and 70.9 ± 7.9 years for those with OD. Of adults with OD, 9.8 % had a prior nasal surgery as compared to 8.1 % of those with normal olfaction, although the difference was not statistically significant. After adjusting for age, gender, race, education, prior stroke, dementia, and self-reported mental health, prior nasal surgery was not significantly associated with OD (OR: 1.14; 95 % CI: 0.77–1.70). Prior nasal surgery was not associated with OD after controlling for covariates. While this study does provide unique insight into the relationship between nasal surgery and OD in nationally representative cohort of older adults, it was limited since the dataset utilized did not contain information on the specific surgery that participants underwent. Therefore, further research with more detailed information on the types of nasal surgeries and sinonasal conditions prior to surgery would further help elucidate the relationship between and nasal surgery and OD.
Keywords: Olfactory function; Nasal surgery; Older adults; Smell impairment; National Social Life, Health, and Aging Project (NSHAP)

25COASMA24

Title: Subtraction CT Improves Detectability of Mandibular Bone Invasion in Oral Squamous Cell Carcinoma,

Mukaigawa, Takashi and Asakura, Koiku and Tsuzuki, Ayaka and Urikura, Atsushi and Yoshida,
The Laryngoscope, volume = 135, number = 5, pages = 1706-1714,
https://onlinelibrary.wiley.com/doi/abs/10.1002/lary.31946,
Abstract: Objective Pretreatment evaluation of bone invasion in head and neck cancer is critical for treatment strategies. We investigated the usefulness of subtraction CT (SCT) in evaluating mandibular bone invasion in oral squamous cell carcinoma (OSCC). Methods This retrospective investigation included patients with OSCC who underwent surgery at the Shizuoka Cancer Center Hospital between 2018 and 2022. We evaluated tumor invasion of the mandibular bone by interpreting conventional computed tomography (CT), SCT, and

magnetic resonance imaging (MRI) and comparing the findings with the pathological examination. Sensitivity and specificity were compared using the McNemar test, whereas Spearman's correlation and Bland–Altman methods were utilized to assess mandibular bone invasion depth. Results A total of 71 patients were enrolled. SCT showed significantly higher sensitivity than conventional CT for evaluating mandibular marrow invasion (97.2\% vs. 80.6\%, $p = 0.031$). In the evaluation of mandibular canal involvement, SCT showed significantly higher specificity than MRI (95.9\% vs. 81.6\%, $p = 0.016$). Furthermore, SCT demonstrated the highest correlation with pathological bone invasion depth (correlation coefficients: CT = 0.933, SCT = 0.950, MRI = 0.908; all $p < 0.05$). Conclusion These results suggest that SCT is more effective than conventional imaging for diagnosing mandibular bone invasion and may be a useful modality for the pretreatment diagnosis of head and neck cancer.

Keywords: clinical research, head and neck, imaging, oral cavity, subtraction CT,

25COASMA25

Title: Effects of Rurality, Socioeconomic Status, and Race on Head and Neck Squamous Cell Carcinoma Outcomes,

Torres-Small, Sofia and Davies, Camron and Kumsa, Fekede Asefa and Maroda, Andrew and Shaban-Nejad,

The Laryngoscope, volume = 135, number = 5, pages = 1715-1723,
https://onlinelibrary.wiley.com/doi/abs/10.1002/lary.31954,

Abstract: Objective To examine how rural residence interacts with SES and race/ethnicity relative to Head and neck squamous cell carcinoma (HNSCC) treatment delay and outcomes. Methods The SEER database was queried for patients aged ≥18 with HNSCC. Out of 164,337 cases, 126,052 remained after exclusions for missing data. Statistical tests performed included Chi-squared tests, log-binomial regression models, and parametric accelerated failure time (AFT) models, with a significance level of $\alpha < 0.05$. Results About 38\% of patients residing in lowest SES census tracts were rural, whereas over 98\% of patients from highest SES tracts were urban. Delayed treatment was associated with shorter median survival [aTR = 0.968, 95\% confidence interval (CI): 0.939, 0.999]. Risk for treatment delay increased with decreasing SES and was greater for those with minoritized race/ethnicity status. Rurality was associated with a lower risk [aRR: 0.917, 95\% CI: 0.892, 0.946] of treatment delays but was not predictive for patient survival (aTR: 1.019 [0.978, 1.061]). Cancer-specific mortality increased with decreasing SES and was higher in patients with minoritized race/ethnicity status. Conclusion Rurality was associated with decreased risk for treatment delay but not with worse survival relative to urban residence, whereas low SES and minority status remained predictive for poor outcome regardless of geographic context (level of evidence: 4). Although these findings argue against HNSCC survival deficits specific to rural populations, there remains concern regarding potential care shortfalls in rural populations not detected in this sample. Confirmatory patient-level analysis should be prioritized to optimize support along the rural/urban divide.

Keywords: head and neck cancer, health disparities, rurality,

25COASMA26

Title: Tunneled Submental Island Flap for Reconstruction of Endoscopic Nasopharyngectomy Defects,

Vuncannon, Jackson R. and Rodas, Alejandra and Daoud, Georges E. and Soriano, Roberto M. and Kaka, Azeem S. and Solares, C. Arturo,

The Laryngoscope, volume = 135, number = 5, pages = 1697-1701,

https://onlinelibrary.wiley.com/doi/abs/10.1002/lary.31931,

Abstract: Endoscopic nasopharyngectomy in the context of recurrent nasopharyngeal carcinoma may require reconstruction with strongly vascularized flaps. This is fundamental to address the volumetric deficit and prevent complications such as carotid blowout syndrome. The submental island flap is well suited for this purpose.

Keywords: nasopharyngectomy, submental artery island flap, skull base reconstruction,

25COASMA27

Title: Serum S100A8/A9 Correlates to Surgery-Free Interval in Idiopathic Subglottic Stenosis,

Mafla, Laura M. and So, Raymond J. and Abd-Elazem, Ibrahim and Collins, Samuel L. and Chan-Li, Yee and Lilly, Gabriela and Lina, Ioan A. and Gelbard, Alexander H. and Hillel, Alexander T. and Motz, Kevin M.,

The Laryngoscope, volume = 135, number = 5, pages = 1724-1731,

https://onlinelibrary.wiley.com/doi/abs/10.1002/lary.31934,

Abstract: Objective Idiopathic subglottic stenosis (iSGS) is a progressive fibrotic condition of the subglottis that presents in women of northern European descent. Endoscopic dilation is a common surgical approach to management of iSGS. The surgery-free interval, or the time between endoscopic dilation procedures is considered an indicator of disease severity. Variations in surgery-free intervals among iSGS patients underscore the necessity for prognostic biomarkers. The objective of this study was to explore serum levels of the damage-associated molecular pattern S100A8/A9 as a prognostic biomarker in iSGS. Methods Serum from 20 iSGS patients and eight healthy controls was collected and S100A8/A9 levels were quantified using an ELISA. Patient data, including demographics and surgery-free intervals, were obtained from medical records. Serum S100A8/A9 levels were compared to surgery-free intervals. S100A8/A9 was also assessed using gene expression and immunofluorescence in iSGS specimens. Results S100A8/A9 was significantly elevated ($p = 0.0413$) in the serum of iSGS patients compared to controls (312.75 vs. 181.49 ng/mL). Linear regression analysis revealed a correlation ($p = 0.009$) between S100A8/A9 levels and endoscopic surgery-free interval. S100A8/A9 was significantly elevated ($p = 0.0011$) in patients with surgery-free intervals less than 1 year (455.2 ± 60.45 ng/mL; $n = 8$) compared to patients with intervals over 1 year ($292.5.93 \pm 162.4$; $n = 6$). Conclusion S100A8/A9 is increased in the serum and tissue of patients with iSGS. In this cohort of iSGS patients, serum S100A8/A9 was associated with surgery-free intervals, potentially representing a prognostic biomarker. Further research within a larger cohort is needed to confirm these findings.

Keywords: idiopathic subglottic stenosis, laryngotracheal stenosis, S100A8/A9, surgery-free interval,

25COASMA28

Title: Inter-rater and Intra-rater Reliability of Glottal Image Capture: A Mobile Application to Quantify Vocal Fold Bowing,

Aboueisha, Mohamed and Jaleel, Zaroug and Baertsch, Hans C. and Sauder, Cara and Merati, Albert L. and Johns, Michael M. and Bhatt, Neel K.,

The Laryngoscope, volume = 135, number = 5, pages = 1732-1736,
https://onlinelibrary.wiley.com/doi/abs/10.1002/lary.31942,

Abstract: Background Age-related vocal atrophy (ARVA) causes vocal fold bowing, impacting communication and quality of life. The assessment of vocal fold bowing is largely subjective. Glottal Image Capture (GlottIC) is a new mobile application that helps quantify vocal fold bowing. We aim through this study to assess its reliability, compare it to manual calculation method, and compare differences between visual-perceptual bowing severity ratings. Methods Ten raters independently quantified Bowing Index (BI) using GlottIC from 10 videostroboscopic images among individuals with ARVA. There was 100\% duplication of images to facilitate intra-rater reliability analyses using Pearson's correlation. Inter-rater reliability was quantified using Intraclass Correlation Coefficient (ICC) for experienced and novice raters. The correlation between manual calculations using ImageJ and GlottIC was analyzed. Results The intra-rater reliability for total BI was strong ($r = 0.822$, $p < 0.001$). The inter-rater reliability for BI, calculated using ICC, was (ICC = 0.720; 95\% CI: 0.579–0.852), indicating good consistency among the raters. Experts had higher ICC (ICC = 0.808; 95\% CI: 0.678–0.906) compared to novice raters (ICC = 0.651; 95\% CI: 0.468–0.816). There was a positive correlation between GlottIC and manual BI ($r = 0.811$, $p < 0.001$). As the BI increased, the bowing severity, based on visual-perceptual ratings, also increased ($p < 0.001$). Conclusion GlottIC is a reliable mobile application that can quantify vocal fold bowing in patients with ARVA with high intra- and inter-rater reliability. GlottIC BI measurments are highly correlated with manual BI and visual-perceptual ratings of bowing severity. Further improvements in reliability may be achieved with more robust rater training and automated technologies.

Keywords: aging larynx, Bowing Index, quantification of vocal fold measures, vocal fold atrophy,

25COASMA29

Title: Using High-Speed Videoendoscopy to Analyze Laryngeal Closure Parameters During Normal Swallow,

Howell, Rebecca J. and Mira, Amna S. and Llico, Andres and McKenna, Victoria S.,

The Laryngoscope, volume = 135, number = 5, pages = 1737-1743,
https://onlinelibrary.wiley.com/doi/abs/10.1002/lary.31945,

Abstract: Objective This pilot study was designed to test the tolerability of a lower scope position and feasibility of custom-designed MATLAB graphical user interface (GUI) used to analyze playback review of laryngeal high-speed videoendoscopy (laryngeal HSV) during healthy volitional dry swallows. We hypothesized this method would conceptually provide time resolution for glottic closure events compared with standard (30 frames per second, fps), and enable a means to measure timing, sequence, and duration of laryngeal movements during swallowing not otherwise visualized. Methods A total of 14 healthy adults (4 male,

22–80 years) participated. We performed laryngeal HSV at 500fps. Measurements included: (i) feasibility and tolerability of the procedure; (ii) identification of a swallowing segment of interest (SOI) for the peak of the swallow; and (iii) description of laryngeal swallowing movements using a GUI. Results Fourteen subjects tolerated the procedure without discomfort and swallow images were able to be analyzed in 12. Using our GUI, mean SOI was 260 ms, yielding 130 frames for analysis (compared with seven in standard laryngoscopy). Vocal fold adduction, vocal fold medialization, and anterior–posterior arytenoid compression to the epiglottis prior to whiteout could be identified and sequenced. Conclusion Participants tolerated a low position of the endoscope during dry volitional swallows. The output of our GUI demonstrated a novel technique for identifying, describing, and sequencing a swallowing SOI. Future studies should investigate laryngeal closure and arytenoid positioning with a bolus and in a range of ages, genders, and etiologies in both healthy and abnormal populations to better understand swallowing physiology.
Keywords: deglutition, HSV, Laryngeal high-speed videoendoscopy, normal swallow, swallowing physiology,

25COASMA30

Title: Correction of Lower Lip Malposition With Fascia Lata Slings Following Anterior Mandibular Resection,

Shahzad, Farooq and Cracchiolo, Jennifer and Allen Jr, Robert J. and Nelson, Jonas A. and Matros, Evan,

The Laryngoscope, volume = 135, number = 5, pages = 1702-1705,
https://onlinelibrary.wiley.com/doi/abs/10.1002/lary.31987,

Abstract: Lower lip malposition can occur after anterior mandibular resection as a result of the loss of soft tissue lip attachments. We report our technique of cranial suspension of the lower lip with fascia lata slings to improve lip position. Correction of lip ptosis results in cessation of drooling, improved oral intake, and restoration of facial aesthetics. **Keywords:** Cranial, Fascia Lata, Lip Incompetence, Lower lip, Malposition, Mandible, Mandibulectomy, Suspension,

25COASMA31

Title: Nationwide Survey on Incidence and Management of Recurrent Respiratory Papillomatosis in Japan,

Murono, Shigeyuki and Kawase, Tomotaka and Matsuzaki, Hiroumi and Hasegawa, Tomohiro and Kurakami,

The Laryngoscope, volume = 135, number = 5, pages = 1744-1751,
https://onlinelibrary.wiley.com/doi/abs/10.1002/lary.31932,

Abstract: Objectives To investigate the incidence, laryngeal distribution, management, and postoperative clinical course of patients with newly diagnosed adult-onset recurrent respiratory papillomatosis (RRP) in Japan. Methods An initial brief questionnaire was sent to 782 institutions, including all 101 core and 627 collaborating institutions providing board certification programs accredited by the Japanese Society of Otorhinolaryngology-Head and Neck Surgery. A detailed questionnaire regarding patient age, sex, Derkay's score, surgery, and postoperative clinical course was sent to 196 institutions caring for patients with either

newly or previously diagnosed RRP. Results A total of 186 patients with newly diagnosed adult-onset RRP from 78 institutions were identified during the present study period (2018–2019), suggesting an annual incidence of 0.20 per 100,000 population in Japan. The true vocal folds were the most frequently affected subsites in the larynx, followed by the false vocal folds, anterior commissure, and laryngeal surface of the epiglottis. The use of cold instruments was the most preferred surgical approach, followed by the carbon dioxide laser and microdebrider. A significant difference in recurrence-free period after the initial surgery was observed between patients with lesions in a single region and those with lesions in multiple regions ($p = 0.001$). Conclusion Here, we estimated the annual incidence of adult-onset RRP for the first time in Japan. To the best of our knowledge, the present study is the largest to identify the laryngeal distribution of lesions, as well as postoperative outcomes after initial surgery in newly diagnosed adult-onset RRP patients.

Keywords: incidence rate, laryngeal distribution, management and outcome, nationwide survey, recurrent respiratory papillomatosis,

25COASMA32

Title: Does the TruBlue Laser Set Microlaryngoscopy Equipment on Fire? A Systematic Evaluation,

Roitman, Ariel and Lunga, Tadeas and Venkatraman, Anumitha and Schroeder, Kristopher M and Thibeault, Susan L and Dailey, Seth H,

The Laryngoscope, volume = 135, number = 5, pages = 1752-1758,
https://onlinelibrary.wiley.com/doi/abs/10.1002/lary.31943,

Abstract: Introduction The risk of fire during laser microlaryngoscopy is well known. However, limited information is available about fire risk with the novel TruBlue laser. This study systematically evaluates its interactions with common surgical supplies, offering valuable insights into safety considerations for surgeons. Material and Methods We used experimental conditions to test the extent to which TruBlue laser energy produces smoke, perforation, or fire in Rüsch®, Medtronic™ and microlaryngeal endotracheal tubes and in surgical pledgets. Results Only the Microlaryngeal Tube (MLT) caught fire. Notably, it happened only when the laser fiber shifted on the tube's surface. Smoke emerged solely from the laser fiber applied to the Medtronic™ shaft and only during continuous contact mode. Cuff perforation and smoke emanating from the shaft occurred in three-quarters of the Rüsch® trials. The pledgets' radiopaque segment exhibited a greater combustibility than other segments ($p < 0.01$). In many of the pledget trials, faster smoke emission occurred with shorter laser-to-target distances ($p < 0.05$). Water-soaked pledgets displayed a reduced rate of smoke production ($p < 0.01$) and string division. Conclusion The Medtronic™ tube assures remarkable safety with a nonignitable shaft and low cuff ignition. The MLT poses the highest ignition risk. Cuff perforation risk is mitigated by maintaining a 0.3-cm distance from the laser fiber tip. Pledget fire risk is mitigated by positioning the radiopaque part away from the laser beam and by soaking the pledget with water. Laser division of the pledgets' string was common.

Keywords: airway surgery, experimental study, fire risk, microlaryngoscopy, surgical supplies, TruBlue laser,

25COASMA33

Title: Churg-Strauss Syndrome: A Case of Laryngeal Presentation,

Serafini, Edoardo and Basso, Margherita and Lupi, Massimo and Marchioni, Daniele and Mattioli, Francesco,

The Laryngoscope, volume = 135, number = 5, pages = 1771-1773,
https://onlinelibrary.wiley.com/doi/abs/10.1002/lary.31935,

Abstract: Eosinophilic granulomatosis with polyangiitis (EGPA), among various organs and systems, can affect the upper respiratory tract. The otolaryngologist must be able to suspect the pathology with the appearance of the first signs and recognize its late complications. Laryngeal involvement is rare and difficult to diagnose. A patient suffering from Churg-Strauss syndrome developed posterior glottic stenosis 5 years after diagnosis. A biopsy of the lesion confirmed the localized recurrence of EGPA. Rituximab therapy prevented further relapse after 12 months of follow-up. In the current literature, only two case reports, both pediatric, deal with laryngeal organic manifestation of the disease. Nonspecific findings, such as corditis or dysphonia, may be found in patients with EGPA in up to 25\% of cases. Thus, even though primary laryngeal manifestation is rare, inflammation can be a common finding. The case herein reported appears to be the first organic Churg Strauss syndrome laryngeal manifestation in an adult patient.

Keywords: eosinophilic granulomatosis with polyangiitis, larynx, posterior glottic stenosis, rituximab,

25COASMA34

Title: Laryngeal Findings in a 20-Month-Old With Cri du Chat Syndrome,

Braunstein, Doris and Jones, Holly and Heffernan, Colleen,

The Laryngoscope, volume = 135, number = 5, pages = 1774-1776,
https://onlinelibrary.wiley.com/doi/abs/10.1002/lary.31941,

Abstract: Laryngeal anatomical variations in Cri du Chat syndrome remain incompletely characterized in the medical literature, with few published photographic documentations. We present a case of a 20-month-old male with confirmed 5p15 deletion who presented with congenital inspiratory stridor and dysphagia. Videofluoroscopic evaluation at 13 months demonstrated aspiration of thin liquids. Microlaryngobronchoscopy revealed a Cormack-Lehane grade 3 view with a retroflexed epiglottis secondary to tight aryepiglottic folds, and laterally positioned false vocal cords resulting in broad, flat ventricles. Bilateral aryepiglottic fold division improved direct laryngoscopic visualization to Cormack-Lehane grade 1. This report provides detailed laryngeal characterization with photographic documentation, contributing to the understanding of airway variations in this syndrome. Recognition of these anatomical features is crucial for optimizing airway management strategies in this patient population.

Keywords: congenital laryngeal anomalies, congenital stridor, Cri du Chat syndrome, pediatric airway management, pediatric otolaryngology,

25COASMA35

Title: Lobectomy vs Sublobar Resection in The Society of Thoracic Surgeons Database: Importance of Patient Factors and Lymph Node Evaluation,

Gavitt A. Woodard, Maria Grau-Sepulveda, Mark W. Onaitis, Brooks V. Udelsman, Elizabeth A. David
The Annals of Thoracic Surgery, Volume 119, Issue 5, 2025, Pages 1071-1081,
https://doi.org/10.1016/j.athoracsur.2025.01.004.
Abstract: Prospective randomized trials have demonstrated noninferior survival between sublobar resection and lobectomy in healthy patients with non-small cell lung cancer with tumors ≤2 cm. However, some patient attributes are not well represented in randomized trials, and uncertainty remains in the widespread applicability of randomized trial nodal dissection protocols. Patients with ≤2 cm, node-negative non-small cell lung cancer (cT1 N0) in The Society of Thoracic Surgeons prospective database were linked to Medicare survival data by using a probabilistic matching algorithm. Survival was assessed by propensity score–weighted Kaplan-Meier analysis. Overall, 20,031 patients were identified, including 11,976 patients who underwent lobectomy, 2586 who underwent segmentectomy, and 5469 who underwent wedge resection. Fewer lymph nodes were sampled in the sublobar resection group (mean, 5.5 vs 12.8), and pathologic upstaging was less common (7.1% vs 14.2%). Overall survival after sublobar and lobar resection was similar within groups understudied in recent trials, including age ≥75 years (P = .07), forced expiratory volume in 1 second of 10% to 59% (P = .14), and Zubrod performance status 2 to 3 (P = .23). When sublobar resection was performed with inadequate nodal evaluation (<2 nodes removed), survival was inferior to survival after lobectomy (P < .001). Among patients with nodal upstaging, lobectomy was not associated with improved survival over sublobar resection (P = .42). The clinical trial finding that sublobar resections achieve survival similar to that seen with lobectomy in early-stage lung cancer appears to apply to older, less healthy patients in a real-world setting, provided adequate lymph node resection is performed. Performing a lobectomy in the setting of nodal upstaging does not obviously improve survival. Further study is warranted to clarify the role of sublobar resection in the general population.

25COASMA36

Title: Minimally Invasive Valve Surgery for Patients With Infective Endocarditis: A Comparative Study,

Connor Raikar, Stanley Wolfe, Luigi F. Lagazzi, Ali Darehzereshki, Nathan Kister, Lawrence Wei,
The Annals of Thoracic Surgery, Volume 119, Issue 5,2025,Pages 1020-1026,
https://doi.org/10.1016/j.athoracsur.2025.01.023.
Abstract: Patients with endocarditis frequently require valve surgical procedure, and despite the recent growth of minimally invasive cardiac surgery (MICS) for complex valve operations, consensus recommendations still suggest conventional sternotomy. The institutional Adult Cardiac Surgery Database of The Society of Thoracic Surgeons (STS) evaluated all patients undergoing valve surgical procedure for endocarditis from July 2016 to March 2024. Patients were stratified by conventional sternotomy vs an MICS approach, including hemisternotomy, right thoracotomy, and robotic-assisted mitral, tricuspid, or aortic valve surgical procedure. Logistic regression assessed the risk-adjusted association with the primary outcomes of STS major morbidity or mortality and the MICS approach by accounting for all covariates in current STS risk models. Of 741 patients undergoing valve

surgical procedure for endocarditis, the median age was 37 years, 582 (78.5%) had a substance use disorder, 210 (28.3%) underwent redo sternotomies, and 166 (22.4%) had redo valve operations. MICS was associated with a higher repair rate for mitral valves (76.3% vs 48%; P < .0001) but a lower rate for tricuspid valve (22.5% vs 44.1%; P < .0001), with no difference for aortic valves (8.3% vs 7.4%; P = .372). Before risk adjustment, MICS was associated with longer cross-clamp times (99 minutes vs 86 minutes; P = 0.019) but a lower incidence of STS major morbidity or mortality (15.4% vs 27.8%; P = 0.019). After robust risk adjustment, age (odds ratio [OR], 1.1; P = 0.008), lung disease (OR, 2.2; P = 0.010), preoperative creatinine (OR, 1.3; P = 0.016), and valve repair vs replacement (OR, 0.17; P = 0.002), but not MICS (OR, 1.2; P = 0.807), were independently associated with STS major morbidity and mortality. MICS valve surgical procedure for endocarditis appears both safe and effective, with repair rates and risk-adjusted outcomes similar to those of open surgical procedure.

25COASMA37

Title: The Association Between Sociodemographic Factors and Delays to Minimally Invasive Surgery for Stage IA-IIIA Non-small Cell Lung Cancer,

Christina M. Stuart, Nicole M. Mott, Michael R. Bronsert, Simran K. Randhawa, Elizabeth A. David,

The Annals of Thoracic Surgery, Volume 119, Issue 5,2025,Pages 1082-1091,
https://doi.org/10.1016/j.athoracsur.2024.12.009.

Abstract: Surgical resection is the gold standard treatment for early-stage non-small cell lung cancer (NSCLC). Prior studies have found that delayed treatment carries risk of disease progression. However, factors that predict delay to surgery are relatively understudied. The aim of this study was to identify characteristics associated with time to surgery. The National Cancer Database was queried for patients with stage IA-IIIA NSCLC who underwent upfront resection from 2017 to 2021. The primary outcome was time to surgery examined as a continuous and categorical variable in which patients were divided into timely (≤6 weeks) and delayed (>6 weeks) surgery cohorts. Across 75,047 patients, the median time to surgery was 41 days (interquartile range, 19-64 days). Of these patients, 39,685 (52.9%) were in the timely cohort and 35,362 (47.1%) were in the delayed cohort. After risk adjustment, significant predictors of increased odds of delayed surgery included African-American race (odds ratio [OR], 1.46; 95% CI, 1.34-1.59), lack of insurance (OR, 1.70; 95% CI, 1.33-2.17), lower educational status (OR, 1.15; 95% CI, 1.04-1.25]), lower household income (OR, 1.40; 95% CI,1.28-1.54), and use of a robotic-assisted approach (OR, 1.21; 95% CI, 1.15-1.27). Patients whose surgery was delayed had significantly increased risk-adjusted odds of upstaging (OR, 1.15; 95% CI, 1.04-1.28), 30-day mortality (OR, 1.24; 95% CI, 1.02-1.52), and 90-day mortality (OR, 1.25; 95% CI, 1.08-1.45]). After risk adjustment for oncologic characteristics, sociodemographic factors are associated with delay to definitive surgery in NSCLC and subsequent increased odds of mortality and pathologic upstaging. Future work should explore strategies to improve availability and accessibility of timely treatment for these patient populations to ameliorate disparities in care for NSCLC.

25COASMA38

Title: Clinical Outcomes and Costs of Robotic-assisted vs Conventional Mitral Valve Repair: A National Analysis,

Joseph Hadaya, Nikhil L. Chervu, Shayan Ebrahimian, Yas Sanaiha, Shannon Nesbit, Richard J. Shemin, Peyman Benharash,

The Annals of Thoracic Surgery, Volume 119, Issue 5,2025,Pages 1011-1019,
https://doi.org/10.1016/j.athoracsur.2024.11.005.

Abstract: Robotic approaches have been increasingly utilized for cardiothoracic operations, though concerns regarding costs remain. We evaluated short-term outcomes and costs of robotic-assisted and conventional mitral valve repair (MV-repair), hypothesizing that cost differences would be mitigated at high-volume programs. Adults undergoing elective MV-repair from 2016 to 2020 were identified in the Nationwide Readmissions Database. Patients with rheumatic heart disease, mitral stenosis, and those undergoing concomitant operations were excluded. Generalized linear models were utilized to evaluate the association between approach and in-hospital mortality, complications, length of stay, costs, and 90-day readmissions. Annual institutional MV-repair volume was modeled using restricted cubic splines, and cost differences subsequently evaluated by volume tertile. Of 40,738 patients, 9.8% underwent robotic-assisted MV-repair. Risk-adjusted outcomes including mortality, stroke, reoperation, respiratory complications, postoperative infection, and readmission were comparable between the 2 groups, while those undergoing robotic-assisted MV-repair had lower rates of nonhome discharge. The median cost of robotic-assisted MV-repair was greater than conventional surgery ($46,800 vs $38,500, P < .001). Despite a 1.3-day decrement (95% CI, 1.1-1.6) in length of stay, robotic-assisted MV-repair was associated with greater risk-adjusted costs by $10,500 (95% CI, $5800-$15,200). Programs in the highest volume tertile exhibited comparable costs for robotic-assisted and conventional MV-repair (cost difference, $5900; 95% CI, –$1200 to $12,200; P > .05). Robotic-assisted MV-repair had comparable short-term outcomes relative to conventional surgery. Despite increased costs of robotic-assisted MV-repair overall, high-volume programs had similar risk-adjusted costs by approach. These findings support the designation and performance of robotic MV-repair at centers of excellence in the United States.

25COASMA39

Title: Does High Standard Uptake Value on Positron Emission Tomography Preclude Sublobar Resection in Stage IA Non-Small Cell Lung Cancer ≤2 cm?,

Shaikha Al-Thani, Abu Nasar, Jonathan Villena-Vargas, Oliver Chow, Sebron Harrison, Benjamin Lee, Nasser Altorki, Jeffrey Port,

The Annals of Thoracic Surgery, Volume 119, Issue 5,2025, Pages 1092-1098,
https://doi.org/10.1016/j.athoracsur.2024.11.007.

Abstract: Recent randomized trials have shown equivalent survival after sublobar resection vs lobectomy in patients with clinical stage IA non-small cell lung cancer (NSCLC) ≤2 cm. High maximum standard uptake value (SUVmax) is a known risk factor in NSCLC, yet limited data exist on whether a high SUV should preclude a sublobar resection. This study aimed to determine whether there is an association between SUVmax and survival based on the extent of parenchymal resection. A retrospective review of a prospectively maintained

institutional database was conducted to identify patients with clinical stage IA NSCLC ≤2 cm (2011-2020) treated with sublobar resection or lobectomy. The primary outcome was cancer-specific survival (CSS). Secondary outcomes were overall survival and disease-free survival. There were 543 patients identified; 36.8% had sublobar resection and 63.2% had lobectomy. Baseline characteristics were similar. Patients who had sublobar resection had significantly worse Eastern Cooperative Oncology Group performance status and higher rates of comorbidities. The 5-year CSS, overall survival, and disease-free survival for the whole cohort were similar between sublobar resection and lobectomy. A receiver operating characteristic curve estimated the SUVmax cutoff point to be 4.15. For the whole cohort, patients with SUVmax >4.15 had worse CSS compared with SUVmax ≤4.15. However, there was no significant difference in 5-year CSS after sublobar resection vs lobectomy in patients with SUVmax ≤4.15 (98% in both groups; P = .77) or patients with SUVmax >4.15 (90% vs 94%, respectively; P = .12). SUVmax may not be a useful clinical determinant of the extent of parenchymal resection in patients with cT1 N0 NSCLC ≤2 cm. Patients treated by sublobar resection had comparable survival to lobectomy, irrespective of positron emission tomography avidity.

25COASMA40

Title: Paravalvular Leak After Transcatheter Aortic Valve Implantation: Results From 3600 Patients,

Nav Warraich, James A. Brown, Eishan Ashwat, Dustin Kliner, Derek Serna-Gallegos, Catalin Toma,

The Annals of Thoracic Surgery, Volume 119, Issue 5,2025, Pages 1037-1044,
https://doi.org/10.1016/j.athoracsur.2025.01.012.

Abstract: Paravalvular leak (PVL) after transcatheter aortic valve implantation (TAVI) is associated with poor outcomes. Mild PVL remains prevalent after TAVI, and its impact on long-term survival is unclear. This study aimed to examine the incidence, impact on survival, and progression of PVL. This was a retrospective, single-institution cohort study of TAVIs between November 2012 and January 2023. Patients were stratified by 30-day PVL severity: none to trace, mild, and moderate to severe. Multivariable logistic regression was performed to identify risk factors associated with increasing PVL severity. Kaplan-Meier survival estimation and Cox proportional hazards regression were performed. A total of 3600 patients underwent TAVI. Of these, 2719 (75.5%) had none to trace PVL, 808 (22.5%) had mild PVL, and 73 (2.0%) had moderate to severe PVL at 30 days. On multivariable logistic regression, later years of valve implantation (2017-2023) were protective against PVL progression. Kaplan-Meier estimates of the 3 groups were significantly different (P < .001) with the moderate to severe group having reduced survival. On Cox regression, moderate to severe PVL was associated with increased mortality (hazard ratio, 1.80; 95% Cl, 1.31-2.46; P < .001), whereas mild PVL was not (hazard ratio, 1.01; 95% CI, 0.89-1.15; P = .88) compared with none to trace PVL. For Kaplan-Meier estimates comparing the none to trace and mild PVL groups alone, landmark analysis showed reduced survival in the mild PVL group after 2 years (P = .03); however, this late reduction in survival in the mild PVL group did not persist on multivariable analysis (P = .14). After TAVI, moderate to severe PVL is

associated with reduced survival compared with none to trace PVL. Mild PVL may result in a delayed survival reduction.

25COASMA41

Title: The role of 18F-FDG PET/CT in detecting synchronous regional and distant metastatic disease in patients with an in-breast tumour recurrence,

Coco J.E.F. Walstra, Robert-Jan Schipper, Adri C. Voogd, Maurice J.C. van der Sangen, Ruben T.N.W. van Duin,

European Journal of Surgical Oncology, Volume 51, Issue 5,2025,109564,
https://doi.org/10.1016/j.ejso.2024.109564.

Abstract: In line with the trend towards minimally invasive, patient-tailored treatment, a selected group of patients with an in-breast tumour recurrence (IBTR) is treated by repeat breast-conserving treatment (BCT). To select eligible patients for repeat BCT, a reliable pre-operative work-up is essential. This study reports on the role of 18F-FDG PET/CT in detecting synchronous regional and distant metastases in patients with IBTR. A nation-wide data query was sent out to all Dutch hospitals offering breast cancer treatment. Breast cancer surgeons from 34 hospitals participated, filling electronic case report forms (eCRFs) on 549 patients treated for IBTR from 2016 to 2017. Of the 549 included patients, 297 were screened using 18F-FDG PET/CT for the presence of distant metastases. Forty of them (13.5 %) presented with synchronous distant metastatic disease. In 168 clinically node-negative patients who underwent 18F-FDG PET/CT, a suspect regional lymph node was found in 18 (10.7 %). Final pathology of these lymph nodes yielded a positive lymph node in 12 patients (7.1 %). Positive predictive value (PPV) of 18F-FDG PET/CT in clinically node-negative patients was 66.7 % and negative predictive value (NPV) was 85.3 %. The clinically relevant percentage of synchronous distant metastatic disease justifies the use of 18F-FDG PET/CT in the workup of patients with an IBTR. Furthermore, 18F-FDG PET/CT can assist in detecting regional axillary lymph node metastases, but requires histopathological confirmation given the moderate PPV, before clinical decisions can be made.

25COASMA42

Title: PET-CT-based host metabolic (PETMet) features are associated with pathologic response in gastroesophageal adenocarcinoma,

Charlie White, Vetri Sudar Jayaprakasam, Megan Tenet, Laura H. Tang, Mark A. Schattner, Yelena Y. Janjigian,

European Journal of Surgical Oncology,Volume 51, Issue 5,2025,109589,
https://doi.org/10.1016/j.ejso.2025.109589.

Abstract: 18F-FDG PET-CT-based host metabolic (PETMet) profiling of non-tumor tissue is a novel approach to incorporate the patient-specific response to cancer into clinical algorithms. A prospectively maintained institutional database of gastroesophageal cancer patients was queried for pretreatment PET-CTs, demographics, and clinicopathologic variables. 18F-FDG PET avidity was measured in 9 non-tumor tissue types (liver, spleen, 4 muscles, 3 fat locations). Logistic and Cox regression were used to model pathologic response (PR) and overall survival (OS) respectively. Classification and regression tree (CART) and random forest modeling were employed to create decision trees and identify

PETMet features associated with outcome. Two-hundred and one patients with distal gastroesophageal (48 %) or gastric (52 %) adenocarcinoma were included. PET-CT-derived scores were independently associated with PR after adjusting for clinical variables. CART and Random Forest methods identified critical split points of non-tumor tissue 18F-FDG avidity that can classify patients and predict PR. PET-CT risk groups created from decision trees predicted PR significantly better than the clinical model ($p < 0.001$). Specifically, an elevated erector spinae-to-gluteal fat 18F-FDG avidity ratio (≥2.7) combined with low 18F-FDG avidity in the spleen (<2.9) and rectus femoris (<0.52) predict PR. No advantage of PET-CT risk groups was seen for predicting OS ($p = 0.155$). Pretreatment host PETMet features may be useful for predicting PR after neoadjuvant therapy in gastroesophageal cancer. Unsupervised decision trees indicate that low 18F-FDG avidity in visceral fat, subcutaneous fat, and muscle result in the most favorable PR, suggesting that systemic hypermetabolism adversely impacts prognosis.

Keywords: Patient metabolic profiling; PETMet; PET-CT; Gastric cancer; Pathologic response

25COASMA43

Title: Long-term oncologic outcomes of robot-assisted versus conventional open esophagectomy for esophageal cancer: Propensity-score matched anaylsis,

Yelee Kwon, Jae Kwang Yun, Yun-Ho Jeon, Yong-Hee Kim,

European Journal of Surgical Oncology, Volume 51, Issue 5,2025,109591,
https://doi.org/10.1016/j.ejso.2025.109591.

Abstract: This study aimed to compare the long-term oncologic outcomes of robot-assisted minimally invasive esophagectomy (RAMIE) with those of conventional open esophagectomy (OE) for esophageal cancer. Between January 2006 and December 2021, 1745 consecutive patients underwent esophagectomy for esophageal cancer at Asan Medical Center, Korea. Among them, we retrieved 1133 patients (mean age 63.1 ± 7.8 years, 86 [7.6 %] women, 1100 [97.1 %] squamous cell carcinomas), who were operated by a single surgeon. These patients were categorized into following two groups based on their surgical approaches: RAMIE (n = 497) and OE (n = 636). The RAMIE and OE groups were matched in a 1:1 ratio using propensity scores. Overall survival (OS) and recurrence-free survival (RFS) were compared between the groups. The median follow-up was 51.8 (24.6–90.2, interquartile) months. Five-year OS (70.7 % vs. 55.0 %, $P < 0.01$) and RFS (63.3 % vs. 50.1 %, $P < 0.01$) rates were significantly higher in RAMIE than in OE group. Following propensity-score matching, 886 patients (443 pairs) were successfully matched, demonstrating no significant intergroup differences, including the pathologic stage. The RAMIE group consistently demonstrated enhanced OS (70.4 % vs. 61.8 %, $P < 0.01$) and RFS (62.8 % vs. 55.8 %, $P = 0.04$) after five years, even after adjustment. The rate of noncancer mortality was significantly higher in the OE group ($P < 0.01$), whereas the rate of esophageal cancer-related mortality showed no significant differences between the groups ($P = 0.25$). RAMIE could be a safer option for patients compared with conventional open esophagectomy with favorable long-term outcomes related to noncancer mortality.

Keywords: Minimally invasive esophagectomy; Robot-assisted esophagectomy; Esophageal cancer; Long-term oncologic outcome; Propensity-score matching

25COASMA44

Title: Benefits of entecavir therapy in HBV-related hepatocellular carcinoma patients with compensated cirrhosis after hepatectomy: A ten-year retrospective cohort study,

Jian Liu, Shilei Bai, Xintong Shi, Tao Yuan, Yongjin Yu, Jianbo Lin, Chun Dai, Yeye Wu, Longjiu Cui,

European Journal of Surgical Oncology, Volume 51, Issue 5,2025,109621,
https://doi.org/10.1016/j.ejso.2025.109621.

Abstract: Data on the impact of antiviral therapy(AVT) on the long-term outcomes of hepatitis B virus(HBV)-related hepatocellular carcinoma(HCC) patients with historically-proved cirrhosis after hepatectomy are limited. We aimed to determine the effect of AVT on resected HCC in the background of HBV-related cirrhosis. A total of 1396 patients with HBV-related cirrhotic HCC undergoing curative resection were categorized into AVT and no-AVT groups retrospectively. Recurrence rates were compared, especially according to the initiation time of AVT, virological response, and low HBV levels. Early and late recurrence was stratified by 2 years postoperatively. The 1-, 3-, 5- and 10-year recurrence rates in AVT group(n = 432) were lower than those in no-AVT group(n = 964, 26 %, 49 %, 65 % and 76 % vs. 29 %, 69 %, 87 % and 92 %,p < 0.001). AVT was an independent factor for late, but not early, recurrence(p < 0.001). The late recurrence rates were similar between patients with only postoperative AVT and those with both pre-and postoperative AVT(p = 0.772). In the AVT group, the late recurrence rates in patients with persistent virological response(PVR) were lower than those in patients with low detectable viral levels(LDV, p = 0.003). Logistic regression analysis showed that the time to virological response(p < 0.001) and HBeAg positivity(p < 0.001) were independently associated with LDV. Patients with spontaneous or treatment-induced undetectable HBV showed the lowest and similar late recurrence rates(p = 0.796). Results were similar in multiple sensitivity analyses. Long-term AVT, regardless of preoperative or postoperative initiation, reduced post-resection late recurrence in patients with HCC and cirrhosis, especially in those with PVR.

Keywords: Hepatocellular carcinoma; Liver cirrhosis; Hepatitis B virus; Entecavir; prognosis

25COASMA45

Title: Assessing the African burden of breast cancer: A demographic analysis using Global Cancer Observatory 2022,

Mengxia Fu, Zhiming Peng, Min Wu, Dapeng Lv, Shuzhen Lyu, Yanping Li,

European Journal of Surgical Oncology, Volume 51, Issue 5,2025,109627,
https://doi.org/10.1016/j.ejso.2025.109627.

Abstract: Breast cancer is a major health issue for women in Africa. This study aims to assess the burden of the disease using the latest estimates from Global Cancer Observatory 2022. Data were sourced from the Global Cancer Observatory 2022. Age-standardized incidence rates (ASIR) and mortality rates (ASMR) per 100,000 person-years were calculated using direct age standardization based on the Segi-Doll World standard population. Pearson's correlation coefficient was employed to assess the relationship between the Human Development Index (HDI) and both incidence and mortality rates. Projections for breast cancer cases and deaths by 2050 were estimated based on global demographic forecasts. In

2022, Africa reported an estimated 198.3 thousand new breast cancer cases and 91.3 thousand deaths. Nigeria reported the highest incidence (32,278) and deaths (16,332). Algeria had the highest ASIR (61.9/100,000) while Cameroon had the highest ASMR (27.4/100,000). ASMR increased with age, surged in individuals over 70 in Africa. Chad had the earliest ASIR peak age at 40–49 years (40.3/100,000) and earliest ASMR peak age at 50–59 years (24.1/100,000). A positive correlation was observed between HDI and incidence rates. Projections suggest that by 2050, Nigeria and Egypt will bear the highest disease burden, with Tanzania and Zambia experiencing nearly 200 % rise in incidence, while Guinea and Niger will see mortality rates surge by over 200 %. Breast cancer mortality is higher in low socio-economic countries. Efforts should focus on low socio-economic countries, implementing rapid intervention measures to mitigate the growing cancer crisis.

Keywords: Breast cancer; Africa; Prediction; Incidence; Mortality

25COASMA46

Title: The role of sentinel lymph biopsy in patients with microinvasive breast cancer: A multicentric study,

Gianluca Vanni, Marco Pellicciaro, Marco Materazzo, Silvia Petrucci, Riccardo Affaniti, Sara Pepe,

European Journal of Surgical Oncology, Volume 51, Issue 5,2025,109601,
https://doi.org/10.1016/j.ejso.2025.109601.

Abstract: Microinvasive breast cancer (MIBC) is a rare tumor. Despite of its good prognosis, which is similar to in situ breast cancer, its management is still similar to invasive tumors. The aim of this study is to assess the prognostic implications of SNLB in MIBC patients and to evaluate the possibility for surgical de-escalation in these patients. A multicentric retrospective study including all patients with MIBC diagnosis who underwent surgery from 2012 to 2022 is carried on. Seven different Italian Breast Units contributed to the study. Preoperative, intraoperative and post operative data were taken into account, including final histological report with tumor staging and oncological outcomes. 261 patients were included. The metastatic rate of sentinel lymph node biopsy (SLNB) was 9.2 % (2.3 % macrometastasis, 6.9 % micrometastasis or isolated tumors cells). Multifocal lesions (p-value: 0.045; OR:1.730), and the absence of hormone receptors (p-value: 0.018; OR:3.658) are all predictors of sentinel lymph node metastasis, while a Ki67 proliferation index <20 % associates with a low risk of nodal metastasis (p-value: 0.035; OR:0.289). Five-years loco-regional recurrence in patients with metastatic sentinel lymph node was comparable to the non-metastatic ones (95.7 % vs 94.1 %; p-value: 0.951). Cox Regression analysis identifies age at diagnosis as a predictive factor of locoregional recurrence at five years (OR 0.831 95%CI: 0.721–0957, p-value: 0.010). MIBC has a favorable prognosis and very low macrometastatic sentinel lymph node rates. The omission of SNLB in patients with MIBC provides a similar overall survival rate, therefore SNLB should be reserved to younger patient with preoperative radiological or clinical suspicion of metastatic lymph nodes.

Keywords: Microinvasive breast cancer; Sentinel lymph node biopsy omission; Surgical de-escalation

25COASMA47

Title: Transcatheter rectal arterial chemoembolization with oxaliplatin and concurrent chemoradiotherapy in patients with locally advanced rectal cancer: A retrospective comparative study,

Weina Yang, Chaofan Li, Jiamin Luo, Yan Feng, He Xiao, Xuemei Li, Dan Jian, Chuan Chen, Lin Lei,

European Journal of Surgical Oncology, Volume 51, Issue 5,2025,109582,
https://doi.org/10.1016/j.ejso.2025.109582.

Abstract: The aim of the study is to assess whether transcatheter rectal arterial chemoembolization (TRACE) with oxaliplatin could increase the pathologic complete response (pCR) rate of locally advanced rectal cancer (LARC) and improve survival outcomes, while minimizing adverse events compared to preoperative chemoradiotherapy (CRT) alone. Eligible LARC patients who received TRACE with oxaliplatin plus chemoradiotherapy (the NATRACE-CRT group) or preoperative CRT alone (the NA-CRT group) were retrospectively selected from the database of our institution. Pathological results, treatment-related adverse events and survival in the two groups were compared. A total of 236 patients were enrolled. The pCR rates were 18.38 % in the NATRACE-CRT group and 14.00 % in the NA-CRT group, with a non-significant difference of 4.38 % (P = 0.473). The median follow-up time was 42 months. The 5-year DFS (75.7 % vs. 73.2 %; P = 0.879) and OS (73.4 % vs. 70.3 %; P = 0.855) rates were comparable between the NATRACE-CRT group and the NA-CRT group. However, the NATRACE-CRT group had significantly fewer patients achieving TRG3 compared to the NA-CRT group (16.18 % vs. 35.00 %; P = 0.001). Furthermore, TRG3 patients in the NATRACE-CRT group exhibited significantly longer OS compared to those in the NA-CRT group (5-year OS: 88.9 % vs 59.5 %; P = 0.016). TRACE with oxaliplatin demonstrates potential in improving treatment response and prognosis of LARC patients with chemoradiotherapy resistance.

Keywords: Locally advanced rectal cancer; Chemoembolization; Neoadjuvant chemoradiotherapy; Pathological complete response; Survival

25COASMA48

Title: Machine learning model based on preoperative contrast-enhanced CT and clinical features to predict perineural invasion in gallbladder carcinoma patients,

Hengchao Liu, Zhenqi Tang, Xue Feng, Yali Cheng, Chen Chen, Dong Zhang, Jianjun Lei, Zhimin Geng, Qi Li,

European Journal of Surgical Oncology, Volume 51, Issue 5,2025,109697,
https://doi.org/10.1016/j.ejso.2025.109697.

Abstract: Perineural invasion (PNI) is an independent prognostic risk factor for gallbladder carcinoma (GBC). However, there is currently no reliable method for the preoperative noninvasive prediction of PNI. This retrospective study included 180 patients with pathologically diagnosed GBC who underwent preoperative contrast-enhanced CT between January 2022 to December 2023 at one high-volume medical center from China. K-Nearest Neighbors (KNN), LightGBM (LGB), Logistic Regression (LR), XGBoost (XGB), Naive Bayes (NB), and Support Vector Machine (SVM) were employed to develop prediction models. The Shapley additive explanations (SHAP) were used to visualize models and rank

the importance of features associated with PNI. Total bilirubin, CA19-9, imaging liver invasion, vascular invasion, T staging and N staging were identified as risk factors for PNI ($P < 0.05$). The LightGBM model demonstrated the improved performance in the testing set, with the AUCs of 0.886 and 0.795 in the training and testing sets, respectively. In four machine learning algorithms prediction models demonstrated improved performance included three imaging features (imaging T staging, N staging, and vascular invasion) and two clinical features (TBIL and CA19-9). When these features were employed to develop the prediction models, the LightGBM model exhibited the higher performance than other machine learning modes in the testing set, with AUCs of 0.843 and 0.802, and ACCs of 0.786 and 0.759 in the training and testing sets, respectively. A machine learning-based prediction model integrating contrast-enhanced CT imaging and clinical features demonstrates good performance and stability in the noninvasive preoperative identification of PNI status in GBC patients.

Keywords: Gallbladder carcinoma; Contrast-enhanced CT; Perineural invasion; Machine learning; Prediction model; LightGBM

25COASMA49

Title: Efficacy and safety of subtotal pelvic peritonectomy for colorectal cancer patients with peritoneal metastasis confined to the pelvic cavity,

Jinghua Tang, Leen Liao, Binyi Xiao, Qiaoqi Sui, Muxu Zheng, Wu Jiang, Kai Han, Lingheng Kong, Zhizhong Pan, Peirong Ding,

European Journal of Surgical Oncology, Volume 51, Issue 5,2025,109703,
https://doi.org/10.1016/j.ejso.2025.109703.

Abstract: Cytoreductive surgery has shown survival benefits for colorectal cancer (CRC) patients with peritoneal metastasis. However, the optimal extent of peritonectomy remains controversial in cases of limited peritoneal metastases. This study modified selective pelvic peritonectomy (SPP) into subtotal pelvic peritonectomy (STPP) for metastasis confined to pelvic cavity, and aimed to evaluate its feasibility, safety, and impact on survival outcomes. CRC patients with limited peritoneal metastasis confined to the pelvic cavity who underwent CC0 (no macroscopic residual cancer remained) resection were included from a prospectively collected database. Surgical complications, disease-free survival (DFS), and overall survival (OS) were analyzed. A total of 67 patients were included (26 in the STPP group and 41 in the SPP group). Clinically, STPP was found to be feasible and without increased surgical complications or mortality rates. At a median follow-up of 33.9 months, the 3-year DFS was 65.9 % and 30.7 % in STPP and SPP groups, respectively ($P = 0.002$). The 3-year OS was 84.1 % and 68.5 % in STPP and SPP groups, respectively ($P = 0.006$). Moreover, STTP was independently associated with improved DFS (HR = 0.351, 95 % CI 0.165–0.745, $P = 0.006$) and OS (HR = 0.324, 95 % CI 0.116–0.902, $P=0.032$). Female gender was also independently associated with poor DFS (HR = 2.146, 95 % CI 1.078–4.271, $P = 0.031$). Among 24 female patients with remaining ovaries, 9 (37.5 %) cases developed metachronous ovarian metastasis, and of these 6 underwent a second operation. Subtotal pelvic peritonectomy is associated with promising long-term outcomes in CRC patients with peritoneal metastasis confined to the pelvic cavity. Prophylactic bilateral oophorectomy should be strongly considered during cytoreductive surgery.

Keywords: Colorectal cancer; Pelvic peritoneal carcinomatosis; Cytoreductive surgery; Subtotal pelvic peritonectomy

25COASMA50

Title: A prospective study of methylated ctDNA in patients undergoing treatment for liver metastases from colorectal cancer,

Louise Raunkilde, Rikke Fredslund Andersen, Caroline Brenner Thomsen, Torben Frøstrup Hansen, Lars Henrik Jensen,

European Journal of Surgical Oncology, Volume 51, Issue 5,2025,109586,
https://doi.org/10.1016/j.ejso.2025.109586.

Abstract: Decision regarding local treatment of colorectal liver metastases (CRLM) is a multidisciplinary assessment, and liver intervention should be performed when the metastases are deemed resectable. There is no standard biomarker to aid neither this decision nor the postoperative treatment decisions. The present prospective, observational study aimed to investigate the potential clinical utility of a combined tumor-specific and organ-specific methylated circulating DNA assay in the perioperative setting of CRLM. The study included 56 cases with CRLM. Blood samples were drawn preoperatively and postoperatively. Multiplex methylation analysis of the markers NPY, KANK1, and GAL3ST3 (meth-ctDNA) was performed using droplet digital PCR. The assay detected preoperative and postoperative meth-ctDNA in 37 % and 46 % of patients, respectively. Patients with negative preoperative meth-ctDNA had a longer median PFS compared to those with positive preoperative meth-ctDNA (HR = 2.2, 95 % CI 1.2–3.9, $p < 0.01$). In a multivariate analysis, preoperative negative meth-ctDNA was identified as a strong independent predictor of PFS (HR = 3.3, 95 % CI 1.5–7.2, $p < 0.01$). Similarly, patients with negative postoperative meth-ctDNA had longer median PFS (HR = 3.0, 95 % CI = 1.6–5.6, $p < 0.001$) and OS (HR = 4.1, 95 % CI 1.9–9.1, $p < 0.001$) compared to those with positive postoperative meth-ctDNA. Preoperative meth-ctDNA may serve as an important biomarker to inform the multidisciplinary assessment and treatment planning of CRLM. Negative meth-ctDNA may indicate the optimal timing for liver intervention, whereas positive meth-ctDNA may indicate initiation or re-orientation of chemotherapy, or immediate local intervention. Our results confirm postoperative negative meth-ctDNA as a strong prognostic marker of survival.

Keywords: Metastatic colorectal cancer; circulating tumor DNA; DNA methylation; Liver metastases; Loco-regional treatment

25COASMA51

Title: Ten years of experience in percutaneous cryoablation for small renal masses in patients aged ≥ 80 years,

Shinya Miyazaki, Atsuko Fujihara, Fumiya Hongo, Takumi Shiraishi, Takashi Ueda, Tsukasa Narukawa,

European Journal of Surgical Oncology, Volume 51, Issue 5,2025,109638,
https://doi.org/10.1016/j.ejso.2025.109638.

Abstract: Small renal masses (SRMs) have been frequently found as incidentaloma in recent decades. Although partial nephrectomy is generally recommended, perioperative adverse events are a concern. As an alternative to partial nephrectomy, percutaneous cryoablation is

minimally invasive for older patients and patients with comorbidities. Reportedly, age at diagnosis may affect the recurrence rate after partial nephrectomy. Given the paucity of reports on whether age is associated with cryoablation outcomes, we aimed to investigate the long-term impact of cryoablation for SRMs performed at different age ranges. This retrospective study included 187 patients who underwent percutaneous cryoablation for SRMs at Kyoto Prefectural University of Medicine during a 10-year period (April 2013 to March 2022). We divided the patients into two groups according to age: Group 1 (<80 years, n = 135) and Group 2 (≥80 years, n = 52). Patient background, post-treatment outcomes, and complications in both groups were retrospectively analyzed during median observation periods of 41 (Group 1) and 36.5 (Group 2) months. Although the tumor diameter was significantly greater in Group 2 than in Group 1 (p = 0.015), there were no significant differences between the two groups in overall, cancer-specific, metastasis-free, and local recurrence-free survival. There were no significant differences in the complication rates or treatment-related decline in renal function between the two groups. Percutaneous cryoablation had no age-related effects on survival, therapeutic outcomes, or complications. These results provide valuable information for deciding on a treatment option for SRMs in an aging society.

Keywords: Renal cell carcinoma; Older; Oncological outcome; Incidentaloma; Aging

25COASMA52

Title: Comparative analysis of oncological and surgical outcomes of robotic versus conventional mastectomy for breast cancer,

Wen-Ling Kuo, Jung-Ju Huang, Chia-Huei Chu, Shu-Chen Chang, Yu-Jr Lin, Yu-Hsuan Chuang,

European Journal of Surgical Oncology, Volume 51, Issue 5,2025,109622,
https://doi.org/10.1016/j.ejso.2025.109622.

Abstract: This study aimed to compare the surgical and oncological outcomes of robotic mastectomy (RM) and conventional mastectomy (CM) for breast cancer. Our institutional registry of women with breast cancer who received RM between 2018 and 2023 and CM between 2016 and 2023 were reviewed. Propensity score matching of clinicopathological variables was used to match 123 RM patients with 123 CM patients. Surgical outcomes, reconstruction type, margin status, complications, recurrence-free survival (RFS), and overall survival (OS) were compared between the 2 groups. Complications with increasing RM experience were also examined. More autologous flap reconstructions were used in RM (67 % vs. 39 %, p < 0.001), but more implant reconstructions were used in CM (61 % vs. 33 %, p < 0.001). The complication rate, especially breast skin necrosis, was lower in the RM group (10 % vs. 26 %, p = 0.002). Nipple-areolar complex necrosis in nipple-sparing mastectomy was similar between the groups (33 % vs. 27 %, p = 0.45). At a median follow-up of 30 months, RFS was comparable between the 2 groups, as was OS (median follow-up 36 months). More RM experience was associated with shorter operation time and lower surgical complication and margin positive rates. The oncological outcomes of RM and CM are similar at a follow-up of about 3 years. RM is associated with a significantly lower rate of breast skin necrosis, and the advantage of RM exists with different types of breast reconstruction. Increasing RM experience leads to improved overall results.

Keywords: Breast cancer; Mastectomy; robotic mastectomy; Robot-assisted mastectomy; Nipple-sparing mastectomy; Small incision breast surgery; Minimally invasive breast surgery

25COASMA53

Title: Up-front resection for hepatocellular carcinoma: Assessing futility in the preoperative setting,

Abdullah Altaf, Mujtaba Khalil, Miho Akabane, Zayed Rashid, Jun Kawashima, Shahzaib Zindani,

European Journal of Surgical Oncology, Volume 51, Issue 5,2025,109594,
https://doi.org/10.1016/j.ejso.2025.109594.

Abstract: We sought to develop a predictive model to preoperatively identify patients with hepatocellular carcinoma (HCC) at risk of undergoing futile upfront liver resection (LR). Patients undergoing curative-intent LR for HCC were identified from a large multi-institutional database. Futile LR was defined by death or disease recurrence within six months postoperatively. Backward logistic regression was performed to identify factors associated with futility. Additionally, binary criteria were established for surgical candidacy, aiming to keep the likelihood of futility below 20 %. Among 1633 patients with HCC, 264 (16.2 %) underwent futile upfront LR. Tumor burden score (TBS) (coefficient: 0.083, 95%CI: 0.067–0.099), alpha-fetoprotein (AFP) (coefficient: 0.254, 95%CI: 0.195–0.310), and albumin-bilirubin (ALBI) grade 2/3 (coefficient: 0.566, 95%CI: 0.420–0.718) were independently associated with an increased risk of futile LR. The model demonstrated strong discrimination and calibration in both derivation and validation cohorts. Low, intermediate, and high-risk groups were determined based on the risk model, each with an escalating likelihood of futility, worse histological features, and worse survival outcomes. Six distinct conditions based on AFP-adjusted-to-TBS criteria were established, all with a futility likelihood of less than 20 %. Patients fulfilling these criteria had significantly better long-term recurrence-free and overall survival. The futility risk model was made available online for wide clinical applicability: (https://altaf-pawlik-hcc-futilityofsurgery-calculator.streamlit.app/). A preoperative risk model and AFP-adjusted-to-TBS criteria were developed and validated to predict the likelihood of futile LR among patients with HCC. This pragmatic clinical tool may assist clinicians in preoperative decision-making, helping them avoid futile surgery unlikely to offer long-term benefits.

Keywords: Hepatocellular carcinoma; Liver resection; Futility; Systemic therapy; Locoregional therapy

25COASMA54

Title: Oncological outcomes after vaginal and robotic-assisted radical trachelectomy in patients with cervical cancer - A single-center prospective cohort study,

Sinor Soltanizadeh, Signe Frahm Bjørn, Ligita Paskeviciute Frøding, Berit Jul Mosgaard, Claus Høgdall,

European Journal of Surgical Oncology, Volume 51, Issue 5,2025,109671,
https://doi.org/10.1016/j.ejso.2025.109671.

Abstract: The aims of this study are to evaluate the oncological outcomes of robotic-assisted radical trachelectomy (RART) compared with radical vaginal trachelectomy (RVT) for

localized early-stage cervical cancer in a national cohort. RVT was introduced in 2003 in Denmark and nationally centralized to Copenhagen Univeristy Hospital. In 2014 the procedure advanced to a robotic-assisted approach. Perioperative and oncological data has been prospectively reported to the Danish Gynecological Cancer Database (DGCD) which is continuously developed and updated. All patients undergoing radical trachelectomy were included in this prospective cohort study. Data was extracted from DGCD and manually validated through electronic medical journals and The Danish Pathology Registry. A total of 206 patients underwent radical trachelectomy, with 78 patients undergoing RART and 128 patients undergoing RVT. No significant differences were observed in the microscopic free margins of the trachelectomy specimens. A total of seven (5.5%) patients undergoing RVT and two (2.6%) patients undergoing RART had recurrences (p = 0.403). No significant differences in recurrence-free survival were found between the groups, both in the unadjusted (HR 0.51 (0.11–2.47)) and adjusted analyses (HR 0.80 (0.16–3.96)). In this large single-center cohort, oncological safety of RART is equal to RVT for patients with localized cervical cancer and a fertility desire.

Keywords: Cervical cancer; Trachelectomy; Recurrence-free survival; Gynecology

25COASMA55

Title: Neoadjuvant chemotherapy and chemoradiotherapy versus chemoradiotherapy alone in high-risk locally advanced rectal cancer: A retrospective comparison of two Dutch tertiary referral centres,

K. van den Berg, E. Banken, J.M. van Rees, L.M. Coolen, M. de Vries, E.L.K. Voogt, J. Rothbarth,

European Journal of Surgical Oncology, Volume 51, Issue 5, 2025, 109699,
https://doi.org/10.1016/j.ejso.2025.109699.

Abstract: The effect of neoadjuvant chemotherapy and chemoradiotherapy in patients with locally advanced rectal cancer, at increased risk of failing current treatment regimens, is unknown. This study compared the complete response rate and long-term survival of these patients treated with or without neoadjuvant chemotherapy prior to chemoradiotherapy. Patients with high-risk locally advanced rectal cancer, who were surgically treated or entered a watch and wait approach after neoadjuvant chemoradiotherapy with or without neoadjuvant chemotherapy in Erasmus Medical Centre or Catharina Hospital between 2016 and 2020, were retrospectively identified. High-risk was defined as the presence of tumour invasion into the mesorectal fascia, grade 4 extramural venous invasion, enlarged lateral lymph nodes, or tumour deposits. The primary endpoint was complete response rate, which was defined as a histopathological complete response or a sustained (during 12 months) clinical complete response. Long-term oncological outcomes were evaluated based on Kaplan-Meier and Cox regression survival analyses. The neoadjuvant chemotherapy group consisted of 64 patients, of whom 61 (95.3 %) were treated with chemotherapy prior to chemoradiotherapy, the chemoradiotherapy group of 194 patients. The complete response rates were 25.0 % and 9.8 %, respectively (P = 0.002). The estimated 3-year overall survival was 92.2 % in the neoadjuvant chemotherapy group versus 66.9 % in the chemoradiotherapy group. Excellent oncological outcomes were observed in patients with high-risk locally advanced rectal cancer selected during a multidisciplinary team (MDT) meeting for neoadjuvant chemotherapy and

chemoradiotherapy. The actual difference with patients treated with chemoradiotherapy alone should be investigated in prospective trials. Pretreatment referral to expert MDTs is encouraged.

Keywords: Rectal cancer; Neoadjuvant chemotherapy; Chemoradiotherapy; Locally advanced

25COASMA56

Title: Efficacy and safety of extended duration postoperative thromboprophylaxis with low molecular weight heparin among subgroups of patients undergoing surgical resection of colorectal cancer: A post-hoc analysis of the PERIOP-01 trial,

Laura Girardi, Ranjeeta Mallick, Tzu-Fei Wang, Marc Carrier, Rebecca Auer,

European Journal of Surgical Oncology, Volume 51, Issue 5,2025,109701,
https://doi.org/10.1016/j.ejso.2025.109701.

Abstract: Extended duration postoperative thromboprophylaxis is suggested by clinical practice guidelines after any cancer-related major abdominal surgeries. However, recent evidence reported relatively low rates of symptomatic venous thromboembolism (VTE) after colorectal cancer surgeries, suggesting the need of a careful risk-benefit assessment in this setting. This is a pre-planned post-hoc analysis of the PERIOP-01 trial which compared extended to standard thromboprophylaxis in patients undergoing surgical resection of localized colorectal cancer. Subgroup analyses were performed based on different baseline characteristics. The primary efficacy and safety outcomes were major VTE and clinically relevant bleeding events, respectively. A total of 614 patients were included in the modified intention-to-treat analysis (307 patients in each group). Major VTE events occurred in 2 % and 1 % of the extended and standard-duration thromboprophylaxis groups, respectively. Clinically relevant bleeding events occurred in 3 % of each group. No specific characteristics were found to be associated with a decreased incidence of major VTE among patients receiving extended thromboprophylaxis. Patients with colon cancer resection receiving extended thromboprophylaxis were at an increased risk of clinically relevant bleeding (HR 2.57, 95%CI 1.25–5.30). Other characteristics that may be associated with an increased incidence of bleeding included age (≥75) (HR 2.37, 95%CI 0.47–11.98) and sex (HR 2.13, 95%CI 0.20–23.17). In the PERIOP-01 trial, extended thromboprophylaxis did not reduce the incidence of major VTE in any subgroups of patients. However, this strategy may be associated with an increased incidence of bleeding among patients with colon cancer, and perhaps among male and elderly patients.

Keywords: Venous thrombosis; Venous thromboembolism; Thromboprophylaxis; Tinzaparin; Abdominal surgery; Colorectal cancer

25COASMA57

Title: Association between ERAS protocol and major postoperative complications and reasons for non-compliance in patients with esophageal cancer,

Christian Geroin, Jacopo Weindelmayer, Serena Camozzi, Barbara Leone, Cecilia Turolo, Maria Bencivenga,

European Journal of Surgical Oncology, Volume 51, Issue 5,2025,109707,
https://doi.org/10.1016/j.ejso.2025.109707.

Abstract: The association between each Enhanced Recovery After Surgery (ERAS) component and the incidence of major postoperative complications following Ivor Lewis or McKeown surgery is understudied. Therefore, we wanted to determine the association between ERAS components, major postoperative complications, and the reasons for non-compliance with the ERAS program. Data were extracted from the prospective ERAS Registry managed by the University of Verona, Italy. We searched and compared the data for postoperative major complications (Clavien-Dindo Classification ≥3B) and reasons for non-compliance with 15 ERAS items in patients undergoing Ivor Lewis or McKeown surgery with radical intent for esophageal or esophagogastric junction cancer. The study sample was 346 patients: 43 (12.4 %) experienced one or more postoperative major complications. When stratified by type of surgery, complications were more frequent after McKeown surgery than after Ivor Lewis surgery (15.5 % and 11.5 %, respectively). Organizational setbacks were the most common reason for non-compliance with the ERAS program. We identified several associations between clinical and patient demographic characteristics and 90-day postsurgical complications. The multivariate model indicated an association between fewer major postoperative complications after Ivor Lewis surgery and adherence to the protocol items "soft diet intake" (adjusted odds ratio [OR], 0.23; 95 % confidence interval [CI], 0.08–0.63) and "urinary catheter removal" (adjusted OR, 0.26; 95 % CI, 0.10–0.63). Major complications are relatively frequent, especially after McKeown surgery. What remains uncertain is whether ERAS items can predict the occurrence of postoperative complications. Adherence to the protocol may be influenced by the co-occurrence of complications, comorbidities, and organizational setbacks.

Keywords: Esophageal cancer; Enhanced recovery after surgery; Major postoperative complications; Surgery; Ivor lewis surgery; McKeown surgery

25COASMA58

Title: Neoadjuvant therapy with triple therapy for centrally located hepatocellular carcinoma,

Wentao Bo, Lixia zhang, Yan Chen, Jinliang Zhang, Haiqing Wang,

European Journal of Surgical Oncology, Volume 51, Issue 5,2025,109588,
https://doi.org/10.1016/j.ejso.2025.109588.

Abstract: Centrally located hepatocellular carcinoma (HCC) is a subtype HCC with special location adjoined hepatic portals. It is difficult to be radically resected with sufficient surgical margin. We discussed whether neoadjuvant therapy could increase surgical margin and reduce recurrence. From January 2018 to September 2023, 106 centrally located HCC patients who underwent radical liver resection were retrospectively included. Neoadjuvant therapy included transarterial chemoembolization (TACE) with programmed death 1 (PD-1) inhibitors plus tyrosine kinase inhibitor (TKI). Surgical margin and long-term outcomes were compared between patients with and without neoadjuvant therapy. 40 patients underwent neoadjuvant therapy and 66 patients underwent surgery alone. In neoadjuvant therapy group, 3 (7.5 %) patients achieved progression disease, 9 (22.5 %) patients achieved stable disease, 13 (32.5 %) achieved partial response and 15 (37.5 %) achieved complete response based on the mRECIST criterion. Ultimately, 36 patients (90 %) underwent subsequent surgical resection in the neoadjuvant therapy group. The neoadjuvant therapy had the advantages of

declining alpha fetoprotein level (5.9 ng/mL vs 50.1 ng/mL, P = 0.001), microvascular invasion rate (MVI) (12.5 % vs 30.3 %, P = 0.036), reducing tumor size to 5.1 ± 2.1 cm from 6.2 ± 2.2 cm (P = 0.021), and increasing more patients with surgical margin>1 cm (30.0 % vs 7.6 %, P = 0.002). The neoadjuvant therapy group reduced tumor recurrence and prolonged overall survival. Multivariate analysis found that neoadjuvant therapy was an independent protective factor for overall survival and recurrence free survival. Neoadjuvant therapy showed advantage of reducing tumor burden and increasing surgical margin for centrally located HCC, resulting in longer overall survival and recurrence free survival.

Keywords: Hepatocellular carcinoma; Neoadjuvant treatment; Centrally located

25COASMA59

Title: Comparison of perioperative outcomes of DaVinci robot and Hugo robot radical prostatectomy: A systematic review and meta-analysis,

Si Ge, Zuoping Wang, Lei Zheng, Yunxiang Li, Lijian Gan, Zhiqiang Zeng, Chunyang Meng,

European Journal of Surgical Oncology, Volume 51, Issue 5,2025,109596,
https://doi.org/10.1016/j.ejso.2025.109596.

Abstract: To compare the safety and efficacy of radical prostatectomy with DaVinci robot and Hugo robot. The system searches Embase, PubMed, Cochrane library, and Web of Science 4 database. The search time ranges from database creation to June 2024. Stata17 was used for statistical analysis. A total of 5 studies were conducted, including 816 patients. The results showed that there was no difference in age, preoperative prostate volume, preoperative PSA level, operation time, estimated blood loss, length of stay, overall complications, urinary incontinence, lymph node yield, and positive margin between DaVinci robot and Hugo robot radical prostatectomy. However, the BMI of DaVinci group was larger than that of Hugo (Effect = 0.47, 95%Cl [0.03, 0.91], P < 0.05). The BMI of the DaVinci group seems to be larger, and Hugo robotic radical prostatectomy seems to be as effective as DaVinci robotic radical prostatectomy. But more well-designed studies are needed to assess the oncology outcomes and cost-effectiveness of both. In addition to this, the accumulation of surgeon experience and the transfer of robotic skills are worthy of further attention.

Keywords: DaVinci robot; Hugo robot; Radical prostatectomy; Meta-analysis

25COASMA60

Title: Phase I trial of phIL12 plasmid intratumoral gene electrotransfer in patients with basal cell carcinoma in head and neck region,

Primoz Strojan, Tanja Jesenko, Masa Omerzel, Crt Jamsek, Ales Groselj, Ursa Lampreht Tratar,

European Journal of Surgical Oncology, Volume 51, Issue 5,2025,109574,
https://doi.org/10.1016/j.ejso.2025.109574.

Abstract: In the treatment of cancer, immunomodulatory approaches are developed to support the organism in fighting cancer or to enhance the immunomodulatory effects of local ablative techniques. To this end, we conducted an interventional, open-label, single-arm Phase I trial to evaluate the safety and tolerability of intratumoral phIL12 plasmid DNA gene electrotransfer as primary objectives. The study was dose-escalating with 3 consecutive

cohorts of 3 patients per phIL12 dose level (0.5 mg/ml, 1 mg/ml or 2 mg/ml) according to a matched 3 + 3 design. Recruitment of patients was staggered. The waiting period was 30 days after treatment of the previous patient, based on the expected duration of acute and subacute toxicity. The results of this phase I clinical trial in basal cell carcinoma demonstrated the feasibility and safety of the phIL12 plasmid by gene electrotransfer. We were able to demonstrate that phIL12 gene electrotransfer induced local IL-12 production, which was accompanied with IFN-γ expression. Triggering of the immune response was demonstrated by increased infiltration of immune cells and some antitumor effect. Based on these data, we would recommend the use of a concentration of 2 mg/ml of the plasmid in future trials. The trial lays the foundation for future Phase II clinical trials in which phIL12 gene electrotransfer is used in combination with local tumor-ablative approaches, such as electrochemotherapy or radiotherapy.

Keywords: Phase I clinical trial; phIL12 plasmid; Interleukin-12; Gene electrotransfer; Basal cell carcinoma

25COASMA61

Title: Current practices and challenges of endoscopic-assisted breast surgery in China: A nationwide cross-sectional survey,

Bingqiu Xiu, Qi Zhang, Xuli Meng, Shuang Hao, Benlong Yang, Junjie Li, Zhi-Ming Shao, Jiong Wu,

European Journal of Surgical Oncology, Volume 51, Issue 5,2025,109620,
https://doi.org/10.1016/j.ejso.2025.109620.

Abstract: Endoscopy-assisted breast surgery is gaining popularity in the treatment of breast cancer owing to its minimally access nature. However, its application in Mainland China varies significantly across regions. We aimed to evaluate the current practices and challenges of endoscopy-assisted breast surgery in Mainland China using a nationwide cross-sectional survey. In 2022, we conducted a comprehensive questionnaire survey across Mainland China regarding the clinical practices of breast surgery in 215 hospitals, 198 responded fully before September 2024 and included for analysis. Data on hospital characteristics, types of EABS performed, agreements on indications and contraindications, complications, and surgeon preferences were collected and analyzed. Of 198 hospitals with complete responses in the endoscopy-assisted breast surgery section, 93 (47.0 %) could perform endoscopy-assisted breast surgery, and 7 (3.5 %) could perform robot-assisted breast surgeries. Hospitals performing endoscopy-assisted breast surgery had more developed breast surgery departments, higher numbers of inpatient beds, and a greater patient population. The median annual number of endoscopy-assisted breast surgery procedures per hospital was 55, with significant variability. Common procedures included endoscopy-assisted breast-conserving surgery and lumpectomy (15.5 % and 30.7 %, respectively). Breast reconstructions constituted 15.5 %. The most commonly reported complications were seroma formation and bleeding. Despite these complications, endoscopy-assisted breast surgery was considered safe and effective, with positive aesthetic and functional outcomes. To the best of our knowledge, this is the largest cross-sectional study on endoscopy-assisted breast surgery-related clinical practices in China, highlighting regional disparities and the need for standardized training and procedures.

Keywords: Endoscopic-assisted breast surgery; Cross-sectional study; Clinical practice; Breast cancer; Surgical volume

25COASMA62

Title: Fit4Surgery app: Home-based prehabilitation app for older patients undergoing elective colorectal cancer surgery,

Lennaert CB. Groen, Thomas GC. Timmers, Freek D. Daams, Hieronymus J. Doodeman, Hermien WH. Schreurs, Emma RJ. Bruns,

European Journal of Surgical Oncology, Volume 51, Issue 5,2025,109691,
https://doi.org/10.1016/j.ejso.2025.109691.

Abstract: Supervised multimodal prehabilitation prior to colorectal cancer (CRC) surgery is associated with reduced complications and enhanced recovery. However, it is labor intensive and expensive. In an aging population with increasing demand and costs on healthcare and staff shortages, home-based prehabilitation (HBP) with an app could be of interest. This study assessed the effectiveness of a Fit4Surgery app in CRC surgery. The app was effectuated in a prospective cohort study of 100 CRC patients ≥60 years from October 2021–December 2022. The primary outcome was preservation or improvement of the 6-minute walking test (6MWT) six weeks postoperative, compared to baseline. Secondary outcomes were 90-day complication and mortality rate, 90-day readmission, length of stay, 6MWT and Short Performance Physical Battery (SPPB) at different timepoints and total costs. Three patients needed urgent surgery, remaining 97 patients (mean age 72) using the app for at least three weeks. The 6MWT was preserved in 74.7 % with a 12.1 m higher mean six weeks postoperative, compared to baseline (p = 0.194). A significant higher 6MWT was observed after prehabilitation and one year postoperative, compared to baseline (p=<0.001). The SPPB was significant higher at all timepoints. Overall 90-day complication rate was 25.8 %, readmission rate 6.3 % and mortality occurred in 2.1 %. Total costs were €518.50 per patient. This is the first study of multimodal HBP by an app for CRC surgery patients with high compliance. Results show promising results regarding functional capacity and a low occurrence of complications, in line with multimodal supervised prehabilitation. This by reducing costs by half.

Keywords: Prehabilitation; Colorectal cancer; Surgery; App

25COASMA63

Title: Clinical value of preoperative circulating tumor DNA before surgery in patients with esophageal squamous cell carcinoma,

Ryota Kobayashi, Satoru Matsuda, Kohei Nakamura, Hirofumi Kawakubo, Keiso Ho, Yosuke Morimoto,

European Journal of Surgical Oncology, Volume 51, Issue 5,2025,109625,
https://doi.org/10.1016/j.ejso.2025.109625.

Abstract: A precise preoperative tumor monitoring method that reflects tumor burden during neoadjuvant treatment is required to guide individualized perioperative treatment strategies for esophageal squamous cell carcinoma (ESCC). This study examined the clinical significance of preoperative circulating tumor DNA (ctDNA) in the plasma of patients undergoing neoadjuvant chemotherapy (NAC) followed by esophagectomy. Plasma samples

were collected longitudinally for ctDNA analysis as well as genomic DNA from primary lesions from patients with histologically confirmed ESCC who received neoadjuvant chemotherapy (NAC) followed by subtotal esophagectomy. Next-generation sequencing was used to identify mutations in both the plasma and primary tumors. We evaluated the relationship between ctDNA alterations and recurrence in patients with locally advanced ESCC. Pretreatment samples from 25 patients (100 %) showed the same mutations in both ctDNA and primary tumors; therefore, they were classified as ctDNA-positive before treatment. In the cohort of 25 patients analyzed, those who tested positive for ctDNA after NAC had a significantly higher risk of recurrence; the 36-month recurrence-free survival rates were 92 % for ctDNA-negative patients and 8 % for ctDNA-positive patients ($p < 0.001$). Preoperative ctDNA status may be a promising prognostic biomarker that can be assessed before surgery in patients with ESCC who received NAC. Expanded cohort validation will allow for more personalized multidisciplinary treatment approaches for ESCC tailored to ctDNA analysis.

Keywords: Circulating tumor DNA; Esophageal squamous cell carcinoma; Liquid biopsy; Neoadjuvant chemotherapy

25COASMA64

Title: Long-term outcomes of hepatopancreatoduodenectomy for perihilar cholangiocarcinoma: A comparative study with conventional hepatectomy,

Sho Kiritani, Yoshikuni Kawaguchi, Yujiro Nishioka, Yuichiro Mihara, Akihiko Ichida, Takeshi Takamoto,

European Journal of Surgical Oncology, Volume 51, Issue 5,2025,109633,
https://doi.org/10.1016/j.ejso.2025.109633.

Abstract: Hepatopancreatoduodenectomy (HPD) is necessary to achieve a reliable margin-negative resection for widespread perihilar cholangiocarcinoma (PhCC), yet data on long-term outcomes following HPD for PhCC remain limited. A retrospective cohort study was conducted on 167 patients with PhCC who underwent surgery with curative-intent between 2000 and 2023. Hepatic resection and extrahepatic bile duct resection (Hr-BDR) were performed for cases presumed to have localized tumors, while HPD was conducted for cases with presumed extensive tumor spread. Short- and long-term outcomes, including surgery details, pathological findings, postoperative complications, survival rates, and recurrence patterns, were compared. Forty-five patients underwent HPD and 122 underwent Hr-BDR. No differences were observed in the T or N factors of the TNM staging between both groups ($P = 0.09$ and 0.09). Overall postoperative significant complications (38 % vs. 34 %, $P = 0.62$), 90-day mortality rates (2 % vs. 2 %, $P = 0.80$), and 5-year cancer-specific survival (45 % vs. 40 %, $P = 0.81$) were comparable between both groups. However, the 5-year survival rate of the HPD group was significantly higher than that of the Hr-BDR group with positive invasive duodenal-side ductal margins (45 % vs. 0 %, $P = 0.03$). Local and remnant bile duct recurrence were significantly less frequent in the HPD than in the Hr-BDR group (20 % vs. 37 %, $P = 0.04$; 11 % vs. 0 %, $P = 0.02$, respectively). Although HPD for widespread PhCC requires careful postoperative management, it has the potential to provide excellent long-term outcomes, and it should be considered proactively.

Keywords: Perihilar cholangiocarcinoma; Hepatopancreatoduodenectomy; Long-term outcome; Local recurrence; Postoperative complication

25COASMA65

Title: Tumour volume analysis applied to imaging and histological examinations in breast cancer,

Angus B. Gordon, Alexander Sheeka, Suzy Cleator, Daniel Leff, Adrian Lim,

European Journal of Surgical Oncology, Volume 51, Issue 5,2025,109578,
https://doi.org/10.1016/j.ejso.2025.109578.

Abstract: Response Evaluation Criteria in Solid Tumours (RECIST) determines partial response (PR) and progressive disease (PD) as a 30 % reduction and 20 % increase in the longest diameter (LD), respectively. Tumour volume analysis (TVA) utilises three diameters to calculate response parameters. We conducted a pilot investigation of patients who underwent neoadjuvant breast cancer treatment and evaluation using RECIST with LD measurements and TVA with three diametric measurements, using the parameters PR (>30 % tumour regression), PD (>20 % tumour growth), and intermediate stable disease (SD). According to TVA, RECIST miscategorised 7 of 28 patients (25 %). We evaluated 145 patients who underwent baseline breast magnetic resonance imaging (MRI), neoadjuvant chemotherapy, presurgical MRI, and surgery and calculated LD and volume from all MRI examinations. Of the 173 patients, 157 had measurable disease at baseline and treatment completion, and 32 were miscategorised (20.4 %). The number of patients with a PR increased from 123 to 150 after TVA. The sensitivity of RECIST-measured responses (95 % confidence interval: 97–100 %) was 100 % for TVA. This altered the staging, as 32 of 157 (20.4 %) patients were allocated to another response group, with fewer cases of SD: 26 patients moved from SD to PR and 6 patients from SD to PD. Measuring a solid mass using LD is fundamentally flawed, as the lesser axes considerably affect the volume, leading to inaccurate response categorisation, with implications for patient management. TVA is a novel method that increases accuracy of tumour size measurement and response to therapy.

Keywords: Tumor volume; Imaging; Histology; Breast cancer

25COASMA66

Title: Efficacy of Neoadjuvant Chemotherapy as pre-habilitation program in advanced epithelial ovarian cancer,

Valentina Ghirardi, Claudia Marchetti, Diana Giannarelli, Alice Zampolini Faustini, Valeria Gallucci,

European Journal of Surgical Oncology, Volume 51, Issue 5,2025,109599,
https://doi.org/10.1016/j.ejso.2025.109599.

Abstract: Approximately 70 % of ovarian cancer patients present at diagnosis with advanced disease(AOC) and impaired clinical conditions, making them not ideal surgical candidates. We aimed to investigate whether neoadjuvant chemotherapy(NACT) can modify pre-operative characteristics of patients at high risk(HR) of perioperative complications, as defined in the Mayo Clinic Algorithm. We also compared their morbidity and survival outcomes with comparable HR women undergoing primary surgery (PCS). We retrospectively collected FIGO stage III and greater AOC patients undergoing either NACT-

interval cytoreductive surgery(HR-NACT) or PCS from 01/2013 to 12/2022. HR features included: Albumin <3.5 g/dL or age≥80 years or age 75–79 and at least one among: ECOG PS > 1, stage IV disease, or complex surgery likely (more than hysterectomy, salpingo-oophorectomy and omentectomy). 400 patients were included. Among them, 298 met the criteria for the HR-NACT group; 203(68.1 %) underwent ICS after 3–4 cycles whislt 95(31.9 %) completed 6 NACT cycles. We reported an improvement in clinical variables in women undergoing 3–4 cycles of NACT: raise of ECOG = 0 rate(53.3 % vs 81.8 %; $p < 0.001$) and median albumin serum levels(3.0 g/dl vs 4.0 g/dl; $p < 0.001$). We identified 102 comparable HR-PCS patients. No difference in intraoperative complications was detected, while a difference was found in severe post-operative complications, favoring patients treated with both 3–4(5.4 % vs 18.6 % $p = 0.0003$) and 6 NACT cycles(7.8 % vs 18.6 %, $p = 0.053$). No difference in both DFS and OS was reported. We offer a rationale to combine non interventional pre-habilitation procedure with short term chemotherapy cycles, aiming to improve pre-operative conditions of selected HR patients.

Keywords: Ovarian cancer; Neoadjuvant chemotherapy; Pre-habilitation; Morbidity

25COASMA67

Title: Can surgeons predict the extent of abdominal surgery based on MRI findings in CRS-HIPEC candidates with colorectal cancer?,

C.J.V. Rijsemus, N.F.M. Kok, A.G.J. Aalbers, B.A. Grotenhuis, E. Berardi, P. Snaebjornsson,

European Journal of Surgical Oncology, Volume 51, Issue 5,2025,109583,
https://doi.org/10.1016/j.ejso.2025.109583.

Abstract: Diffusion-weighted MRI (DW-MRI) is a promising tool for selecting patients with colorectal peritoneal metastases for cytoreductive surgery (CRS). This study investigated whether surgeons can predict the extent of CRS based on preoperative MRI findings. This single-centre retrospective study included patients who underwent CRS-HIPEC after preoperative MRI. An expert abdominal radiologist showed MR images to three experienced surgeons, who independently predicted the probability of achieving a complete resection by scoring which of 29 anatomical structures would be resected during CRS-HIPEC. Other predictions were surgery duration, number of anastomoses and CRS-HIPEC resulting in a stoma. Predictions were confirmed using surgical reports and histopathology. Data from 29 patients were analyzed. The median surgical PCI was 6 [range 0–19]. Complete resection was achieved in all patients with a total of 216 structures resected. All three surgeons had a negative predicting value (NPV) above 75% for most anatomical structures, and a positive predicting value (PPV) ranging from moderate (50%–75%) to good (>75%). The PPV for CRS-HIPEC resulting in a stoma ranged between 71% and 100%, and for colon anastomoses between 57% and 77%. The ICC indicated good to excellent (≥0.75) agreement among surgeons' predictions for most structures. Based on DW-MRI, the abdominal radiologist and surgeon are good at predicting the extent of the cytoreductive surgical procedure. Surgeons can use MRI findings for surgical planning and patient expectation management. However, adhesions and fibrosis interpreted as possible tumors during surgery and not clearly depicted small metastases on MRI can lead to more resections than anticipated.

Keywords: (DW)MRI; Peritoneal metastases; Colorectal cancer; PCI; CRS-HIPEC

25COASMA68

Title: Clinical implications of disappearing pancreatic cancer liver metastases: Lessons from colorectal liver metastases,

Aya Maekawa, Kojiro Omiya, Atsushi Oba, Yosuke Inoue, Yuki Hirose, Kosuke Kobayashi, Yoshihiro Ono,

European Journal of Surgical Oncology, Volume 51, Issue 5,2025,109635,
https://doi.org/10.1016/j.ejso.2025.109635.

Abstract: The efficacy of local control for pancreatic cancer liver metastases (PCLM), including surgical treatment, remains controversial, with no consensus on the management and clinical significance of disappearing liver metastases (DLMs). This study aimed to evaluate the clinical implications of DLMs in treating PCLM after multi-agent chemotherapy, utilizing contrast-enhanced imaging modalities. A retrospective analysis was conducted on patients who underwent curative resection for pancreatic cancer with synchronous or metachronous liver metastases between 2014 and 2023. Surgical indications were based on our recently reported ABCD criteria (Anatomical/Biological/Conditional/Duration). Both contrast-enhanced computed tomography (CE-CT) and gadolinium ethoxybenzyl diethylenetriamine pentaacetic acid-enhanced magnetic resonance imaging (EOB-MRI) were used to monitor metastatic lesions in the liver. DLMs were defined as tumors undetected on CE-CT post-chemotherapy. A total of 58 lesions in 29 patients with PCLM who underwent surgical resection were evaluated. Of the 13 lesions evident on CE-CT, 76.9 % (10/13) contained clinically/pathologically residual tumors. Of the 45 DLMs, 16 (35.6 %) had residual tumors. Twenty-six DLMs (57.8 %) were detected on EOB-MRI or intraoperative screening (contrast-enhanced ultrasonography and palpation), with 42.3 % (11/26) being residual tumors. Nineteen DLMs were undetectable by any modality, of which 26.3 % (5/19) were confirmed to be residual tumors with a median follow-up of 32 months. The median overall survival from initiating treatment for PCLM was 48.5 months. Integrating EOB-MRI into preoperative evaluations for PCLM enhances the detection of clinically relevant DLMs. Our findings highlight the potential benefits of considering an image-guided surgical approach in selected patients.

Keywords: Metastatic pancreatic cancer; Liver metastases; EOB-MRI; Chemotherapy; Surgical resection

25COASMA69

Title: Identification of a gene signature and prediction of overall survival of patients with stage IV colorectal cancer using a novel machine learning approach,

Abdullah Altaf, Jun Kawashima, Mujtaba Khalil, Hunter Stecko, Zayed Rashid, Matthew Kalady, Timothy M. Pawlik,

European Journal of Surgical Oncology, Volume 51, Issue 5,2025,109718,
https://doi.org/10.1016/j.ejso.2025.109718.

Abstract: We sought to characterize unique gene signature patterns associated with worse overall survival (OS) among patients with stage IV colorectal cancer (CRC) using a machine learning (ML) approach. Data from the AACR GENIE registry were analyzed for genetic variations (somatic mutations, structural variants and copy number alterations) among patients with CRC. Adult patients (≥18 years) with histologically confirmed stage IV CRC

who underwent next-generation sequencing were included. An eXtreme Gradient Boosting (XGBoost) model was developed to predict OS and the relative importance of different genetic alterations was determined using SHapley Additive exPlanations (SHAP) algorithm. Among 688 patients with stage IV CRC, 54.4 % were male (n = 374) with a median age of 55 years (IQR, 46–64). An XGBoost model developed using the 200 most frequent genetic alterations demonstrated good performance to predict OS with a c-index of 0.701 (95 % CI: 0.675–0.726) on 5-fold cross-validation. The model achieved time-dependent AUC of 0.742, 0.757 and 0.793 at 12-, 24- and 36-months, respectively. The SHAP algorithm identified the top 20 genetic alterations most strongly predictive of worse OS among stage IV CRC patients. Based on the 20-gene signature, individuals at high risk had worse 12- and 36-month OS versus low-risk patients (82.6 % vs. 97.1 % and 30.1 % vs. 72.6 %, respectively; $p < 0.001$). The XGBoost ML model identified a unique gene signature that accurately risk stratified stage IV CRC patients. ML models that incorporate molecular information represent an opportunity to predict long-term outcomes and potentially identify novel therapeutic targets for stage IV CRC patients.

Keywords: Colorectal cancer; Gene signature; Overall survival; Therapeutic target; Machine learning

25COASMA70

Title: Intraoperative electron radiotherapy (IOERT) in colorectal cancer: Updated systematic review of techniques, oncological outcomes and complications,

Abhinav Tiwari, Sheah Lin Lee, Tom MacCabe, Michal Woyton, Charles T. West, Rohan Micklethwaite,

European Journal of Surgical Oncology, Volume 51, Issue 5,2025,109724,
https://doi.org/10.1016/j.ejso.2025.109724.

Abstract: Intra-operative electron radiotherapy (IOERT) directly delivers a large fraction of radiation to at-risk margins during surgery. However, the precise benefit of IOERT in patients with locally advanced and locally recurrent colorectal cancer (LACC/LRCC) is unclear. This study aimed to provide an updated summary of the current evidence available regarding IOERT as part of multi-modality treatment of LACC and LRCC. This systematic review update was prospectively registered on PROSPERO (CRD42023438184). An electronic literature search was carried out using Ovid (MEDLINE), EMBASE, Web of Science, and the Cochrane Library databases for studies from July 2011 to April 2024. The inclusion criteria were adult patients who received IOERT as part of multi-modal treatment for LACC or LRCC. The primary outcome was overall survival (OS), disease free survival (DFS) and local control (LC) at 5 years. Secondary outcomes included post-operative complications. 16 new studies were identified since the previous analysis, and included (study population 1912 patients) of which two were prospective. High heterogeneity prevented meta-analysis of outcomes except for 5-year OS which suggested a non-significant benefit favouring IOERT. Significant methodological concerns were identified making interpretations challenging, however patients with LACC or LRCC with an R1 resection margin showed a favourable 5-year OS (40 % and 18 % respectively) when compared to current evidence. Although limited by a lack of appropriately conducted randomised

evidence, IOERT-containing multi-modality treatment may improve oncological outcomes in LACC and LRCC patients with R1 resections.

25COASMA71

Title: A proposed framework of strategies to overcome challenges to surgical quality assurance in oncology trials (SQA-Onc.),

J.W. Butterworth, P.R. Boshier, S. Mavroveli, J.V. Reynolds, Young-Woo Kim, G.B. Hanna, European Journal of Surgical Oncology, Volume 51, Issue 5,2025,109593,
https://doi.org/10.1016/j.ejso.2025.109593.

Abstract: Randomised controlled trials (RCTs) with surgical interventions frequently lack a framework to ensure surgical quality. We aimed to investigate surgical quality assurance (SQA) in oesophagogastric oncology trials and to develop a translatable framework of strategies to overcome challenges in the design and implementation of SQA. Seventy-one peer-nominated, international, expert trial stakeholders included surgeons; oncologists; trial managers and trial methodologists. Semi-structured interviews were conducted with expert stakeholders examining challenges to SQA in oncology trials followed by a Delphi process to gain consensus on mitigating strategies. Relevant expert consensus strategies were selected for inclusion within a separate written survey and Delphi process in the active ADDICT RCT. Expert consensus was reached for 59 strategies to overcome challenges to SQA in oncology trials. 19 of these strategies were selected for inclusion within the ADDICT survey and Delphi process, of which 14 (74 %) gained consensus amongst ADDICT trial stakeholders across two Delphi rounds, indicating their relevance within an active surgical oncology RCT. Prominent mitigating strategies included operative monitoring using photographs and/or videos with a structured objective assessment tool. Summarising the expert Delphi consensus allowed formulation of a framework of strategies to overcome challenges to SQA in oncology trials (SQA-Onc.) In this first international expert consensus within this area, agreement was reached for 59 strategies to overcome challenges to implementation of SQA. The proposed SQA-Onc. tool is intended to support SQA measures within future trials. Validating this framework within the next generation of RCTs should be the focus of future research.

Keywords: Quality assurance; Oesophagogastric surgery; Oncology trials; Challenges; Strategies; ADDICT trial

25COASMA72

Title: Nomogram for predicting postoperative temporomandibular joint degeneration after mandibulectomy for oral cavity cancer: a study on patients using CT and MRI data,

T.-Y. Tseng, A. Y.-H. Lin, P.-Y. Chou, C.-H. Toh, Y.-M. Wu, C.-H. Yeh,
International Journal of Oral and Maxillofacial Surgery, Volume 54, Issue 5,2025,Pages 395-403,
https://doi.org/10.1016/j.ijom.2024.10.010.

Abstract: The aim of this study was to develop a model for predicting the risk of postoperative temporomandibular joint osteoarthritis (TMJOA) in patients receiving a segmental or marginal mandibulectomy for oral cavity cancer . A total of 371 patients with

buccal or gingival cancer who underwent mandibulectomy were included in this retrospective cohort study. Demographic data, computed tomography, and magnetic resonance images were reviewed. Univariate and multivariate Cox regression analyses were performed to develop a nomogram to predict post-mandibulectomy TMJOA. TMJOA was identified in 81 of the 371 patients at 2 years and 107 at 4 years. The predictors of post-mandibulectomy TMJOA were segmental mandibulectomy (hazard ratio (HR) 2.51, 95% confidence interval (CI) 1.64–3.83, P < 0.001), age ≥ 62.5 years (HR 2.28, 95% CI 1.53–3.40, P < 0.001), BMI < 24.1 kg/m2 (HR 2.13, 95% CI 1.45–3.13, P < 0.001), and American Joint Committee on Cancer stage IVa/IVb (HR 2.21, 95% CI 1.38–3.56, P = 0.001). The nomogram developed in this study exhibited good predictive capacity (area under the curve 0.742, 95% CI 0.679–0.804). The proposed model for predicting post-mandibulectomy TMJOA in patients with buccal or gingival cancer can identify high-risk individuals for early preventive oral rehabilitation.

Keywords: Temporomandibular joint disorders; Mouth neoplasms; Nomograms; Magnetic resonance imaging; X-ray computed tomography

25COASMA73

Title: Validation of 'total face approach' (TFA) three-dimensional cephalometry for the diagnosis of dentofacial dysmorphisms and correlation with clinical diagnosis,

C. Zilio, A. Tel, G. Perrotti, T. Testori, S. Sembronio, M. Robiony,
International Journal of Oral and Maxillofacial Surgery,Volume 54, Issue 5,2025,Pages 420-429,
https://doi.org/10.1016/j.ijom.2024.10.002.

Abstract: The last decades have witnessed significant improvements in orthognathic surgery, but a true standardization of cephalometric analysis to guide clinical assessment in three-dimensional (3D) virtual planning is still lacking. Therefore, the aim of this study was to validate the 'total face approach' (TFA) 3D cephalometric model for the diagnosis of dysmorphia and to analyse its correlation with the clinical diagnosis and virtual surgical planning performed in the Maxillofacial Surgery Clinic in Udine. This model was validated by studying different cephalometric points in three modules (vertical dimensions, sagittal dimensions, and symmetry) and their sections. Each section of the different modules evaluates the range of the studied patient according to the TFA analysis executed in Planmeca Romexis software and compares it with the ProPlan CMF data. The results of the statistical analysis defined the degree of concordance for each point studied. An overall high correlation was demonstrated for each of the cephalometric categories (weighted kappa between 0.442 and 0.642 in vertical dimension, between 0.587 and 1 in sagittal dimension, and between 0.773 and 1 in symmetry). The TFA model can be considered a valuable guide for the diagnosis of dysmorphia and 3D virtual planning of orthognathic maxillofacial surgery.

Keywords: Cephalometry; Orthognathic surgery; Dentofacial deformities; Computer-generated 3D imaging; Orthodontics

25COASMA74

Title: Inflammatory breast cancer response to modern neoadjuvant chemotherapy: Tumor response and survival outcomes,

Dorsa Mousa-Doust, Amy Bazzarelli, Melina Deban, Carol Dingee, Jieun Newman-Bremang,
The American Journal of Surgery, Volume 243,2025,116288,
https://doi.org/10.1016/j.amjsurg.2025.116288.

Abstract: Inflammatory breast cancer (IBC) is a rare, aggressive form of breast cancer. This study evaluates oncologic outcomes in IBC patients treated with modern multimodal treatment. A retrospective review analyzed clinicopathologic data of 5063 patients, 646 of whom underwent NAC followed by surgery between 2012 and 2024. Survival outcomes were compared across biologic subtypes. Twenty-six cases of T4dM0 IBC were identified, with 57.7 % HER-2 positive, 26.9 % ER positive/HER-2 negative, and 15.4 % ER negative/HER-2 negative. The total pCR rate was highest in HER-2 positive (53.3 %) and lowest in ER-positive/HER-2 negative patients ($p = 0.036$). Among 19 patients with ≥3 years of follow-up, 47 % experienced recurrence (78 % distant and 22 % locoregional) and 42 % died of breast cancer. No significant differences in locoregional recurrence, or survival outcomes were found across subtypes. pCR has limited prognostic value in IBC. Although HER-2 positive patients are more likely to achieve pCR, this does not necessarily translate into improved outcomes.

Keywords: Inflammatory breast cancer; Neoadjuvant chemotherapy; Pathologic complete response; Tumor biology; Tumor recurrence; Survival outcome

25COASMA75

Title: Expert consensus on the clinical practice of sleeve gastrectomy in China using the modified Delphi method,

Peirong Tian, Boyu Tao, Mengyi Li, Yang Liu, Jingli Liu, Jia Liu, Peng Zhang, Zhongtao Zhang,
Asian Journal of Surgery, Volume 48, Issue 5,2025, Pages 2918-2926,
https://doi.org/10.1016/j.asjsur.2024.11.211.

Abstract: Sleeve gastrectomy (SG) is the most commonly performed bariatric surgery worldwide, including in China. Despite its prevalence, significant variations exist in its practice. This consensus aims to standardize SG practices in China. A modified Delphi method was employed to gather expert opinions from 50 Chinese bariatric surgeons. Participants voted on 80 statements covering indications, contraindications, preoperative/postoperative management, and surgical techniques. Consensus was achieved on 54 out of 80 statements. Key areas include SG being the preferred choice for patients with high surgical risk and severe obesity. Agreement was reached on surgical techniques such as staple line reinforcement and the management of hiatal hernias found during surgery. Consensus was also achieved on aspects of preoperative and postoperative care, including routine endoscopy and the use of the enhanced recovery after surgery (ERAS) protocol. This consensus provides valuable guidelines for standardizing SG practices in China. It provides evidence-based recommendations to standardize SG practice, improve outcomes, and guide future research directions.

Keywords: Delphi method; Metabolic and bariatric surgery; Sleeve gastrectomy; Obesity

25COASMA76

Title: Iatrogenic vascular injuries in inguinal hernia repair: A comprehensive analysis of incidence, management, and outcomes,

Zhui Li, Yangyang Feng, Chuli Jiang, Gaoxiang Fan, Yu Zhao, Wei Ren,

Asian Journal of Surgery,Volume 48, Issue 5,2025,Pages 2882-2890,
https://doi.org/10.1016/j.asjsur.2024.07.201.

Abstract: Iatrogenic vascular injuries associated with inguinal herniorrhaphy are seldom documented. This study sought to provide a thorough analysis of the types, underlying mechanisms, treatment approaches, results, and mortality hazards linked to such vascular injuries during the repair of inguinal hernias. Thirteen cases of vascular injury among 3988 inguinal hernia repair patients were retrospectively analyzed from 2012 to 2023. The data included demographic information, injury types, surgical details, patient presentations, diagnostic methods, management strategies, and outcomes. Factors contributing to mortality risk were identified via univariate analysis. The incidence of vascular injuries was 0.075 %, with 92.31 % being penetrating injuries and 7.69 % being blunt injuries. Common mechanisms included intraoperative dissections, trocar-related injuries, and mechanical mesh fixation. Treatment approaches included anastomosis, transplantation, endovascular therapy, ligation, and conservative methods. The 30-day mortality rate was 23.07 %, primarily due to hemorrhage-induced multiorgan failure. Late complications included anastomotic restenosis, graft aneurysms, testicular atrophy, and hernia recurrence. Iatrogenic vascular injuries during inguinal herniorrhaphy, though rare, pose significant risks of mortality and complications. Timely identification, intervention, and long-term monitoring are vital for improving outcomes. This study offers insights into managing complex vascular challenges in hernia repair, with the goal of improving patient outcomes.

Keywords: Iatrogenic vascular injuries; Inguinal hernia repair; Retrospective analysis; Surgical complications

25COASMA77

Title: Achieving ideal surgical outcomes by identifying the dominant supratrochlear artery for forehead flap harvesting: A comparative study,

Wentian Xiao, Liuhanghang Cheng, Sally Ng, Hua Li, Shaoqing Feng, Yixin Zhang, Peiru Min,

Asian Journal of Surgery, Volume 48, Issue 5,2025,Pages 2911-2917,
https://doi.org/10.1016/j.asjsur.2024.11.165.

Abstract: Despite being considered the golden standard for nasal reconstruction for decades, there has been a lack of detailed investigation into the hemodynamic differences between bilateral supratrochlear vessels during forehead flap procedures. In this study, the authors utilized infrared thermography (IRT) to identify the dominant supratrochlear vessel as the nourished pedicle, aiming to achieve optimal surgical outcomes. A total of 24 regular and 40 pre-expanded forehead flaps, consecutively included from October 2017 to February 2023, were retrospectively divided into two groups for analysis. In group A (11 regular and 23 pre-expanded flaps), bilateral supratrochlear arteries were identified using infrared thermography (IRT) and color Doppler ultrasound (CDU), with the flap designed based on the dominant side. In group B (13 regular and 17 pre-expanded flaps), the flap was designed directly at the

ipsilateral side. Vascular disparities and surgical outcomes were compared. Among the 34 flaps in group A, bilateral hemodynamic disparities were observed in 13 flaps (38.2 %), comprising of 3 regular flaps (27.2 %) and 10 pre-expanded flaps (43.5 %). The complication incidences for group A is lower than that for group B (5/34 VS 9/30, $p < 0.05$). The complication rate between regular and pre-expanded flaps was 3/24 versus 11/40, $p < 0.05$. All complications resulted in a delayed pedicle division. The potential asymmetry of supratrochlear arteries could significantly impact the prognosis of nasal reconstruction with forehead flaps, especially within tissue expansion technique. It is essential to identify the dominant side to achieve optimized surgical outcomes.

Keywords: Forehead flap; Supratrochlear vessel; Vascular navigation; Infrared thermography; Nasal reconstruction

List of Serials
Abstracted in COAS
COAS, Volume- 2 Issue No. 5, 2025

1. American Journal of Otolaryngology, Volume 46, Issue 3, 2025
2. American Journal of Roentgenology, Vol-224, issue-3, 2025
3. Anaesthesia Critical Care & Pain Medicine, Volume 44, Issue 3, 2025
4. Annals of Oncology, Vol.-36, issue-4, 2025
5. Anticancer Research, Volume 45, issue 5, 2025
6. Archives of Pathology and Laboratory Medicine, Vol.-149,issue-4, 2025
7. Asian Journal of Surgery, Volume 48, Issue 5, 2025
8. Blood , Vol.-145, issue-8,9 and 10, 2025
9. British Journal of Anaesthesia, Volume 134, Issue 5, 2025
10. Cancer Cytopathology , Vol-133, issue-5 and , 2025
11. Cancer Gene Therapy, Volume 32, Issue 4, 2025
12. Cancer, Volume 131, Issue 8,9, 2025
13. Carcinogenesis, Volume 46, Issue 2, 2025
14. European Journal of Surgical Oncology, Volume 51, Issue 5, 2025
15. International Journal of Cancer ,Vol-156 , issue- 8 and 9, 2025
16. International Journal of Oral and Maxillofacial Surgery, Volume 54, Issue 5, 2025
17. JAMA.; Vol.-333, Issue- 13,14 and 15, 2025
18. Journal of American Chemical Society, Volume 147, Issue 14,15,16.17, 2025
19. Journal of Cardiothoracic and Vascular Anesthesia, Volume 39, Issue 5, 2025
20. Journal of Clinical Anesthesia, Volume 104, 2025
21. Journal of Clinical Oncology, Volume 43, Issue-7 and 8, 2025
22. Journal of Intensive Care Medicine, Vol. 40, Number-5, 2025
23. Medical Oncology, Vol.- 42, issue-4, 2025
24. Nature Cell Biology, Volume 27, Issue 4, 2025
25. New England Journal of Medicine ,Vol. 392, Issue13,14 and 15 , 2025
26. The American Journal of Surgery, Volume 243, 2025
27. The American Journal of Surgical Pathology, Vol.-49, issue-5, 2025
28. The Annals of Thoracic Surgery, Volume 119, Issue 5, 2025
29. The Laryngoscope, Volume 135, number 5, 2025
30. Toxicology Letter, Volume 407, 2025

May 2025, Volume 2 Issue 5

Current Oncological Abstract Service (COAS)

Chittaranjan National Cancer Institute
(An Autonomous Body under Govt. of India, Ministry of Health & Family Welfare)
1st Campus,Hazra: 37,S.P.Mukherjee Road, Kolkata-700026
2nd Campus,New Town: Street Number 299, DJ Block, Action Area I,New Town, Kolkata-700160